

https://dspace.org/

Towards a multi-proxy holocene palaeoenvironmental and palaeoclimatic reconstruction for Eastern Lesotho

Fitchett, Jennifer Myfanwy

2016-01-20
http://hdl.handle.net/10539/19361

Downloaded from a DSpace repository. https://dspace.org/

Towards a Multi-Proxy Holocene Palaeoenvironmental and Palaeoclimatic Reconstruction for Eastern Lesotho

Jennifer Myfanwy Fitchett



Mafadi Summit, eastern Lesotho highlands

A Thesis submitted in fulfilment of the academic requirements for the degree of Doctor of Philosophy

School of Geography, Archaeology and Environmental Studies

University of the Witwatersrand, Johannesburg

October 2015

DECLARATION

I hereby declare that this thesis is my own, unaided work, except where otherwise acknowledged. It is being submitted for the degree of Doctor of Philosophy in Science at the University of the Witwatersrand, Johannesburg. I have not submitted this work previously, for the purpose of obtaining any degree, qualification or otherwise, at this or any other university



12/10/2015

Jennifer Myfanwy Fitchett

Date

ABSTRACT

The eastern Lesotho highlands observe climate patterns distinct from adjacent lower altitude regions, representing a niche environment with unique biodiversity, comprising well-adapted but restricted biomes. With a heavy reliance on subsistence agriculture, Lesotho faces risks to both the economy and individual livelihoods, should current rates of climate change persist or intensify. Furthermore, eastern Lesotho serves as southern Africa's primary water catchment, with precipitation exceeding evaporation. Any changes in the climate and hydrological systems, as are likely under climate change scenarios, would compromise biomes, livelihoods, and water security both locally and regionally. Climate change research in eastern Lesotho, is thus of particular value, yet meteorological data are sparse and the palaeoenvironmental history remains poorly resolved.

This research presents the first multi-proxy Holocene palaeoenvironmental and palaeoclimatic reconstruction for eastern Lesotho. This reconstruction is developed from the results from pollen, diatom and sediment analyses, extracted from sediment cores obtained from two peat bogs at Sani Valley (~2,800 m.asl) and Mafadi Wetland (~3,390 m.asl), and from an exposed gully-sidewall profile at Sekhokong (~2,950 m.asl), approximately 1km south of the Sani Valley site. The reconstructions are temporally constrained by AMS radiocarbon dates obtained for all three sites.

Mafadi Wetland demonstrates marked differences to the lower altitude sites, including slower sedimentation rates, a decrease in pollen and diatom taxa diversity, and an increase in the relative abundance of ice-tolerant diatom taxa. The microtopography of the three sites influences the rates of sedimentation, sediment properties, pollen composition, and distinct palaeoenvironmental and palaeoclimatic reconstructions for each site. The Sekhokong record commences in the late Pleistocene, with a wet period from ~13,180-10,850 cal. yr BP, interrupted by a dry period from ~13,080-12,830 cal. yr BP. From ~10,550-6,420 cal. yr BP, the Sekhokong record indicates a drier climate with a slow transition to warmer, wetter conditions. The Mafadi Wetland record commences with cold, wet conditions from ~8,140-7,580 cal. yr BP, followed by a warmer, drier period from ~7,520-6,680 cal. yr BP. Thereafter, greater microclimatic differences are apparent. For Sekhokong, warmer, dry conditions are inferred for ~6,420-6,000 cal. yr BP, followed by cold, wet conditions from ~6,000-5,450 cal. yr BP. Warmer, dry conditions commence earlier at Mafadi Wetland, from ~6,160-5,700 cal. yr BP, coinciding with the initiation of a longer wet period at Sani Valley, from ~6,200-4,900 cal. yr BP. At Sekhokong, a dry, warmer period follows from ~5,450-3,700 cal. yr BP. At Sani Valley, drier conditions are evident from ~4,770-4,470 cal. yr BP, followed by a cold, wet period from ~4,460-2,260 cal. yr BP. For Mafadi Wetland, these cold, wet conditions endure longer, from ~5,600-1,100 cal. yr BP. This overlaps with similarly cool, wet conditions at Sekhokong, from ~3,650-1,200 cal. yr BP. By contrast, dry conditions are evident at Sani Valley, from ~2,260-1,350 cal. yr BP. For all three sites, ~1,000 cal. yr BP to present is characterised by progressive drying, with discrete wet events. Pronounced cold events are detected at ~12,660 cal. yr BP, ~8,400-8,000 cal. yr BP and ~150 cal. yr BP.

The results of this study indicate similarities with records from adjacent studies in western Lesotho and South Africa, although with notable variability in the timing of events. The palaeoenvironmental reconstructions for eastern Lesotho, and their comparison with existing studies, provide valuable information to improve the understanding of southern African Holocene climates, and to facilitate the development of high resolution, accurate climate models for the eastern Lesotho region.

ACKNOWLEDGEMENTS

My thanks first go to my three supervisors, Prof Stefan Grab, Prof Marion Bamford and Prof Anson Mackay. They have encouraged, challenged and supported me throughout this degree, and have developed both my critical thought and my academic writing. Specific thanks to Stefan for sharing his invaluable knowledge of the eastern Lesotho highlands, his enthusiastic fieldwork assistance, and his financial support for much of the fieldwork and AMS dating costs; to Marion for inviting me to use the pollen laboratory at the Evolutionary Studies Institute, making this project feasible given restricted funding; and to Anson for making my time at UCL both academically stimulating and truly enjoyable, for covering the funding for additional diatom samples analysed at UCL, and for his continued support from across the world during my thesis write-up. In addition to my supervisors, many thanks go to Prof Louis Scott for his assistance in the identification of pollen grains, and to Prof Jasper Knight for his advice regarding the sediment analysis.

Pilot projects often face difficulties in obtaining permits to conduct work. I am grateful to the Lesotho Department for the Environment and Lineo Lerotholi for their assistance in granting me fieldwork permits for the project. To reach the Mafadi Wetland site, a helicopter flight-path over a KwaZulu-Natal Wildlife managed area was required, and I thus am grateful for the flight-path permission granted facilitating access to the site. Thanks to the pilots from Westline Aviation for their assistance in obtaining flight permits, and in transporting the team safely to and from the site.

Pilot projects also require considerable funding to enable a thorough and rigorous scientific approach. I therefore gratefully acknowledge the National Research Foundation for my Innovation PhD scholarship which covered much of my South African research costs; the Oppenheimer Memorial Trust which provided the funding to cover the split-site component of my PhD conducted at UCL; the DST/NRF Centre for Excellence in Palaeosciences which provided funding for the Mafadi Wetland fieldtrip and for AMS radiocarbon dates; and the Scholarships Office, the School of Geography, Archaeology and Environmental Studies, and the WITS Research Office, which funded my attendance at international conferences, where I presented two oral papers and a poster.

I have received assistance from incredible laboratory staff throughout my degree. Many thanks go to Petrus Chakane at the Evolutionary Sciences Institute for his assistance with pollen preparation; Janet Hope and Tula Maxted in the Geography Department at UCL; and Thandizwe Nsimbi in the School of Geography, Archaeology and Environmental Studies at WITS.

Immense thanks go to my family. To my mother, Anne, and sister, Meg, for proofreading first drafts of my chapters, feeding me when I'm too tired to cook, making coffee when I'm falling asleep, and providing sounding-boards from very different academic backgrounds. Thanks to my family in the UK: B, Laurence, Jack, Miri and Issy, who provided a home-base during the split-site component of my PhD. Thanks to my gran, who took a keen interest in my work, proven by my birthday card making mention of carbon dating!

Last, but not least, thanks to the friends who have encouraged me and stimulated valuable conversation throughout my degree: Donna Koch, Raeesa Moolla and Gijsbert Hoogendoorn at Wits, and Kelly Cheshire, Jen Adams, Stef Goodrich, Janet Hope, Luca Marazzi and Kevin Roe at UCL. Particular thanks to Kelly, a PhD student at UCL, who despite being in a different Hemisphere, has shared every step of the second half of my PhD with me, with unending support and enthusiasm.

TABLE OF CONTENTS

Abstract iii
Acknowledgements iv
List of Figures ix
List of Tables xiii
List of Acronyms xiv
List of Naming and Style Conventions xv
1. Introduction 1
1.1 Background 1
1.2 Palaeoenvironmental Proxies 3
1.2.1 AMS Radiocarbon Dating 5
1.2.2 Sediments: Total Organic Carbon, Carbonates and Particle Size 5
1.2.3 Pollen 7
1.2.4 Diatoms 10
1.4 Contribution to Knowledge 13
1.5 Study Aims and Objectives 14
1.6 Structure of the Thesis 16
2. Literature Review 18
2.1 Introduction 18
2.2 The Development of Palaeoenvironmental Work in Southern Africa 19
2.2.1 Southern African Palaeoenvironmental Proxies 20
2.2.2 Key Debates on Southern African Palaeoenvironmental Change 34
2.2.3 The Future of Southern African Palaeoenvironmental Research: The Importance of Application 43
2.3 Palaeoclimatic History of eastern Lesotho 47
2.3.1 The Archaeological Record 49
2.3.2 The Palaeogeomorphological Record 56
2.3.3. The Palaeoenvironmental Record: Proxy Evidence 60
2.3.4 Synthesis of Palaeoclimatic Change in Lesotho 64
2.4 Synopsis 66
2.4.1 Holocene Palaeoenvironmental Change in Southern Africa 66
2.4.2 Research Gaps: Avenues for Future Work 68
3. Regional Setting 70
3.1 Introduction 70
3.2 The Eastern Lesotho Highlands 70
3.2.1 Descriptive Geography 70
3.2.2 Geology and Geomorphology 72

3.2.3 Climate 77
3.2.4 Vegetation 82
3.2.5 Hydrology 85
3.3.6 Environmental Problems 86
3.3 Contemporary Environments of the Specific Study Sites 89
3.3.1 Sani Valley 90
3.3.2 Sekhokong 93
3.3.3 Mafadi Wetland 97
3.4 Conclusion 101
4. Methods 102
4.1 Introduction 102
4.2 Study Site Selection 102
4.3 Field Work 107
4.4 Laboratory work 112
4.4.1 Age Determination 113
4.4.2 Sediment Analysis 114
4.4.3 Pollen Preparation 117
4.4.4 Diatom Preparation 119
4.5 Statistical Analysis 120
4.5.1 Statistical Analysis of Diatom and Pollen Results 120
4.5.2 Statistical Analysis of Sediment Results 124
4.5.3 Statistical Analysis of AMS Dates 128
4.6 Conclusion 130
5. Results 131
5.1 Introduction 131
5.2 Sani Valley 132
5.2.1 Chronology and Sediment Accumulation 132
5.2.2 Stratigraphy and Sediment Properties 133
5.2.3 Pollen Analysis 138
5.2.4 Diatom Analysis 143
5.2.5 Multi-Proxy Synthesis 148
5.3 Sekhokong 150
5.3.1 Chronology and Sediment Accumulation 150
5.3.2 Stratigraphy and Sediment Properties 151
5.3.3 Pollen Analysis 157
5.3.4 Diatom Analysis 162
5.3.5 Multi-Proxy Synthesis 168

5.4 Mafadi Wetland 171
5.4.1 Chronology and Sediment Accumulation 171
5.4.2 Stratigraphy and Sediment Properties 172
5.4.3 Pollen Analysis 177
5.4.4 Diatom Analysis 183
5.4.5 Multi-Proxy Synthesis 188
5.4.6 Samples from a Diatomite Outcrop 191
5.5 Conclusion 197
6. Discussion 200
6.1 Introduction 200
6.2 Multi-Proxy Environmental and Climatic Inferences 201
6.2.1 Pollen 202
6.2.2 Diatoms 213
6.2.3 Sediments 222
6.3 Palaeoenvironmental Reconstructions 229
6.3.1 Sani Valley 230
6.3.2 Sekhokong 235
6.3.3 Mafadi Wetland 240
6.4 Lesotho Holocene Synthesis 246
6.4.1 Comparison Between Sites 248
6.4.2 Comparison with other studies in Lesotho 253
6.5 Regional to Global Comparisons 267
6.5.1 Comparison of Proxy composition 267
6.5.2 Comparison the Synchronicity of Climatic Events 268
6.6 Future Research Trajectories 272
7. Conclusion 277
7.1 Introduction 277
7.2 Achievement of Study Objectives 277
7.3 Regional Significance 281
7.5 Application of Findings 283
7.6 Synthesis 283
References 285
Appendix A: Laboratory Methods 322
A.1 Pollen Preparation 322
A.2 Diatom Preparation 323
A.3 Sediment Preparation 324
Appendix B: Raw Proxy Data 325

B.1 Sani Valley Mastersizer Particle Size Results 325
B.2 Sani Valley Pollen Counts 327
B.3 Sani Valley Diatom Counts 329
B.4 Sekhokong Mastersizer Particle Size Results 330
B.5 Sekhokong Pollen Counts 332
B.6 Sekhokong Diatom Counts 334
B.7 Mafadi Wetland Mastersizer Particle Size Results 338
B.8 Mafadi Wetland Pollen Counts 340
B.9 Mafadi Wetland Diatom Counts 342
B.10 Mafadi Diatomite Outcrop Mastersizer Particle Size Results 346
B.11 Mafadi Diatomite Outcrop Pollen Counts 348
B.12 Mafadi Diatomite Outcrop Diatom Counts 350
Appendix C: Additional Data Analysis 352
C.1 Principal Components Analysis Output 352
C.1.1 Sani Valley Pollen PCA 352
C.1.2 Sani Valley Diatom PCA 353
C.1.3 Sekhokong Pollen PCA 354
C.1.4 Sekhokong Diatom PCA 355
C.1.5 Mafadi Wetland Pollen PCA 357
C.1.6 Mafadi Wetland Diatom PCA 358
C.2 Skewness: Kurtosis Plots 360
C.2.1 Sani Valley 360
C.2.2 Sekhokong 360
C.2.3 Mafadi Wetland 361

LIST OF FIGURES

Figure 1.1: Examples of a range of pollen grains from the eastern Lesotho highlands under light microscope…… 8

Figure 1.2: Examples of a range of diatom valves from the eastern Lesotho highlands under light microscope. Scale bar represents 10µm…… 11

Figure 2.1: Locations of prominent southern African sites at which published palaeoenvironmental reconstructions have been undertaken…… 20

Figure 2.2: Number of proxies used in published palaeoenvironmental reconstructions for southern Africa: 1950-2015. Data derived from and cross-checked using Google Scholar, Science Direct and Web of Knowledge…… 21

Figure 2.3: The location of southern African sites at which published pollen-based environmental reconstructions have been undertaken…… 24

Figure 2.4: Southern African sites at which published diatom-based environmental reconstructions have been undertaken..... 27

Figure 2.5: The location of archaeological, geomorphological and palaeoenvironmental study sites in Lesotho from which published palaeoclimatic inferences have been made…… 48

Figure 2.6: Palaeoclimatic inferences from geomorphological, archaeological and palaeoenvironmental studies from eastern Lesotho..... 65

Figure 2.7: Maps demonstrating palaeoclimatic data across southern Africa for 1,000 cal. yr intervals throughout the Holocene, indicating spatial and temporal variations in climate throughout the period (Burrough & Thomas, 2013)…… 68

Figure 3.1: Location of the three study sites in eastern Lesotho…… 71

Figure 3.2: Thurfur formed due to mechanisms associated with ground freeze…… 75

Figure 3.3: Light snowfall in eastern Lesotho…… 80

Figure 3.4: Variations in vegetation with altitude across Lesotho (after Killick, 199, p. 24)…… 84

Figure 3.5: Southern African vegetation zones delineated by altitude and aridity (after Scott, 1982a)..... 84

Figure 3.6: Sheep in an already overgrazed grassland, close to Sani Valley…… 87

Figure 3.7: Extensive gullying on a north-facing slope of the Sekhokong Mountain Range. …… 88

Figure 3.8: Topographical map indicating the location of the Sani Valley (adapted from map code 2929CB Sani Pass and 2929CA Sani Pass (West)). Study site indicated by red circle…… 90

Figure 3.9: Google Earth Image of the region surrounding the Sani Valley site. Site marked by a red circle. 91

Figure 3.10: PVC pipe inserted into the raised bog, and the resultant standing water with algae…… 92

Figure 3.11: Topographical map indicating the position of the Sekhokong study site (adapted from map code 2929CB Sani Pass). Study site indicated by red circle…… 93

Figure 3.12: Google Earth Image of the region surrounding the Sekhokong site. Site marked by a red circle…… 94

Figure 3.13: Gully erosion exposing a sediment sequence of >5m at the selected study site…… 95

Figure 3.14: Topographical map indicating the location of the Mafadi Wetland site (adapted from map code 2929AB Champagne Castle). Study site indicated by red circle…… 97

Figure 3.15: The sparse vegetation near Mafadi Summit…… 98

Figure 3.16: Grazing sheep adjacent to the gullied river, and an ice rat outside its burrow in the gullied riverbank..... 100

Figure 3.17: Google Earth Image of the region surrounding the Mafadi site. Site marked by a red circle…. 101

Figure 4.1: The Sani Valley sampling site..... 104
Figure 4.2: The Mafadi Wetland sampling site, marked by white diatomite beds..... 105
Figure 4.3: The Sekhokong sampling site..... 106
Figure 4.4: Coring procedure for (a) consolidated and (b) unconsolidated sediments..... 109
Figure 4.5: Position of the two sampling sites adjacent to Mafadi Summit, from which one core was taken at Mafadi Wetland site and two from Mafadi Diatomite site..... 111
Figure 4.6: Summarised process of sediment preparation undertaken to determine colour, organic and carbonate content, and particle size distribution..... 117
Figure 4.7: Summarised procedure of pollen preparation (after Faegri et al., 1989)..... 118
Figure 4.8: Summarised process of diatom preparation undertaken..... 119
Figure 5.1: BACON output for the Sani Valley profile, providing interpolated ages for depths throughout the core..... 133
Figure 5.2: Stratigraphic log and photograph of core from Sani Valley..... 134
Figure 5.3: Changes in sediment properties throughout the Sani Valley profile..... 135
Figure 5.4: CONISS output separating samples from the Sani Valley profile on the basis of variations in sediment properties across the samples..... 136
Figure 5.5: CONISS zonation for the Sani Valley profile on the basis of pollen results..... 139
Figure 5.6: PCA biplot for pollen results from the Sani Valley profile..... 140
Figure 5.7: Stratigraphic diagram of the pollen results for the Sani Valley profile, ordered by PC1 species scores, and with curves indicating the PC1 and PC2 sample scores..... 142
Figure 5.8: CONISS output separating the Sani Valley profile according to variations in relative abundances in diatoms throughout..... 144
Figure 5.9: PCA biplot for the diatom results from the Sani Valley profile..... 145
Figure 5.10: Stratigraphic diagram of the relative abundance of diatoms throughout the Sani Valley profile, arranged by PC1 species score, with curves demonstrating PC1 and PC2 sample scores..... 147
Figure 5.11: Multi-proxy stratigraphic plot for the Sani Valley sequence..... 149
Figure 5.12: BACON output for the Sekhokong profile, providing interpolated ages for depths throughout the core..... 151
Figure 5.13: Stratigraphic log and photograph of core from Sekhokong..... 152
Figure 5.14: Stratigraphic plot demonstrating changes in sedimentary properties throughout the Sekhokong profile..... 155
Figure 5.15: CONISS output separating the Sekhokong profile into zones on the basis of changes in the sedimentary properties..... 156
Figure 5.16: CONISS output separating the Sekhokong profile into zones based on the relative abundance of pollen throughout..... 158
Figure 5.17: PCA biplot for the pollen results from the Sekhokong profile..... 159
Figure 5.18: Stratigraphic plot demonstrating changes in pollen throughout the Sekhokong profile, with species arranged by PC1 species score, and curves for the PC1 and PC2 sample scores..... 161
Figure 5.19: CONISS output separating the Sekhokong profile into zones based on the diatom results..... 164
Figure 5.20: PCA biplot for the diatom results from the Sekhokong profile..... 164
Figure 5.21: Stratigraphic diagram of the diatom results from the Sekhokong profile, with species ordered by PC1 species score and curves for the PC1 and PC2 sample scores..... 167
Figure 5.22: Multi-proxy stratigraphic diagram for Sekhokong..... 169

Figure 5.23: BACON output for the Mafadi Wetland profile, providing interpolated ages for depths throughout the core…… 172
Figure 5.24: Stratigraphic diagram of the sedimentary properties throughout the Mafadi Wetland profile…… 173
Figure 5.25: Stratigraphic log and photograph of core from Mafadi Wetland…… 174
Figure 5.26: CONISS output separating the Mafadi Wetland profile into zones based on differences in sedimentary characteristics throughout…… 175
Figure 5.27: CONISS output separating the Mafadi Wetland profile into zones based on the pollen results…… 179
Figure 5.28: PCA biplot for pollen results from the Mafadi Wetland profile…… 180
Figure 5.29: Stratigraphic diagram of the pollen results for the Mafadi Wetland profile, with species ordered according to the PC1 species scores, and curves for PC1 and PC2 sample scores…… 181
Figure 5.30: CONISS output dividing the Mafadi Wetland profile into zones based on changes in diatom species composition throughout…… 185
Figure 5.31: PCA biplot for diatom results from the Mafadi Wetland profile…… 185
Figure 5.32: Stratigraphic diagram of the diatom results from the Mafadi Wetland profile, with species ordered by their PC1 species scores and curves for PC1 and PC2 sample scores…… 187
Figure 5.33: Multi-proxy stratigraphic diagram for the Mafadi Wetland profile…… 190
Figure 5.34: Stratigraphic diagram of the pollen results from the core obtained from the Mafadi Diatomite Outcrop. A discontinuity or overlap of unknown depth occurs between the two sections…… 193
Figure 5.35: Photograph of samples from the diatomite bed diluted by 100x, demonstrating the high concentration of diatom valves remaining…… 194
Figure 5.36: Stratigraphic diagram of diatom results from the Mafadi Diatomite Outcrop. A discontinuity or overlap of unknown depth exists between the two sections…… 195
Figure 6.1: Pollen sequence from ~6,000 cal. BP - present at Sani Valley, plotted against age, grouped according to ecology, and zoned according to the CONISS output for pollen. Black circles represent the appearance of 1-5 pollen grains from the particular species…… 206
Figure 6.2: Pollen sequence from ~13,200 cal. BP - present at Sekhokong, plotted against age, grouped according to ecology, and zoned according to the CONISS output for pollen. Black circles represent the appearance of 1-5 pollen grains from the particular species…… 207
Figure 6.3: Pollen sequence from ~8,140 cal. BP - present at Mafadi Wetland, plotted against age, grouped according to ecology, and zoned according to the CONISS output for pollen. Black circles represent the appearance of 1-5 pollen grains from the particular species…… 208
Figure 6.4: The likely trajectories of *Podocarpus* and *Olea* pollen into the central Lesotho valleys during warm periods, and photograph illustrating such fragmented forest growth in Drakensberg valleys…… 209
Figure 6.5: Diatom sequence from ~6,000 cal. BP - present at Sani Valley, plotted against age, grouped according to habitat, and zoned according to the CONISS output for pollen at Sani Valley…… 219
Figure 6.6: Diatom sequence from ~13,200 cal. BP - present at Sekhokong, plotted against age, grouped according to habitat, and zoned according to the CONISS output for pollen at Sekhokong…… 220
Figure 6.7: Diatom sequence from ~8,140 cal. BP - present at Mafadi Wetland, plotted against age, grouped according to habitat, and zoned according to the CONISS output for pollen at Mafadi Wetland…… 221
Figure 6.8: Changes in sediment properties from ~6,000 cal. BP - present at Sani Valley, plotted against age and zoned according to the CONISS output for Sani Valley pollen…… 226

Figure 6.9: Changes in sediment properties from ~13,200 cal. BP - present at Sekhokong, plotted against age and zoned according to the CONISS output for Sekhokong pollen…… 227

Figure 6.10: Changes in sediment properties from ~8,140 cal. BP - present at Mafadi Wetland, plotted against age and zoned according to the CONISS output for Mafadi Wetland pollen…… 228

Figure 6.11: Summary diagram indicating the wetter and drier, and extreme cold and warmer periods at Sani Valley from ~6,000 cal. yr BP - present, indicated by the pollen, diatom and sediment records. Cold 40, 50, 60, 70 refer to the index of percentage composition of Fragilaria diatom species; warm 75, 80 refer to the percentage species richness for pollen….. 234

Figure 6.12: Summary diagram indicating the wet and dry, and cold and warm periods at Sekhokong from ~13,180 cal. yr - present, indicated by the pollen, diatom and sediment records. Cold 40, 50, 60, 70 refer to the index of percentage composition of Fragilaria diatom species; warm 75, 80 refer to the percentage species richness for pollen …… 239

Figure 6.13: Summary diagram indicating the wet and dry, and cold and warm periods at Mafadi Wetland from ~8,140 cal. yr - present, indicated by the pollen, diatom and sediment records Cold 40, 50, 60, 70 refer to the index of percentage composition of Fragilaria diatom species; warm 75, 80 refer to the percentage species richness for pollen…… 243

Figure 6.14: Reconstructed periods of dry and wet conditions, and warmer and extremely cold temperatures for Sani Valley, Sekhokong and Mafadi Wetland, and for the published proxy work for Lesotho…….. 247

Figure 6.15: Age-depth relationship for the three study sites…… 250

Figure 6.16: Van Zinderen Bakker's (1955) pollen diagram. The following changes in names of pollen taxa should be noted: Umbelliferae = Apiaceae, Compositae = Asteraceae, Gramineae = Poaceae…… 254

* All photographs, diagrams, graphs and images are the authors own unless stated otherwise.

LIST OF TABLES

Table 2.1: Known periods of occupation at Stone Age sites in Lesotho…… 50

Table 3.1: Geological time scale for eastern Lesotho (after Schmitz & Rooyani, 1987)…… 73

Table 3.2: Active and inactive cryogenic landforms in the eastern Lesotho highlands (after Grab et al., 2012)..... 76

Table 3.3: The most common floral families in the DAC and Lesotho by number of species (after Carbutt & Edwards, 2004)…… 83

Table 3.4: Summary of the key geographic attributes of the three study sites…… 90

Table 3.5: Plants at the Sani Valley Site (on the raised bog) identified by Carbutt (2004)…… 93

Table 3.6: Vegetation transects for the Sekhokong Wetlands (Deschamps, 2006)…… 96

Table 3.7: Species identified at Mafadi Wetland…… 99

Table 4.1: Samples for which AMS dates were obtained…… 114

Table 4.2: Size grades of sedimentary particles (after Briggs, 1977[2], p. 56; Masselink et al., 2014[1], p. 107)…… 126

Table 4.3: Descriptive terms for Soil Statistics (after Briggs, 1977)…… 127

Table 5.1: AMS radiocarbon dates acquired for the Sani Valley profile…… 133

Table 5.2: Sediment properties for the Sani Valley profile…… 137

Table 5.3: Frequency of occurrence of pollen identified from the Sani Valley sequence…… 139

Table 5.4: Frequency of occurrence of diatoms identified in the Sani Valley profile…… 144

Table 5.5: AMS radiocarbon dates acquired for the Sekhokong profile…… 150

Table 5.6: Summary of sedimentary changes throughout the Sekhokong profile…… 153

Table 5.7: Frequency of occurrence of pollen grains throughout the Sekhokong profile…… 158

Table 5.8: Percentage occurrence of diatom species throughout the Sekhokong profile…… 163

Table 5.9: AMS radiocarbon dates acquired for the Mafadi Wetland profile…… 171

Table 5.10: Summary of sedimentary changes throughout the Mafadi Wetland profile…… 176

Table 5.11: Percentage occurrence of pollen grains throughout the Mafadi Wetland profile…… 178

Table 5.12: Percentage occurrence of diatom species throughout the Mafadi Wetland profile…… 184

Table 5.13: Change in sedimentary properties throughout the core obtained from the Mafadi Diatomite Outcrop…… 192

Table 6.1: Habitat and autecological characteristics of the diatoms identified in the eastern Lesotho diatom sequences presented in this study…… 213

Table 6.2: Climate reconstruction from Sani Valley, Sekhokong and Mafadi Wetland compared with the periods of human occupation at sites in Lesotho, as presented in the archaeological record…… 261

Table 6.3: Palaeoenvironmental reconstructions published for Braamhoek Wetland…… 263

List of Acronyms

AMS: Accelerator Mass Spectrometer

CONISS: Constrained Incremental Sum of Squares

CSAG: Climate Systems Analysis Group

DAC: Drakensberg Alpine Centre

DCA: Detrended Correspondence Analysis

ENSO: El Niño Southern Oscillation

EPILOG: Land, Oceans, Glacier Programme

FAO: Food and Agricultural Organization

IPCC: Intergovernmental Panel on Climate Change

ITCZ: Inter-Tropical Convergence Zone

KZN: KwaZulu-Natal

LGM: Last Glacial Maximum

LOI: Loss on Ignition

PC: Principal Component

PCA: Principal Components Analysis

SIO: South Indian Oscillation

SOP: Standard Operating Procedure

SRZ: Summer Rainfall Zone

U.V.: Ultra Violet

WRZ: Winter Rainfall Zone

YRZ: Year-round Rainfall Zone

List of Naming and Style Conventions

± cal. yr BP: measured, calibrated AMS dates acquired from Beta Analytic; years before present

~ cal. yr BP: interpolated, calibrated AMS dates calculated using the BACON model; years before present

yr BP: un-calibrated age-dates presented in publications

kyr: kiloyears, retained in the context of events by that name (eg. 8.2 kyr event)

m.asl: meters above sea level

PVC tube: tubes made from polyvinyl chloride, a hard plastic

GPS: Global Positioning System; often used to refer to a device which relies on GPS technology to determine ones location.

Fragilaria pinnata/ construens: the group of morphologically indistinguishable and ecologically similar diatom species *Staurisorella pinnata* and *Fragilaria construens.*

Cheno-Am: the group of morphologically indistinguishable and ecologically similar pollen grains from the Chenopodiaceae and Amaranthaceae families

1. INTRODUCTION

1.1 BACKGROUND

Palaeoclimatology refers to the study and inference of climates prior to the period of instrumental weather recording, and is most often informed by palaeoecology, the study of past changes in vegetation and fauna using fossil proxies (Bradley, 1999; Jones et al., 2009). With projections of global temperature increases in the order of 2.6–4.8°C by the end of the 21st century, studying the nature and extent of both contemporary and historic climate change is becoming critically important (Jones et al., 2009; IPCC, 2013). Establishing and understanding climate change is particularly important for developing regions, such as southern Africa, that, due to their relatively low adaptive capacity, are likely to struggle with consequent physical and social challenges in future decades (Smith et al., 2003; Ziervogel & Calder, 2003). To improve the capacity to plan, manage, and adapt to climate change in such regions, it is necessary to understand the nature and magnitude of past changes in climate over time periods ranging from recent decades to thousands of years, as it provides considerable amounts of information on rates of change, patterns of variability, and feedback systems (Jones et al., 2009; Meadows, 2014). Climate change research in the eastern Lesotho highlands region of southern Africa, and its potential to inform adaptation, is of particular value. With a heavy reliance on subsistence agriculture, Lesotho faces the prospect of significant economic loss and a sustained threat to livelihoods should current rates of climate change persist or intensify (Ziervogel & Calder, 2003; Bell, 2011). Furthermore, the eastern Lesotho highlands serve as southern Africa's primary water catchment, one of the few catchments in southern Africa where precipitation exceeds evaporation (Zunckel, 2003; Carbutt & Edwards, 2006). Any change in this hydrological system is thus of considerable importance to the southern African region as a whole.

An understanding of how climate change has impacted on geophysical components of the landscape is reasonably comprehensive where long-term climate records are available (Meadows, 1988; Grab, 2010). However, in remote mountain regions such as those of Lesotho, where long term climate monitoring – covering several decades or longer – is absent, most discussions concerning 'Global Change Science' have been premised on

extrapolated assumptions from southern African lowland regions and Northern Hemisphere alpine environments (Boelhouwers & Meiklejohn, 2002; Mulder & Grab, 2009; Borg, 2012). Such approaches, while valuable in providing generalised estimates of both past and present conditions, are unable to quantify the precise rate and magnitude of any climate variability or change (Boelhouwers & Meiklejohn, 2002). In the absence of quantitative climate data, and as the rate and magnitude of climate variability and change at higher altitudes may not necessarily match those recorded at adjacent lower altitude regions (Pepin, 2000; Pepin & Losleben, 2002; Grab, 2013), it becomes difficult to develop high resolution climate models and long term forecasts, particularly in determining vulnerability to drought and extreme climatic events. For any region, palaeoenvironmental work is beneficial in that it provides the only approach to explore climatic change and cycles throughout the Holocene (Meadows, 2012; Meadows, 2014), the geological epoch spanning 11,700 cal. yr BP to present (Burrough & Thomas, 2013). As long-term meteorological data for eastern Lesotho are scarce, a palaeoecological approach involving climate and environmental proxies is essential, as it provides the only historical climate information (Grab & Nash, 2010).

In addition to the contribution that palaeoecological studies in the region would make to an improved understanding of southern African Holocene climate change, the eastern Lesotho region is particularly well positioned for detailed analyses into late Quaternary synoptic climate fluctuations and associated ecological changes at high altitude (Mills et al., 2012). The region receives moisture both from the Indian Ocean in the form of convective storms in summer, and through mid-latitude cyclones moving across the country from the Western Cape region during autumn-winter-spring (Mulder & Grab, 2009; Nash & Grab, 2010; Mills et al., 2012). As a topographic barrier controlling the penetration dynamics of these two moisture systems, and with annual snow and ice, the region has the potential to capture signals of these relatively low latitude occurrences of westerly frontal systems, and any changes in their relative strength (Mills et al., 2012).

The high altitude and frequent occurrence of frost and snowfalls in the eastern Lesotho region during colder months induces a particularly marginal environment for plant growth (Carbutt & Edwards, 2006). Not only are a specific group of species able to survive the harsh environmental conditions, but any changes in climate can potentially lead to the extirpation

of certain plant groups (Carbutt & Edwards, 2006; Inouye, 2008). While plants at lower altitudes could respond to warming climates by moving upslope to cooler environments, at the summits of these mountain ranges there is no higher altitude to which plants could relocate during periods of warming, and so may suffer heat stress (Parmesan & Yohe, 2003). The exploration of long-term climate and environmental change in this particular region is thus both of academic interest, and of considerable value for adaptation policy as these changes under contemporary conditions are manifested as shifts in regions suitable for grazing.

1.2 Palaeoenvironmental Proxies

A key approach to reconstructing past environments for periods before meteorological recording, is the use of biological and abiotic proxies, variations of which can act as analogues for environmental and climate shifts (Meadows, 2014). An increasing range of proxies are being used, including but not limited to: remains of previously living organisms such as charcoal, fossil pollen, diatoms, phytoliths, ostracods, gastropods and cladocera; and archives from organisms that have long life-spans, including tree rings and corals (Battarbee, 2000; Armstrong & Brasier, 2005; Meadows, 2014). The archives from which these proxies can be isolated for analysis are also varied, including sediments cored from wetlands, lakes and oceans; ice cores; stalagmites; packrat and hyrax middens; and coprolites (Meadows, 2014). *Chapter 2 (Literature Review)* provides an overview of climate and environmental proxies used in southern Africa and their relative advantages and limitations in the southern African context. Here a brief overview of the three proxies used in this study – pollen, diatoms and sedimentary proxies of total organic content and particle size – is presented to familiarise the reader with the variation in their characteristics and application in palaeoenvironmental reconstruction.

In order to use environmental proxies obtained from archives that cover long time periods, assumptions need to be made regarding the relationships between modern and past communities of those proxies (Fritz et al., 1991; Battarbee, 2000). The most common of these is the Principle of Uniformitarianism, developed originally in Hutton's (1795) *Theory of the Earth,* and expanded upon by Lyell's (1830) *Principles of Geology*, which argues that the

natural processes that operate today have operated universally and throughout geological time (Roberts, 2014; Meadows, 2012; Knight & Harrison, 2014). Using the 'present as the key to the past' requires modern analogues of the identified past ecological communities and abiotic features, from which to infer their environment, climate, and driving forces (Roberts, 2014; Meadows, 2012). The assumptions that need to be met to use the Principle of Uniformitarianism in the fields of palaeoecology include:

1. We understand the environmental factors governing present-day plant and animal distributions
2. Plant and animal ecological affinities have not changed through time
3. Present (and past) distributions of these plants and animals are (and were) in equilibrium
4. Modern analogues of these distributions of plants and animals exist
5. The origin (taphonomy) of a plant or animal fossil assemblage can be established, and that…
6. … this assemblage is not biased by contamination or differential preservation
7. Plant and animal fossils can be identified to a meaningful level of taxonomic resolution

[after Roberts, 2014, p.32]

Efforts are being made to improve the level of taxonomic resolution of identified fossils, to prevent contamination, and to calibrate contemporary marker assemblages with contemporary communities, such as the relationship between the pollen grains in top soil to species counts of the surrounding vegetation. However, concerns remain about the uncautioned use of the Principle of Uniformitarianism (Meadows, 2014). For very long time scales, there is a considerable risk of extinction, resulting in an absence of contemporary analogues, and relationships between extinct and surviving species would be unknown (Roberts, 2014). At more recent time scales, the application of the Principle of Uniformitarianism to the Anthropocene, the late Holocene period marked by human influence on the environment and climate (Steffen et al., 2007) spanning a disputed time period (Rose, 2015), is met with concern as it is argued that the current CO_2 levels and the extent of human disturbance to the environment are sufficient that there is no past analogue of current activity (Meadows, 2012; Knight & Harrison, 2014). However, not all

proxies are as severely affected by human influence on the environment, and efforts have been made to integrate training sets from pre-anthropogenic environments to overcome these problems (Juggins, 2013). With no clear theory to replace Uniformitarianism, and with the need to use some present clues to understand the past, it is of value to understand and remain conscious of these limitations, but value remains in using this approach (Jackson, 2012; Knight & Harrison, 2014).

1.2.1 AMS Radiocarbon Dating

To facilitate situating a palaeoenvironmental reconstruction within ecological history, and to make comparisons with existing studies, it is necessary to determine the chronology. To temporally constrain the sediment profiles and derived palaeoenvironmental reconstructions, Accelerator Mass Spectrometer (AMS) radiocarbon dating is used due to the significant carbon content of the sediment (Walker, 2005). During the lifetime of a plant, the ratio of ^{14}C assimilated, relative to other carbon isotopes, is in isotopic equilibrium with the percentage of ^{14}C ions in the atmosphere (Fairbanks et al., 2005). Once the plant has died the uptake of ^{14}C ceases, and the percentage of ^{14}C begins to decline as radioactive decay occurs, with a half-life of 5,730 ±40 years (Fairbanks et al., 2005; Walker, 2005). Based on the half-life, the limit of routine measurements using carbon dating is ca. 45,000 yr BP, which is not problematic for Holocene research (Higham, 1999; Walker, 2005). AMS dating measures the relative number of ^{14}C ions in comparison with the more rare ^{12}C and ^{13}C ions in the sample using a tandem accelerator system, and can subsequently determine the length of the period of radio-active decay (Walker, 2005). Due to variations in atmospheric concentrations of ^{14}C over both short and long time periods due to changes in solar and geomagnetic activity, together with differences in ^{14}C concentrations between the Northern and Southern Hemispheres, calibration of AMS dates is critical (McCormack et al., 2004; Fairbanks et al., 2005).

1.2.2 Sediments: Total Organic Carbon, Carbonates and Particle Size

Sediments are primarily used in palaeoenvironmental reconstructions for the proxies they hold, with the sediment itself often sieved, digested and discarded from the solution (Bell & Walker, 2013). The sediments themselves, however, are also a useful proxy for past changes in climate and environment (Briggs, 1977). Sediments are a product of weathering,

deposition and decomposition, all of which are predominantly influenced by the climatic and environmental conditions in a location over a given time period. A commonly used proxy from sediments is the percentage organic composition (Heiri et al., 2001; Meyers & Teranes, 2001). Sediments with particularly high organic content, such as peat, indicate environments with a specifically defined climatic profile of high moisture and low temperatures, while the rate of peat formation provides higher resolution information of climatic conditions (Meadows, 1988; Bell & Walker, 2013). More broadly, in the southern African context, the relative presence or absence of organic content in the sediments has be used to infer the relative amounts of available moisture in that environment for a particular time period (Meadows, 1988; Heiri et al., 2001; Meyers & Teranes, 2001). The percentage composition of carbonate in sediment samples can similarly be determined, indicating biotic and abiotic carbonate development, providing a coarse proxy for relative temperature changes (Heiri et al., 2001). The abiotic component of the sediments is also of value, as the sediment particle size distribution is an indicator of the weathering, transportational and depositional environments (Briggs, 1977). Sediments with larger proportions of small silt- and clay-sized sediment particles tend to originate from wetland conditions, and indicate wetter periods, while larger sand- and gravel-sized particles are more indicative of dry periods, with limited vegetation cover and resultant colluviation (Bell & Walker, 2013). Sediment particle size can also provide information about the depositional environment, and provide clues as to whether fluvial or aeolian transport dominated the system at a particular time, and from this the climate drivers responsible (Briggs, 1977).

In isolation, sediments are limited as an environmental and climatic proxy, as they do not directly convey any information about changes in the biotic environment, the threshold levels, or community responses (Bell & Walker, 2013). Rather, sediments provide information more directly on the climate drivers behind these changes, and so in combination with environmental proxies, are useful in corroborating evidence (Bell & Walker, 2013). Sediments are further limited in their application to palaeoenvironmental studies in that they predominantly reflect moisture changes, and inferences of temperature are difficult to impossible unless geochemical work or micro-sedimentology is undertaken (Marker, 1994; Meyers & Teranes, 2001). Therefore, to conduct a holistic environmental reconstruction, sediment characteristics need to be paired with proxies that can convey

more direct information on absolute temperatures (Bell & Walker, 2013). Despite their limitations, sediments are an integral part of the environment at any point in time, and as the dominant component in a sediment core, it is a waste not to use them as an additional environmental proxy.

1.2.3 POLLEN

Flowering terrestrial plants produce pollen in great quantities, of which only a small proportion is utilised for reproductive purposes (Moore & Webb, 1978; Bennett & Willis, 2001). The remaining pollen grains are deposited on soil and water surfaces, where they can accumulate over long periods in the sedimentary record (Bennett & Willis, 2001). The outer layer of the pollen grain wall, the exine, is composed of a highly resistant substance called sporopollenin, which preserves the structuring of pollen grains within the sedimentary layer for many hundreds of thousands of years (West, 1968; Moore & Webb, 1978; Bennett & Willis, 2001). This exine layer retains a morphology and sculpturing specific to the taxon that produces it, facilitating identification of the original plant when the pollen grains have been chemically isolated from the surrounding sediment (Faegri et al., 1989). Typically ranging in size from 10-100µm, pollen grains require light or scanning electron microscopy for identification, at magnifications greater than 400x (Faegri et al., 1989; Bennet & Willis, 2001). Identification requires a reference collection of pollen grains collected from plants in that particular botanical region, and is made on the basis of comparison of shape, size and texture of the pollen grain, together with number, shape and symmetry of apertures on the surface of the remaining fossil pollen grain (Erdtman, 1943; West, 1968). Identification is seldom achieved to a higher resolution than genus, due to similarities in pollen grains between species (West, 1968; Birks & Birks, 2014). Light microscope photographs of a selection of pollen grains commonly found in samples from this study are presented in *Figure 1.1.*



a. Asteraceae b. Crassula c. Geraniaceae

d. Cyperaceae e. Cheno-Am f. Poaceae

Figure 1.1: Examples of a range of pollen grains from the eastern Lesotho highlands under light microscope.

The pollen rain (the collection of pollen grains deposited at a particular site) is an index of the plant type that produced it, and thus the fossil pollen assemblage is an indication of the vegetation type that produced it (Erdtman, 1943; Birks & Birks, 2014). Pollen assemblages identified from multiple layers throughout a sedimentary record can therefore provide an overview of the vegetation and environmental development through time, with environmental attributes inferred using the Principle of Uniformitarianism (Faegri et al., 1989; Bennett & Willis, 2001). Due to the large number of well understood contemporary analogues and ecology of modern plants, the identification of pollen of an individual species, the reconstruction of the population of that species through time, and the concurrent reconstruction of the broader community of plants, provides a detailed vegetation reconstruction, particularly for the Holocene (Birks & Birks, 2014). In making such a large number of assumptions it is important to understand the uncertainties involved, and to understand the limitations of these assumptions both in theory and practice (Faegri et al., 1989). Jackson (2012) presents a conceptual model for these limitations, grouping them by proxy source, vector, diagenesis and analysis. The first two groups are specific to a particular locality or region, while the latter two are of global

significance. For eastern Lesotho, the high altitude environment ensures a comparatively smaller radius for the proxy source, for both wind and faunal vectors. As a pioneering study in the region, the diagenesis is, to an extent, uncertain, and the analysis can potentially be limited by the use of broader regional pollen reference collections.

The greatest challenges in pollen analysis involve determining the relationships between pollen rain and the vegetation that produced it, and between pollen rain and fossil pollen composition (Scott et al., 2012; Birks & Birks, 2014; Meadows, 2014). This involves differences in the volumes of pollen produced, their dispersal, their deposition and incorporation into the sediment, and their identification and analysis (Hicks, 2001; Jackson, 2012; Roberts, 2014). Plants produce pollen in varying quantities, depending on their reproductive strategies, methods of pollination, and strength of the plant (Faegri et al., 1989). Consequently, a large count of a specific taxon from the pollen rain does not necessarily indicate its abundance in the local region, nor does a low count always reflect a rare species (Erdtman, 1943; Bennett & Willis, 2001). Differential dispersal, referred to by Jackson (2012) as the vector component, involves pollen grains from some plant species travelling greater distances than others, depending on the size of the pollen grain, the method of transportation, and the topography of the landscape (Prentice, 1985; Hicks, 2001; Traverse, 2007; Jackson, 2012). While mean transportation distances can be calculated for pollen grains according to their size, dispersal method and topography, they do not account for the potential for multiple stages of deposition, as could potentially occur should pollen land in a river, and be deposited downstream (Jackson, 2012). Pollen rain for a particular site consequently frequently reflects a combination of both local and regional vegetation, and environmental inferences therefore need to incorporate these differences in transportational characteristics (Jackson, 2012). The 'Neves effect' theoretically isolates long-distance wind pollinated plants, from plants that produce pollen grains that are transported shorter distances due to their larger size, or because they are pollinated by insects (Prentice, 1985; Traverse, 2007). To overcome this, pollen traps should ideally be established close to the study site to test the fidelity of contemporary deposits with the local vegetation, and to determine the likely range of pollen dispersal (Hill, 1996; Renaut & Bamford, 2006; Herzschuh, 2007). Effective palaeopalynology also requires that pollen grains have been well preserved throughout the sequence, and that preservation rates are

equal among the different taxa (Faegri et al., 1989). This is not always the case, and often the differences in morphology and size of fossil grains result in differential preservation (Faegri et al., 1989). Finally, the distances travelled by pollen grains can be considerable, particularly for wind pollinated plants (Erdtman, 1943; Bennett & Willis, 2001). The species distribution of a sample could thus reflect the local environment at that site, or the environment of a broader region (Bennett & Willis, 2001; Scott et al., 2012). Therefore questions remain concerning authenticity of zero counts in a pollen sequence, the validity of statistically attributed rare species, and the over-estimation of plants that produce large quantities of readily preserved pollen (Walanus & Nalepka, 2013; Meadows, 2014).

1.2.4 DIATOMS

Diatoms are a group of microscopic unicellular algae that form part of the class Bacillariophyceae (Barber & Haworth, 1981; Stoermer & Smol, 2004). They have siliceous cell walls, composed of two valves that make up a frustule, which range in size from ~2-200µm (Harwood, 2004; Stoermer & Smol, 2004). This silica structure is highly resistant, and given the right conditions, fossil diatoms are well preserved (Barber & Haworth, 1981; Stoermer & Smol, 2004). Diatoms are present in almost all aquatic habitats, and due to their successful preservation, are often abundant in ocean, lake and wetland sediments (Battarbee et al., 2001; Stoermer & Smol, 2004). There are estimated to be over 10,000 species of diatoms, of which a large proportion are ecologically sensitive, making them a particularly valuable palaeoenvironmental proxy (Battarbee et al., 2001; Stoermer & Smol, 2004). Their ecological sensitivity is in part due to their rapid reproduction and short life-spans (a few days to a week), allowing their communities to respond rapidly to environmental stresses and change (Stevenson & Pan, 2004). Diatoms can be identified on the basis of morphology, beginning with a broad classification into centric (*Figure 1.2a*) and pennate (*Figure 1.2d-f*) groups (Battarbee et al., 2001). Thereafter, the more specific shape, length and breadth, frequency of striations, pattern of striations and presence of a raphe are used to identify diatoms to species level (Barber & Haworth, 1981; Battarbee et al., 2001; *Figure 1.2*). This high resolution of identification allows for more precise environmental interpretation, as it segregates species that may have slightly different environmental preferences and tolerances (Mackay et al., 2003). Diatoms are unique in their palaeoecological value within the algal community, as many of the other algal classes

have more than one stage within their life cycle with highly variable ontogeny, cannot be distinguished without special reproductive structures, or cannot be distinguished without culturing (Stevenson & Pan, 2004). When diatoms accumulate rapidly in an environment with otherwise slow sedimentation, a thick white sediment layer almost entirely comprised of diatoms, called diatomite, can form on the surface, and when sufficiently compressed, can form a lightweight sedimentary rock (Barber & Haworth, 1981; Harwood, 2004). It is estimated that one cubic inch of diatomite contains 40-70 million diatoms, providing a valuable palaeoenvironmental reference (Harwood, 2004). However, the formation of diatomite can occur rapidly, and in such cases is of little palaeoenvironmental interest as the diatoms would represent only a short time period (Harwood, 2004).

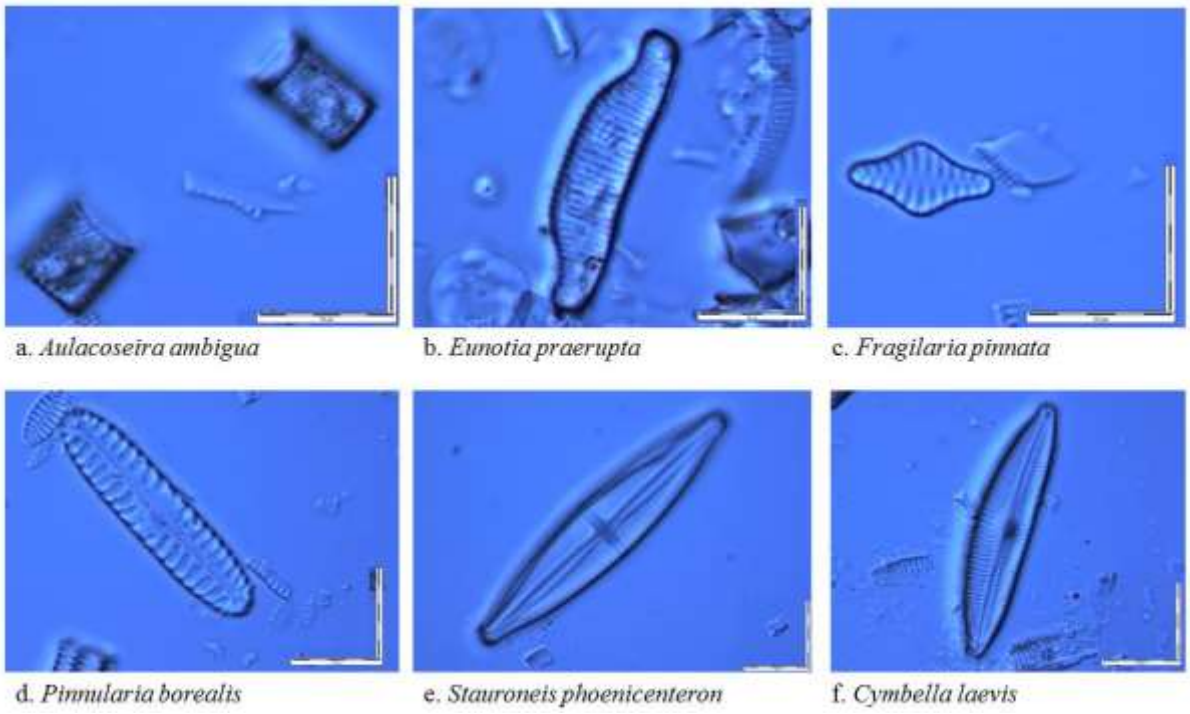


Figure 1.2: Examples of a range of diatom valves from the eastern Lesotho highlands under light microscope. Scale bar represents 10µm.

There are two principal habitats that diatoms occupy: moist or submerged surfaces in which benthic diatoms reside, and deep open water in which planktonic diatoms are found (Round et al., 1990). A third habitat is drier damp surfaces, inhabited by aerophilous species (Johansen, 2004). These habitat differences represent the broadest categorisation for the ecology of different diatom species. Diatoms respond to a far larger range of environmental

variables, including temperature, nutrient concentrations, pollution levels, pH and herbivory, with each species having a specifically defined set of thresholds for many of these attributes (Battarbee et al., 2001; Stevenson & Pan, 2004; Mackay et al., 2003). Diatom communities, and their change through time, can thus be used to determine local climate- and environmentally-driven changes within a waterbody, while pollen records reflect environmental changes at larger scales (Battarbee et al., 2001). These environmental factors can be distinguished on a hierarchical framework, separating the proximal factors that directly affect diatom species composition, including light, nitrogen, phosphorous, pH, temperature and the presence of toxic substances, from the higher level factors such as geology that restrict the effects of the lower level factors by controlling factors such as pH, concentration of nitrates and phosphates (Stevenson & Pan, 2004). The development of autecological indices, which outline the environmental preferences of each species, is invaluable in facilitating the inference of the predominant environmental drivers of changes in diatom communities over time (Stevenson & Pan, 2004; Mackay et al., 2003).

With their highly specific morphology facilitating identification to species level, and the large suite of environmental conditions for which they provide accurate indication, diatoms represent a valuable environmental proxy. However, while for pollen even a layperson has a conception of the environmental preferences of the associated plant, and can visualise both the landscape and associated environment of a lack of trees, or abundance of grass, the ecological traits of diatoms are poorly understood even within the scientific community (Stoermer & Smol, 2004). Over the last few decades, considerable emphasis has been placed on developing training sets and transfer functions, to relate communities of living diatoms to their specific aquatic habitat, facilitating an improved understanding of environmental influences (Fritz et al., 1991; Stevenson & Pan, 2004; Juggins, 2013). While diatom analysis does not encounter the problems of differential production, and the provenance of wind-blown particles, issues of poor preservation and potentially differential preservation create statistical uncertainties, particularly in lake environments (Mackay et al., 2003).

1.4 Contribution to Knowledge

The academic output in the reconstruction of past climates and environments in southern Africa is sparsely distributed due to a paucity of sites with well-preserved fossil proxies (Neumann et al., 2008; Scott et al., 2012), and the late Quaternary environmental record remains uncertain, and at best undefined for much of the Lesotho highlands (Grab et al., 2005). The majority of the Quaternary environmental reconstructions for the Lesotho region stem from the rich archaeological heritage (cf. Carter, 1976; Plug, 1993; Mitchell et al., 1994, 1998, 2011; Mitchell, 1996a; Cain, 2009; Stewart et al., 2012; Roberts et al., 2013). This archaeological work has included inferences on possible past climatic situations (Mitchell et al., 1998), but the temporal resolution and the quantification of past climates lacks detail. The only detailed Holocene palaeoenvironmental records for western Lesotho are based on charcoal assemblages and isotope analysis on grazer tooth enamel in the Phuthiatsana-ea-Thaba Bosiu basin (Esterhuysen and Mitchell, 1996; Smith et al., 2002; Roberts et al., 2013) and on sedimentary and phytolith records from an exposed sedimentary sequence in a gully of the Tsoaing Basin (Grab et al., 2005). From central Lesotho, palaeoenvironmental inferences have been made from phytolith and stable isotope analyses for Likoaeng open-air shelter (Parker et al., 2011). The only continuous palaeoenvironmental reconstruction from eastern Lesotho (Van Zinderen Bakker, 1955), is a pollen record from an unspecified location, examined at coarse sampling and taxonomic resolution, and an absence of age-dates.

A variety of Quaternary periglacial and glacial studies from Lesotho's eastern high mountain region have indicated colder, and possibly relatively wet conditions during the late Pleistocene (incl. Harper, 1969; Grab, 2002a; Mills and Grab, 2005; Mills et al., 2009a) and Holocene neoglacial episodes (Grab, 2000). However, the absence of age-dates for many of these periglacial studies, the lack of consistent temporal chronologies, and the disputed interpretation of landforms have limited their palaeoenvironmental value (Boelhouwers & Meiklejohn, 2002). Where Holocene sedimentary sequences have been described together with age-dates in the eastern mountains of Lesotho (Hanvey & Marker, 1994; Marker, 1994, 1995, 1998), the absence of pollen, diatoms or other environmental proxy markers has limited the potential for a more detailed and higher resolution environmental and climatic

reconstruction (Grab et al., 2005). The only published record analysing fossil pollen from a sedimentary sequence in the Maluti Mountains (Van Zinderen Bakker, 1955) is limited in its palaeoenvironmental value owing to the absence of any age-dates, and the low sampling-resolution.

The existing palaeoecological and palaeoclimatic research in southern Africa provides a detailed foundation on which to base future work. It also highlights critical gaps in current knowledge. While numerous studies have been undertaken in the west and southern Cape, the Highveld interior and KwaZulu-Natal, no such work has been undertaken in eastern Lesotho at a high enough resolution or with accurate age-dates. Although it has been noted that studying alpine regions in order to determine differing altitudinal rates of species relocation during periods of climate shifts is important (Van Zinderen Bakker & Coetzee, 1988), no such research has yet been undertaken in high altitude southern Africa. Norström et al. (2009, 2014) make mention of likely shifts in the position of the westerly belt during the Last Glacial Maximum (LGM), but no studies to date have examined the effect that the strength and position of mid-latitudes have had on the palaeoenvironmental record for regions affected by regular winter snowfalls. Finally, while the work at Tswaing Crater (Metcalfe, 1993; Kristen et al., 2007), Braamhoek Wetland (Norström et al., 2009, 2014; Finné et al., 2010) and Wonderkrater (Backwell et al., 2014) have highlighted the value in conducting multi-proxy palaeoenvironmental studies, few have been undertaken.

1.5 Study Aims and Objectives

To address the aforementioned gaps in the literature, the primary aim of this PhD project is to utilise a multi-proxy approach, using palaeoecological and palaeosedimentological archives, to construct a high resolution palaeoenvironmental record for the eastern Lesotho highlands region. The work is undertaken through the extraction of sediment cores from three sites in the eastern Lesotho highlands, at Sani Valley, Sekhokong and Mafadi Wetland. This is followed by the examination of sediment, fossil pollen and diatoms subsampled at regular intervals throughout the sediment cores, temporally constrained by AMS radiocarbon dating. This multi-proxy approach facilitates a high resolution Holocene environmental and climatic reconstruction to be undertaken as a pioneering study in the

region. Findings from these environmental proxies extracted from the sediment are compared with the existing archaeological records for the broader Lesotho region, to determine any links between environmental and climate changes and the pulses of human occupation observed. Results are also compared with studies at adjacent lower altitude sites, so as to determine environmental lapse rates and population resilience thresholds.

The specific objectives of this study are:

1) To determine suitable sites, and extract sediment cores from peat bogs at three locations in eastern Lesotho constrained by altitude, latitude and depth of sediment.
2) To determine the species composition, richness and frequency from fossil pollen grains and diatoms isolated from high resolution sampling of discrete layers subsampled from the cores from each site;
    a. To determine changes in the frequency of each species throughout the depth of each core, and infer any dominant shifts in vegetation
    b. To determine differences in species composition and change between the study sites
3) To determine the sediment characteristics in each of the subsampled sediment layers, including the organic and carbonate composition and the particle size distribution of each sample
    a. To determine changes in the sediment properties throughout the core
    b. To determine changes in depositional environments throughout the core
4) To temporally constrain the observed changes in sedimentology and proxy species composition through AMS dating of selected subsamples from cores from each of the study sites.
5) To infer changes in past environments and climates from the shifts in species composition of fossil pollen and diatoms, and from the sedimentological changes through statistical analysis
    a. To determine the dominant environmental drivers responsible for the changes in proxies throughout the time period represented by the sediment cores
    b. To use the multiple proxies to corroborate results, and to provide information on a greater range of environmental variables.

1.6 Structure of the Thesis

This introductory chapter presents the background to this study, exploring the need for palaeoenvironmental work to improve our understanding of climate change, and in particular, emphasising the need for such work to be undertaken in eastern Lesotho. A brief overview of each of the environmental proxies used in this study is then presented, to familiarise the reader with their application. The contribution of this study to the broader palaeoenvironmental knowledge of southern Africa is outlined, followed by the study aims and objectives.

The literature review chapter begins by exploring the development of palaeoenvironmental work in southern Africa, the proxies used, and the archives from which these proxies have been isolated. The key debates within the southern African palaeoscientific community are briefly synthesised. The existing palaeoenvironmental and palaeoclimatic knowledge for eastern Lesotho is then interrogated, synthesising the existing scientific knowledge to which this study will contribute. The current understanding of palaeoenvironmental and palaeoclimatic changes throughout the Holocene period in southern Africa is then explored.

The regional setting chapter is aimed at acquainting a reader unfamiliar with eastern Lesotho with the regional setting for this research. This chapter begins with a description of the geography of eastern Lesotho, including the location, geology, climate, vegetation, hydrology, and environmental issues. The chapter then provides a more detailed account of the micro-environment at each of the study sites, including their location, geomorphological setting and vegetation.

The methods chapter begins with a justification of the selection of the study sites used in this study. This is followed by a detailed account of the methods used in performing the palaeoenvironmental reconstructions, commencing with an outline of the methods used in the field to extract the sediment cores from which the proxies were isolated. The laboratory procedures are outlined, including the methods for the isolation of pollen and preparation of pollen slides, the diatom preparation, sediment analysis and age determination, the details of which are presented in Appendix A. The statistical methods used once pollen and

diatom communities had been determined are then described, including indirect ordination, classification of samples and visual representation. The statistical analysis of sediment results, and the statistical handling of the AMS dates are then presented.

The results chapter presents the stratigraphic changes in sediment, pollen and diatom composition for the sediment profiles, plotted against the depth in the profile, from each of the three study sites. Statistical analyses of these changes are then presented. This is structured by study site, with changes in each of the proxies presented independently for each of the sites.

The discussion chapter integrates the environmental information from the proxies for each of the study sites providing an environmental reconstruction through key time slices. In this chapter an altitudinal comparison is made across the three study sites, from which more regional environmental changes and climate variations for the eastern Lesotho highlands are inferred. Comparisons are also made to similar environmental reconstructions undertaken in Lesotho, and at lower altitude adjacent sites in southern Africa. Key environmental and climatic events of global significance which are detected in the eastern Lesotho record are then explored. The chapter concludes with an overview of the limitations of the study.

The conclusion reflects on the key findings of the study, and the extent to which the study aims have been achieved. As this study is the first large-scale palaeoenvironmental study conducted in eastern Lesotho, this chapter provides some insight into prioritising the avenues for future research, both at these study sites, and in the broader eastern Lesotho region.

2. Literature Review

2.1 Introduction

Southern Africa spans the tropical, subtropical and temperate belts, at the convergence of the Indian, Atlantic and Southern Oceans. These atmospheric, oceanographic and latitudinal influences result in distinct summer, winter and year-round rainfall regions, and arid through to humid environments across longitudinal transects for the southern African sub-continent (Carr et al., 2006; Chase and Meadows, 2007; Neukom et al., 2014). The region hosts a rich and diverse variety of plants and animals, with nine biomes and three global biodiversity hotspots (Mucina and Rutherford, 2006). These distinct bioregions are likely to have each experienced varied palaeoenvironmental shifts throughout the Holocene, and through glacial to interglacial cycles (Willis et al., 2005; Chase & Meadows, 2007; Scott et al., 2012). Compared with much of the Northern Hemisphere, historical and documentary evidence of past climates and environments is limited both temporally and spatially, placing greater importance on information from palaeoenvironmental proxies (Grab & Nash, 2010; Neukom et al., 2014). Regional climate and vegetation variability provides immense scope for palaeoenvironmental and palaeoclimatic work in southern Africa (Scott et al., 2012). Relative to the numerous biogeographical zones, the paucity of information is problematic from a modelling perspective, yet despite the immense value of palaeoclimatic evidence to inform climate models, little work has been undertaken in this field (Chase & Meadows, 2007; Scott et al., 2012). Recent attempts at climate modelling using palaeoenvironmental reconstructions and proxy data continue to raise more questions than arguably are solved, which while valuable in providing direction for future research, highlights further the problems of paucity of data (cf. Kohfeld et al., 2013; Sime et al., 2013). Furthermore, much of the existing southern African palaeoenvironmental work to date has focussed on the identification of pattern within and across datasets, rather than the underlying drivers.

This chapter explores the existing literature on palaeoenvironmental change in southern Africa for the late Quaternary. The development of palaeoenvironmental work in southern Africa is outlined, to familiarise the reader with key sites and proxies used. The use of pollen, diatoms and sedimentary properties as palaeoenvironmental proxies in southern

Africa is then critically assessed, outlining their value as climate and environmental proxies in the southern African context, and the benefit of further work using these proxies. The key debates within southern African palaeoenvironmental science are then presented, namely the nature and extent of Quaternary sea-level rise in southern Africa; shifts in the extent of the westerly belt; temperature, moisture and potential glaciation during the LGM; and the extent of synchronicity between major climate and environmental shifts in southern Africa and those of the Northern Hemisphere. The section concludes with the future trajectories of palaeoenvironmental science in southern Africa. The chapter then provides a synthesis of the palaeoenvironmental history of eastern Lesotho, exploring the existing literature from the disciplines of archaeology, geomorphology and palaeobotany. Finally the current understanding of Holocene climate shifts for southern Africa is presented, outlining periods for which there is consensus or disagreement regarding past climates and their associated environments.

2.2 The Development of Palaeoenvironmental Work in Southern Africa

The inference of past environments and climates through the analysis of climate proxies isolated from sediment profiles was initiated comparatively late in southern Africa when compared to work elsewhere in the world (Scott, 1982a,b; Van Zinderen Bakker & Coetzee, 1988; Meadows, 2015). Pioneering studies conducted by Van Zinderen Bakker (1955), Martin (1959, 1968), Coetzee (1967), Schalke (1973), and Scott (1976, 1982a), were limited by a lack of precise dating techniques, and by the considerably rich and varied flora of the region, for which no pollen collections existed (Scott, 1989; Van Zinderen Bakker & Coetzee, 1988). In recent years, studies have benefitted from access to increasingly affordable high precision dating facilities, and considerable pollen, phytolith and diatom collections to facilitate the identification of proxies (Kristen et al., 2007). Despite these advances, there remain relatively few studies, given the geographical and botanical diversity of the region, and consequently, considerable gaps in the research exist (Kristen et al., 2007; Neumann et al., 2008). This is due to the scarcity of appropriate study sites, with uninterrupted, undisturbed sediment profiles that contain sufficient concentrations of fossil proxies to produce statistically significant analyses (Martin, 1968; Livingstone, 1975; Van Zinderen Bakker & Coetzee, 1988; Kristen et al., 2007; Neumann et al., 2008). Unlike much of Europe,

where numerous palaeoecological studies have been undertaken due to the wealth of palaeoenvironmental archives, much of southern Africa is too arid to support the preservation of fossil pollen or to host communities of aquatic microfossil proxies such as diatoms, ostracods and foraminifera (Livingstone, 1975; Scott, 1989; Chase & Meadows, 2007; Meadows, 2015). Consequently, research has largely been confined to wetlands in the more humid regions, and isolated springs in the interior (Scott, 1989; Neumann et al., 2008; Meadows, 2015; *Figure 2.1*).

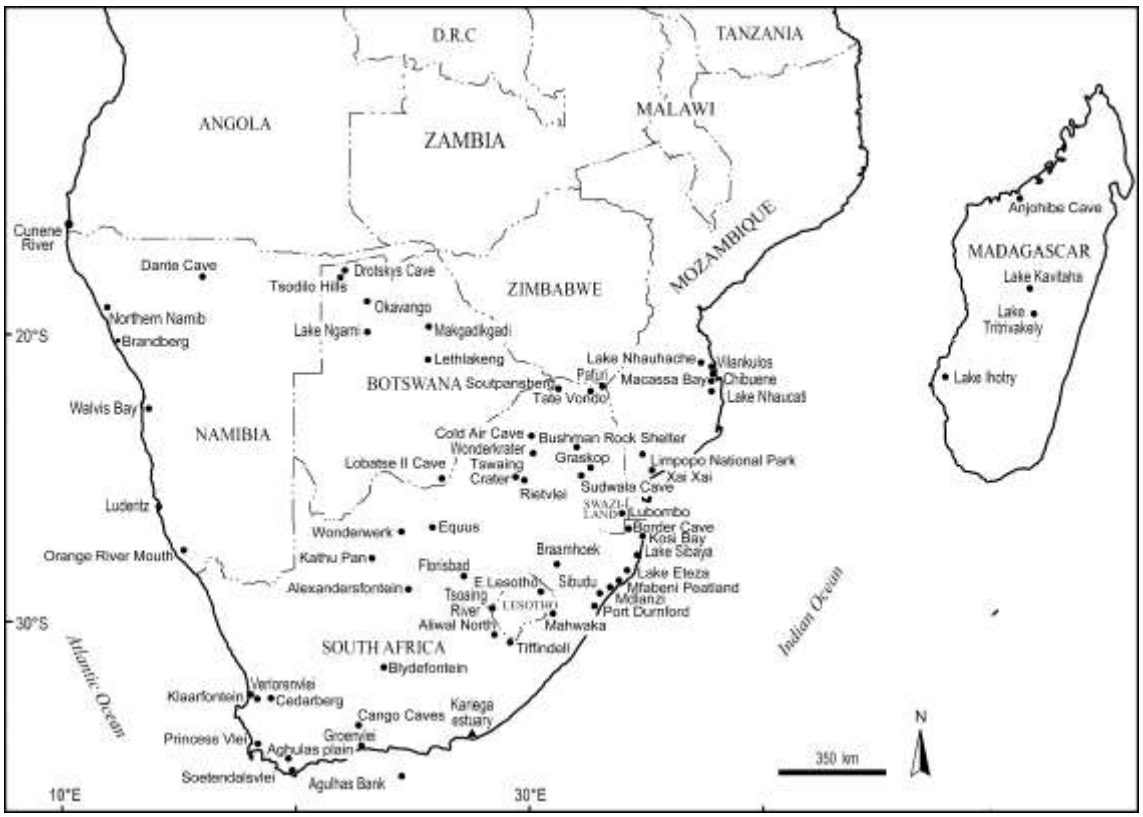


Figure 2.1: Locations of prominent southern African sites at which published palaeoenvironmental reconstructions have been undertaken.

2.2.1 Southern African Palaeoenvironmental Proxies

Southern African palaeoenvironmental studies have experienced considerable growth in the number of papers published, sites explored, and proxies used, since the early work of Van Zinderen Bakker (Meadows, 2007, 2015). Pollen is the most commonly used proxy for southern African palaeoenvironmental reconstructions, but more recently there has been an increasing use of isotopes, geochemistry and diatoms (*Figure 2.2*; Chase & Meadows,

2007; Scott et al., 2012). In particular, since the early 1990s, there has been an increase in the use of speleothems as a palaeoenvironmental archive, which affords high resolution isotope analysis, supported by temporally well constrained chronologies (cf. Holmgren et al., 1995, 1999, 2001, 2003; Brook et al., 1999; Repinski et al., 1999; Finch et al., 2001; Lee-Thorp et al., 2001; Sundqvist et al., 2013; Green et al., 2015). Isotopes are also increasingly used from a range of archives including sediment cores, hyrax middens, and shells and bones at archaeological sites (Cohen et al., 1992; Cohen & Tyson, 1995; Johnson et al., 1997; Abell & Plug, 2000; Chase et al., 2012; Weldeab et al., 2013; Meadows, 2014). The increasing diversity of palaeoenvironmental proxies being used, both across all published work and within individual studies, highlights an increase in available funding and international collaboration (Chase & Meadows, 2007; Meadows, 2007). This enables a wider range of palaeoenvironmental variables, tipping points, and stressors to be analysed, and facilitates multi-proxy work (Meadows, 2014). The few studies utilising foraminifera (Strachan et al., 2014, 2015), phytoliths (Burrough et al., 2012), dinoflagellate cysts (Dupont et al., 2004) and biomarkers (Norström et al., 2014; Carr et al., 2015), would suggest that there is a greater wealth of palaeoenvironmental proxies available in southern Africa than has typically been used; these too have much potential to improve our understanding of the late Quaternary palaeoenvironmental and palaeoclimatic history of southern Africa.

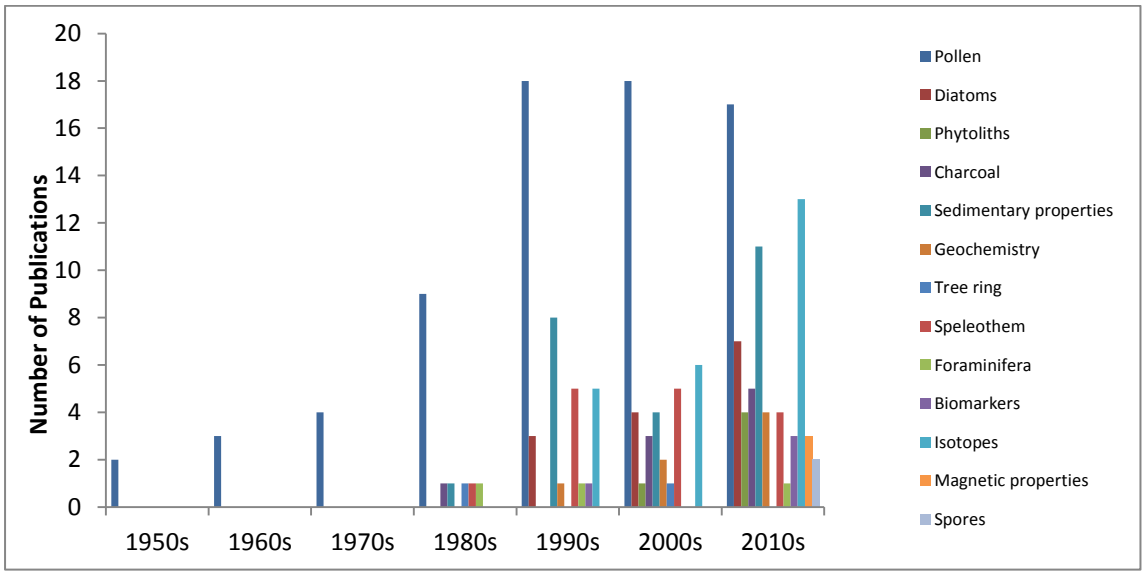


Figure 2.2: Number of proxies used in published palaeoenvironmental reconstructions for southern Africa: 1950-2015. Data derived from and cross-checked using Google Scholar, Science Direct and Web of Knowledge.

2.2.1.1 The use of Pollen in Southern African Palaeoenvironmental Reconstructions

The inception of southern African palaeoenvironmental palynology followed Van Zinderen Bakker's arrival in South Africa in 1947, with the subsequent development of a pollen analysis laboratory at the University of Orange Free State (Van Zinderen Bakker, 1995; Meadows, 2007). Van Zinderen Bakker's early work was largely exploratory in nature, including low resolution pollen analysis from Florisbad (Van Zinderen Bakker, 1957) and from the eastern Lesotho highlands (Van Zinderen Bakker, 1955), with a large focus on the east African mountains due to the more suitable environments for pollen preservation (Coetzee, 1967; Coetzee & Vogel, 1967; Van Zinderen Bakker, 1969, 1972; Van Zinderen Bakker & Coetzee, 1988). Pollen analysis thus has a considerably longer history than for many other proxies in southern Africa (*Figure 2.2*), providing sufficient material for review papers based on pollen analyses alone, covering themes including: Quaternary environmental change in southern Africa (Van Zinderen Bakker & Butzer, 1973); a synthesis of pollen studies conducted across east, central and southern Africa (Van Zinderen Bakker & Coetzee, 1988); climate change since the LGM (Scott, 1989); late Quaternary warming (Scott, 1993); the palaeoenvironmental history of the Cape Floristic Region (Meadows & Sugden, 1993); grassland development through glacial and interglacial periods (Scott, 2002); and climate change in southern Africa over the past 26,000 cal. yr (Scott et al., 2012). There are also several review papers that, while not limited to pollen, rely heavily on results from this proxy, including analyses of results on the Pleistocene-Holocene transition in southern Africa (Scott et al., 1995), and review papers on past climates of the winter-rainfall region of the Western Cape (Meadows & Baxter, 1999; Chase & Meadows, 2007).

Many of the sites from which earlier pollen-based palaeoenvironmental records were developed have been re-analysed several times, either due to their value across numerous environmental changes of interest, or to improve sampling techniques, resolution, and to integrate newer dating techniques (*Figure 2.3*). Florisbad, located in the interior of South Africa, is the first southern African site where Van Zinderen Bakker undertook pollen analysis for the purpose of reconstructing past climates, using sediment samples extracted from an exposed profile from past archaeological work at the site (Van Zinderen Bakker, 1957). Re-analysing pollen obtained from 'fresh' exposures at the site, Van Zinderen Bakker (1989, 1995) reflected on methodological errors in originally using samples that had been

exposed for long periods, and two new pollen records were presented for the site. A re-analysis of botanical evidence at Florisbad, including both pollen and phytoliths, was later undertaken (Scott & Rossouw, 2005), and also a more detailed analysis of the Holocene records from Florisbad (Scott & Nyakale, 2002), as much of Van Zinderen Bakker's work focussed on the Pleistocene.

Another site in the South African interior which has received much interest is Wonderkrater, with initial pollen results published from the late 1970s (Scott & Vogel, 1978; Scott 1982a). A more detailed pollen analysis was presented five years later (Scott & Thackeray, 1987), and a re-investigation of the age interpretations for the site reported some two decades later (Scott et al., 2003). In the most recent decade, the site has received renewed attention, including an analysis of the evidence for the Younger Dryas (Thackeray & Scott, 2006); an investigation into the geomorphology of the site, with implications on the validity of pollen records (McCarthy et al., 2010); a transfer function to relate modern vegetation to the pollen records (Truc et al., 2013); and a multi-proxy analysis of the excavated archaeological material from the site, including analyses of pollen, charcoal and phytoliths (Backwell et al., 2014).

The third site in the interior of South Africa to receive renewed attention is Tswaing Crater, although the first reference to pollen changes throughout the sequence (Partridge et al., 1993) was relatively broad. A more detailed analysis of the pollen from the Tswaing Crater profile was later produced (Scott, 1999b), together with a comparison with the pollen record from Wonderkrater (Scott, 1999a). A higher resolution pollen analysis limited to the Holocene portion of the profile has recently been reported (Metwally et al., 2014). The site has also received continued re-investigation using a range of proxies, including diatoms (Metcalfe, 1993), geochemistry (Kristen et al., 2007), and biomarkers (Schmidt et al., 2014).

At the coast, pollen from the estuarine site of Verlorenvlei was investigated intensively throughout the 1990s by Meadows (Baxter & Meadows, 1994, 1999; Meadows et al., 1994, 1996), and the site has more recently been used in the analysis of diatoms to explore changes in the strength of the westerlies (Stager et al., 2012), and biomarkers and stable isotopes to confirm changes in sea-level rise (Carr et al., 2015). While these re-analyses of

key sites are valuable in applying state-of-the-art techniques, and in improving the temporal resolution of reconstructions, in a region for which palaeoenvironmental studies remain scarce (*Figure 2.3*), such efforts are often at the cost of work in new locations.

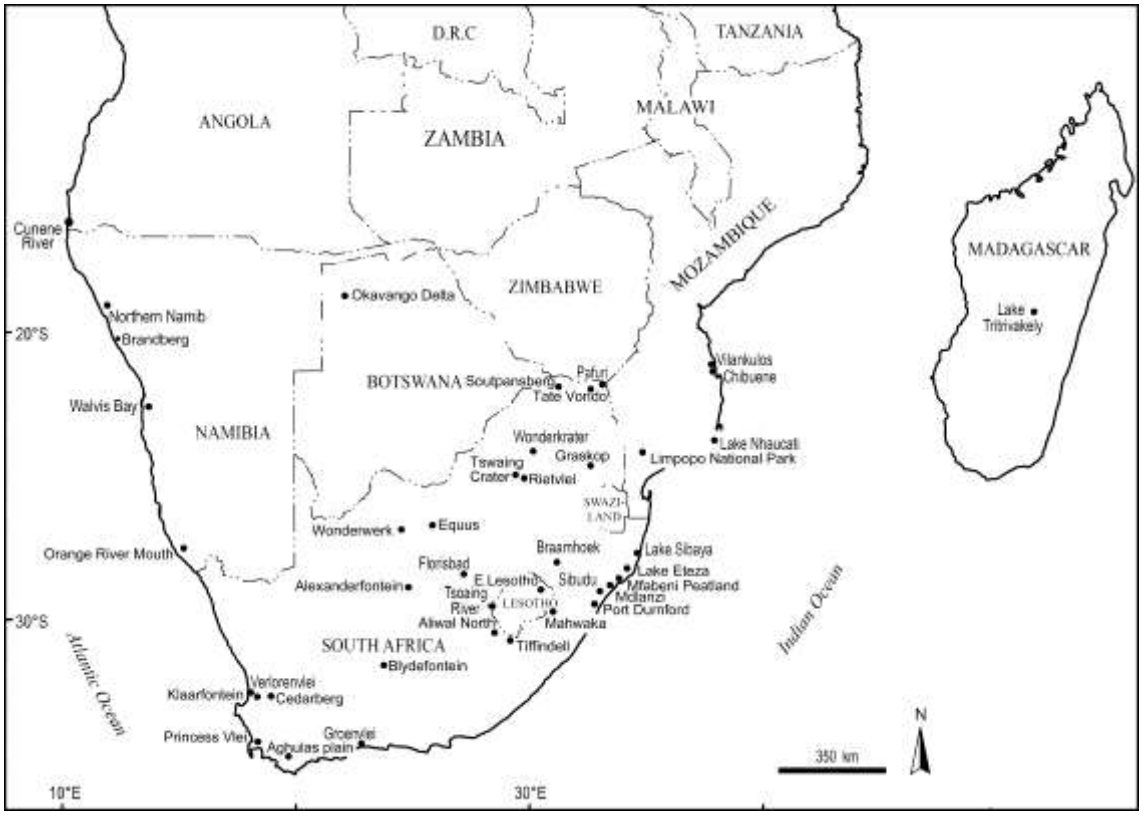


Figure 2.3: The location of southern African sites at which published pollen-based environmental reconstructions have been undertaken.

The expansion of pollen-based palaeoenvironmental reconstructions into new regions and sites appears to have formed one of the primary trajectories of palynological research in southern Africa throughout the last decade (*Figure 2.3*). Extensive work has been undertaken in the KwaZulu-Natal Province of South Africa, at Mfabeni peatland (Finch & Hill, 2008), Lake Sibaya (Neumann et al., 2008), Lake Eteza (Neumann et al., 2010) and in the Mahwaqa Mountains (Neumann et al., 2014). Moving further inland to the Free State Province, pollen analysis has formed an integral part of a multi-proxy analysis from Braamhoek Wetland (Norström et al., 2009, 2014). Pollen records spanning the past few hundred years have been presented for locations in the Kruger National Park (Ekblom et al., 2008; Gillson & Ekblom, 2009), while further north, analyses from southern Mozambique span similar durations (Ekblom et al., 2014a,b). Pollen analysis for the Okavango Basin in

Botswana spans a longer period, with an oldest date of 9,000 cal. yr BP reported (Nash et al., 2006). Off the main landmass of southern Africa, new pollen records have also been presented from Mauritius (De Boer et al., 2013). These pollen records are largely restricted to the eastern region of southern Africa, due to the wetter climate, facilitating pollen preservation (Finch & Hill, 2008; Neumann et al., 2010; Scott et al., 2012).

Perhaps the greatest development in the use of pollen as a palaeoenvironmental proxy in southern Africa has been the use of hyrax middens as an archive, facilitating pollen-based environmental reconstructions for areas too arid to support well preserved pollen within sedimentary records (Scott & Bousman, 1990; Scott et al., 2004; Chase et al., 2012; Meadows, 2014). This archive was originally investigated and then adopted by Scott in the 1990s (cf. Scott & Bousman, 1990; Scott & Vogel, 1992; Bousman & Scott, 1994; Scott, 1994, 1996), in an attempt to produce palaeoenvironmental reconstructions for regions where sedimentary records produced no viable pollen records. Later work included the use of the archive in the driest locations in southern Africa where few plants and animals currently exist, and proxies are almost absent, including the Namib Desert (Scott et al., 2004; Gil-Romera et al., 2006, 2007), and the Karoo (Scott et al., 2005). Much of the recent work using hyrax middens as pollen archives has involved high resolution analyses from middens extracted from the Cederberg Mountains, improving the climatic and environmental history for the southwestern Cape (Scott & Woodborne, 2007; Meadows et al., 2010; Chase et al., 2011, 2013, 2015a,b; Quick et al., 2011). In addition to pollen, these archives contain well preserved microcharcoal (Chase et al., 2015a), and stable nitrogen and carbon isotopes (Scott & Vogel, 2000; Chase et al., 2011, 2013, 2015a) that can be used in refining palaeoenvironmental reconstructions (Chase et al., 2012). The high resolution of analyses facilitated using this archive, together with the feasibility of work in arid regions which it affords, has made an invaluable contribution to current and future pollen-based climate change reconstructions in southern Africa (Chase et al., 2012).

Notably, while many of the sites identified by Van Zinderen Bakker have been revisited, and an increased effort has been placed on making pollen-based environmental reconstructions for a broader set of sites across southern Africa, no palynological work has been undertaken in the eastern Lesotho highlands since Van Zinderen Bakker's (1955) exploratory report of

the alpine mires. The improvements in pollen analytical work and in the potential for age determination, warrant further investigation in this region (Mitchell et al., 1998; Scott & Nyakale, 2002).

2.2.1.2 The use of Diatoms in Southern African Palaeoenvironmental Reconstructions

The identification and classification of southern African diatom species and their ecologies for the purpose of contemporary water quality monitoring developed considerably from the 1950s to 1980s, commencing with the extensive work of Cholnoky (Harding & Taylor, 2011). This work continued with Giffen's (1966) focus on diatoms as indicators of estuarine health, and the work of Schoemann and Archibald in continuing the development of diatom reference collections initiated by Cholnoky, detailed in great depth in the numerous volumes of their *Diatom Flora of Southern Africa* (Schoeman & Archibald, 1976). Despite the resultant database for the identification of diatom flora and their ecologies, there remained little use of diatoms in palaeoenvironmental studies, with the record from Tswaing Crater (Metcalfe, 1993) representing the first diatom profile assessing palaeoenvironmental change over long time periods (Partridge et al., 1993). Over the past decade, diatoms have increasingly been used as an additional environmental proxy to complement pollen, geochemical or isotope analyses from sediment profiles (cf. Huntsman-Mapila et al., 2006; Kirsten, 2008, 2014; Ekblom et al., 2008; Gillson & Ekblom, 2009; Gordon et al., 2012; Holmgren et al., 2012; Norström et al., 2012). Treated merely as a corroborating source of evidence, the environmental inferences from changes in diatom communities reported in these studies are often limited to assessments of freshwater versus brackish species, or planktonic versus benthic communities, with little to no interpretation of the temperature, nutrient or pH signals.

Despite the recent increase in the use of diatoms as palaeoenvironmental indicators, their appearance in the southern African palaeoenvironmental literature remains sparse when compared to pollen or stable isotopes, arguably due to the small proportion of sediment cores from southern Africa with well-preserved diatoms (Neumann et al., 2010; *Figure 2.2, 2.4*). This is partly because of the restricted locality of living diatoms that would subsequently appear in the sedimentary record, compared to the more ubiquitous fossil

pollen that originates from plants communities more consistently distributed across the terrestrial landscape, and the deposited pollen which often originates from a larger radius (Metcalfe, 1993; Finné et al., 2010). Second, even in regions where diatoms exist at present, poor preservation of their fossils can result in their absence for distinct periods in long-term sedimentary profiles (Finné et al., 2010; Gordon et al., 2012). As siliceous microfossils, diatoms are sensitive to the pH of percolating water, dissolving when exposed to alkaline waters, and are sensitive to mechanical abrasion from coarse sediment particles (Finné et al., 2010; Neumann et al., 2010; Gordon et al., 2012). Damage extensive enough to prevent counting was noted for Tswaing Crater (Metcalfe, 1993), Lake Eteza (Neumann et al., 2010), Soetendalsvlei (Gordon et al., 2012), and the Limpopo River floodplain (Sitoe et al., 2015). Third, diatoms can also be destroyed through siliceous uptake occurring during plant growth, resulting in low diatom concentrations at Braamhoek Wetland (Finné et al., 2010).

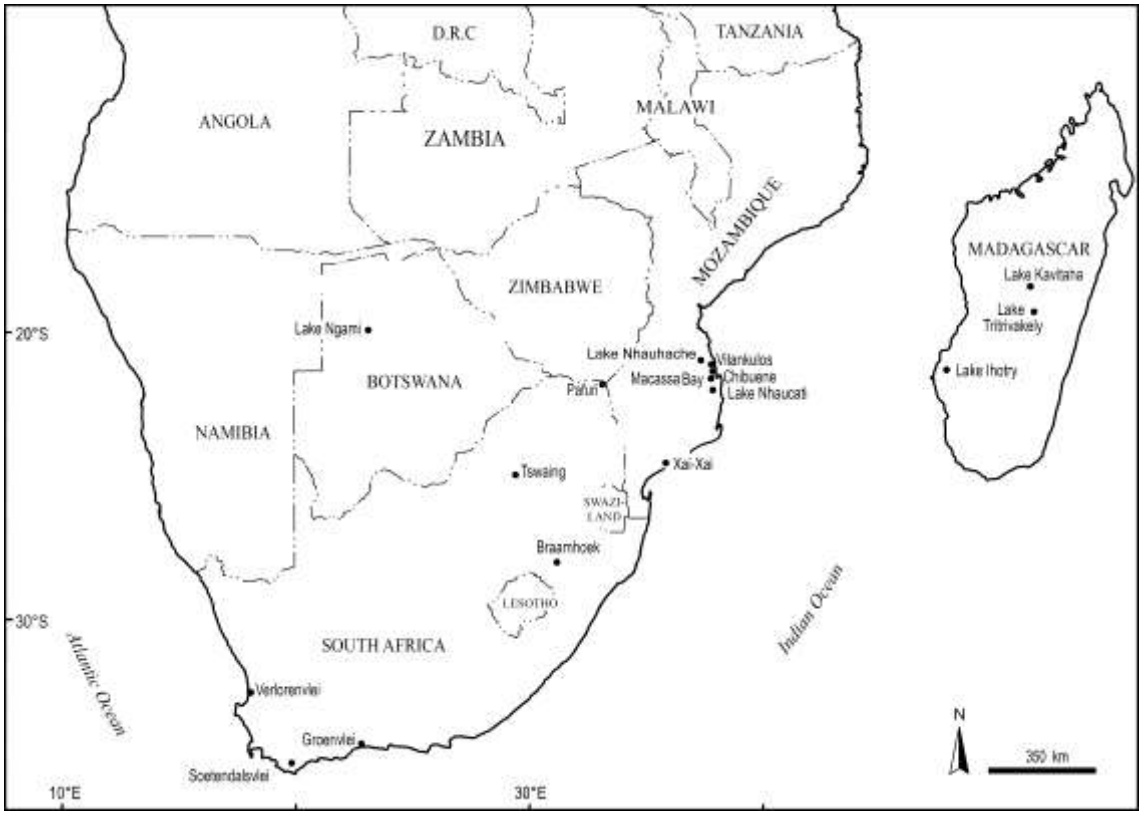


Figure 2.4: Southern African sites at which published diatom-based environmental reconstructions have been undertaken.

The use of diatoms for southern African palaeoenvironmental reconstructions has largely been restricted to lakes or palaeolakes and estuaries (Figure 2.4), using the ecology of the

identified diatoms to reconstruct changes in water depth and in the relative influence of marine conditions respectively. Diatoms from sediment profiles spanning over 100,000 years were analysed for Lake Tritrivakely in Madagascar (Gasse & Van Campo, 1998) and Tswaing Crater (Metcalfe, 1993), both demonstrating long-term hydrological changes, and associated broader environmental changes for their region. For Lake Tritrivakely, pollen and diatoms are analysed from a 40m sediment sequence extracted from the crater-lake, presently occupied by an ombrotrophic marsh in dry years (Gasse & Van Campo, 1998). The top 13m of the sediment profile are dated to span the period from 41,000 yr BP to present, and the basal date is inferred from comparison to the Vostok ice core to 150,000 yr BP (Gasse & Van Campo, 1998, 2001). Using these proxies, a reconstruction of temperature, moisture and vegetation history is provided, spanning the last interglacial to glacial cycle, reflecting changes between lake and marsh conditions (Gasse & Van Campo, 1998). The Tswaing Crater profile is 200m in length, spanning the past 180,000 yr (Metcalfe, 1993). Work was undertaken by a team of scientists to develop palaeoenvironmental reconstructions from this sequence, presented in a set of individual papers for each proxy (Partridge et al., 1993), with continued palaeoenvironmental work at the site most recently including a higher resolution pollen analysis for the Holocene (Metwally et al., 2014). The diatom record reflects an increase in salinity and alkalinity throughout the profile, paralleled by the sediment mineralogy, and accounting for the contemporary salt pan (Metcalfe, 1993). Broader environmental inferences from the record include relatively wet conditions during the last interglacial, indicated by the presence of diatoms, suggesting a well-mixed lake over the period; for the LGM, dry conditions are inferred from the absence of diatoms in the profile throughout this period (Metcalfe, 1993). A third study using diatoms, together with geochemistry, from palaeo-lake Ngami in northwest Botswana explored palaeoenvironmental shifts for a comparatively shorter 4.6m profile spanning the past 42,000 cal. yr BP (Huntsman-Mapila et al., 2006). Analysis of the ecology of fossil diatom composition of the sequence was used to corroborate geochemistry results indicative of high and low lake levels, while also providing evidence of fluctuations in salinity, pH and macrophyte presence in the lake over time (Huntsman-Mapila et al., 2006).

A methodological approach relying almost exclusively on ratios of planktonic to benthic diatom communities seems to characterise the more recent diatom-based reconstructions

of lake level change in southern Africa. Analyses of lake-level changes in the Kruger Park over the past 1,500 cal. yr using diatoms are presented as part of broader studies on rainfall variability and vegetation changes in the region, based on pollen and charcoal analyses. These studies separate periods of high percentages of planktonic diatoms (indicative of deeper water) from those with larger proportions of benthic and/or halophilous species (suggesting shallow conditions), with *Cyclotella meneghiana* used in both studies as an indicator species for shifts between the two states (Ekblom et al., 2008; Gillson & Ekblom, 2009). Similarly, a study primarily determining changes in the water level of Lake Nhauhache in southern Mozambique explores the relationship between planktonic versus benthic and/or halophilous diatoms, although places a greater emphasis on relationships between halophilous and planktonic species (Holmgren et al., 2012). Although more complex inferences are presented here than for the Kruger Park profiles, including hydrological changes from wetland to lake structure, there is little exploration of the other ecological markers of the species identified (Holmgren et al., 2012). An analysis of the diatoms from the profile extracted from Lake Sibaya (analysed for pollen by Neumann et al., 2008), explicitly relies on the percentage of planktonic species to represent lacustrine responses to changes in the ratio of precipitation and evaporation (Stager et al., 2013). It is argued that a high percentage of planktonic species would occur under conditions of deeper water or reduced water clarity, both resulting from increased precipitation, relative to evaporation (Stager et al., 2013). Notably, the results from the diatom analysis presented by Stager et al. (2013) are not temporally consistent with the environmental inferences made on the basis of pollen presented by Neumann et al. (2008), which was ascribed to improved dating in the later study, rather than differences in environmental conditions inferred from the proxy records.

Where studies exploring changes in lake levels rely on the ratios of planktonic species, studies in estuaries and coastal environments report almost exclusively the ratios between freshwater and marine species. These studies include a 10,000 cal. yr profile from Soetendalsvlei, a coastal lake on the southern Cape coast of South Africa, from which peaks in marine and brackish species were used to constrain periods of mid-Holocene sea-level high-stands from the freshwater conditions otherwise dominating the site (Gordon et al., 2012). Analyses of diatoms, in conjunction with sediment properties, stable isotopes and

mineral magnetic properties, from Macassa Bay in Mozambique, similarly rely on the ratio of freshwater to marine species to determine periods of marine incursions (Norström et al., 2012). Notably, while the profile is dominated by the marine genus *Pseudopodosira,* many of the species identified are extinct, indicating reworking and deposition from the Neogene bedrock (Norström et al., 2012). Pollen from Verlorenvlei was used to construct a Holocene sea-level curve for the southwest coast (Baxter & Meadows, 1999), that was later confirmed with an analysis of the ratio between freshwater and brackish diatoms from a Verlorenvlei core (Stager et al., 2012). A study of diatoms from the Limpopo River floodplain in Mozambique explores the transition from an ox-bow lake to terrestrial conditions, but notes periodic inundation of the lake by marine water (Sitoe et al., 2015). Masters and Doctoral research undertaken in lakes on the southern Cape coastal plain use diatoms to reconstruct periods of sea level fluctuation, together with discrete climate anomalies during the Little Ice Age, and evidence for the remobilisation of sand dunes (Kirsten, 2008, 2014).

Analysis of diatoms from inland wetlands remains restricted to the environmental reconstruction at Braamhoek Wetland in the Free State Province of South Africa, based on pollen and phytoliths (Finné et al., 2010). This study complemented the pollen, charcoal and isotope analyses for the site (Norström et al., 2009, 2014), but relied heavily on phytolith rather than diatom evidence due to the considerable proportion of damaged and dissolved diatom valves (Finné et al., 2010). They do, however, report on shifts from more dominant planktonic species during the Pleistocene/Holocene transition, to benthic and aerophilic diatoms that characterise the modern wetland, with three phases of greater water depth than at present, ascribed to changes in humidity (Finné et al., 2010). While Van Zinderen Bakker (1955) recorded the relative presence of diatoms in his pollen analysis for an unidentified site in the eastern Lesotho highlands, no further work was undertaken to determine the diatom species or their ecological preferences.

There has been a marked increase in the use of diatoms for palaeoenvironmental reconstructions in southern Africa over the past two decades, particularly within multi-proxy studies. Recent work, however, restricts the potential value of these climate and environmental proxies through focusing only on broad ecological divisions, and often limits analysis to one key environmental shift. The location of studies using diatoms for

palaeoenvironmental work in southern Africa is presently limited almost entirely to lakes and coastal sites. Given that diatoms are of immense value to understanding the environmental history at such sites, increased inclusion of these proxies at inland wetland localities is encouraged, in particular with a greater emphasis to explore changes across a broader range of ecological affinities.

2.2.1.3 The use of Sedimentary Records in Southern African Palaeoenvironmental Reconstructions

The use of sediment properties, namely the percentage of organic and carbonate content obtained through Loss on Ignition (LOI) and sediment size, for palaeoenvironmental work in southern Africa is broadly classified into three groups for this section. The first group covers the application of sediment properties in palaeoenvironmental reconstructions where no other proxies are available. The second group includes studies for which other proxies are available, but are not analysed due to a lack of facilities or expertise. These appear no longer to be independently published, as a greater access to resources and expertise through collaborative work between institutions has become more feasible, and hence more common. The third category comprises studies that include the analysis of sediment properties together with another 'primary' proxy of environmental significance. Sediment properties here are either provided solely as part of the description of the core, or are included to provide additional information regarding the profile from which the proxies originate, and are often used to corroborate the inferences made from these other proxies.

Studies categorised into the first group, wherein sediment properties are used in environmental reconstruction as no other proxies are available, are largely from hyper-arid conditions that do not support the growth of plants or animals, or that do not support the preservation of these proxies (Chase & Meadows, 2007; Burrough & Thomas, 2013). Many of these study more broadly examine landforms themselves, for which sediment analysis provides more detail regarding periods and rates of formation. This is the case for sand the dunes occupying much of the Kalahari and Namib deserts, as well as coastal regions of southern Africa (Roberts et al., 2009; Burrough & Thomas, 2013). Sediment properties are used to determine distinct periods of coastal dune formation, from which extensive

luminescence age-dating is used to constrain the timing, as has been done for St Lucia, KwaZulu-Natal (Sudan et al., 2004) and in the Maputaland dune field (Botha & Porat, 2007; Porat & Botha, 2008), as well as for exploring signals of the African Humid Period in the Kalahari (Burrough & Thomas, 2013). For the Skeleton Coast in Namibia, sediment particle size has a significant relationship between dune spacing and height, providing information about wind strength and dynamics responsible for dune production (Lancaster, 1982). Sediment properties from coversands and aeolianite deposits, such as those found in the Wilderness region of the Eastern Cape, can similarly provide information about the extent of past depositional environments, provided that they can be accurately dated (Bateman et al., 2004; Holmes et al., 2007). For all of these studies, of greater importance than the sediment properties, is the ability to obtain accurate high resolution dates for the features, and thus the focus of much research is on improving the dating methods, rather than obtaining further sedimentological information (Burrough & Thomas, 2013). Developments in the sedimentological component include the use of geochemistry to improve the identification of individual depositional events, and to better understand the sediment provenance (Bateman et al., 2004; Carr et al., 2015).

The second category of studies, that rely on sedimentary properties to reconstruct past climates and environments, even though other proxies are available, due to restrictions on funding and the scarcity of expertise in a broader range of proxies. This approach has largely ceased as increasingly southern African palaeoenvironmental studies have involved multi-disciplinary teams of scientists from a broader range of institutions, thus providing greater access to expertise and equipment (Scott et al., 2012; Meadows, 2014). Relying entirely on sediment properties to reconstruct past climates, a study was undertaken using a sediment profile extracted off the coast of Walvis Bay, with sediment particle size used to determine aridity and wind strength over Namibia (Stuut et al., 2002). Earlier work includes analyses of sediment profiles from Sani Top (Sekhokong) and Tlaaeng in Lesotho, from which periods of wet and dry conditions were inferred, with suggestions of associated temperatures (Marker, 1994, 1995). A preliminary environmental reconstruction for Vankerversvlei on the southern coast of South Africa was presented by Irving and Meadows (1997), relying entirely on sediment properties, but making reference to the presence of pollen in the record. These

studies are limited in their application in inferring climatic and environmental changeover time (Grab et al., 2005).

Many palaeoenvironmental reconstructions in southern Africa that analyse biotic proxy evidence extracted from sediment profiles, report the sediment properties of the sediment profile together with these biological proxy results. In some cases this is only a brief reference to the lithological changes throughout the core (cf. Martin, 1968; Shi et al., 1998; Neumann et al., 2008, 2010, 2011; Gilson & Ekblom, 2009; Holmgren et al., 2012). In such cases, the sedimentary descriptions are usually limited to a broad sediment type and colour, and do not use scientific tests for particle size and organic content. Therefore, they cannot be considered an environmental proxy, nor are implications of changes in lithology considered from an environmental or climate perspective. Where the sedimentary properties have been tested scientifically (with varying levels of robustness), the environmental inferences are often limited (Carr et al., 2006; Norström et al., 2012). In this instance, the sedimentary properties are often described in the results or represented on stratigraphic diagrams along with the primary proxy, but these properties are not used to corroborate the results of the primary proxy. In some cases, however, the sediment properties are treated as an additional proxy, and changes in sediment size and the proportional composition of organics and carbonates are considered for their environmental implication, and used to corroborate results from primary proxy (cf. Meadows et al., 1996; Gasse & Van Campo, 1998; Baxter & Meadows, 1999; Rosen et al., 1999; Carr et al., 2006, 2015; Huntsman-Mapila et al., 2006; Gordon et al., 2012; Norström et al., 2012; Stager et al., 2012, 2013; Walther & Neumann, 2011; Sitoe et al., 2015).

Sediment cores form the archive for the analysed proxies in a large proportion of studies, yet no investigation of changes in the sedimentary properties throughout the profile is presented (cf. Scott, 1982a, 1989, 1999a, 2002; Finch & Hill, 2008; Norström et al., 2009; Breman et al., 2011; De Boer et al., 2013; Metwally et al., 2014; Strachan et al., 2014). In some cases, the specific focus on vegetation shifts means only pollen is of direct interest, as is the case for the reconstruction of forest history in Maputuland (Finch & Hill, 2008) or grassland development (Scott, 2002). There are also study sites for which sedimentary properties of the profile have already been detailed, such as the pollen records from

Tswaing Crater (Scott, 1999a; Metwally et al., 2014) where a detailed sedimentary account is provided by Kristen et al. (2007). For studies aiming to provide a general environmental reconstruction, any additional proxies are of value in detecting periods of environmental change, and corroborating potential drivers of such change. With recent trends towards multi-proxy studies (Meadows, 2014), sediment properties provide a proxy present in all cores, that requires relatively low cost and expertise to analyse (Heiri et al., 2001). It would thus be of value for studies relying on proxies from sediment core archives to explore the sedimentary properties, and reflect on the extent to which these agree with the primary proxy of interest (Reinwarth et al., 2012; Baker et al., 2014). Although standalone sedimentary analyses are discouraged, such work would improve the understanding of variations in sediment properties within the southern African palaeoclimatic history, and strengthen the value of this proxy.

2.2.2 Key Debates on Southern African Palaeoenvironmental Change

2.2.2.1 Sea level change

Debates regarding the extent and timing of sea level changes throughout geological time are not unique to southern Africa (Hendey & Volman, 1986). Due to the relative tectonic stability of southern Africa throughout the late Quaternary, the region is well placed for analyses into sea-level rise resulting from changes in the extent of polar ice mass (Hendey & Volman, 1986; Ramsay & Cooper, 2002; Carr et al., 2010). The determination of sea-level changes cannot be undertaken within this study as it inherently requires coastal archives, and changes in sea level do not directly influence the environmental and hydrological history of the eastern Lesotho highlands throughout the late Quaternary, as they would have for coastal locations (Baxter & Meadows, 1999). However, debates concerning the timing and extent of sea level change in southern Africa are of relevance to the interior, as it provides information on the nature and duration of the interglacial warm periods at a hemispheric scale (Carr et al., 2010).

Early work on past sea-level high-stands relied on the identification and dating of geomorphological markers of palaeo-coastlines including wave-cut platforms, coastal dune complexes, diamondiferous marine sediments, beachrocks, and sites where marine

sediments are exposed (cf. Martin, 1962; Maud, 1968; Hendey & Volman, 1986; Marker, 1987; Ramsay, 1995). Extensive debate persists regarding the validity of identifying such markers, and age-dates ascribed to them (Ramsay & Cooper, 2002; Carr et al., 2010). This was followed by efforts to synthesise a range of sea-level proxies from across the southern African coastline, of which Ramsay and Cooper's (2002) sea-level curve is the most widely referenced. This sea-level curve demonstrated a strong relationship in the extent and timing of sea level shifts with those of the Caribbean for much of the past 200,000 yr, with the exception of interglacial high-stands, for which significant deviations in timing were noted. The issue of deviations in the timing of sea-level high-stands during the last interglacial, has subsequently been resolved by Carr (2010), thereby presenting a record more consistent with global records throughout glacial and interglacial cycles.

In addition to concerns relating to the reliability of identification and dating, geomorphological features of sea-level high-stands are limited in that they reflect only discrete periods in palaeoenvironmental history of extremes in sea-levels, and many reflect the last interglacial. There has consequently been an increasing effort to find proxies for sea-level change within sediment profiles extracted from coastal sites, that can track both increasing and decreasing sea levels, and detect lower-amplitude shifts at a higher temporal resolution. The first of these southern African palaeoenvironmental reconstructions to trace sea-levels is the work of Meadows et al. (1996), briefly exploring evidence for a mid-Holocene sea-level high-stand based on pollen records from Verlorenvlei. This record is subsequently explored in further detail by Baxter and Meadows (1999) and included in Ramsay and Cooper's (2002) sea level synthesis. This sea-level high-stand from 8,000-4,300 cal. yr BP for Verlorenvlei has been confirmed through further analysis of an 8,000 cal. yr profile of biomarkers and stable isotopes from the site (Carr et al., 2015). A study using diatoms, geochemistry and stable isotopes from a profile extracted from Soetendalsvlei on the south coast of South Africa, provides evidence for two distinct sea-level high-stands at ~8,000 cal. yr BP and ~4,000 cal. yr BP, separated by a period centred at ~6,000 cal. yr BP, in which the region was characterised by freshwater conditions, that resumed by ~1,800 cal. yr BP (Gordon et al., 2012). This is in broad agreement with earlier findings for the south Cape coast from the Keurbooms estuary (Reddering, 1988) and from Knysna (Marker & Miller, 1993). For the east coast, a late Holocene foraminifera record from the Kariega Estuary was

investigated, detecting a marine transgression before 1,110 cal. yr BP, followed by oscillations within a 0.5m amplitude until 300 cal. yr BP, after which a stable sea-level has been maintained (Strachan et al., 2014).

2.2.2.2 Shifts in the extent of the winter rainfall zone

For the southern half of the region, the most important synoptic scale changes that are likely to have occurred during the late Quaternary are shifts in the position and strength of the westerly belt, with resultant influences on the position of the Winter Rainfall Zone (WRZ) and the associated flora (Barrable et al., 1998; Chase & Meadows, 2007; Stager et al., 2012). The contemporary WRZ, located in the southwestern Cape, is an important geographical region as a Southern Hemisphere example of a Mediterranean-type climate (Barrable et al., 1998). The region is characterised by high floristic diversity, and is the endemic habitat of the majority of the Fynbos species, a biome constrained by the position of the regular intrusion of mid-latitude cyclones (Barrable et al., 1998; Chase & Meadows, 2007). The WRZ is thus climatically and ecologically distinct from the Summer Rainfall Zone (SRZ) which comprises the majority of the country (Stager et al., 2013), but is arguably distinct also from the year-round rainfall zone (YRZ), located along the south coast of the country, despite similarities in vegetation (Van Zinderen Bakker, 1976; Barrable et al., 1998; Carr et al., 2006; Chase & Meadows, 2007). It is argued that during glacial periods, the increase in Antarctic sea ice would have resulted in a northward shift in the westerlies and a resultant increase in the winter-rainfall zone (Van Zinderen Bakker, 1976; Cockroft et al., 1987; Stuut et al., 2002; Chase & Meadows, 2007), while there are concerns that a retreat in the westerlies under climate change may result in a greater incidence of drought in the WRZ (Stager et al., 2012). It is difficult to obtain direct information pertaining to the seasonality of rainfall for a particular region from climate proxies, which instead reflect broader fluctuations in total precipitation (Chase et al., 2015a). There is thus on-going debate concerning the nature and extent of such geographic shifts in the position of westerlies (Chase & Meadows, 2007).

The position of frequent westerly belt intrusions in southern Africa during the late Quaternary, in response to changes in sea ice extent, has been of palaeoenvironmental

interest for many decades, initiated by the work of Van Zinderen Bakker (1976), Tyson (1986) and Cockroft et al. (1987). Van Zinderen Bakker (1976) originally suggested an expansion of Mediterranean Cape flora and the associated WRZ as far north as ~24°S, encompassing Namibia and the Free State during the LGM. This was later revisited, and Van Zinderen Bakker (1983) conceded that while he still argued that considerably stronger westerlies occurred during the LGM, the westerly belt and associated vegetation probably did not extend as far north as originally proposed (Chase & Meadows, 2007). More recently, studies within the southern Cape region have led to some consensus that the strength of the westerly belt and the resultant WRZ expanded in both northerly (Barrable et al., 1998; Chase & Meadows, 2007; Stager et al., 2012) and easterly (Carr et al., 2006; Chase & Meadows, 2007) directions, although the geographic limits of these shifts remain uncertain. Changes in the extent of the westerly belt are not only of importance to the WRZ, but also influence the frequency and intensity of mid-latitude cyclones moving into the interior regions of South Africa. Pollen, diatom and phytolith records from Braamhoek Wetland, located north of the WRZ in the Free State Province of South Africa, provide evidence for a greater influence of mid-latitude cyclones, associated with a northward shift of the westerly belt towards the South African interior during the terminal Pleistocene (Norstöm et al., 2009, 2014; Finné et al., 2010). This is in agreement with palaeogeomorphological evidence for eastern Lesotho indicating an increased intensity of mid-latitude cyclones reaching the Lesotho highlands during the late Pleistocene (Mills et al., 2012). Recently, the palaeoenvironmental work involving changes in synoptic patterns throughout the late Quaternary has involved exploring the role of shifts in the Inter-Tropical Convergence Zone (ITCZ) on the SRZ, from diatom records at Lake Sibaya (Stager et al., 2013), and from the pollen record from Wonderkrater (Truc et al., 2013). The role of the strength of the easterly waves, and associated ocean upwelling in drought periods, has also been explored for the winter-rainfall zone, based on pollen, microcharcoal and stable carbon and nitrogen isotope records extracted from a hyrax midden at Swartruggens Mountains in the Western Cape (Chase et al., 2015a). This demonstrated that Holocene fluctuations in the easterly waves are associated with variability in summer rainfall, (Chase et al., 2015a). Debates regarding changes in the strength of synoptic features are of critical importance to climate modellers, and many of the specifics remain unresolved for southern Africa and the Southern Hemisphere (Fletcher & Moreno, 2012). Climate models would therefore benefit from

greater collection of high temporal-resolution records across transects covering the WRZ, YRZ and SRZ (Chase and Meadows 2007).

2.2.2.3 Similarity of Northern and Southern Hemisphere Late Quaternary Climate Shifts

There remains ongoing debate amongst the palaeoenvironmental science community concerning the extent to which Northern Hemisphere climate events have contemporaneous Southern Hemisphere equivalents (Holmgren et al., 2003; Scott et al., 2012; Truc et al., 2013). Improvements in high resolution dating provide the capacity to resolve these debates, but through refined chronological reconstructions, regional differences in southern African climatic histories have been revealed (Tyson & Lindesay, 1992; Holmgren et al., 2003). Climate events that have been verified for the Northern Hemisphere, but remain unconfirmed for southern Africa, include the African Humid Period (Burrough & Thomas, 2013), and cold relapses including Younger Dryas (Peteet, 1995; Thackeray & Scott, 2006), the '8.2 kyr' event (Smith et al., 2002), and the Little Ice Age (Tyson et al., 2000). There is not yet conclusive published evidence of distinct, temporally synchronous '4.1 kyr' or '2.8 kyr' cold events (Mayewski et al., 2004; Wanner et al., 2015). Unresolved questions include whether such events occurred in southern Africa, and the specific environmental conditions potentially associated with them.

The most notable debate has focussed on the existence of a Younger Dryas cool period interrupting the warming period following the LGM, from 13,000-11,500 cal. yr BP (Abell & Plug, 2000). Analysing pollen records from a range of sites within the interior of South Africa, Scott et al. (1995) reported that if there were a Younger Dryas event in southern Africa, the effect of it would have been too small to be registered in the pollen record. Records for a Younger Dryas cold event were, however, detected in oxygen isotope and aragonite-calcite ratios from molluscs in Elands Bay, indicating colder sea temperatures (Cohen et al., 1992); dinoflagellate cysts from the Cunene River Mouth indicating depressed sea surface temperatures (Dupont et al., 2004); oxygen isotopes from giant land snails at Bushmans' Rock shelter indicating colder air temperatures (Abell & Plug, 2000); and stable carbon and nitrogen isotopes from hyrax middens similarly indicating lower temperatures for the WRZ (Quick et al., 2011). Notably, both Dupont et al. (2004) and Quick et al. (2011)

remarked on distinct isotope signals for a Younger Dryas event, but no pollen signal from the same sample, suggesting that vegetation may have remained relatively stable throughout this period. While speleothems hold the potential for higher resolution climate reconstructions, stalagmites analysed from Cold Air Cave had a depositional hiatus covering this period, although it was argued that this might reflect drier conditions associated with the event (Holmgren et al., 2003). In a re-evaluation of the pollen record from Wonderkrater, with improved chronological detail, Thackeray and Scott (2006) found three samples close in age to the Northern Hemisphere Younger Dryas, during which a cold reversal was notable (Truc et al., 2013). Multivariate analysis on this re-analysed pollen record quantified the temperature incursion to 6 ±2°C (Truc et al., 2013). More recently, a Younger Dryas signal has been detected in the Sudwala Cave speleothem isotope record, associated with wet conditions (Green et al., 2015), while a multi-proxy analysis of a sediment core from Braamhoek Wetland indicates a Younger Dryas cold period paired with dry conditions (Norström et al., 2014). Increasing evidence supports the existence of a Younger Dryas event in southern Africa, but the climatic conditions during this event remain unclear, and are likely to have been regionally varied, requiring further high resolution studies across a broad selection of regions to determine the nature of these variations (Chase et al., 2011).

A more recently emerging debate concerns the existence of conditions indicative of a southern African extension of the African Humid Period recorded for East Africa, occurring in the early Holocene, within the period ~14,800-5,500 cal. yr BP (Chase et al., 2009; Burrough & Thomas, 2013). Evidence is presented from hyrax middens in Namibia, suggesting the existence of an early Holocene moist period, with the inference that the African Humid Period extended as far south as 23° in Namibia (Chase et al., 2009). The extensive aridity in the Kalahari during this period poses contradictory evidence, and while there are lake high-stands in the Makgadikgadi dated to this period, it is argued that these are fed from distant sources (Burrough & Thomas, 2013). Although not referred to specifically as the African Humid Period, and with varying time periods throughout the early Holocene, reference has been made to humid periods following the postglacial warming, with evidence from peat development (Meadows, 1988), the Caledon River charcoals

(Esterhuysen & Mitchell, 1996; Esterhuysen et al., 1999), and pollen across the South African interior (Van Zinderen Bakker & Coetzee, 1988; Scott, 1993; Lewis, 2005).

Considerable evidence for the Little Ice Age cold period exists for southern Africa, from AD 1300-1800 (cf. Talma et al., 1974; Herbert, 1987; Talma & Vogel, 1992; Tyson & Lindesay, 1992; Brook et al., 1999; Holmgren et al., 2003; Sundqvist et al., 2013; Zinke et al., 2014). The majority of studies presenting evidence for this event are based on stable isotopes from speleothems, due to the high resolution afforded (cf. Talma & Vogel, 1992; Brook et al., 1999; Holmgren et al., 1999, 2001, 2003; Repinski et al., 1999; Tyson et al., 2000; Lee-Thorp et al., 2001; Sundqvist et al., 2013). While the existence of a Little Ice Age event has been confirmed across much of the region, the associated climatic conditions remain unclear. Evidence suggests that broadly, dry conditions occurred during the Little Ice Age in the SRZ (Lee-Thorpe et al., 2001; Holmgren et al., 1999; Ekblom et al., 2008; Gillson & Ekblom, 2009; Neumann et al., 2010), while wet conditions were experienced in the WRZ (Stager et al., 2012; Weldeab et al., 2013), supporting Tyson and Lindesay's (1992) original model. The temperature decrease for this period remains to be quantitatively constrained. Suggestions of temperatures 1°C colder during the Little Ice Age and 3°C warmer in the prior Medieval Warm Period (Tyson et al., 2000), remain unconfirmed against evidence of more severe cooling, as this event reflects the most pronounced $\delta^{18}O$ deviation within the 25,000 yr Cold Air Cave record (Holmgren et al., 2003).

2.2.2.4 The Last Glacial Maximum: Temperatures, Moisture and Glaciation

A Northern Hemisphere climate event that is undisputed to have influenced the southern African palaeoenvironment is the LGM (Chase & Meadows, 2007). Debates continue regarding the exact time period the event spanned, the timing of the coldest conditions, the moisture conditions during the LGM, and evidence for glaciation at high altitude locations during the period. Many of these debates overlap with disputes on the extent of the westerlies discussed in *Section 2.2.2.2*, and with the evidence for glaciation discussed in Section *2.3.2*. Thus, presented here are the broader debates concerning the LGM that have arisen from evidence provided through the increase of archives, proxies and locations studied across southern Africa.

The time period spanning the LGM in southern Africa has been unclear. Studies have defined the period for the purpose of analysis of specific datasets as centred around 18,000 yr BP (Meadows & Linder, 1993; Meadows & Sugden, 1993), roughly equivalent to 21,000 cal. yr BP (Partridge et al., 1997), or with a broader range, such as between 21,000-17,000 cal. yr BP (Partridge et al., 1999). The ranges are also inconsistent between studies, including 20,000-16,000 cal. yr BP (Deacon & Lancaster, 1988) and 21,000-17,000 cal. yr BP (Partridge et al., 1993). Chase and Meadows (2007) suggest that for ease of comparison, both within southern African records, and in comparison with records from elsewhere, the Land, Oceans, Glaciers Programme (EPILOG) definition be used, that conservatively places the LGM within a range of 24,000-18,000 cal. yr BP (Chase & Meadows, 2007). The timing of the coldest period within the LGM also remains unresolved, with pollen from Elim in the Free State indicating coldest periods at ~18,000-17,000 cal. yr BP (Scott, 1999a), confirmed by speleothem isotope records from Cold Air Cave (Holmgren et al., 2003). A statistical re-analysis of 27 pollen records spanning the Namib Desert, Namaqualand, Western Cape Fynbos, east coast woodland, Karoo grassland, upland grassland, dry woodland, and sub-humid woodland ecozones in southern Africa suggests that there may have been two periods of coldest temperatures during the LGM, at ~24,000 cal. yr BP and ~17,000 cal. yr BP (Scott et al., 2012). With dates for LGM conditions in southern Africa spanning such a long period, it remains unclear whether this event is contemporary with the Northern Hemisphere LGM, or whether some lag period exists.

Many southern African palaeoenvironmental studies report cooler temperatures during the LGM, but are unable to quantify, or do not report, the temperature depression relative to contemporary conditions (cf. Scott, 1982a; Shi et al., 1998; Scott & Vogel, 2000; Neumann et al., 2014; Norström et al., 2014). One of the earliest reports of a quantified temperature depression for the LGM was an indication of conditions 5-6°C cooler than present in interior highveld during LGM based on the pollen record from Wonderkrater (Scott, 1982a). A review and synthetic reconstruction of climatic conditions during the LGM (Partridge, 1999), similarly suggests an overall temperature decrease of 5°C throughout the LGM in southern Africa between latitudes of 24°-33°S. This reconstruction was based primarily on the records of Talma & Vogel (1992) who suggest a decrease of 6°C, Heaton et al. (1986) suggesting a 5.2°C depression, and Stute & Talma (1997) reporting a 5.3°C decline, all relative to

contemporary mean temperatures (Partridge, 1999). A significantly greater temperature departure of 7-8°C for the LGM is suggested based on palaeogeomorphological evidence from high altitude sites in the Western Cape Mountains (Boelhouwers & Meilklejohn, 2002). The suggestion of an even more extreme temperature depression of 10°C is based on possible moraines from the Eastern Cape Drakensberg (Lewis & Illinger, 2001). Isotope analysis from the Cold Air Cave speleothem facilitated much higher resolution proxy analysis and dating, and suggests a temperature increase of 5.7°C from the terminal Pleistocene to Holocene (Holmgren et al., 2003). A more recent statistical reanalysis of the improved pollen records for Wonderkrater (Thackeray & Scott, 2007) would reconfirm the lower estimates, reporting a temperature depression of 6 ±2°C during the LGM. The extremely cold LGM temperatures implied from the palaeogeomorphological evidence may be due to misconceptions on the moisture levels during the LGM, highlighting the importance of understanding both temperature and precipitation changes (Mills et al., 2012).

If the temperature depression during the LGM were to have been ~6°C, wetter conditions would need to have occurred in the eastern Lesotho highlands to have produced the periglacial and glacial features observed on south-facing slopes, which was attributed to a shift in the westerlies (Rojas et al., 2009; Mills et al., 2012). The broad understanding of moisture conditions during the LGM, however, was of drier conditions in the SRZ but wetter in the WRZ (Partridge, 1999). The dry LGM in the SRZ is supported by records from Mfabeni Peatlands in Kwa-Zulu-Natal (Finch & Hill, 2008; Baker et al., 2014), Tswaing Crater in the interior (Metcalfe, 1993; Partridge et al., 1993), together with numerous other inland sites including Wonderkrater, Rietvlei, Tate Vondo, Elim, Equus Cave, Boomplaas (Scott 1989), and Braamhoek Wetland (Norström et al., 2009). Offshore pollen records obtained from the Cunene River Mouth suggest that southwestern Africa was also dry during the LGM. Records from the southern region of the country, originally argued to be homogenously wetter during the LGM, highlight local variations in moisture levels during this period (Barrable et al., 1998; Chase & Meadows, 2007). The first distinction is between the YRZ and WRZ: previously considered to have experienced similar climatic changes throughout much of the late Quaternary, but evidence suggests that conditions during the LGM were drier in the YRZ but wetter in the WRZ (Carr et al. 2006; Chase & Meadows, 2007). Further variation exists within the WRZ, with models integrating palaeoenvironmental proxy data indicating that the

western coastal zone was cool and moist, while the southern region was colder and drier (Barrable et al. 1998). Considerable temporal variations within the LGM may exist, as the Cederberg isotope records suggest a dry late LGM period (Chase et al. 2011).

As the LGM was associated with a temperature depression of at least 5° in southern Africa, questions of possible glaciation in alpine regions of southern Africa have been debated frequently over the past few decades (cf. Sparrow, 1967; Harper, 1969, Marker & Whittington, 1971; Marker, 1991; Grab, 1996a,b, 1999, 2000, 2002a,c; Grab & Hall, 1996; Boelhouwers & Meiklejohn, 2002; Sumner, 2004b; Mills et al., 2009a). As much of the alpine region of southern Africa is located in eastern Lesotho, the intricacies of these debates are presented in *Section 2.3.2*. Notably, however, glacial moraines identified from the south-facing slopes of the Leqooa (Mills et al. 2009a) and Sekhokong Mountain Ranges (Mills et al., 2009b) in eastern Lesotho, dated to within the period of the LGM provide the first temporally constrained and thus far undisputed evidence for niche glaciation. Widespread glaciation in the eastern Lesotho highlands, and glaciation in other regions of southern Africa during the LGM, has been contested (Boelhouwers & Meiklejohn, 2002; Mills, 2009b).

Aside from a study for off-shore Namibia reporting increases in wind flux during the LGM (Shi et al., 1998), little further information regarding the climate dynamics for this period exist. Considerable work to improve the chronology of the LGM event, and associated climatic fluctuations during the period, is still required (Chase & Meadows, 2007; Chase et al., 2011). Research to quantify the climatic conditions during the LGM relative to the contemporary state, and to understand the regional variations in LGM climates and their drivers, also warrants attention (Barrable et al., 1998). While this study is limited to the Holocene, the LGM conditions provide a backdrop to the environmental and climatic conditions during this period, and thus cannot be ignored in a Holocene study such as this.

2.2.3 The Future of Southern African Palaeoenvironmental Research: The Importance of Application

Southern African regional palaeoenvironmental reconstructions remain relatively limited in quantity, owing to numerous factors including the comparatively late inception of the discipline in the region, difficulties in obtaining suitable archives in drought prone regions,

and limitations in skills and expertise (Neumann et al., 2008; Meadows, 2014). Adapted from Scott et al. (2012, p. 101), these limitations can be summarised as: 1) a scarcity of appropriate sites with well preserved, representative proxies; 2) the use of poor dating techniques, and/or low temporal resolution; 3) sub-regional ecological differences, many of which are unaccounted for in the palaeoenvironmental literature; 4) varied levels of, and often inadequate, taxonomic resolution in fossil identification; 5) non-uniform presentation of palaeoenvironmental evidence; and 6) non-uniform methods for the interpretation of results. As a developing discipline, the future of Quaternary palaeoenvironmental research in southern Africa necessarily needs to address these problems in an holistic manner (Scott et al., 2012; Meadows, 2014). There has however been a key shift in academic focus since the inception of palaeoenvironmental work in the 1960s, with climate change interpretations increasingly taking greatest importance (Meadows, 2007). Much of the immediate future of palaeoenvironmental work thus arguably involves the application of an understanding of palaeoenvironments to contemporary management, including global climate modelling, ecological monitoring through the determination of critical thresholds and an understanding of the role of fire, and the attribution of human influence to environmental changes (Willis et al., 2005; Meadows, 2012; Gillson, 2015a,b).

The first application of palaeoenvironmental data in southern Africa was in the validation of climate models. The first southern African conceptual climate model to include both surface and upper air dynamics for the contemporary climate was compared with the, albeit sparse, palaeoclimatic reconstructions for the region (Cockroft et al., 1987). From the correlation between model simulations and palaeoclimatic evidence, support was provided for the conceptual palaeoclimatic model proposed by Tyson (1986). At a smaller geographical scale, and with a greater volume of palaeoclimatic work for comparison, Barrable et al. (1998) evaluated the palaeoclimatic evidence for the southern African WRZ against climate model simulations, and confirmed a difference in moisture conditions within the WRZ during the LGM. It was argued that such correlations between models and proxy data have the potential to improve both methods, as proxy data can validate the climate model output and provide further data to improve the reliability of projections, while the model data can improve explanations of the synoptic drivers of palaeoclimatic changes, and indicate locations for which palaeoclimatic studies would be of particular value in determining

regional patterns in past climates (Barrable et al., 1998). Despite the value of such work, and the use of palaeoclimatic data to validate the IPCC climate models (Meadows, 2012, 2014), detailed work in southern Africa remains to be forthcoming.

The second application of palaeoenvironmental work is in improving the ecological understanding of ecosystems through exploring the dynamics of their changes over long time-periods, although the adoption of palaeoenvironmental evidence by ecologists has arguably been overdue (Willis et al., 2005; Meadows, 2012; Gillson, 2015b). The value of understanding the long-term history of ecological systems is most apparent with regard to the management of grasslands, as decisions inherently require the nature of grassland development to be understood, because anthropogenic development through deforestation would have significantly different implications to the existence of grasslands in the region prior to permanent human occupation (Meadows & Linder, 1993; Scott, 2002; Gillson, 2015a). Management decisions that relied on the assumption that grasslands were anthropogenically initiated, have been critiqued by palaeoenvironmental evidence from pollen, phytoliths and stable isotopes of southern African grasslands dating back to the Tertiary (Scott, 2002), presence of Afromontane grasslands prior to permanent human occupation in southern Africa (Meadows & Linder, 1993), and a progressive shift from C_4 dominated grassland and open savannah to C_3 thicket, forest and densely wooded saVannah in KwaZulu-Natal (Gillson, 2015a). Studies of the ecological histories in other biomes include an analysis of the palaeoenvironmental history of the Cape Floristic Kingdom (Meadows & Sugden, 1993), and of *Podocarpus* forest history in Maputuland (Finch & Hill, 2008). It can further be argued that studies that do not intend to provide purely ecological information from palaeoenvironmental proxies would be of great value to ecologists in determining historical vegetation communities, and drivers of their shifts (Willis et al. 2005; Meadows, 2012).

Of increasing interest within the grassland history of southern Africa is the role of fire, and the relationships between fire intensity and vegetation composition (Duffin, 2008; Ekblom & Gillson, 2010). An empirical relationship between charcoal deposits in surface sediment samples from Kruger National Park and the proximity of fires, area of fires and fire intensity was developed (Duffin et al., 2008), from which palaeoenvironmental records were

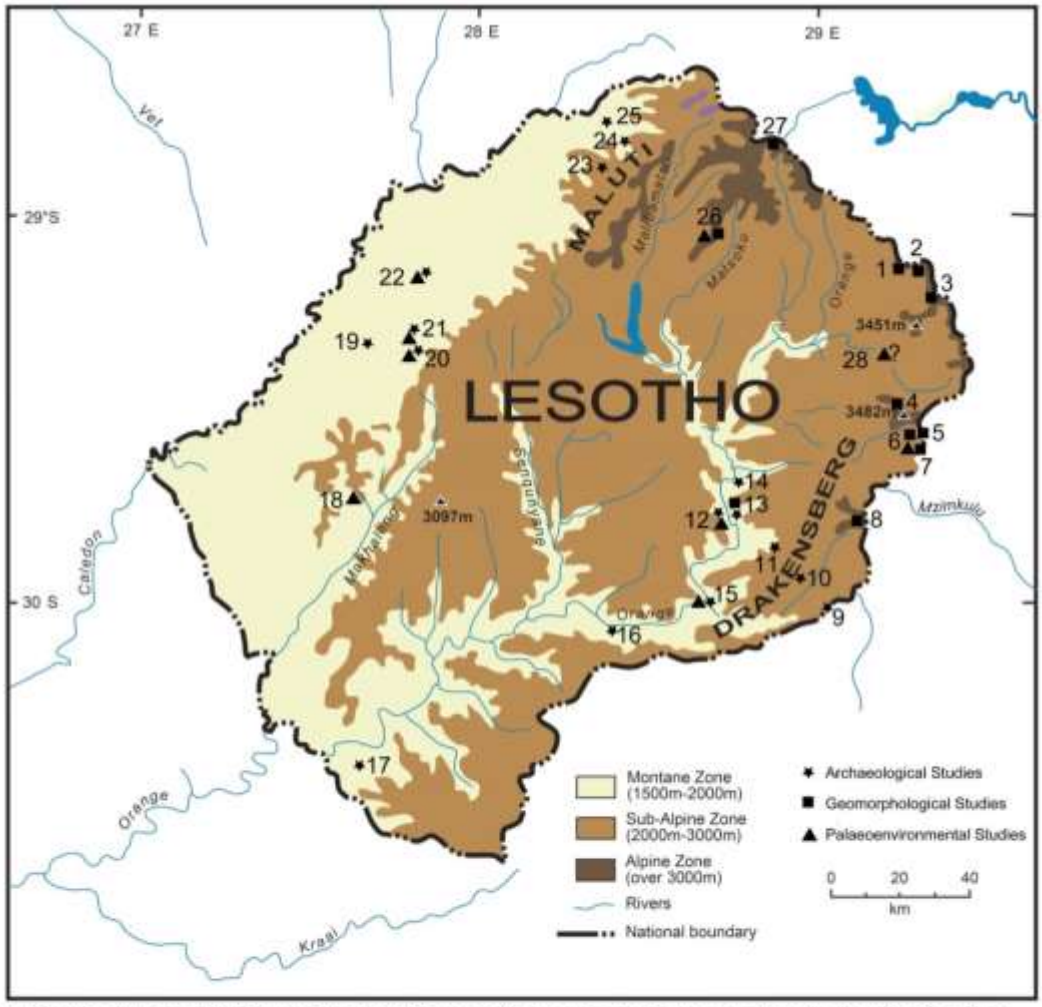
compared, reporting higher fire intensity related to higher percentages of herbaceous cover and lower percentages of woody plant growth (Duffin, 2008). Further work in the Kruger National Park challenged the assumption that fire suppresses tree seedling growth and hence encourages grasslands, through finding that in grassland-dominated periods the high frequency of fire appears to shift the system to a saVannah environment through increasing woody recruitment, while during saVannah-dominated periods fire limits woody recruitment and retains the environment in a saVannah state (Ekblom & Gillson, 2010). A record spanning a longer period, covering the mid- to late-Holocene for Graskop and Versailles in Mpumalanga Province, South Africa, found that fire was rare during the grassland dominated period prior to 4,000 cal. yr BP, but that fire incidence increases from 600 cal. yr BP following a decrease in *Podocarpus* pollen, and spiked in the last 70 years due to human influence (Breman et al., 2011). At the scale of interglacial-glacial cycles, a study of charcoal from a core off the coast of Namibia found six periods of heightened fire incidence over the past 170,000 cal. yr, coinciding with precessional forcing of north-south shifts in the ITCZ and notably occurred during periods with wetter and cooler climates, assumed to be due to changes in rainfall seasonality (Daniau et al., 2012). A more complete understanding of the dynamics between vegetation and fire throughout periods of vegetation change enables improved ecosystem fire management, and these developments in palaeoecological fire studies offer an example of the value of palaeoenvironmental work to ecologists (Ekblom & Gillson, 2010).

The third application of palaeoenvironmental work to contemporary management is in determining the influence of prolonged anthropogenic settlement on the natural environment, which has been facilitated through improvements in sampling resolution and dating accuracy to capture environmental changes over the past few centuries (Baxter & Meadows, 1999; Neumann et al., 2008; Reinwarth et al., 2013; Neumann et al., 2014). This is particularly important in regions with a high level of human occupation, as progressively the anthropogenic effect on vegetation changes has exceeded those of climate shifts (Neumann et al., 2011), influencing the success of management decisions (Gillson, 2015a). The relative anthropogenic and climatic influences on the shift from afromontane forest to grassland in the Western Cape was inferred on the basis of species richness from fossil pollen in the Winterberg escarpment region, which demonstrated that climatic shifts

remained the most dominant drivers even in the late Holocene (Meadows & Linder, 1993). By contrast, considerable human influence is noted in regions that experienced sudden shifts to agricultural land-use (Meadows et al., 1996; Neumann et al., 2008). Pollen records demonstrated a sudden, marked appearance of cereals at Verlorenvlei (Meadows et al., 1996; Baxter & Meadows, 1999), the adjacent Klaarfontein Springs (Meadows & Baxter, 2001), Lake Sibaya (Neumann et al., 2008), and in present-day Kruger National Park (Gillson & Ekblom, 2009), all dating to the 19th and 20th centuries. Further evidence of anthropogenic impacts includes increases in algae synchronous with the introduction of cereal pollen at Lake Sibaya (Neumann et al., 2008), the appearance of pine pollen from the 19th century in the core from Mahwaqa Mountain, indicating the introduction of alien plants to the region (Neumann et al., 2014), and an increase in sediment and nutrient deposition in Eilandvlei from the 19th century onwards, a possible consequence of agriculture and associated soil erosion (Reinwarth et al., 2013). Through quantifying anthropogenic influence on the environment and the relative influence of climatic shifts over long time periods, more informed management decisions can be made (Gillson, 2015a,b).

2.3 Palaeoclimatic History of eastern Lesotho

The late Quaternary environmental record remains uncertain and at best undefined for much of the Lesotho highlands (Grab et al., 2005; Roberts et al., 2013), and is based almost entirely on archaeological and geomorphological evidence (*Figure 2.5*; Parker et al., 2011). The majority of the palaeoenvironmental evidence for the Lesotho region stems from its rich archaeological heritage, and is often based on material derived from discrete periods during which occupation of a specific site occurred (cf. Carter, 1976; Plug, 1993; Mitchell et al., 1994, 1998, 2011; Mitchell, 1995, 1996a; Plug et al., 2003, 2010; Cain, 2009; Parker et al., 2011; Stewart et al., 2012; Roberts et al., 2013). This archaeological work includes numerous inferences of possible palaeoclimatic changes throughout the late Quaternary (Mitchell et al., 1998), but the chronological temporal continuity and the quantification of past climates lacks detail (Mitchell, 1996a; Parker et al., 2011).



1. Mafadi; 2. Njesuthi; 3. Popple Peak; 4. Thabana Ntlenyana; 5. Tsatsa-la-Manguaung; 6. Sani Top; 7. Sekhokong; 8. Leqooa; 9. Belleview; 10. Ha Soloja; 11. Moshebi's Shelter; 12. Likoaeng; 13. Sehonghong; 14. Mashai; 15. Melikane; 16. Bohlahla; 17. Masitise; 18. Tsoaing River; 19. Leqhetsoana; 20. Tloutle; 21. Ha Makotoko; 22. Ntloana Tsoana; 23. Liphofung; 24. Muela; 25. Hololo Crossing; 26. Tlaeeng; 27. West of Mont Aux Sources; 28. Eastern Lesotho Wetland

Figure 2.5: The location of archaeological, geomorphological and palaeoenvironmental study sites in Lesotho from which published palaeoclimatic inferences have been made.

A variety of Quaternary periglacial and glacial studies from Lesotho's eastern high mountain region have indicated colder conditions during the late Pleistocene (Harper, 1969; Grab, 2002a; Mills and Grab, 2005; Mills et al., 2009a,b) and Holocene neoglacial episodes (Grab, 2000). However, the absence of age-dates for many of these features, lack of consistent temporal chronologies, and disputed interpretation of landforms, have limited their palaeoenvironmental value (Boelhouwers & Meiklejohn, 2002; Mills et al., 2009b; Roberts et al., 2013). Where Holocene sedimentary sequences have been described together with age-dates for the eastern mountains of Lesotho (Hanvey & Marker, 1994; Marker, 1994,

1995, 1998), the absence of analysis of environmental proxies has limited the potential for a more detailed and higher resolution environmental and climatic reconstruction (Grab & Hall, 1996; Parker et al., 2011). The paucity of palaeoenvironmental work in the region (*Figure 2.5*) stems largely from the difficulty in accessing sites in the mountainous terrain, and considerable logistical challenges in extracting material (Mitchell, 1992). This section explores current understandings of the late Quaternary palaeoclimatic history of the region, critically analysing the evidence published to date.

2.3.1 The Archaeological Record

The selection of locations for settlement by Early through to Late Stone Age communities in southern Africa necessarily involved considerations of the climate, natural environment, and resource availability, as these factors presented varied opportunities and threats at each location (Carter, 1976; Mitchell, 1995; Plug, 1997; Plug et al., 2003). These considerations would have been particularly pertinent to the eastern Lesotho highlands, with rapid altitude changes over short distances, and associated climate and vegetation variability, resulting in potential settlement locations across gradients of increasing climate threats and decreasing opportunity (Carter, 1976; Mitchell 1995, 1996a). During colder periods, the highest altitude sites would have become completely unsuitable for occupation due to the harsh climate, poor vegetation cover and an associated decrease in animal populations, while occupants at the lower altitude sites would rely more heavily on microtopographical factors including aspect (Carter, 1976; Mitchell, 1995; Plug, 1997; Mitchell et al., 1998). Under warmer conditions, the higher altitude sites could be re-occupied, and lower altitude sites would become more permanently occupied (Mitchell, 1995). This selective use of eastern Lesotho shelters by Stone Age communities based on their climatic suitability, results in pulses of occupation in the archaeological record (Carter, 1976; Mitchell, 1992; *Table 2.1*). These occupation pulses can be associated more closely with changes in climate in Lesotho, than is possible at lower altitude sites, where climates are tolerable and resources are available even during cold or dry periods (Carter, 1976; Mitchell, 1992, 1995; Stewart et al., 2012). Inferences on climate change can thus be made from evidence on the timing and duration of occupation pulses at Stone Age sites in the eastern Lesotho highlands (Carter, 1976; Mitchell, 1995). Due to the scarcity of palaeoenvironmental reconstructions for the region, these climate inferences from the archaeological record provide a valuable resource.

Table 2.1: Known periods of occupation at Stone Age sites in Lesotho.

Author	Year	Site	Figure reference	Occupation Periods
Mitchell et al.	1994	Hololo	2.5:25	AD 1660 (cal.) AD 1640 (cal.)
Mitchell et al.	1994	Bohlahla	2.5:16	AD 1885-1914 (cal.) AD 1179 (cal.)
Mitchell et al.	1994	Tloutle	2.5:20	AD 1272-1305 (cal.) AD 1446-1638 (cal.)
Esterhuysen & Mitchell	1996	Ha Makotoko	2.5:21	10,000-8,370 yr BP
Esterhuysen & Mitchell	1996	Ntloana Tsoana	2.5:22	12,100-8,780 yr BP
Esterhuysen & Mitchell	1996	Tloutle	2.5:20	9,000-5,000 yr BP
Mitchell	1996a	Sehonghong	2.5:13	~6,000 yr BP ~7,000 yr BP ~10,000 yr BP ~ 11,000 yr BP ~12,000-12,500 yr BP ~20,000 yr BP ~25,000 yr BP
Mitchell	1996b	Sehonghong	2.5:13	AD 850-1870 (cal.)
Mitchell et al.	1998	Sehonghong	2.5:13	12,500-12,000 yr BP ~11,000 yr BP 9,800-9,300 yr BP
Mitchell et al.	2011	Likoaeng	2.5:12	1700-1000 BC (cal.) 1000-200 BC (cal.) AD 100 BC-250 (cal.) AD 800-899 (cal.)
Parker	2011	Likoaeng	2.5:12	>3,380-2,860 cal. yr BP 2,860-2,440 cal. yr BP 2,510-2,150 cal. yr BP 2,070-1,600 cal. yr BP 1,260-1,070 cal. yr BP
Stewart et al.	2012	Melikane	2.5: 15	~80,000 cal. yr BP ~60,000 cal. yr BP ~50,000 cal. yr BP ~46,000-38,000 cal. yr BP ~24,000 cal. yr BP ~9,000 cal. yr BP ~3,000 cal. yr BP ~1,800 cal. yr BP
Roberts et al.	2013	Ntloana Tsoana	2.5:22	~61,000 cal. yr BP 57,000 cal. yr BP 14,200-9,600 cal. yr BP

Archaeological work in eastern Lesotho experienced a relatively late inception, resulting from problems endemic to field-based research in the region: difficulty in accessing sites due to the high altitude, deeply dissected landscape, and a lack of institutional knowledge (Mitchell, 1992; Arthur et al., 2011). The first significant contribution to an understanding of Stone Age occupation in the eastern Lesotho highlands was made by Carter (1970, 1976), with a specific aim of understanding occupation patterns resulting from changes in the

natural environment, driven by climate change (Carter, 1976; Mitchell, 1992; Mitchell et al., 1998). While some aspects of the methodology have been critiqued, this work importantly confirmed that occupation stretched back to the Early Stone Age, and that the highlands did not represent an enclave only recently inhabited, but rather that occupation over this time period was highly pulsed (Mitchell, 1992, 1996; Cain, 2009). Carter's work also hypothesised that the occupational pulses detected for sites across Lesotho did not reflect periods of permanent occupation, but rather that these sites were occupied seasonally, many only in spring and summer, with a set of sites at lower altitude or improved aspect being used in winter (Carter, 1976; Mitchell, 1992). The development of the Southern Perimeter Road and the Lesotho Highlands Water Scheme initiated a more intensive developer-funded archaeological effort in the region from the late 1980s (Mitchell et al., 1994; Arthur et al., 2011). This included further work on the timing and seasonal patterns of human occupation in the region, based on excavations at predominantly shelter sites (cf. Carter, 1969, 1976; Mitchell, 1992, 1995, 1996; Mitchell et al., 1994, 1998; Esterhuysen & Mitchell, 1996; Stewart et al., 2012; Roberts et al., 2013), and with later work on open air sites (Plug, 1997; Plug et al., 2003, 2010; Mitchell et al., 2011; Parker et al., 2011). These studies have largely supported the initial findings and inferences of Carter, while improving the resolution of detail. The environmental inferences from these studies are explored in this section, beginning with long-term patterns of occupation and absence at these sites, followed by evidence for the seasonal occupation of sites, and finally evidence of human influence on the environment. A small body of archaeological work undertaken in the region has analysed palaeoecological proxies for the periods of settlement (cf. Esterhuysen & Mitchell, 1996; Parker et al., 2011; Roberts et al., 2013). This will be discussed predominantly under the palaeoecological section to follow.

It has been posited that Stone Age settlement in the eastern Lesotho highlands would occur under two dominant environmental conditions: first, arid conditions that would force people into the moist highlands in search of water and surviving plants and animals (Plug & Mitchell, 2008; Stewart et al., 2012; Roberts et al., 2013); second, temperatures warm enough to support a varied vegetation and consequent range of animals, and to prevent extensive snow cover (Carter, 1976; Plug, 1997; Mitchell et al., 1998; Stewart et al., 2012). These conditions could occur simultaneously, with temperature and precipitation being

interconnected. With limited capacity for improved warmth, settlement under arid cold conditions could not occur at the highest altitudes as temperatures would be intolerably cold, preventing plant growth and deterring animals; warm conditions would only attract settlement if it were sufficiently warm, with enough moisture, to support a varied ecology (Carter, 1976; Mitchell, 1995, 1996; Plug, 1997). Pulsed occupation throughout the Pleistocene and Holocene has commonly been observed for archaeological sites across Lesotho, and for many the periods of absence are greater than those of occupation (Carter, 1976; Mitchell, 1996a; Plug, 1997; Stewart et al., 2012). For the highest altitude sites, such as Belleview (Figure 2.5:9), Moshebi's Shelter (Figure 2.5:11) and Ha Soloja (Figure 2.5:10), occupation ceases at known periods of particularly cold conditions, most recently during the LGM (Mitchell, 1992, 1995; Plug et al., 2003). Occupation resumes during warm periods, as is most clearly noted for Likoaeng (Mitchell, 1992, 1995; Plug et al., 2003; Mitchell et al., 2011). For lower altitude sites, including Sehonghong (Figure 2.5:13) and Melikane (Figure 2.5:15), there remains evidence of occupation throughout very cold periods including the LGM, although it is suggested that this evidence of occupation reflects visits of short-duration for the purposes of hunting (Mitchell, 1995). While it would appear that occupation has been more intensive and of longer duration at most sites in Lesotho since the mid-Holocene (Plug, 1997), notably, there are no clear overlaps in periods of occupation or absence amongst the eastern Lesotho sites, nor for the broader southern African sites (Mitchell, 1996b; *Table 2.1*). Therefore, first, the microclimate and microtopography of the settlement is important (Mitchell, 1995). Second, a far greater set of influencing factors are likely to be responsible for the selection of sites and timing of occupation than climate and associated environment alone (Plug, 1997). Third, these pulses of occupation may critically involve seasonal movements between sites both within Lesotho, and farther afield (Carter, 1976; Mitchell, 1995). Carter's early environmental inferences from the occupation pulses were supported by radiocarbon dates for peat formation and increased spring activity indicative of wetter periods, while rock falls were considered as evidence for cold periods (Carter, 1976). More recent verification of environmental signals has included the use of phytoliths (Mitchell et al., 2011), faunal remains (Plug et al., 2003, 2010), geochemistry (Stewart et al., 2011) and stable isotopes (Roberts et al., 2013).

Carter (1976) originally suggested that evidence of occupation at sites in Lesotho may only reflect periods of a seasonal duration, and that movements between two or more sites may have occurred during annual periods. This hypothesis was supported by observations of seasonal movements between eastern Lesotho and low altitude sites in KwaZulu-Natal in the late 19th century, with the highest altitude or coldest site being used in spring and summer but a warmer site used in winter each year (Carter et al., 1988; Mitchell, 1995). Patterns of seasonal occupation across a range of sites with varied climates explains continuous evidence for human occupation in Lesotho over long time periods, particularly throughout known cold periods (Mitchell, 1992, 1995). There are three key examples of seasonal occupation shifts in eastern Lesotho: Sehonghong and Melikane (Carter, 1976; Mitchell, 1995); Belleview and lower altitude sites in KwaZulu-Natal (Carter, 1976); and Likoaeng (Figure 2.5:12; Plug et al., 2010; Mitchell et al., 2011). Sehonghong and Melikane are both situated on the Senqu/Orange River, but Sehonghong has a considerably colder climate as it is west facing, compared to north-facing Melikane (Carter et al., 1988; Mitchell, 1992). The synchronous dates of occupation at the two sites suggests that people migrated seasonally between the two, using Sehonghong in summer and Melikane in the colder winter months during interglacial periods (Mitchell, 1995), while during the LGM it is likely that both sites were used only briefly in summer (Mitchell, 1996a). This seasonal pattern of use is supported by evidence of fish, flower heads and grasses found at Sehonghong, but not at Melikane, indicating preferential occupation of this site in spring (Carter et al., 1988; Mitchell, 1992, 1995). At the higher altitude sites on the eastern escarpment, including Belleview, Moshebi's Shelter and Ha Soloja, a different system of seasonal movement appears to have occurred, across far greater distances, covering a transect from the eastern Lesotho highlands to the KwaZulu-Natal lowlands (Carter, 1970; Mitchell, 1992). The high altitude Lesotho sites would have been used only briefly in summer, with movement through the mist-belt and tall-grassveld of KwaZulu-Natal, and coast-wards to the thornveld during winter months (Carter, 1970, 1976; Mitchell, 1992). The larger distances to be travelled and more extreme cold temperatures at the escarpment sites explain the complete abandonment of high altitude sites during the LGM (Carter, 1976; Mitchell, 1996a; Mitchell et al., 1998). It remains unexplained by archaeologists, however, why these communities would not have remained in the thornveld year-round, as there appeared to have been sufficient resource availability and suitable environmental conditions (Mitchell,

1996a), but this may relate to increased risks from animals, pests and vector borne diseases during summer months (Blaylock, 2004; Craig et al., 2004).

Likoaeng is one of the few open-air sites in Lesotho for which archaeological records have been reported, with remains of mammals, birds, reptiles and molluscs, demonstrating a shift from hunting to fishing at the site at ~4,000 cal. yr BP (Plug et al., 2003; Parker et al., 2011). Higher resolution seasonal occupation is evident from Likoaeng, where fish bones provide evidence of deliberate occupation of a site timed by recurrent biological events (Plug et al., 2003, 2010; Mitchell et al., 2011; Parker et al., 2011). The late Holocene deposits at this site are dominated by large numbers of fish bones (1.3 million counted), suggesting that the site was occupied specifically to intercept the spawning runs (Mitchell et al., 2011). The species of fish from these deposits demonstrated a marked shift in dominance from the smallmouth yellowfish (*Labeobarbus aeneus*) to the Orange River mudfish (*Labeo capensis*) over time, with the Orange River mudfish accounting for the majority of fish bones after 560 cal. yr BP (Plug et al., 2010). Notably, these fish have different spawning times, centred in mid-summer for the smallmouth yellowfish and early spring for Orange River mudfish (Plug et al., 2010). This means that the timing of occupation of Likoaeng was not only based on a highly predictable phenological event, but that they made a preference for different spawning groups based most likely on the availability of food elsewhere (Plug et al., 2010; Mitchell et al., 2011). The shift to spring-spawning fish is therefore indicative of a food shortage in other regions at the end of winter (Mitchell et al., 2011). It is of further interest that once occupation had shifted to early spring, only those fish were consumed, indicating that they did not remain at the site for the summer-spawning smallmouth yellowfish, suggesting that the site was only ever used for short periods (Plug et al., 2010). It was thus hypothesised that Likoaeng may have been a third stop in the seasonal movement between Sehonghong and Melikane (Mitchell et al., 2011). Over longer time periods, occupation at Likoaeng appears to have been interrupted primarily by periods of flooding, rather than changes in temperature or snowfall (Mitchell et al., 2011).

Archaeological evidence of human occupation in Lesotho during the late Holocene can also provide information on more recent, non-climate driven environmental change that occurred due to increasing anthropogenic stress on the environment (Plug, 1997). Faunal

records from Likoaeng indicate the first introduction of domesticated animals into the region, including sheep, at 1285 ± 40 cal. yr BP (Plug et al., 2003; Parker et al., 2011). Evidence from Likoaeng also indicates a reduction in fish size, posited to have occurred due to the introduction of rainbow trout into the river, which together with increased sedimentation, reduced the competitive advantage of these endemic species (Mitchell et al., 2011). Charcoal records from western Lesotho indicate the late Holocene introduction of species more commonly observed at the site today, including weed-invasive firewoods (Esterhuysen & Mitchell, 1996). While such evidence of anthropogenic environmental change is common for lower altitude sites (*Section 2.2.3*), the human impact on Lesotho remains more limited.

The palaeoenvironmental significance of these occupation pulses identified in the archaeological record, together with evidence of seasonal movement between sites, implies that an ameliorating climate would have been necessary for these Stone Age occupants of high altitude sites to survive (Mitchell, 1996a). Although it seems reasonable that these occupation pulses and seasonal movements were driven predominantly by climatic changes in the eastern Lesotho highlands, it is impossible to quantify the extent of any climatic influence, or to account for all non-environmental drivers (Humphreys, 1987; Mitchell, 1996a). Social interactions between different communities and changes in food and landscape preference could alter settlement patterns and occupation pulses entirely, independent of changes in climate and vegetation (Plug, 1997; Plug et al., 2010; Roberts et al., 2013). Where settlement location and consequent occupation pulses were driven by climate changes, it is difficult to determine whether these were shifts in temperature, precipitation or both (Carter, 1976; Roberts et al., 2013). As already outlined, it is posited that occupation in the eastern Lesotho highlands would occur during warmer periods when temperatures are tolerable and promote diversity in plants and animals, or during periods of drought when the moisture available in the highlands was a valuable and necessary resource, surpassing the detriments of having to endure the cold (Carter, 1976; Mitchell, 1995; Roberts et al., 2013). For most of the sites there is insufficient evidence to interpret independently the dominant drivers at any point in time, and thus many of the climate inferences based on occupation cycles are dependent on palaeoclimatic information from the site or from elsewhere in southern Africa (Carter, 1976; Mitchell et al., 2011).

Consequently, there have been continued calls (Mitchell, 1996a) and recent efforts made to extract palaeobotanical climate proxies including charcoal, faunal remains, phytoliths and stable isotopes from material recovered from archaeological excavations in the region, the results of which are examined in *Section 2.3.3.*

2.3.2 The Palaeogeomorphological Record

The eastern Lesotho highlands host an impressive array of glacial and periglacial geomorphic features, that developed during cold periods as recent as the Little Ice Age, extending to the LGM, and even earlier glaciations over hundreds of thousands of years (Grab, 2000, 2002a; Boelhouwers & Meiklejohn, 2002; Grab & Mills, 2011). The sustained cold temperatures in interglacial periods, and resultant scarcity of vegetation and human influence, have preserved many of these features, such that their positive identification can provide evidence for the cold events which produced them (Grab, 1996a). As these features in the eastern Lesotho highlands are relatively unique in southern Africa, they have attracted considerable research focus over recent decades (Grab, 1996a; Boelhouwers & Meiklejohn, 2002). However, much of the feature identification and their associated palaeoenvironmental and palaeoclimatic inferences has been contentious (Grab, 1999; Boelhouwers & Meiklejohn, 2002; Mills et al., 2009b). These issues are increasingly addressed through improved scientific rigour, facilitating the use of these palaeogeomorphological features in elucidating information on the coldest periods in southern Africa's Quaternary history, for a region where little supporting palaeoenvironmental evidence exists (Boelhouwers & Meiklejohn, 2002; Hall, 2010).

The most contentious palaeogeomorphologic features in eastern Lesotho are those interpreted to be of glacial origin (Sparrow, 1967; Harper, 1969; Boelhouwers & Meiklejohn, 2002; Hall, 2010). Many critiques of such glacial interpretations arise from the predominantly qualitative approach utilised, and difficulties in positive identification and age-dating of these features (Boelhouwers & Meiklejohn, 2002). A more scientifically rigorous approach to method and interpretation was adopted in the analysis of small moraines in high altitude south-facing slopes, providing robust evidence for their glacial origin (Mills & Grab, 2005; Mills et al., 2009a,b; Hall, 2010). Moraine-like features were identified on the south-facing slopes of the Tsatsa-La-Mangaung (Figure 2.5:5; Mills & Grab,

2005), Leqooa (Figure 2.5:8; Mills et al., 2009a) and Sekhokong Mountain Ranges (Figure 2.5:7; Mills et al., 2009b). Various possible origins of the landforms were considered, including mass movement, fluvial processes, nivation, and weathering processes for debris production (Mills & Grab, 2005; Mills et al., 2009b; Hall, 2010). From these studies, evidence was presented for niche glaciation, dated to the LGM (Mills & Grab, 2005; Mills et al., 2009a,b). While the accuracy of the term 'niche glaciation' has been queried (Hall, 2010), the evidence from these moraines for small-scale, spatially restricted glaciers during the LGM remains undisputed to date.

Evidence of contemporary and relict periglacial features in the eastern Lesotho highlands is more widely accepted (Butzer, 1973; Roqvist, 1990; Boelhouwers & Meiklejohn, 2002; Boelhouwers et al., 2002). Periglacial environments are defined as a "wide range of cold, non-glacial conditions, regardless of their proximity to a glacier, either in time or space" (French, 1996, p. 3). The eastern Lesotho highlands are described as a marginal periglacial environment (Hanvey & Marker, 1992; Boelhouwers, 1994; Grab, 2002c), with contemporary periglacial geomorphological features still developing due to ongoing seasonal and diurnal frost action (Grab, 1996b, 2005). Landforms include thufur (Harper, 1969; Sparrow, 1971; Grab, 2005), alpine turf exfoliation pans (Grab, 2010), needle ice mounds (Grab, 2002c), and miniature sorted patterned ground (Grab, 1996a). Inactive periglacial landforms dating back to colder periods are generally larger in scale than their contemporary counterparts, formed through more prolonged periods of sub-zero ground and air temperatures (Grab, 2002a; Grab et al. 2012), and include small pronival ramparts (Grab & Mills, 2011), large sorted patterned ground (Boelhouwers, 1994; Grab, 2002a; Sumner, 2004a), stone-banked lobes (Grab, 2000), blockfields and blockstreams (Grab, 1999; Boelhouwers et al., 2002; Sumner, 2004b). Similar to the contested glacial evidence, greater insolation on north-facing slopes requires that the majority of such features are situated on south-facing slopes (Grab, 1999, 2000; Boelhouwers, 2003; Sumner, 2004a,b). The larger relict periglacial features could indicate the existence of permafrost during their genesis, most likely during the LGM, albeit localised and formed over a short, discontinuous duration (Grab, 2002a).

All of these palaeo-periglacial phenomena indicate colder conditions than at present, with the size of the feature and possible genesis providing possible indications as to the magnitude of the temperature depression (Grab, 2002a; Grab et al., 2012; Mills et al., 2012). Palaeoenvironmental interpretations of the associated precipitation levels during these cold periods, however, are conflicting (Hanvey & Marker, 1992; Boelhouwers & Meiklejohn, 2002; Mills et al., 2009a; Grab et al., 2012). Boelhouwers and Meiklejohn (2002) suggested that depositional periglacial features, including large patterned ground, solifluction mantles and blockstreams were indicative of dry, cold conditions at the time of formation, while erosional features would be indicative of wetter conditions during cold periods. Openwork block accumulations identified near Thabana Ntlenyana (Figure 2.5:4) support this hypothesis, as they arguably require minimal snow cover for development, requiring lower precipitation than at present (Sumner, 2004b). Evidence of a blockstream near Sani Pass (Figure 2.5:6) was inferred to have developed under conditions of lower snowfall, but required moister conditions than at present (Boelhouwers et al., 2002). Depositional features indicative of periglacial conditions, including large sorted patterned ground near Mafadi Summit (Figure 2.5:1) and Thabana Ntlenyana, and pronival ramparts at Thabana Ntlenyana, imply wet conditions during their formation (Grab, 2002a; Grab & Mills, 2011). In addition, small glaciers would have required greater snow cover, implying an increase in precipitation, at least throughout winter months, during the LGM (Sparrow, 1967; Mills & Grab, 2005; Mills et al., 2009a,b). The uncertain moisture inferences from periglacial features, derives from the relationship between temperature and moisture in developing these features: temperature influences the percentage of precipitation falling as snow, while the moisture levels control the maximum potential precipitation (Mills et al., 2012). Using glacier reconstructions from five sites in the eastern Lesotho highlands to calculate Equilibrium Line Altitudes, climate models indicate a shift in the timing of precipitation to the cold-season resulting in a 28% increase in solid precipitation (Mills et al., 2012). For such glacial moraines to have developed without an increase in precipitation, a temperature depression of at least 8°C would have been required in order for the total annual precipitation to fall exclusively as snow (Mills et al., 2012). Such a temperature decrease is not only inconsistent with proxy data for the lower-altitude regions of southern Africa, but would have resulted in considerable permafrost, for which there remains insufficient evidence (Sumner, 2004a,b; Mills et al., 2012). Evidence from periglacial and glacial features

from the eastern Lesotho highlands, combined with climate modelling, suggests a temperature depression of 5-6°C (Boelhouwers et al, 2002; Grab, 2002a; Mills et al., 2009a,b, 2012), and an increase in aseasonal precipitation during the LGM, driven by a shift in the position of the westerlies (Mills & Grab, 2005; Mills et al., 2009a,b, 2012). While many of the relict periglacial features are assumed to originate during the LGM, it should be noted that stone banked lobes on higher summits above 3,300m.asl are believed to have formed during a cold neoglacial period (Grab, 2002a), and pronival ramparts dated to AD 300-1000 (Grab & Mills, 2011), are similarly indicative of moist cold periods.

Where archaeological work provides information for discrete pulsed events during which the climate was sufficiently warm to encourage human occupation, geomorphological features provide evidence for single discrete cold events. The restricted climatic requirements for the formation of these features, can facilitate improved quantification of climatic change during these cold periods (Grab, 2002a; Mills et al., 2012). The continued debates in the literature concerning these cold-climate geomorphic features highlight many unresolved uncertainties as to their identification, processes, and environmental drivers, with an over-reliance on Northern Hemisphere analogues (Grab & Hall, 1996; Boelhouwers et al., 2002; Hall, 2010, 2012; Knight, 2012). The identification of features may become increasingly difficult to address as landscape disturbance increases as a consequence of greater human and livestock pressure in the region (Grab, 1996a; Grab & Nüsser, 2001). Temporal constraint for the period of landform formation is critical if such debates are ever to be adequately resolved, yet age-dating remains a challenge due to an absence of datable material (Boelhouwers & Meiklejohn, 2002; Mills, 2006) and the large costs involved (Mills, 2006). Age-dates obtained for pronival ramparts and moraines have confirmed the timing of development of these features, and improved the potential for palaeoenvironmental inferences made from these features (Mills & Grab, 2005; Mills et al., 2009a,b, 2012). As is the case with archaeological evidence, long-term continuous palaeoenvironmental reconstructions, based on proxy data, would be of benefit to improve the palaeoclimatic inferences made from geomorphic features (Boelhouwers & Meiklejohn, 2002; Mills et al., 2012). This could be achieved through the provision of corroborating environmental evidence, and in filling the large temporal gaps between cold periods reflected by these

features (Boelhouwers et al., 2002; Boelhouwers & Meiklejohn, 2002; Mills et al., 2009, 2012).

2.3.3. The Palaeoenvironmental Record: Proxy Evidence

Despite repeated calls for detailed continuous palaeoenvironmental records to be investigated from the bogs of eastern Lesotho, such research remains limited (Mitchell, 1996a; Mitchell et al., 1998; Grab et al., 2005). The only fossil pollen palaeoenvironmental reconstruction for the eastern Lesotho highlands (Van Zinderen Bakker, 1955) is limited by an absence of age-dates, poor resolution of sampling, and no information on the location of the site. Fluctuations in Holocene climate have been reconstructed on the basis of sedimentary sequences in eastern Lesotho (Marker, 1994, 1995, 1998), but without environmental proxies the environmental inferences made remain speculative (Grab et al., 2005). The majority of studies that have explored changes in palaeoenvironmental proxies over time are from the western Lesotho lowlands (Esterhuysen & Mitchell, 1996; Grab et al., 2005; Roberts et al., 2013). Many of these studies rely on material from archaeological excavations, which, while of value in constraining the climatic and environmental conditions during occupation, do not reflect the conditions during periods of absence (Roberts et al., 2013). Archaeological material is further compromised by human bias in the material brought to shelters, often not directly reflecting the broader spectrum of vegetation of the environment but rather preferences for fuel, food and bedding material (Esterhuysen & Mitchell, 1996; Parker et al., 2011). The results of the published proxy-based environmental reconstructions for eastern and western Lesotho are presented, with commentary on their value in determining the climatic and environmental change of Lesotho during the late Quaternary.

As part of a broader, preliminary study of the wetlands in eastern Lesotho, Van Zinderen Bakker (1955) presents results of pollen from a sediment profile 90-100cm in length, extracted from an unidentified wetland. The primary findings of the pollen analysis reflect a shift from Cyperaceae dominated samples at the bottom of the profile to a proportion of Poaceae (Gramineae) near the top, argued to represent a regional decrease in moisture over the period represented by the profile (Van Zinderen Bakker, 1955). In addition to Poaceae and Cyperaceae pollen, Asteraceae (Compositae) pollen is noted throughout the

profile, but any environmental significance is dismissed as the pollen grains are argued to be exclusively insect-transported (Van Zinderen Bakker, 1955). Occasional presence of *Podocarpus* pollen is noted, but inferred to be transported by wind from temperate forests in the lower-altitude KwaZulu-Natal Drakensberg. The period during which the regional drying would have occurred, and the timing of the *Podocarpus* pollen intrusion, remains unclear due to the absence of an age-dated chronology. In a later, more detailed, vegetation analysis for the eastern Lesotho bogs, Van Zinderen Bakker and Werger (1974) present a basal date for a peat bog in eastern Lesotho of 8,020 ±80 yr BP, which could potentially be related to this profile, but due to a lack of site details for either study, is impossible to confirm. This was, however, preliminary work in the region that no doubt was intended to be followed up by a wealth of future studies given the availability of well-preserved pollen and diatoms (Van Zinderen Bakker, 1955).

Sedimentary sequences with alternating layers of organic rich clays, peat, and gravels, exposed by extensive gullying at Sani Top (Sekhokong) and Tlaeeng (Figure 2.5:26) were investigated for palaeoclimatic signals (Marker, 1994, 1995, 1998). Interpreting the sequence to represent dry periods through the layers of orange-coloured gravels, and wet periods for the organic rich clay and peat layers, a chronology of precipitation fluctuations for the eastern Lesotho region was developed, constrained by radiocarbon dates (Marker, 1995, 1998). The profile suggested cold conditions prior to 13,500 yr BP, a warm and wet period from 13,500-9,000 yr BP, drier and potentially colder conditions from 9,000-5,000 yr BP, and warmer wet conditions from 5,000-1,000 yr BP (Marker, 1998). The methodology requires critical review, as the samples were not pre-dried, and organic material was determined by burning the samples at only 105°C rather than the standard 550°C (Heiri et al., 2001), which accounts for results of percentage organic content that were, by Marker's own admission, exceptionally high (Marker, 1994). Nonetheless, distinct differences in colour and texture between the gravels and organic-rich sediments are recorded (Marker, 1994, 1995). With the profile temporally constrained through the provision of valuable age-dates for sedimentation in the region, the additional analysis of the contrasting sediment types provides some understanding of Holocene precipitation changes in the eastern Lesotho highlands. The analysis of additional proxy data from the sequence would have had

the potential to confirm the climatic inferences and provide information on concurrent environmental changes (Grab et al., 2005).

The third study deliberately aimed at reconstructing the palaeoenvironment of Lesotho was undertaken on a 13m deep gully sidewall in the Tsoaing River Basin (Figure 2.5:18), western Lesotho (Grab et al., 2005). Pollen and phytoliths were extracted for analysis from nine distinct sedimentary layers within the sequence, with dates ranging from 12,000-4,000 cal. yr BP (Grab et al., 2005). Insufficient pollen was available for counting, with representative samples only for the bottom two layers of the sequence, possibly indicating oxidation under seasonal dry conditions, unsuitable to pollen preservation, for the remaining layers (Grab et al., 2005). The environmental reconstruction was therefore made primarily from the phytolith data, indicating a rapid transition to dry conditions from 8,600-8,450 cal. yr BP, with wetter conditions by 7,000 cal. yr BP and again after 4,500 cal. yr BP (Grab et al., 2005). The absence of pollen for much of the sequence, the limited information available from the phytoliths, and the low sampling resolution, restricts the value of this work in developing a robust palaeoenvironmental chronology.

The analysis of environmental proxies from sediments excavated from archaeological sites provides further palaeoenvironmental information for Lesotho (Esterhuysen & Mitchell, 1996; Smith et al., 2002; Parker et al., 2011; Roberts et al., 2013). Holocene charcoal assemblages were analysed from archaeological excavations at three shelters on a tributary of the Caledon River in western Lesotho: Tloutle (Figure 2.5:20), Ha Makotoko (Figure 2.5:21) and Ntloana Tsoana (Figure 2.5:22; Esterhuysen & Mitchell, 1996; Esterhuysen et al., 1999). Considerable differences in species composition were noted between Tloutle, located closer to the river, and Ha Makotoko and Ntloana Tsoana throughout the periods of occupation, highlighting the influence of microclimates within small geographic areas in Lesotho (Esterhuysen & Mitchell, 1996). Ha Makotoko and Ntloana Tsoana had charcoal evidence of species well adapted to cold and drought, including *Protea sp.*, *Leucosidea sericea*, *Rhamnus prinoides*, *Rhus sp*, *Passerina montana* and *Erica sp*, while the species composition from Tloutle was indicative of more mesic woodland, including high percentages of *Olea africana, Celtis africana*, *Maytenus heterophylla*, *Rhus sp*. and small percentages of *Podocarpus* (Esterhusyen & Mitchell, 1996). Examining changes throughout

the periods of occupation, two mesic periods were identified by the appearance of *Podocarpus* charcoal: the first was centred at 8,700 yr BP, possibly the result of a continued increase in moisture from 10,000 yr BP; the second, from 6,900-5,000 cal. yr BP, reflected an even wetter period (Esterhuysen & Mitchell, 1996; Esterhuysen et al., 1999). These wet periods were separated by dry conditions, characterised by the appearance of *Euphorbia sp*. and increases in charcoal from *Buddleia sp*. and *Passerina montana* (Esterhusyen & Mitchell, 1996).

Analyses of stable carbon and oxygen isotopes from ungulates, and stable carbon isotopes from organic material provides further palaeoenvironmental evidence for these three sites (Smith et al., 2002; Roberts et al., 2013). The isotopic values for herbivores reflect the proportion of C_3:C_4 vegetation consumed, from which the vegetation balance at the site can be inferred (Smith et al., 2002). Evidence for the three Caledon River sites within Lesotho indicate a progressive warming from 16,000-6,000 cal. yr BP, marked by considerable fluctuations, notably including periods sufficiently cool to encourage the growth of C_3 plants, from 16,000-14,000 cal. yr BP, 10,200-9,600 cal. yr BP, and 8,400-8,000 cal. yr BP (Smith et al., 2002). A more recent study of stable carbon isotopes provides further environmental proxy data for Ntloana Tsoana and Tloutle, for the period spanning the Pleistocene-Holocene transition (Roberts et al., 2013). The $\delta^{13}C$ values are distinct for C_3 and C_4 plants, and the ratio of C_3:C_4 plants is related to temperature, which in Lesotho is altitudinally constrained, with C_3 plants found largely in the cold high altitude regions, and C_4 plants predominating in the warmer lowlands (Roberts et al., 2013). Isotope analysis confirms predominantly C_3 vegetation during the LGM, followed by a progressive increase in the proportion of C_4 plants (Roberts et al., 2013). Within this period of overall warming, the Pleistocene-Holocene transition was marked by rapid temperature fluctuations of as much as 4°C from 11,200-9,500 cal. yr BP, with at least three cycles of warming and cooling reflected in the carbon isotope record (Roberts et al., 2013). More stable, warm conditions were attained by 9,500 cal. yr BP (Roberts et al., 2013). In addition to providing valuable proxy evidence for the period preceding the charcoal record reported by Esterhuysen and Mitchell (1996), this record notably demonstrates the existence of very cold periods and extreme climatic fluctuations during longer periods of occupation, which, without proxy data, would have assumed to reflect continuous moderate conditions (Roberts et al., 2013).

Caution must be used when interpreting environmental proxy data from archaeological sites, particularly in the case of shelters, as the species composition depends on what people selectively brought into the shelter (Esterhuysen & Mitchell, 1996). Depending on the intended use of the plant material, biases may exist, and species that were common in the area may not appear at all (Esterhuysen & Mitchell, 1996).

Evidence of environmental and climate change at Likoaeng open air shelter is derived from phytoliths and stable carbon isotopes, from a 3m stratified sequence, spanning periods of both occupation and absence over the period 3,400-1,070 cal. yr BP (Parker et al., 2011). Results suggest a warm period dominated by C_4 Panicoid and Chloridoid types from the beginning of the sequence to 2,960 cal. yr BP (Parker et al., 2011). This is followed by an abrupt neoglacial cooling period from 2,960-2,160 cal. yr BP, dominated by C_3 Pooid grassland, with the presence of *Erica* and *Euryops sp* (Parker et al., 2011). Thereafter, the environment is characterised by a mixture of C_3 and C_4 species, until 1600 cal. BP, followed by a return to the original environment dominated by C_4 Panicoid and Chloridoid (Parker, 2011). This proxy evidence complements findings on occupation pulses at the site based on mammal and fish remains (Plug et al., 2003, 2010; Mitchell et al., 2011), and while occupational hiatuses at the site resulted from flooding rather than unsuitable temperatures, unlike most archaeologically derived environmental reconstructions, the record spans both occupation and absence (Parker, 2011).

2.3.4 Synthesis of Palaeoclimatic Change in Lesotho

Combining evidence from archaeological, geomorphological and palaeoenvironmental archives, highlights considerable variability in temperature and precipitation throughout the late Quaternary (*Figure 2.6*). While there are conflicting interpretations in the available records, these often occur where coarse-resolution long-term records do not detect the intricacies of higher resolution records spanning shorter time periods (*Figure 2.6*). Most notable is the lack of any high resolution, long-term records that can bridge the gap between these, and resolve apparent conflicts.

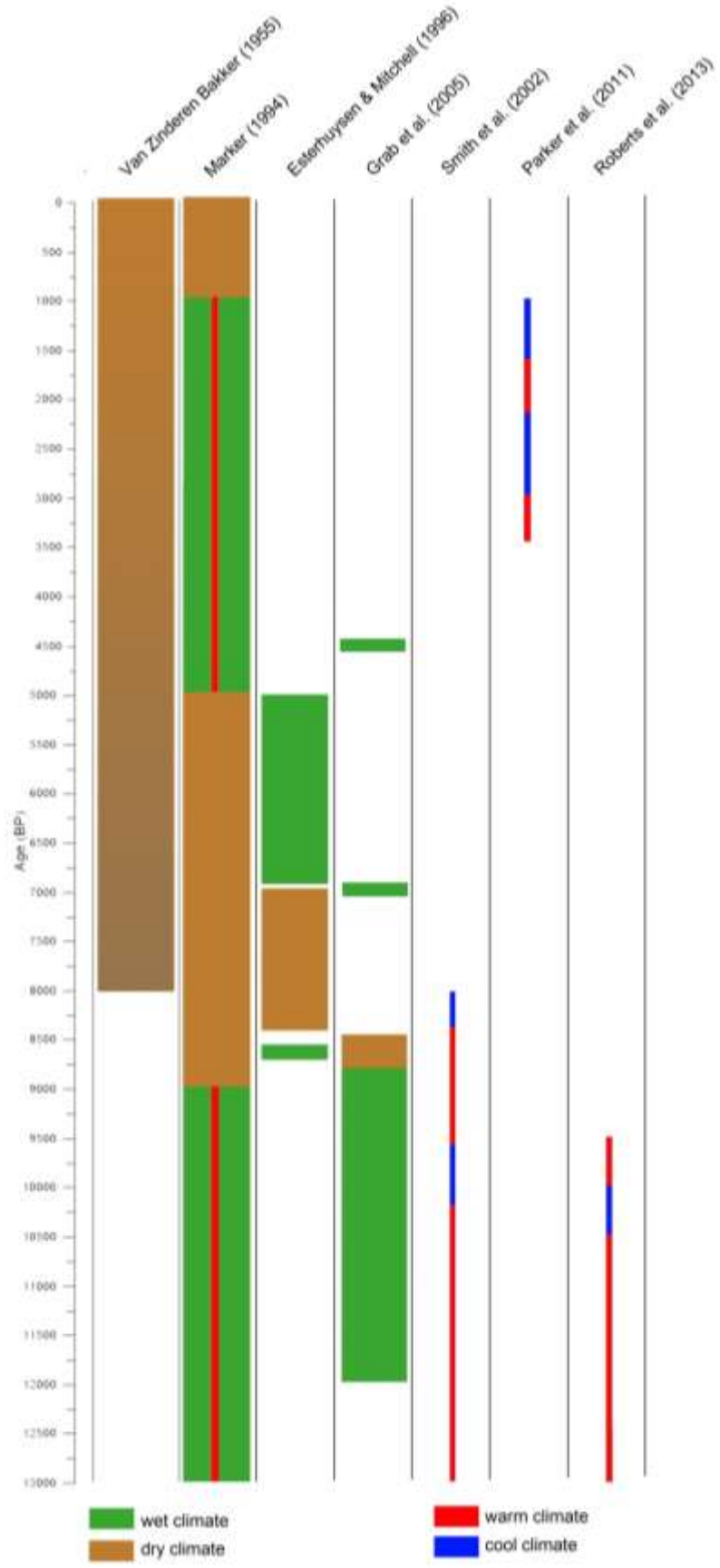


Figure 2.6: Palaeoclimatic inferences from geomorphological, archaeological and palaeoenvironmental studies from eastern Lesotho.

The reconstruction of the palaeoclimatic and palaeoenvironmental history of Lesotho relies predominantly on archaeological and geomorphologic evidence (Grab et al., 2005). Both sources of evidence are produced through pulsed events: in the case of archaeology, these are recurrent periods of usually warmer temperatures, whereas for geomorphology each feature reflects a single pulse of cold conditions (Mills et al., 2009a,b; Roberts et al., 2013). When combined, palaeogeomorphological and archaeological evidence can be used to infer the timing of both cold and warm events, however, they are collectively unable to provide a complete climatic and environmental history for the region, as the climatic extremes they represent are often short-lived, and are influenced significantly by the conditions leading into and out of the events they document (Mills & Grab, 2011; Parker et al., 2011; Roberts et al., 2013). Such evidence is also limited in that past climate changes cannot be accurately quantified, but are rather inferred from the broader characteristics. Thus, while tremendously valuable in defining these extremes, and useful in determining broad patterns of environmental change where no other data exist, these records are not of absolute value (Grab et al., 2005). A continuous, well dated palaeoecological record is thus essential for determining the nature of climate changes and the associated environment during which these extreme events took place, during the periods leading up to these events, and the smaller fluctuations between them (Mitchell, 1996a; Grab et al., 2005). Due to the complexity of the temperature-precipitation relationship in the Quaternary history of eastern Lesotho, it would be beneficial for such records to employ multiple proxies, to untangle the relative influences of these different climate influences (Roberts et al., 2013). Finally, the large differences in geomorphic features, human occupation, and present-day environments at sites within close proximity to each other, highlight distinct microclimatic differences, requiring detailed analyses across many sites (Esterhuysen and Mitchell, 1996). Only when we are able to do this will we develop a high resolution understanding of past climates at specific sites, and the palaeo-lapse rates that govern them.

2.4 Synopsis

2.4.1 Holocene Palaeoenvironmental Change in Southern Africa

Compared to the rest of the Quaternary, the Holocene has been a period of relative climate stability (Hannah, 2010; Burrough & Thomas, 2013). The period is, however, marked by fine-

resolution variability, driven by multiple controls, and with considerable regional variation, both globally and in southern Africa (Mayewski et al., 2004; Chase & Meadows, 2007; Truc et al., 2013). A broad outline of the sequence of global climatic events throughout the Holocene includes post-glacial climate amelioration, the Younger Dryas cold period, the Holocene climatic optimum, the Medieval Warm Period and Little Ice Age, and the period of anthropogenic influence (Hannah, 2010; Wanner et al., 2015). Further events detected in regionally-specific records, with questionable broader influence, include the '8.2 kyr' cold event and the African Humid Period (Alley et al., 1997; Hannah, 2010; Burrough & Thomas, 2013). The influence of a Younger Dryas cooling period and the African Humid Period in southern African proxy records is discussed in *Section 2.2.2.3,* together with the regional variability in climate during the Little Ice Age and Medieval Warm Period. The anthropogenic influence on the natural environment, and its manifestation in the proxy record, are explored in *Section 2.2.3*. The only evidence in the southern African palaeoenvironmental records for the abrupt '8.2 kyr' cold event detected in the Greenland Ice Cores for the Northern Hemisphere Atlantic (Alley et al., 1997; Alley & Ágústsdóttir, 2005), is notably from stable carbon and oxygen isotope records from western Lesotho in the Caledon River Valley (Smith et al., 2002), with recent confirmation from the De Rif hyrax midden record from the Cederberg (Chase et al., 2015b). By contrast, there is extensive evidence for the Holocene Altithermal period in southern Africa (cf. Avery, 1993; Scott, 1993; Marker, 1994, 1998; Esterhuysen & Mitchell, 1996; Partridge et al., 1999; Finch & Hill, 2008; Scott et al., 2012; Chase et al., 2013; Truc et al., 2013), although the timing and duration of this event varies between records, with potential regional similarities (Scott, 1993).

As is evident from the literature presented throughout this review, there appears to be considerable spatial and temporal variability in the reconstructed Holocene climates of southern Africa. Even within small geographic regions, with common climate seasonality, changes in the climate signal during events such as the Little Ice Age are different across space, with variations in the timing of the event, and in quantifications of the climatic conditions (Barrable et al., 1998; Chase & Meadows, 2007; Scott et al., 2012; *Figure 2.7*). This may be owing to the numerous synoptic drivers of both contemporary and past southern African climates, with changes in their strength and shifts in their regional influence over time (Mayewski et al., 2004). The dominant synoptic features central to

southern African palaeoenvironmental debates include the westerlies (Tyson & Lindesay, 1992; Chase & Meadows, 2007; Mills et al., 2012; Chase et al., 2013), tropical easterlies (Chase et al., 2015a), the position of the ITCZ (Chase & Meadows, 2007; Burrough & Thomas, 2013) and the Congo Air Boundary (Burrough and Thomas, 2013). Modelling efforts to improve the understanding of these synoptic features, paired with larger palaeoenvironmental databases, should aid in explaining some of these regional inconsistencies (Barrable et al., 1998; Chase & Meadows, 2007; Mills et al., 2012).

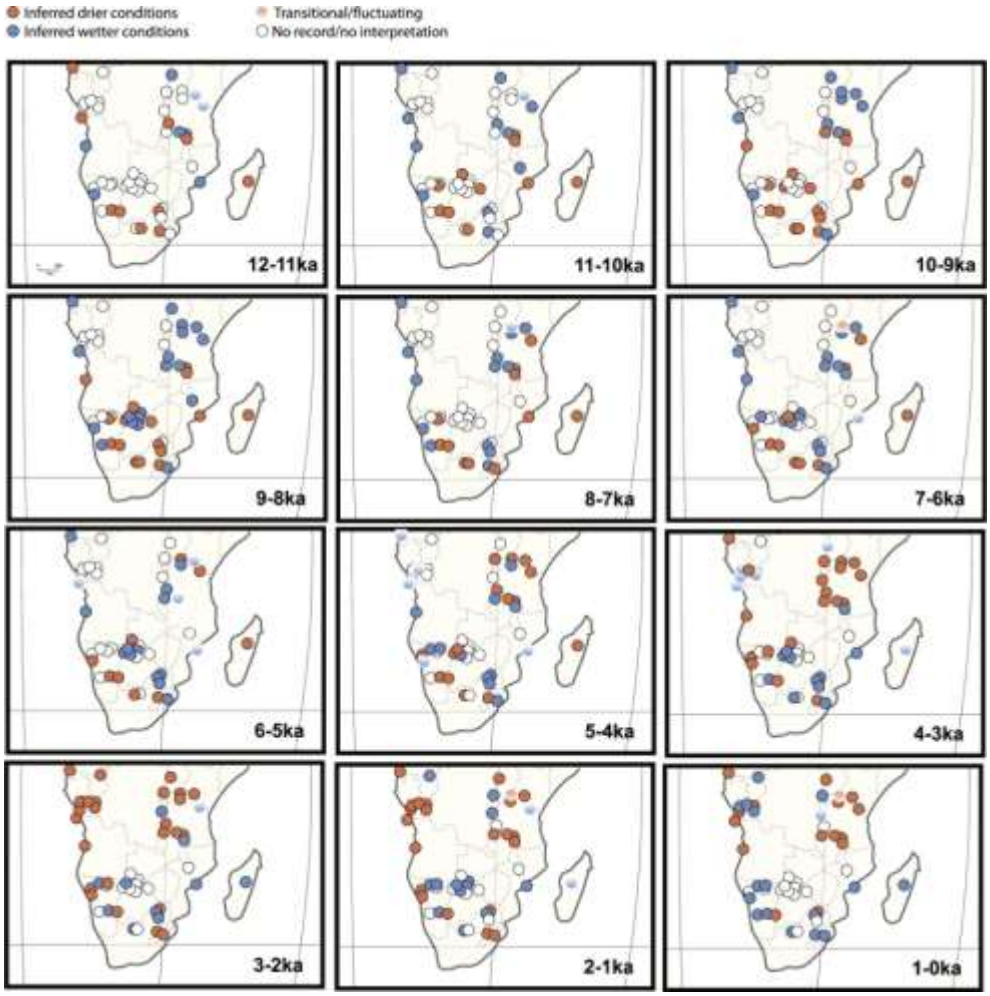


Figure 2.7: Maps demonstrating palaeoclimatic data across southern Africa for 1,000 cal. yr intervals throughout the Holocene, indicating spatial and temporal variations in climate throughout the period (Burrough & Thomas, 2013).

2.4.2 Research Gaps: Avenues for Future Work

The large variation in the palaeoclimatic histories of different regions in southern Africa highlights the importance for continued research in southern Africa (Chase & Meadows,

2007). To determine the role of climate drivers in influencing locally-specific environmental variability, and to explore the role of such fluctuations within broader regional Holocene change, a larger dataset including previously excluded regions, is essential (Mitchell, 1996a; Burrough & Thomas, 2013). Due to the demonstrated palaeo- and contemporary-climate variability within individual regions of southern Africa, it is important to not only undertake research in under-explored regions, but to understand the local topographic and environmental variability (Esterhuysen & Mitchell, 1996; Barrable et al., 1998). This can be achieved through studying palaeoenvironmental records from a range of sites within geographically small, but environmentally diverse regions (Roberts et al., 2013). To this end, the eastern Lesotho highlands present an important region for palaeoenvironmental research, as the topography promotes considerable micro-climatic and micro-environmental variability across small geographic areas (Esterhuysen & Mitchell, 1996; Mills et al., 2009a).

To improve the spatial resolution of palaeoenvironmental research in southern Africa, it is necessary to explore a broader range of archives and proxies (Scott et al., 2012). Considerable work has been undertaken using hyrax middens as an archive in regions too arid for pollen preservation in sediment sequences (Chase et al., 2012). A broader range of palaeoenvironmental proxies is also increasingly being used, as is explored in *Section 2.2.1*, facilitating the corroboration of results, and the investigation of environmental variables that were previously only coarsely inferred. These adVances in the use of new proxies and archives present invaluable opportunities to palaeoenvironmental science in the region (Meadows, 2014). It is also important to explore archives that have been identified, yet not thoroughly investigated. A much bigger focus of palaeopalynology in southern Africa has involved the re-analysis of former sites, profiles, and results to improve the temporal constraint, sampling resolution and interpretation of results (*Section 2.2.1.1*). The repeated calls for an analysis of pollen and diatoms from the high altitude bogs of eastern Lesotho (Esterhuysen & Mitchell, 1996; Mitchell, 1996a; Mitchell et al., 1998), and the problems in age-constraints, and poor proxy information and resolution of results from existing studies, highlights the significant need for further research in this region (Grab et al., 2005).

3. Regional Setting

3.1 Introduction

This study presents a Holocene palaeoenvironmental reconstruction for eastern Lesotho. As the only comparable palaeoecological study for eastern Lesotho, undertaken by Van Zinderen Bakker (1955), was not dated and did not disclose the locations of the study sites, considerable knowledge gaps remain; yet there is much potential for palaeoenvironmental research. The primary challenge in study site selection is access to remote sites in this mountainous region. The three study sites at Sani Valley, Sekhokong and Mafadi Wetland were selected, differentiated predominantly by altitude, facilitating comparisons of environmental lapse rates and an investigation of ecological resilience at high altitudes under changing climates. The justification for the selection of the three study sites, together with the field methods used at each site, appears in *Chapter 4.* What follows in this chapter is a description of contemporary geography of the Kingdom of Lesotho, and of the three selected study sites. This description is limited to the geographic features of interest to this study, and thus does not explicitly cover topics of the history, social and economic status, or cultural and religious practices in the country.

3.2 The Eastern Lesotho Highlands

3.2.1 Descriptive Geography

Lesotho is located between the co-ordinates 28°30'–30°40'S and 27°00'–29°30'E, and covers a terrestrial area of 30,355km^2 (Rydgren, 1988; Grab & Linde, 2014; *Figure 3.1*). The country is landlocked, entirely surrounded by the provinces of the Free State, KwaZulu-Natal and the Eastern Cape of the Republic of South Africa. Lesotho is classified into four main physiographic zones: the western lowlands, ranging in elevation from 1,500-1,800m.asl, the foothills ranging from 2,000-2,500m.asl, the Senqu River valley, and the eastern highlands which include elevations greater than 2,500m.asl (Smit, 1967; Schmitz & Rooyani, 1987; Grab & Linde, 2014). The eastern highlands comprise 75-80% of the total land area, but the majority of the population lives in the lowlands, where the climate, soils and topography are most suitable for agriculture (Mitchell, 1992; Ziervogel, 2004; Letšela, 2008; Grab & Linde,

2014). The lowest elevation of 1,400m.asl is located within the western lowlands at the confluence of the Orange and Makhaleng Rivers along the southwestern border with South Africa (Marake et al., 1998; Sene et al., 1998; *Figure 3.1*).



Figure 3.1: Location of the three study sites in eastern Lesotho.

The highest mountain range in southern Africa is situated in eastern Lesotho, with the highest peak (3,482m.asl) at Thabana Ntlenyana (Grab et al., 2009). The high altitude and steep slopes contribute to a set of flora and fauna markedly different from those observed for much of southern Africa. Eastern Lesotho accounts for a substantial portion of the Drakensberg Alpine Centre (DAC) – a biome listed as a centre of endemism – and thus increasing efforts have been made to protect and understand the biodiversity of the region. Consequently, a portion of eastern Lesotho has been included in the uKhahlamba Drakensberg Park, a World Heritage Site (Grab & Nüsser, 2001). However, despite 50% of

the species of plants and animals occurring only in this region, and its hosting 32 endemic birds and 11 endemic mammals, only 5% of the DAC is currently within the protected area (Zunckel, 2003; Carbutt & Edwards, 2004).

Due to the steep slopes throughout eastern Lesotho, the marginal winter climate and poor soil conditions, only 10% of the terrestrial area of Lesotho is arable (Letšela, 2008). Despite the limited amount of arable land, 76-85% of the population lives in rural areas of Lesotho, and subsistence agriculture and livestock farming form a substantial component of the livelihood of the population (Ziervogel & Calder, 2003; Bisaro et al., 2010; Mpholo et al., 2012). With the predominance of subsistence farming, the agricultural sector accounts for 60-70% of the labour force, but only 10% of the Gross Domestic Product (Gwimbi et al., 2012). The principal crops of maize, sorghum and wheat account for 85% of the cultivated area, while livestock accounts for 30% of the total agricultural output (Gwimbi et al., 2012). Livestock ownership has increased considerably over the past three decades, due to the return of former mineworkers from South Africa owing to fewer employment opportunities within the mining sector (Zunckel, 2003). Agriculture is predominantly rain-fed, with only 1% of crop production irrigated (Hydén & Sekoli, 2001; Ziervogel & Calder, 2003; FAO, 2011).

3.2.2 Geology and Geomorphology

The eastern Lesotho Drakensberg is a deeply dissected plateau, with elevations ranging from 2,290-3,484m.asl (Magill, 1987; Nüsser & Grab, 2002). All exposed and underlying rock in the eastern Lesotho Drakensberg forms part of the Karoo Supergroup (Mitchell, 1992; *Table 3.1*). This includes the Drakensberg Group flood basalts of Upper Triassic to Jurassic age, intruded by fine grained dolerite dykes, underlain by the Stormberg group of sandstone including the Clarens Formation which is exposed to an altitude of 2,500m.asl, and the underlying Elliot and Molteno Formations (Schmitz & Rooyani, 1989; *Table 3.1*). The Stormberg series was formed during the late Permian to the early Jurassic, commencing with the development of the Molteno Formation through fluvial deposition of coarse sediments onto the Burgersdorp Formation of the Beaufort Group (Schmitz & Rooyani, 1987; Hancox & Rubidge, 2001; *Table 3.1*). The Elliot Formation was formed from the Late Triassic to early Jurassic periods, under an increasingly arid period dominated by aeolian processes (Eriksson, 1981; Schmitz & Rooyani, 1989; *Table 3.1*).

Table 3.1: Geological time scale for eastern Lesotho (after Schmitz & Rooyani, 1987).

Years	Era	Period	Epoch	Supergroup	Group	Formation
Present	Cenozoic	Quaternary	Holocene			
			Pleistocene			
2mya		Tertiary	Pliocene			
			Miocene			
			Oligocene			
			Eocene			
			Paleocene			
65mya	Mesozoic	Cretaceous				
135mya		Jurassic	Late			
			Middle	KAROO	Drakensberg	Lesotho
			Early		Stormberg	Clarens
190mya		Triassic	Late			Elliot
			Middle			Molteno
			Early		Beaufort	Burgersdorp
240mya	Paleozoic	Permian				
					Ecca	
						Dwyka
280mya		Carboniferous				

The Clarens Formation is the only component of the Stormberg series which is visible in Lesotho, and its outcrops are largely restricted to the western Lesotho lowlands (Eriksson, 1981; Schmitz & Rooyani, 1989; *Table 3.1*). This sandstone layer was formed from aeolian deposits in the late Triassic to early Jurassic, with sedimentation ceasing approximately 182 million years ago, preceding the break-up of Gondwanaland (Eriksson, 1981; McCarthy & Rubidge, 2005; *Table 3.1*). During an explosive volcanic phase from 187-155 million years ago, approximately coinciding with the break-up of Gondwanaland, horizontal lava flows extruding from fissures in the Clarens Formation formed the resistant overlying Drakensberg Group basalts (Schmitz & Rooyani, 1987; *Table 3.1*). The Drakensberg Group basalts extend

to a maximum thickness of 1,600m, and cover the region of the eastern Lesotho highlands, with the remaining eroded basalt plateaus of the Drakensberg group having formed the Maluti and Drakensberg ranges (Schmitz & Rooyani, 1987; Marake et al., 1998; McCarthy & Rubidge, 2005). Partridge and Maude (1987) estimated that some 300m of basalt have been removed through erosion over time; this however remains contentious.

No discernible faulting or tilting has occurred since the development of the Clarens Formation sandstone, but persistent weaknesses in the basalt have developed vertical shear zones and linearments (Marsh, 1987; Brackley et al., 1991). The intersection of these linearments, as mapped in the geological surveys of Lesotho, corresponds closely with the locations of many of the spring-fed wetlands in the Lesotho highlands (Mills et al., 2009b). While the volcanic period that formed the Drakensberg Formation basalts terminated in the early Jurassic, infrequent volcanic eruptions and smaller gaseous eruptions have continued, hypothesized to result from the Quathlamba mantle hotspot (Hartnady, 1985). Earthquakes are uncommon but not unheard of in the region, but the epicentres do not clearly correlate with the geological properties (Schmitz & Rooyani, 1987).

There are 26 soil types in Lesotho, of which 80% are restricted to altitudes greater than 2,000m.asl (Nixon, 1973; Schmitz & Rooyani, 1987). The predominant soil orders in eastern Lesotho are Mollisols and Lithosols, while Alfisols are more common in the lowlands and foothills (Schmitz & Rooyani, 1987). The horizontally layered basalts of the eastern Lesotho highlands weather to a loamy regolith that supports grass and heath alpine vegetation (Boelhouwers & Meiklejohn, 2002). Thin layers of silty loams are found in the interfluves, whist thick colluvial mantles are present on many of the valley floors (Sumner, 2004b). The moist eastern Lesotho highlands have a large network of alpine peat wetlands, rich in organic material due to the cooler climate, waterlogging, and the dominance of tall grass vegetation (Schmitz & Rooyani, 1987; Schwabe, 1995). These peat layers are often interspersed with layers of orange gravels, that formed due to the oxidation of iron in the basalt (Hanvey & Marker, 1994). The basalt bedrock is rich in K_2O, CaO and P_2O_5, so the resultant soils have high percentages of potash, phosphoric acid and nitrogen (Van Zinderen Bakker, 1955).

The eastern Lesotho highlands are classified as a marginal periglacial environment, and an array of active cryogenic landforms (*Table 3.2*) that do not require permafrost can be found at higher altitudes (Grab 2002b, 2010; Nel & Sumner, 2008). There is a marked valley asymmetry in the east-west oriented valleys in the highlands, with considerably steeper south-facing slopes resulting in more rapid denudation (Sumner, 2004b; Borg, 2012). These slopes encourage the development of many of these cryogenic landforms, including sorted patterned ground, block deposits, teracettes, stone polygons and earth hummocks (Hanvey & Marker, 1992; Boelhouwers et al., 2002; Grab, 2010). Needle ice and ice lenses are active periglacial agents in the region. Periglacial processes result in the development of small cryogenic mounds (earth hummocks/ thurfur) (*Figure 3.2*), and pan-like depressions – both of which are particularly common in the wetlands (Grab, 2002b, 2005, 2010).



Figure 3.2: Thurfur formed due to mechanisms associated with ground freeze.

In addition to the geomorphological formations produced by contemporary cryogenic activity, a range of palaeogeomorphologic features of colder past environments (*Table 3.2*) remain on display across the landscape of the eastern Lesotho highlands (Boelhouwers & Meiklejohn, 2002; Mills, 2009b). These can be separated into a group of features indicative

of dry, cold periods, including large patterned ground, solifluction mantles and blockstreams (Boelhouwers & Meiklejohn, 2002). The second group includes geomorphic features that suggest wetter cold periods such as nivation hollows, cirques and cryoplantation terraces (Boelhouwers & Meiklejohn, 2002). Due to continued landscape change and disruption on both large and local scales, these features often attract controversy in their identification and the interpretation of their environmental drivers, a problem compounded by the difficulty in dating them (Butzer, 1973; Boelhouwers et al., 2002; Mills et al., 2009a).

Table 3.2: Active and inactive cryogenic landforms in the eastern Lesotho highlands (after Grab et al., 2012).

Geomorphological Feature	**Active/ Contemporary**	**Inactive/ Relic**
Earth hummocks (thurfur)	X	
Flarks	X	
Sorted patterned ground	Miniature	Large
Miniature non-sorted patterned ground	X	
Terraces and terracettes	X	
Needle-ice pans and cryo-deflation	X	
Needle ice: sediment movement and associated landforms	X	
Ploughing boulders	X	
Segregation ice and ice lenses	X	
Solifluction lobes	X	X
Stone-banked lobes	X	X
Turf exfoliation	X	
Turf exfoliation pans	X	
Cryoplanation		X
Cryoturbation and 'periglacial' soils		X
Glacial erosional phenomena		X
Glacial deposition phenomena		X
Nivation processes and phenomena		X
Openwork block deposits		X
Pronival ramparts		X
Cryoclastic scree		X
Valley asymmetry		X

3.2.3 CLIMATE

Climate data for Lesotho, and eastern Lesotho in particular, are scarce (Tyson et al., 1976; Mulder & Grab, 2009). There remains an insufficient coverage of weather recording stations relative to the varied climate across region, and historical data represent an even more sparse set of locations of uncertain accuracy (Boelhouwers & Meiklejohn, 2002; Grab et al., 2009). However, despite the lack of climate data, much has been written on the climate of eastern Lesotho, with an interest driven by the high altitude, the influence of aspect, and the role of the broader synoptic drivers (Grab et al., 2009; Grab & Linde, 2014). Much of this work relies on recording stations set up and managed by researchers for the duration of a project at a specific study location, so they tend not to reflect long-term climate patterns or climatic trends of the broader region (cf. Preston-Whyte, 1971; Tyson et al., 1976; Grab, 2002c, 2010; Nel & Sumner, 2005, 2008; Mpholo et al., 2012). Due to the lack of a robust meteorological network, and the rapid change in altitude and aspect within small areas, interpolation of both climate data and the requisite lapse rates must be made with caution (Grab, 1997; Boelhouwers & Meiklejohn, 2002). What follows is an overview of the climate on the basis of reports from both the permanent meteorological recording stations, and from short-term meteorological observations made by scientists, often in the process of studies on topics that required recorded daily meteorological conditions. A focus is made on the climate of eastern Lesotho, as it is directly relevant to this study.

The contemporary climate of eastern Lesotho can be described as a distinct seasonal alpine climate with cool wet summers and cold dry winters (Grab, 2010), classified as Köppen codes of Cbf by Boelhouwers (2003) and Cwb by Borg (2012). Broadly, along a trajectory from the eastern Lesotho highlands to the western lowlands, temperatures increase while rainfall and humidity decreases. The climate of eastern Lesotho, as well as the broader country, is influenced predominantly by altitude and distance from the rain-shadow of the Drakensberg Mountains, but there is considerable local variation arising from aspect and temperature inversions (Mitchell, 1992; Roberts et al., 2013). Aspect alone accounts for a 50% difference between the amount of solar radiation received on north- versus south-facing slopes in winter, while in summer there is little difference in radiation due to the high solar angle (Mills et al., 2009b). Synoptic conditions also play a role in meteorological conditions at a daily to weekly scale, with cold fronts resulting in sudden temperature

decreases of approximately 10°C which persist for 2-4 days at a time, often accompanied by snow and frost (Deschamps, 2006; Grab & Nash, 2010). Recurrent fog and mist occur in the eastern highlands due to humid conditions, and the effect of sudden altitudinal increases at the escarpment (Van Zinderen Bakker 1955; Sene et al., 1998; Nüsser & Grab, 2002).

Due to the high altitude, eastern Lesotho experiences some of the coldest temperatures in southern Africa (FAO, 2011). There is a large difference in temperatures between the eastern highlands and the lowlands to the west, with a mean annual temperature of 15°C in the lowlands, but <6°C in the highest summits; and mean mid-winter minimum temperatures of 4.3°C in the lowlands and -6.1°C in the highlands (Grab & Nash, 2010; Mills et al., 2012). The mean temperature at Sani Top for the period 2001-2005 is recorded at 5.8°C (Nel & Sumner, 2008). The lowest recorded temperature for eastern Lesotho is -20.4°C at Letseng-La-Draai, which occurred on 12 June 1967 (Nüsser & Grab, 2002). Lapse rates for eastern Lesotho remain uncertain, with the terrestrial lapse rate of 8°C.km^{-1} suggested by Ambrose (1976) exceeding the lapse rate measured for northern Lesotho by Grab (1997) of 6.2°C.km^{-1}, with considerable variation in lapse rates between the sub-alpine and alpine zones. It has been suggested that these lapse rates may be sensitive to variations in wind intensity, and to the passing of mid-latitude cyclones (Grab, 1997, 2013; Grab & Simpson, 2000).

Precipitation records similarly suffer from the sparse network of meteorological stations, and data for the eastern Lesotho highlands arises predominantly from research projects of relatively short duration. Figures for mean annual precipitation in eastern Lesotho thus have a considerable range (Nash & Grab, 2010), between 750mm.yr^{-1} reported by Nel and Sumner (2005), and the more widely cited 1600mm.yr^{-1} by Sene et al. (1998). These differences may, in part, be due to the considerable inter-annual variation in precipitation, driven by the El Niño Southern Oscillation (ENSO), the South Indian Oscillation (SIO), and more regional synoptic fluctuations (Hydén & Sekoli, 2001; FAO, 2011), with the recordings made by Nel and Sumner (2005) having spanned a known regional dry period. A decline in total annual rainfall is observed on an east-west transect across Lesotho, with an average of only ~500mm.yr^{-1} in the central interior of Lesotho (Grab & Deschamps, 2004; Bisaro et al., 2010). Precipitation in the Lesotho lowlands demonstrates a strong correlation with rainfall

in South Africa's SRZ, significant relationships between summer rainfall and the SIO, and correlations between drought events and ENSO conditions (Hydén & Sekoli, 2001; Nash & Grab, 2010; FAO, 2011).

Precipitation in eastern Lesotho is strongly seasonal, with 70-80% falling between November and March, and less than 10% between May and August (Boelhouwers & Meiklejohn, 2002; Grab & Deschamps, 2004; Borg, 2012). Summer precipitation is predominantly in the form of convection storms, controlled by the subtropical high pressure belt, with a smaller proportion of the summer rainfall occurring as lighter orographic rain or drizzle, resulting from an influx of moist maritime air from the east (Sene et al., 1998; Deschamps, 2006; Nash & Grab, 2010). As these storms are predominantly convective in nature, 60% occur between 13:00-21:00h (Nel & Sumner, 2008). These storms involve thunder on an average of 90 days per year, and a lightning strike frequency of 10 strikes per km^2 (Sene et al., 1998; Letšela, 2008). High pressure systems dominate in winter, resulting in dry conditions and particularly low atmospheric humidity, which decrease further under the influence of westerly winds (Killick, 1963; Deschamps, 2006; Nash & Grab, 2010).

Most precipitation above ~3,000m.asl between May and September falls as snow, accounting for less than 10% of total annual precipitation (Nel & Sumner, 2008). These snowfalls are driven by frontal perturbations in the westerlies (Mills et al., 2009b; Grab & Linde, 2014). Particularly heavy snow events occur in the highlands either as a result of cut-off lows, or as the Indian Ocean high pressure ridges behind a cold front (Grab & Simpson, 2000; Mulder & Grab, 2009). In the eastern Lesotho highlands, moderate to light snow falls on average 2-8 times per year (*Figure 3.3*), while in the lowlands snowfall occurs only once in every 2-3 years (Boehouwers & Meiklejohn, 2002; Grab & Nash, 2010; Grab & Linde, 2014). Satellite image analysis indicates that the highest incidence and most widespread snowfalls occur from June to August (Mulder & Grab, 2008; Grab & Linde, 2014). Although individual snowfalls account for snow depths usually less than 5cm (Grab & Linde, 2014), snow can remain for a few days on north-facing slopes, and several weeks on south-facing slopes, particularly at high altitudes in mid-winter (Deschamps, 2006; Mulder & Grab, 2009). The longest mean snow cover duration is averaged for July at 11 days, followed by June at

9.8 days and August at 9.7 days for the period 2003-2010 (Grab & Linde, 2014). This persistent snow cover insulates the underlying ground from frost (Grab et al., 2009).



Figure 3.3: Light snowfall in eastern Lesotho.

Due to the high altitude and relatively high latitude, combined with high insolation and clear skies, strong diurnal heating occurs, resulting in diurnal frost cycles in winter at moderate altitudes, and prolonged freezing at altitudes greater than 3,000m.asl (Hanvey & Marker, 1992; Boelhouwers & Meiklejohn, 2002). Ground level freezing occurs in the highlands at an average of 180-200 days per annum (Grab & Deschamps, 2004; Mills et al., 2009a). Seasonal frost begins in March in the highlands, with heavy frosts frequently recorded for more than 120 days per year. By contrast, the lowlands experience an average of 31 frost days per year (Grab & Nash, 2010).

Lesotho is amongst the windiest countries in Africa (Mpholo et al., 2012). The strongest winds are experienced in late winter due to the frontal systems associated with the

westerlies, while wind speeds are lowest in the wet summer months (Grab, 2002a, 2010). For eastern Lesotho, the most complete wind data available is for the Sani Valley, reflecting a range in wind speeds for 2001 from 3.39m.s^{-1} in March to 8.09m.s^{-1} in August, with maximum gust speeds of 26.75m.s^{-1} recorded in April, August and September (Grab, 2010). These wind speeds are corroborated by a second study conducted over 2001-2002, reporting that March was the least windy month at an average 3.6m.s^{-1}, while the strongest mean wind speeds of 7.47m.s^{-1} were recorded for August (Mpholo et al., 2012). The mean annual wind speed for the Sani Valley is calculated at 5.37m.s^{-1} for 2001 and 5.63m.s^{-1} for 2002, tentatively suggesting little interannual variability in wind speed. Wind direction varies both throughout the day, and over the course of the year in the Sani Valley (Sene et al., 1998; Deschamps, 2006). Summer winds dominate from the east and northeast, bearing moisture from the Indian Ocean, while the winter winds are predominantly north-westerly (Sene et al., 1998; Grab, 2010). Under clear conditions, a marked diurnal variation in wind direction is observed, with easterly winds during the day due to the overflow of plain-mountain circulation, but north-westerly gradient winds channeled by the northwest-southeast aligned Sani Valley occur from 21:00h at night (Preston-Whyte, 1971). In addition, berg winds are experienced, particularly in winter, resulting from large prefrontal disturbances due to the westerlies, which are associated with low humidity and temperature increases of up to 5°C (Deschamps, 2006).

Reports of contemporary climate change over recent decades are hindered by the lack of climate data, and are largely restricted to an analysis of human perceptions based on interviews with elderly members of rural communities, conveying their subjective descriptions of changes in climate patterns. Farmers and the elderly who were interviewed by Bharwani et al. (2007) describe long term climate changes in the Lesotho highlands, including more snow in winter but warmer summers, corroborated by satellite imagery (Grab & Linde, 2014). Changes in rainfall patterns have also been observed, and are reported to include more frequent drought, particularly in January and December, and a delayed but more intense rainfall season (Bharwani et al., 2007). Projections for temperature changes throughout much of the century are based on data from the current meteorological stations across Lesotho, and are largely consistent (FAO, 2011; Gwimbi et al., 2012). The Lesotho Meteorological Service projects a 1°C increase in T_{mean} by 2030, 1.5-2°C

by 2050 and 2.5-3.5°C by 2080, averaged for the whole country (FAO, 2011). Projections made by the Climate Systems Analysis Group (CSAG) of the University of Cape Town project increases in mean temperature for Lesotho of 2-2.5°C by 2046-2065, and 3.5-4.5°C by 2080-2099 (FAO, 2011). Separating the lowlands from the highlands, Gwimbi et al. (2012) project temperature increases of 1-2°C by 2050 for the lowlands, but slower temperature increases for the mountain regions. The Lesotho Meteorological Service and CSAG agree on projections of significant decreases in winter rainfall; but although CSAG suggest increasing rainfall throughout the months October to March, the Lesotho Meteorological Service subdivide this period and project gradually increasing spring rainfall, but no change in rainfall for summer or autumn months (FAO, 2011).

3.2.4 VEGETATION

The High Drakensberg is floristically the only true alpine area in southern Africa (Linder, 1990), and is one of southern Africa's primary biodiversity hotspots (Cowling & Hilton Taylor 1994; Carbutt & Edwards, 2004; Grab 2010). Due to the high altitude, rapid changes in altitude and aspect, and the high moisture levels, the High Drakensberg, and in particular eastern Lesotho, is home to a considerable number of endemic and near endemic species, as well as considerable species richness and diversity (Carbutt & Edwards, 2004; Letšela, 2008). The region forms part of the DAC, which in addition to the Lesotho Drakensberg, includes the Eastern Cape Drakensberg, the Witteberge, the KwaZulu-Natal Drakensberg, and the eastern Free State (Carbutt & Edwards, 2004). Within the DAC, 13% of species are endemic, and 24% near endemic, with over 2,800 specific and infraspecific native taxa (Carbutt & Edwards, 2004). The angiosperm flora of the Lesotho Drakensberg region of the DAC contains 95 families, 526 genera and 1,537 species, of which only 6% are exotics (Carbutt & Edwards, 2004). The ten most common families in the DAC, and the five most common families in Lesotho are listed in *Table 3.3*.

Table 3.3: The most common floral families in the DAC and Lesotho by number of species (after Carbutt & Edwards, 2004).

Drakensberg Alpine Centre		Lesotho
Name	# Species	Name
1. Asteraceae	430	1. Asteraceae
2. Poaceae	267	2. Poaceae
3. Fabaceae	136	3. Scrophulariaceae
4. Scrophulariaceae	133	4. Fabaceae
5. Orchidaceae	130	5. Liliaceae
6. Cyperaceae	122	
7. Iridaceae	97	
8. Asclepiadaceae	87	
9. Hyacinthaceae	55	
10. Asphodelaceae	50	

As a result of considerable altitudinal and climatic differences between the eastern Lesotho highlands and western lowlands, there is a considerable vegetation gradient across Lesotho (*Figures 3.4, 3.5*). Western Lesotho is considerably drier, but due to the lower altitude, has the potential to support scrub forest (*Figure 3.4;* Van Zinderen Bakker, 1955). Eastern Lesotho is wetter, with numerous small high altitude wetlands consisting of grasses, sedges and mosses (*Figure 3.4;* Magill, 1987; Schwabe, 1995; Grab, 2002a). The vegetation composition in eastern Lesotho is determined predominantly by altitude and slope aspect, and the resultant climate, rather than by soil type (Carbutt & Edwards, 2004). The alpine belt of eastern Lesotho, from 2,865-3,482m.asl, is classified as a grassland biome (Lesotho Highland Basalt Grassland, GD8) with both tussock and meadow grasses (*Figure 3.4*), dominated by *Merxmuellera*, *Festuca*, *Danthonia* and *Pentaschistis* and interspersed by the woody shrubs *Erica* and *Helichrysum* (Backéus, 1989; Nüsser & Grab, 2002; Mucina & Rutherford, 2006; Grab, 2010).

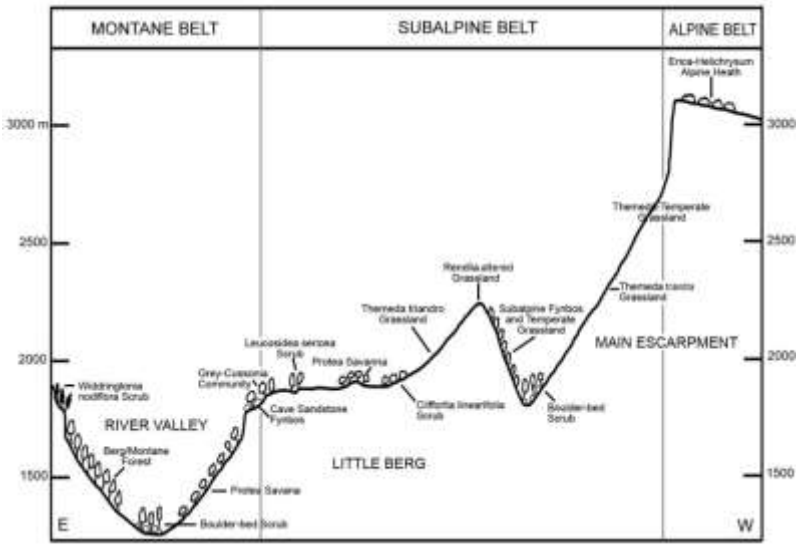


Figure 3.4: Variations in vegetation with altitude across Lesotho (after Killick, 199, p. 24).

Trees are limited to small patches in protected valleys in western Lesotho, not exceeding altitudes of 2,200m.asl, while shrubs in eastern Lesotho seldom reach heights greater than 0.5m due to altitudinal constraints (*Figure 3.5*; Van Zinderen Bakker & Werger, 1974; Plug, 1997; Mitchell et al., 1998; Nüsser & Grab, 2002). The climax community on the summits of eastern Lesotho (above 3,200m.asl) is *Erica-Helichrysum* Alpine Heathland, with dwarf shrubs; at the highest peaks (>3,400m.asl) plant cover is particularly sparse, if not completely absent (*Figure 3.4*; Killick, 1978; Grab, 1996a).

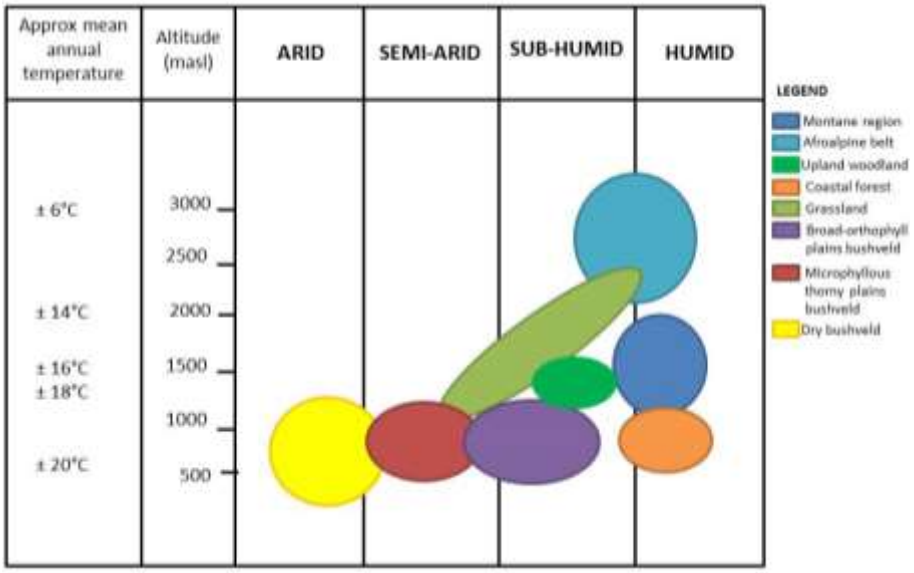


Figure 3.5: Southern African vegetation zones delineated by altitude and aridity (after Scott, 1982a).

3.2.5 HYDROLOGY

Eastern Lesotho has one of the only catchments in southern Africa where long-term annual precipitation exceeds evaporation (Zunckel, 2003). The region is the source of the Tugela/ Orange/ Senqu Rivers, with run-off from smaller tributaries in the eastern Lesotho highlands contributing more than half the volume of the Orange/ Senqu River (Sene et al., 1998; Zunckel, 2003; Letšela, 2008). Water is a lucrative natural resource to Lesotho, and has boosted the local economy considerably by providing much needed foreign income since the inception of the Lesotho Highlands Water Project in the 1980s, that transfers water from the Katse Dam to South Africa and provides hydropower to Lesotho (Letšela, 2008; Haas et al., 2010). With the development of a further four dams and a larger system of tunnels, the region has become a major source of freshwater for the more water-stressed regions of southern Africa (Haas et al., 2010; Arthur et al., 2011; FAO, 2011).

Van Zinderen Bakker (1955) referred to eastern Lesotho as the "barren boggy wastes", describing the extensive network of wetlands situated across the landscape of eastern Lesotho at altitudes of greater than 2,750m.asl (Schwabe, 1995). These wetlands are ubiquitous as a result of the cool, moist climatic conditions, and a large number of springs (Meadows, 1988; Schwabe, 1995; Grab & Deschamps, 2004; Grundling et al., 2015). The wetlands can be categorised into the organic rich bogs, in which only atmospheric water leaves or enters the system, and the more minerogenic fens, that receive water input from the surrounding soil (Schwabe, 1995; Nüsser & Grab, 2002; Du Preez & Brown, 2011). Many of the alpine wetlands of eastern Lesotho are undergoing a transition from bog to fen, as a result of climate warming and increased erosion, affecting both the hydrological input and the organic content (Schwabe, 1995; Grab & Deschamps, 2004; Grundling et al., 2015). These alpine wetlands are unique in Africa due to the extensive peat horizons, and represent the only alpine wetlands in southern Africa with contemporary peat formation (Nüsser & Grab, 2002; Grab, 2012). Peat is classified as a soil with a minimum of 20% organic material, and is produced through the decomposition of sedges and grasses, which are common in the highlands (Backéus, 1989; Schwabe, 1995). Due to the cool temperatures, peat formation in the eastern Lesotho highlands occurs slowly, with an estimated accumulation rate of 0.25mm.yr^{-1} (Van Zinderen Bakker & Werger, 1974; Du Preez & Brown, 2011).

The peat mires of eastern Lesotho are dominated by tussock grasses, sedges and herbs, with meadow vegetation usually occurring in wetlands situated at the lower slope positions (Backéus, 1989; Schwabe, 1995; Grab & Deschamps, 2004; Grab, 2012). The eastern Lesotho bogs have considerably less moss than those of the Northern Hemisphere (Schwabe, 1995), but the mosses present are notably endemics, including the Bartramiaceae family which is not found elsewhere in Africa (Magill, 1987). Some of the mires contain pools of deeper water within their greater extents, which are referred to as flarks (Backéus, 1989) or mire pools (Van Zinderen Bakker & Werger, 1974); these have alkaline waters and can contain more aquatic species due to their depth (Van Zinderen Bakker, 1955). The alpine wetlands have occasionally been reported as containing diatomite, which is uncommon in southern Africa, and provides a useful palaeoenvironmental archive (Van Zinderen Bakker & Werger, 1974; Mitchell, 1996a).

In addition to their intrinsic value, through their biodiversity, the alpine wetlands are also of direct hydrological importance (Schwabe, 1995). These wetlands control ground water storage and discharge and flood flow attenuation (Schwabe, 1995). They stabilise soil, and retain both sediments and toxins, while facilitating nutrient removal and transformation (Schwabe, 1995). The wetlands are also important in organic matter production and export, predominantly through the development of peat (Schwabe, 1995; Nüsser & Grab, 2002). Despite their considerable importance, it is estimated that 65% of Lesotho's wetlands are damaged, with 49% containing plants that suggest disturbance (Schwabe, 1995). Much of this disturbance is as a result the vegetation disruption through overgrazing and trampling, and soil erosion discussed below.

3.3.6 Environmental Problems

Although the eastern Lesotho highlands represent one of the most endemic-rich regions within the DAC, which itself is a biogeographical area of high ecological value, only 1% of the Lesotho Highlands Grassland belt is statutorily conserved (Du Preez & Brown, 2011). One of the most pressing environmental issues in eastern Lesotho is the degradation of natural vegetation, and the necessity of management intervention (Letšela, 2008). Biodiversity of the DAC, and in particular eastern Lesotho, is threatened by a combination of over-stocking and associated over-grazing; cropping in locations unsuited to agriculture, such as steep

slopes; the introduction and spread of invasive exotic plants (eg. *Chrysocoma ciliata*); human population growth and associated pressures on available land; uncontrolled burning; and large scale soil erosion (Nüsser & Grab, 2002; Carbutt & Edwards, 2006; Letšela, 2008). Grassland degradation, primarily as a result of livestock grazing, is a concern for the species richness and diversity of vegetation in eastern Lesotho (Quinlan, 1995; Grab & Deschamps, 2004; Letšela, 2008; *Figure 3.6*). Concerns of grassland degradation were first raised in the 1930s Ecological Survey of Lesotho, and have remained a management concern over the decades with the implementation of the Drakensberg/Maluti Catchment Conservation Project in 1987, and the proclamation of the Range Management Area in 1991 (Quinlan, 1995). This aligns with the increasing use of the high altitude grasslands as a common pool pastoral resource, and the resultant environmental shift from grass to shrub due to overgrazing (Nüsser & Grab, 2002; Grab & Deschamps, 2004). This clearly requires greater management of this common pool resource, to ensure its sustainability for both the grazers and the natural environment (Quinlan, 1995; Nüsser & Grab, 2002). Despite being at the heart of the problem, often the solutions of local stock owners have been of equivalent, if not greater, value than the formal managerial responses, involving a transhumance system derived from seasonal movement between areas, based on observations of biological and climate factors, and their economic success (Quinlan, 1995).



Figure 3.6: Sheep in an already overgrazed grassland, close to Sani Valley.

Lesotho is considered to be one of the most eroded countries in the world, with a 1980s approximation of net erosion ranging from 100-2000 tons.km^{-2}.year^{-1} (Heine, 1987). The erosion problems, particularly in eastern Lesotho, are similar to the problem of grassland degradation in that they have primarily been attributed to livestock grazing, resulting from overstocking of 50-300% (Heine, 1987). The results of overgrazing have a circular effect, whereby vegetation is removed, facilitating rapid erosion, which in turn reduces the potential for grassland restoration (Heine, 1987; Grab & Deschamps, 2004). Formed through extensive soil erosion, deep gullies are widespread through eastern Lesotho (Heine, 1987; Hanvey & Marker, 1994; Grab et al., 2005; *Figure 3.7*). The age of these gullies is unclear; Heine (1987) argues that they developed during the last 100-150 years, as there are no reports of them from the first missionaries who entered the country, but Showers (2005) demonstrates some missionary reports mentioning gully-like features, and suggests they may be much older. Aerial photographs suggest that the most active period of gully development in the region was from AD 1951-1961, and can be attributed to higher than normal rainfall (Stromquist et al., 1985). Today gullies are common on the wetlands at the foot of north-facing slopes in eastern Lesotho, with causes for continued erosion attributed to a combination of trampling pressure, livestock grazing and rodent burrowing (Nüsser & Grab, 2002; Grab & Deschamps, 2004). A contemporary study on rates of gully denudation on one of these wetlands quantified an 8-13cm erosion rate over 18 months (Grab & Deschamps, 2004).



Figure 3.7: Extensive gullying on a north-facing slope of the Sekhokong Mountain Range.

Although the introduction of domesticated livestock into eastern Lesotho for grazing purposes has attracted much attention due to the environmental degradation resulting from their grazing and trampling, small mammals also contribute to soil and vegetation degradation (Grab & Deschamps, 2004; Grab, 2005; Mokotjomela et al., 2009). Ice rats (*Otomys sloggetti robertsi*) have extensive burrow systems within many wetland soils (Grab, 2005; Hinze et al., 2006). While there remains debate as to the level of habitat deterioration attributable to the ice rats (cf. Mokotjomela et al., 2009; Grab, 2012), their burrowing leads to destabilisation of sediments, particularly adjacent to gullies, and they are known to reduce the height of herbaceous plants through selective foraging (Mokotjomela et al., 2009). Of concern is the expansion of suitable habitat for the ice rat owing to the degradation of vegetation and drying of wetlands towards the centre of these systems (Grab & Deschamps, 2004; Du Preez & Brown, 2011).

With the degradation of natural vegetation through a combination of direct factors including overgrazing, and indirect factors such as consequent soil erosion, the introduction and spread of opportunistic invasive species is facilitated (Rouget et al., 2004). This is of particular concern with the rapid increase in the agricultural use of land, and under climate change scenarios, as these invasives are likely to spread because of their wider environmental tolerances (Carbutt & Edwards, 2004; Rouget et al., 2004). The most widely recognised invasive species is the Karroid shrub *Chrysocoma ciliata*, which rapidly establishes itself within environmentally degraded areas including gullies and ice rat burrowed regions, and dominates the grassland regions under periods of severe climatic stress such as droughts (Grab & Deschamps, 2004; Letšela, 2008; Carbutt, 2012). Despite the potential threat of invasive species replacing the natural indigenous vegetation, much remains unknown about them.

3.3 Contemporary Environments of the Specific Study Sites

The three study sites in this study can be broadly classified as alpine environments, with characteristic low temperatures throughout the year, and niche vegetation constrained by these climatic conditions (*Table 3.4*). The Sani Valley and Sekhokong sites are located within 10km of one another and at similar altitudes, and thus their mean annual climates are near

identical. Their microtopography, however, is different, resulting in subtle differences in climate and associated flora. More importantly though, their geomorphological characteristics are very different, offering a core spanning a comparatively short period for Sani Valley, relative to the considerably longer period spanned for Sekhokong. The Mafadi Wetland site is located at a distance of 27km, and an altitude approximately 500m higher than these two sites, and represents the altitudinal limit for vegetation growth in the eastern Lesotho highlands. The justification for the selection of these sites is presented in the *Chapter 4 (Methods)*. Here the contemporary environment at each of the sites is outlined, based on a combination of the literature and observations made during the fieldwork at each site.

Table 3.4: Summary of the key geographic attributes of the three study sites.

Site	GPS coordinates	Elevation	Site description	Core description
Sani Valley	29°37'S 29°14'E	2,900m.asl	Raised wetland on a large valley-floor meadow, surrounded by hills	Very rich peat throughout
Sekhokong	29°36.517'S 29°15.897'E	2,920m.asl	Deep gully wall along a stream channel on the north-facing slope of the Sekhokong Range, with meadow-wetland surrounding it.	Alternating layers of rich peat and coarse orange coloured sediment.
Mafadi Wetland	29°11'58''S 29°21'04.1''E	3,390m.asl	Bowl shaped topography with spring-fed wetland and a stream running through it. Diatomite outcrops	Alternating levels of peat, clay and diatomite.

3.3.1 SANI VALLEY

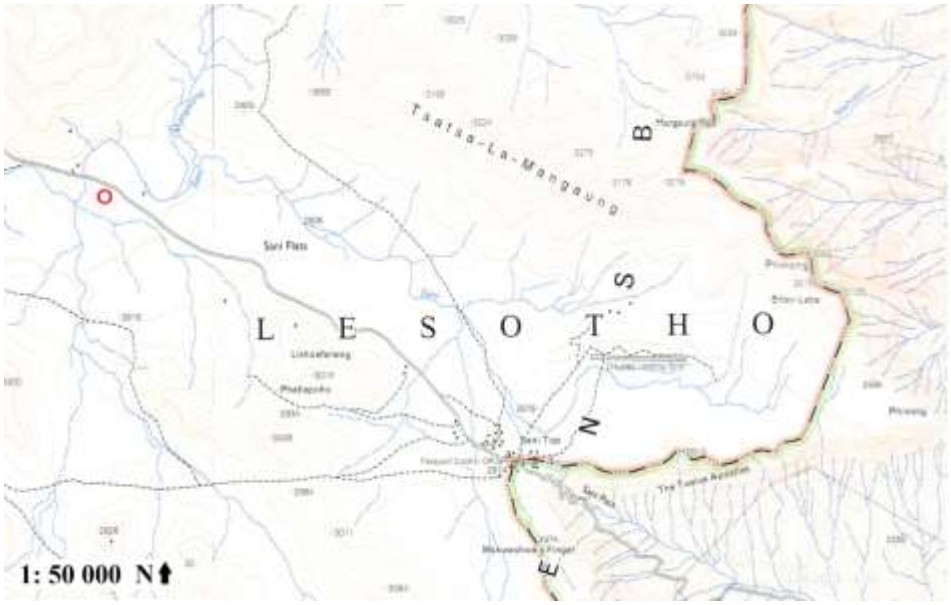


Figure 3.8: Topographical map indicating the location of the Sani Valley (adapted from map code 2929CB Sani Pass and 2929CA Sani Pass (West)). Study site indicated by red circle.

The Sani Valley site for this study is located approximately 5km west of the Sani Top border post, directly adjacent to the Mokhotlong road and south of the Sani River (*Figure 3.8*). The site represents an unusually large wetland compared to the small wetlands more typical in eastern Lesotho (Figure 3.9), with a large area of meadow-grasses and sedges surrounded by gentle basalt hills. In the centre of the wetland is a raised bog, with surface moisture at the summit (similar to those described by Schwabe, 1995). This mound appears to represent a hydralaccolith, and is probably situated above the intersection of large lineations giving rise to the spring and possibly cryogenically raised mound.



Figure 3.9: Google Earth Image of the region surrounding the Sani Valley site. Site marked by a red circle.

A narrow PVC pipe had recently been inserted into the mound, presumably for the extraction of spring water (*Figure 3.10*). The strong outflow of water from this artificial pipe has induced rapid gully erosion in the resultant channel, revealing an exposure of rich peat (sediment with a high proportion of peat) approximately 1m in depth. It was from this gullied section that the sediment core for this project was extracted. The water flowing from this pipe extended for a radius of a few meters, with large quantities of algae growing in the

standing water. The mound is surrounded by thurfur fields and large expanses of short grassed meadows interspersed with clusters of short sedges and herbs.



Figure 3.10: PVC pipe inserted into the raised bog, and the resultant standing water with algae.

Mean annual air temperature estimates for Sani Top range from 3-7°C (Borg, 2012), with results from temperature readings for 2004 of 5.8°C (Nel & Sumner, 2008), while mean annual rainfall was measured at 750mm/yr for 2002-2003 (Nel & Sumner, 2005). The hills surrounding the wetland protect it from much of the wind in the region. The raised bog has a limited diversity of vegetation, ranging from grass and herbs, to sedges more indicative of wetland conditions, and semi-aquatic to aquatic species in the exposed water, many of which are endemic to the DAC (*Table 3.5*). The site is home to a large population of ice rats, that are thought to be responsible for soil erosion and diminished size of the plants at the site (Mokotjomela et al., 2009). There is considerable grazing pressure from sheep, cattle and horses in the area, which together with their associated trampling, results in loss of vegetation and soil erosion (Mokotjomela et al., 2009).

Table 3.5: Plants at the Sani Valley Site (on the raised bog) identified by Carbutt (2004).

Species	Family	Classification
Aponogeton junceus	Aponogetonaceae	Aquatic
Nostoc sp.	Nostocaceae	
Agrostis subulifolia	Poaceae	Grass
Cotula paludosa	Asteraceae	Herb
Haplocarpha nervosa	Asteraceae	
Limosella vesiculosa	Scrophulariaceae	
Lobelia galpinii	Lobeliaceae	
Ranunculus meyeri	Ranunculaceae	
Ranunculus multifidus	Ranunculaceae	
Rhodohypoxis rubella	Hypoxidaceae	
Trifolium burchellianum	Fabaceae	
Isolepis seacea	Cyperaceae	Sedge
Bryum pseudotriquetum	Bryaceae	Semi-aquatic

3.3.2 SEKHOKONG

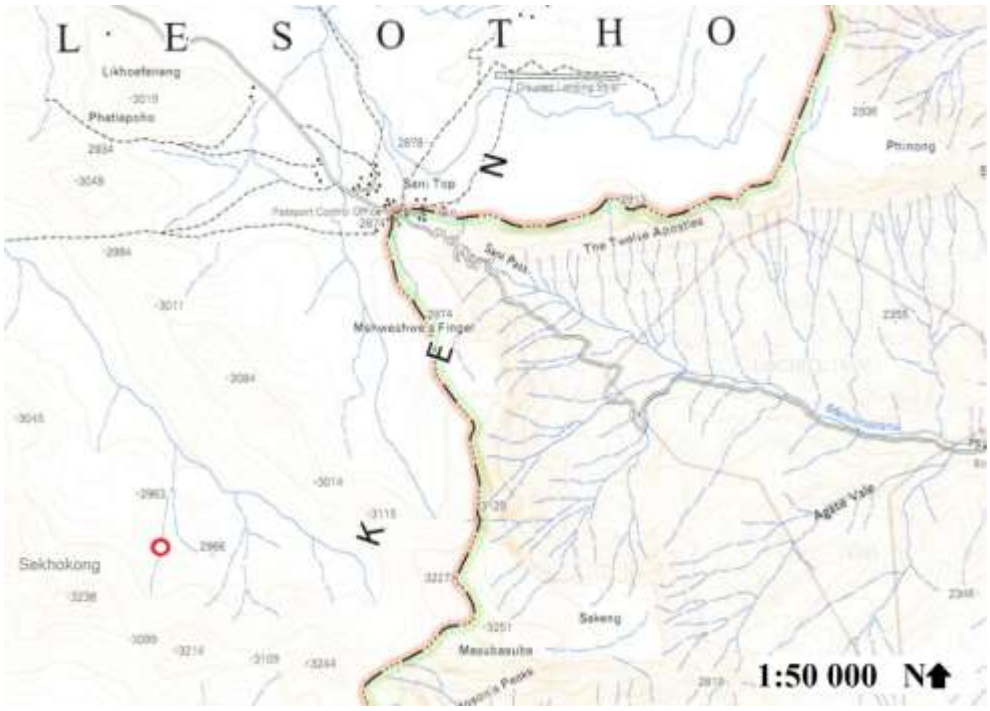


Figure 3.11: Topographical map indicating the position of the Sekhokong study site (adapted from map code 2929CB Sani Pass). Study site indicated by red circle.

The Sekhokong site is located approximately 3.5km southwest of the Sani Top border post, on the north-facing slope of the Sekhokong Range (*Figure 3.11*), just south of its highest point at Hudson's Peak (Marker & Whittington, 1974; Deschamps, 2006). This north-facing slope has at least four valley heads eroded into it, separated by basalt ridges (*Figure 3.12*; Deschamps, 2006). These were originally identified by Marker (1994) as glacial cirques, a theory that has subsequently been disproven due to the predominance of equator-facing landforms of this morphology (Mills et al., 2009b; Borg, 2012). They are now believed to have been formed over a considerably longer time, through a range of geomorphological processes, with the position most likely determined by underlying joint networks promoting enhanced weathering (Mills et al., 2009b).



Figure 3.12: Google earth image of the region surrounding the Sekhokong site. Site marked by a red circle.

The valley heads or hollows are approximately 800m wide and 1200m deep, with relatively flat valley floors of meadow grass with scattered but extensive thurfur fields (Marker & Whittington, 1971; Marker, 1994; Deschamps, 2006). Each of these valley floor wetlands has a tributary stream flowing from the Sekhokong Range, many of which have cut deep gullies into the sediment, with maximum depths closest to the valley head (*Figure 3.12*; Marker,

1994; Grab & Deschamps, 2004; Deschamps, 2006). The coring site was in one of these gullies (Deschamps, 2006: valley head 3; Marker, 1994: hollow C), that provided an exposed sedimentary sequence of more than 4m in depth, with alternating colluvial and peat layers (Grab & Deschamps, 2004; Marker, 1994; *Figure 3.13*). A sedimentary sequence from this gully (and others) has been investigated by Marker (1994, 1995, 1998), but it was limited to sedimentary description. Benefit could thus be gained from the analysis of palaeoecological proxies, and an improved dating chronology, while allowing direct comparison with these earlier studies.



Figure 3.13: Gully erosion exposing a sediment sequence of >5m at the selected study site.

The climate at the Sekhokong site is similar to that of the Sani Valley site. The greatest climate variation between the two sites is differences in wind patterns, resulting from the somewhat different topographic settings that would control site-specific air flow. Changes in wind direction and intensity could in turn affect temperature and evaporation. Broadly described, the vegetation is similar to that at the Sani Valley site, with large expanses of meadow grass, increased sedge cover towards the more water saturated regions of the wetland, and *Erica-Helichrysum* shrubs closer to the mountain backwall (Marker & Whittington, 1971; Grab & Deschamps, 2004). Vegetation transects within the wetland (crossing the gully) undertaken by Deschamps (2006) reveal far greater species diversity than at the Sani Valley site (*Table 3.6*).

Table 3.6: Vegetation transects for the Sekhokong Wetlands (Deschamps, 2006).

Species	Family	Classification	Valley head
Trifolium burchellianum	Fabaceae	Dryland	1,2,4,5
Selago flanaganii	Scrophulariaceae		2,3,4,5
Helichrysum subglomeratum	Asteraceae		1,2,3,4,5
Helichrysum flanaganii	Asteraceae		1,2,3,4
Geranium multisectum	Geraniaceae		1,2,3,4,5
Anthospermum basutocum	Rubiaceae		2,3,4
Helichrysum aureum var. aureum	Asteraceae		1,2
Helicchrysum sessillodes	Asteraceae		1,2
Erica sp.	Ericaceae		1
Erica dominans	Ericaceae		2,3,4
Centella asiatica	Apiaceae		2,3,4
Alchemilla woodii	Rosaceae		1,2,5
Senecio inaequadens	Asteraceae		2,4,5
Helichrysum milifordiae	Asteraceae		1
Crassula sp.	Crassulaceae		1
Delosperma sp.	Aizoaceae	Shrubs	1
Helichrysum trilineatum	Asteraceae		1,2,3,4
Chrysocoma ciliate	Asteraceae		1,2,3,4
Eumorphia sericea	Anthemideae		1,2,3,4
Polygala amatymbica	Polygalaceae		2
Merxmuellera drakensbergensis	Poaceae	Grass	1,2,4
Haplocarpha nervosa	Asteraceae	Wetland	1,2,3,4,5
Ranunculus multifidus	Ranunculaceae		2,3,4
Rhodohypoxys rubella	Hypoxidaceae		5
Saniella verna	Hypoxidaceae		1,2
Kniphofia caulescens	Xanthorrhoaeceae	Wetland	2,3,4
Aponogeton sp.	Aponogetonaceae		1,2
Wurmbea elatlor	Colchicaceae		1,2
Limosella major	Scrophulariaceae		1,3,4,5
Ranunculus meyeri	Ranunculaceae		1,2,3,4,5
Sebaea filiformis	Gentianaceae		1,2
Lobelia ± filiformis	Campanulaceae		1,3,4,5
Rhodohypoxis rubella	Hypoxidaceae		1,2,4
Cotula paludosa	Asteraceae		1,2,3,4,5
Alepidea ± pusilla	Apiaceae		1,2
Oxalis obliquifolia	Oxalidaceae		5

The extensive gully erosion alone points to severe environmental degradation at the site, and is of concern for subsequent environmental problems such as increased sediment loads reducing water flow. The site is grazed from October to June by horses, cattle, sheep and goats, resulting in vegetation loss and soil erosion (Deschamps, 2006). Ice rats are also common at this site, and are increasing their habitat range as erosion degrades the wetland structure and increases the proportion of drier areas, although this is argued to result in regeneration of vegetation over longer time periods (Grab & Deschamps, 2004; Grab, 2012). There are also notable quantities of the karroid invasive *Chrysocoma ciliata* shrub, which is thought to colonise regions that have undergone environmental deterioration (Deschamps, 2006; Mills, 2006). However, this is one case in which environmental degradation is of benefit to those studying environmental change, as without the severe gully erosion it would not have been possible to extract sediments from such a deep profile, given the logistical constraints in this relatively inaccessible location.

3.3.3 MAFADI WETLAND



Figure 3.14: Topographical map indicating the location of the Mafadi Wetland site (adapted from map code 2929AB Champagne Castle). Study site indicated by red circle.

Mafadi Summit is situated at the border between South Africa and Lesotho, and at an altitude of 3,450m.asl, represents the highest peak in South Africa and the third highest peak in Lesotho (Grab, 1999; Bristow, 2010). To the south of the summit, within Lesotho, is

a bowl shaped depression with a small non-perennial stream and a spring-fed wetland, the highest altitude wetland in southern Africa (*Figure 3.14*). Marked across Mafadi Wetland are bright white sediment exposure surfaces, that represent rich beds of diatomite. Vegetation within the wetland consists of meadow grasses and sedges, but consists mostly of shrubs on the slopes, thinning out towards the highest summits, suggesting proximity to the altitudinal limit of vegetation growth in this part of southern Africa (Grab, 1996a; *Figure 3.15*).



Figure 3.15: The sparse vegetation near Mafadi Summit.

The climate at Mafadi Wetland is considerably harsher than at the Sani Valley and Sekhokong sites, owing to the higher altitude. No long-term climate studies have been undertaken at Mafadi Wetland or the summit region yet, and thus interpolated from the lower altitude Letseng-la-Draai is an annual mean temperature of 4°C, with mean temperatures for January of ca. 9°C and July of -2°C; in winter temperatures may drop to as low as -15°C (Grab, 1996a, 2002c). There are considerable diurnal temperature variations, with diurnal soil freezing occurring between March and October (Grab, 2000). The ground is continuously frozen from June to August, to depths of as much as 34cm in places (Grab, 1996a, 2000). Rainfall is inferred to be similar to that of much of the eastern escarpment, exceeding 1000mm per year (Grab, 1999). Wind intensity and direction have not yet been quantitatively measured, but from experience winds are particularly strong on the summit.

However, the study site itself, located within a topographic depression, is relatively well protected from the much stronger winds near the summit interfluves.

The vegetation, while very sparse, is similar in composition to that of the Sani Valley and Sekhokong sites, dominated by alpine grasses, sedges and *Erica-Helichrysum* heath (Grab, 2000). Notable at the Mafadi Wetland site are the dwarfed sizes of these plants compared to their lower altitude analogues, a result of the harsh climatic conditions. As no previous vegetation data for Mafadi Wetland exist, vegetation surveys were undertaken during the fieldwork for this project, producing the species list in *Table 3.7*. There is lower species diversity than for Sekhokong, reflecting the harsher environmental conditions. The diatomite beds were of particular interest as no palaeoenvironmental work has been undertaken in eastern Lesotho using diatoms as a proxy (Mitchell, 1996a).

Table 3.7: Species identified at Mafadi Wetland.

Species	**Family**	**Classification**
Festuca costata	Poaceae	Grass
Harochloa falx	Poaceae	
Merxmuellera drakensbergensis	Poaceae	
Pentaschistis oreodoxa	Poaceae	
Cyperus sp.	Cyperaceae	Sedge
Pycreus cooperi	Cyperaceae	
Berkheya multijuga	Asteraceae	Shrub
Chrysocoma ciliata	Asteraceae	
Cotula paludosa	Asteraceae	
Crassula sp.	Crassulaceae	
Erica sp.	Ericaceae	
Euphorbia clavariodes	Euphorbiaceae	
Helichrysum flanaganii	Asteraceae	
Helichrysum sp.	Asteraceae	
Kalanchoe sp.	Crassulaceae	
Lotonis galpinii	Fabaceae	
Monsonia attenuata	Geraniaceae	
Rhodohypoxis baurii	Hypoxidaceae	

Due to the high altitude and resultant cold temperatures, Mafadi Summit is host to a large number of relict and active cryogenic landforms, including but not limited to blockstreams and debris deposits, miniature sorted stripes, sorted patterned ground, and thurfur (Grab, 1996a,b, 1999, 2002). These landforms provide valuable evidence for extreme cold events, the potential existence of permafrost in the region, and the nature and extent of palaeo-lapse rates (Grab, 1996a,b, 1999, 2002). Unfortunately these cryogenic landforms and the wetland are being damaged by the increasing numbers of livestock and people utilizing the area (Grab, 1996a). Recent gullying has occurred along the stream banks, which have further been degraded by trampling and ice rat burrowing (*Figure 3.16*).



Figure 3.16: Grazing sheep adjacent to the gullied river, and an ice rat outside its burrow in the gullied riverbank.

Mafadi Wetland represents the highest altitude wetland in southern Africa. The site forms part of a network of high altitude wetlands all at elevations of greater than 3,000m.asl, in adjacent lower altitude valleys, spanning an east-west transect which terminates at the escarpment (Figure 3.17). The presence of diatomite beds, and the depths of sediment profiles in these adjacent wetlands, has yet to be determined. Future work is intended in this region, to explore the value of these archives, and develop an east-west transect of palaeoenvironmental records for the highest altitude wetlands in southern Africa, to better explore palaeoclimatic and palaeoecological lapse rates.



Figure 3.17: Google earth image of the region surrounding the Mafadi site. Site marked by a red circle.

3.4 Conclusion

Eastern Lesotho provides an important environmental setting for palaeoenvironmental work due to the high altitude, with resultant harsh climate and niche vegetation communities. Situated at the extremes of the altitudinal ranges of many species, and vegetation itself, palaeoenvironmental research holds the potential to explore highly responsive ecological boundaries and palaeoenvironmental lapse rates. The large network of peat-rich wetlands is unique to eastern Lesotho, and contain a wealth of palaeoenvironmental proxies. There are many environmental threats to the eastern Lesotho highlands, requiring integrated management, particularly under climate change, to ensure sustainability of the natural environment and human populations.

4. METHODS

4.1 INTRODUCTION

This chapter outlines the key methods used in the acquisition and analysis of data in this study. Palaeoenvironmental studies have been of global interest over the past century, through which many standard methods have been developed. Using these standard methods where possible allows for reproducible experiments, but also for a more accurate comparison between different studies. For this reason, standard methods for pollen and diatom sample preparation, microscopy and statistics were used. The fieldwork involved a number of logistical constraints due to difficulty in accessing sites, and the requirement of permits. It was therefore not feasible to use the well-established fieldwork methods, but rather a more creative approach to sediment extraction was developed. The methods used were based on work undertaken in similar environmental settings elsewhere, and precautions were taken to ensure that the extracted sediment samples received the minimum possible contamination. This chapter begins with a justification for the selection of the study sites for the study. Further details on the contemporary environments of each of the study sites can be found in the *Regional Setting* chapter. Following this are the fieldwork methods undertaken, the laboratory procedures, and the methods of statistical analysis.

4.2 STUDY SITE SELECTION

The paucity of research directly exploring the palaeoclimatic history of eastern Lesotho provides considerable choice in site selection for this study (Grab et al., 2005). While the potential for palaeoenvironmental work in southern Africa has been limited largely by arid environments, and a consequent lack of sites with well-preserved proxy records (Livingstone, 1975; Scott, 1989; Neumann et al., 2008), eastern Lesotho has sufficient precipitation to support a large network of wetland systems (Schwabe, 1995; Grab, 2010). Bog systems similar to those in eastern Lesotho have been documented as maintaining particularly well-preserved pollen and diatom assemblages, and reflect temporally constrained local climatic and environmental changes (Aaby, 1976; Booth & Jackson, 2003; Langdon et al., 2003). The high altitude of the eastern Lesotho region, and the considerable

altitudinal variation within this highland area, presents the need to improve the understanding of climatic and environmental lapse rates, both contemporary and past. Alpine regions also facilitate the investigation into differing altitudinal rates of species' relocation during periods of climate change (Van Zinderen Bakker & Coetzee, 1988). As a consequence it was decided that sites with a considerable altitudinal range should be selected to quantify these high altitude lapse rates, to detect the past altitudinal ranges of plant species, and to facilitate improved comparisons with lower altitude sites surrounding eastern Lesotho.

The first two study sites selected therefore are both bog systems, separated by an altitude of 400m (2,900m.asl at Sani Valley and 3,400m.asl at Mafadi Wetland), and a distance of 27km. The lower of the two sites is located in the Sani Valley, in close proximity to the Sani Top border post. Sani Valley is relatively easy to access by 4x4, allowing for experimentation with different field methods. The chosen site is a slightly raised bog system, which due to artificial piping of the spring, has experienced rapid erosion over recent years, exposing a 1.2m deep gully wall to core (*Figure 4.1*). The site has been the focus of previous environmental research, with thorough documentation of contemporary flora and fauna (Carbutt, 2004; Schwaibold & Pillay, 2006; Mokotjomela et al., 2009). This provides an ideal location for Holocene palynological work, as comparisons with the contemporary species are possible. Sani Top has also been the focus of contemporary climate studies over recent decades, providing the potential for valuable comparisons with current climate patterns (Preston-Whyte, 1972; Grab, 2005; Nel & Sumner, 2004, 2008; Mpholo et al., 2012). Similarly detailed records of contemporary vegetation (Killick, 1978; Boelhouwers & Hall, 1990; Grab 1994; Grab et al., 1999), and both contemporary and palaeogeomorphological features indicative of frost conditions (Boelhowers et al., 2002; Grab, 2010) have been published. Situated at the foot of a range of hills, the study site is well protected from wind, reducing the contamination of pollen from adjacent regions (*Figure 4.1*).

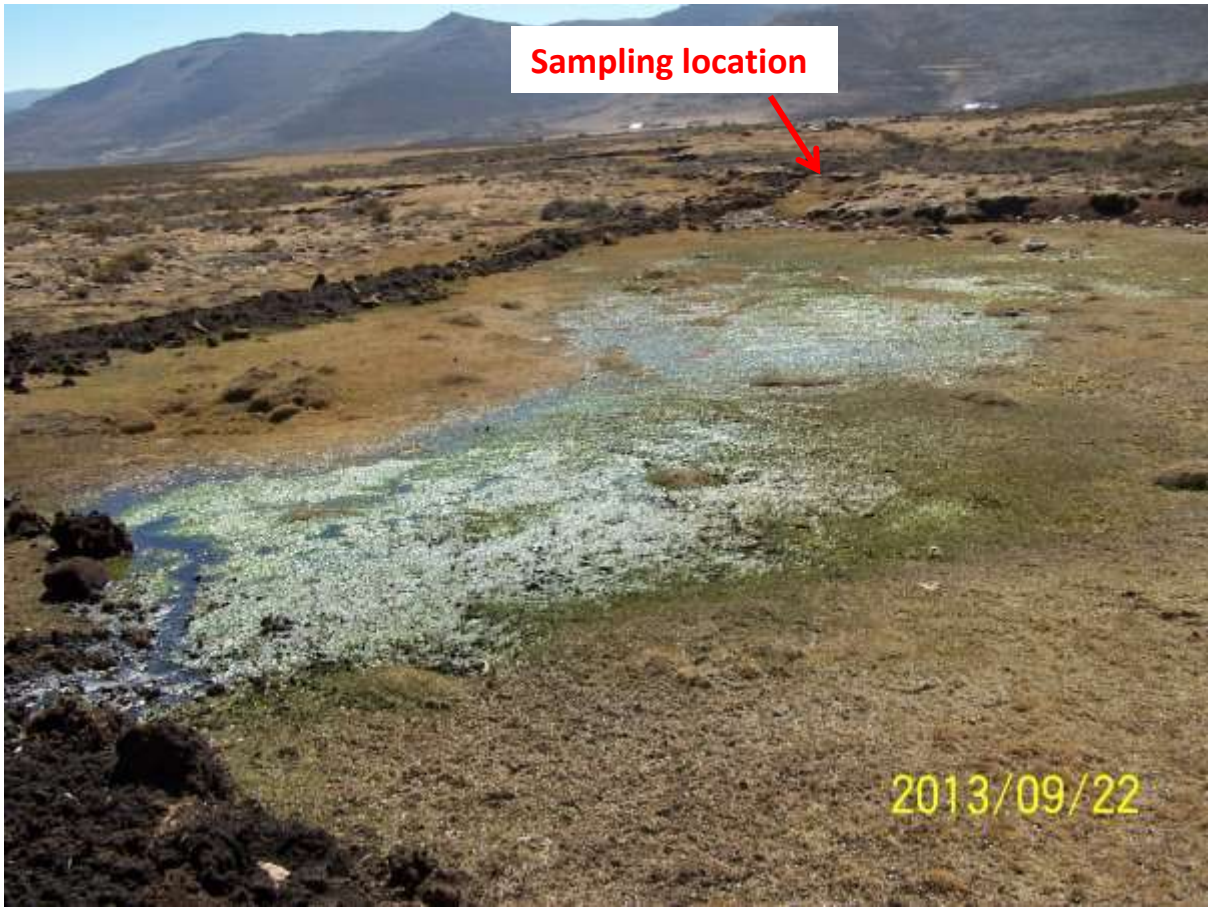


Figure 4.1: The Sani Valley sampling site.

The second bog site is located adjacent to Mafadi Summit. At an altitude of 3,400m.asl the site is southern Africa's highest wetland, and thus provides an invaluable palaeoenvironmental record for southern Africa. Mafadi Wetland is situated within a large depression, surrounded by hills on three sides, therefore is similarly well suited for collecting highly representative local pollen (*Figure 4.2*). Together with the pollen record from the Sani Valley site, this facilitates comparisons of altitudinal shifts in plant communities during periods of climatic change. In addition to the pollen record, the sediment profile at Mafadi Wetland has thick diatomite horizons (*Figure 4.2*), which are rare for both the Lesotho alpine region, and the broader southern African landscape. Diatoms provide a second palaeoenvironmental proxy, from which the moisture regime of the Holocene can be reconstructed. Finally, due to its high altitude, a number of previous studies have been undertaken on the palaeogeomorphology of Mafadi Summit (Grab, 1996a, 1999, 2002a,c; Grab et al., 2009). Conducting a multi-proxy environmental reconstruction has the potential to contribute to many of the debates on the timing and

nature of past climate changes that the palaeogeomorphological studies in the region have raised (Boelhouwers & Meiklejohn, 2002).



Figure 4.2: The Mafadi Wetland sampling site, marked by white diatomite beds.

Both of the bog sites revealed thick coarse gravel horizons at a depth of just over 100cm, which prevented deeper coring. It was consequently decided that there would be value in sampling from a third site with a considerably deeper sediment profile, so that any climate and environmental fluctuations observed in the shorter records could be understood within patterns of longer term Holocene change. The most extensively documented deep sediment profiles from eastern Lesotho were investigated by Marker (1994). This system of deep incised gully walls in a set of three valleys of the Sekhokong Mountains was classified by Marker (1994, 1995, 1998) based on sediment properties signifying changes in rainfall volumes. However, as few age-dates were obtained, and no environmental proxies were used, the climate inferences could not be further validated. Situated approximately 1km from the Sani Valley site, the Sekhokong gully walls, reaching a depth of over 5m, provide an

ideal site against which the late Holocene results from the other two sites can be compared (*Figure 4.3*). The contemporary vegetation of the site has been documented in detail, as has the nature of the erosion of the gully system and glacial moraine features (Grab & Deschamps, 2004; Deschamps, 2006; Mills et al., 2009b). Similar to the Sani Valley site, this facilitates high accuracy comparisons between past and present vegetation, and allows for this study to be situated within the broader environmental research in the region.

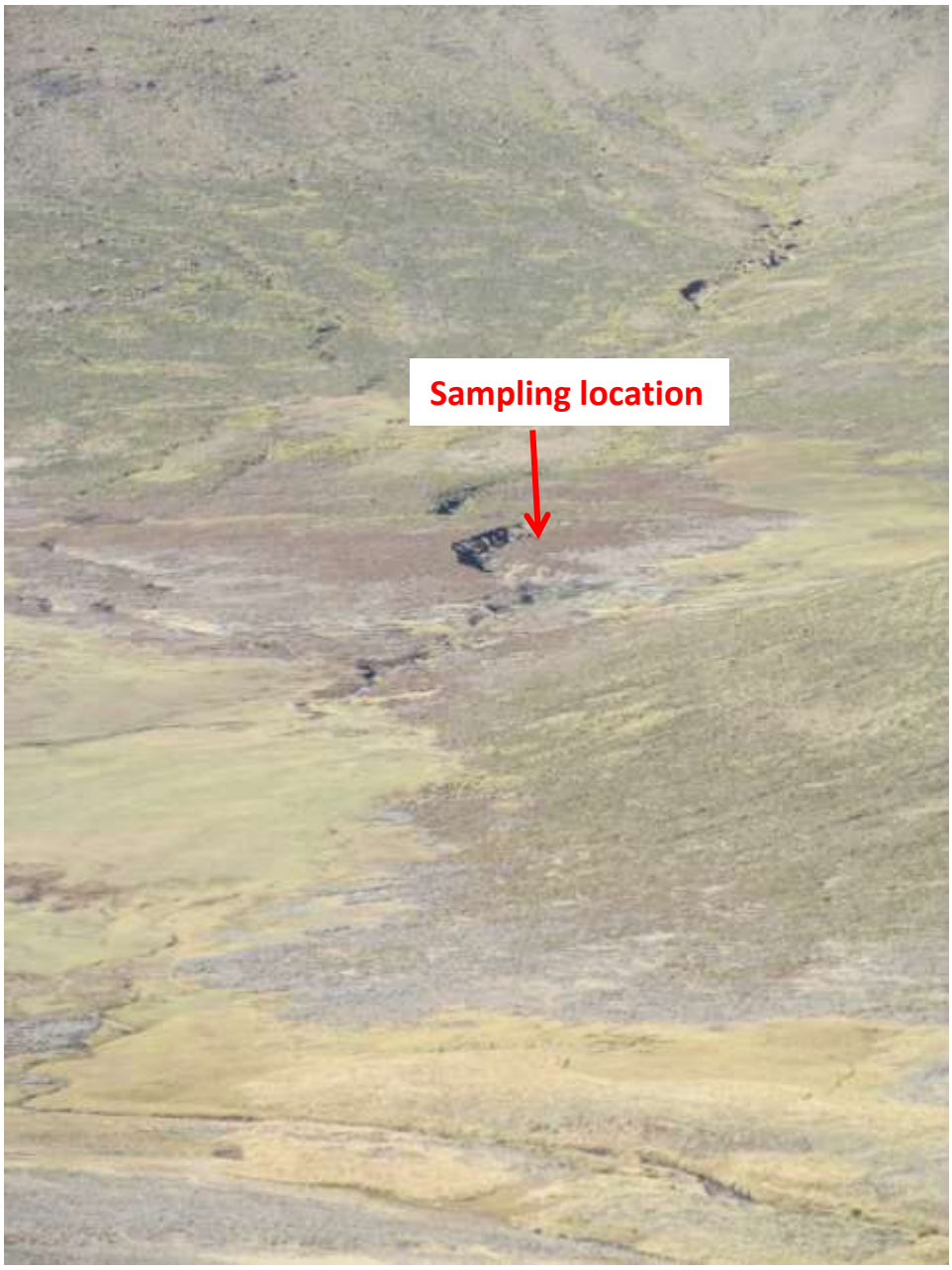


Figure 4.3: The Sekhokong sampling site.

4.3 Field Work

Field work for this study was undertaken during three field trips to Lesotho; one to each of the study sites. The primary aim of the fieldtrips was to acquire sediment profiles of a minimum of 100cm depth, from locations at the aforementioned study sites, which were likely to contain well preserved proxy material. GPS co-ordinates were taken for each of the coring locations using a Garmin® eTrex® 20. Elevation was obtained both from the GPS, and an altimeter calibrated at the nearest spot height at each site. Due to poor accessibility of the sites, equipment was limited to items that could be carried while hiking.

Due to the nature of the sediment types at the three sites, and the restrictions in transporting equipment, experimental and investigational work had to be undertaken in order to determine the most suitable coring method. Vibracorers, which are used extensively in palaeoecological work in South Africa (cf. Meadows et al., 1996; Baxter & Meadows, 1999; Meadows & Baxter, 2001; Carr et al., 2006; Norström et al. 2009; Quick, 2013), were not suitable due to their size and weight. Furthermore, the soft peat found at the Sani Valley site would have experienced considerable compression in using a Vibracorer for extraction, resulting in a disturbed sediment profile (Norström et al., 2009). Similar problems of disturbance in using the Vibracorer would have been experienced when extracting the powdery diatomite from the Mafadi Wetland site. Another popular coring method in South Africa utilises manual Russian Corers (cf. Finch & Hill, 2008; Ekblom & Gillson, 2010; Norström et al., 2012). As this instrument is considerably smaller and lighter than the Vibracorer, we took it into the field for experimentation. The spongy peat material, however, prevented the Russian Corer from being drilled in to a depth of greater than 0.5m. Furthermore, the sticky clay components adhered to the sides of the corer when rotating the flange, resulting in considerable contamination of adjacent layers, and the sediment profiles extracted demonstrated evidence of substantial compression of sediments.

To achieve the extraction of uncontaminated, well preserved sediment profiles, while meeting the equipment weight and size restrictions, a method of extracting sediment from exposed gully walls was utilised at each of the three sites, as undertaken by Grab et al. (2005), described visually in Figure 4.4. The gully walls were prepared by digging vertically back from the gully wall to remove all surface material to prevent contamination, and to

provide a vertical profiling position (Grab et al., 2005). The first vertical centimetre of the newly cleaned face was then sliced away using a 10cm wide stainless steel scraper, to ensure that there was no contamination between individual sedimentary units (Grab et al., 2005; Grab & Mills, 2011). A series of photographs was then taken, with scale measures, to record the sediment profiles as they appeared in situ (Grab et al., 2005). The depth of each lamination was recorded and described (Grab et al., 2005).

Where the top material was relatively cohesive, a core was then extracted from behind this face (*Figure 4.4a*). These cores comprised 0.5m long 75mm diameter PVC tubes that were sliced in half longitudinally. The tube was hammered down into the sediment approximately 1cm behind the cleaned gully face (*Figure 4.4a*). The core was then extracted from the gully wall, and the face of the extracted core was cleaned by slicing away the surplus 1cm sediment, using the cleaned stainless steel scraper (*Figure 4.4a*). The profile in the sediment was compared with the cleaned sediment profile adjacent to the position of the extracted core. If the two profiles were consistent in depth and appearance of individual sedimentary units, the core was labelled with the site name and core number, wrapped in plastic 'clingwrap' to prevent contamination, and covered in aluminium foil for additional protection from sunlight (*Figure 4.4a*). If a core was not deemed to be consistent with the adjacent gully profile, or if it had any discontinuities (as often occurred when cores intercepted underlying ice rat burrows), the core would be discarded and another core extracted from an adjacent location to ensure that any disruption of the profile and bioturbation due to burrowing would be avoided (Schwaibold & Pillay, 2006; Grab, 2012).

In some cases, complete cores could not be extracted. This occurred in conditions in which the top layer of sediment was not cohesive, a thick layer at some depth was not cohesive, or a thick gravel lenses prevented coring. In these instances, sediments were extracted directly from the exposed gully face, as described by Grab et al. (2005) for the Tsoaing River basin in eastern Lesotho, and detailed in Figure 4.4b. The gully face was prepared as for the coring, but thereafter individual samples were extracted horizontally from the gully face and stored individually (*Figure 4.4b*).

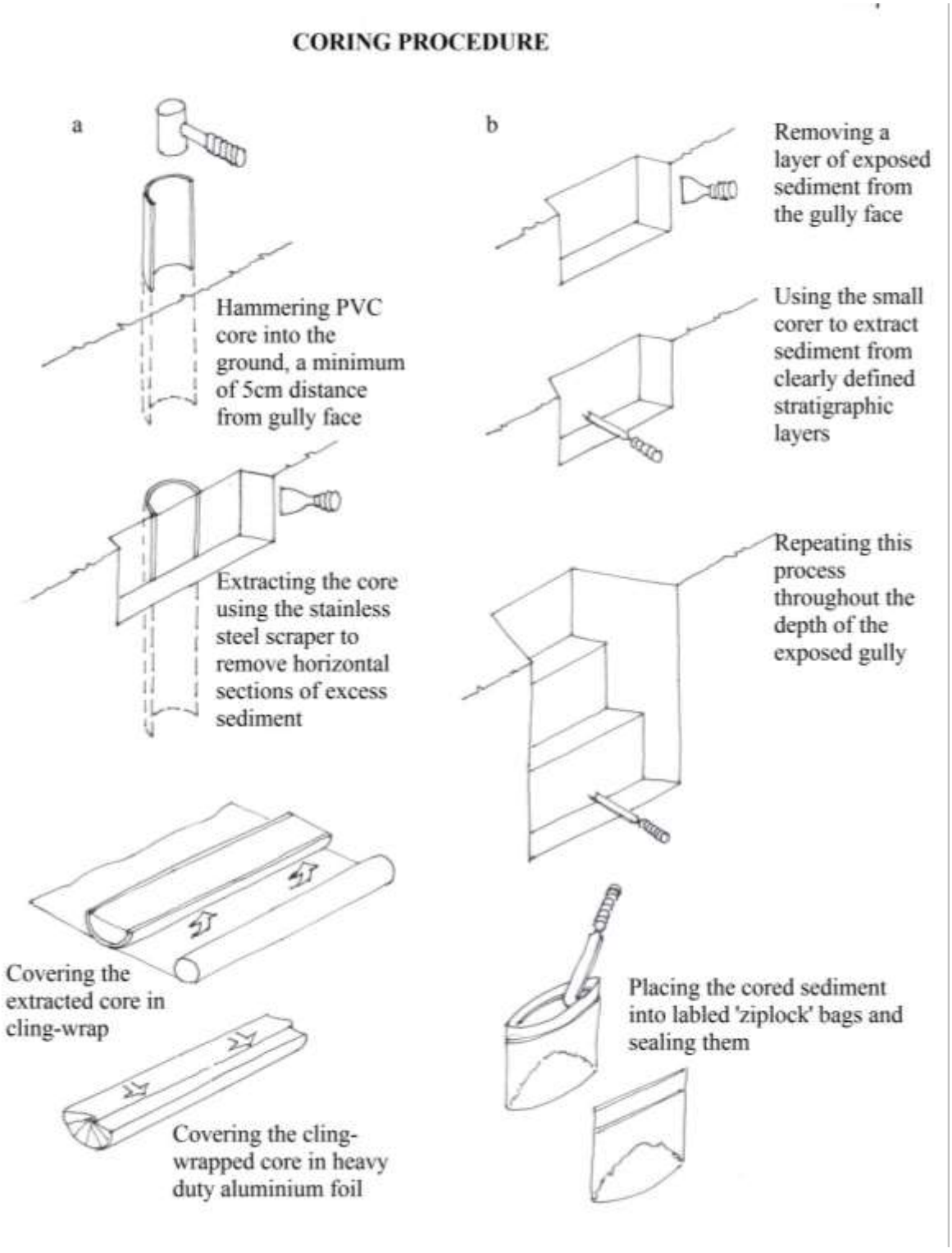


Figure 4.4: Coring procedure for (a) consolidated and (b) unconsolidated sediments.

At the Mafadi Wetland site, where cores extended to depths of only 1m, continuous sequences of sediment samples were extracted at consecutive depths of 3cm, using long, thin spatulas. The sediment was placed into “ziplock” bags, sealed, and labelled with the site

name, sample number and depth. At the Sekhokong site, a 5m gully wall was exposed. Consecutive sediment extraction of 3cm depths was not possible due to time constraints. Rather, the gully wall profile was recorded, with each of the sedimentary units measured for their depth and coded according to sediment type. A minimum of one sample was extracted from each distinct layer, with a minimum depth of 1cm. For layers of a depth of 7cm or more, two samples were collected, one at the bottom of the section and one at the top. For layers of a depth of 10cm or more, three samples were collected; from the top, middle and bottom. Where possible, samples represented a depth of 3cm or less. This resulted in a sampling frequency of 5-10cm throughout the profile. These sediment samples were likewise placed into "ziplock" bags, sealed, and labelled with the site name, sample number and depth. The cores and sample bags were refrigerated at temperatures below 4°C immediately on return to the laboratory, and remained refrigerated until subsampling could take place.

The first coring trip was undertaken at the Sani Valley site (29°33'34'' S, 29°14'36'' E) in September 2014. As the site is adjacent to the road, it was possible to test and compare different coring methods, from which the Russian Corer was found to be unsuitable. Two cores were extracted from the gully wall, at a distance of 3m apart. The first core, taken at the highest point in the gully system was 1.2m in length, sampled using three PVC tubes. The second core, taken at a more recently eroded section of the gully was only 1m in length, sampled using two PVC tubes. The second core did not provide further valuable stratigraphic or sedimentological information and hence was excluded from this study.

The second coring trip was conducted in April 2014, at the Mafadi Wetland site (29°11'59'' S, 29°21'03'' E). Due to its remote, high altitude location, Mafadi Wetland is not accessible by 4x4 vehicles. While the site can be accessed by hiking or on horseback, both methods were not feasible due to the weight of equipment required, and because this would not ensure sufficiently careful transportation of the cores and sediment samples collected. The trip was consequently made by helicopter. Due to the high altitude, the weight allowance was restrictive and thus the coring method developed at the Sani Valley site thus proved ideal. Three cores were obtained from the Mafadi Wetland site during the course of the fieldtrip. The first was cored from an incised riverbed, reaching a depth of 1.4m, collected in

a series of three PVC tubes (*Figure 4.5*). The second and third cores were taken at a diatomite outcrop located further up the hill, with samples extracted from an exposed face (*Figure 4.5*). The first of these two was located uphill, with the 1m profile terminating at the approximate altitude of the top of the second profile. These profiles were horizontally sampled continuously at 3cm intervals. Sediments from these horizontal excavations were stored in ziplock bags. Further down the profile, where material was more cohesive, cores were taken.

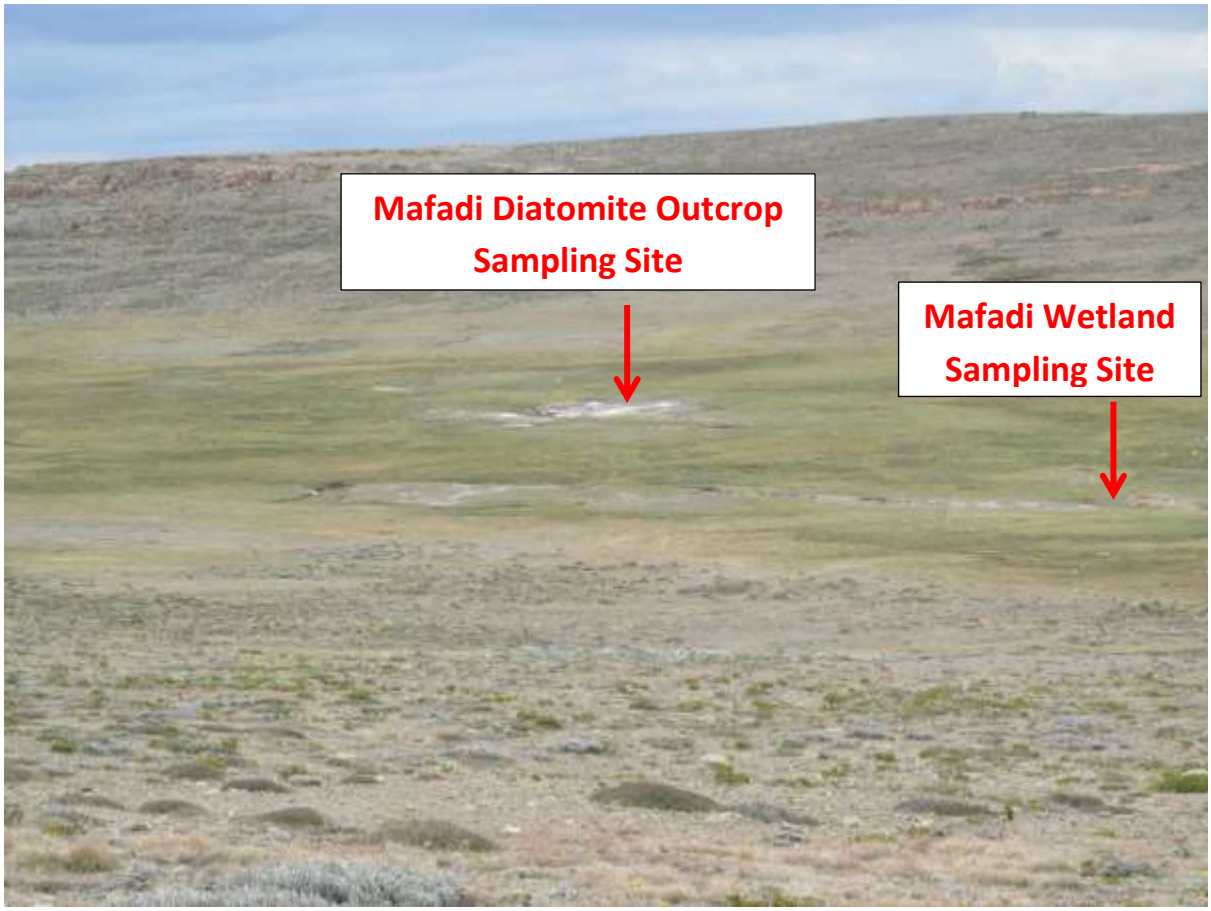


Figure 4.5: Position of the two sampling sites adjacent to Mafadi Summit, from which one core was taken at Mafadi Wetland site and two from Mafadi Diatomite site.

The third coring trip was undertaken in May 2014, at the Sekhokong site (29°36'13'' S, 29°15'32'' E). This site is not accessible by vehicles, and required a 3.5km hike traversing the hills separating the site from the Sani Top border post. The site revealed the incised river bed gully walls extending to a depth of 5m described by Marker (1994). Due to the thick gravel horizons, vertical coring using PVC tubes was not feasible. All samples were extracted

horizontally, as described for Mafadi Wetland. Samples were collected across the 5m profile depth, with a minimum frequency of one sample per distinct lamination, and additional samples in thick sedimentary units. This yielded a total of 44 samples from depths spanning the vertical extent of the gully.

As all of the fieldwork was undertaken within the Kingdom of Lesotho, permission for research was obtained from the Lesotho Government Department of the Environment. The conditions of the permission granted required each of the sites to be accessed by foot or helicopter; for samples removed from Lesotho to be of no economic value; and for all research findings to be shared with the Lesotho Government. To access the Mafadi Wetland site by helicopter, the flight path inevitably had to cross airspace over KwaZulu-Natal (KZN) Wildlife Protected Areas. We were required to apply for flight permission from KZN Wildlife, granted on condition that this would be a one-off flight, and that we mitigated any harm to the environment as best as possible, which involved reaching maximum flying altitude before flying over the protected area, and making the trip at a time outside of the peak tourism period. Helicopter flight times were further restricted by weather conditions, and required careful planning to ensure a safe flight with minimal damage to the natural environment.

4.4 Laboratory work

The sediment samples were subsampled for pollen, diatom and sediment analysis, and underwent AMS radiocarbon dating. To facilitate accurate comparison between different proxies, and the assignment of highly precise AMS dates, each subsample was divided into four sections and stored separately for each type of analysis. This ensured that all comparisons between proxies, together with the age-dates, would be for the same layer. These subsamples were stored in sealed glass test tubes and refrigerated at temperatures below 4°C, until they could be processed, to prevent decay and microbial activity (Faegri et al., 1989; Haberyan, 1987; Stager et al., 2003). All subsampling took place in a pressure controlled laboratory to prevent contamination from local contemporary pollen (Moore & Webb, 1978; Faegri et al., 1989).

For the cored profiles, subsamples were isolated using a scalpel to slice 2cm sections perpendicular to the core length, extracted at 2-5cm intervals. Any sediment that was in contact with either the PVC tube, or on the exposed face was removed using the scalpel and discarded to reduce the risk of contamination (Renberg, 1990). The scalpel was washed and rinsed with distilled water between each use to prevent contamination (Renberg, 1990). Each slice was then divided into four groups for each of the respective laboratory processes. The samples that were extracted from the gully face were stored individually from their extraction in the field and required no further sub-sampling. Rather, for each layer, sediments were transferred into four individual test tubes using a stainless steel spatula, sealed with rubber caps and refrigerated until analysis. The spatula was washed and rinsed with distilled water between samples.

All laboratory procedures for the AMS radiocarbon dating, sediment, pollen, and diatom, analyses were undertaken using standard methods. These are briefly outlined below, and explained in detail in *Appendix A.*

4.4.1 Age Determination

In order to quantify the time periods in which the environmental changes revealed by the diatoms, pollen and sediment characteristics took place, the chronology requires constraining. The age of the bottom of each core, and the age of sub-samples at various levels throughout the core similarly need to be independently determined, to use an age-depth model to understand the rate at which sediments have accumulated (Parnell et al., 2008, 2011; Blaauw, 2010). While a number of methods exist for determining the age of sediment through the proportion of isotopes that decay over time, the large number of peat samples and considerable percentage of organic material in the remaining samples, favoured the use of radiocarbon dating (Walker, 2005).

Vials containing between 1-3g of subsampled sediments from selected depths in the core were sent to *Beta Analytic* for AMS dating, and the calibration of dates. *Beta Analytic* was selected as it is an ISO 17025:2005 accredited company, ensuring high precision results. Dating on bulk organic matter rather than macro-plant remains was instructed for all samples to ensure consistency between sites with varying plant matter (Neumann et al.,

2010, 2014). While dating of intact macro-plant remains would potentially provide a more accurately constrained date, because these remains could not be identified, they risked representing contaminant material such as roots from a higher level in the core (Borojevic, 2011). Dating was undertaken in two stages due to funding constraints, and the benefits of establishing range-finder dates. In the first stage, basal dates were acquired for the two Mafadi profiles, the Sani Valley profile and the Sekhokong profile to determine the period of the Holocene covered at each site (*Table 4.1*). Thereafter, with an understanding of the time period in consideration, a second set of dates was acquired for approximate middle and top sections of each of the cores, and for depths at which abrupt environmental changes are indicated by the pollen, diatom and sediment analysis (*Table 4.1*). The depth of the samples for which dates were obtained is outlined in *Table 4.1*.

Table 4.1: Samples for which AMS dates were obtained.

Site	Sample Number	Mid-point depth (cm)	Type of Accumulation
Sani Valley	S10	18	Peat
	S13	38	Peat
	S5	57	Peat
	S21	78	Peat
	S27	107	Peat
Mafadi Wetland and Diatomite Bed	M7	19	Diatomite rich peat
	M13	41	Diatomite rich clay
	M19	59	Diatomite rich clay
	M32	84	Diatomite rich sand
	M38	103	Diatomite rich sand and gravel
	M77	* bottom of diatomite bed	Diatomite rich peat
Sekhokong	SK3	16.5	Peat
	SK7	45.5	Organic rich clay
	SK11	75.5	Peat
	SK14	107.5	Iron rich sand and gravel
	SK21	134.5	Organic rich clay
	SK25	202.5	Clay
	SK30	267.5	Peat
	SK31	287.5	Peat
	SK34	327.5	Peat
	SK38	412.5	Clay
	SK41	472.5	Peat

4.4.2 Sediment Analysis

For use as a third environmental proxy, sediments were classified on the basis of colour, organic content, carbonate content and particle size, in order to relate their composition and weathering processes to periods of distinct climatic change. In particular, sedimentary units of distinct sediment properties can demonstrate shifts in rainfall amount, intensity, temperature and depositional environment, and have the potential to corroborate the

findings of pollen and diatom analysis (Meadows, 1988; Heiri et al., 2001; Meyers & Teranes, 2001; Bell & Walker, 2013). Furthermore, as the majority of the palaeoclimatological work undertaken in eastern Lesotho adopted either a geomorphological or archaeological approach, the sediment record provides a crucial link between this work and previous studies (Mitchell, 1996a; Marker, 1998).

The sediment types that comprise each of the subsamples were first classified in terms of colour. This was done by means of comparison against the Munsell colour chart (Deaton, 1987; Rossel et al., 2006). Due to the high moisture content of samples derived from wetlands – common to all samples in this study – there was likely to be considerable difference in colour between the 'wet samples' as they originate from the field, and the 'dry samples' that have been oven-dried. For consistency with existing studies in eastern Lesotho, and following standard methods, Munsell colour chart comparisons were determined using wet samples, and thereafter sediment samples were oven dried (Marker, 1994; Rossel et al., 2006).

The second level of sediment classification is made on the basis of the organic content of each subsample (Heiri et al., 2001; Meyers & Teranes, 2001). The total organic content of the sample is approximated through the process of LOI, whereby the organic content of each sediment subsample is burned off, and the weight difference measured (Dean, 1999; Heiri et al., 2001). The method used for LOI follows the discussion of Heiri et al. (2001), ensuring reproducible and comparable results and is outlined in detail in *Appendix A.3*. The difference in weights, once the weight of the crucible has been accounted for, represents the proportion of the organic content:

$$LOI_{550} = \frac{Dw_{105} - Dw_{550}}{Dw_{105}} \; x \; 100$$

For southern Africa, subsamples with a high organic content typically signify humid periods, while samples with lower organic content tend to accumulate during drier periods (Meadows, 1988; Marker, 1994; Meyers & Teranes, 2001). The change in percentage

organic content with depth for each core can thus tentatively be used as a proxy for changes in moisture levels (Meadows 1988; Meyers & Teranes, 2001).

In addition to determining the organic content of sediment samples, a further step of LOI can be undertaken to quantify the weight of carbonates (Dean, 1999; Heiri et al., 2001). During the diatom preparation, fizzing that occurred when HCl was added to many of the samples indicated the presence of carbonates, and thus warranted this step (Battarbee & Kneen, 1982). To determine the percentage carbonate content, the mass of the carbonate in the sample is first estimated, assuming a molecular mass for CO_2 of 44g.mol^{-1} and for CO_3^{2-} of 60g.mol^{-1} (Dean, 1999; Heiri et al., 2001). The percentage carbonate in the sample is then the mass of carbonates divided by the total dry mass:

$$LOI_{950} = \frac{Mass_{CO_3{}^{2-}}}{Dw_{105}}\ x\ 100$$

$$Mass_{CO_3{}^{2-}} = Dw_{550} - Dw_{950}\ x\ 1.36$$

The percentage carbonate composition in the sediment provides information on both the moisture availability, and the moisture pH (Dean, 1999). Changes in carbonate percentage throughout the core are thus of interest in corroborating the results from diatom analysis.

The third classification is made on the basis of particle size, measured through laser diffraction using the Malvern Mastersizer 3000©. It should be noted that the particle sizes measured include both the abiotic sediments, and the fossilised biotic components including diatoms. Sediments that have undergone LOI at 550°C and 950°C are immersed in water, subjected to ultrasonic stirring to disperse clays and other agglomerated sediments, and flow past a set of lasers that measure the resultant refraction of light in the red and blue wavelengths (Konert & Vandenberghe, 1997; Sperazza et al., 2004; Ryżak & Bieganowski, 2011). The scattering of light as the sediments pass the lasers is measured and converted into a measure of the number of particles within a particular size category (Ryżak & Bieganowski, 2011). To ensure consistency between measurements and facilitate

comparisons of particle size throughout the sediment cores, a single Standard Operating Procedure (SOP) was developed and used for all of the samples from each of the sites (Ryżak & Bieganowski, 2011). The SOP for the study was based on experimental manual runs using samples from both the Mafadi Diatomite samples and the Sekhokong samples, to ensure the most consistent set of readings across both. Advice on the use and duration of the ultrasonic phase was obtained in consultation with technicians from Malvern (Truter pers comm., 2014). The details of the SOP are listed in *Appendix A.3*. The Mastersizer size outputs were subsequently analysed for each of the subsamples within each profile, to determine changes in particle size and associated sedimentation processes over the respective periods of the Holocene (Briggs, 1977). A flow-chart of the sediment analysis is presented in *Figure 4.6*, with a detailed description in *Appendix A.3*.

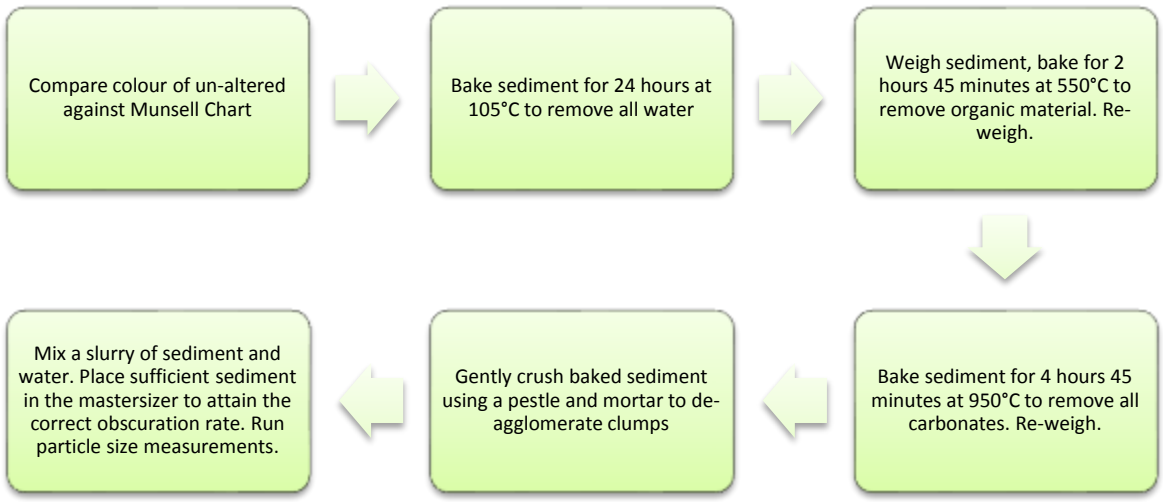


Figure 4.6: Summarised process of sediment preparation undertaken to determine colour, organic and carbonate content, and particle size distribution.

4.4.3 Pollen Preparation

Pollen preparation was undertaken in the laboratories of the Evolutionary Studies Institute at the University of the Witwatersrand, Johannesburg. The isolation of pollen grains required the removal and/or dissolution of all non-pollen components of the sediment subsample (Faegri et al., 1989). The methods undertaken for the pollen isolation are standard, as described by Erdtman (1943), Moore and Webb (1978), Faegri et al. (1989) and Bradley (1999), and adapted by the University of the Free State and the University of the

Witwatersrand to be best suited to southern African sediments (Scott, 1982a). Two slides were prepared per sub-sample to ensure that there were sufficient pollen grains from each subsample for counting, for all non-sterile layers. A summarised flow-chart of the procedure is presented in *Figure 4.7*, and a detailed step-by-step procedure is listed in *Appendix A.1*.

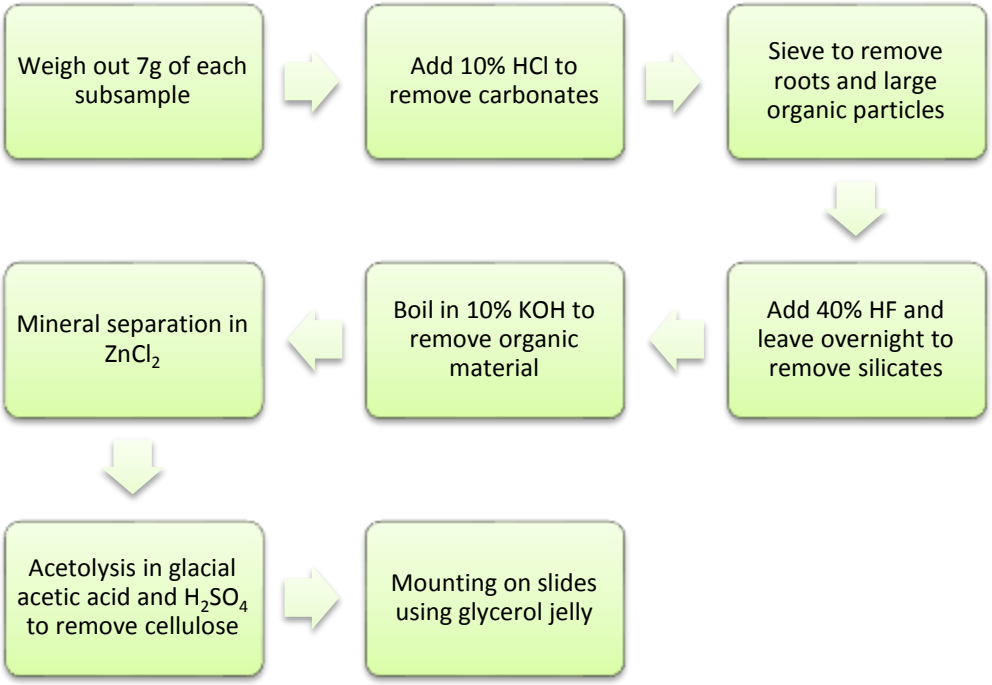


Figure 4.7: Summarised procedure of pollen preparation (after Faegri et al., 1989).

Once mounted on slides, the pollen grains can be identified on the basis of morphology and sculpturing using a light microscope (Faegri et al., 1989; Bradley, 1999). General scanning for pollen grains was undertaken at a magnification of 400x, while the identification of pollen grains and photography occasionally required further magnification under oil immersion at 1000x. For each subsample a minimum of 250 pollen grains were counted in transects of the slide to ensure accurate representation (Bradley, 1999). If there were fewer than 250 pollen grains on one slide, the second slide from that sample was counted, and this was recorded. Pollen grains of each taxon counted were photographed to facilitate identification. In cases where pollen grains could not be identified, the photomicrographs were used to consult with pollen experts, and compare with more complete pollen reference collections.

4.4.4 Diatom Preparation

Diatom preparation, and all diatom work for this thesis, was undertaken in the laboratories of the Department of Geography at University College London. Methods for diatom isolation for identification similarly followed standard procedures, as outlined in Setty (1966), Bolli et al. (1989) and Andren et al. (2007), adapted by University College London for the use of a water bath for the simultaneous preparation of large numbers of samples (Renberg, 1990; Battarbee et al. 2001), and to include the use of microsphere markers to determine diatom concentration (Battarbee & Kneen, 1982). For some of the organic-rich samples a second set of slides was produced with the solutions diluted by 10x to prevent crowding of slides by diatoms and clay particles, facilitating more accurate identification. A summarised flow chart of the procedure is outlined in *Figure 4.8*, and a detailed step-by-step method appears in *Appendix A.2*.

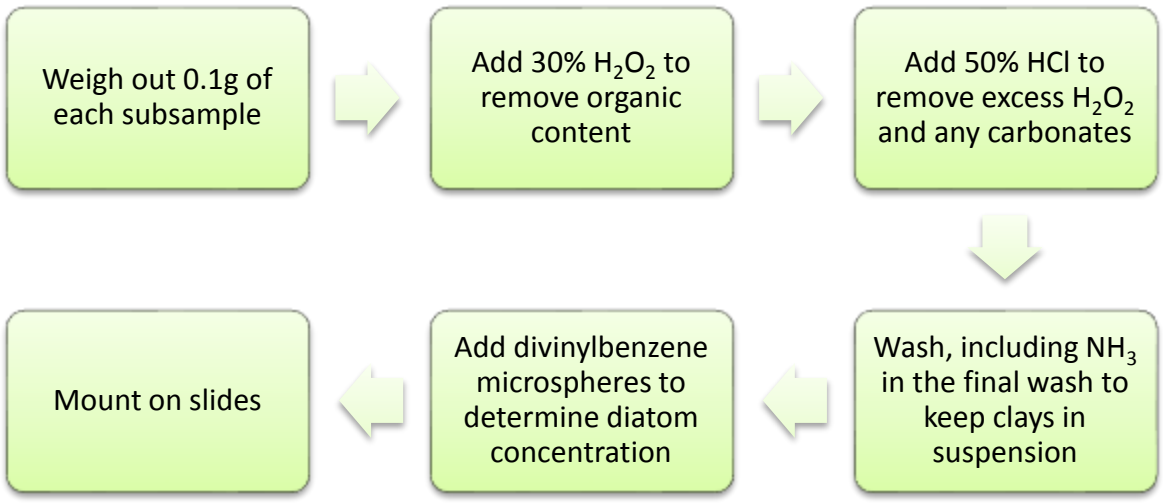


Figure 4.8: Summarised process of diatom preparation undertaken.

Identification was undertaken using a light microscope, with bright-field phase contrast oil immersion at a magnification of 1000x. Particular note was taken of the length, breadth, frequency of striae, striae pattern, and the presence of a raphe (Barber & Haworth, 1981; Battarbee et al., 2001). This allowed for discrimination to be made between species in the identification process. A minimum of 300 diatom valves were counted per sample, in equally spaced transects across the slide. Identification was made to species level, with comparison made to international diatom reference material (Patrick & Reimer, 1975; Krammer &

Lange-Bertalot, 1986; Snoeijs & Balashova, 1998; Camburn & Charles, 2000; Kramer, 2002), and more local reference texts for southern Africa (Schoeman & Archibald, 1976; Harding & Taylor, 2011; Matlala et al., 2011) and Lesotho (Schoeman, 1973) where possible. In instances when species of a similar morphology but different taxonomy were found in the international and local reference material, preference was made for the local collections. While counting the 300 diatom valves per sample, the number of microspheres observed simultaneously was recorded, to facilitate the calculation of diatom concentration. This would be useful to note if notable differences in diatom concentration were observed within profiles, or between the three sites.

$$Diatom\ Concentration = \frac{\#\ microspheres\ introduced\ x\ \#\ diatoms\ counted}{\#\ microspheres\ counted}$$

4.5 Statistical Analysis

4.5.1 Statistical Analysis of Diatom and Pollen Results

The aim of statistical analysis in this research is to determine periods in which the environmental and/or climatic conditions have remained stable, and those in which notable change has occurred (Finkelstein et al., 2005; Smol et al., 2012). This can be achieved through clustering samples that demonstrate the greatest similarity in diatom or pollen species distributions (Stevenson & Pan, 2004; Legendre & Birks, 2012a). The two principal methods used to achieve this are the investigation of gradients of change through ordination, and the clustering of adjacent samples using CONISS (Constrained Incremental Sum of Squares) (Grimm, 1987; Stevenson & Pan, 2004; Finkelstein et al., 2005). From these analyses, periods of environmental change can be compared with local, regional and international recorded periods of change, and the causal factors can be explored (Finkelstein et al., 2005). Through plotting the relative abundance of pollen and diatom species in each of the samples, these periods of change and clusters of samples can be visually explored. All statistical analysis has been undertaken using the statistical coding interface R (Venables & Smith, 2015), with the exception of the diatom and pollen plots produced using C2 (Juggins, 2007).

In preparation for the statistical analysis, all species that occur with a frequency of less than 2% throughout the cores for a particular site are removed from the counts for that site to prevent the disproportionate influence of rare species (Mackay et al., 2012; Simpson & Birks, 2012). The mid-point depth for each sample is then added to the table, in place of the depth range. For the indirect ordination and clustering, a square root transformation is performed on the dataset prior to the analysis to down-weight any groups of species with disproportionately high species counts (Lepš & Šmilauer, 2003; Legendre & Birks, 2012b). This ensures that species with consistently high scores do not unduly influence the environmental gradient, through reducing those by a proportionally larger amount than the smaller species (Legendre & Birks, 2012b). It also assists in better approximating a Gaussian distribution before analysis commences (Lepš & Šmilauer, 2003; Legendre & Birks, 2012b).

4.5.1.1 Indirect Ordination Methods

Ordination of vegetation samples refers to their arrangement in a two dimensional space relative to each other, based on similarity in species composition and potentially together with the associated environmental conditions (Kent & Coker, 1992; Stevenson & Pan 2004). The more frequently used form of ordination is that of indirect ordination, or gradient analysis, whereby the variation in samples is studied independent of environmental data (Kent & Coker, 1992; Stevenson & Pan, 2004; Legendre & Birks, 2012b). This method is suitable for palaeoenvironmental research in which changes in species composition over time are used to infer the environmental drivers (Lepš & Šmilauer, 2003; Stevenson & Pan, 2004).

Ordination plots all of the samples in a three-dimensional space, on a set of axes. These axes are produced in descending order of importance, with the first axis explaining more of the variation in samples than all subsequent axes, and placed as a trajectory through the longest dimension of the three-dimensional cloud of data points (Legendre & Birks, 2012b). The second axis explains less than the first, but more than those subsequent to the second, and so forth, to a number of axes smaller than or equal to the number of samples (Legendre & Birks, 2012b). The distances between points on the resultant graph can then be taken as a measure of their similarity, with points closer together demonstrating a large similarity in

species composition, those further apart suggesting a large dissimilarity (Legendre & Birks, 2012b). For Principal Components Analysis (PCA), points separated by an angle of 180° behave in an opposite manner to one another, whereas points separated by an angle of 90° should have no similarity.

To determine the appropriate indirect ordination method, it is first necessary to determine whether the species data are linear or unimodal in nature (Ter Braak, 1987; Lepš & Šmilauer, 2003). Unimodal data tend to be observed along long environmental gradients, and demonstrate a low diversity of each sample (alpha-diversity), but a large change in species over the environmental gradient (beta-diversity). By contrast, linear data would more likely be ordered along a shorter environmental gradient, would have high species diversity within each sample, but would demonstrate far less of a change between samples. For unimodal data, Detrended Correspondence Analysis (DCA) would be used, while for linear data, PCA would be more appropriate (Lepš & Šmilauer, 2003). For DCA, a process of 'detrending' is undertaken to remove the arch effect, which as a function of the quadratic relationship between the first and second axis, has the potential to produce a false signal (Birks et al, 2012). Detrending is undertaken through dividing the first axis into a number of segments, and recalculating the second axis scores for each segment to average zero (Legendre & Birks, 2012b). To determine whether the data are unimodal or linear, and consequently to select the appropriate ordination method, the amount of species change between samples needs to be determined by running DCA, and examining the beta-diversity scores produced in SD units (Mackay et al., 2013). If the first axis of the ordination results has a beta-diversity value of four or more SD units, the data are likely to be unimodal, and DCA is the appropriate method (Mackay et al., 2013). If the beta-diversity values for the first axis are less than three SD units, then the data are likely linear, and PCA would be a more appropriate method (Mackay et al., 2013).

Once the PCA or DCA is complete, bi-plots are produced (Lepš & Šmilauer, 2003). These plots situate the data points in two-dimensional space relative to the first and second principal components (Lepš & Šmilauer, 2003). The species names are then overlaid, based on their species scores relative to the first and second principal components (Lepš & Šmilauer, 2003). This facilitates visual exploration of the clustering of samples, and enables

the species dominant in those clusters to be identified simultaneously. In addition to the bi-plots, the sample scores for principal components 1 and 2 are recorded and plotted in the diatom and pollen diagrams to demonstrate the periods of change in the diatom or pollen communities at that site over the study period (Legendre & Birks, 2012b). Stratigraphic diagrams with the principal component 1 and 2 sample scores for pollen and diatoms are then plotted for each site adjacent to the sediment properties, to explore the multi-proxy responses in the environmental changes (Mackay et al., 2013). Finally, the species scores are extracted, and used to order the list of species for diatom and pollen stratigraphic diagrams (Bangs et al., 2000; Antoniades et al., 2005; Juggins, 2007).

4.5.1.1 CLUSTERING

The aim of clustering in palaeoenvironmental datasets is to partition groups of samples according to similarity, in order to identify clearly defined periods of environmental change to explore, and to examine the relationships between these groups (Legendre & Birks, 2012a). Unlike discrimination, in which the number of groups is known a priori, in classification the number of optimal groups is unknown, resulting in unsupervised pattern recognition (Finkelstein et al., 2005; Legendre & Birks, 2012a). There remains debate in the palaeo-scientific community as to whether unsupervised pattern recognition should be preferred over a scientist's visual pattern recognition based on expert knowledge of the location and species (Lamentowicz et al., 2005). However, the lack of human bias in classification allows for reproducibility in experiments which is particularly valuable when studying multiple proxies at more than one study site (Finkelstein et al., 2005).

For the purpose of this study, hierarchical agglomerative clustering is utilised, which involves fusing individual samples to form groups, and small groups to form larger groups, with local similarity prevailing over larger differences, and then arranging those groups on a hierarchical system, displayed as a dendrogram (Finkelstein et al., 2005; Legendre & Birks, 2012a). This study uses the clustering method most common in palaeoecological studies – CONISS (Grimm, 1987; Legendre & Birks, 2012a). CONISS has the advantage of requiring the samples to remain in their original order, which is imperative when working with core data in which clusters need to be true to the depth of samples (Legendre & Birks, 2012a). CONISS

clustering is paired with the Wards minimum variance algorithm distance measure between samples (Finkelstein et al., 2005; Kaufman & Rousseeuw, 2009). To determine the optimal number of groups, silhouette plots are created for all possible group numbers (Rousseeuw, 1987; Kaufman & Rousseeuw, 2009). These plots represent the silhouette width, a measure of each sample and all other samples in the cluster compared to the same measure for samples in the nearest cluster. A silhouette plot with values closest to 1 suggest an optimal number of clusters, while negative values suggest that samples are currently in the wrong cluster, and values close to 0 suggest that samples may fall between clusters (Rousseeuw, 1987; Kaufman & Rousseeuw, 2009). The dendrogram produced by CONISS is then colour-coded to delineate the separation of clusters, and this colour coding is then added to those samples in the PCA/DCA biplot, to provide a complementary analysis (Kent & Coker, 1992; Finkelstein et al., 2005).

4.5.1.3 Visual Representation

Standard pollen and diatom plots are produced using C2, plotting the counts of each species of diatom/pollen against depth throughout the core (Juggins, 2007). The sample scores from the first and second principal components from the PCA/DCA are plotted to indicate periods of change in species composition (Legendre & Birks, 2012b; Mackay et al., 2013). The species are arranged according to their species scores in order to demonstrate a clear gradient of change (Bangs et al., 2000; Antoniades et al., 2005). Zones are demonstrated on the graph on the basis of the CONISS cluster analysis for each of the proxies (Finkelstein et al., 2005). The stratigraphic diagrams in the *Discussion Chapter* are plotted against age to facilitate comparison with studies in adjacent regions, with species grouped according to their ecological traits to enhance environmental inferences and further facilitate comparison with existing published palaeoenvironmental reconstructions for the region.

4.5.2 Statistical Analysis of Sediment Results

Once the percentage organic content and carbonate content of each of the subsamples has been calculated, the change in their percentage throughout the total depth of the core can be explored. This can be done visually through plotting the percentage composition against depth using the programme C2 as for the pollen and diatom counts (Juggins, 2007). Unified

periods of change in organic and carbonate composition are then calculated using CONISS (Grimm, 1987).

Statistical analysis of the sediment particle size output from the Mastersizer involves determining the nature of the distribution of sediment sizes within each subsample, as well as the changes in particle sizes throughout each core (Marker, 1994; Masselink et al., 2014). Sediment samples tend to have a log-normal distribution based on the large range in particle sizes from a few microns for clays through to a couple of centimetres for boulders (Briggs, 1977; Masselink et al., 2014), and are thus commonly classified according to the Phi Scale (*Table 4.2*), defined by:

$$\Phi = -\log_2 d$$

(where d = diameter of particle)

As a negative logarithmic scale, coarsest sizes have the lowest values, and a one unit increase is equivalent to reducing the particle size by 50% (Briggs, 1977; *Table 4.2*). This not only means that the differences in one unit are of considerable range in absolute sizes, but that a small change in a small grain size is viewed as equivalent to a relatively large change in a large grain size, which is more accurate given the implications on weathering processes (Briggs, 1977).

Key sediment statistics describe the central tendency, and the scatter and non-normality of the log-normal distribution (Saarinen & Petterson, 2006). The central tendency of the sediment sample is described in terms of the mean (Briggs, 1977; Saarinen & Petterson, 2006). The mean is arithmetically calculated as the sum of the sizes of each measured particle, divided by the total number of particles (Saarinen & Petterson, 2006). The mean value is classified according to the Wentworth Scale, and increases in the mean reveal a sample with smaller particle sizes than a smaller mean would (Briggs, 1977; Masselink et al., 2014; *Table 4.2*). A sample can contain a range of particle sizes, and thus the mean alone is often of little value in determining long term changes in particle size, nor their associated depositional environment.

Table 4.2: Size grades of sedimentary particles (after Briggs, 1977[2], p. 56; Masselink et al., 2014[1], p. 107).

Phi size (ϕ)	Micrometers (µm)	Wentworth Scale[1]	Wentworth Scale[2]
-6.0	64 000.00		Cobbles
-5.5	44 800.00		
-5.0	32 000.00	Pebbles	Coarse gravel
-4.5	22 400.00		
-4.0	16 000.00		
-3.5	11 200.00		Medium gravel
-3.0	8 000.00		
-2.5	5 600.00		
-2.0	4 000.00	Granules	Fine gravel
-1.5	2 800.00		
-1.0	2 000.00		
-0.5	1 400.00		
0.0	1 000.00		Coarse sand
0.5	710.00		
1.0	500.00		
1.5	355.00	Sand	Medium sand
2.0	250.00		
2.5	180.00		
3.0	125.00		Fine sand
3.5	90.00		
4.0	63.00		
4.5	45.00		Coarse silt
5.0	32.00		
5.5	23.00	Silt	
6.0	16.00		Medium silt
6.5	11.00		
7.0	8.00		
7.5	5.50		Fine silt
8.0	4.00		
8.5	2.75		
9.0	2.00	Clay	
9.5	1.38		Clay
10.0	1.00		

Sorting is a measure of the scatter of the distribution, calculated as the standard deviation of the sample mean (Saarinen & Petterson, 2006; *Table 4.3*). A sample with a large sorting value would have a greater width of the distribution than normal, and would reflect poorly sorted sediments (Saarinen & Petterson, 2006). The sorting of a sample is related to the ability of the transporting agent to segregate its load according to size (Briggs, 1977).

$$Sorting = \sigma = \frac{\varphi_{84} - \varphi_{16}}{4} + \frac{\varphi_{95} - \varphi_{5}}{6.6}$$

Skewness is a measure of the symmetry of the distribution around the mean (Saarinen & Petterson, 2006; *Table 4.3*). For an absolutely normal distribution, the mean and median

would be located at the same point; the larger the difference between the mean and median the larger the skewness (Saarinen & Petterson, 2006).. Positively (or fine) skewed distributions have more smaller grained material than would be present in a normal distribution; negatively skewed (or coarse) distributions have more large grained material than in a normal distribution (Briggs, 1977; Saarinen & Petterson, 2006). The skewness of a sample is calculated:

$$Skewness = \frac{\varphi_{16}+\varphi_{84}-2\varphi_{50}}{2(\varphi_{84}-\varphi_{16})} + \frac{\varphi_{5}+\varphi_{95}-2\varphi_{50}}{2(\varphi_{95}-\varphi_{5})}$$

Kurtosis describes the height of the peak of the distribution (Saarinen & Petterson, 2006). A normal distribution is described as mesokurtic (Saarinen & Petterson, 2006; Masselink et al., 2014; *Table 4.3*). A distribution with a curve flatter than a normal distribution is referred to as playtykurtic, while one more peaked than normal is termed leptokurtic (Saarinen & Petterson, 2006; Masselink et al., 2014; *Table 4.3*). The kurtosis of a sample is calculated:

$$Kurtosis = \frac{\varphi_{95}+\varphi_{5}}{2.44(\varphi_{75}-\varphi_{25})}$$

Table 4.3: Descriptive terms for Soil Statistics (after Briggs, 1977).

Sorting (σ)		**Kurtosis**		**Skewness**	
<0.35	Very well sorted	<0.67	Very playtykurtic	-1.0 – -0.3	Very coarse skewed
0.35-0.50	Well sorted	0.67-0.90	Playtykurtic	-0.3 – -0.1	Coarse skewed
0.50-0.70	Moderately well sorted	0.90-1.11	Mesokurtic	-0.1 – 0.1	Symmetrical
0.70-1.00	Moderately sorted	1.11-1.50	Leptokurtic	0.1 – 0.3	Fine skewed
1.00-2.00	Poorly sorted	1.50-3.00	Very leptokurtic	0.3 – 1.0	Very fine skewed
2.00-4.00	Very poorly sorted	>3.00	Extremely leptokurtic		
>4.00	Extremely poorly sorted				

Biplots of these sediment statistics can be used to distinguish sediments that derive from different depositional environments. In particular, plots of skewness versus kurtosis can differentiate between fluvial and other depositional environments (Briggs, 1977).

In addition to statistics analysing the distribution of particle sizes for each subsample, the Malvern Mastersizer 3000 additionally provides an output of the percentage of sediment particles that are smaller than each half-unit on the Phi Scale. When these have been

converted to the percentage of sediment particles in each Phi Scale category, these categories can each be plotted against depth similar to pollen and diatoms using C2, to visually determine relative changes in each particle size category over the study period (Juggins, 2007). The particle sizes can then be grouped according to the Wentworth scale and plotted against depth to compare relative changes in the clay, silt and sand composition over the study period. For the purpose of this, the Wentworth scale presented in Masselink et al. (2014) is used. Such analysis of changes in proportion of different sediment sizes provides insight into changing depositional environments.

For multi-proxy analysis and the comparison of the sediment results with those from pollen and diatom analysis, the diatom and pollen PCA curves are plotted together with the organic and carbonate composition and sediment statistics (mean, sorting, skewness and kurtosis, or the relative percentage sizes within Wentworth categories), against depth. This facilitates visual corroboration of the environmental proxies with the sediment data, and for the climatic drivers responsible for these environmental changes to be further confirmed or contested.

4.5.3 Statistical Analysis of AMS Dates

4.5.3.1 Calibration

Calibration of the age-dates to account for periods of time in which atmospheric ^{14}C was not in equilibrium with contemporary atmospheric ^{14}C, and for the inter-hemispheric differences (Hogg et al., 2013), was undertaken by *Beta Analytic.* The calibrated 'conventional dates' provided by *Beta Analytic* use the SHCal13 database, and thus no further calibration nor adjustment of dates was required for this study (Hogg et al., 2013).

4.5.3.2 Age-Depth Model

In understanding past climates, quantifying the dates of events in which changes in environmental proxies are observed, and the rates of such changes, is crucial (Parnell et al., 2011). However, the dating of palaeosediment samples is costly, and often not all of the samples in a core have sufficient organic material for carbon dating to be undertaken (Blaauw & Christen, 2011). It is therefore necessary to interpolate values for the missing dates as accurately as possible, while taking into account errors from changing accumulation

rates, the extraction of the sediment, and the dating process itself (Parnell et al., 2008, 2011; Blaauw, 2010). In the past decade there has been a considerable effort to develop more complex Bayesian age-depth models to replace the 'classical' methods of more basic linear interpolation (Blaauw, 2010; Parnell et al., 2011), which are problematic in that radiocarbon age uncertainties are not included, the uncertainties for undated depths (the depth of the sample, for example) are not addressed, and outlying dates often have to simply be ignored (Parnell et al., 2011). Bayesian models that address these uncertainties use a Markov Chain Monte Carlo algorithm to estimate sediment accumulation rates, and account for factors including the depth of the sample, the depth spanned by the sample, and the radiocarbon age uncertainty (Parnell et al., 2008). Bayesian models are critiqued for their required use of prior knowledge about a system (priors), which is not included in the data, and which is therefore likely to be subjective (Parnell et al., 2011). For radiocarbon dating these priors involve assumptions of accumulation rate uniformity, which not only are used objectively on all samples and sites, but furthermore are often assumptions made throughout a study (Parnell et al., 2011). The benefits in more accurately representing natural changes in accumulation rate, and the acceptability of these priors, make Bayesian age-depth models appropriate for this study.

The Bayesian age-depth model used in this study is the BACON model developed by Blaauw and Christen (2011). This model was selected because unlike the Bchron model (Parnell et al., 2008), BACON was built with an emphasis on the evolution and shape of the accumulation rate of sediments throughout the sediment profile, with prior accumulation rates based iteratively on each previous rate (Blaauw & Christen, 2011). This process is achieved through the division of the core across a specified minimum and maximum depth into a large number of thin theoretical sections for which accumulation rates and times are estimated, based on knowledge of all known dates, together with their age uncertainty and depth (Blaauw & Christen, 2011). The process of accumulation rate estimation is achieved through running millions of self-adjusting Markov Chain Monte Carlo iterations on the gamma distribution (Blaauw & Christen, 2011). Outliers are identified and addressed using the Student's t-distribution (Blaauw & Christen, 2011). The model produces an interpolation curve for the core, with the calibrated distributions of individual dates, and the 95%

probabilities of the model, together with an output of interpolated dates for each centimetre of the core (Blaauw & Christen, 2011).

4.6 CONCLUSION

A multi-proxy approach allows for the investigation of the long term change in a broader range of environmental variables than is possible with a single record, and for the corroboration of results. Using standard methods in sediment preparation and analysis facilitates reproducibility of results and improved comparisons between sites, as errors are understood and accounted for. Many of the difficulties faced throughout the methodological processes are of value to future studies in the region, as this essentially forms a pioneering study for high altitude palaeoenvironmental work in the eastern Lesotho wetlands.

5. RESULTS

5.1 INTRODUCTION

This study involves the use of palaeoenvironmental proxies to reconstruct changes in climate and environment throughout the Holocene in eastern Lesotho. Three proxies were used: pollen, diatoms, and sedimentary properties, including percentage organic content, percentage carbonate content, and particle size. All three of these proxies were analysed for each of the three study sites, located in the Sani Valley, Sekhokong Mountains, and Mafadi Wetland. The changes in sedimentary properties, pollen and diatoms for each site are temporally constrained using sets of AMS dates acquired for samples distributed across the profiles. This chapter presents the results of these analyses, structured first by study site, and second by the proxies. For each site, the chronology and sediment accumulation rates are presented, followed by stratigraphy and sediment properties, pollen analysis and diatom analysis. For each of the sites, the section concludes with a multi-proxy synthesis. The interpretation of these results, from which an environmental reconstruction is developed, is presented in *Chapter 6 (Discussion)*.

Throughout this chapter, pollen and diatom stratigraphic diagrams are presented with species ordered by their species scores from PCA, with plots for the species score order for the first and second principal components. CONISS cluster analysis was performed on each of the proxies for each of the sites, and thus in this chapter, zones for each proxy are defined and discussed. CONISS was then performed using data from all of the proxies to determine site-based stratigraphic zones, which are presented at the end of each site section, and are used in the discussion. The PCA biplots for each proxy at each site are colour-coded according to their CONISS output. Subsamples from each of the sites are numbered consistently across the three proxies, but numbered according to the order in which they were extracted, and are not necessarily stratigraphically consistent. All stratigraphic diagrams are hence made on the basis of subsample depth. For age-dates of samples, dates are represented in years before present, with ‘cal. yr BP’ used where the calibrated AMS date provided by Beta Analytic for a particular sub-sample is cited, and ‘~cal. yr BP’ used for all interpolated dates, produced using the BACON model, with calibrated

AMS dates from Beta Analytic used as input values. It should be noted that there are two cases in which species have been grouped for the purpose of analysis. For pollen the 'Cheno-Am' grouping commonly used in the literature has been adopted for the families Chenopodiaceae and Amaranthaceae, that have similar pollen grain morphology and sufficiently similar ecologies to warrant them to be treated as a single unit (Scott et al., 2002). For diatoms, *Fragilaria pinnata* and *Fragilaria construens* have been combined into a single group '*Fragilaria pinnata/ construens*'. This is partially due to the difficulties in accurately differentiating the two species when observed in girdle view, but more critically as their similar ecologies make the proportional differences between them irrelevant, obscuring PCA results for other species. For the sake of this grouping the renamed *Staurosirella pinnata* (*Ehrenberg*) will remain referred to as *Fragilaria pinnata*.

5.2 Sani Valley

5.2.1 Chronology and Sediment Accumulation

Five AMS dates were obtained for the Sani Valley site (*Table 5.1*), with selection of samples for dating made on the basis of notable changes in pollen and diatom principal component (PC) 1 curves, and in sediment properties. These dates range from 250 ±30 cal. yr BP at a mean depth of 18cm, to 3,990 ±30 cal. yr BP at 78cm mean depth. An erroneous date (WITSS27) obtained for the bottom of the core (111cm) was excluded by the BACON model, and consequently omitted from this study, as two older dates were obtained for samples closer to the surface, providing an age-depth profile consistent with those for other sites in the eastern Lesotho Highlands (Van Zinderen Bakker & Werger, 1974; Marker, 1994). Due to insufficient sediment remaining from this depth, no further dates for the bottom of the core could be acquired. The age of the bottom of the core is consequently unknown, but from interpolations using the BACON model and fluctuations in rates of accumulation from the nearby Sekhokong site, the bottom of the core is estimated to date to ~6,200 cal. yr BP.

Table 5.1: AMS radiocarbon dates acquired for the Sani Valley profile.

Laboratory ID	^{14}C Age (yr BP)	Age (cal. yr BP)	1σ Uncertainty (yr)	2σ calibrated age range (BP)	Mean Depth (cm)	Sample thickness	d13C
WITSS10	270	250	±30	310-270	18	3cm	-26.3
WITSS13	700	680	±30	660-555	38	3cm	-26.5
WITSS5	1,630	1,610	±30	1,535-1,375	57	3cm	-26.0
WITSS21	4,020	3,990	±30	4,330-4,295	78	3cm	-26.9
WITSS27	1,570	1,550	±30	1,430-1,315	111	3cm	-26.5

The BACON model estimates the mean accumulation rate throughout the sequence to 40yr.cm^{-1} (*Figure 5.1*). Notable is a period of very slow sediment accumulation in the middle of the sequence, from 1,610 ± 30 cal. yr BP to 3,990 ± 30 cal. yr BP, during which time only 19cm of sediment accumulated, with a mean rate of 125yr.cm^{-1}. Comparatively slow and consistent sediment accumulation occurred subsequent to, and following, this period.

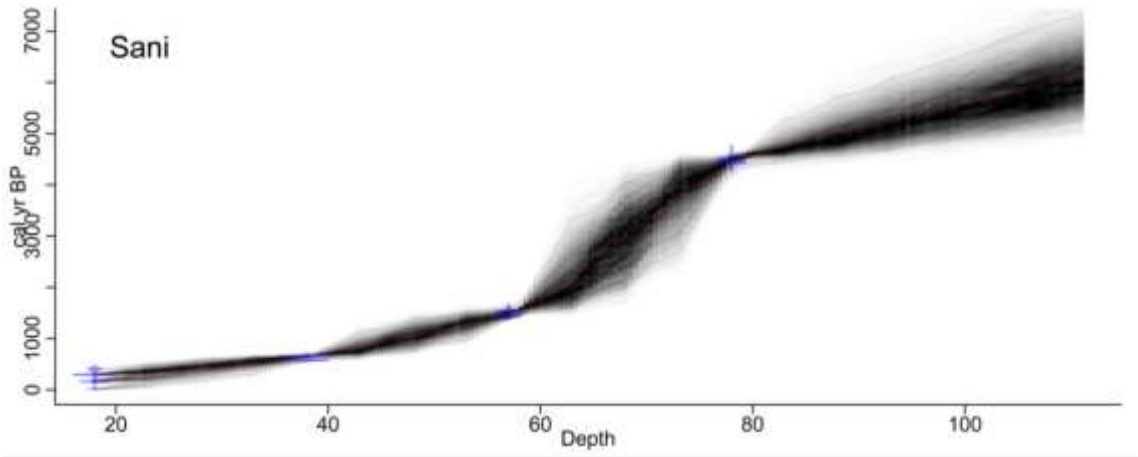


Figure 5.1: BACON output for the Sani Valley profile, providing interpolated ages for depths throughout the core.

5.2.2 Stratigraphy and Sediment Properties

Preliminary observations of the extracted core from the Sani Valley site suggested that the contemporary landscape dominated by a peat bog characterises much of the profile (*Figure 5.2*). Dark brown to black sediment is found throughout the core, the texture of which suggests a substantial organic content, with peat layers near the top of the profile, and decomposed organic clays from the middle down (*Figure 5.2; Table 5.2*). Coring at the site was terminated at a depth of just over 110cm (*Figure 5.3*) due to an impenetrable layer of

coarse grey gravels cemented by dark grey-green clay, that could not be sampled. The sediment properties from a total of 40 samples were examined.

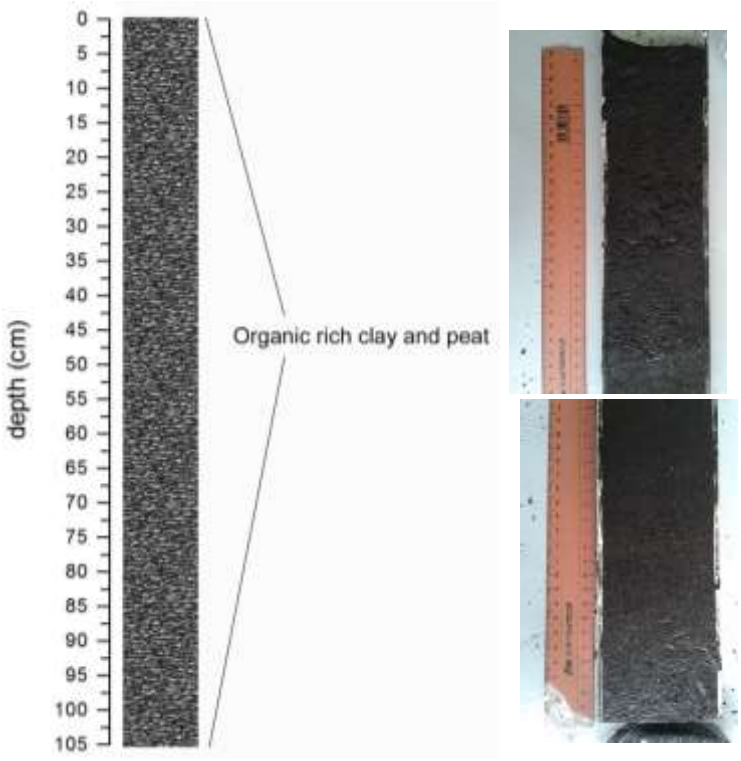


Figure 5.2: Stratigraphic log and photograph of core from Sani Valley

The results of the first stage of LOI indicate greater variability in the percentage organic content of the sediment throughout the profile than was expected, but ranging from 23-80%, indicates the presence of peat and organic clay throughout the sequence (*Figure 5.3*). Two peaks in percentage organic content (>50%) are apparent in the profile, the first extending from 20.5-50.5cm (~240-1,150 cal. yr BP) and the second from 68-88cm (~2,970-5,020 cal. yr BP). The periods between these peaks, preceding and following them, comprise sediments with an organic content less than half of the total weight. The percentage carbonate composition demonstrates far greater fluctuation throughout the profile, but seldom exceeds 5%. The sequence is dominated sand- and silt-sized particles, with fluctuations in the percentage composition of these two groups, and a notable decrease in percentage sand particles and equivalent increase in percentage silt particles from 23-59cm (~300-1,690 cal. yr BP). Although for much of the profile clay particle sizes account for less than 5% of the total, a peak of 12% is observed at a depth of 57cm (~1,490 cal. yr BP).

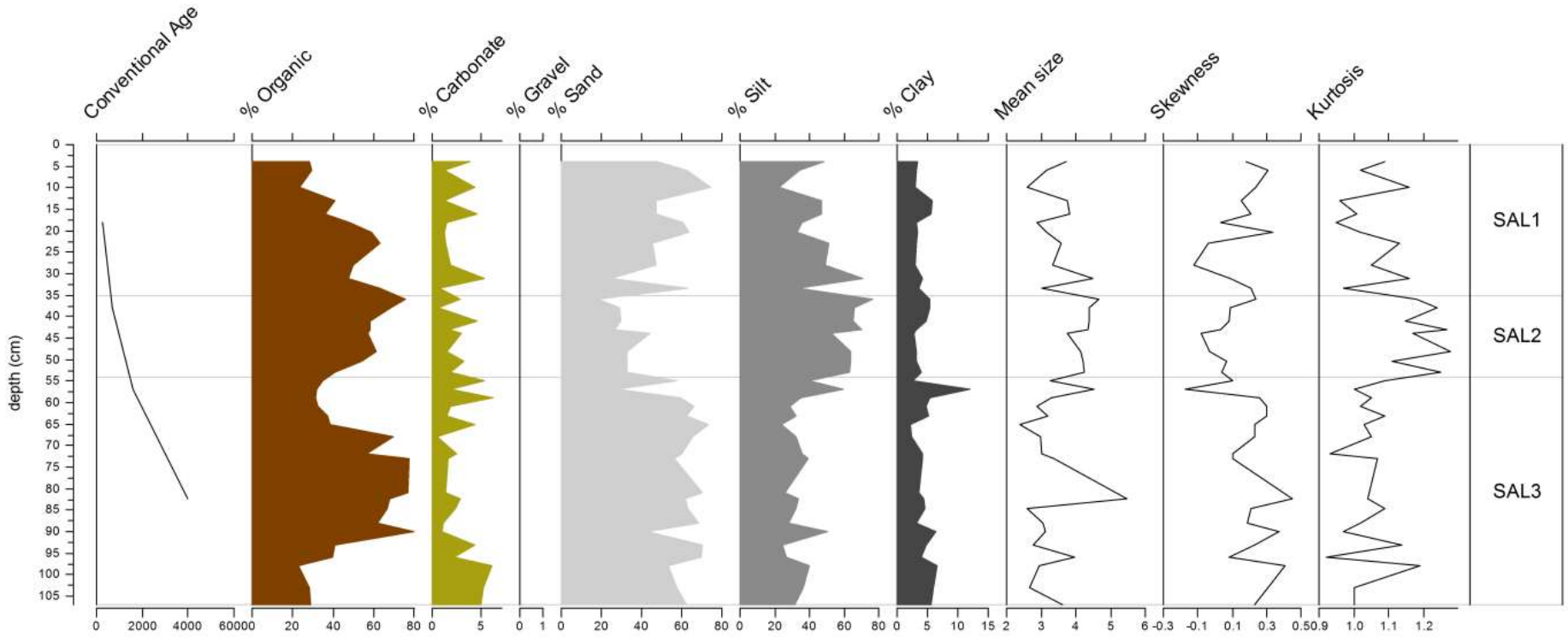


Figure 5.3: Changes in sediment properties throughout the Sani Valley profile.

The CONISS clustering separates the profile into three groups, named here as SAL1, SAL2 and SAL3 (*Figure 5.4*). The separation between SAL1 and SAL2 occurs at a mean depth of 35cm (~570 cal. yr BP), marked by the highest percentage organic content for the late Holocene at the site, and concurrent with a peak in sand-sized particles, and a decrease in mean particle size and percentage silt particles (*Figures 5.3, 5.4*). The division between SAL2 and SAL3 occurs at a mean depth of 54cm (~1,340 cal. yr BP), at which point there is no change in direction of change in the percentage organic content, but a sudden peak in percent sand-sized particles and carbonate content, and decrease in mean particle size and percent silt-sized particles (*Figures 5.3, 5.4*).

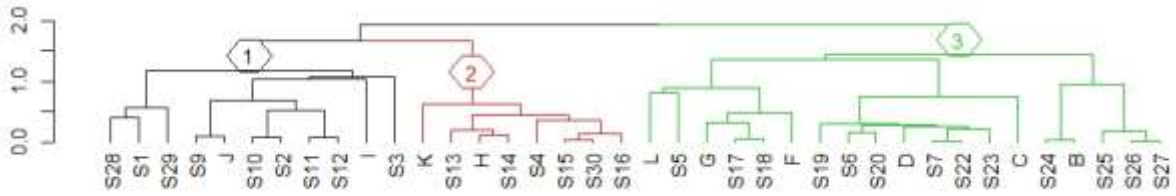


Figure 5.4: CONISS output separating samples from the Sani Valley profile on the basis of variations in sediment properties across the samples.

SAL3 (107-55cm; ~6,200-1,370 cal. yr BP) is characterised by relatively consistent sediment particle size distributions across samples, with 60-80% sand, 20-40% silt and <5% clay, but terminates with a sudden peak in silt- and clay-sized particles and a decrease in sand (*Figure 5.3*). Notable, given the relatively stable percentage composition of the various particle size groups, are the large fluctuations in mean particle size, with a pronounced peak at 78cm (~4,460 cal. yr BP; *Figure 5.3*). This peak in mean particle size, which may be influenced by the size of diatom valves, is concurrent with a peak in percentage organic content, and a decrease in carbonate composition. The percentage of both organic and carbonate composition varies considerably throughout this zone, with the second of the two aforementioned organic peaks contained in this zone, surrounded by periods of particularly low (<30%) organic content. These three distinct clusters of low, high and low organic content are separated by CONISS in subgroups, from depths 107-93cm, 90-68cm and 65-55cm (*Figure 5.4*).

Table 5.2: Sediment properties for the Sani Valley profile.

Sample Number	Depth	Mean	SD	Skewness	Kurtosis	Texture	Munsell
S28	3-5	very fine grained	poorly sorted	fine skewed	mesokurtic	sandy loam	10YR 4/1
S1	6	very fine grained	poorly sorted	strongly fine skewed	mesokurtic	loamy sand	10YR 4/4
S29	9-11	fine grained	poorly sorted	fine skewed	leptokurtic	loamy sand	10YR 4/1
S9	12-14	very fine grained	poorly sorted	fine skewed	mesokurtic	sandy loam	10YR 3/4
J	15-17	very fine grained	poorly sorted	fine skewed	mesokurtic	sandy loam	2.5Y 3/1
S10	17-19	fine grained	very poorly sorted	near symmetrical	mesokurtic	loamy sand	10YR 2/2
S2	19-22	very fine grained	poorly sorted	strongly fine skewed	mesokurtic	loamy sand	10YR 3/3
S11	22-24	very fine grained	poorly sorted	near symmetrical	leptokurtic	sandy loam	10YR 3/3
S12	27-29	very fine grained	very poorly sorted	coarse skewed	mesokurtic	sandy loam	10YR 3/6
I	30-32	coarse silt	poorly sorted	near symmetrical	leptokurtic	silty loam	10YR 3/3
S3	32-35	very fine grained	very poorly sorted	fine skewed	mesokurtic	loamy sand	10YR 3/3
K	35-37	coarse silt	poorly sorted	fine skewed	leptokurtic	silty loam	10YR 3/2
S13	37-39	coarse silt	poorly sorted	near symmetrical	leptokurtic	sandy loam	10YR 3/3
H	40-42	coarse silt	poorly sorted	near symmetrical	leptokurtic	sandy loam	10YR 3/2
S14	42-44	coarse silt	poorly sorted	near symmetrical	leptokurtic	sandy loam	10YR 3/3
S4	43-45.5	very fine grained	very poorly sorted	near symmetrical	leptokurtic	sandy loam	10YR 3/4
S15	47-49	coarse silt	poorly sorted	near symmetrical	leptokurtic	sandy loam	10YR 3/4
S30	49-52	coarse silt	poorly sorted	near symmetrical	leptokurtic	sandy loam	10YR 3/2
S16	52-54	coarse silt	poorly sorted	near symmetrical	leptokurtic	sandy loam	10YR 3/2
L	54-56	very fine grained	poorly sorted	fine skewed	mesokurtic	loamy sand	10YR 3/1
S5	56-58	coarse silt	very poorly sorted	coarse skewed	mesokurtic	silty loam	10YR 3/2
G	58-60	very fine grained	very poorly sorted	fine skewed	mesokurtic	loamy sand	10YR 3/1
S17	60-62	fine grained	very poorly sorted	strongly fine skewed	mesokurtic	loamy sand	10YR 2/2
S18	62-64	very fine grained	very poorly sorted	strongly fine skewed	mesokurtic	loamy sand	10YR 2/2
F	64-66	fine grained	poorly sorted	fine skewed	mesokurtic	loamy sand	10YR 2/1
S19	67-69	fine grained	poorly sorted	fine skewed	mesokurtic	loamy sand	10YR 3/2
S6	71-73	very fine grained	very poorly sorted	fine skewed	mesokurtic	loamy sand	10YR 2/2
S20	72-74	very fine grained	very poorly sorted	fine skewed	mesokurtic	sandy loam	10YR 2/2
S21	77-79	medium silt	poorly sorted	strongly fine skewed	mesokurtic	silt	10YR 2/2
D	80-82	fine grained	very poorly sorted	fine skewed	mesokurtic	loamy sand	2.5Y 2.5/1
S7	81.5-83.5	very fine grained	very poorly sorted	fine skewed	mesokurtic	loamy sand	10YR 3/1
S22	83.5-85.5	very fine grained	very poorly sorted	strongly fine skewed	mesokurtic	loamy sand	10YR 3/3
S23	87-89	fine grained	very poorly sorted	fine skewed	leptokurtic	loamy sand	10YR 2/2
C	89-92	very fine grained	very poorly sorted	near symmetrical	mesokurtic	sandy loam	10YR 2/1
S24	92-94	fine grained	very poorly sorted	strongly fine skewed	leptokurtic	loamy sand	10YR 3/3
B	95-97	fine grained	very poorly sorted	strongly fine skewed	mesokurtic	loamy sand	10YR 2/1
S25	97-99	very fine grained	very poorly sorted	fine skewed	mesokurtic	sandy loam	10YR 2/1
S26	102-104	very fine grained	very poorly sorted	fine skewed	mesokurtic	sandy loam	10YR 2/1
S27	106-108	very fine grained	very poorly sorted	fine skewed	mesokurtic	loamy sand	10YR 3/1
S8	109.5-112	very fine grained	very poorly sorted	fine skewed	mesokurtic	sandy loam	2.5Y 3/2

SAL2 (53-36cm; ~1,310-590 cal. yr BP) has relatively consistent low percentages (<40%) of sand-sized particles, higher percentages (>50%) of silt-sized particles, and mean particle sizes seldom fluctuating outside of a 4-5ϕ unit bracket, compared to the full profile (*Figure 5.3*). The percentage organic content rapidly increases throughout this zone. Carbonate percentages remain low, but continue to fluctuate considerably. Notable is the particularly high kurtosis values, indicative of a large variation in sediment sizes within each subsample in this zone.

SAL1 (33cm - surface; ~540 cal. yr BP - present) is characterised by a gradual decrease in percent organic content to approximately 30% at present (*Figure 5.3*). This occurs concurrently with an increase in the percentage sand-sized particles, and a relative decrease in silt-sized particles. A relatively recent peak in percentage clay, silt and organic material, concurrent with a decrease in sand-sized particles occurred between mean depths of 13-16cm (<200 cal. yr BP; *Figure 5.3*).

5.2.3 Pollen Analysis

Pollen grains from a total of 25 taxa were identified from a total of 30 samples spanning the depth of the Sani Valley core (*Table 5.3*). The sequence is dominated by Cyperaceae*,* with high proportions of Asteraceae and Poaceae*.* Plant families that represent 1% or more of the profile include *Crassula,* Aizoaceae, Cheno-Am, Caryophylaceae and Apiaceae (*Table 5.3*)*.* Maximum counts for each of the pollen grains across the individual samples are significantly higher than their average occurrence through the sequence, but largely follow the same order of frequency. This is indicative of conditions similar to the contemporary environment comprising a large bog with meadow grasses and scattered communities of small shrubs persisting throughout the mid- to late-Holocene at this site.

Table 5.3: Frequency of occurrence of pollen identified from the Sani Valley sequence.

Pollen type (family/genera)	% Occurrence in core	Maximum individual sample %
Cyperaceae	52.9	78.2
Asteraceae	17.6	42.4
Poaceae	16.8	31.1
Crassula spp.	3.3	10.6
Aizoaceae	1.4	4.2
Cheno-Am	1.9	3.6
Caryophylaceae	1.2	4.7
Apiaceae	1.1	4.8
Pentzia spp.	0.8	2.0
Indigofera spp.	0.7	4
Liliaceae	0.5	1.6
Olea sp.	0.5	2.4
Typha spp.	0.4	2.8
Gentianaceae	0.4	2.4
Vernonia spp.	0.4	2.4
Chrysocoma sp.	0.2	1.2
Acanthaceae	0.2	0.8
Passerina spp.	0.2	1.2
Malvaceae	0.1	1.2
Anthospermum spp.	0.1	1.2
Podocarpus sp.	0.1	0.8
Geraniaceae	0.1	0.4
Pinus sp.	0.1	0.8
Ericaceae	<0.1	0.4
Widdringtonia spp.	<0.1	0.4

The CONISS output for the pollen results from the Sani Valley site divides the profile into three groups, named here as SAP1, SAP2 and SAP3 (*Figure 5.5*). The division between SAP1 and SAP2 occurs at a relatively shallow mean depth of 16cm (<200 cal. yr BP), while SAP2 and SAP3 are separated at a mean depth of 55cm (~1,390 cal. yr BP), roughly equivalent to the separation between SAL2 and SAL3 (*Figure 5.5*). All three clusters have two distinct subgroups, dividing samples 6-13cm; 18-44cm from 48-53cm; and 57-82.5cm from 84.5-111cm (*Figure 5.5*).

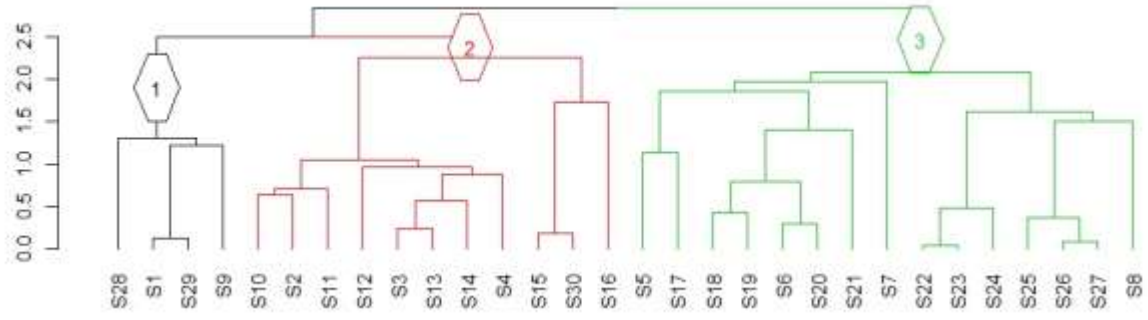


Figure 5.5: CONISS zonation for the Sani Valley profile on the basis of pollen results.

The zones identified by CONISS are largely consistent with the clustering observed in the PCA biplot constructed for the samples and species distributions against principal

components 1 and 2 (*Figure 5.6*). Samples grouped as SAP1 are largely located in quadrant 3 of the biplot, strongly affiliated with Cyperaceae, and to a lesser extent with Caryophylaceae. Samples from SAP2 are distributed predominantly in quadrant 2, characterised predominantly by Asteraceae. Samples from SAP2 are arranged across quadrants 1 and 4, influenced to a relatively equal extent by all of the remaining pollen groups.

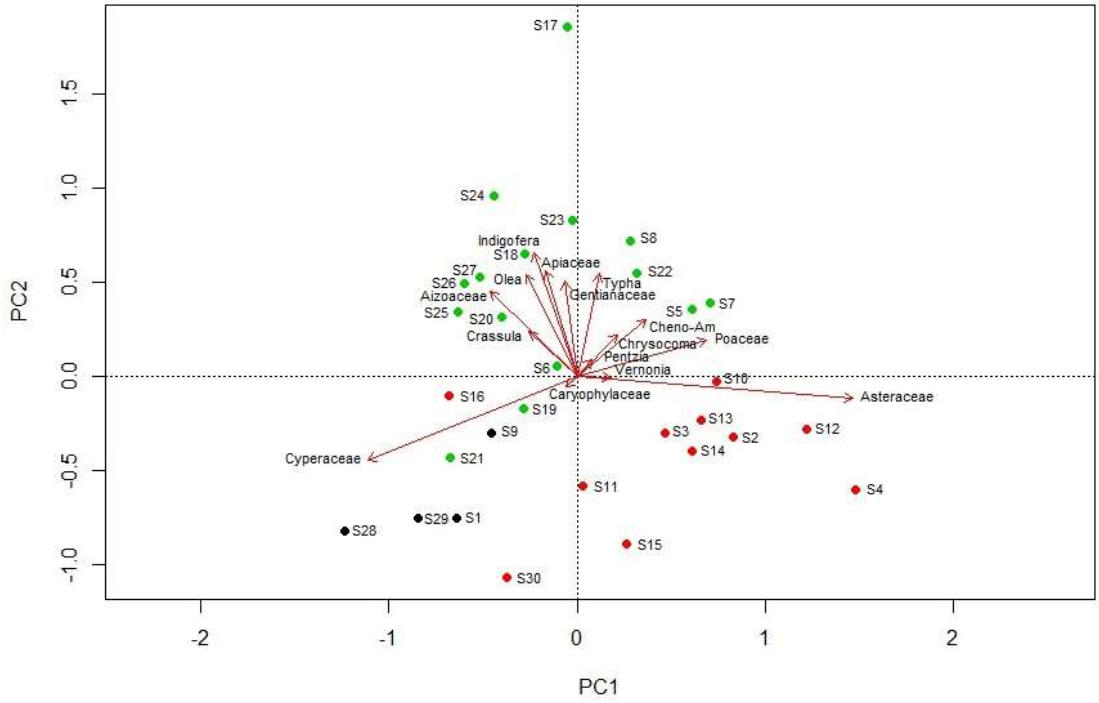


Figure 5.6: PCA biplot for pollen results from the Sani Valley profile.

PC1 accounts for 36.2% of the variance in samples on the basis of their pollen species distribution. PC1 species scores are ordered at extremes from Cyperaceae with large negative PC1 scores to Asteraceae with large positive PC1 scores, that dominated SAP1 and SAP2 respectively (*Figure 5.7*). PC1 includes a gradual transition through the species that dominated SAP3. PC2 accounts for a further 18.0% of the variance between samples, reaching a cumulative variance of 54.2% explained between the two. PC2 largely segregates SAP1 and SAP2 from SAP3, transitioning from the abundant Cyperaceae and Asteraceae typical of the contemporary environment represented by negative PC2 scores, to the presently less extensive herb communities of *Indigofera,* Apiaceae and *Typha,* which have increasing positive PC2 scores (*Figure 5.6*).

SAP3 (111-56cm; ~6,200-1,400 cal. yr BP) is dominated by Cyperaceae, with percentages of Asteraceae and Poaceae pollen remaining below 20% for much of the zone (*Figure 5.7*). A notable decrease in the PC1 curve, shifting to negative values, occurs at a depth of 78cm (~4,460 cal. yr BP), driven by a peak in Cyperaceae, and the lowest percentage of Asteraceae throughout the zone (*Figure 5.7*). The zone appears largely to indicate warm, wet conditions, with small pulses of drought conditions and a transition to dry conditions at its termination. SAP3 has the greatest species diversity, with continuous presence of the majority of the pollen groups from the site throughout the zone (*Figure 5.7*). Particularly notable is the counts of ~5% Aizoaceae throughout this zone, which thereafter largely disappears from the site (*Figure 5.7*). Gentianaceae, *Olea, Typha* and *Indigofera* are similarly more dominant in SAP3 than any other zone. A distinct peak in the PC2 curve is observed towards the termination of SAP3 at a depth of 61cm (~1,980 cal. yr BP, *Figure 5.7*), driven by the peak in the shrub species Asteraceae, *Crassula,* Poaceae, Caryophylaceae, *Vernonia,* Cheno-Am, Gentianaceae and Apiaceae mentioned above. This peak lags slightly from a peak in Apiaceae, *Indigofera, Pentzia and Olea* (*Figure 5.7*).

SAP2 (54-16.5cm; ~1,350-200 cal. yr BP) has the highest proportions of Asteraceae pollen throughout the sequence, paired with lower percentages of Cyperaceae. Poaceae percentages continue to fluctuate, but are at their highest level throughout the sequence (*Figure 5.7*). The PC1 curve is positive for much of SAP2, tracking the larger proportions of the grassland and shrub components in place of the sedges, indicative of comparatively drier conditions overall. A sudden peak in Caryophylaceae, Asteraceae, Aizoaceae and *Typha* is apparent at a depth of 23cm (~330 cal. yr BP), indicative of a rapid but short-lived increase in shrub vegetation (*Figure 5.7*). The bottom of the zone (~1,350 cal. yr BP) is marked by a peak in *Crassula, Olea, Indigofera,* Caryophylaceae and Cyperaceae, but low proportions of Asteraceae and Poaceae, suggesting a short-lived particularly moist period (*Figure 5.7*).

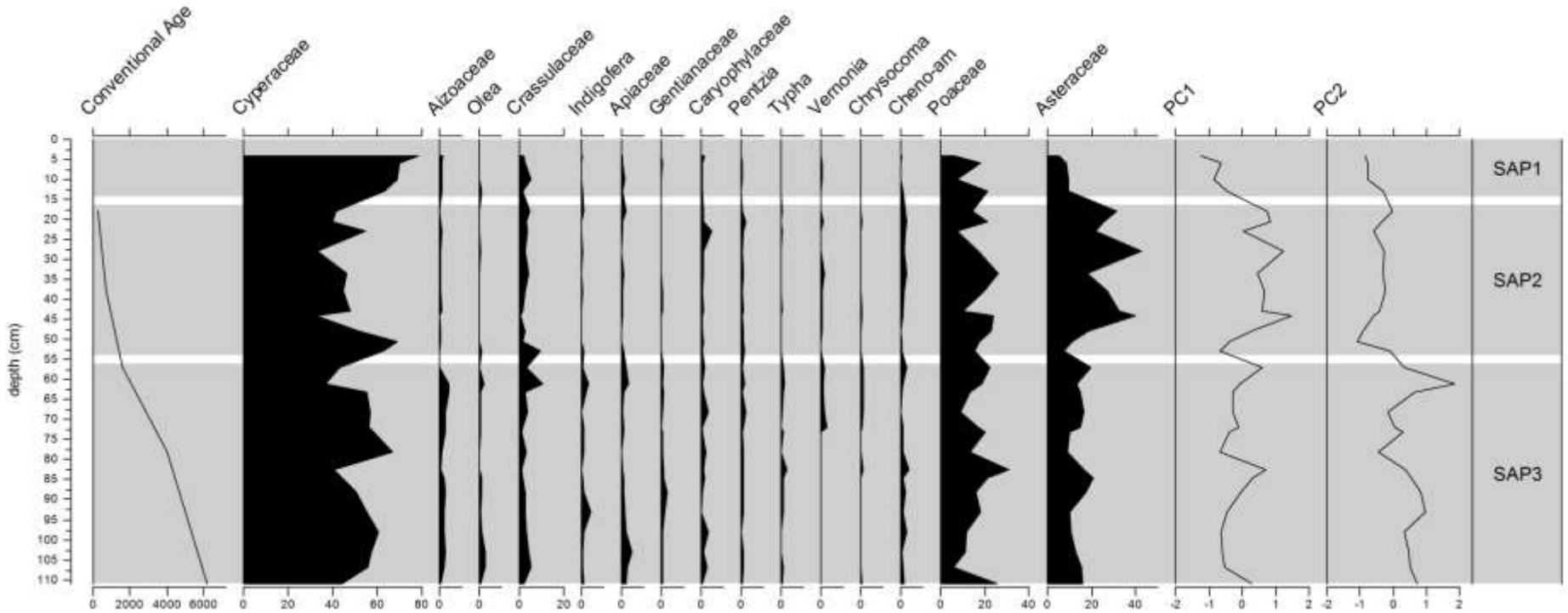


Figure 5.7: Stratigraphic diagram of the pollen results for the Sani Valley profile, ordered by PC1 species scores, and with curves indicating the PC1 and PC2 sample scores.

SAP1 (14.5cm - surface; ~145 cal. yr BP - present), similar to SAP3, is dominated by Cyperaceae, which increases rapidly from approximately 60% of the pollen count to just under 80% in the modern samples (*Figure 5.7*). Asteraceae percentages are particularly low, but largely stable during this period. By contrast, the relative abundance of Poaceae varies considerably, with peaks exceeding 20% at the beginning and end of the zone, separated by a minimum abundance of 7.4% at a depth of 10cm (<100 cal. yr BP; *Figure 5.7*). This decrease in Poaceae occurs concurrently with an increase in *Crassula*, which remains relatively abundant throughout this zone (*Figure 5.7*). The predominance of Cyperaceae would suggest relatively wet conditions throughout this zone.

5.2.4 Diatom Analysis

It was initially assumed, based on prior investigation at the site, that there would not be sufficient diatom valves to count in the samples from Sani Valley. Once sub-sampling had been undertaken for pollen and sediment analysis and for age-dating, the remaining 10 discrete subsamples from the profile were prepared for exploratory diatom analysis. It was discovered that these initial assumptions were incorrect as there were sufficient diatom valves in each subsample for counting. As this was the first of the cores obtained for the project, and material from this core required trial-and-error testing to optimise the pollen and sediment analysis, no further subsamples could be processed for diatom analysis. The use of diatoms as an environmental proxy for this site is consequently limited by the small number of subsamples (n=10), but the information that does exist has the potential to corroborate findings from the other proxies.

Despite the small number of samples, diatoms representing a total of 33 different species were identified from the Sani Valley sequence (*Table 5.4*). The most common species throughout the sequence was *Fragilaria famelica. Diploneis parma* accounted for a further 16.7% of identified diatoms in the core, while species with frequencies of more than 5% include *Cymbella laevis and Pinnularia gentilis.* A total of 13 species were observed with frequencies between 1-5%, indicating relatively high species richness.

Table 5.4: Frequency of occurrence of diatoms identified in the Sani Valley profile.

Diatom species	% occurrence in core	Maximum individual sample %
Fragilaria famelica Kützing	34.6	65.1
Diploneis parma Cleve	16.7	32.0
Cymbella laevis Nägeli	6.5	20.8
Pinnularia gentilis Donkin	5.7	7.9
Diploneis ovalis Hilse	4.9	11.0
Hantzschia amphioxys Ehrenberg	3.8	15.5
Eunotia bilunaris Ehrenberg	3.1	8.1
Pinnularia divergentissima Grunow	2.9	6.2
Fragilaria construens Ehrenberg	2.7	20.3
Pinnularia borealis Ehrenberg	2.4	10.9
Eunotia praerupta Ehrenberg	2.1	4.3
Cymbella gracilis Ehrenberg	1.7	4.0
Navicula minima Grunow	1.5	7.4
Achnanthes minutissima Kützing	1.3	6.9
Sellaphora pupula Kützing	1.2	4.6
Gomphonema parvulum Kützing	1.1	2.0
Denticula kuetzingii Grunow	1.0	6.2
Navicula laevissima Kützing	0.9	4.3
Caloneis silicula Ehrenberg	0.9	4.3
Gomphonema gracile Ehrenberg	0.8	2.0
Navicula trivialis Lange-Bertalot	0.7	3.3
Fragilaria pinnata Ehrenberg (Staurosirella pinnata)	0.6	3.3
Pinnularia viridis Ehrenberg	0.5	4.0
Stauroneis phoenicenteron Ehrenberg	0.5	1.0
Pinnularia intermedia Lagerstedt	0.5	2.0
Aulacoseira ambigua Grunow	0.4	1.6
Gomphonema bohemicum Hustedt	0.3	1.3
Cymbella selesiaca Bleisch	0.3	1.9
Nitzschia palea Kützing	0.3	1.3
Navicula explanata Hustedt	0.1	0.7
Stauroneis producta Cleve	0.1	0.7
Navicula pygmaea Kützing	<0.1	0.3

CONISS separated the 10 samples into four zones based on changes in diatom composition, named here as SAD1, SAD2, SAD3 and SAD4 (*Figure 5.8*). Zone SAD1 includes the top portion of the profile, from 16-31cm, accounting for the past ~590 cal. yr BP (*Figure 5.8*). Zone SAD2 comprises only one sample, located at a mean depth of 36cm (~590 cal. yr BP; *Figure 5.8*). SAD3 spans depths of 59-75cm (~1,250-4,320 cal. yr BP; *Figure 5.8*). SAD4 represents the largest group of samples, extending from 81-105cm (~4,370-6,200 cal. yr BP; *Figure 5.8*).

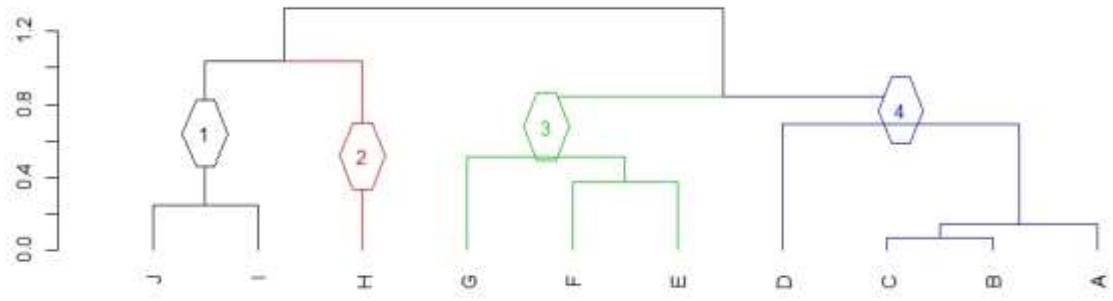


Figure 5.8: CONISS output separating the Sani Valley profile according to variations in relative abundances in diatoms throughout.

As with the pollen from the Sani Valley site, the CONISS output for the diatom analysis demonstrates a good fit with the observed clustering in the PCA biplot for components 1 and 2 (*Figure 5.9*). Samples grouped into zone SAD1 are located in the 3rd and 4th quadrants, driven predominantly by the *Fragilaria pinnata/ construens* group, and influenced by *Caloneis silicula, Achnanthes minutissima, Sellaphora pupula, Eunotia bilunaris, Navicula laevissima, Navicula trivialis and Navicula minima* (*Figure 5.9*). Sample H which makes up zone SAD2 is situated on the boundary of quadrants 2 and 3, with the lowest PC2 value, influenced by *Cymbella laevis* (*Figure 5.9*). Samples comprising SAD3 are located in quadrant 1, driven by *Hantzschia amphioxys, Pinnularia borealis, Diploneis parma, Diploneis ovalis and Pinnularia gentilis* (*Figure 5.9*). SAD4 samples are located in quadrant 2, driven by *Eunotia praerupta* and *Fragilaria famelica* (*Figure 5.9*). Thus the limited number of samples analysed for diatoms spanned the full profile, and demonstrated significant differences in species composition throughout.

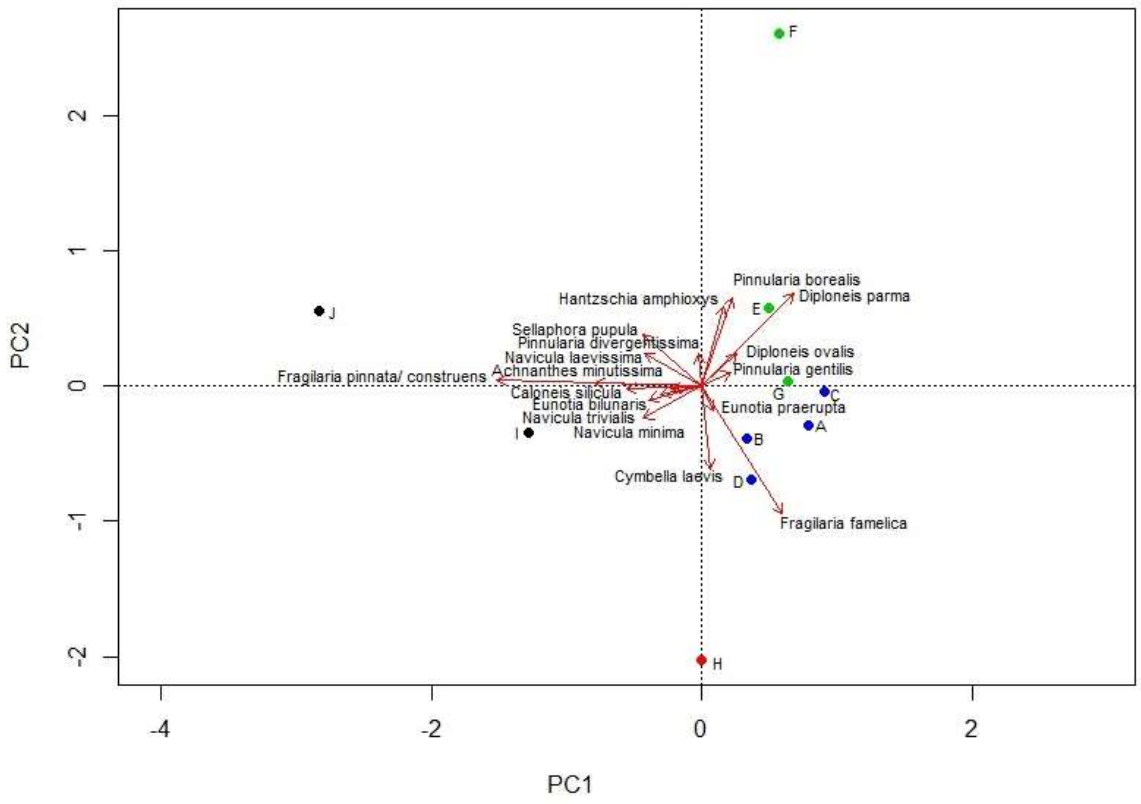


Figure 5.9: PCA biplot for the diatom results from the Sani Valley profile.

PC1 accounts for 41.2% of the variation in diatom species composition throughout the core. Diatom results plotted in order of species score for PC1, demonstrate a transition from *Fragilaria pinnata and construens* and *Achnanthes minutissima* with negative scores through to *Fragilaria famelica* and *Diploneis parma* with positive PC1 axis scores (*Figure 5.10*). Zones SAD4 (105-81cm; ~6,200-4,370 cal. yr BP) and SAD3 (75-59cm; ~4,320-1,250 cal. yr BP) are characterised by relatively consistent positive PC1 sample scores, while SAD2 (41cm; ~1,200-640 cal. yr BP) and SAD1 (31-16cm; 590 cal. yr BP - present) demonstrate a rapid decrease in PC1 sample scores over time (*Figure 5.10*). *Fragilaria famelica* maintained a relative abundance of approximately 40% through SAD4, SAD3 and SAD2, while *Diploneis parma* maintained a consistent proportion of approximately 20% only in SAD4 and SAD3 (*Figure 5.10*). PC1 sample scores demonstrate their peak in SAD4, driven in part by a peak in *Diploneis parma,* combined with peaks in *Diploneis ovalis* and *Pinnularia gentilis* (*Figure 5.10*). The decrease in PC1 scores in SAD2 from positive to zero, and through SAD1 from zero to strongly negative, are driven by an increase in *Fragilaria pinnata/ construens,* replacing the decreasing *Cymbella laevis, Fragilaria famelica* and *Diploneis parma* counts (*Figure 5.10*).

PC2 accounts for 23.7% of the variance, with distinct differences in each CONISS zone. Species scores for PC2 indicate a transition from *Fragilaria famelica* and *Cymbella laevis* to *Hantzschia amphioxys, Pinnularia borealis* and *Diploneis parma* (*Figure 5.10*). Relatively stable PC2 scores are maintained throughout SAD4, with the environment dominated by *Fragilaria famelica, Diploneis Parma, Cymbella laevis, Diploneis ovalis* and *Pinnularia gentilis* (*Figure 5.10*). The highest PC2 value occurs within SAD3, at a depth of 65cm (~2,550 cal. yr BP), characterised by the highest counts of *Diploneis parma, Pinnularia borealis and Hantzschia amphioxys,* and the lowest counts of *Fragilaria famelica* and *Cymbella laevis* in the profile (*Figure 5.10*). This peak is preceded and followed by significantly lower PC2 scores, resulting from environments dominated by *Fragilaria famelica* (*Figure 5.10*). SAD2 is marked by the lowest PC2 score, associated with the highest count of *Cymbella laevis,* large proportions of *Fragilaria famelica,* and the lowest count of *Diploneis parma* (*Figure 5.10*). SAD1 is characterised by an increase in the PC2 score over time, which appears to result mainly from a decrease in *Cymbella laevis* and *Fragilaria famelica* (*Figure 5.10*).

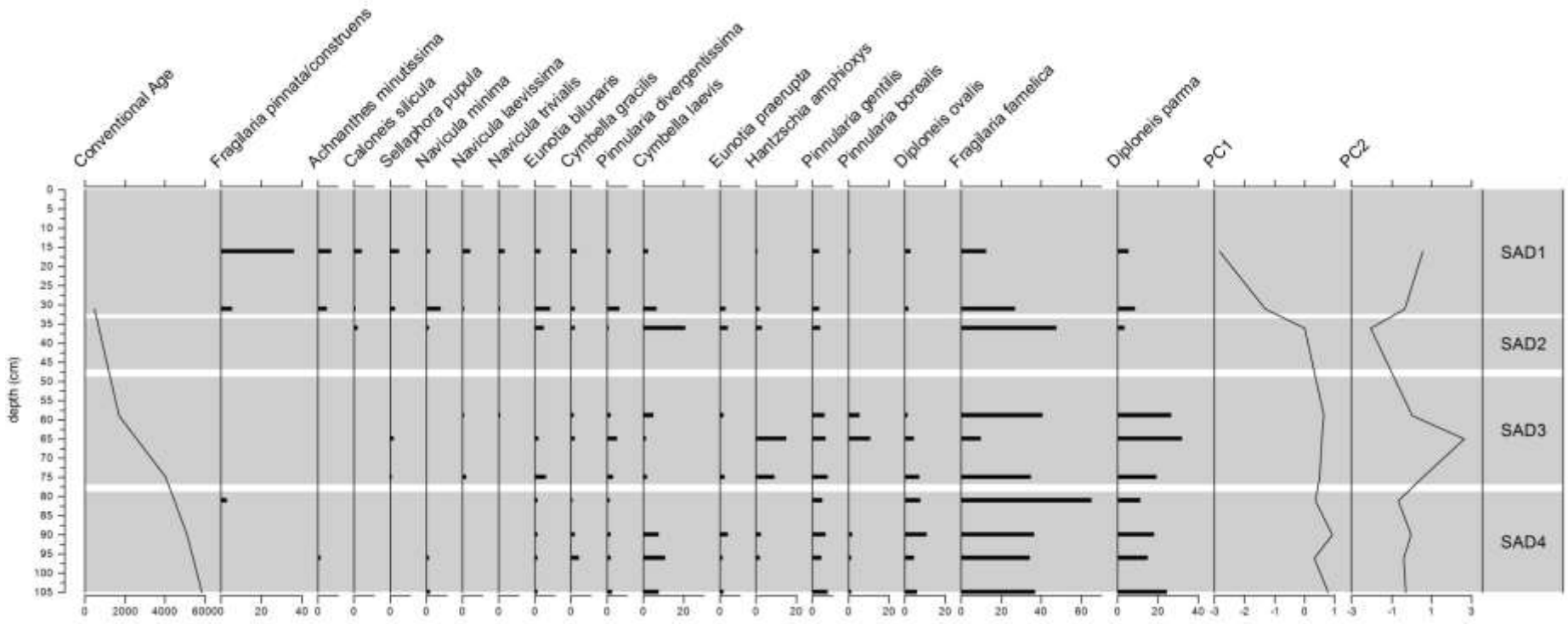


Figure 5.10: Stratigraphic diagram of the relative abundance of diatoms throughout the Sani Valley profile, arranged by PC1 species score, with curves demonstrating PC1 and PC2 sample scores.

5.2.5 Multi-Proxy Synthesis

The three pollen zones identified using CONISS, and presented in *Section 5.2.3* are used as a basis for the multi-proxy analysis presented in *Figure 5.11*.

SAP3 (111-56cm; ~6,200-1,400 cal. yr BP) is marked by consistent diatom PC1 scores, but a peak in diatom PC2 from 81-75cm (~4,650-4,030 cal. yr BP) reflecting an increase in the relative abundance of *Fragilaria famelica* (*Figure 5.11*). Three peaks in pollen PC1 sample scores occur during this zone, at the beginning, at 78cm (~4,200 cal. yr BP), and at the end of the zone (*Figure 5.11*). The latter is preceded by a high-amplitude peak in pollen PC2 from 93-88cm (~5,270-5,020 cal. yr BP) and a decrease in the percentage organic composition of sediments and silt-sized particles, compensated by a peak in sand-sized particles (*Figure 5.11*). A prolonged peak in the percentage organic composition occurs over a depth of 88-73cm (~5,020-3,750 cal. yr BP), coinciding with low percentage composition of carbonates (*Figure 5.11*). The middle of this period is marked by a peak in silt- and clay-sized particles, and an absence of sand-sized particles, at a depth of 78cm, coinciding with the second peak in pollen PC1 scores (*Figure 5.11*).

SAP2 (54-16.5cm; ~1,350-200 cal. yr BP) is marked by relatively consistent percentages of clay-sized sediments, and of the pollen PC2 curve (*Figure 5.11*). The percentage carbonates fluctuates rapidly throughout this zone, but within a small range of values (*Figure 5.11*). The first half of the zone (45-31cm; ~900-480 cal. yr BP) is characterised by consistent diatom PC1 scores and a decrease in diatom PC2 scores, while the second half of the zone is marked by a decrease in diatom PC1 scores and an increase in diatom PC2 scores (*Figure 5.11*). While the pollen PC2 curve remains relatively constant throughout this zone, the pollen PC1 curve fluctuates considerably (*Figure 5.11*). The percentage organic content increases at the beginning of the zone and decreases at its termination, with the highest percentage at approximately the middle of the zone (36cm, 590 cal. yr BP; *Figure 5.11*). This coincides with a peak in silt-and clay-sized particles, and a decrease in sand-sized particles, but is preceded by a larger-amplitude peak in sand-sized particles and decrease in silt-sized particles (*Figure 5.11*).

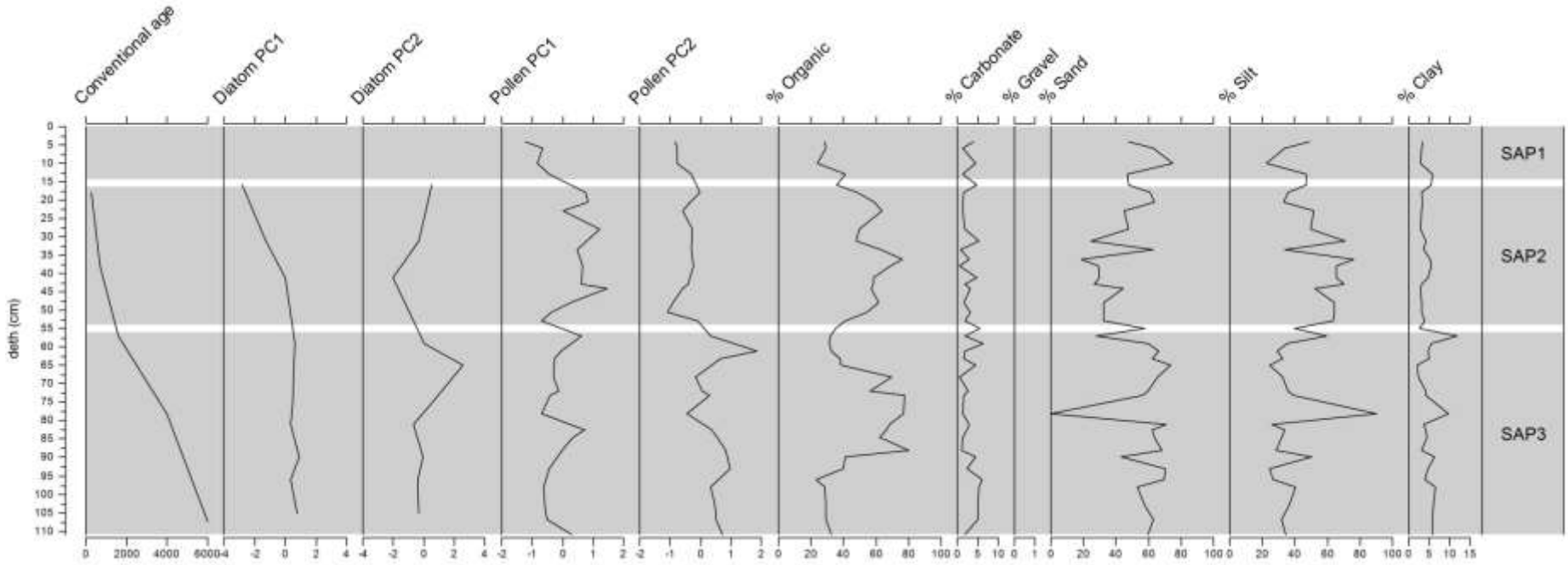


Figure 5.11: Multi-proxy stratigraphic plot for the Sani Valley sequence.

SAP1 (14.5cm - surface; ~145 cal. yr BP - present), is marked by a decline in pollen PC1 and the percentage organic content (*Figure 5.11*). The percentage of sand-sized particles increases and subsequently decreases throughout this zone, with a peak at 10cm (~110 cal. yr BP), a pattern mirrored by the percentage of silt-sized particles (*Figure 5.11*). The percentage carbonate content continues to fluctuate throughout this zone (*Figure 5.11*). No samples from this zone were analysed for diatoms.

5.3 Sekhokong

5.3.1 Chronology and Sediment Accumulation

AMS dates were acquired for a total of 11 samples, distributed throughout the 4.75m sequence at positions of notable abrupt changes in more than one of the proxies, in order to best temporally constrain this considerably longer record (*Table 5.5*). The dates range from 1,440 ±30 cal. yr BP at a depth of 16.5cm to 13,180 ±40 cal. yr BP at a depth of 472.5cm, representing the bottom of the profile (*Table 5.5*). The earliest, but stratigraphically inconsistent, date is 1,380 ±30 cal. yr BP for a depth of 45.5cm (*Table 5.5*). The BACON model treated this date as an outlier, and excluded it for the purpose of modelling accumulation rates. The top sample from the sequence is interpolated to reflect contemporary sediments. The Sekhokong sequence therefore provides a transect through the Holocene, commencing at the end of the Pleistocene-Holocene transition.

Table 5.5: AMS radiocarbon dates acquired for the Sekhokong profile.

Laboratory ID	^{14}C Age (yr BP)	Age (cal. yr BP)	1σ Uncertainty (yr)	2σ calibrated age range (BP)	Mean depth (cm)	Sample Thickness	d13C
SK3	1,430	1,440	±30	1,345-1,335	16.5	5cm	-24.5
SK7	1,380	1,380	±30	1,300-1,260	45.5	5cm	-25.1
SK11	2,660	2,680	±30	2,780-2740	75.5	5cm	-24.0
SK14	3,110	3,100	±30	3,360-3,175	107.5	5cm	-25.3
SK21	3,130	3,130	±30	3,375-3,215	134.5	3cm	-25.3
SK25	5,470	5,450	±30	6,258-6,180	202.5	5cm	-26.5
SK30	6,420	6,420	±30	7,4115-7,350	267.5	5cm	-24.8
SK31	6,500	6,470	±30	7,425-7,272	287.5	5cm	-26.8
SK34	10,610	10,550	±30	12,555-12,420	327.5	5cm	-28.9
SK38	12,720	12,660	±40	13,185-12,910	412.5	5cm	-28.5
SK41	13,200	13,180	±40	13,930-13,725	472.5	5cm	-26.0

A mean accumulation rate for the complete sequence of 20yr.cm^{-1} is calculated using the BACON model (*Figure 5.12*). Similar to the Sani Valley profile, periods of slower sediment accumulation are observed, with the most extreme of these occurring in the mid-early Holocene between 6,470 ±30 cal. yr BP to 10,550 ±40 cal. yr BP, during which only 40cm of sediment accumulated (*Figure 5.12, Table 5.5*). The age-depth model cannot account for sediment loss which may well have occurred during this time, and could explain this slow accumulation in part. This should be considered with caution, as it may influence the interpretations made from proxies within this layer. Accumulation occurs at a more constant, relatively rapid, rate towards the late-Holocene, with a mean accumulation rate of 29yr.cm^{-1} from the surface to a depth of 107.5cm, and the early Holocene with depths of 327.5-472.5cm ranging in date from 10,550 ±30 cal. yr BP to 13,180 ±40 cal. yr BP (*Figure 5.12*).

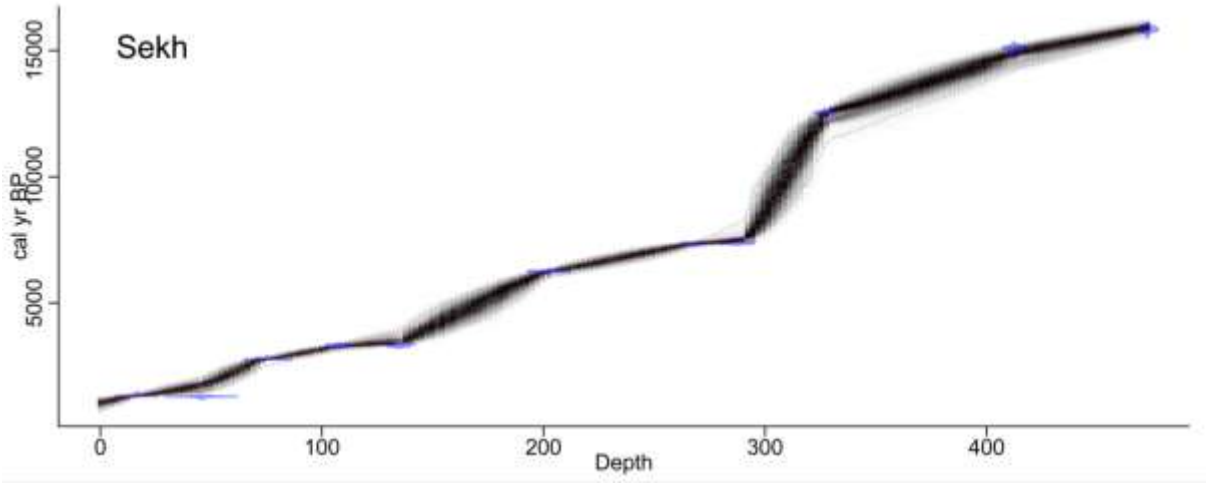


Figure 5.12: BACON output for the Sekhokong profile, providing interpolated ages for depths throughout the core.

5.3.2 Stratigraphy and Sediment Properties

Unlike the Sani Valley profile, which uniformly comprises dark coloured sediment rich in organic material, the Sekhokong profile comprises alternating clearly-defined layers of coarse orange-coloured gravels, dark black moist peat through to organic clay, and green-grey fine clays (*Figure 5.13*). Results from LOI, Mastersizer sediment particle size measurements, and comparisons with the Munsell colour chart for 43 samples spanning the

profile confirm numerous rapid fluctuations in organic content, carbonate content, particle size and colour throughout the sequence (*Table 5.6*).

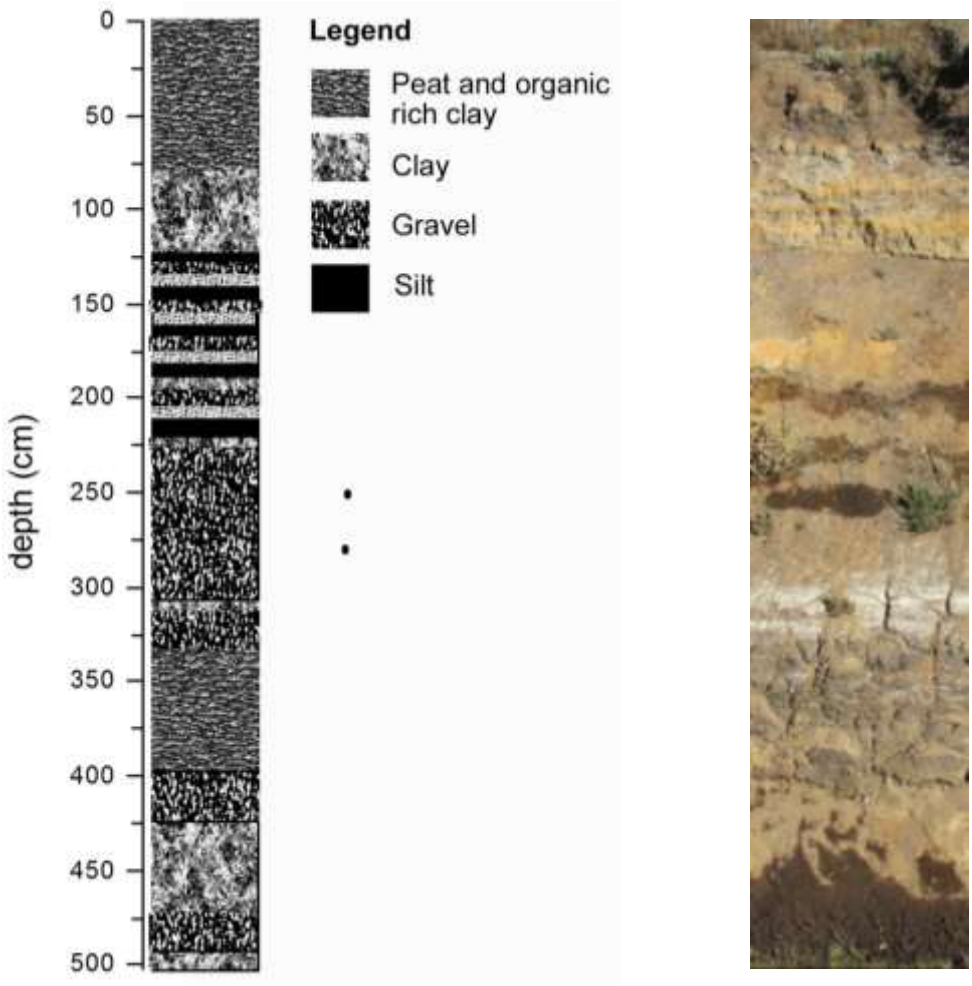


Figure 5.13: Stratigraphic log and photograph of core from Sekhokong

Coring terminated at a depth of 475cm, at a layer of impenetrable coarse gravel and dark grey clay, similar to the bottom of the Sani Valley profile (*Table 5.6*). This layer of clay and gravel was situated close to the bottom of the gulley face where the steam flowed. On the opposite side of the stream, comparison of the individual sedimentary layers suggested that a further 10cm of exposed sediment was present before the gravel and clay layer, which more closely corresponded with the layer of bedrock. This sediment was sampled, but would require extensive dating to be accurately compared with the samples from the opposite stream bank, and thus these samples are not included in this study.

Table 5.6: Summary of sedimentary changes throughout the Sekhokong profile.

Sample number	Depth	Mean	SD	Skewness	Kurtosis	Texture	Munsell
SK1	0-5	very fine grained	poorly sorted	near symmetrical	Leptokurtic	sandy loam	7.5YR 3/2
SK2	7-12	fine grained	poorly sorted	near symmetrical	Leptokurtic	loamy sand	10YR 3/2
SK3	14-19	very fine grained	poorly sorted	near symmetrical	Leptokurtic	loamy sand	5YR 2.5/2
SK4	20-25	very fine grained	poorly sorted	fine skewed	Leptokurtic	loamy sand	5YR 2.5/1
SK5	29-34	very fine grained	very poorly sorted	fine skewed	Leptokurtic	sandy loam	5YR 2.5/1
SK6	35-40	very fine grained	very poorly sorted	near symmetrical	Mesokurtic	sandy loam	5YR 2.5/2
SK7	42-47	medium grained	moderately sorted	coarse skewed	Leptokurtic	sand	7.5YR 3/2
SK8	50-55	very fine grained	poorly sorted	near symmetrical	Leptokurtic	sandy loam	5YR 3/2
SK9	58-62	fine grained	very poorly sorted	near symmetrical	Leptokurtic	loamy sand	5YR 3/3
SK10	65-70	fine grained	poorly sorted	near symmetrical	Mesokurtic	loamy sand	5YR 2.5/2
SK11	72-77	medium silt	poorly sorted	strongly fine skewed	Mesokurtic	silty loam	5YR 2.5/1
SK12	83-88	fine grained	very poorly sorted	fine skewed	Mesokurtic	loamy sand	5YR 4/1
SK13	93-100	very fine grained	very poorly sorted	fine skewed	Mesokurtic	sandy loam	5YR 3/1
SK14	105-110	medium grained	moderately sorted	skewed	Leptokurtic	sand	10YR 4/6
SK15	114-118	very fine grained	poorly sorted	fine skewed	Mesokurtic	loamy sand	10YR 3/6
SK16	119-120	fine grained	very poorly sorted	fine skewed	Playtykurtic	loamy sand	10YR 2/2
SK17	122-123	medium silt	poorly sorted	strongly fine skewed	Mesokurtic	silty loam	10YR 3/6
SK19	124-125	very fine grained	poorly sorted	fine skewed	Mesokurtic	sandy loam	10YR 3/2
SK20	126-127	very fine grained	very poorly sorted	near symmetrical	Leptokurtic	sandy loam	10YR 3/6
SK21	133-136	medium silt	poorly sorted	strongly fine skewed	Mesokurtic	silt	10YR 3/1
SK22	143-146	medium grained	very poorly sorted	strongly fine skewed	Mesokurtic	loamy sand	5YR 2.5/2
SK23	157-161	medium grained	very poorly sorted	fine skewed	Playtykurtic	loamy sand	10YR 4/6
SK24	185-190	very fine grained	poorly sorted	near symmetrical	Mesokurtic	sandy loam	5YR 2.5/2
SK25	200-205	fine grained	poorly sorted	fine skewed	Mesokurtic	loamy sand	10YR 3/6
SK26	211-212	medium silt	poorly sorted	strongly fine skewed	Mesokurtic	silt	10YR 3/1
SK27	220-225	very fine grained	poorly sorted	near symmetrical	Mesokurtic	loamy sand	5YR 3/3
SK28	230-235	fine grained	very poorly sorted	near symmetrical	Mesokurtic	loamy sand	10YR 3/6
SK29	245-250	coarse silt	poorly sorted	fine skewed	Leptokurtic	silty loam	10YR 2/1
SK30	265-270	coarse silt	poorly sorted	fine skewed	Leptokurtic	sandy loam	10YR 3/1
SK31	285-290	coarse silt	very poorly sorted	fine skewed	Mesokurtic	sandy loam	10YR 2/1
SK32	300-305	coarse silt	very poorly sorted	near symmetrical	Mesokurtic	sandy loam	10YR 2/2
SK33	307-310	very fine grained	poorly sorted	fine skewed	Leptokurtic	sandy loam	10YR 5/3
SK34	325-330	coarse silt	poorly sorted	near symmetrical	Leptokurtic	silty loam	5YR 3/1
SK35	355-360	medium silt	poorly sorted	fine skewed	Mesokurtic	silty loam	5YR 2.5/1
SK36	385-390	medium silt	poorly sorted	fine skewed	Mesokurtic	silty loam	10YR 2/1
SK37	395-400	coarse silt	poorly sorted	fine skewed	Mesokurtic	silty loam	10YR 2/1
SK38	410-415	coarse silt	poorly sorted	fine skewed	Leptokurtic	sandy loam	10YR 3/1
SK39	425-430	very fine grained	poorly sorted	near symmetrical	Leptokurtic	loamy sand	10YR 5/2
SK40	455-460	very fine grained	very poorly sorted	near symmetrical	Leptokurtic	sandy loam	10YR 4/2
SK41	470-475	very fine grained	poorly sorted	fine skewed	Leptokurtic	sandy loam	10YR 5/2
SK42	480-485	coarse silt	poorly sorted	fine skewed	Leptokurtic	silty loam	5YR 3/1
SK43	495-500	coarse silt	poorly sorted	fine skewed	Leptokurtic	silty loam	10YR 2/1
SK44	500-505	very fine grained	poorly sorted	fine skewed	Leptokurtic	sandy loam	10YR 3/6

A period with large percentage of organic material (>45%) is noted for the depths 457.5-387.5cm of the profile (*Figure 5.14*). AMS dates were acquired for these two constraining depths, placing this period between 12,660 ±40 cal. yr BP and 10,550 ±30 cal. yr BP, directly preceding the onset of the early Holocene period of slow accumulation mentioned previously. Within this period, organic percentage composition of greater than 75% is observed from depths of 427.5-397.5cm (~11,750-10,850 cal. yr BP; *Figure 5.14*). A second, far less extreme (>30%), peak in percentage organic content is observed for the late Holocene, from depths of 31.5-22.5cm (~1,560-1,430 cal. yr BP; *Figure 5.14*). These are the two most dominant of a total of 13 peaks in percentage organic content throughout the sequence (*Figure 5.14*). The relative percentages of sand-, silt- and clay-sized particles demonstrates considerably greater fluctuation in the most recent third of the Holocene, from depths of 134.5-2.5cm (~3,520-103 cal. yr BP) than during the early to middle Holocene (*Figure 5.14*). Greater percentages of gravel-sized particles are observed for this period, although also fluctuating considerably (*Figure 5.14*). Gravel-sized particles cease at a depth of 211.5cm (~5,320 cal. yr BP; *Figure 5.14*). Aside from the introduction of gravel, the sequence is dominated more by rapid low-amplitude fluctuations than by long-term trends in any particular direction (*Figure 5.14*).

CONISS performed on the percentage organic content, percentage carbonate content, and particle size results from Sekhokong divides the profile into three zones, named here as SKL1, SKL2 and SKL3 (*Figure 5.15*). The division between SKL1 and SKL2 occurs at a mean depth of 121cm (~3,390 cal. yr BP), marked by an abrupt decrease in sand-sized particles, a peak in silt- and clay-sized particles, and one of the two largest-amplitude peaks in skewness throughout the profile (*Figures 5.14, 5.15*). Both the percentage organic component and the percentage of carbonates demonstrate small peaks at this depth, and gravel sized particles are absent (*Figure 5.14*). The division between SKL2 and SKL3 occurs at a mean depth of 313cm (~6,970 cal. yr BP), coinciding with slight peaks in organic component and clay, and an abrupt decrease in silt-sized particles (*Figures 5.14, 5.15*). Within zone SKL2 is a notable sub-division at a mean depth of 227.5cm (~5,490 cal. yr BP) marking the onset of gravel-sized particles and a sustained peak in sand-sized particles, concurrent with low percentages of silt and clay sized particles, and very low carbonate percentages (*Figures 5.14, 5.15*).

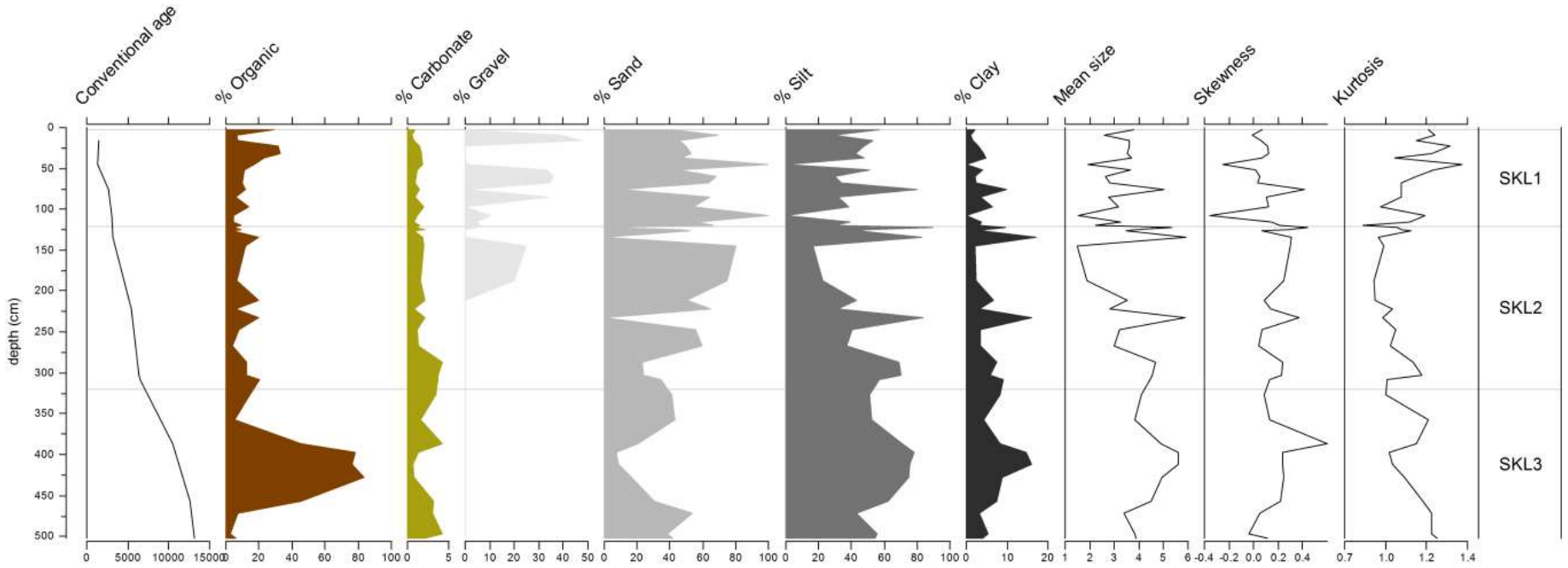


Figure 5.14: Stratigraphic plot demonstrating changes in sedimentary properties throughout the Sekhokong profile.

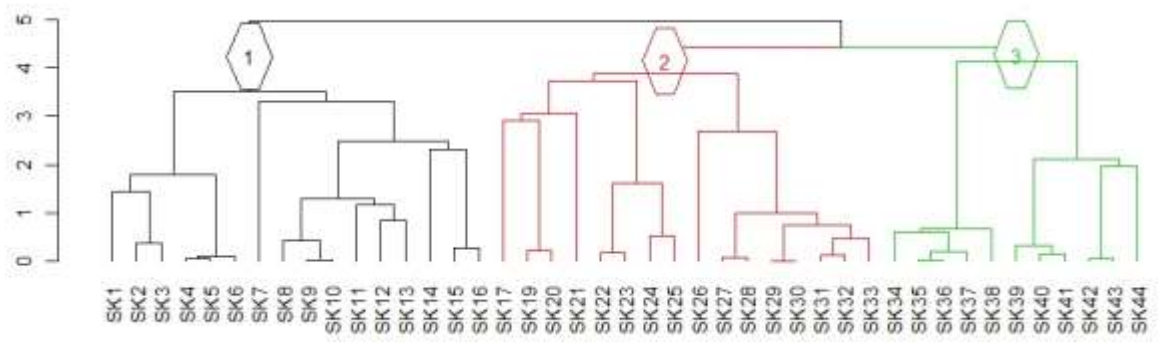


Figure 5.15: CONISS output separating the Sekhokong profile into zones on the basis of changes in the sedimentary properties.

Zone SKL3 (502.5-327.5cm; ~13,180-8,270 cal. yr BP) is characterised by the highest proportion of carbonates throughout the sequence, and a high organic content (*Figure 5.14*). The large peak in organic material for the sequence discussed previously is centred in this zone, and is coupled with smaller amplitude, more abrupt peaks in silt and clay, and simultaneous decreases in sand-sized particles and carbonates (*Figure 5.14*). The zone is dominated by silt-sized particles, which experience their largest concentrations for the profile in this zone (*Figure 5.14*). There are no gravel-sized particles in this zone. Overall, this zone most closely resembles the organic-rich sediments which dominate the Sani Valley sequence.

Zone SKL2 (308.5-122.5cm; ~8,210-3,420 cal. yr BP) is characterised by low carbonate percentages throughout (*Figure 5.14*). There is an overall decrease in the proportion of sand-sized particles, compensated by an increase in silt-sized particles throughout the depth of this zone, which appears to be a continuation of sediment particle size observed for zone SKL3, but which terminates with the increase in sand-sized particles and rapid fluctuations of zone SKL1 (*Figure 5.14*). No gravel-sized particles are measured for the bottom half of the zone, but they make a sudden appearance at a mean sample depth of 187.5cm (~4,790 cal. yr BP), at which point they account for 20% of the sample particle size distribution (*Figure 5.14*). The rest of the zone is marked by large proportions of gravel, dominating the sediment particle size distribution in many samples (*Figure 5.14*). This gravel dominance is paired with a large proportion of sand-sized particles, but low percentages of silt- and clay-sized particles (*Figure 5.14*). Immediately preceding the appearance of gravel is an abrupt

short-lived peak in silt- and clay-sized particles, accompanied by lower amplitude peaks in organic and carbonate percentages, and an absence of sand-sized particles (*Figure 5.14*).

Zone SKL1 (119.5cm - surface; ~3,380 cal. yr BP - present) is characterised by the lowest proportions of carbonate and clay throughout the sequence (*Figure 5.14*). By contrast, the highest proportions of sand- and gravel-sized particles occur within this zone, but with large-amplitude, short-lived fluctuations throughout the zone (*Figure 5.14*). The large fluctuations in sediment particle size are predominantly confined to this zone (*Figure 5.14*). The percentage organic content of sediment remains below 10% for much of the zone, with the exception of two marked peaks of 20% or higher at mean depths of 37.5-22.5cm (~1,640-1,430 cal. yr BP) and 2.5cm (~103 cal. yr BP; *Figure 5.14*). Skewness in the sediment particle size distribution decreases throughout the profile, indicating a decreasing proportion of large particles, while kurtosis increases, indicating particle size distributions that are more closely centred around the mean (*Figure 5.14*).

5.3.3 Pollen Analysis

Similar to Sani Valley, the sequence from Sekhokong is dominated by Poaceae*,* Cyperaceae and Asteraceae*,* with Poaceae accounting for the largest species count for this sequence at 49.2% (*Table 5.7*). This indicates greater grassland dominance in proportion to the size of the wetland than at the Sani Valley site, which is consistent with the contemporary environment. Pollen grains from a total of 24 different taxa were identified across the 43 samples spanning the profile. It is notable, given the considerably longer time period covered and the larger topographically defined area in which the site is located, that there are not considerably more plant families accounted for here than at the Sani Valley site. This could suggest that the location, and broader region of eastern Lesotho, have experienced repeated cycles within a clearly-defined niche environment over time. However, a limitation of all pollen work is the relatively poor resolution of taxon identification. Much of the larger contemporary species count at Sekhokong, compared to Sani Valley was at a family and genus level (*Table 3.6*). There is less of an extreme difference between the mean and maximum counts for each pollen type, which can be accounted for by the cyclical nature of the environmental shifts at this site over time, rather than a continued shift in a single direction.

Table 5.7: Frequency of occurrence of pollen grains throughout the Sekhokong profile.

Pollen type (family/genera)	% occurrence in core	Maximum individual sample %
Poaceae	49.2	65.6
Cyperaceae	21.0	36.4
Asteraceae	19.2	34.4
Crassula spp.	5.0	24.8
Cheno-Am	1.2	3.6
Pentzia spp.	1.1	4.4
Aizoaceae	1.0	5.6
Apiaceae	0.8	4.0
Liliaceae	0.6	4.4
Anthospermum spp.	0.4	3.2
Caryophylaceae	0.3	2.8
Indigofera spp.	0.1	1.0
Olea sp.	0.1	2.8
Passerina spp.	<0.1	0.7
Ericaceae	<0.1	0.4
Acanthaceae	<0.1	0.4
Malvaceae	<0.1	0.4
Geraniaceae	<0.1	0.4
Podocarpus sp.	<0.1	0.4
Vernonia	<0.1*	0.4
Amaranthaceae	<0.1	0.4
Agricultural grass	<0.1*	0.4
Chrysocoma sp.	<0.1*	0.4
Gentianaceae	<0.1	0.4

* grouped by their family (Asteraceae and Poaceae respectively)

CONISS analysis on the pollen data obtained from the Sekhokong samples separates the sequence into three primary zones (*Figure 5.16*). Zone SKP3 represents the transition from the late Pleistocene to the early Holocene, extending from the bottom of the core at 542.5cm (~13,180 cal. yr BP) to a depth of 302.5 (~6,420 cal. yr BP; *Figure 5.16*). This is followed by SKP2, a particularly long zone of 28 samples, from a depth of 287.5cm (~6,130 cal. yr BP) to 16.5cm (~1,340 cal. yr BP; *Figure 5.16*). The first zone, SKP1, is brief encompassing only the top two samples, extending from a depth of 9.5cm (~1,030 cal. yr BP) to the surface (*Figure 5.16*).

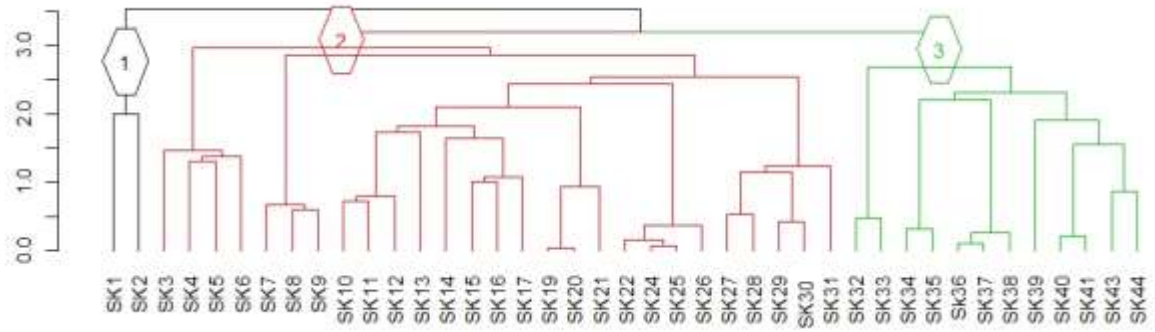


Figure 5.16: CONISS output separating the Sekhokong profile into zones based on the relative abundance of pollen throughout.

The PCA biplot for principal components 1 and 2 demonstrates the considerable difference between SKP1 and the rest of the sequence (*Figure 5.17*). The two SKP1 samples are located in the 3rd quadrant, with strongly negative PC1 scores (*Figure 5.17*). They appear to have affinities with *Olea*, *Vernonia*, *Anthospermum* and *Crassula* (*Figure 5.17*). Samples from SKP2 and SKP3 are centred around a PC1 score of zero with a greater range in PC2 scores (*Figure 5.17*. SKP2 and SKP3 samples and are less clearly clustered by their zones, with samples from both zones found across all four quadrants. The majority of SKP2 samples are, however, located in quadrants 2 and 3 with negative PC2 values, while SKP3 samples are largely situated in quadrants 4 and 1 with positive PC2 scores (*Figure 5.17*). SKP2 samples display greater affinities for Poaceae, Liliaceae, *Pentzia* and Apiaceae, while SKP3 samples have a greater association with Cyperaceae, Caryophylaceae and Cheno-Am (*Figure 5.17*).

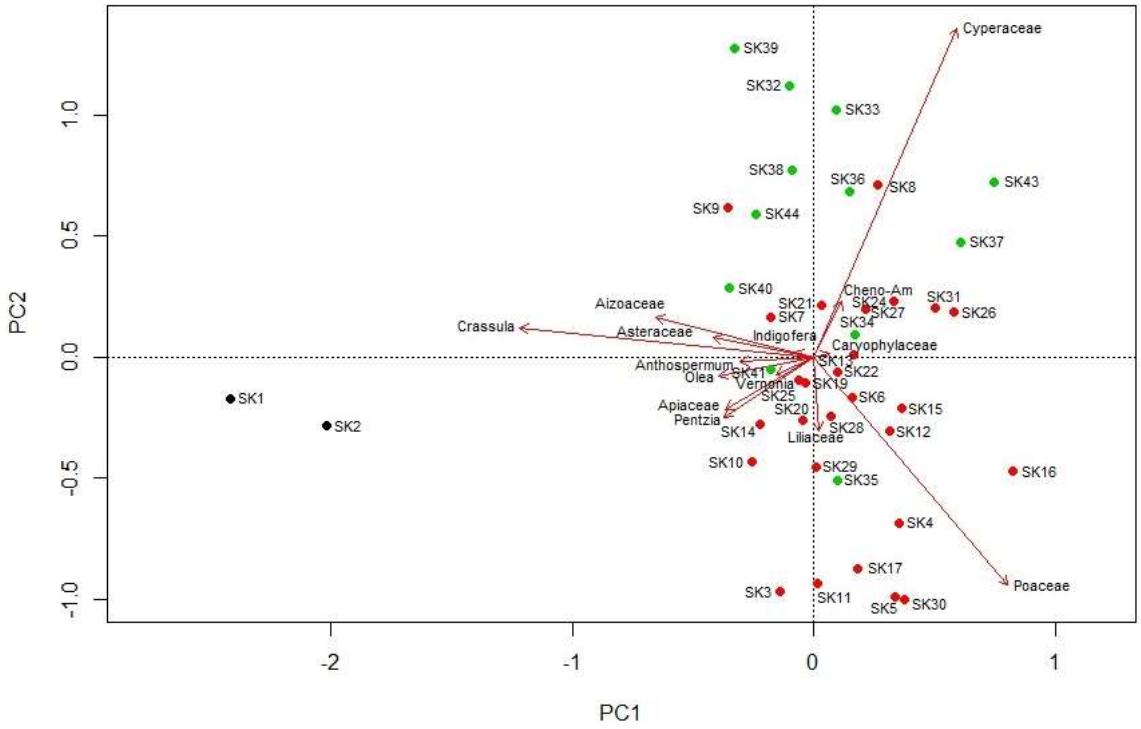


Figure 5.17: PCA biplot for the pollen results from the Sekhokong profile.

PC1 accounts for 26.6% of the observed variance in pollen counts across samples. Ordering the species by their PC1 species score, *Crassula*, Aizoaceae and Asteraceae are distinguished most strongly from Cheno-Am, Cyperaceae and Poaceae (*Figure 5.17*). The similarity in species scores for Cyperaceae and Poaceae are notable for PC1, as they represent typically opposing environmental conditions of wetland and grassland respectively. Marked by the

extreme isolation of the SKP1 samples, PC1 appears to be driven by the difference between the contemporary, anthropogenically influenced drier landscape, and palaeo-vegetation, rather than the environmental drivers responsible for long term fluctuations within the palaeo-vegetation. PC2 accounts for 22.2% of the observed variance in relative pollen abundance across samples, and together with PC1, explains a cumulative total of 48.8%. Arranged by species score for PC2, Poaceae and Cyperaceae are separated by extremes in species score, separating a dominance of grass from communities of sedges and shrubs (*Figure 5.17*). The differences between SKP3 and SKP2 are more apparent when analysing PC2, with a shift from positive to negative PC2 scores.

Zones SKP3 (502.5-302.5cm; ~13,180-6,470 cal. yr BP) and SKP2 (287.5-16.5cm; ~6,420-1,200 cal. yr BP) are similar in their relative abundance of the different pollen groups, with relatively consistent PC1 scores throughout (*Figure 5.18*). As indicated on the PCA biplot (*Figure 5.17*), there are larger percentages of Poaceae in SKP2 than SKP3, and for SKP2, Poaceae is the dominant plant type. *Pentzia*, Cheno-Am and Asteraceae are present throughout SKP3, while the proportion of Cyperaceae fluctuates between 10-30%. Poaceae is less dominant throughout SKP3, with proportions of Cyperaceae and Asteraceae, and a continued presence of Cheno-Am pollen (*Figure 5.18*). SKP3 is marked by three peaks in Cyperaceae counts, with maxima at depths of 502.5cm (~13,180 cal. yr BP), 397.5cm (~10,850 cal. yr BP) and 308.5cm (~6,470 cal. yr BP), all of which are concurrent with low relative abundances of Poaceae (*Figure 5.18*). These peaks in Cyperaceae are separated by peaks in relative abundance of Poaceae, and decreases in Cyperaceae and Asteraceae pollen (*Figure 5.18*). Notable are peaks in *Crassula* throughout zone SKP3, which are not in phase with Cyperaceae and Asteraceae, but more closely resemble the timing of peaks in Poaceae, despite the positive PC2 species score (*Figure 5.17*). For SKP2, peaks in Poaceae are apparent at the beginning and end of the zone, while Poaceae pollen reaches lowest concentrations at a depth of 60cm (~2,270 cal. yr BP), concurrent with the peak in Cyperaceae, potentially indicative of a short period of wetland retreat (*Figure 5.18*). While the proportion of Poaceae pollen remains relatively stable, there is considerable fluctuation in Cyperaceae abundance throughout the zone (*Figure 5.18*). Although comparatively more stable, the relative abundance of Asteraceae and *Crassula* fluctuate throughout this zone, with relatively similar timing in their peaks (*Figure 5.18*).

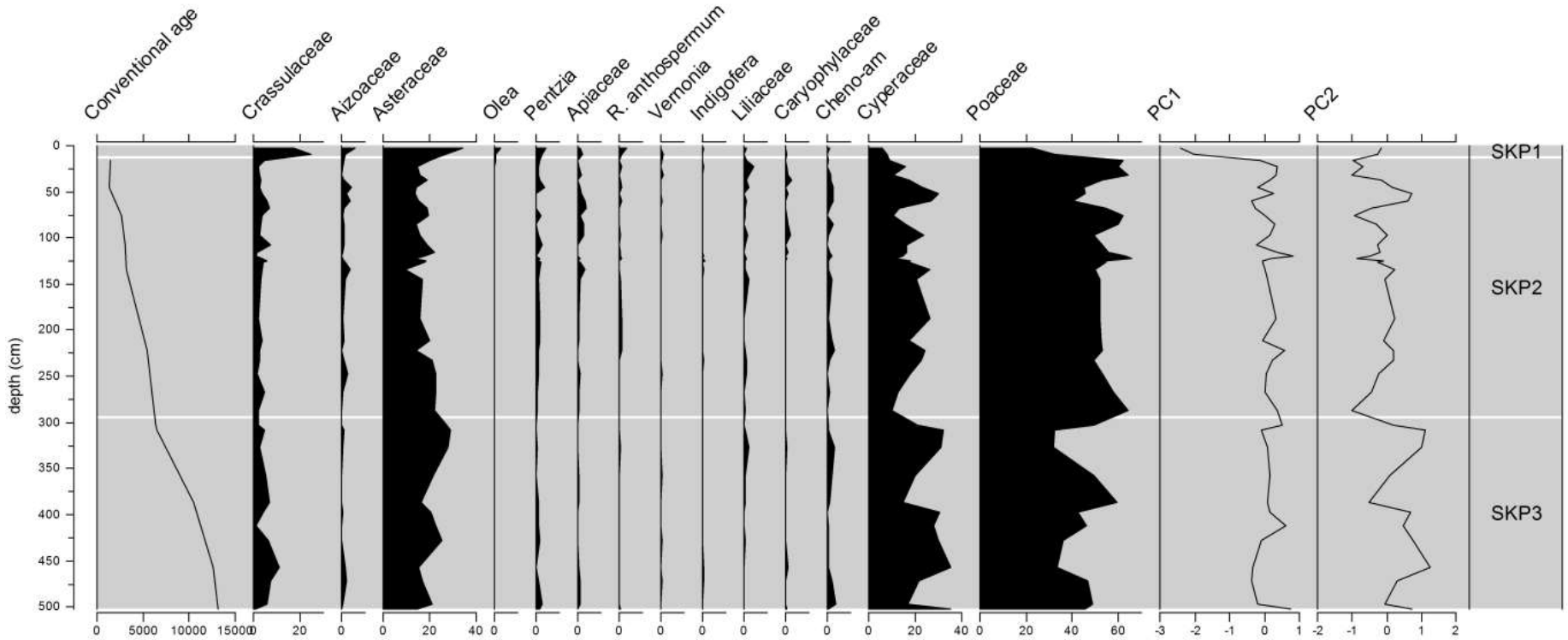


Figure 5.18: Stratigraphic plot demonstrating changes in pollen throughout the Sekhokong profile, with species arranged by PC1 species score, and curves for the PC1 and PC2 sample scores.

SKP1 (~1,150 cal yr. BP - present) is marked by a sudden peak in *Crassula* pollen, which reflecting greater than 20% of the total pollen composition of this zone, is of an order of ten times the maximum relative abundance of the taxon throughout the remainder of the sequence (*Figure 5.18*). Paired with the unusually high *Crassula* count, are large-amplitude peaks in Aizoaceae and Asteraceae, again with quantities greater than those represented within samples at depths lower in the sequence (*Figure 5.18*). Although with smaller-amplitude peaks, *Pentzia*, Apiaceae, *Anthospermum* and *Vernonia* contribute to the species composition in this zone, distinguishing SKP1 from the previous zones (*Figure 5.18*). During this period, Cyperaceae and Poaceae pollen proportions are at their minima for the sequence (*Figure 5.18*). Notably the tree species, *Olea*, is present only in this zone, but is present also at the Sani Valley site, despite both sites being situated above the contemporary tree line (*Figure 5.18*).

5.3.4 Diatom Analysis

Diatom valves from a total of 39 species have been identified from 43 samples spanning the Sekhokong sequence, with large similarities in species composition between the Sani Valley and Sekhokong profiles (*Table 5.8*). Similar to the Sani Valley site (*Table 5.4*), the diatom assemblages identified from Sekhokong are dominated by *Fragilaria famelica*, with relatively large proportions of *Diploneis parma* and *Cymbella laevis.* Specific to the Sekhokong site are larger proportions of *Eunotia bilunaris*, *Hantzschia amphioxys* and *Pinnularia divergentissima,* all aerophilic diatoms (*Table 5.8*). Notable are the species *Fragilaria pinnata*, *Cymbella laevis*, *Fragilaria construens* and *Aulacoseira ambigua*, for which the maximum percentage contributions within an individual sample are considerably larger than the mean percent occurrences within the core, suggesting the existence of key periods during the time period represented by the profile, which were particularly more suitable for their concurrent or independent growth.

Table 5.8: Percentage occurrence of diatom species throughout the Sekhokong profile.

Diatom species	% occurrence in core	Maximum individual sample %
Fragilaria famelica Kützing (Synedra famelica)	26.4	86.8
Eunotia bilunaris Ehrenberg	8.2	36.7
Hantzschia amphioxys Ehrenberg	7.4	17.9
Pinnularia divergentissima Grunow	6.6	18.5
Diploneis parma Cleve	5.7	19.0
Pinnularia borealis Ehrenberg	5.3	13.6
Pinnularia gentilis Donkin	4.4	10.2
Eunotia praerupta Ehrenberg	3.7	10.2
Navicula minima Grunow	3.6	13.3
Fragilaria pinnata Ehrenberg (Staurosirella pinnata)	3.6	26.8
Cymbella gracilis Ehrenberg	3.4	10.6
Cymbella laevis Nägeli	3.0	21.9
Fragilaria construens Ehrenberg	2.6	19.0
Achnanthes minutissima Kützing	2.3	12.5
Gomphonema parvulum Kützing	2.3	9.6
Stauroneis phoenicenteron Ehrenberg	1.7	5.5
Aulacoseira ambigua Grunow	1.6	19.0
Eunotia exigua Brébisson ex Kützing	1.5	10.0
Navicula laevissima Kützing	1.2	5.9
Diploneis ovalis Hilse	1.1	5.5
Navicula explanata Hustedt	1.0	6.6
Sellaphora pupula Kützing	1.0	5.6
Gomphonema gracile	0.9	6.6
Caloneis silicula Ehrenberg	0.7	3.7
Nitzschia palea Kützing	0.4	2.9
Cymbella cistula	0.4	3.9
Stauroneis product	0.4	2.8
Cymbella selesiaca	0.4	5.6
Navicula trivialis Lange-Bertalot	0.4	2.0
Pinnularia viridis Ehrenberg	0.2	3.3
Gomphonema bohemicum Hustedt	0.2	3.8
Denticula kuetzingii Grunow	0.2	1.6
Diploneis didyma	0.1	2.9
Navicula salinarum	0.1	1.9
Navicula pygmaea Kützing	0.1	1.0
Pinnularia intermedia Lagerstedt	0.1	1.0
Achnanthes coartata	<0.1	1.0
Navicula insociabilis Krasske	<0.1	0.7
Gomphonema exigua	<0.1	0.7

CONISS for diatom results from Sekhokong divides the sequence into four zones of relatively equivalent size (*Figure 5.19*). Zone SKD4 represents the lowest portion of the core from the bottom of the profile at 542cm (~13,180 cal. yr BP) to a depth of 327.5cm (~7,460 cal. yr BP), and can be separated into two subzones at a mean depth of 405cm (~11,170 cal. yr BP; *Figure 5.19*). Zone SKD3 covers the portion of the sequence of the core from 308.5-134.5cm (~6,470-3,520 cal. yr BP), and can be subdivided into lower-order zones at a mean depth of 257.5cm (~5,870 cal. yr BP; *Figure 5.19*). Zone SKD2 comprises the smallest group of samples, extending from a depth of 126.5 (3,450 cal. yr BP) to 107.5cm (~3,270 cal. yr BP; *Figure 5.19*). Zone SKD1 extends from a depth 96.5cm (~3,110 cal. yr BP) to the surface, and has two clearly delineated sub-zones separated at a mean depth of 56cm (~2,130 cal. yr BP; *Figure 5.19*). The large number of hierarchical splits is representative of the numerous sedimentary lenses, which are believed to be environmentally driven.

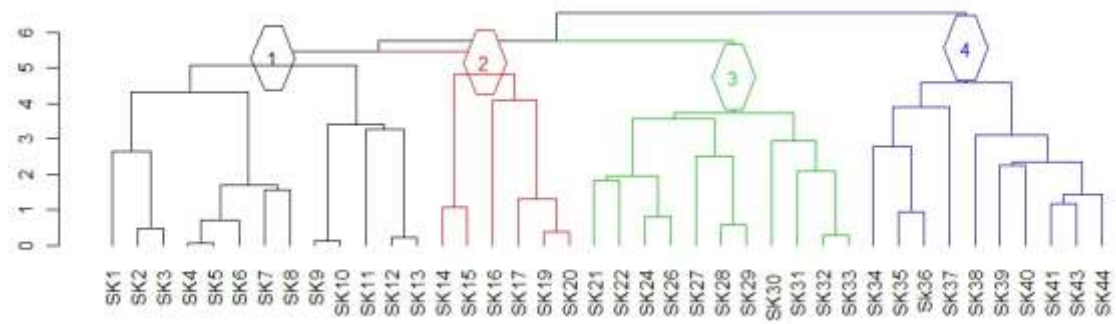


Figure 5.19: CONISS output separating the Sekhokong profile into zones based on the diatom results.

Samples from zones SKD2 and SKD4 are fairly distinctly clustered in the PCA biplot of principal components 1 and 2 (*Figure 5.20*). Samples from zone SKD2 are predominantly situated in quadrant 3, along a gradient of negative PC2 scores, demonstrating a strong affinity with *Fragilaria famelica* and *Achnanthes minutissima* (*Figure 5.20*). Samples from SKD4 appear in quadrants 1 and 2, similarly along a gradient of PC2 sores, influenced by a large number of species, but with strongest affinity with *Eunotia bilunaris*, *Cymbella laevis, Aulacoseira ambigua* and *Fragilaria pinnata/ construens* (*Figure 5.20*). Samples from zones SKD1 and SKD3 are scattered predominantly across quadrants 1 and 4, across gradients of positive PC2 scores (*Figure 5.20*). Their distinction, outside of the constraints of stratigraphy, is therefore likely to be represented in lower order principal components.

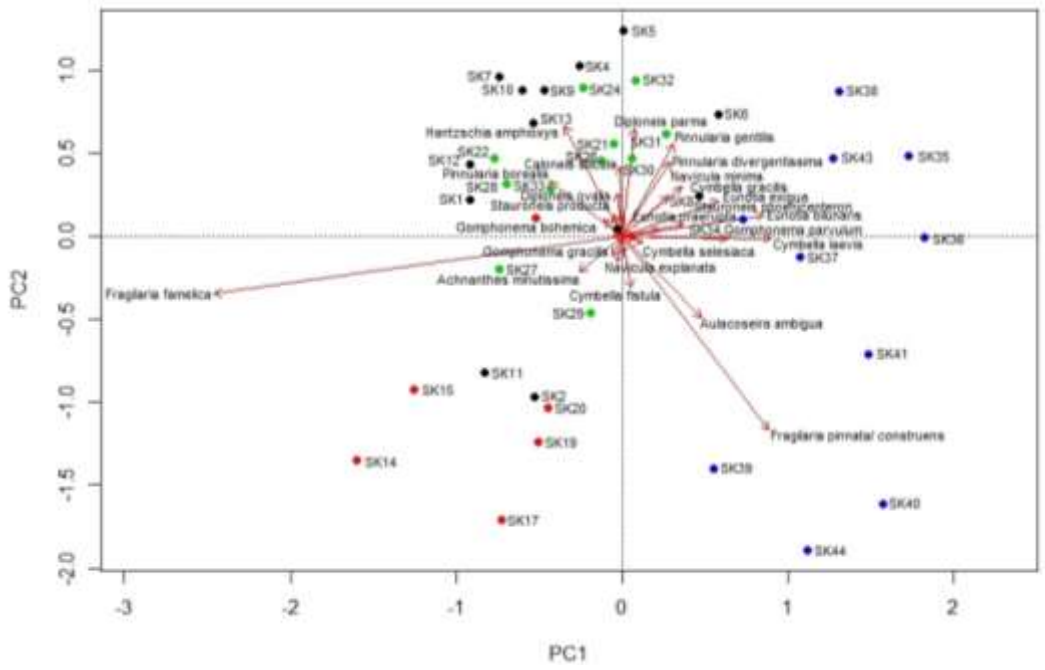


Figure 5.20: PCA biplot for the diatom results from the Sekhokong profile.

PC1 accounts for 35.0% of the observed variation in diatom species composition across samples from the Sekhokong profile. Arranged by species score for PC1, samples are differentiated by a change from conditions dominated by *Fragilaria famelica*, *Pinnularia borealis*, *Hantzschia amphioxys* and *Achnanthes minutissima* to environments characterised by *Fragilaria pinnata/ construens*, *Cymbella laevis* and *Eunotia bilunaris* (*Figure 5.21*). A notable decrease in PC1 scores is apparent throughout the profile, driven by a significant increase in the relative abundance of *Fragilaria famelica*, paired with less extreme decreases in *Fragilaria pinnata/ construens*, *Cymbella laevis* and *Eunotia bilunaris* (*Figure 5.21*). A slight increase in PC1 scores at the top of the sequence appears to be driven by an abrupt decrease in *Fragilaria famelica* and a peak in *Eunotia bilunaris* (*Figure 5.21*). PC2 accounts for 13.3% of the observed variance in diatom species composition across the samples from Sekhokong, and together with PC1, a cumulative total of 48.3% of the variance. Species scores from PC2 separate *Fragilaria pinnata/ construens*, *Aulacoseira ambigua* and *Fragilaria famelica* from *Hantzschia amphioxys*, *Diploneis parma*, *Pinnularia gentilis* and *Pinnularia divergentissima* (*Figure 5.20*). Far greater fluctuation in PC2 scores occurs throughout the profile than was observed for PC1 scores (*Figure 5.21*).

Zone SKD4, (502.5-327.5cm; ~13,180-8,270 cal. yr BP) is distinguished by a low relative abundance of *Fragilaria famelica* (*Figure 5.21*). In place of *Fragilaria famelica*, the zone is dominated by a group of species with the highest PC1 species scores, including *Fragilaria pinnata/ construens*, *Cymbella laevis* and *Eunotia bilunaris* (*Figure 5.21*). PC1 scores are characterised by two prolonged high-amplitude peaks in this zone. The first, peak extending from a depth of 497.5-457.5cm (~13,080-12,660 cal. yr BP), with its maximum point at 457.5cm, is characterised by large proportions of *Fragilaria pinnata/ construens* (*Figure 5.21*). The second peak, extending from 412.5-357.5cm (~13,300-9,020 cal. yr BP), with a maximum at a depth of 387.5cm (~10,550 cal. yr BP) is driven by larger percentages of *Eunotia bilunaris* and *Cymbella laevis* (*Figure 5.21*). A decrease in PC1 scores between these peaks is driven by an increased abundance (21.2%) of *Fragilaria famelica* at a depth of 427.5cm (~11,750 cal. yr BP; *Figure 5.21*). Elevated PC2 scores characterise SKD4, dominated by a decrease in *Fragilaria pinnata/ construens* and *Aulacoseira ambigua*, and a slight increase in *Hantzschia amphioxys* (*Figure 5.21*). The bottom half of SKD4 represents the only

section of the profile with significant percentage of *Aulacoseira ambigua*, a planktonic species which favours deeper waters (*Figure 5.21*).

Zone SKD3 (308.5-134.5cm; ~8,210-3,510 cal. yr BP) is characterised by the introduction of *Fragilaria famelica*, initiating the continued increase in the relative abundance of this species witnessed throughout the rest of the profile (*Figure 5.21*). The largest relative abundance of *Pinnularia borealis* and *Hantzschia amphioxys* throughout the sequence occur in this zone, paired with the lowest relative abundance of *Fragilaria pinnata/ construens*, *Cymbella laevis* and *Eunotia bilunaris* (*Figure 5.21*). PC1 scores decrease throughout this zone, with three negative peaks, at depths of 144.5cm (~3,730 cal. yr BP), 222.5cm (~5,450 cal. yr BP) and 308.5cm (~6,470 cal. yr BP; *Figure 5.21*). All three incursions in PC1 sample scores coincide with peaks in *Fragilaria famelica* abundance, while the upper two also coincide with peaks in *Pinnularia borealis* and *Hantzschia amphioxys* (*Figure 5.21*). SKD3, which is marked by a low abundance of *Fragilaria pinnata/ construens* and near-absent *Aulacoseira ambigua*, has a relatively consistent positive PC2 score, with 5-20% of the core represented by each of *Hantzschia amphioxys*, *Diploneis parma*, *Pinnularia gentilis*, *Pinnularia divergentissima* and *Pinnularia borealis* (*Figure 5.21*).

Zone SKD2 (126.5-107.5cm; ~3,460-3,220 cal. yr BP) contains the highest relative abundance of *Fragilaria famelica* for the sequence, comprising over 50% of the species count in all samples (*Figure 5.21*). PC1 scores decrease rapidly throughout this zone, driven by an increase in *Fragilaria famelica* (*Figure 5.21*). The decrease in the PC1 curve has a brief interruption with a peak at 119.5cm (~3,380 cal. yr BP), driven by abrupt peaks in the relative abundance of the positively loaded *Fragilaria pinnata/ construens*, *Gomphonema parvulum*, *Eunotia exigua* and *Stauroneis phoenicenteron* (*Figure 5.21*). Low PC2 scores dominate SKD2, punctuated by a sudden, short-lived peak, driven by a short-lived increase in abundance of *Hantzschia amphioxys*, *Diploneis parma*, *Pinnularia gentilis* and *Pinnularia divergentissima* (*Figure 5.21*). The low PC2 scores at the beginning of SKD2 are marked by peaks in *Fragilaria pinnata/ construens* and *Achnanthes minutissima*, while the peak at the end of the zone corresponds with the largest peak in *Fragilaria famelica* observed across the whole sequence (*Figure 5.21*).

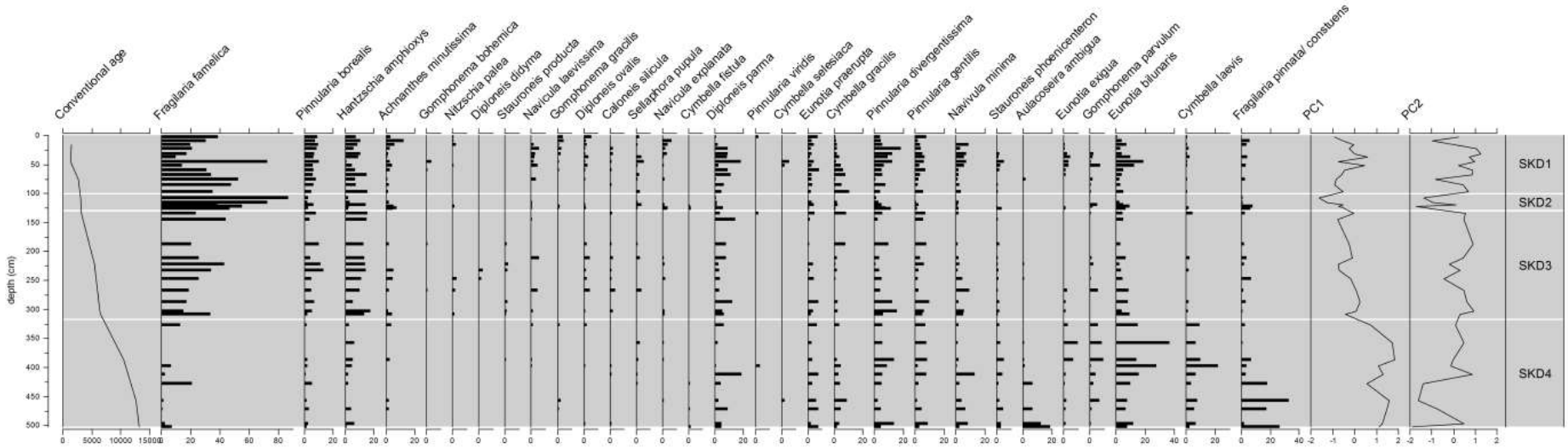


Figure 5.21: Stratigraphic diagram of the diatom results from the Sekhokong profile, with species ordered by PC1 species score and curves for the PC1 and PC2 sample scores.

Zone SKD1 (96.5cm - surface; ~3,170 cal. yr BP - present) is dominated by *Fragilaria famelica* throughout, even at the lowest concentration of the species at a depth of 37.5cm (~1,640 cal. yr BP; *Figure 5.21*). *Fragilaria famelica* decreases from ~50% at the beginning of the zone to a minimum of 17% at 37.5cm, but re-emerges thereafter, reaching a relative abundance of 39% at the surface (*Figure 5.21*). The period of lowest concentrations in *Fragilaria famelica* coincides with a decrease in *Hantzschia amphioxys*, but with peaks in the abundance of *Eunotia bilunaris*, *Gomphonema parvulum*, *Eunotia exigua*, *Stauroneis phoenicenteron*, *Navicula minima*, *Pinnularia gentilis*, *Pinnularia divergentissima*, and *Diploneis parma* (*Figure 5.21*). *Pinnularia borealis* and *Fragilaria pinnata/ construens* demonstrate little change through this zone, with relative abundances of 5-10% and 0-5% respectively (*Figure 5.21*). The most rapid and highest amplitude fluctuations in PC2 scores are observed in zone SKD1, driven by the periodic presence of *Fragilaria pinnata/ construens*, and largely coinciding with decreases in abundance of *Hantzschia amphioxys* and *Diploneis parma* (*Figure 5.21*).

5.3.5 Multi-Proxy Synthesis

The three zones from the CONISS analysis of the pollen sequence for Sekhokong are used to separate the multi-proxy plot (*Figure 5.22*). The Sekhokong profile demonstrates progressive shifts in pollen and diatom communities, and in sediment particle size, throughout the late Quaternary (*Figure 5.22*). A decrease in pollen PC2 scores is noted throughout the profile, reflecting a gradual decline in the proportion of Cyperaceae pollen (*Figure 5.22*). Diatom PC1 scores decrease more notably throughout the profile, driven by a change from an environment dominated by *Fragilaria pinnata/ construens*, *Cymbella laevis* and *Eunotia bilunaris,* to one comprised of a far greater relative abundance of *Fragilaria famelica, Pinnularia bilunaris* and *Hantzschia amphioxys* (*Figure 5.22*). Throughout the profile, the proportion of silt- and clay-sized particles decreases, replaced by greater percentages of sand-sized particles and the introduction of gravel-sized particles (*Figure 5.22*).

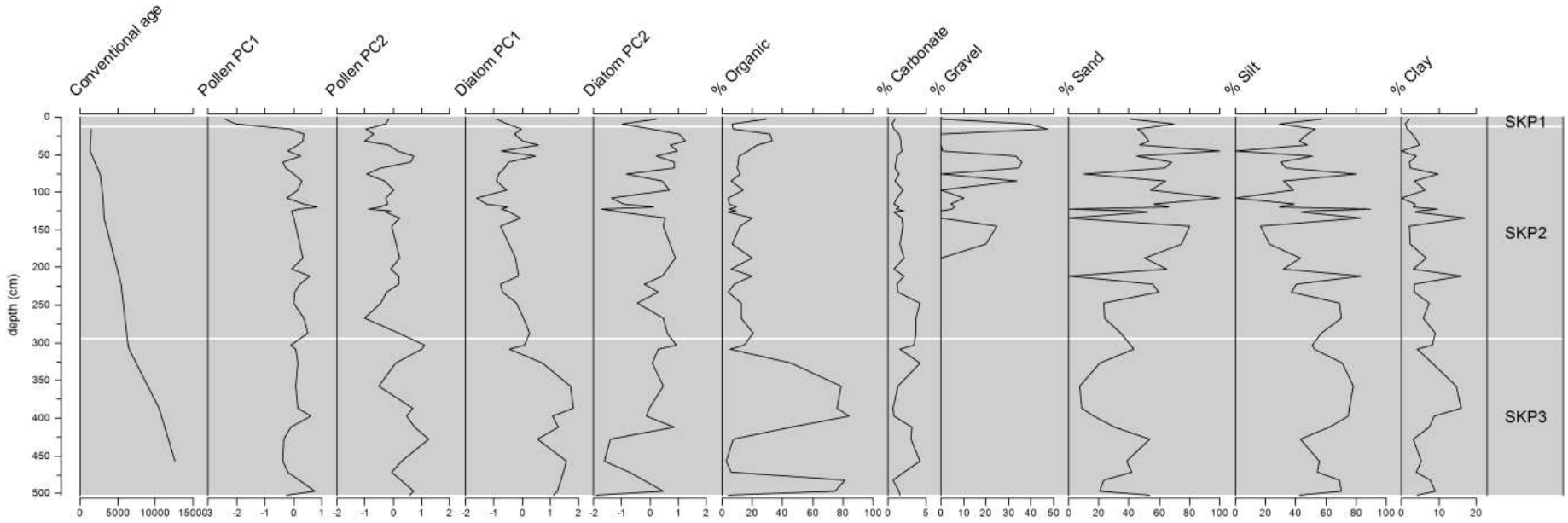


Figure 5.22: Multi-proxy stratigraphic diagram for Sekhokong.

Zones SKP3 (502.5-302.5cm; ~13,180-6,470 cal. yr BP) is marked by large amplitude fluctuations in the sediment characteristics, but relatively consistent pollen PC1 scores (*Figure 5.22*). Pollen PC2 scores approximately mirror the diatom PC1 scores, while the diatom PC2 scores track the pattern of fluctuations of the percentage organic content of the sediment for the first half of the zone (*Figure 5.22*). The prolonged peak in the percentage organic content from 397-357cm (~10,850-9,020 cal. yr BP), however, is simultaneous with a progressive increase in diatom PC2 scores (*Figure 5.22*). The percentage silt- and clay-sized particles both mirror the fluctuations in the percentage of sand-sized particles throughout the zone (*Figure 5.22*).

SKP2 (287.5-16.5cm; ~6,420-1,200 cal. yr BP) can be divided into two distinct sub-zones, with the latter marked by the appearance of gravel sized particles at 169cm (~4,220 cal. yr BP; *Figure 5.22*). The first half of the zone is characterised by relatively consistent pollen PC1 and PC2 scores, diatom PC1 and PC2 scores, and percentage composition of carbonates (*Figure 5.22*). The percentage of sand-sized particles increases throughout the first half of this zone, while the percentage of silt-sized particles decreases (*Figure 5.22*). These trends are marked by an abrupt peak in silt-and clay-sized particles, and a simultaneous drop in sand-sized particles at 211.5cm (~5,320 cal. yr BP; *Figure 5.22*). The second half of the zone is characterised by rapid, high-amplitude fluctuations in all of the proxy variables (*Figure 5.22*). There are two notable peaks in the percentage of sand-sized particles, at 122.5cm (~3,410 cal. yr BP) and 45.5cm (~1,750 cal. yr BP; *Figure 5.22*). The former is contemporary with a drop in pollen PC2, diatom PC1 and the percentage organic content, while the latter coincides with a drop in pollen PC1 and diatom PC1, and a peak in diatom PC2, and marks the beginning of a peak in carbonates and a decrease in the percentage carbonate content (*Figure 5.22*).

SKP1 (~1,150 cal yr. BP - present) is marked by a large decline in pollen PC1, simultaneous with smaller amplitude decreases in diatom PC1, and the percentages of gravel- and sand-sized particles, and increases in pollen PC2, diatom PC2, the percentage organic content, percentage carbonate content, and in the percent of silt- and clay-sized particles (*Figure 5.22*).

5.4 MAFADI WETLAND

5.4.1 CHRONOLOGY AND SEDIMENT ACCUMULATION

A total of five AMS dates were acquired for the Mafadi Wetland profile, distributed at largely regular intervals throughout the profile, with depths for age-dates selected on the basis of occurrences of peaks in more than one proxy (*Table 5.9*). These dates constrain the 103cm profile to the last 7,140 ±30 cal. yr BP, while the youngest date of 870 ±30 cal. yr BP obtained at a depth of 7cm would suggest that the sequence extends to the contemporary environment at the surface. All of the dates acquired were in sequence, and fit within the BACON model, with no outliers statistically identified. Notably, although 8cm shorter in depth, this profile covers a significantly longer time period than that of the sequence from Sani Valley, even with largest extrapolated bottom-date for that core, with older dates consistently acquired at comparable depths throughout the Mafadi Wetland core.

Table 5.9: AMS radiocarbon dates acquired for the Mafadi Wetland profile.

Laboratory ID	^{14}C Age (yr BP)	Age (cal. yr BP)	1σ Uncertainty (yr)	2σ calibrated age range (BP)	Mean Depth (cm)	Sample Thickness	d13C
M3	900	870	±30	790-680	7	3cm	-26.6
M13	1,310	1,280	±30	1,270-1,205	41	3cm	-26.8
M19	5,020	4,960	±30	5,710-5,675	59	3cm	-28.5
M32	6,660	6,650	±30	7,565-7,435	84	3cm	-25.8
M38	7,160	7,140	±30	7,970-7,925	103	3cm	-26.3

The accumulation rate calculated by the BACON model is averaged for the sequence at 100yr.cm^{-1} (*Figure 5.23*). This slow accumulation compared to the lower-altitude sites is most likely a function of the lower temperatures at this site due to the 400m higher altitude, but may additionally reflect the influence of deflation. Temperature would play a large role in the accumulation rate at all three sites due to their contemporary peat-dominated sediment, and considerable organic content throughout the profiles, requiring warm temperatures to facilitate plant growth, and for sufficient humidity to develop peat. Similar to both the Sani Valley and Sekhokong sites, there is a marked period of particularly slow accumulation, potentially coupled with sediment loss, which extends from 1,280 ±30 cal. yr BP to 4,960 ±30 cal. yr BP (*Figure 5.23*). During this period, only 18cm of sediment accumulated, yielding an accumulation rate less than half of the mean, at 205yr.cm^{-1}. Before

and after this period of slow accumulation, periods of consistent, and more rapid accumulation are noted (*Figure 5.23*).

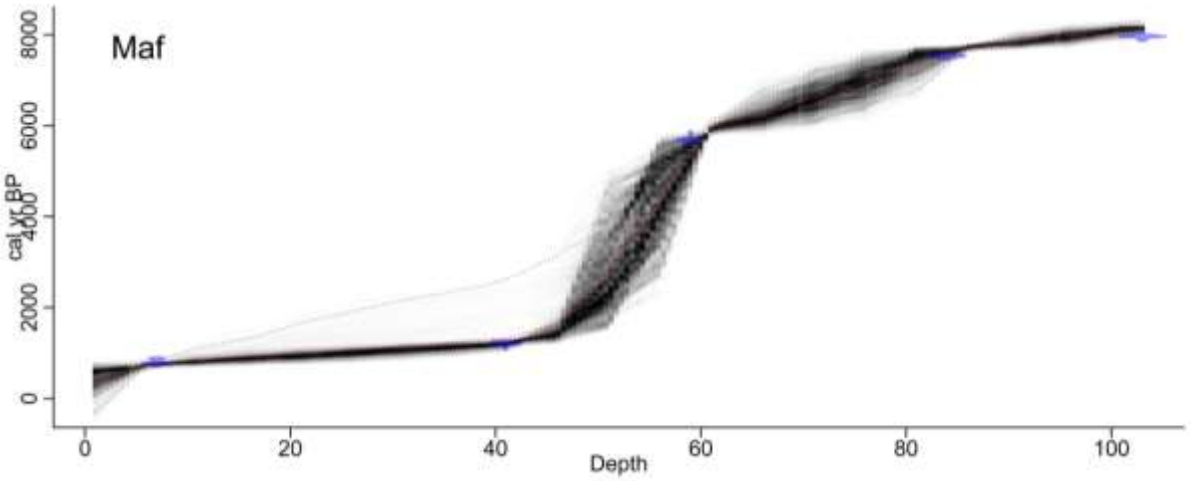


Figure 5.23: BACON output for the Mafadi Wetland profile, providing interpolated ages for depths throughout the core.

5.4.2 Stratigraphy and Sediment Properties

The profile from Mafadi Wetland contains considerably lower percentages of organic material across the 38 samples than in the profiles from Sani Valley and Sekhokong (*Figure 5.24*). The largest proportion of organic material occurs in the top samples which represent the contemporary environment (*Figure 5.24*). This peak marks the culmination of continued increase in organic material throughout the profile, particularly in the top 25cm, covering the approximate period of ~1,060 cal. yr BP to present (*Figure 5.24*). A large decrease in the organic and carbonate component of the sediment occurs from a depth of 38-25cm (~1,270-1,060 cal. yr BP), paired with a sudden decrease in the mean particles size and the proportion of silt-sized particles (*Figure 5.24*). The lower percentage organic content at Mafadi Wetland may, in part, be explained by the considerable diatomite content, indicated by the lighter colour of the sediment (*Table 5.10*), which would necessarily result in a lower LOI results as these silica frustules remain in the sample. There is a slight increase in silt- and decrease in sand-sized particles throughout the profile, although this is obscured by large amplitude fluctuations (*Figure 5.24*). Similar to Sani Valley, there are no gravel-sized particles in the sequence.

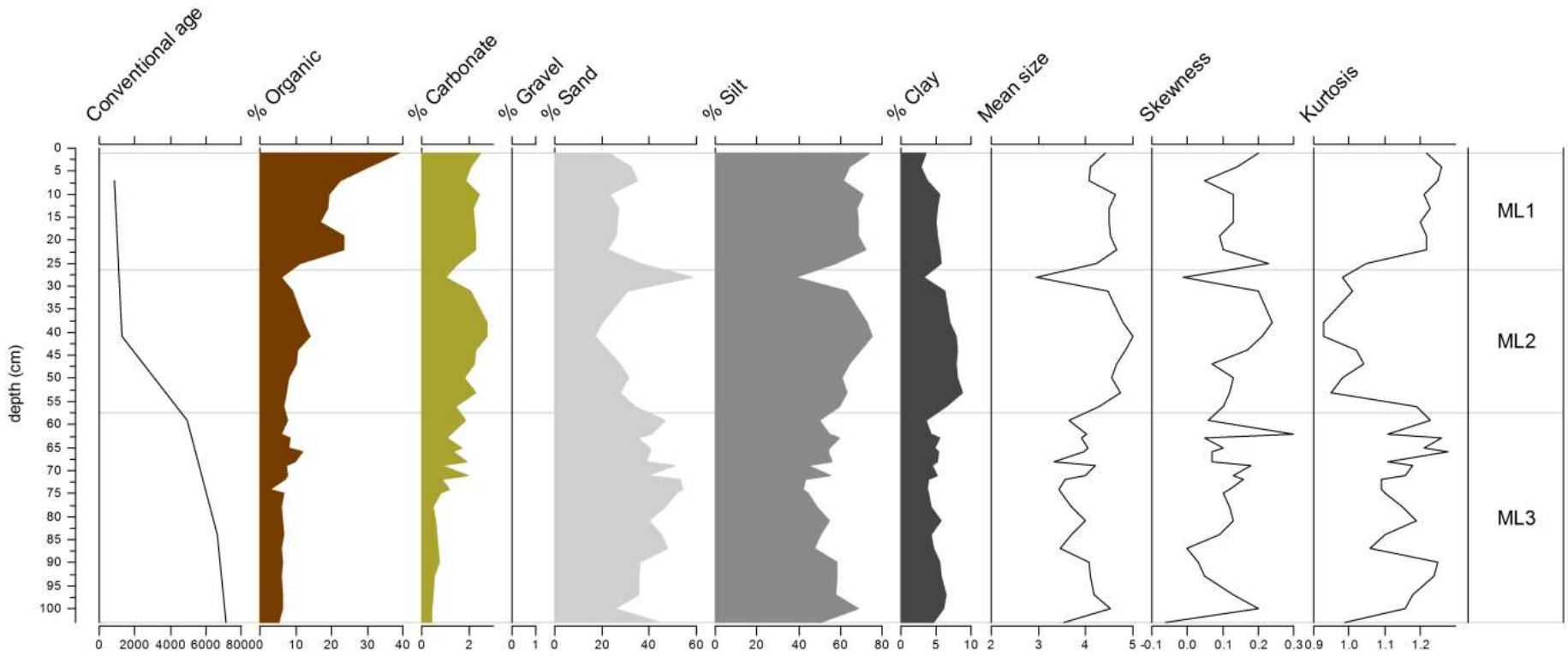


Figure 5.24: Stratigraphic diagram of the sedimentary properties throughout the Mafadi Wetland profile.

Skewness of the sediment particle size distributions of each of the samples is highly varied throughout the profile, demonstrating a fluctuation between samples with disproportionate volumes of fines, and those with a disproportionate percentage of coarse material (*Figure 5.24*). This too, may be influenced by the considerable concentration of diatoms, which would indiscriminately reflect 'particle sizes' of diatoms rather than sediment grains (*Figure 5.25*).

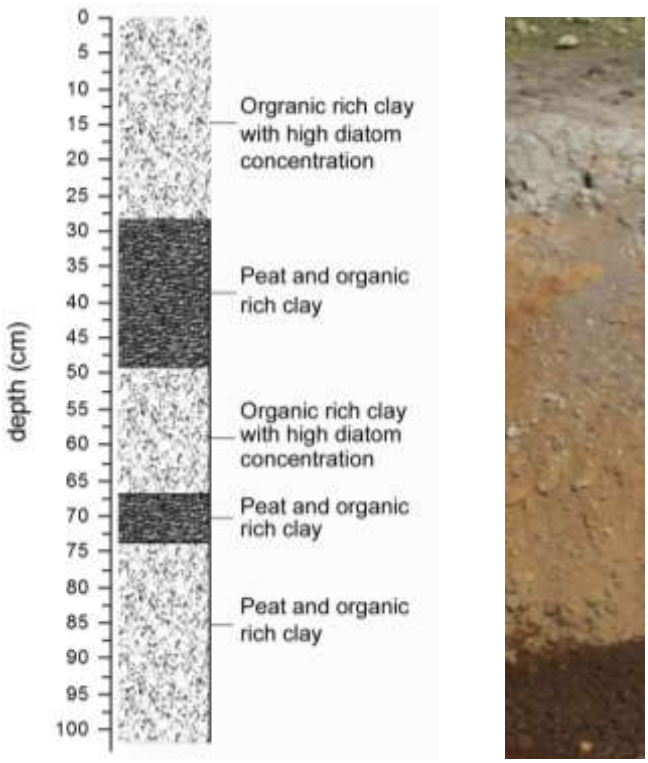


Figure 5.25: Stratigraphic log and photograph of core from Mafadi Wetland

CONISS separates the samples from the Mafadi Wetland profile into three zones based on their sediment properties (*Figure 5.26*). ML3 extends from the bottom of the core at 103cm (~8,140 cal. yr BP) to a depth of 59cm (~5,300 cal. yr BP), with three clearly-defined sub-groups separated at mean depths of 71.5cm (~6,650 cal. yr BP) and 88.5cm (~7,780 cal. yr BP; *Figure 5.26*). The separation of zones ML2 and ML3 at a mean depth of 57.5cm (~4,800 cal. yr BP) most notably coincides with the commencement of the period of particularly slow accumulation, despite no age-date data being included in the CONISS analysis, indicating coinciding changes in other sedimentary properties (*Figures 5.24, 5.26*). A peak in sand-sized particles and low intensity peaks in carbonates and organics also coincide with the division of these two zones (*Figures 5.24*). The first two zones, ML1 and ML2, cover roughly the top

half of the profile. They are separated at a mean depth of 26.5cm (~1,090 cal. yr BP), which is marked by a sudden, short-lived, peak in sand-sized particles, concurrent with the lowest relative abundance of organic, carbonate, silt, clay and mean particle size of the profile (*Figure 5.24*).

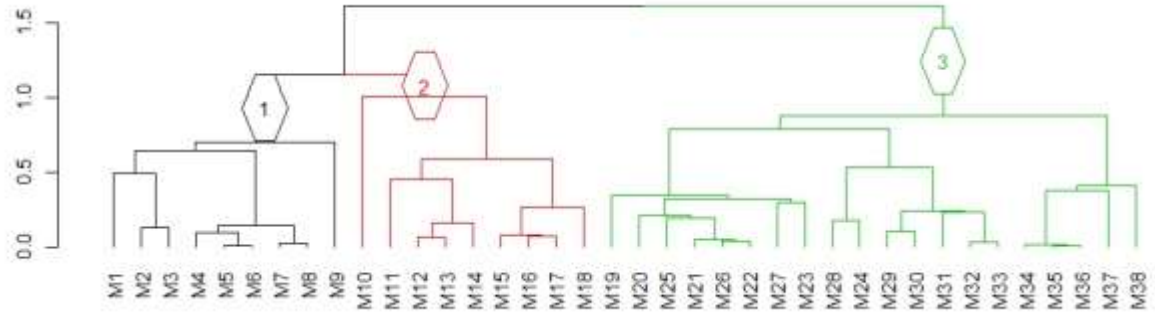


Figure 5.26: CONISS output separating the Mafadi Wetland profile into zones based on differences in sedimentary characteristics throughout.

ML3 (103-59cm; ~8,140-4,850 cal. yr BP) is marked by low proportions of carbonates, organic content and clay-sized particles throughout the zone, in comparison with the rest of the sequence (*Figure 5.24*). All three sediment properties exhibit rapid, low-amplitude fluctuations towards the end of the zone, from a depth of 72-65cm (~6,680-6,200 cal. yr BP; *Figure 5.24*). Silt-sized sediment particles are dominant in zone ML3, although the relative abundance of silt-sized particles is considerably lower in this zone than the rest of the profile, compensated by a larger proportion of sand-sized particles (*Figure 5.24*). The sediment particle size distribution is positively skewed for much of this zone, indicating a disproportionate amount of sand-sized particles than are represented by the mean (*Figure 5.24*). Overall, ML3 has little fluctuation in sediment properties, and is characterised by relatively stable rates of accumulation.

Table 5.10: Summary of sedimentary changes throughout the Mafadi Wetland profile.

Sample Number	Depth	Mean	SD	Skewness	Kurtosis	Texture	Munsell
M1	0-2	coarse silt	poorly sorted	fine skewed	Leptokurtic	sandy loam	7.5 YR 6/4
M2	3-5	coarse silt	poorly sorted	fine skewed	Leptokurtic	sandy loam	7.5 YR 6/4
M3	6-8	coarse silt	poorly sorted	near symmetrical	Leptokurtic	sandy loam	5YR 4/3
M4	9-11	coarse silt	poorly sorted	fine skewed	Leptokurtic	silty loam	10YR 4/4
M5	12-14	coarse silt	poorly sorted	fine skewed	Leptokurtic	sandy loam	5YR 5/2
M6	15-17	coarse silt	poorly sorted	fine skewed	leptokurtic	sandy loam	5YR 5/2
M7	18-20	coarse silt	poorly sorted	near symmetrical	leptokurtic	silty loam	7.5YR 5/2
M8	21-23	coarse silt	poorly sorted	fine skewed	leptokurtic	silty loam	7.5YR 5/3
M9	24-26	coarse silt	poorly sorted	fine skewed	mesokurtic	sandy loam	7.5 YR 5/2
M10	27-29	fine grained	very poorly sorted	near symmetrical	mesokurtic	loamy sand	7.5 YR 4/6
M11	30-32	coarse silt	poorly sorted	fine skewed	mesokurtic	sandy loam	10YR 5/6
M12	37-39	medium silt	poorly sorted	fine skewed	mesokurtic	silty loam	10YR 5/3
M13	40-42	medium silt	poorly sorted	fine skewed	mesokurtic	silty loam	7.5YR 5/3
M14	43-45	coarse silt	poorly sorted	fine skewed	mesokurtic	silty loam	10YR 5/2
M15	46-48	coarse silt	very poorly sorted	near symmetrical	mesokurtic	silty loam	10YR 5/2
M16	49-51	coarse silt	very poorly sorted	fine skewed	mesokurtic	sandy loam	7.5YR 5/3
M17	52-54	coarse silt	very poorly sorted	fine skewed	mesokurtic	silty loam	7.5 YR 6/4
M18	55-57	coarse silt	poorly sorted	fine skewed	leptokurtic	sandy loam	7.5YR 5/2
M19	58-60	very fine grained	poorly sorted	near symmetrical	leptokurtic	sandy loam	7.5 YR 6/4
M20	61-63	coarse silt	poorly sorted	strongly fine skewed	leptokurtic	sandy loam	7.5YR 6/4
M21	64-66	very fine grained	poorly sorted	near symmetrical	leptokurtic	sandy loam	7.5 YR 5/3
M22	67-69	coarse silt	poorly sorted	fine skewed	leptokurtic	sandy loam	10YR 5/2
M23	70-72	very fine grained	poorly sorted	near symmetrical	leptokurtic	sandy loam	10YR 5/3
M24	73-75	very fine grained	poorly sorted	near symmetrical	leptokurtic	loamy sand	10YR 4/6
M25	62-64	coarse silt	poorly sorted	fine skewed	leptokurtic	sandy loam	10YR 5/3
M26	65-67	coarse silt	poorly sorted	fine skewed	leptokurtic	sandy loam	7.5 YR 5/2
M27	68-70	very fine grained	poorly sorted	fine skewed	mesokurtic	sandy loam	7.5YR 3/4
M28	71-73	very fine grained	poorly sorted	fine skewed	mesokurtic	sandy loam	7.5YR 6/4
M29	74-76	very fine grained	poorly sorted	fine skewed	mesokurtic	sandy loam	7.5YR 5/4
M30	77-79	very fine grained	poorly sorted	fine skewed	leptokurtic	sandy loam	7.5YR 5/6
M31	80-82	coarse silt	poorly sorted	fine skewed	leptokurtic	sandy loam	7.5YR 6/4
M32	83-85	very fine grained	poorly sorted	near symmetrical	mesokurtic	sandy loam	7.5YR 5/4
M33	86-88	very fine grained	very poorly sorted	near symmetrical	mesokurtic	sandy loam	7.5YR 5/8
M34	89-91	coarse silt	poorly sorted	near symmetrical	leptokurtic	sandy loam	7.5YR 6/6
M35	92-94	coarse silt	poorly sorted	near symmetrical	leptokurtic	sandy loam	7.5YR 6/8
M36	96-98	coarse silt	poorly sorted	fine skewed	leptokurtic	sandy loam	7.5YR 5/8
M37	99-101	coarse silt	poorly sorted	fine skewed	leptokurtic	sandy loam	7.5YR 5/8
M38	102-104	very fine grained	very poorly sorted	near symmetrical	mesokurtic	sandy loam	7.5YR 5/4

ML2 (56-28cm; ~4,790-1,110 cal. yr BP) contains large proportions of silt-sized sediment particles, and the greatest abundance of clay-sized particles throughout the sequence (*Figure 5.24*). The percentage composition of both organic material and carbonates

increases throughout much of the zone, but decreases considerably at the termination (*Figure 5.24*). There is a peak in the percentage organic content, percent of carbonate content and the abundance of silt-sized particles at a depth of 41cm (~1,320 cal. yr BP), concurrent with a decrease in sand-sized particles (*Figure 5.24*). This is followed by a mirroring of this pattern, which persists to the end of the zone (*Figure 5.24*). These events follow the termination of the period of slow accumulation.

ML1 (25cm - surface; ~1,060 cal. yr BP - present) is characterised by the maximum percentage organic content in the sequence, which rapidly increases throughout the zone (*Figure 5.24*). There is a relatively high, largely consistent, proportion of carbonates within the sediments from each sample (*Figure 5.24*). Silt-sized particles dominate the particle size distribution, which together with the large percentage organic content and dark sediment colour, is indicative of peat, while the proportion of clay-sized particles decreases throughout the zone (*Figure 5.24*). The mean particle size is relatively stable throughout zone ML1, with the exception of a notable decrease from relatively stable mean particle size, except for a decrease from 7-4cm (~760-590 cal. yr BP), simultaneous with a decline in carbonate and a peak in the larger sand-sized particles (*Figure 5.24*).

5.4.3 Pollen Analysis

The pollen grains identified from the Mafadi Wetland profile are dominated by the Poaceae, Cyperaceae and Asteraceae families, similar to the profiles from Sani Valley and Sekhokong (*Table 5.11*). This again is typical of the continued presence of a wetland surrounded by meadow grasses throughout the early- to late-Holocene. There is a lower diversity in pollen taxa than was observed for the lower altitude sites, with only a small proportion of pollen grains from the Mafadi Wetland samples occurring with a frequency of more than 1% throughout the sequence. A total of 20 pollen grains from different taxa were identified across the 38 samples spanning the profile.

Table 5.11: Percentage occurrence of pollen grains throughout the Mafadi Wetland profile.

Pollen type (family/genera)	% Occurrence in core	Maximum individual sample %
Poaceae	43.6	70.5
Cyperaceae	23.5	49.2
Asteraceae	22.2	41.1
Crassula spp.	4.5	8.4
Apiaceae	1.3	5.2
Cheno-Am	1.0	3.6
Pentzia spp.	0.9	2.8
Anthospermum spp.	0.7	2.8
Aizoaceae	0.6	2
Indigofera spp.	0.6	3.4
Liliaceae	0.4	2.0
Passerina spp.	0.2	1.0
Caryophylaceae	0.2	1.6
Acanthaceae	0.1	2.3
Typha spp.	0.1	1.2
Vernonia spp.	0.1	0.6
Ericaceae	0.1	0.4
Podocarpus sp.	<0.1	0.8
Malvaceae	<0.1	0.4
Stoebe spp.*	<0.1	0.4

*Accumulated with Asteraceae for pollen diagrams

CONISS separates the samples from the Mafadi Wetland profile into four zones on the basis of changes in the relative abundance of the identified pollen (*Figure 5.27*). CONISS and PCA function only on samples with non-zero counts, and thus this analysis is applied only to sample numbers M1-M31. M32-M38 all had insufficient pollen for counting (>20 pollen grains counted across duplicate slides from each sample). The absence of pollen is, however, a 'similarity' between the samples, and thus while they could not be statistically clustered using CONISS, an artificial manually created zone MP5 is defined including these samples, for the purpose of comparison with the other proxies. Zone MP5 extends from a depth of 103-84cm (~8,140-7,580 cal. yr BP). Zone MP4 covers the portion of the sequence from 81-72cm (~7,380-6,680 cal. yr BP), marking the terminal depth of samples containing sufficient pollen for counting (*Figure 5.27*). Zone MP3 includes seven samples, and extends from a depth of 71-62cm (~6,610-6,010 cal. yr BP; *Figure 5.27*). Zones MP1 and MP2 comprise larger sets of samples than zones MP3 and MP4, and are separated at a mean depth of 26.5cm (~1,080 cal. yr BP; *Figure 5.27*).

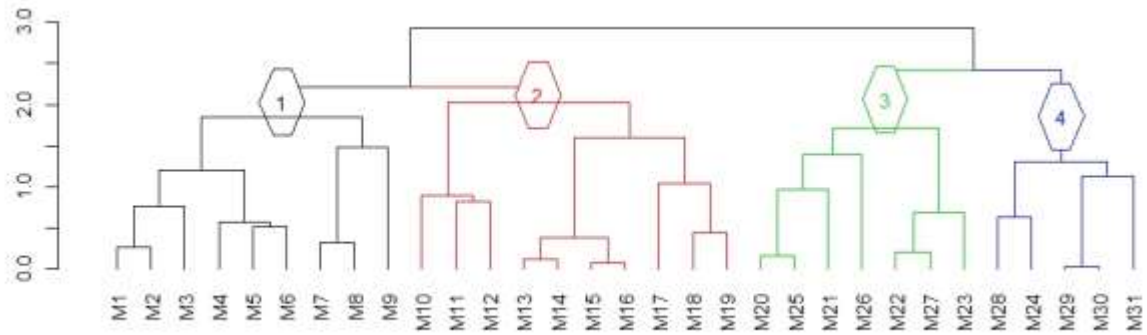


Figure 5.27: CONISS output separating the Mafadi Wetland profile into zones based on the pollen results.

The inclusion of the samples for which there was insufficient pollen for a representative count resulted in PCA separating non-pollen samples from those with pollen, with all variance in pollen species distribution represented on PC2. This plot is thus not of value, and thus is not included in this thesis. The PCA biplot therefore includes only samples M1-M31 (*Figure 5.28*). The zones identified through CONISS analysis are not as clearly visible as clusters in the PCA biplot for principal components 1 and 2 (*Figure 5.28*), as they were for the proxies at the lower altitude sites (*Figures 5.6, 5.17*). Samples from zones MP1 and MP2 are distributed across quadrants 2, 3 and 4, with PC1 scores just below zero and spanning a gradient of PC2 scores (*Figure 5.28*). Broadly, samples from zone MP1 demonstrate a stronger affinity with Apiaceae, *Anthospermum* and *Pentzia*, while MP2 samples appear driven more strongly by Poaceae and *Indigofera* (*Figure 5.28*). Zone MP3 samples are distributed predominantly within the first quadrant, with two samples located in the second quadrant, again with relatively constrained PC1 scores, but a range of PC2 scores (*Figure 5.28*). These samples demonstrate a strong affinity with Asteraceae, with a smaller influence from *Crassula* and Acanthaceae (*Figure 5.27*). Samples from zone MP4 are largely located in quadrant 2, together with the species vectors for Cyperaceae and Aizoaceae (*Figure 5.28*).

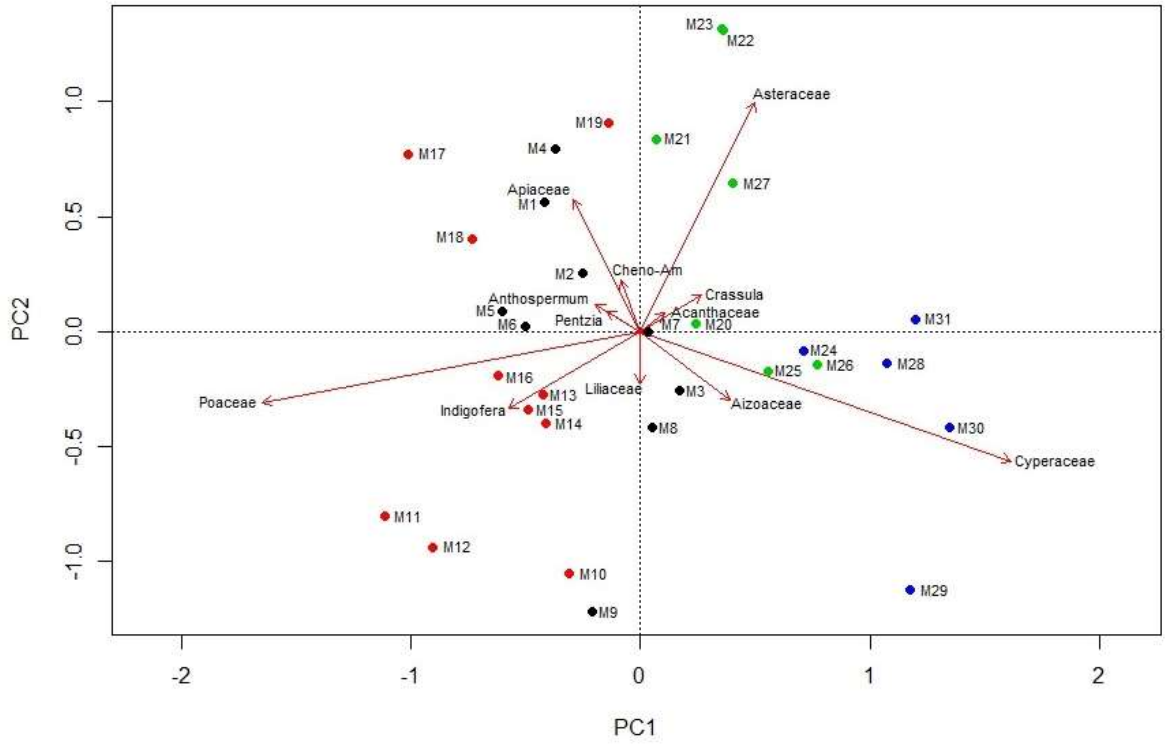


Figure 5.28: PCA biplot for pollen results from the Mafadi Wetland profile.

PC1 accounts for 29.1% of the observed variance in the relative abundance of pollen across species. Species scores from PC1 separate Poaceae, *Indigofera* and Apiaceae with very negative scores, from Asteraceae and Cyperaceae with positive scores (*Figure 5.29*). A decrease in PC1 sample scores is observed through zones MP4 to MP3 (*Figure 5.29*). This is followed by a stabilization of PC1 scores at ca. -1 through MP2, and an increase throughout MP1 (*Figure 5.29*). These changes are driven predominantly by fluctuations in the relative abundance of Poaceae, Cyperaceae and Asteraceae. PC2 accounts for 26.3% of the observed variance in pollen for the Mafadi Wetland profile. Arranging species by their PC2 species scores, Cyperaceae and Poaceae are coupled, and separated from Asteraceae, which has the highest species scores (*Figure 5.28*). The PC2 sample score curve largely follows the relative abundance of Asteraceae pollen, capturing many of the fluctuations (*Figure 5.29*). These peaks in Asteraceae are often concurrent with peaks in Apiaceae, Cheno-Am, *Crassula*, *Anthospermum* and *Pentzia* (*Figure 5.29*).

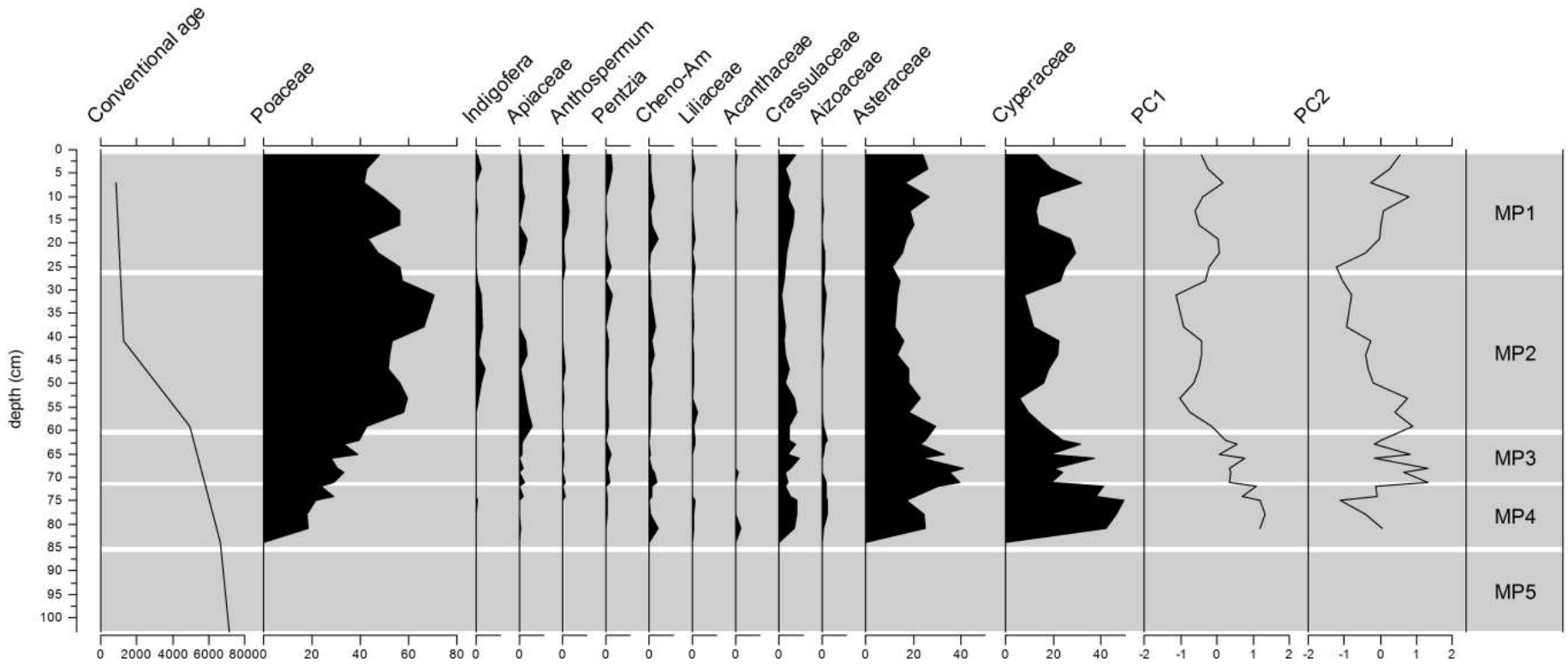


Figure 5.29: Stratigraphic diagram of the pollen results for the Mafadi Wetland profile, with species ordered according to the PC1 species scores, and curves for PC1 and PC2 sample scores.

Zone MP5 (103-84cm; ~8,140-7,580 cal. yr BP) has insufficient pollen for representative counting, with less than 20 grains counted between two duplicate slides for each sample, representing less than 10% of the required minimum (*Figure 5.29*). Zone MP4 (81-72cm; ~7,520-6,680 cal. yr BP) is dominated by Cyperaceae, which maintains a relative abundance of over 40% throughout all of the samples in the zone (*Figure 5.29*). There is a peak in Asteraceae pollen from 81-78cm (~7,380-7,130 cal. yr BP), and a second peak at the termination of the zone (*Figure 5.29*). Although Poaceae increases throughout the zone, the relative abundance remains at its minimum for the sequence (*Figure 5.29*). By contrast, the highest percentages of *Crassula* for the sequence are maintained throughout much of the zone (*Figure 5.29*). Peaks in Cheno-Am and Acanthaceae are notable, concurrent with the peaks in Asteraceae (*Figure 5.29*).

Zone MP3 (71-62cm; ~6,610-5,700 cal. yr BP) has the largest relative abundance of Asteraceae pollen in the sequence, despite its continued decrease throughout the zone (*Figure 5.29*). There are two short-lived peaks in Cyperaceae pollen at depths of 66cm (~6,270 cal. yr BP) and 63cm (~6,070 cal. yr BP), during which the concentration temporarily doubles (*Figure 5.29*). The PC1 sample score curve is interrupted by two peaks. The older of these, at a depth of 69cm (~6,470 cal. yr BP), coincides with peaks in the relative abundance of Cyperaceae and Asteraceae pollen, and a decrease in Poaceae (*Figure 5.29*). The second, at 63cm (~6,070 cal. yr BP), is driven by peaks in Cyperaceae, Aizoaceae and *Crassula* pollen, and an abrupt decrease in Poaceae (*Figure 5.29*). Zones MP4 and MP3 are characterised by a rapid increase in Poaceae, and a corresponding decrease in the relative abundance of Cyperaceae (*Figure 5.29*).

Zone MP2 (59-28cm; ~5,600-1,110 cal. yr BP) is dominated by Poaceae pollen, with the largest relative abundance of Poaceae for the sequence, exceeding 40% throughout all samples (*Figure 5.29*). There are two sustained peaks in Poaceae concentration, the first from 56-50cm (~4,050-2,620 cal. yr BP) and the second from 38-31cm (~1,270-1,160 cal. yr BP; *Figure 5.29*). These peaks in relative abundance of Poaceae are paired with decreases in Cyperaceae of a roughly equivalent proportion. The Poaceae peaks are separated by a peak in the relative abundance of Cyperaceae pollen (*Figure 5.29*). Asteraceae pollen concentration decreases throughout much of the zone, with small amplitude fluctuations

(*Figure 5.29*). The PC1 sample scores follow the concentration of Cyperaceae, with a slight decrease driven by the changing concentration of Asteraceae (*Figure 5.29*). Notable, yet small, concentrations of *Indigofera* and Apiaceae appear from this zone onwards (*Figure 5.29*).

Zone MP1 (25cm - surface; ~1,060 cal. yr BP - present) is characterised by a significant decrease in the relative abundance of Poaceae pollen, concurrent with an increase in Asteraceae (*Figure 5.29*). The decrease in Poaceae is interrupted by a peak in concentration from 16-10cm (~920-820 cal. yr BP), which is concurrent with a decrease in Cyperaceae (*Figure 5.29*). Poaceae concentration demonstrates a slight increase in the samples closest to the surface (4cm - surface; 590 - present), again paired with a comparable decrease in the percentage of Cyperaceae pollen (*Figure 5.29*). The PC1 sample score curve largely tracks the changes in Cyperaceae throughout this zone, with peaks at 10cm (~820 cal. yr BP) and the surface, both concurrent with peaks in Cyperaceae (*Figure 5.29*). The increase in Asteraceae throughout MP1 is marked by one notable interruption at a depth of 7cm (~760 cal. yr BP), simultaneous with the termination of the decrease in Poaceae and the large peak in Cyperaceae (*Figure 5.29*).

5.4.4 Diatom Analysis

The diatom composition at Mafadi Wetland is markedly different from that of the lower altitude sites. Where the Sani and Sekhokong profiles are dominated by *Fragilaria famelica* (*Tables 5.4, 5.8*), this species has a mean occurrence of only 1% throughout the Mafadi Wetland profile (*Table 5.12*), with a maximum relative abundance of 4.3% at a depth of 66cm (~6,270 cal. yr BP). *Aulacoseira ambigua*, which occurred in small percentages at the lower altitude sites, is the second most dominant species at Mafadi Wetland. This deep water species would suggest a larger proportion of standing surface water than at Sani Valley or Sekhokong. *Fragilaria pinnata* and *Fragilaria construens* are the most abundant diatoms species at Mafadi Wetland, individually ranked 1st and 3rd. Diatoms from a total of 37 different species have been identified from the 38 samples for the Mafadi Wetland core, 16 of which have a mean occurrence of 1% or more throughout the profile (*Table 5.12*). Notably, unlike the pollen record, sufficient diatom valves for counting were found in samples from all depths of the profile.

Table 5.12: Percentage occurrence of diatom species throughout the Mafadi Wetland profile.

Diatom species	% occurrence in core	Maximum individual sample %
Fragilaria pinnata Ehrenberg (Staurosirella pinnata)	22.4	46.1
Aulacoseira ambigua Grunow	19.3	52.2
Fragilaria construens Ehrenberg	19.0	51.4
Eunotia praerupta Ehrenberg	8.3	24.4
Pinnularia divergentissima Grunow	3.7	8.5
Eunotia bilunaris Ehrenberg	3.1	8.9
Pinnularia borealis Ehrenberg	3.1	8.5
Cymbella laevis Nägeli	3.0	7.3
Gomphonema parvulum Kützing	2.9	11.3
Pinnularia gentilis Donkin	2.2	4.9
Cymbella gracilis Ehrenberg	1.9	6.0
Navicula laevissima Kützing	1.7	5.7
Pinnularia viridis Ehrenberg	1.3	4.2
Stauroneis phoenicenteron Ehrenberg	1.1	4.3
Fragilaria famelica Kützing (Synedra famelica)	1.0	4.3
Achnanthes minutissima Kützing	1.0	4.0
Diploneis ovalis Hilse	0.9	2.7
Eunotia exigua (Brébisson ex Kützing)	0.8	3.3
Hantzschia amphioxys Ehrenberg	0.6	2.3
Navicula minima Grunow	0.5	3.6
Gomphonema gracile Ehrenberg	0.3	2.3
Cymbella selesiaca Bleisch	0.3	1.3
Sellaphora pupula Kützing	0.2	2.6
Gomphonema bohemicum Hustedt	0.2	2.0
Cyclotella meneghiniana Kützing	0.2	1.3
Navicula trivialis Lange-Bertalot	0.2	1.3
Navicula salinarum Grunow	0.1	1.0
Nitzschia palea Kützing	0.1	1.0
Navicula pygmaea Kützing	0.1	1.0
Pinnularia intermedia Lagerstedt	0.1	1.3
Caloneis silicula Ehrenberg	0.1	0.7
Denticula kuetzingii Grunow	0.1	1.3
Navicula explanata Hustedt	0.1	1
Diploneis parma Cleve	0.1	1.3
Stauroneis producta Cleve	<0.1	0.7
Amphora sp.	<0.1	0.3
Navicula insociabilis Krasske	<0.1	0.3

CONISS analysis divides the Mafadi Wetland diatom sequence into five zones (*Figure 5.30*). Zone MD5 extends from the bottom of the core at 103cm (~8,140 cal. yr BP) to a depth of 93cm (~7,900 cal. yr BP; *Figure 5.30*). The shortest zone, MD4, covers depths 90-87cm (~7,820-7,750 cal. yr BP; *Figure 5.30*). MD3 includes 14 samples, and spans from a depth of 84cm (~7,580 cal. yr BP) to 59cm (~5,300 cal. yr BP), with subzones separated at a mean depth of 74.5cm (~6,860 cal. yr BP; *Figure 5.30*). Zone MD2 extends from 56-31cm (~4,340-1,160 cal. yr BP; *Figure 5.30*). MD1 extends from a depth of 28cm (~1,110 cal. yr BP) to the surface, with two subzones separated at a mean depth of 14.5cm (~900 cal. yr BP; *Figure 5.30*).

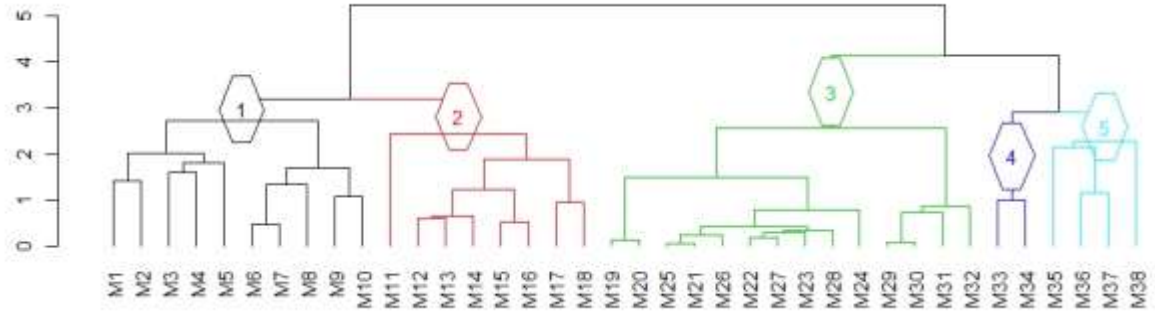


Figure 5.30: CONISS output dividing the Mafadi Wetland profile into zones based on changes in diatom species composition throughout.

The zones delineated by CONISS correspond closely with clusters in samples on the PCA biplot for principal components 1 and 2 (*Figure 5.31*). Samples from zones MD4 and MD5 are both located in the 4th quadrant, with no corresponding species vector (*Figure 5.31*). Zone MD3 has the largest number of samples, all of which are clustered in quadrants 1 and 2 (*Figure 5.31*). These samples demonstrate a strong affinity with *Eunotia praerupta*, but are situated together with vectors for all of the remaining the species (*Figure 5.31*). Samples from MD2 are situated along a line of relatively constant PC1 score crossing quadrants 3 and 4 (*Figure 5.31*). They appear to be closely affiliated with *Aulacoseira ambigua* and *Fragilaria pinnata/ construens* (*Figure 5.31*). Zone MD1 samples are situated in the third quadrant, and reflect a strong association with *Aulacoseira ambigua* and *Sellaphora pupula* (*Figure 5.31*).

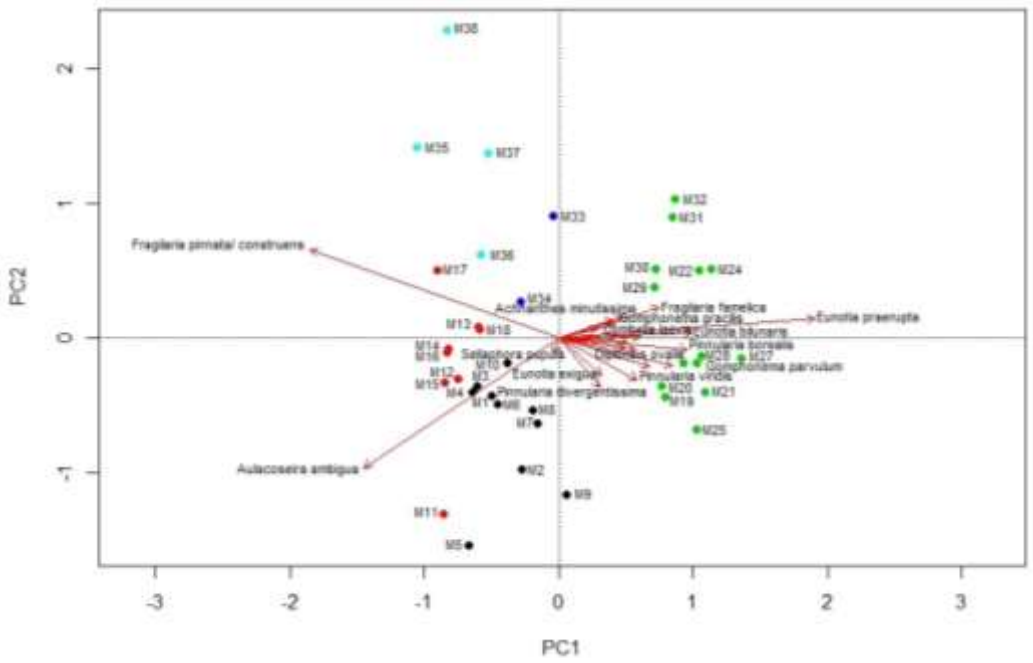


Figure 5.31: PCA biplot for diatom results from the Mafadi Wetland profile.

PC1 accounts for 68.1% of the variance in diatom species across samples, and largely segregates zones MD5 (103-93cm; ~8,140-7,880 cal. yr BP), MD4 (90-87cm; ~7,830-7,690 cal. yr BP), MD2 (56-31cm; ~4,800-1,160 cal. yr BP) and MD1 (28cm - surface; ~1,110 cal. yr BP to present), all of which are affiliated almost exclusively with *Fragilaria pinnata/ construens* and *Aulacoseira ambigua*, from MD3 (84-59cm; ~7,640-4,850 cal. yr BP) which is dominated by *Eunotia praerupta*, and influenced by the majority of the remaining species (*Figure 5.32*). The PC1 sample score curve remains negative for much of the profile, influenced by the dominance of *Fragilaria pinnata/ construens* and *Aulacoseira ambigua*, with a peak across MD3 dominated by *Eunotia praerupta*, and smaller amplitude peaks in the relative abundances of all of the remaining species (*Figure 5.32*). Smaller peaks in the PC1 curve are observed between 100-97cm (~8,070-8,000 cal. yr BP) and at a depth of 25cm (~1,060 cal. yr BP), similarly driven by a decrease in the relative abundance of *Fragilaria pinnata/ construens* and *Aulacoseira ambigua*, but peaks in the percentage composition of all remaining species (*Figure 5.32*). There appears an almost mutually exclusive relationship between the two groups of species, with a disappearance in many species during peaks of *Fragilaria pinnata/ construens* and *Aulacoseira ambigua* (*Figure 5.32*).

PC2 accounts for only 8.5% of the observed variance in diatom species composition across the profile. There is little variance in species scores on the second principal component axis, which separates *Aulacoseira ambigua* and *Fragilaria pinnata/ construens* at the two extremes (*Figure 5.31*). As these two species demonstrate considerable similarities in the timing of their changes in relative abundance, the PC2 sample score curve largely tracks the fluctuations in *Fragilaria pinnata/ construens* concentration, punctuated by extreme changes in relative abundance of *Aulacoseira ambigua* (*Figure 5.32*). There is a general decrease in PC2 scores throughout the profile, driven by a slight decrease in *Fragilaria pinnata/ construens*, and a more noticeable increase in *Aulacoseira ambigua* (*Figure 5.32*). An increase in *Pinnularia divergentissima* and a decrease in *Eunotia praerupta* can also be noted, strengthening this trend (*Figure 5.32*).

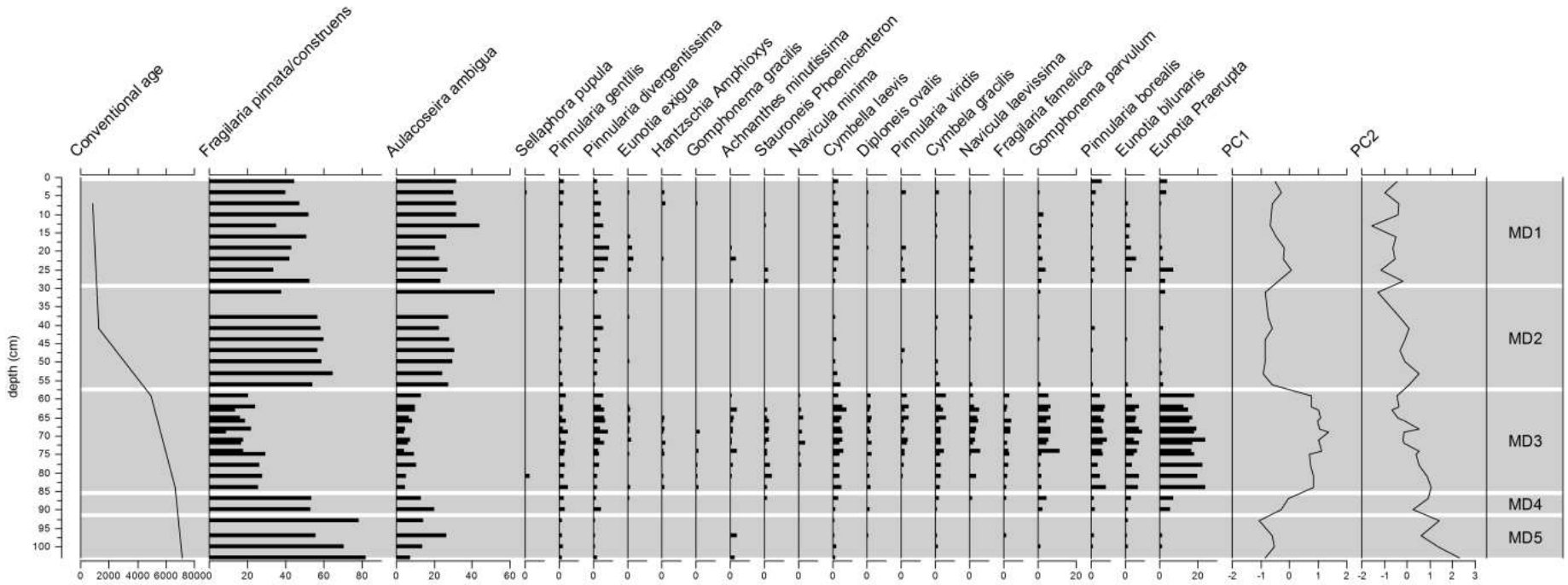


Figure 5.32: Stratigraphic diagram of the diatom results from the Mafadi Wetland profile, with species ordered by their PC1 species scores and curves for PC1 and PC2 sample scores.

5.4.5 Multi-Proxy Synthesis

Progressive shifts in proxies are more apparent for the Mafadi Wetland profile than persistent fluctuations for common time periods across more than one proxy (*Figure 5.33*). An increase in organic material, carbonates and the proportion of silt-sized particles occurs throughout the upper portion of the profile, while a decrease in pollen PC1, reflecting an increase in Poaceae and decrease in Cyperaceae is most obvious through the middle of the profile (*Figure 5.33*). CONISS output dividing the Mafadi Wetland profile based on the pollen sequence separates five zones, with zone MP5 characterised by an absence of pollen (*Figure 5.33*).

Zone MP5 (103-84cm; ~8,140-7,580 cal. yr BP) is characterised by an absence of pollen and particularly low percentages of carbonates and organic matter (*Figure 5.33*). A peak in the proportion of silt-sized particles occurs at 100cm (~8,070 cal. yr BP), compensated by a decrease in sand-sized particles, contemporary with a peak in diatom PC1, reflecting a peak in *Aulacoseira ambigua* (*Figure 5.33*). Diatom PC1 increases rapidly throughout the second half of the zone, indicating the transition from *Fragilaria pinnata/ construens* and *Aulacoseira ambigua* which dominate the section of the profile from 103-93cm (~8,140-7,900 cal. yr BP), to the rest of the sequences, dominated by *Eunotia praerupta* (*Figure 5.33*). The proportion of sand-sized particles increases throughout the zone, while the proportion of silt-sized particles decreases (*Figure 5.33*). Very little change in the proportion of clay-sized particles can be noted in the zone (*Figure 5.33*).

Zone MP4 (81-72cm; ~7,520-6,680 cal. yr BP) is marked by the re-emergence of pollen. Diatom PC1 increases throughout the zone, while diatom PC2 decreases (*Figure 5.33*). This zone comprises the first half of the period of highest diatom PC1 scores in the profile. The percentage carbonate and organic composition remains constant until the end of the zone, at which point large amplitude fluctuations in the sediment variables commence.

Zone MP3 (71-62cm; ~6,610-5,700 cal. yr BP) comprises the second half of the peak in diatom PC1 scores, which remain relatively constant throughout the period (*Figure 5.33*). Diatom PC2 scores and pollen PC1 scores decrease throughout this zone (*Figure 5.33*). Pollen PC2 scores fluctuate rapidly throughout the zone, as do the percentage composition

of carbonate and percentage of silt- and sand-sized particles (*Figure 5.33*). The percentage organic content and the percentage of clay-sized particles remain relatively constant throughout this zone (*Figure 5.3*).

Zone MP2 (59-28cm; ~5,600-1,110 cal. yr BP) is marked by greater stability across the three proxies (*Figure 5.33*). Diatom PC1 and PC2 scores mimic the pattern of MP5, with low PC1 scores and a decrease in PC2 scores (*Figure 5.33*). Pollen PC1 scores demonstrate three distinct peaks, at the beginning, middle and end of the zone, while pollen PC2 scores decrease throughout the period (*Figure 5.33*). The percentage composition of both organics and carbonates increases throughout the zone, with marked decreases at the end of the zone (*Figure 5.33*). The percentages of silt- and clay-sized particles experience a peak and subsequent decrease in this zone, with highest values at 41cm (~1,320 cal. yr BP; *Figure 5.33*). This pattern is mirrored by the percentage sand-sized particles (*Figure 5.33*).

Zone MP1 (25cm - surface; ~1,060 cal. yr BP - present) commences with a large, short-lived peak in the proportion of sand-sized particles, concurrent with a decrease in the proportion of silt- and clay-sized particles, and of the percentages of organic materials and carbonates (*Figure 5.33*). The proportion of sand in this peak is greater than observed elsewhere in the profile, while the decrease in silt-sized particles is to the lowest proportion (*Figure 5.33*). The zone is marked by the most rapid increases in the percentage organic material in the profile, and an increase in pollen PC2 indicating an increase in Asteraceae coupled with a decreasing abundance of Poaceae (*Figure 5.33*). Little change is noted for the diatom principal component curves and pollen PC1 (*Figure 5.33*). Within this relative stability throughout the zone is a peak in the proportion of sand-sized particles at a depth of 7cm, concurrent with peaks in pollen PC1 and diatom PC2, indicating an increased abundance of Cyperaceae pollen and of *Fragilaria pinnata/ construens* (*Figure 5.33*). A simultaneous temporary decrease is noted in the proportion of silt- and clay-sized particles, and of pollen PC2, indicating a lower abundance of Asteraceae (*Figure 5.33*).

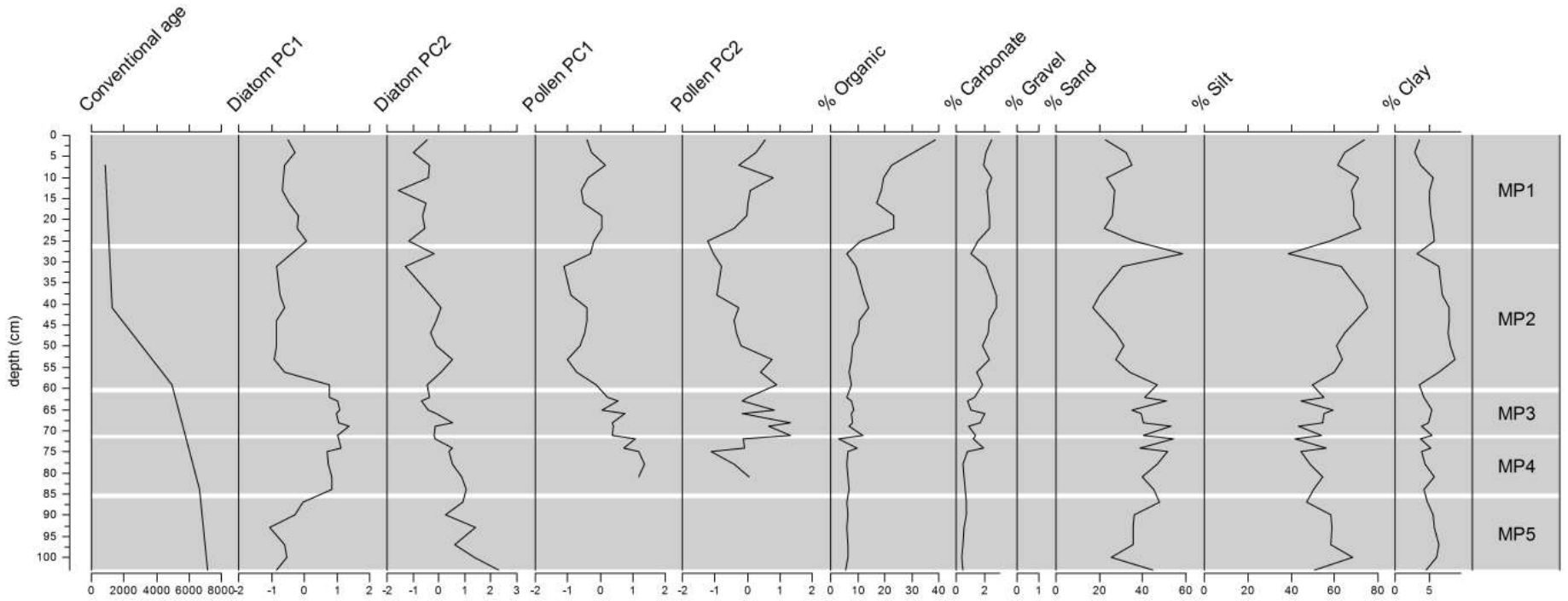


Figure 5.33: Multi-proxy stratigraphic diagram for the Mafadi Wetland profile.

5.4.6 Samples from a Diatomite Outcrop

A second core was acquired for the region adjacent to Mafadi Summit, from a diatomite bed situated 20m perpendicular to the stream, some 400m from the Mafadi Wetland site, and at approximately 50m.asl higher altitude (Figure 4.5). It was of interest to note differences in the diatom communities and sediment properties between the diatomite beds, of which there were many across the wetland periphery, and the more peat dominated wetland centre. A single continuous core could not be obtained due to the poor agglomeration of the material, and an adjacent large pond. Two cores were taken from adjacent points on a slope, which most likely overlap stratigraphically, but represent a continuous sequence through the diatomite bed when intersected. These profiles comprise a total of 38 samples. To determine the extent of the period of overlap, a high resolution set of dates would be required for the samples of equivalent altitude. Furthermore, to understand the rates of deposition of the diatomite, which could have occurred in abrupt pulses rather than continuously, high resolution dating would be required throughout the 1.5m. This was not financially possible for this project, and so remains work to be completed in future. A single date for the bottom sample of the lower of the two cores was obtained, at 3,680 ±30 cal. yr BP, which due to the comparable depths cored, indicates relatively more rapid deposition than in the more organic-rich sediment from the river bank.

Presented here are the sediment, pollen and diatom results from each of the individual samples obtained from the two sections of cores, which are of interest as an insight into the properties of high altitude diatomite in eastern Lesotho, rather than of palaeoenvironmental value. Sediments through much of the two sections of the core are of a light grey to slightly pink colour, typical of diatomite (*Table 5.13*). Particle sizes are larger than that of the peat material which is common in the eastern Lesotho wetlands, but for many of the samples has a near symmetrical skewness, indicating an even distribution around this mean than for the peat samples (*Table 5.13*). The organic component of the sequence is relatively consistent at below 20%, with the exception of the top samples from the lower section, which has considerably higher percentage organic content (40-55%), indicating a relatively thin peat layer (*Table 5.13*). The percentage carbonate composition remains below 3% throughout both sections of the sequence (*Table 5.13*).

Table 5.13: Change in sedimentary properties throughout the core obtained from the Mafadi Diatomite Outcrop.

Sample Number	Depth	Mean	SD	Skewness	Kurtosis	Texture	Munsell	% organic	% carbonate
M39	0-3	coarse silt	poorly sorted	near symmetrical	mesokurtic	silty loam	10YR 6/1	11.06	1.55
M40	3-6	medium silt	poorly sorted	fine skewed	playtykurtic	silty loam	7.5YR 7/1	12.46	1.24
M41	6-9	medium silt	poorly sorted	near symmetrical	playtykurtic	silty loam	5YR 7/1	12.73	1.85
M42	9-12	medium silt	poorly sorted	near symmetrical	playtykurtic	silty loam	10YR 6/1	12.22	1.87
M43	12-15	medium silt	poorly sorted	near symmetrical	playtykurtic	silty loam	7.5 YR 5/1	10.99	1.55
M44	15-18	medium silt	poorly sorted	near symmetrical	mesokurtic	silty loam	5YR 7/1	9.01	2.25
M45	18-21	medium silt	poorly sorted	coarse skewed	mesokurtic	silty loam	7.5 YR 6/3	8.40	2.03
M46	21-24	coarse silt	very poorly sorted	near symmetrical	mesokurtic	silty loam	7.5 YR 6/3	8.85	2.05
M47	24-27	medium silt	poorly sorted	near symmetrical	mesokurtic	silty loam	5YR 5/2	8.88	2.17
M48	27-30	medium silt	poorly sorted	coarse skewed	mesokurtic	silty loam	7.5 YR 6/3	8.72	2.27
M49	30-33	medium silt	poorly sorted	near symmetrical	mesokurtic	silty loam	10 YR 5/2	8.97	2.24
M50	33-36	medium silt	very poorly sorted	near symmetrical	mesokurtic	silty loam	10 YR 5/3	9.58	2.65
M51	36-39	medium silt	very poorly sorted	near symmetrical	leptokurtic	silty loam	10 YR 4/3	11.67	2.02
M52	39-42	medium silt	poorly sorted	coarse skewed	leptokurtic	silty loam	7.5 YR 5/2	13.98	2.34
M53	42-45	coarse silt	very poorly sorted	near symmetrical	mesokurtic	silty loam	10 YR 5/2	13.41	2.41
M54	45-48	coarse silt	very poorly sorted	near symmetrical	mesokurtic	silty loam	10 YR 4/2	23.87	2.05
M55	48-51	coarse silt	very poorly sorted	coarse skewed	mesokurtic	coarse silt	7.5 YR 3/3	17.04	2.21
M56	51-54	coarse silt	very poorly sorted	near symmetrical	mesokurtic	silty loam	10 YR 3/2	16.05	2.26
M57	0-3	coarse silt	poorly sorted	fine skewed	leptokurtic	sandy loam	7.5 YR 5/2	56.07	0.19
M58	3-6	coarse silt	poorly sorted	fine skewed	leptokurtic	sandy loam	7.5 YR 4/3	58.03	0
M59	6-9	coarse silt	poorly sorted	strongly fine skewed	leptokurtic	sandy loam	5 YR 4/2	54.68	0
M60	9-12	medium silt	poorly sorted	strongly fine skewed	mesokurtic	Silt	5 YR 4/2	53.48	0
M61	12-15	coarse silt	poorly sorted	fine skewed	mesokurtic	silty loam	7.5 YR 4/3	48.39	0.46
M62	15-18	medium silt	poorly sorted	fine skewed	mesokurtic	silty loam	10 YR 3/4	40.20	0.46
M63	18-21	medium silt	poorly sorted	fine skewed	playtykurtic	silty loam	7.5YR 3/3	54.32	0.91
M64	21-24	medium silt	poorly sorted	near symmetrical	playtykurtic	silty loam	7.5 YR 6/3	18.76	1.28
M65	24-27	medium silt	poorly sorted	near symmetrical	playtykurtic	silty loam	7.5 YR 7/3	15.68	1.47
M66	27-30	medium silt	very poorly sorted	coarse skewed	mesokurtic	silty loam	7.5 YR 7/2	16.41	1.63
M67	30-33	medium silt	poorly sorted	near symmetrical	playtykurtic	silty loam	7.5 YR 7/3	16.26	1.27
M68	33-36	medium silt	poorly sorted	near symmetrical	mesokurtic	silty loam	7.5 YR 6/3	20.22	1.49
M69	36-39	medium silt	poorly sorted	near symmetrical	playtykurtic	silty loam	7.5 YR 6/3	14.59	1.59
M70	39-42	medium silt	poorly sorted	near symmetrical	playtykurtic	silty loam	7.5 YR 7/2	14.92	2.11
M71	42-45	medium silt	poorly sorted	near symmetrical	mesokurtic	silty loam	10 YR 7/4	13.81	1.32
M72	45-48	medium silt	poorly sorted	near symmetrical	mesokurtic	silty loam	10 YR 7/3	12.23	1.32
M73	48-51	medium silt	poorly sorted	near symmetrical	mesokurtic	silty loam	7.5 YR 7/3	12.21	1.22
M74	51-54	medium silt	poorly sorted	near symmetrical	mesokurtic	silty loam	7.5 YR 8/3	13.14	1.30
M75	54-57	fine silt	poorly sorted	near symmetrical	playtykurtic	Silt	10 YR 7/2	16.041	1.16
M76	57-60	coarse silt	very poorly sorted	coarse skewed	mesokurtic	silty loam	7.5 YR 7/3	16.75	1.34
M77	60-63	fine silt	poorly sorted	fine skewed	mesokurtic	Silt	10 YR 6/4	14.78	1.66

5.4.6.1 POLLEN

The pollen sequence from Mafadi Diatomite Outcrop is dominated by Poaceae (*Figure 5.34*), with considerably higher relative abundance of Poaceae than for the Mafadi Wetland sequence (*Figure 5.29*), or for the two lower altitude sites (*Figures 5.7, 5.18*).

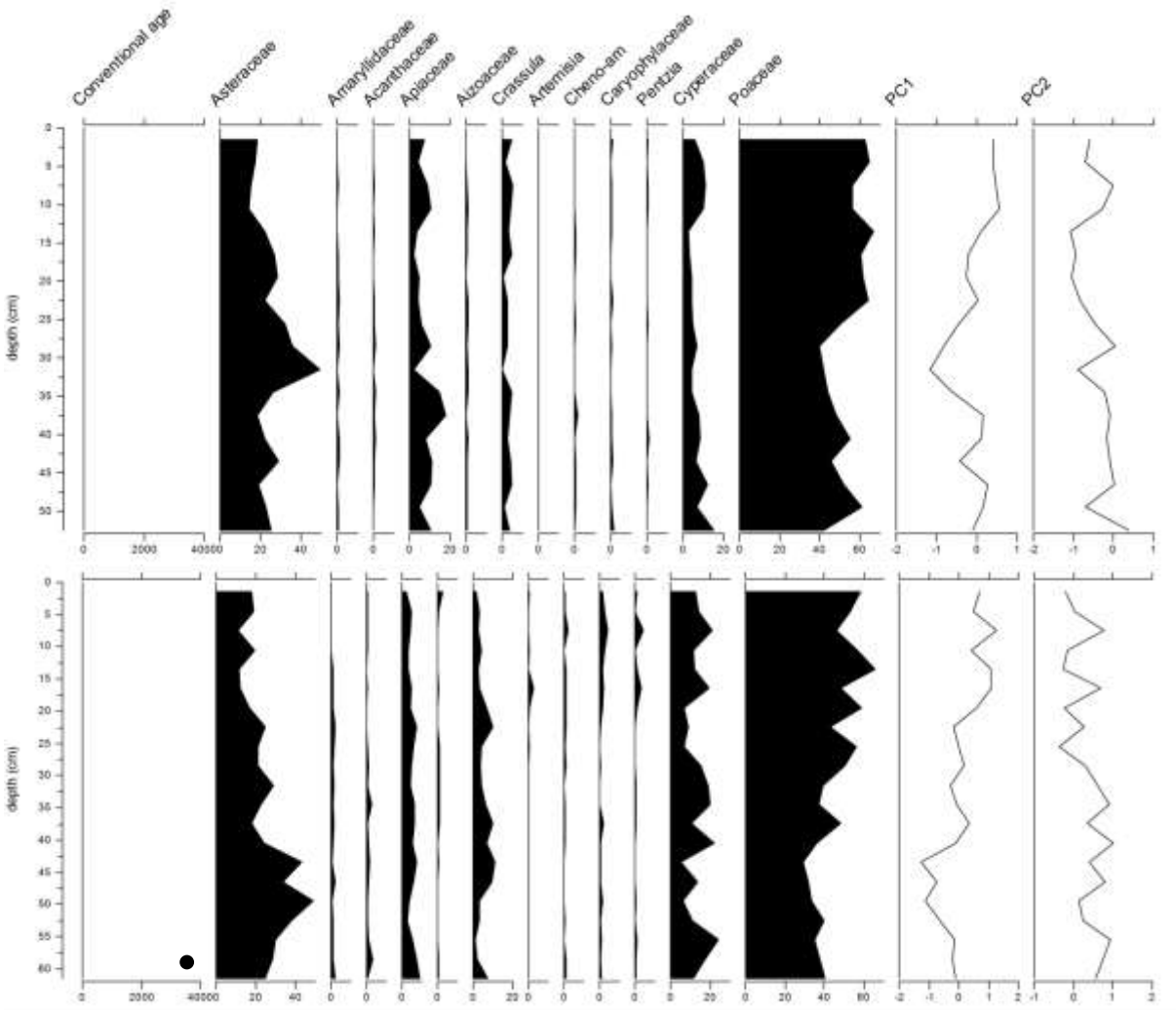


Figure 5.34: Stratigraphic diagram of the pollen results from the core obtained from the Mafadi Diatomite Outcrop. A discontinuity or overlap of unknown depth occurs between the two sections.

Notably, there is a small proportion of Cyperaceae pollen throughout the sequence (*Figure 5.34*). This could suggest that the diatomite outcrop has been situated upslope from the bog for the duration of the sequence. The relative abundance of Cyperaceae pollen through the lower section of the sequence is higher than in the top section, but marked by clearly-defined fluctuations throughout (*Figure 5.34*). Asteraceae is more abundant than

Cyperaceae throughout the sequence, but concentration of the two demonstrates similar timing in shifts (*Figure 5.34*). This could indicate wet-dry cycles during which the wetland periphery shifted up and down slope. A low abundance in Cyperaceae relative to Poaceae would generally suggest a dominance of grassland proportional to the wetland environment, but given the markedly different pollen distribution from the Mafadi Wetland sequence (*Figure 5.29*), which would have received the same wind-blown pollen distributions, this is unlikely. Rather, it would appear that the diatomite itself may be better suited to preserving Poaceae pollen than Cyperaceae, possibly due to the coarser sediment particles.

5.4.6.2 DIATOMS

As with pollen, the species diversity of diatoms throughout the two sections of the sequence is considerably smaller than that for the Mafadi Wetland sequence. There is, however, a far greater concentration of diatoms from these samples, with all of the samples from the sequence requiring 100x dilution before counting could occur, and many samples requiring further dilution thereafter (*Figure 5.35*).

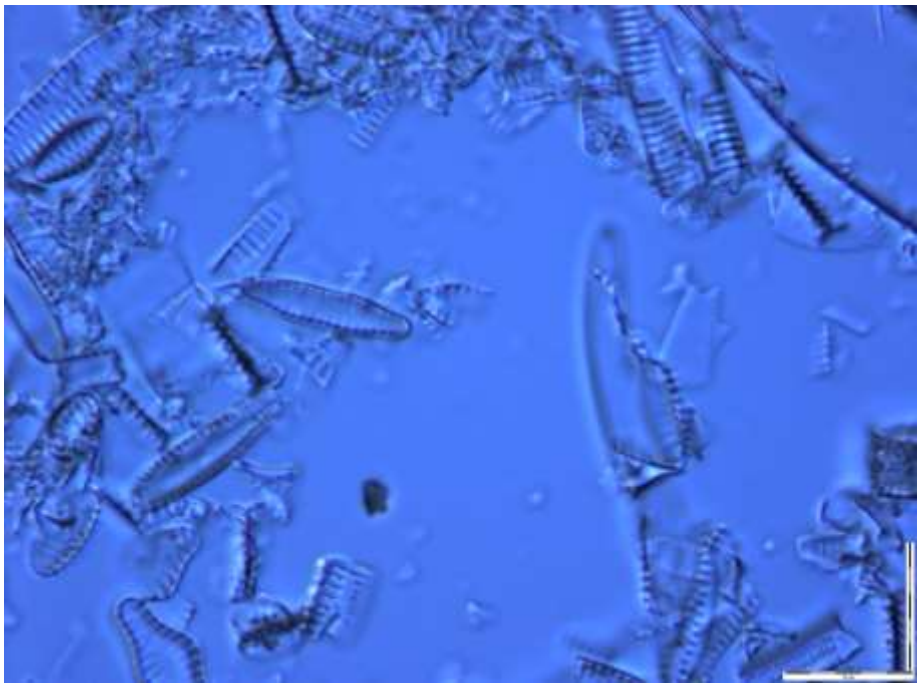


Figure 5.35: Photograph of samples from the diatomite bed diluted by 100x, demonstrating the high concentration of diatom valves remaining.

The sequence is almost entirely dominated by *Fragilaria pinnata/ construens*, ranging in relative abundance from 60-90% (*Figure 5.36*). As with the Mafadi Wetland sequence (*Figure 5.32*), *Aulacoseira ambigua* is present throughout the two sections, but in smaller quantities, ranging from 5-30% (*Figure 5.36*).

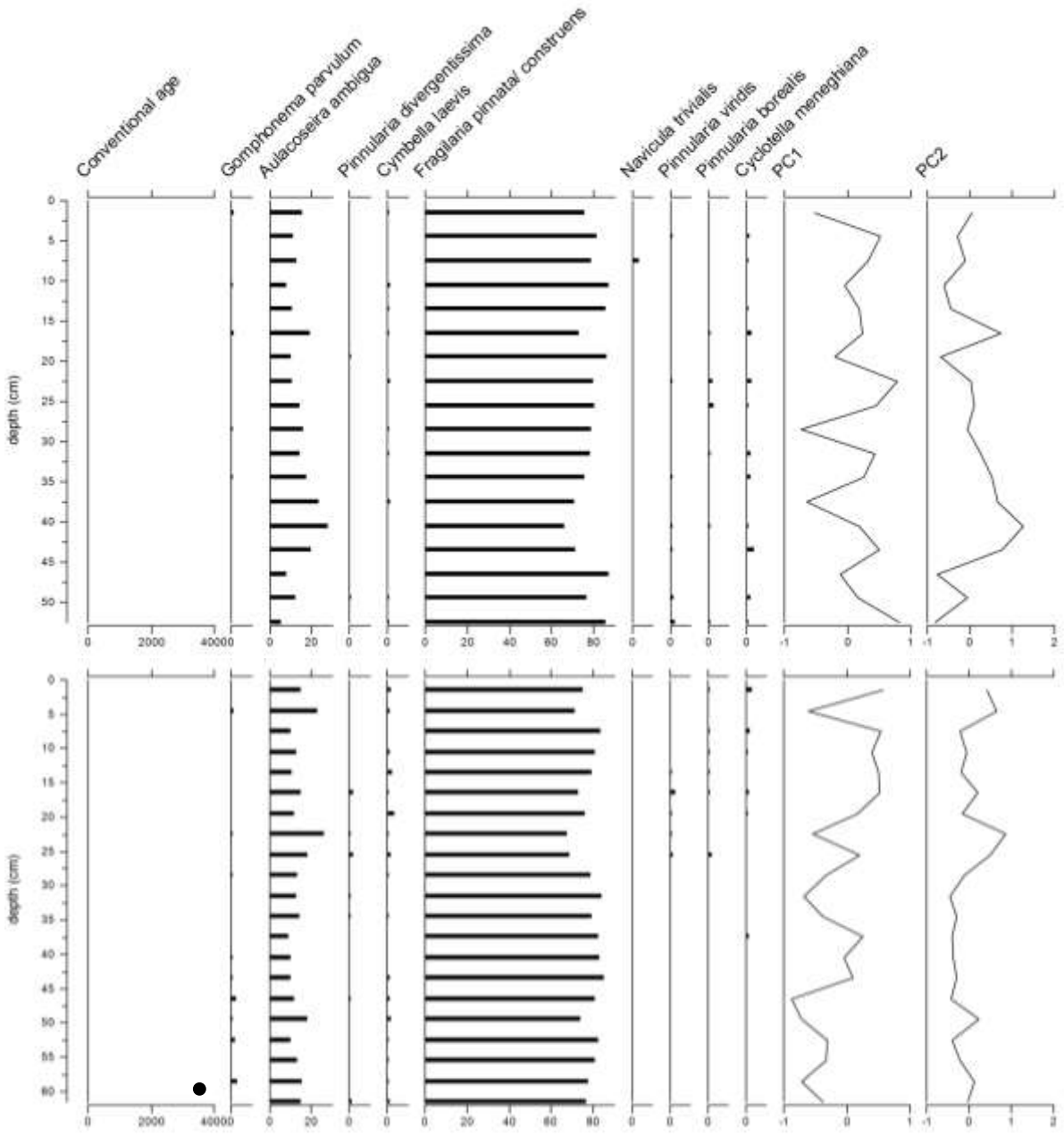


Figure 5.36: Stratigraphic diagram of diatom results from the Mafadi Diatomite Outcrop. A discontinuity or overlap of unknown depth exists between the two sections.

The presence of *Aulacoseira ambigua* throughout the sequence would re-affirm that the low percentage of Cyperaceae pollen is not indicative of a decrease in wetland size, as the

species requires relatively deep water. The lower percentages of *Aulacoseira ambigua* in this core could, however, indicate that it is located at the wetland edge. Unlike the Mafadi Wetland sequence, there is a poor synchrony between peaks in *Aulacoseira ambigua* and *Fragilaria pinnata/ construens*, and often throughout this sequence their percentage contributions demonstrate an inverse relationship (*Figure 5.36*). The PC1 curve appears largely to track the change in concentration of *Fragilaria pinnata/ construens*, while the PC2 curve follows fluctuations in *Aulacoseira ambigua* (*Figure 5.36*). Notably, *Eunotia praerupta*, which demonstrated pulses inverse to those of *Aulacoseira ambigua* and *Fragilaria pinnata/ construens* for the Mafadi Wetland profile (*Figure 5.32*), is absent throughout this sequence. Concentrations of all other diatom species are particularly low throughout the sequence, but the re-emergence of species appears often to occur simultaneously (*Figure 5.36*).

5.4.6.3 Multi-Proxy Observations

The sequence from the diatomite outcrop has far greater consistency in sediment characteristics, and lower species diversity for both pollen and diatoms, than observed for the adjacent core obtained from Mafadi Wetland. This suggests that this profile reflects very local conditions within the diatomite outcrop, rather than the environmental and climatic conditions of the broader area downslope from the adjacent Mafadi Summit, which are likely to be reflected more clearly in the Mafadi Wetland profile. There is a notably small proportion of Cyperaceae pollen throughout the core, which would in many situations indicate drier conditions. The high diatom concentration, and the presence of >5% *Aulacoseira ambigua*, indicates that the location remained wet throughout the period covered by the sequence, although could potentially include spring-driven pulses in diatom accumulation to form diatomite. Regardless, any influence of temperature on Cyperaceae and the other shrub species would necessarily also have affected the Mafadi Wetland site some 400m away, and as the pollen grains are wind-transported, they would have had similar compositions at the time of deposition. The dominance of Poaceae, and small percentages of Cyperaceae, is thus likely a result from the sediment type, with the larger coarse particles typical of the diatomite not supporting the preservation of Cyperaceae and other pollen. While the absence of high resolution dates, and the potential that the sequence was produced through discrete short-lived events of rapid diatomite formation,

makes the sequence of little palaeoenvironmental value, it is of interest to understand the differences in composition of the diatomite and peat sequences in eastern Lesotho.

5.5 Conclusion

The results from the multi-proxy analysis of the sediment cores obtained from three study sites at Sani Valley, Sekhokong and Mafadi Wetland are presented in this chapter. These sequences span varying proportions of the Holocene, dating back to ~6,200 cal. yr BP, ~13,180 cal. yr BP and ~8,140 cal. yr BP respectively. The rate of sediment accumulation is considerably slower at Mafadi Wetland than at Sani Valley and Sekhokong. Pollen and diatom species diversity and composition are more similar for Sani Valley and Sekhokong than for Mafadi Wetland, with greater species diversity at the two lower altitude sites. These differences in accumulation rate and species diversity of pollen and diatoms reflect the influence of altitude and topographic setting on the temperatures and associated environments in the eastern Lesotho highlands.

The 111cm profile from Sani Valley reflects the existence of a peat bog throughout the past ~6,200 cal. yr BP. Sediments are dark in colour, dominated by silt-sized particles and large proportions of organic material throughout the depth of the core. Cyperaceae pollen is dominant throughout the core, together with smaller but notable proportions of Asteraceae and Poaceae. Diatom results span a lower temporal resolution than the pollen and sediment records, but are dominated by *Fragilaria famelica, Diploneis parma* and *Cymbella laevis,* with the introduction of a greater relative abundance of *Fragilaria pinnata/ construens* in the samples from more shallow depths. The profile is characterised by relatively low-amplitude fluctuations over long time-periods rather than any long-term persistent change in a uniform direction.

The Sekhokong profile is considerably longer with a depth of 472.5cm, and spans the late Pleistocene/ Holocene transition, extending from ~13,180 cal. yr BP to present. This profile is marked by persistent fluctuations between orange coarse grained sediments, the dark-coloured silt-sized organic rich sediments which are ubiquitous at Sani Valley, and grey clay-

sized sediments. These fluctuations in sediment properties increase in both amplitude and frequency in the late Holocene from ~3,520 cal. yr BP to present. The profile is dominated by Poaceae, Cyperaceae and Asteraceae pollen similar to Sani Valley, although with a greater relative abundance of Poaceae throughout the sequence. This is consistent with the differences in local topography of the two sites, as the wetland dominates the Sani Valley site, while far greater expanses of meadow grasses are observed in the contemporary Sekhokong site. Notable is an abrupt decrease in Cyperaceae and Poaceae in the surface samples, replaced by *Crassula,* Aizoaceae, and a greater relative abundance of Asteraceae, together with the emergence of a large group of plant types which are scarce for much of the profile. Diatom results demonstrate a progressive shift from an aquatic environment dominated by *Fragilaria pinnata/ construens, Cymbella laevis* and *Eunotia bilunaris* in the early Holocene to an environment with an increasing relative abundance of *Fragilaria famelica, Pinnularia borealis* and *Hantzschia amphioxys* from the middle to late Holocene.

The profile from the stream bank at Mafadi Wetland, while shortest in depth (103cm), extends to the early Holocene commencing at ~8,140 cal. yr BP. The sediments from the Mafadi Wetland profile contain a relatively lower percentage of organic matter and carbonates than at Sani Valley and Sekhokong, despite being similarly situated in a peat bog. This is likely due to the large concentration of diatoms in the sediment. The profile is dominated by silt-sized sediments, and the proportion of silt-sized particles, organic matter and carbonates increases throughout the profile. The pollen record, similar to that of Sekhokong, is dominated by Poaceae, combined with a large abundance of Cyperaceae and Asteraceae. Notably, pollen is too scarce for statistically robust counting in the lowermost section of the profile, suggesting an absence of vegetation at the site during the mid to early Holocene. Diatoms are present throughout the core, and are dominated by *Fragilaria pinnata/ construens*, *Aulacoseira ambigua* and *Eunotia praerupta*. Notably, two largely discrete diatom communities exist, with clearly marked fluctuations between the two occurring throughout the profile. The first community comprises *Fragilaria pinnata/ construens* and *Aulacoseira ambigua,* which are present throughout the profile but demonstrate notable peaks. The second community is dominated by *Eunotia praerupta*, *Eunotia bilunaris*, *Pinnularia borealis* and *Gomphonema parvulum*, but includes all of the

remaining diatom species present, which make discrete appearances in the profile during periods of lower abundance of the first community.

A second core was obtained from the Mafadi Wetland site, but due to the need for a greater frequency of dates than was feasible for this project, the results are of little palaeoenvironmental value. Pollen and diatom results indicate sedimentary conditions which are not conducive to the uniform preservation of all proxies deposited. The similarity in sedimentary properties throughout the sequence may indicate that it was produced rapidly, through a series of pulses in diatom productivity.

In the *Discussion Chapter*, that follows, the environmental drivers responsible for the changes in sediment properties, pollen and diatoms at the three sites presented here are explored, constrained by the age-date model. Through interpreting these results, Holocene environmental reconstructions are developed for each of the sites. From these environmental reconstructions, broader environmental and climate changes for the eastern Lesotho region can be explored, while determining the influence of altitude, micro-topography and environmental lapse rates.

6. DISCUSSION

6.1 INTRODUCTION

The primary aim of this study is to develop a multi-proxy Holocene palaeoenvironmental and palaeoclimatic reconstruction for eastern Lesotho. The need for such research is highlighted through the knowledge gaps identified in *Chapter 2 (Literature Review).* The results of the pollen, diatom and sediment analyses of sediment profiles extracted from sites at Sani Valley, Sekhokong and Mafadi Wetland are presented in *Chapter 5 (Results).* This chapter develops palaeoenvironmental reconstructions for each site, and explores Holocene climatic shifts for the broader region, based on inferences of the environmental proxy changes reflected in these results. The chapter begins with an exploration of the potential for, assumptions in, and theoretical background to environmental and climatic inferences made on the basis of the results from the three proxies. Palaeoenvironmental reconstructions based on these inferences are accordingly presented for each of the three study sites, divided by time intervals determined by the CONISS analysis for pollen presented in *Chapter 5.* This is followed by a regional synthesis in which the palaeoenvironmental reconstructions for the three sites are compared in order to explore the influence of altitude and topographical differences. The palaeoenvironmental implications from this study are also compared with the archaeological, geomorphological and palaeoecological information for Lesotho outlined in *Chapter 2,* and with palaeoenvironmental reconstructions from lower-altitude sites in the adjacent South African regions. Comparisons are then made with relevant palaeoenvironmental studies elsewhere in southern Africa and globally, to determine and verify temporally synchronous climatic events. Finally, the prospects for future work are explored, based on the successes and difficulties experienced in this study.

As this chapter presents interpretations of the results, all proxy changes are plotted here against age rather than depth, facilitating the analysis of temporal changes in climate and the environment. To make environmental reconstructions on the basis of more than one proxy, a standardised set of profile zones needs to be selected to delineate the temporal divisions to be discussed (Finkelstein et al., 2005). The CONISS output for the pollen results

is used for this purpose. The reason is twofold: first, pollen analyses were conducted at the highest, and most consistent resolution across the three profiles (Finkelstein et al., 2005); second, the fossil pollen record represents both the local environment of the specific wetland, and the broader regional environment, and is thus more likely to reflect broader environmental changes than the progression of the wetland alone (Van Zinderen Bakker, 1955; Gasse & Van Campo, 1998; Norström et al., 2009). Finally, while this adopts an objective statistical approach, exploring changes in proxy group composition through depth, based on the PCA species scores, this chapter also qualitatively assesses the ecologies and habitats of the biotic proxies in order to infer environmental and climate drivers responsible for their shifts, both individually and as communities, over time.

6.2 Multi-Proxy Environmental and Climatic Inferences

To develop a robust and sound environmental reconstruction based on proxy evidence, it is important to understand the environmental preferences and thresholds of the source organisms of these proxies (Jones et al., 2009). Such an understanding relies on information regarding the contemporary distribution, particularly of living diatoms and the plants from which fossil pollen is derived, but also of various sedimentary conditions (Fritz et al., 1991; Norström et al., 2009; Juggins, 2013). To further constrain the environmental preferences of these proxies, future work should involve testing these environmental thresholds and developing transfer functions (Juggins et al., 2013; Truc et al., 2013). For now, such inferences on environmental and climate change are made from shifts in diatom communities are made on the basis of existing literature on diatom distributions in Lesotho (Schoeman, 1973) and southern Africa (Harding & Taylor, 2011), as well as in highland regions at a broader global scale (cf. Lotter & Bigler, 2000; Karst-Riddoch et al., 2005; Westover et al., 2006; Panizzo et al., 2007; Ohlendorf et al., 2000; McGlynn et al., 2010). Environmental inferences made from changes in fossil pollen composition are in accordance with published southern African pollen-based palaeoenvironmental reconstructions from wetland environments (cf. Gasse & Van Campo, 1998; Scott & Rossouw, 2005; Finch & Hill, 2008; Norström et al., 2009, 2014; Truc et al., 2013; Neumann et al., 2014) and an understanding of the contemporary vegetation comprising the eastern Lesotho alpine mires (Schwabe, 1995; Carbutt & Edwards, 2004, 2006; Grundling et al., 2015). This section

outlines these environmental preferences and tolerances, developing the foundation for the environmental reconstructions that follow.

Obtained from the same environment, there is a degree of inter-relationship between the three proxies (Lotter & Birks, 2003). The percentage organic content of the sediments is determined, in part, by vegetation type, diversity and density at a particular time, which is reflected in the fossil pollen record (Baker et al., 2014). Similarly, vegetation of the area in and around a wetland has the capacity to influence the diatom community within the wetland, both directly through influencing the proportion of epiphytic species, and indirectly through influencing the pH, nutrient and oxygen availability, and light penetration (Lotter & Birks, 2003; Mackay et al., 2012). These interrelationships will be discussed throughout this chapter.

6.2.1 POLLEN

The interpretation of the pollen results must be undertaken in the context of the southern African landscape and vegetation, and more specifically the high alpine wetland setting of eastern Lesotho (Van Zinderen Bakker & Werger, 1974; Scott, 1982a). The extent to which the fossil pollen composition of a sample or profile represents a regional rather than local area, depends on both the type of pollen transport, and on the local topography with associated implications on wind transport (Van Zinderen Bakker, 1955; Norström et al., 2009). Although the pollen composition of the sediment profiles will reflect a radius of vegetation far greater than that of the wetland, the steep mountains separating the region from the Lesotho lowlands to the west and the escarpment to the east, provide barriers to the long-distance transport of pollen. Thus the fossil pollen assemblage is likely predominantly sourced from the Lesotho highlands, representing a flora typical of the DAC (Carbutt & Edwards, 2004). What follows is an interpretation of the various fossil pollen flora based on literature describing the vegetation of contemporary eastern Lesotho wetlands (Van Zinderen Bakker, 1955; Schwabe, 1995; Carbutt & Edwards, 2004), and from pollen analysis undertaken at other lower altitude southern African wetlands (cf. Scott & Rossouw, 2005; Norström et al., 2009, 2014; Truc et al., 2013). It is important to note that, unlike lower altitude sites where species composition can be used to infer temperature changes, in the eastern Lesotho highlands even temperature increases of ~3°C during the

Medieval Warm Period and 5°C during the Holocene Altithermal (Tyson et al., 2000; Truc et al., 2013) are unlikely to prevent seasonal frost, as evidenced by the preservation of periglacial features in the region (Mills et al., 2009a). Temperature increases of the magnitudes modelled for the Holocene Altithermal (Truc et al., 2013) would similarly not have been sufficient to result in a shift of the tree-line to the altitude of the study sites (Van Zinderen Bakker, 1955; Grundling et al., 2015). Variation in contemporary vegetation between Mafadi Wetland and the lower altitude Sekhokong and Sani Valley sites involve species-level differences that would not be detected at the family- to genera-resolution which pollen affords (Quick et al., 2011; Quick, 2013). However, it is noted from the differences in contemporary species, and changes in species richness throughout the pollen sequences for the three sites (taken as a total count of different pollen taxa counted for each sample), that the warmer temperatures at lower altitude sites promote greater species diversity (Schwabe, 1995; Carbutt & Edwards, 2004). From an ecological perspective, periods of climate warming are associated with an expansion of the geographical range of plants to both higher altitudes and latitudes, which, for a region with limited plant diversity due to extreme cold temperatures, would increase the species diversity (Kudo, 1991; Walker et al., 1995; Inouye, 2008). Consequently, an increase in species diversity at any of the study sites in a set of adjacent samples is crudely inferred here as indicating warmer temperatures.

The three most common pollen types identified at all three sites are Cyperaceae, Poaceae and Asteraceae. These are typically the most common group of pollen types at southern African wetland sites (Gasse & Van Campo, 1998; Norström et al., 2009, 2014; Neumann et al., 2014), and reflect the most dominant contemporary plants in eastern Lesotho wetlands (Van Zinderen Bakker, 1955; Schwabe, 1995; Carbutt & Edwards, 2004). It is therefore the relative shifts in the abundance of each of these plant families, rather than their combined dominance, which is of palaeoenvironmental interest. Cyperaceae (sedges) is a semi-aquatic plant family, indicative of wet marsh conditions in which they thrive (Van Zinderen Bakker, 1955; Scott & Nyakale., 2002; Norström et al., 2009). A relative increase in the percentage of Cyperaceae pollen, relative to non-aquatic species, reflects a wet climate with an increase in the spatial extent of the wetland, potentially including both surface moisture and shallow standing water (Van Zinderen Bakker, 1955; Schwabe, 1995; Norström et al., 2009). An

increase in Cyperaceae pollen therefore implies wetter conditions, both locally and more regionally (Scott & Nyakale, 2002; Duffin et al., 2008). Poaceae, the family of grass species, is typical of the alpine grasslands that dominate much of the Lesotho highlands (Carbutt & Edwards, 2004). A relative increase in Poaceae pollen reflects a proportional increase in grassland area, and when paired with a decrease in Cyperaceae pollen, locally implies wetland desiccation (Van Zinderen Bakker, 1955; Norström et al., 2009; Neumann et al., 2011). In the early eastern Lesotho palynological work, Van Zinderen Bakker (1955) excluded Asteraceae (Compositae) from analysis as it was thought to be insect transported, and hence argued to be of only local significance. More nuanced interpretations are now being made. In the southern African context, Asteraceae are found to favour less pronounced rainfall seasonality, preferring moderate rainfall year round (Coetzee, 1967; Scott, 1999a). By contrast, Poaceae favour a greater proportion of summer rainfall (Scott, 2002). Consequently, while on their own, Poaceae and Asteraceae may be less climatically informative due to their diverse ecological ranges (Chase et al., 2015a), the ratio between Asteraceae and Poaceae is used (*Figures 6.1-6.3*) to determine the strength of precipitation seasonality (Coetzee, 1967; Scott, 2002, 2009; Norström et al., 2009). Where possible, Asteraceae fossil pollen has been identified to genus-level to facilitate a more accurate interpretation of changes within this plant family over time (Scott, 1982b).

The remainder of the fossil pollen sum for the three sites comprises smaller relative abundances from a range of plant families. At all three sites, periods of heightened species diversity are noted throughout the profiles (*Figures 6.1-6.3*), comprising increases in the relative abundance of pollen from small, flowering shrubs. These distinct increases in species diversity, most notable for Sekhokong and Mafadi Wetland, are interpreted as indicating discrete periods of warmer temperatures. It is, however, possible that these peaks in species diversity reflect an increase in wind speed, which would expand the radius from which pollen at the site originates (Jackson, 2012; Scott et al., 2012; Birks & Birks, 2014). Such a change would, however, require additional evidence to support increased strength of the westerly belt. Fossil pollen taxa which comprise a smaller percentage composition within the sequences from each of the sites provide further palaeoenvironmental information based on their individual ecological preferences. Similar to Cyperaceae, Apiaceae, *Typha* and Gentianaceae are semi-aquatic families, and an

increase in their percentage composition reflects an increase in moisture (Scott, 1989, 2002; Neumann et al., 2010). Furthermore, as aquatic species, fluctuations in their relative pollen abundance are more indicative of the plant communities within the wetland itself, rather than the broader alpine region (Norström et al., 2009). Cheno-Am (the group of morphologically indistinguishable Chenopodiaceae and Amaranthaceae), Aizoaceae, Acanthaceae, *Crassula, Chrysocoma* and *Stoebe,* by contrast, reflect dry conditions (Scott, 1989, 2002; Scott et al., 2005; Truc et al., 2013; Chase et al., 2015a). In particular, Cheno-Am reflects an increase in evaporation, rather than, necessarily, a decrease in precipitation (Scott, 1999a; Norström et al., 2009). Considering seasonality, the increased presence of Fynbos species, including *Erica*, *Anthospermum*, *Passerina* and *Stoebe,* indicates shifts to colder and wetter conditions, as these species are best suited to the Cape Floristic Kingdom in the WRZ (Scott, 1999a; Norström et al., 2009; Truc et al., 2013; Backwell et al., 2014; Neumann et al., 2014). To interpret environmental and climatic changes which the pollen sequences for each site represent, pollen counts are plotted against age, and arranged according to broad ecological groups, ranging from those requiring wet conditions to those which tolerate dry conditions, followed by the tree species and the ratio of Asteraceae to Poaceae (*Figures 6.1, 6.2, 6.3*).

In addition to contemporary species found in the eastern Lesotho highlands region, which is situated above the tree-line, fossil pollen from three tree species was found intermittently in the sequences from all three sites: *Olea, Podocarpus* and *Pinus* (*Figures 6.1-6.3*). There are contemporary forests of both *Podocarpus* and *Olea* trees in the western Lesotho lowlands, the lower altitude Drakensberg valleys, and in KwaZulu-Natal (Esterhuysen & Mitchell, 1996; Grab et al., 2005; Norström et al., 2009; Neumann et al., 2014). It is unlikely that temperatures in the eastern Lesotho highlands were sufficiently warm at any time during the Holocene for the tree-line to have moved sufficiently up-slope for either of these tree species to grow within the pollen-catchments of these wetlands, and furthermore, the steep mountain slopes and thin soils would have been unsuitable for such tree populations (Van Zinderen Bakker, 1955; Körner, 2012; Grundling et al., 2015). Thus, the presence of tree pollen in these sediment profiles cannot be interpreted as the intrusion of these species into the alpine region (Hicks, 2001).

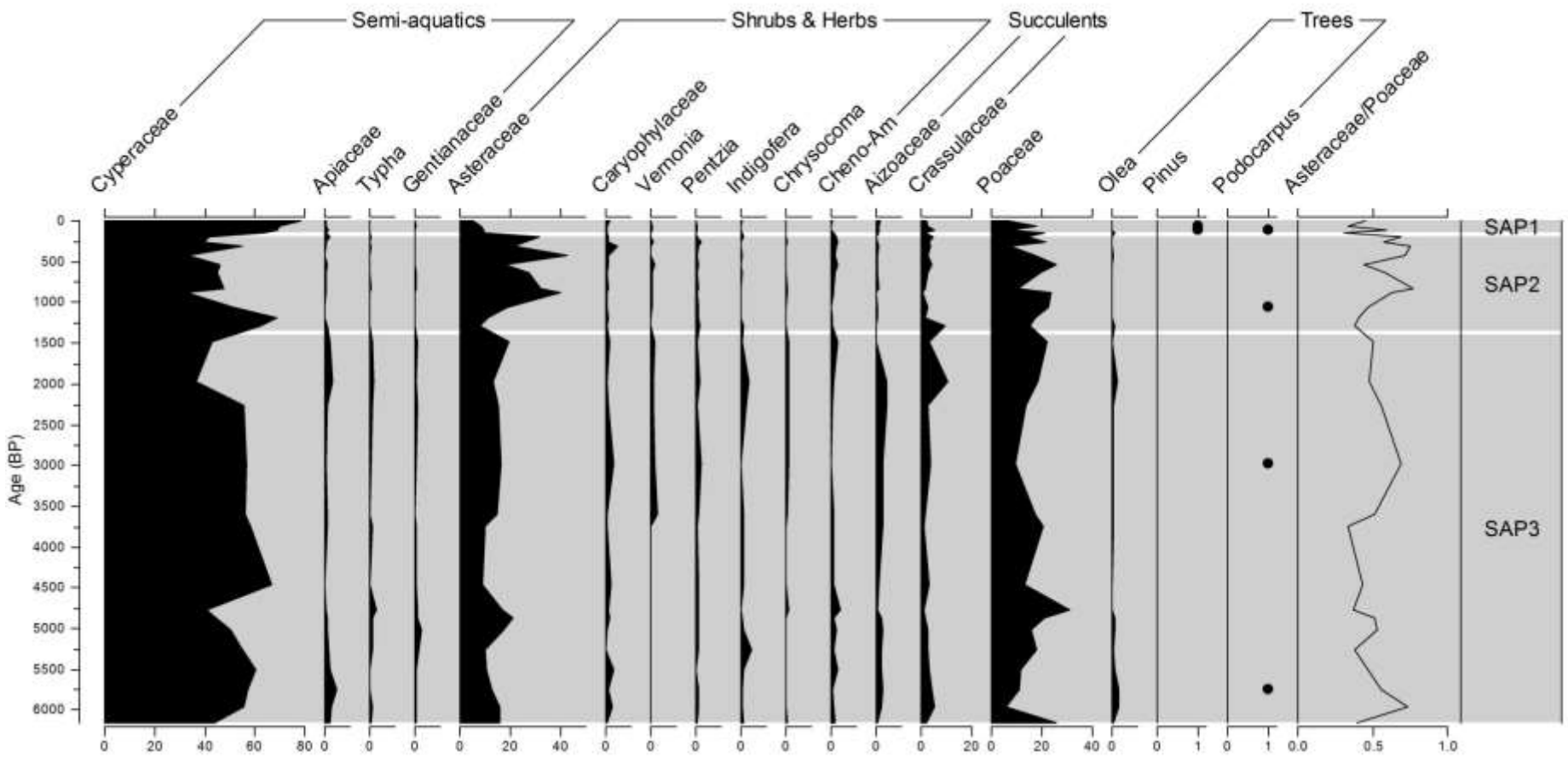


Figure 6.1: Pollen sequence from ~6,000 cal. BP - present at Sani Valley, plotted against age, grouped according to ecology, and zoned according to the CONISS output for pollen. Black circles represent the appearance of 1-5 pollen grains from the particular species.

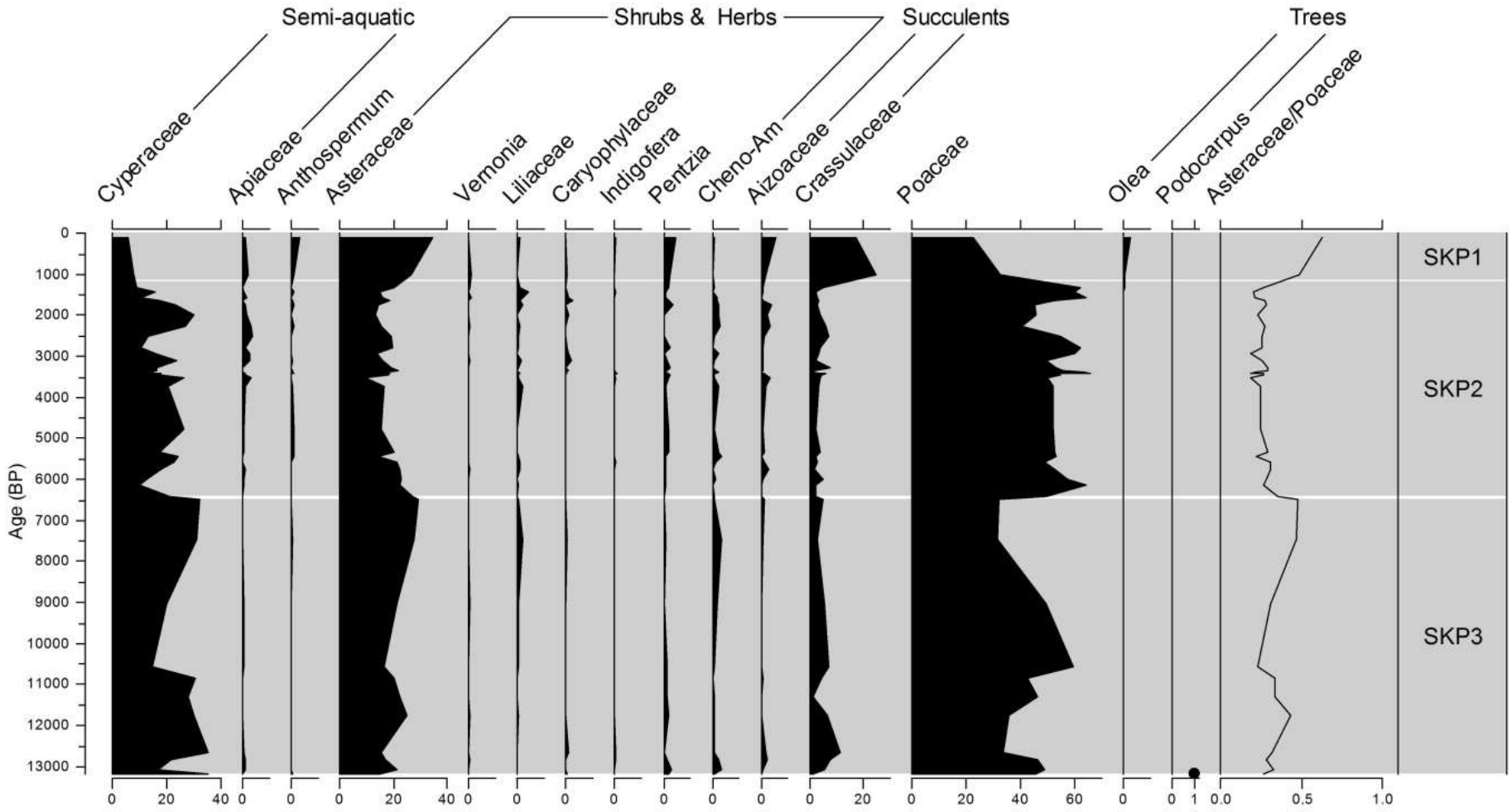


Figure 6.2: Pollen sequence from ~13,200 cal. BP - present at Sekhokong, plotted against age, grouped according to ecology, and zoned according to the CONISS output for pollen. Black circles represent the appearance of 1-5 pollen grains from the particular species.

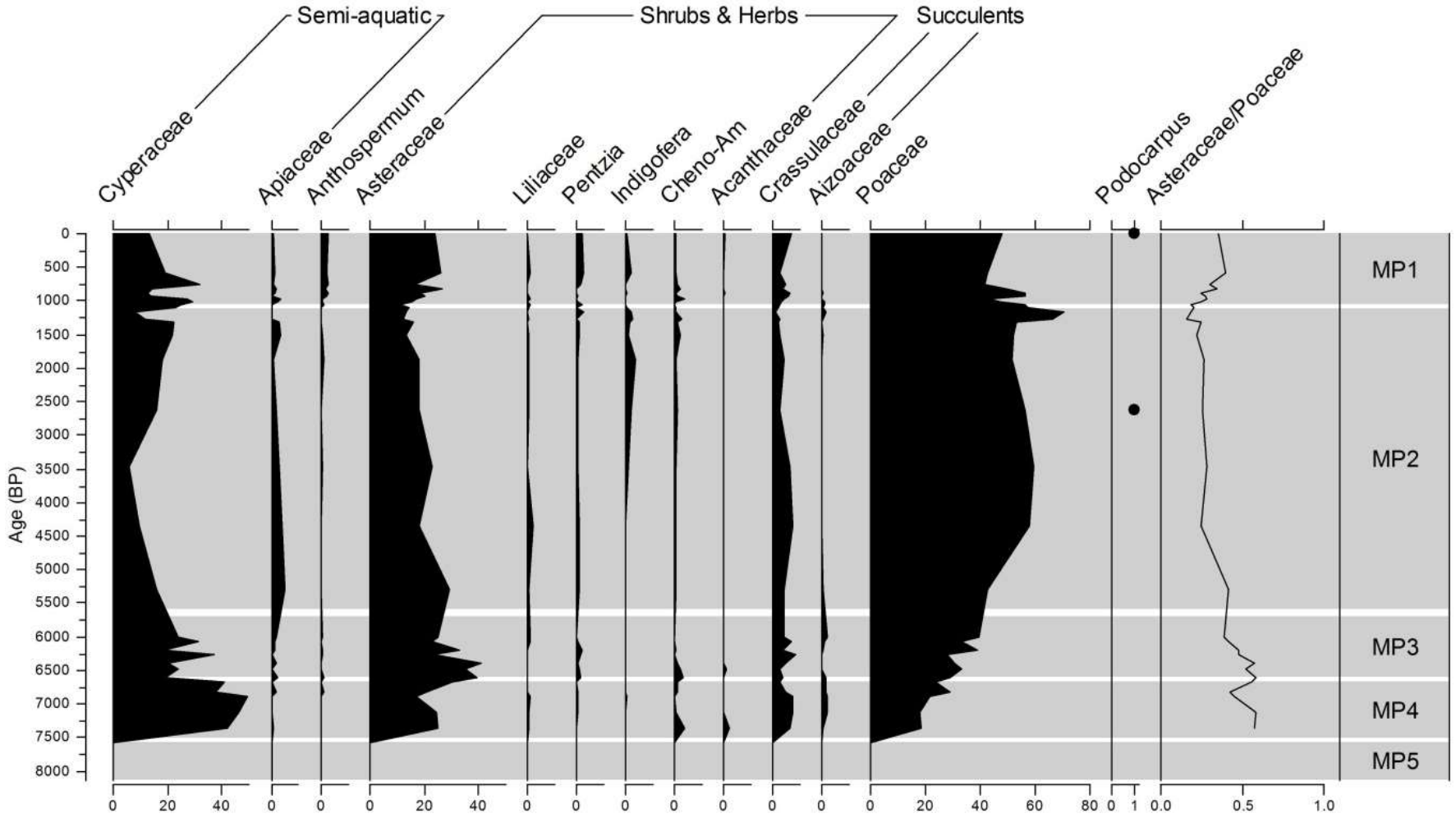


Figure 6.3: Pollen sequence from ~8,140 cal. BP - present at Mafadi Wetland, plotted against age, grouped according to ecology, and zoned according to the CONISS output for pollen. Black circles represent the appearance of 1-5 pollen grains from the particular species.

The presence of tree species in the pollen record rather predominantly reflects a change in the pollen transport dynamics (Hicks, 2001). This could involve an increase in temperature and/or precipitation which would encourage a slight upslope shift in the extent of these forests in surrounding mountain valleys of central Lesotho and adjacent KwaZulu-Natal, thus increasing the probability of pollen transport to the eastern Lesotho wetlands (Esterhuysen & Mitchell, 1996; *Figure 6.4*). This paired with, or replaced by, an increase in the westerly wind regime to facilitate the transport of tree pollen across greater distances. Given the dominant westerly airflow and less abrupt topography to the west of the study sites, it is most likely that this pollen is derived from the lowlands to the west (Stromquist et al., 1985). The increased the westerly wind regime would thus require a strengthening of the westerly belt, a phenomenon which has previously been argued to influence the regional climate during the late Quaternary (Norström et al., 2009; Mills et al., 2012).

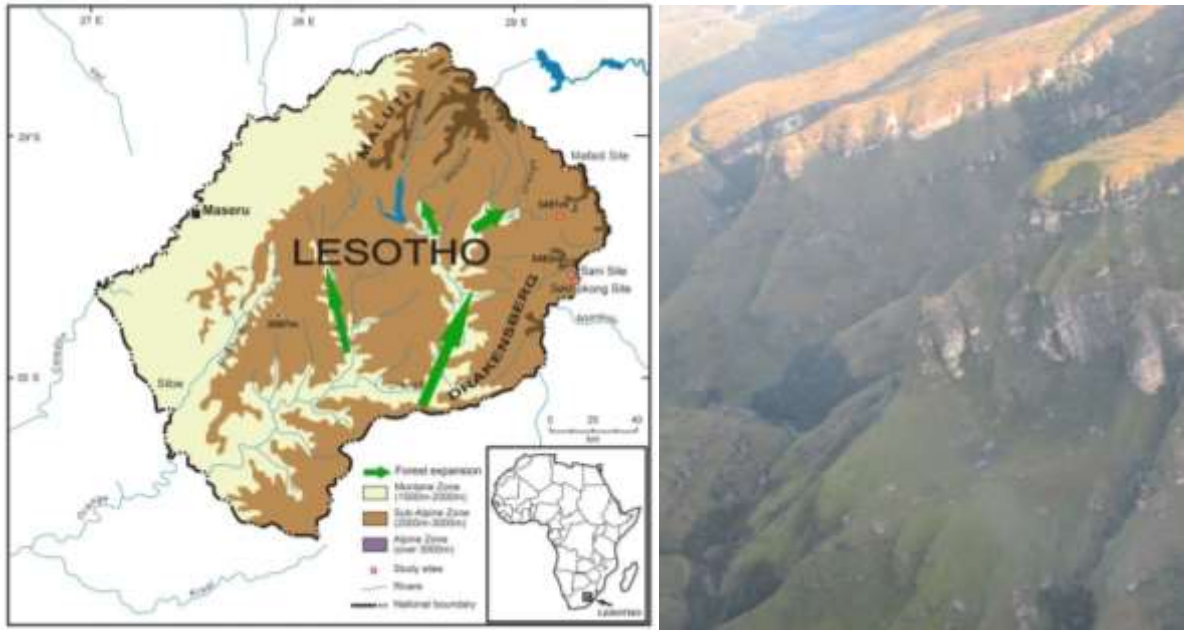


Figure 6.4: The likely trajectories of *Podocarpus* and *Olea* pollen into the central Lesotho valleys during warm periods, and photograph illustrating such fragmented forest growth in Drakensberg valleys.

It is notable that, under any climatic interpretation, one would expect that peaks in tree pollen of the individual species would occur concurrently, yet this is seldom the case for any of the eastern Lesotho pollen records. Furthermore, while Grab et al. (2005) report

Podocarpus pollen from their profile in western Lesotho between 6,900-5,000 cal. yr BP, contemporaneous with the *Podocarpus* charcoal in the same region reported by Esterhuysen and Mitchell (1996), *Podocarpus* pollen appears only once during this period in the pollen record presented here, and only in the Sani Valley profile (*Figure 6.*1). While climatic changes could increase the probability of tree pollen being transported to eastern Lesotho, this would entail a high level of chance. Therefore, no direct robust climate inferences can be made from the presence or absence of tree pollen.

Three pollen grain types from the eastern Lesotho sequences are of interest from the perspective of alien and invasive species. The first of these is pine, which appears in the top three samples from Sani Valley (>2% for samples in layers 2 and 3, ~110 cal. yr BP- present; *Figure 6.1*), and in the top sample from Mafadi Wetland (<2%; >100 cal. yr BP; *Appendix B.8*). Pine was introduced to southern Africa 300 years ago (Van Wilgen & Richardson, 2012), but commercial forestry in the KwaZulu-Natal was initiated in the mid-20th century (Turner & Plater, 2004; Stager et al., 2013). The age-dates for the sediment samples containing *Pinus* pollen are therefore temporally consistent with the introduction of pine in adjacent regions, and this pollen was likely transported by wind from lower altitude plantations. The second pollen type of interest is *Olea*, which is found intermittently at relative abundances of greater than 2% throughout the profiles from each of the three study sites (*Figures 6.1-6.3*). It is often assumed to be an alien species (Grab et al., 2005), but established African wild olive trees were present in the KwaZulu-Natal uplands when early navigators and missionaries visited the area as early as AD 1576 (Bird, 1965), and it appears regularly in the archaeological charcoal record from western Lesotho (Esterhuysen & Mitchell, 1996), and from Braamhoek Wetland in the adjacent Free State Province of South Africa (Norström et al., 2009; 2014). There is no reason to believe that the *Olea* pollen represents any species other than the African wild olive, and thus this pollen is not of interest from the perspective of species invasions (Scott, 1982a,b). The third pollen type, Asteraceae *Chrysocoma*, most likely reflects *Chrysocoma cilliata,* which is widely described as a karroid invasive which colonises areas in eastern Lesotho during periods of drought (Grab & Deschamps, 2004; Letšela, 2008). Evidence of this pollen throughout the 6,000-year sequence from Sani Valley (*Figure 6.1*) would suggest that this may not be a human induced invasive, but rather that the species has a natural environmental niche in the eastern

Lesotho highlands. This supports the more recent classification of *Chrysocoma cilliata*, together with *Artemisia afra* and *Stoebe vulgaris*, as native species to the DAC, which become prolific under changing climatic conditions (Carbutt, 2012). It is, however, interesting that the *Chrysocoma* pollen is present throughout a full sequence at Sani Valley, at Sekhokong only in samples from the past ~350 cal. yr BP (with relative abundance <2%, *Appendix B.5*), and does not appear in the pollen sequence for Mafadi Wetland. This further indicates the niche habitat of this species, and potentially indicates a weak tolerance to cold temperatures. The presence of these 'invasive' species in the pollen record in the niche environment of the eastern Lesotho highlands, illustrates the value of palaeoenvironmental work in clarifying ecological debates (Gillson et al., 2008). This is of critical importance as climate change is argued to increase the susceptibility of an ecosystem to alien vegetation invasions (Gillson et al., 2008; Carbutt, 2012).

PCA fits a linear model to a set of data-points arranged in a multi-dimensional cloud of points, transferring it to a representation in two-dimensions (Kent & Coker, 1992; Stevenson & Pan 2004). Consequently, it provides an interpretation of the major similarities in behaviour of species without human interpretive bias (Stevenson & Pan, 2004). PCA is not, however, able to isolate environmental conditions for each axis, or even for the first axis in all cases, but facilitates a relatively quick interpretation of the results presented in *Chapter 5*. Even in those cases, it remains of interest to see where the greatest axis of change sits, and the resultant order of species according to that axis. For the Sani Valley pollen sequence, PC1 separates Cyperaceae with very negative scores, from Poaceae, Asteraceae and Cheno-Am with strong positive scores (*Figure 5.7*). While Aizoaceae and *Crassula* are positioned alongside Cyperaceae with negative scores, this principal component largely reflects a transition from wet to dry conditions. PC2 separates the dominant species – Cyperaceae, Poaceae and Asteraceae (together with the differentiated Asteraceae genera) from the more under-represented taxa. This suggests a temperature gradient, with warmer temperatures encouraging greater species diversity, associated with positive PC2 scores. This could also imply an increase in the westerly wind regime, expanding the region from which pollen in the profile originates.

For Sekhokong, PC1 separates a range of small shrub species from the dominant Cyperaceae and Poaceae pollen (*Figure 5.18*). Marked by the extreme isolation of the two SKP1 samples, PC1 appears to be driven by differences between the contemporary and palaeo-vegetation, rather than the environmental drivers responsible for long term fluctuations in vegetation, and associated broader environmental and climatic changes. Recent vegetation shifts may indicate the role of human and livestock influence in changing the wetland properties and encouraging greater species diversity (Schwabe, 1995; Grab & Deschamps, 2004). This may coincide with the beginning of the intensive gully erosion at this site (Marker, 1994; Grab & Deschamps, 2004). PC2 separates Cyperaceae from Poaceae with extremes in axis scores, indicating transitions between drier conditions facilitating predominant grasslands, and wetter conditions under which the moist to shallow water area of the wetland expands. The positive axis scores of *Crassula*, Aizoaceae and Cheno-Am together with Cyperaceae, however, are not consistent with this interpretation. PC2 might therefore not represent a clear, uniform climatic shift.

The Mafadi Wetland pollen sequence reflects considerably lower species diversity throughout, likely driven by the cooler temperatures at this higher altitude site (Carbutt & Edwards, 2004). A much smaller group of plants can survive the colder conditions and greater incidence of frost at Mafadi Wetland, and under cold periods even fewer species are likely to have been present (Grab, 1996a). The limitation of the family-level resolution of pollen analysis prevents a more detailed understanding of the dynamics in individual plant species habitat ranges under colder and warmer climates, or the comparison of specific species at high and lower altitude sites (Quick et al., 2011; Quick, 2013). PC1 separates Poaceae from Cyperaceae, Asteraceae and many of the small shrubs, indicating a variation in the dominance of grassland relative to marsh conditions, which is possibly moisture driven, but the selection of underrepresented dry- and wet-climate shrubs paired with Cyperaceae and Poaceae pollen respectively, confuse this (*Figure 5.29*). PC2 is similar to that for Sekhokong, separating Cyperaceae and Poaceae from the lesser-represented shrubs, potentially indicating a temperature gradient, with warm conditions reflected by positive PC2 scores. The bottom zone of the Mafadi Wetland profile has a marked absence of pollen, and hence could not be included in the PCA (*Figure 5.29*).

6.2.2 DIATOMS

Diatom species composition is influenced by a range of environmental factors, including inter-species competition regarding temperature, precipitation, pH, pollution, conductivity and the habitat which their environment provides (Mackay et al., 2003; Stoermer & Smol, 2004). As diatoms can be identified to species level, an understanding of the diatom community composition in a particular sample, and changes throughout a sequence, can facilitate inferences regarding the climatic and environmental conditions of the aquatic habitat based on similarities in the autecology of co-existing species (Battarbee et al., 2001; Stoermer & Smol, 2004; Stevenson & Pan, 2004). The diatoms extracted and identified from the sediment profiles at Sani Valley, Sekhokong and Mafadi Wetland represent a range of environmental attributes and habitats, with notable overlaps between sites as well as species unique in this study to a particular site (*Table 6.1*). While this large selection of environmental indicators is of value in tracking specific environmental changes, diatom communities often change in response to a range of different interacting drivers, and without transfer functions one runs the risk of imprecise interpretation (Fritz et al., 1991; Juggins, 2013). These characteristics are thus used only where necessary to explain the observed principal components, and to explore changes in communities which cannot be explained by broader, more regional, environmental drivers.

Table 6.1: Habitat and autecological characteristics of the diatoms identified in the eastern Lesotho diatom sequences presented in this study.

Diatom Species	Site	Habitat	Additional notes on Ecology
Achnanthes minutissima	Mafadi, Sekhokong, Sani	Epiphytic (Huntsman-Mapila et al. 2006)	Presence of macrophytes (Gasse & Van Campo, 1998), low pollution (Schoeman, 1973; Mackay et al., 2012), common in upland streams (Walsh & Wepener, 2009)
Aulacoseira ambigua	Mafadi, Sekhokong	Planktonic (Holmgren et al., 2012)	Shallow to deep alkaline water (Gasse & Van Campo, 1998; Sitoe et al., 2015)
Caloneis silicula	Sekhokong, Sani	Benthic (Harding & Taylor, 2011)	Alkaline water (Schoeman, 1973)
Cymbela gracilis	Mafadi, Sekhokong, Sani	Benthic (western diatoms)	Low electrolyte content (Harding & Taylor, 2011)
Cymbella cistula	Sekhokong	Epiphytic epipelic (Harding & Taylor, 2011)	Oxygen rich (Schoeman, 1973)
Cymbella laevis	Mafadi, Sekhokong, Sani	Epiphytic (Schoemann, 1973)	Alkaline water (Schoeman, 1973)
Cymbella selesiaca	Sekhokong	Benthic (Gillson & Ekblom, 2009)	Tolerates polluted water (Harding & Taylor, 2011), high electrolytes (Huntsman-Mapila et al., 2006)
Diploneis didyma	Sekhokong	Epipelic (Denys, 1994)	Found in brackish waters (Sitoe et al., 2015)
Diploneis ovalis	Mafadi, Sekhokong, Sani	Aerophillic, benthic (Caljon & Cocquyt, 1992)	Alkaline water (Schoeman, 1973)
Diploneis parma	Sekhokong,	Aerophilic (Gell & Little,	

	Sani	2007)	
Eunotia bilunaris	Mafadi, Sekhokong, Sani	Epiphytic (Gasse & Van Campo, 2001)	Freshwater, low electrolytes (Norström et al., 2012; Gasse & Van Campo 2001)
Eunotia exigua	Mafadi, Sekhokong	Benthic, moist environments (western diatoms)	Very acidic water (Harding & Taylor, 2011)
Eunotia praerupta	Mafadi, Sekhokong, Sani	Aerophilic (Cocquyt, 2007); benthic (Finné et al. 2010)	Acidic water (Schoeman, 1973), tolerates drying (Cocquyt, 2007)
Fragilaria famelica	Mafadi, Sekhokong, Sani	Benthic (western diatoms)	Alkaline water (Schoeman, 1973), tolerates prolonged snow (Wang et al., 2013)
Fragilaria pinnata/ construens	Mafadi, Sekhokong, Sani	Facultative planktonic (Sonneman et al. 1999)	Low alkalinity, dominant in very cold waters (low water temperature optimum) (Schmidt et al., 2004; Cocquyt, 2007), tolerates ice (Ohlendorf et al., 2000; Wang et al., 2013)
Gomphonema bohemica	Sekhokong	Epiphytic (Hargan et al., 2015)	Freshwater, moderate pollution (Craticula, n.d.)
Gomphonema gracile	Mafadi, Sekhokong	Epiphytic (Gasse, 1986)	Acidic water (Gasse & Van Campo, 1998)
Gomphonema parvulum	Mafadi, Sekhokong	Epiphytic, epipelic, epilithic (Gasse & Van Campo, 1998; Sonneman et al. 1999); benthic (Caljon & Cocquyt, 1992)	Alkaline water (Gasse & Van Campo, 1998; Schoemann Lesotho), tolerant of very polluted water (Cocquyt, 2007; Walsh & Wepener, 2009; Oberg et al., 2013)
Hantzschia Amphioxys	Mafadi, Sekhokong, Sani	Aerophilic (Sonneman et al., 1999)	Tolerates extreme drying (Sitoe et al., 2015; Mackay et al., 2012)
Navicula explanata	Sekhokong	Epiphytic (Foged, 1964)	
Navicula laevissima	Mafadi, Sekhokong, Sani	Epiphytic (Karst Riddoch et al., 2005)	Eutrophic freshwater (Poulíčková et al., 2008)
Navicula minima	Mafadi, Sekhokong Sani	Epilithic (Camargo & Jiménez, 2007)	Tolerates polluted water (Harding & Taylor, 2011), alkaline water (Schoeman, 1973)
Navicula trivialis	Sani	Benthic (Caljon & Cocquyt, 1992)	Alkaline water, tolerates pollution (Craticula, n.d.)
Nitzschia palea	Sekhokong	Epilithic & epipelic (Sonneman et al. 1999)	Tolerates pollution (Schoeman, 1973; Walsh & Wepener, 2009)
Pinnularia borealis	Mafadi, Sekhokong, Sani	Aerophilic (Sitoe et al., 2015); epiphytic (Gasse & Van Campo, 2001)	Cold, acidic water (Cocquyt, 2007)
Pinnularia divergentissima	Mafadi, Sekhokong, Sani	Aerophilic (Holmgren et al., 2012)	Acidic water (Schoeman, 1973), montane environments (Harding & Taylor, 2011)
Pinnularia gentilis	Mafadi, Sekhokong, Sani	Epipelic (Lee & Yoon, 2003)	Mesotrophic (Yang, 1990)
Pinnularia viridis	Mafadi, Sekhokong	Benthic (Gasse & Van Campo, 1998)	Mesotrophic (Yang, 1990), slightly acidic (Schoeman, 1973)
Sellaphora pupula	Mafadi, Sekhokong, Sani	Epipelic and epilithic (Sonneman et al. 1999)	Presence of macrophytes (Gasse & Van Campo, 1998), tolerates very polluted water (Harding & Taylor, 2011, Schoeman, 1973)
Stauroneis phoenicenteron	Mafadi, Sekhokong	Benthic (Caljon & Cocquyt, 1992)	Acidic water (Gasse & Van Campo, 1998), tolerates pollution (Schoeman, 1973)
Stauroneis producta	Sekhokong	Aerophillic (Gasse & Van Campo, 1998)	Acidic water (Gasse & Van Campo, 1998, 2001)

Diatoms are arguably relatively poor indicators of temperature (Anderson, 2000), and as with pollen in the high alpine wetlands of eastern Lesotho, diatoms representative of warm conditions are unlikely to exist, as their minimum temperature thresholds are unlikely to be met even under past periods of warming. However, the *Fragilaria* species in the diatom sequences from the eastern Lesotho wetlands are potentially of value in detecting periods

of particularly cold temperatures. The *Fragilaria* group of species (*Fragilariods*) are r-strategists, which can survive under periods of stress and rapid climatic and environmental change (Schmidt et al., 2004; McGlynn et al., 2010). The *Fragilaria pinnata/ construens* group are common in environments that experience rapid temperature changes (Ohlendorf et al., 2000; Panizzo et al., 2007; McGlynn et al., 2010). Notably, they are common in high alpine lakes, are often the dominant species in very cold water with a preference for cold water temperatures, and survive prolonged periods of ice cover (Ohlendorf et al., 2000; Schmidt et al., 2004; Coquyt, 2007; Wang et al., 2013). In eastern Lesotho, increases in the relative abundance of *Fragilaria pinnata/ construens* appear to be associated predominantly with conditions of greater frequency of ice occurrence (Schoeman, 1973), which is confirmed by their greater relative abundance in the diatom sequence from higher altitude, and consequently more ice-prone, Mafadi Wetland, than the sequences from Sekhokong or Sani Valley (*Tables 5.4, 5.8, 5.12*). *Fragilaria famelica* similarly tolerates very cold water and is common in high altitude water bodies, but differs from the *pinnata/ construens* group in that it tolerates prolonged snow cover rather than ice conditions (Wang et al., 2013). This reflects a preference for slightly warmer conditions than those which *Fragilaria pinnata/ construens* tolerate, and potentially an increase in precipitation or a shift to a larger proportion of winter precipitation. Larger relative abundances of the *Fragilaria* group, and in particular their dominance for particular samples, is thus interpreted to represent periods of particularly cold temperatures, which only ice- and snow-tolerant diatoms will survive (Ohlendorf et al., 2000). While a reduction of the relative abundance of these species suggests an amelioration of the climate, their absence does not necessarily imply warm conditions, as they are usually replaced by aerophilic species. This shift is of importance from a habitat perspective, as a shift from benthic/ facultative planktonic diatoms to aerophilic species is indicative of a moisture rather than temperature transition (Gell & Little, 2007; Finné et al., 2009; Sitoe et al., 2015). Interestingly there is a notable similarity between the diatom species composition in these three eastern Lesotho wetlands, and diatom assemblages from the Canadian Arctic (Antoniades et al., 2005; Karst-Riddoch et al., 2005; Hargan et al., 2015), representing both the cosmopolitan nature of the distribution and the influence of cold temperatures in restricting species composition. As noted in *Table 6.1*, *Fragilaria pinnata/ construens* additionally have a preference for acidic waters, while *Fragilaria famelica* demonstrate a preference in Lesotho for alkaline water (Schoeman,

1973). However, the co-existence of these species with other diatoms of varying pH preference, makes this interpretation unlikely. Only if it they were paired with similarly alkalophilous or acidophilous species, is a pH inference made on the basis of the presence of these species. Finally, r-strategists are argued to be more tolerant of high ultra-violet (U.V.) Radiation, which is inferred to be responsible for periods of predominant *Fragilaria* species in the Rwenzori Mountains of Uganda (Panizzo et al., 2008). While changes in U.V. strength may induce further stress in a harsh environment, the palaeogeomorphological evidence from the region supporting periods of prolonged ice cover (Grab, 1996a; Boelhouwers & Meiklejohn, 2002; Mills et al., 2011), would support the ice- and temperature-based interpretation.

On the basis of these habitat preferences and autecologies of the individual diatom species in the profile, inferences can be made regarding the environmental factors which the dominant principal components most likely represent. For Sani Valley, diatom analysis was performed for only a few samples, and thus the interpretation of PCA results must be made with caution. PC1 separates *Fragilaria pinnata/ construens, Achnanthes minutissima, Caloneis silicula, Sellaphora pupula* and *Navicula minima,* with negative PC1 scores, from *Diploneis parma, Fragilaria famelica, Diploneis Ovalis, Pinnularia borealis, Pinnularia gentilis* and *Hantzschia Amphioxys,* with positive scores (*Figure 5.10*). This appears largely to reflect a shift to species more tolerant of alkaline water and higher levels of pollution. The timing of the shift to strongly negative PC1 scores coincides with the introduction of livestock to eastern Lesotho which could be responsible for the increased alkalinity and organic pollution (Parker et al., 2011). PC2 separates *Fragilaria famelica, Cymbella laevis* and *Navicula minima,* with the lowest negative scores, from *Diploneis Parma, Pinnularia borealis* and *Hantzschia amphioxys,* with the highest positive scores. This reflects a shift from benthic species to aerophilic species, which can be inferred as representing a transition between dry and wet conditions.

The PC1 axis for Sekhokong is difficult to interpret as there are no clear similarities in the autecologies of the species situated comparatively closely on the axis. PC1 separates *Fragilaria famelica, Pinnularia borealis, Hantzschia amphioxys* and *Achnanthes minutissima,* with most extreme negative scores, from *Fragilaria pinnata/ construens*, *Cymbella laevis,*

Eunotia bilunaris, Gomphonema parvulum and *Eunotia exigua,* with the most positive scores (*Figure 5.21*). Notably, this separates the two *Fragilaria* groups, which could suggest shifts between conditions favouring snow and those dominated by ice, reflecting a temperature transition paired with a shift in seasonality to a greater proportion of cold-season precipitation. However, as *Fragilaria famelica, Pinnularia borealis* and *Hantzschia amphioxys* all share positive PC1 scores (*Figure 5.21*), there is some contradiction as the snow preference of *Fragilaria famelica* typically requires increased moisture input, or a change in seasonality of precipitation to favour snow, while *Pinnularia borealis* and *Hantzschia amphioxys* are aerophilic species indicative of dry conditions. The Sekhokong diatom PC2 axis separates *Fragilaria pinnata/ construens*, *Aulacoseira ambigua, Fragilaria famelica* and *Achnanthes minutissima,* with negative scores, from *Hantzschia amphioxys, Diploneis parma, Pinnularia gentilis, Pinnularia divergentissima, Caloneis silicula* and *Pinnularia borealis,* with positive scores. This segregates the planktonic and facultative planktonic species from the aerophilic species, therefore the PC2 axis represents a moisture gradient between the two.

The Mafadi Wetland diatom sequence is interesting in that it cycles between periods dominated by *Aulacoseira ambigua* and *Fragilaria pinnata/ construens*, and periods with low relative abundances of these two groups but dominated by all of the remaining species. PC1 separates *Aulacoseira ambigua* and *Fragilaria pinnata/ construens* with negative species scores from all of the rest of the diatom species in the profile, which are assigned positive species scores (*Figure 5.32*). Notable are the species which have the highest positive PC1 species scores – *Eunotia praerupta, Eunotia bilunaris* and *Pinnularia borealis* (*Figure 5.32*). These three species tolerate dry conditions and, separated at extremes from the planktonic *Aulacoseira ambigua* and facultative planktonic *Fragilaria pinnata/ construens* group, represent a pattern of pulsing, rather than progressive transition, between wet and dry conditions. PC2 separates *Aulacoseira ambigua* and *Pinnularia divergentissima* with very negative species scores from *Fragilaria pinnata/ construens, Fragilaria famelica, Achnanthes minutissima* and *Eunotia praerupta* with very positive scores. The *Fragilaria* group, while facultative planktonics, are littoral species which frequently attach to plants (Schmidt et al., 2004). *Achnanthes minutissima* and *Eunotia praerupta* are epiphytic diatoms, and thus thrive in conditions with the presence of macrophytes (Gasse & Van Campo, 1998).

Therefore, this axis represents a transition between higher and lower plant density in the water body, suggesting a decrease in turbidity or a change in water temperature.

The majority of palaeoenvironmental reconstructions made on the basis of diatom analysis in southern Africa rely predominantly, and often entirely, on environmental inferences made on the basis of the habitat preferences of diatom communities (cf. Gasse & Van Campo, 1998; Ekblom et al., 2008; Gillson & Ekblom, 2009; Finné et al., 2010; Holmgren et al., 2012; Stager et al., 2013). In a wetland environment this is a valuable approach as the dominant environmental changes are likely to involve changes in the size and water depth of the wetland, including shifts from shallow standing water, through to a moist wetland with a greater presence of macrophytes, to a dry environment in which diatoms are exposed directly to air (Gasse & Van Campo, 1998; Stager et al., 2013). Furthermore, using an equivalent approach facilitates comparison with other studies. Therefore, the interpretation of the diatom results in this study for the purpose of developing a palaeoenvironmental reconstruction for each of the sites, and in turn the region, will be made on the basis of the habitat groups of the species present. However, where appropriate, reference will be made to individual species and their specific ecologies. The diatom sequences for the three sites are consequently presented in *Figures 6.5-6.7*, plotted according to the age of the samples and divided into zones according to the pollen CONISS output for each site. The species are grouped according to their habitats, ranging from the wettest to the driest conditions, for consistency with the pollen diagrams (*Figures 6.5-6.7*). For all three sites there are notable fluctuations between planktonic, benthic and epiphytic environments representing wet periods, and drier environments dominated by aerophilic species.

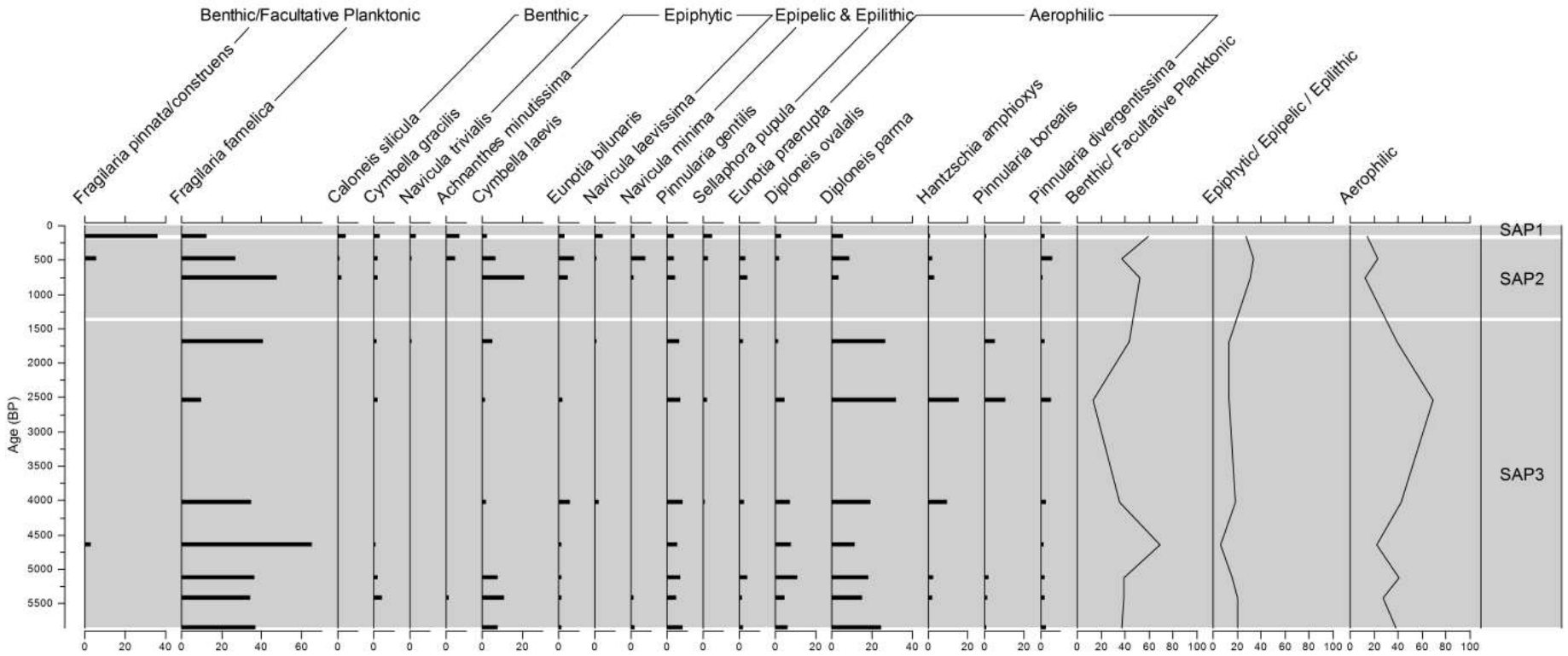


Figure 6.5: Diatom sequence from ~6,000 cal. BP - present at Sani Valley, plotted against age, grouped according to habitat, and zoned according to the CONISS output for pollen at Sani Valley.

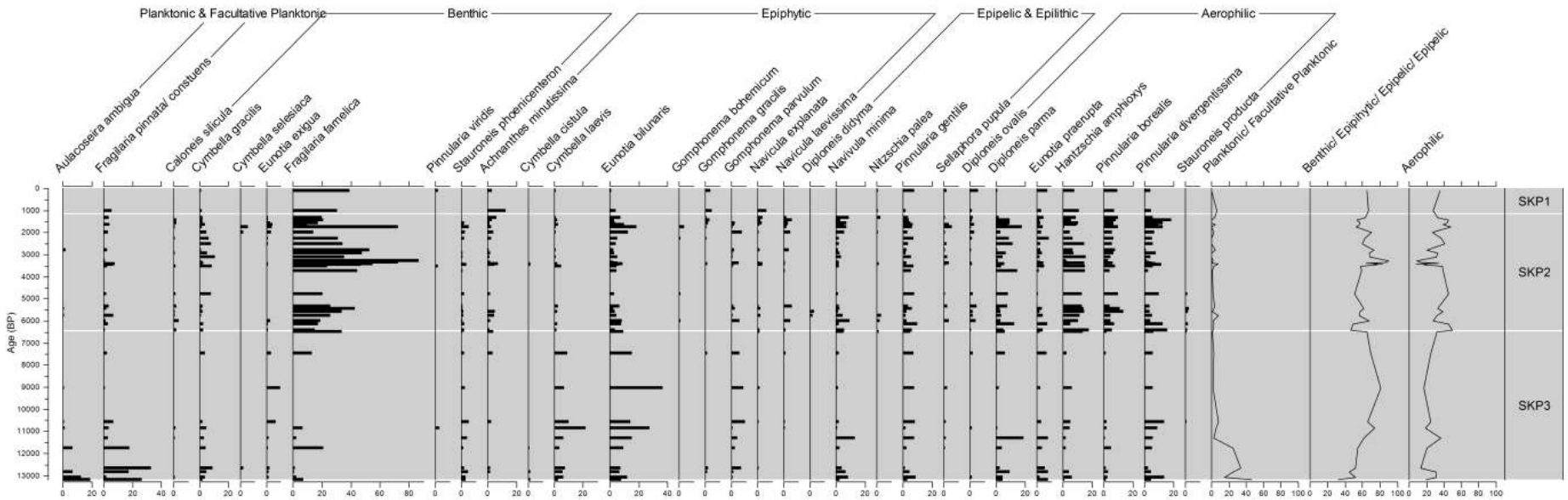


Figure 6.6: Diatom sequence from ~13,200 cal. BP - present at Sekhokong, plotted against age, grouped according to habitat, and zoned according to the CONISS output for pollen at Sekhokong.

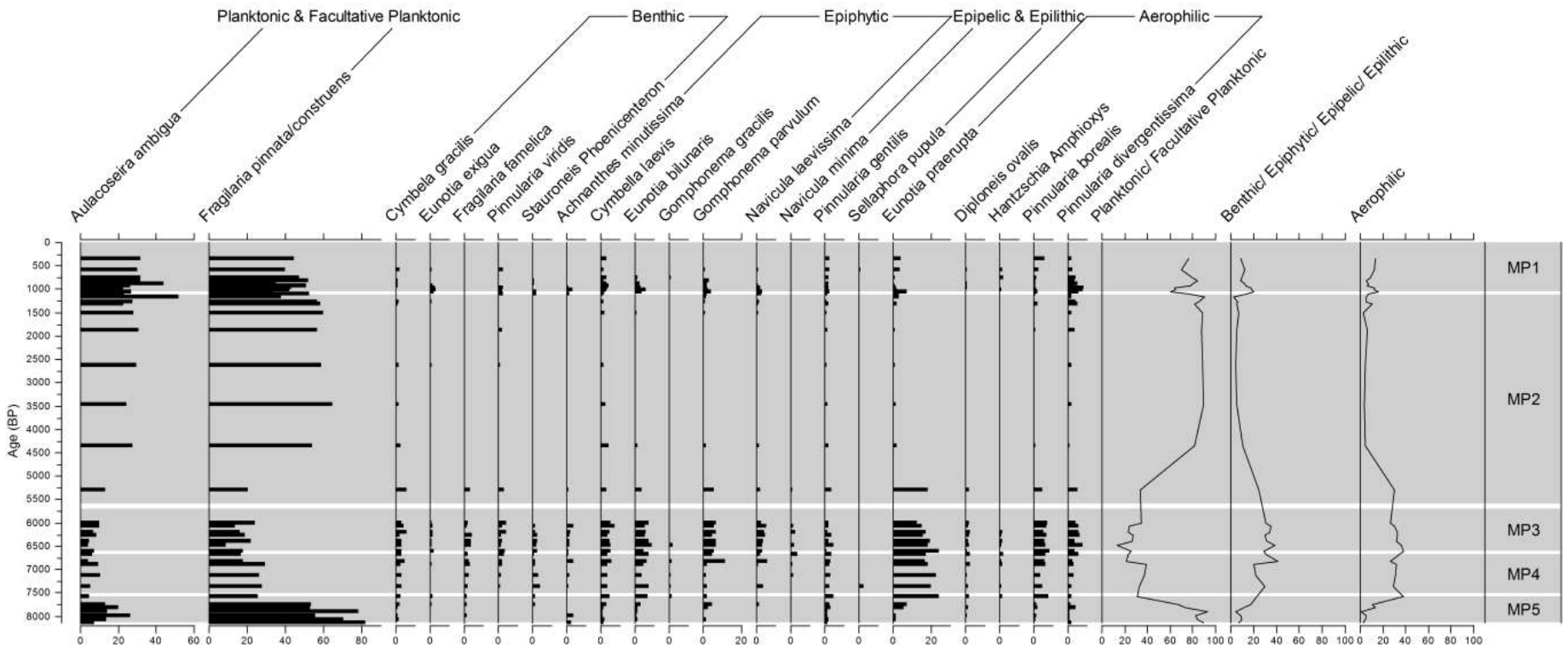


Figure 6.7: Diatom sequence from ~8,140 cal. BP - present at Mafadi Wetland, plotted against age, grouped according to habitat, and zoned according to the CONISS output for pollen at Mafadi Wetland.

It is also of interest to explore the extent to which the diatoms in each of the wetlands were influenced by the plants surrounding the wetland, and from the broader region (Lotter & Birks, 2003; Mackay et al., 2012). Redundancy analysis was therefore undertaken for the diatom counts, using pollen principal component sample scores to represent pollen as a single explanatory factor (Legendre & Birks, 2012b; Mackay et al., 2012). For Mafadi Wetland, an exceptionally high, statistically significant, 49.4% ($p>0.001$) of the diatom variation is explained by the pollen PC1 sample scores. For Sekhokong, a considerably lower, yet statistically significant, 13.3% ($p>0.0001$) of the variation in diatom composition is explained by the pollen principal component sample scores. Such analysis could not be undertaken in a robust and consistent manner for Sani Valley as the samples for pollen and diatom analysis were mutually exclusive, and hence no results are reported. The disparity in explanatory strength between the results from Mafadi Wetland and Sekhokong could reflect the size of the 'pollen catchment' at each site. At Mafadi Wetland, the bowl shaped topography of the area immediately surrounding the wetland, and its location between two of the highest summits in southern Africa, means that the pollen deposited in the wetland was probably predominantly from immediate surrounds (Grab, 1996a, 1999). Sekhokong, by contrast, is situated at the foot of a steep mountain slope in a long, wide valley, at a lower altitude (Marker, 1994; Grab & Deschamps, 2004). It is therefore more likely for the pollen deposited in this wetland to represent a considerably larger region of vegetation. If this is the case, a smaller proportion of the pollen would in turn have originated from the wetland itself, and so only a lower proportion of the pollen present would have the potential to explain the diatoms in the wetland. To further obscure the results, the contemporary wetland at Sekhokong, at 1.78km^2, is a larger than the Mafadi Wetland (0.6km^2), so diatoms with a range of micro-environments could be present in the profile.

6.2.3 Sediments

While many southern African palaeoenvironmental reconstructions have included in their methodology and results the determination of sediment particle size and the LOI calculations of the percentage composition, few use these data in their palaeoenvironmental interpretations (cf. Martin, 1968; Shi et al., 1998; Neumann et al., 2008, 2010, 2011; Gilson & Ekblom, 2009, Holmgren et al., 2012). There is consequently limited literature on which to base the interpretation of sedimentary properties in southern

Africa for palaeoenvironmental reconstruction. However, unlike biological proxies, such as pollen and diatoms, for which varied communities exists in an array of locations, the same selection of sedimentary properties – organic content, carbonate content and particle size distribution – exists in all sedimentary profiles, and thus it is only the relative changes of these which require interpretation (Heiri et al., 2001; Reinwarth et al., 2012). Fortunately, previous palaeoenvironmental work in Lesotho has relied strongly on sediment based climate inferences (cf. Van Zinderen Bakker, 1955; Van Zinderen Bakker & Werger, 1974; Marker, 1994, 1995, 1998; Grab et al., 2005), and hence location specific inferences can be made here. The characteristics of variation in sediment properties, from which climatic and environmental inference can be made, have been outlined in the *Introductory Chapter* (*Section 1.2.2*) and the *Methods Chapter* (*Section 4.4.2*). A summary of the interpretation of these properties, highlighting the inferences which can be made from them, is presented.

The percentage organic content and percentage carbonate content for each sample were determined using LOI, and the results presented reflect changes in both of these variables over time at all three sites (*Sections 5.2.2, 5.3.2, 5.4.2*). While many studies determine the organic content of sediments using LOI the results are often used only in matching dates for adjacent cores for which different tests are undertaken, rather than to make environmental inferences from the organic content itself (cf. Neumann et al., 2008; Norström et al., 2009). Organic content of the sediment sample is, however, of climatic and environmental interest, although in many cases the signal is difficult to interpret (Heiri et al., 2001; Battarbee et al., 2002; Baker et al., 2014). For wetlands, including those in the eastern Lesotho highlands, the significant peat content implies that the organic content of the sediment record is inherently linked to the conditions which favour the formation of peat, and the vegetation production required (Van Zinderen Bakker & Werger, 1974; Marker, 1994; Irving & Meadows, 1997; Baker et al., 2014). For much of the Northern Hemisphere, peatlands are located in cool climates, where depressed temperatures slow down microbial decomposition and allow peat to accumulate (Baker et al., 2014). In much of southern Africa, it is often conditions of warm temperatures, paired with higher precipitation, which encourage peat development through high rates of primary production exceeding the elevated decomposition rate (Baker et al., 2014). The eastern Lesotho highlands comprise a large network of peat mires as the environment is particularly conducive to peat production,

given relatively high precipitation levels facilitating primary production, but cool temperatures depressing rates of microbial decay (Van Zinderen Bakker & Werger, 1974; Baker et al., 2014). With moisture presenting the limiting factor in southern Africa, peat formation is consequently predominantly driven by periods of greater moisture (Meadows, 1988; Marker, 1994; Baker et al., 2014). The alpine environment of eastern Lesotho restricts plant growth increasingly with altitude due to the associated low temperatures, and thus locations with slightly warmer conditions will experience more rapid peat accumulation due to the raised primary production (Van Zinderen Bakker & Werger, 1974; Schwabe, 1995). It should be noted that the eastern Lesotho peat mires are markedly different from those in the Northern Hemisphere, due to their flora of sedges rather than *Sphagnum* moss (Schwabe, 1995). Cyperaceae is notably more sensitive to changes in moisture level than *Sphagnum*, further emphasising the relationship between moisture levels, peat development and the organic content of sediments (Gorham, 1957; Schwabe, 1995). Furthermore, the extent to which the Cyperaceae pollen curve tracks the organic sediment content curves for all three sites, is explained.

The percentage composition of carbonates in the sediment samples, and the change throughout the sediment profile, is less well understood from a climatic perspective. This is in part because a range of environmental conditions can facilitate carbonate accumulation, but more as this relies on the surrounding rock and sediment composition (Milliman et al., 2012). Rather, changes in the carbonate content of the sediments can play a role in controlling the potential plant and diatom communities, through influencing the pH and conductivity of water and soil (Battarbee et al., 2002).

The particle size distribution of each sediment sample, and the associated relative composition of particles within the size categories of gravel, sand, silt and clay, relates to the transport and depositional environment (Briggs, 1977). The interpretation is thus specific to an environment, and the relative variations in the transportational energy between various systems (Masselink et al., 2014). Based on existing interpretations for wetlands in the eastern Lesotho highlands, large particle sizes (sand and gravels) reflect drier periods, while smaller particle sizes are indicative of moist conditions, as they are dominant in the marshy wetlands with low transportational energy (Marker, 1994, 1998).

The fine green-grey clays at the base of the Sekhokong sequence (*Table 5.6*) are similar to those reported for the bottom layer of previously published sediment sequences in eastern Lesotho, argued to reflect shallow lacustrine conditions (Van Zinderen Bakker & Werger, 1978; Marker, 1994). The skewness and kurtosis of the particle size distribution for a sample can reflect the depositional environment for that period, and changes in these skewness-kurtosis relationships between samples can indicate changes in the depositional environment throughout the profile (Briggs et al., 1977; Masselink et al., 2014). However, these samples indicate a continual, low-energy depositional system, and do not indicate a change from the spring-fed wetland environment over time (*Appendix C.2*). In summary, a high percentage organic content, and high percentage composition of silt- and clay-sized particles are interpreted as reflecting a relatively moist environment. A higher percentage composition of gravel- and sand-sized particles by contrast represents periods of drier climate, with a greater proportion of weathered detritus, from more exposed regoliths under conditions of lower vegetation, easily transported into the wetland. The sediment results are re-plotted against age, with zones delineated by the CONISS output for the pollen results for each site (*Figures 6.8, 6.9, 6.10*).

The profile from Sekhokong has a larger range in particle size, and a greater mean particle size for many samples (*Figure 6.9*). There is also considerably faster accumulation at Sekhokong (20yr.cm^{-1}) than at Sani Valley (40yr.cm^{-1}) and Mafadi Wetland (100yr.cm^{-1}). This is largely due to the greater colluvial input at Sekhokong, due to the microtopographical setting. Whereas the Mafadi Wetland is situated at the bottom of a bowl shaped depression formed within gentle slopes and the Sani Valley site at the centre of a wide valley floor, the Sekhokong site is located at the foot of a steep slope of a mountain range. Similar mountains surround the Sani Valley site, but due to the greater distance from the slopes, the wetland does not derive much sediment input from the slopes. For all three sites, and particularly at Sekhokong, the colluvial input will increase during drier periods, as drought will result in the removal of vegetation off the slopes which would otherwise stabilise the sand and gravel particles. The lower organic content in sediments from the majority of samples throughout the Sekhokong profile in comparison to Mafadi Wetland and Sani Valley further confirms the colluvial input at this site.

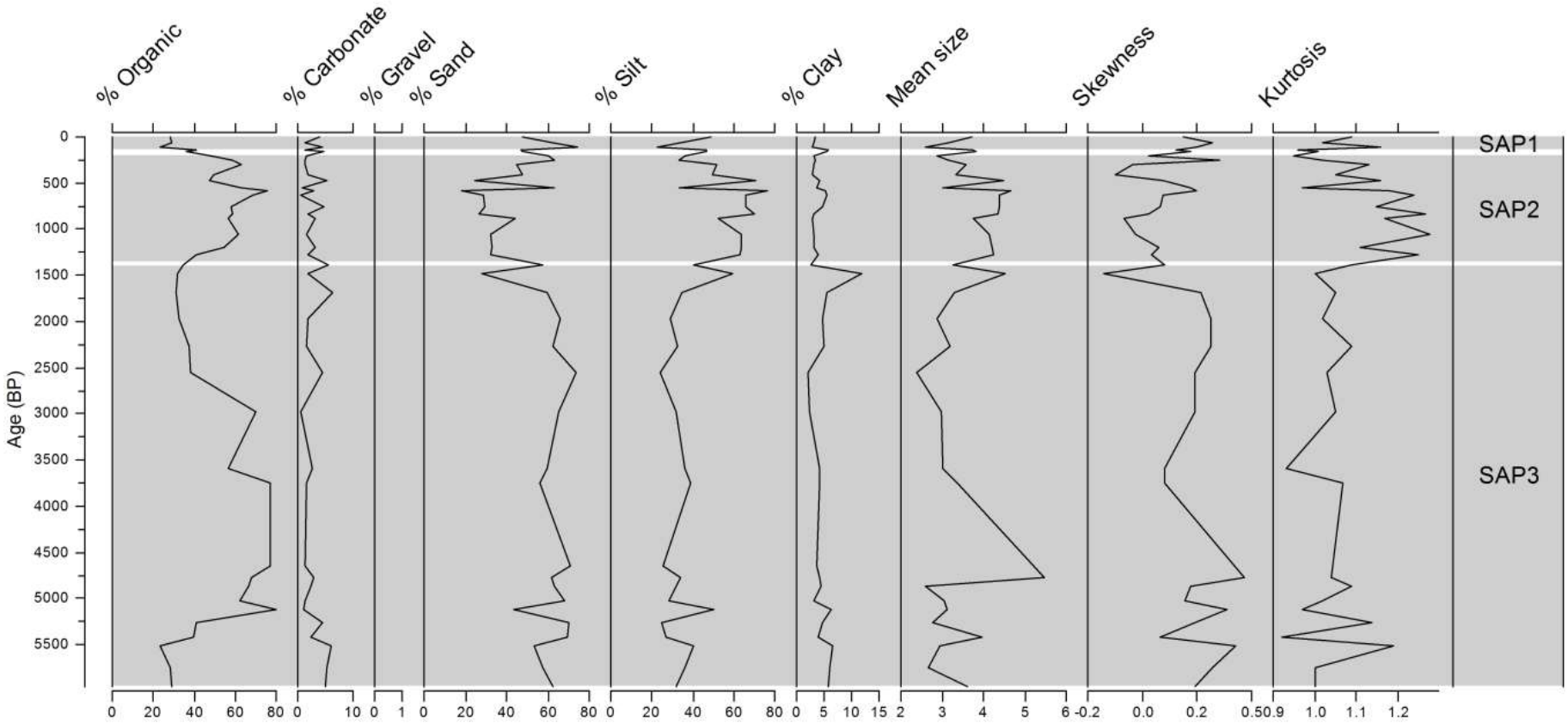


Figure 6.8: Changes in sediment properties from ~6,000 cal. BP - present at Sani Valley, plotted against age and zoned according to the CONISS output for Sani Valley pollen.

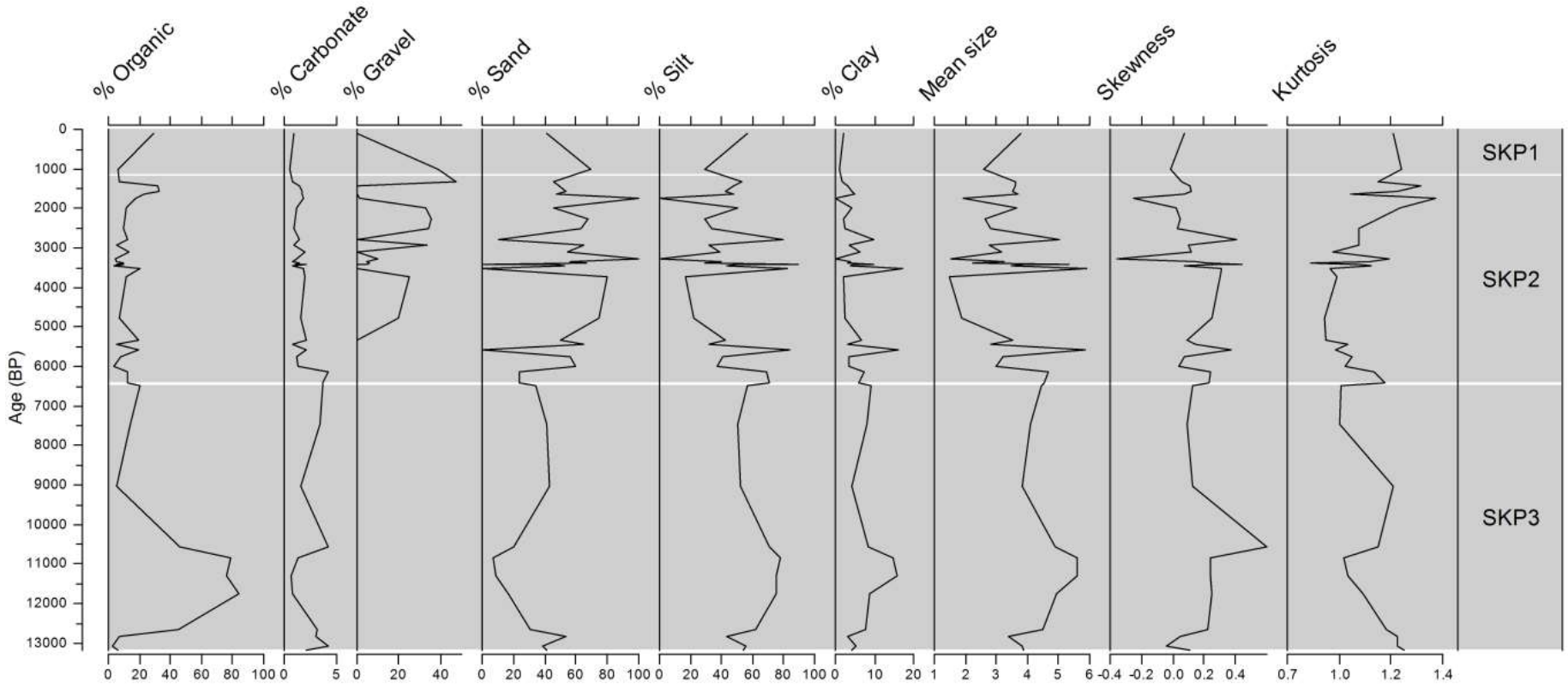


Figure 6.9: Changes in sediment properties from ~13,200 cal. BP - present at Sekhokong, plotted against age and zoned according to the CONISS output for Sekhokong pollen.

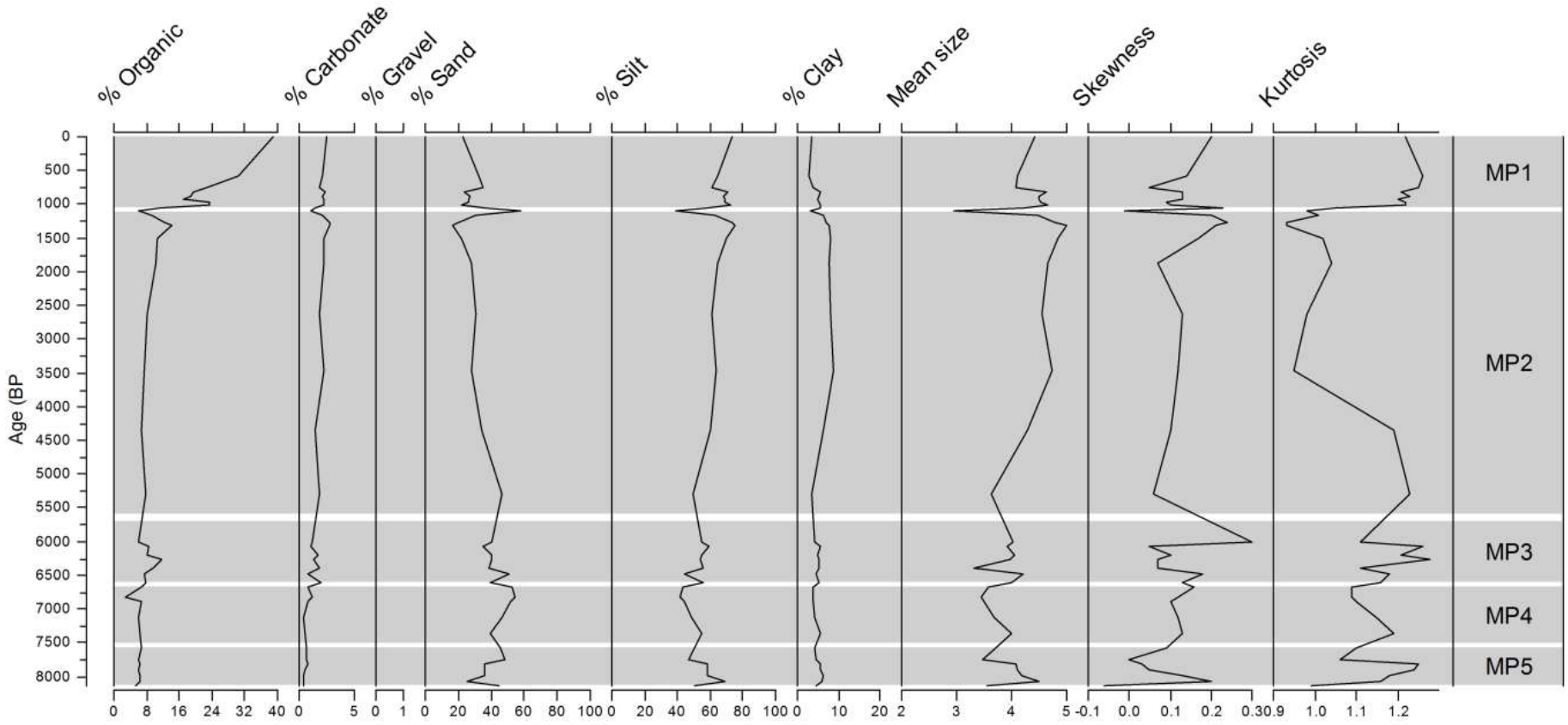


Figure 6.10: Changes in sediment properties from ~8,140 cal. BP - present at Mafadi Wetland, plotted against age and zoned according to the CONISS output for Mafadi Wetland pollen.

The differences in sediment rates are influenced to a smaller extent by the altitude and associated temperature differences between the sites. As all three sediment profiles have a high mean percentage of organic content, comprising both peat and organic clays (*Figures 6.8-6.10*), the vegetation density, and the rate of vegetation deposition and decomposition, play a role in the accumulation of sediment (Van Zinderen Bakker & Werger, 1974; Schwabe, 1995). The particularly slow sediment accumulation rates at Mafadi Wetland, in comparison to those at Sekhokong and Sani Valley, may be explained by the cooler temperatures which result in sparser vegetation cover, smaller plants, and slower peat formation (Schwabe, 1995; Baker et al., 2014). The greater mean organic content of the sediments from Sani Valley, in comparison to Mafadi Wetland, further confirm this interpretation.

6.3 Palaeoenvironmental Reconstructions

Presented in this section are the palaeoenvironmental and palaeoclimatic reconstructions for each of the three study sites: Sani Valley, Sekhokong and Mafadi Wetland. These reconstructions are made on the basis of collective evidence from the pollen, diatom and sediment results, relying on interpretations outlined in *Section 6.2*. The time divisions used to structure *Sections 6.3.1*, *6.3.2* and *6.3.3.* are derived from the CONISS output for the pollen results from each site, making adjustments in cases where there are additional samples for which sediment information was obtained between two separating pollen samples. For all three sites, summary stratigraphic diagrams are presented, which provide evidence for dry periods based on dry tolerant pollen taxa, aerophilic diatoms, and the percentage composition of gravel- and sand-sized sediment particles, and evidence for wet periods from semi-aquatic pollen, planktonic and facultative planktonic diatoms, the percentage organic composition of the sediments, and the percentage composition of silt- and clay-sized particles in the sediment record (*Figures 6.11, 6.12, 6.13*). Inferences of cold periods are made on the basis of cumulative percentage composition of *Fragilaria* diatoms >50, >60 and >70%; inferences of warm periods are made on the basis of increased species diversity, reflecting samples in which >75% and >80% of the total number of pollen types represented in the profile appear.

6.3.1 SANI VALLEY

SAP3: ~6,200-1,400 cal. yr BP

Zone SAP3 commences with a wet period, dominated by Cyperaceae pollen, and *Fragilaria famelica* paired with a group of epiphytic diatoms, suggesting an extensive wetland area (*Figures 6.1, 6.5*). There is a low percentage organic content which persists until the end of this period, but the highest percentage of carbonates in the sediments for the profile appears in this period (*Figure 6.8*). This wet period was probably accompanied by warmer temperatures, indicated by the high species diversity reflected by the pollen record, and the appearance of *Olea* and *Podocarpus* pollen from trees that would have been able to grow farther upslope in the deep valleys of central Lesotho (*Figure 6.4*), increasing the probability of their pollen reaching eastern Lesotho. This warm and moist period could represent a weak signal for the terminal phase of the Holocene Altithermal, which due to the cold temperatures across the eastern Lesotho highlands would not have been sufficiently warm to exceed the thresholds of a broader group of less cold tolerant plants and diatoms to encourage their growth at these sites. This moist warm period is disrupted by an abrupt dry period from ~4,770-4,470 cal. yr BP, with a 20% decrease in Cyperaceae pollen and peaks in Asteraceae and Poaceae (with a slight Poaceae lag to the end of this period), suggesting a rapid reduction in the wetland area and an expansion of grassland (*Figure 6.1*). This event is accompanied by peaks in *Chrysocoma* and Cheno-Am pollen (*Figure 6.1*), both of which are drought resistant plants, indicating that this vegetation shift and reduction in the wetland size was driven by a reduction in precipitation. Due to the lower sampling frequency, there is no diatom information for this abrupt event.

A second more prolonged, and possibly wetter, moist period is established by ~4,460 cal. yr BP, with over 50% of the pollen sum comprising Cyperaceae pollen, a peak in the benthic/ facultative diatom species *Fragilaria famelica*, and the emergence of *Fragilaria pinnata/ construens* (*Figures 6.1, 6.5*). This would suggest an expansion of the wetland area, potentially comprising shallow surface water, and possibly forming pools or flarks (Backéus, 1989) in the centre of the wetland area. The presence of both snow-tolerant *Fragilaria famelica* and ice-tolerant *Fragilaria pinnata/ construens* would suggest that this was a cold, wet period. This is supported by the pollen record which reflects lower species diversity

than for the first wet period (*Figure 6.1*). The percentage organic content of sediments is high throughout this period, likely driven by the increase in moisture (*Figure 6.8*). The middle of the zone is marked by the appearance of *Podocarpus* pollen, coinciding with the lowest relative abundance of Poaceae pollen in the zone (*Figure 6.1*). With cold conditions inferred for this period, it is unlikely that *Podocarpus* forests would have moved upslope into the central Lesotho valleys, despite the wetter conditions. The inference of cold, moist conditions, the high Asteraceae: Poaceae ratio, and in particular the decrease in Poaceae pollen coinciding with the *Podocarpus* peak (*Figure 6.1*), rather suggests an increase in the strength of the westerly belt, which would increase the strength of the westerly wind regime across Lesotho and increase the probability of tree pollen being transported from the forests in the western Lesotho lowlands.

At ~2,260 cal. yr BP an abrupt termination of the wet period occurs, indicated by a sudden decline in Cyperaceae, the emergence of greater percentages of succulent *Crassula* and drought tolerant Cheno-Am, and by a peak in Asteraceae and Poaceae (*Figure 6.1*). The diatom record reflects a shift from facultative planktonic and benthic species to epipelic and epilithic, and dominant aerophilic species, supporting an inference of a termination of the wet period (*Figure 6.5*). This is interpreted as a substantial reduction in the wetland area, and a drying within the remaining portion of wetland, to only surface moisture. This is paired with a large increase in the proportion of the area covered by grassland, with the Asteraceae: Poaceae record indicating a shift to summer rainfall dynamics. This dry period persists to the end of the zone.

SAP2: ~1,350-200 cal. yr BP

Zone SAP2 commences with a re-emergence of wet conditions, with peaks in Cyperaceae and facultative planktonic, benthic and epiphytic diatoms, and with a large percentage composition of organic material (*Figures 6.1, 6.5, 6.8*). This suggests the re-emergence of wetland conditions, and the re-introduction of shallow surface water, possibly associated with warmer temperatures. Notable is the anomalous peak in succulent *Crassula* pollen (*Figure 6.1*), which could reflect an increase in evaporation paired with the higher precipitation during the period, and possibly associated with large areas of surface water

exposed to evaporation. The zone reflects an overall decrease in moisture over the time period, with decreases in Cyperaceae pollen, benthic/facultative planktonic *Fragilaria famelica* and epiphytic *Cymbella laevis* (*Figures 6.1, 6.5*). This is paired with an increase in Asteraceae, Cheno-Am, *Crassula* and re-emergence of the aerophilic diatom group, suggesting a progressive drying of the wetland, supporting the shift to grassland conditions (*Figures 6.1, 6.5*). This drying period is, however, marked by large fluctuations in the pollen record, and even greater fluctuations in sediment particle size, indicating high frequency fluctuations in precipitation, with markedly wet periods from ~1,350-1,150 cal. yr BP, ~840-550 cal. yr BP and at ~304 cal. yr BP (*Figures 6.1, 6.8*).

SAP1: ~160 cal. yr BP – Present

Zone SAP1 commences with a peak in *Fragilaria pinnata/ construens* at ~160 cal. yr BP (*Figure 6.5*). This species is dominant throughout the Mafadi Wetland sequence, and at the commencement of the Sekhokong record, and is indicative of very cold conditions, is common in the east African high alpine lakes, and most notably is tolerant of prolonged ice (Ohlendorf et al., 2000; McGlynn et al., 2010; Wang et al., 2013). This is inferred as a marked cold period, which presents evidence for a Little Ice Age event in eastern Lesotho. Associated with this cold period is a peak in the otherwise decreasing percentage organic content paired with a peak in Cyperaceae, and decrease in Poaceae and Asteraceae (*Figure 6.1*), suggesting wetter conditions for this event. This is simultaneous with an increase in epiphytic species, notably emergence of *Achnanthes minutissima* (*Figure 6.5*), suggesting that the wetland was dominated by a large population of macrophytes, supported by the wetter climatic conditions. Notably, this event is also coincident with an increase in the Asteraceae: Poaceae ratio to >0.5 (*Figure 6.1*), indicating a weakening of the summer rainfall pattern, and a shift in the westerly belt. This would suggest that this was a cold, wet period, with an increase in the strength and influence of the westerly belt (Mills et al., 2012). The appearance of *Pinus*, *Podocarpus* and *Olea* pollen during this period (*Figure 6.1*) may have resulted from the preceding Medieval Warm Period (AD <1300), as these trees would have required time to establish in the higher altitude central Lesotho valleys, and similarly would not have disappeared immediately at the onset of the cold event. However, the increase in the westerlies would increase the strength of the westerly wind regime, facilitating the

transport of tree pollen from the western Lesotho lowlands. The coinciding pollen from all three tree types, and with the greatest proportion of tree pollen in the sequence, may suggest the combination of these two climatic drivers.

A progressive increase in moisture, indicated by an increasing proportion of Cyperaceae pollen, and a decrease in Asteraceae and Poaceae (*Figure 6.1*), is responsible for the continued expansion of the wetland to its contemporary spatial extent. This is paired with an increase in the sediment proportion of silt, and a slight increase in the percentage organic content after it had reached its minimum, further providing evidence for an increase in wetland extent. This period is marked by an increase in the species diversity of the pollen record (*Figure 6.1*), which reflects warming after the cold period contemporary with the Little Ice Age. There is also evidence from the diatom record that may suggest human influence on the local environment as the region became utilised for the grazing of sheep, goats and cattle (Grab & Deschamps, 2004; Showers, 2005). While there is only one diatom sample for this zone, dominated by the *Fragilaria pinnata/ construens* group which was used to infer the cold period synchronous with the Little Ice Age event, the autecologies of the remaining diatoms from this sample are of interest, relating to the abrupt change in PC1 scores (*Figure 5.11*). These diatoms indicate a shift from pH neutral and acidophilous species which dominate the rest of the profile, to alkalophilous species in this zone (*Figure 6.5*). This is paired with a peak in pollution tolerant species (*Table 6.1*). Evidence of domestic livestock in the Lesotho highlands was detected by 1,070 cal. yr BP in the Likoaeng record (Parker et al., 2011), while historical records suggest the introduction of sheep and goats into the high mountains by AD ~1890 (Van Zinderen Bakker, 1981; Grab & Deschamps, 2004; Showers, 2005), so by this time it is likely that there was a large population of sheep, at least on a seasonal basis, contributing organic pollution, and changing the water quality at the site. Evidence of human disturbance outside of the site is presented with the introduction of *Pinus* pollen, indicating the increased extent of the forestry industry in KwaZulu-Natal (Turner & Plater, 2004). The summary stratigraphic diagram indicating dry and wet indicators, and inferences of cold and warm conditions is presented in *Figure 6.11*.

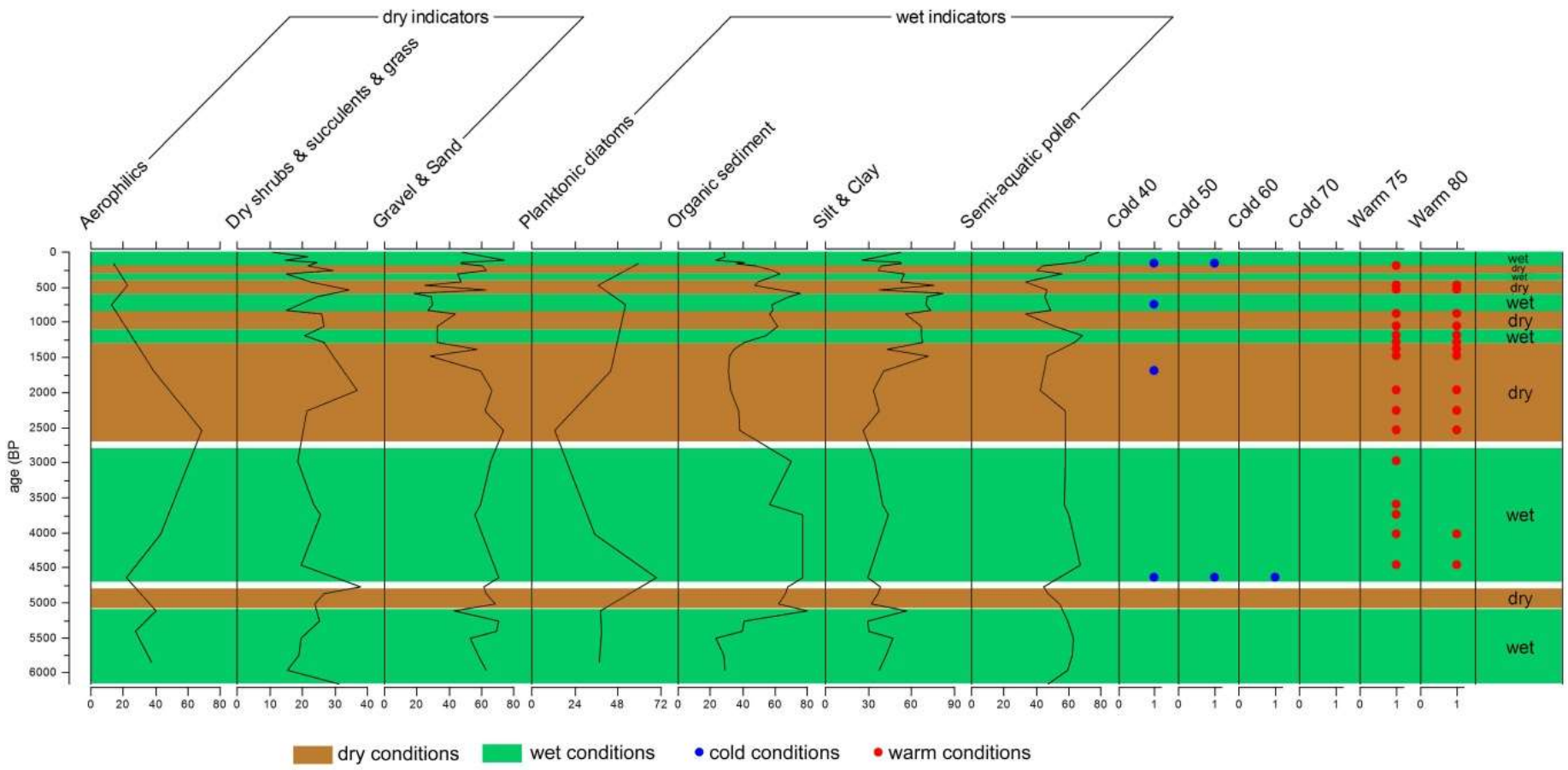


Figure 6.11: Summary diagram indicating the wetter and drier, and extreme cold and warmer periods at Sani Valley from ~6,000 cal. yr BP - present, indicated by the pollen, diatom and sediment records. Cold 40, 50, 60, 70 refer to the index of percentage composition of Fragilaria diatom species; warm 75, 80 refer to the percentage species richness for pollen.

6.3.2 SEKHOKONG

The CONISS output for Sekhokong produced comparatively few statistically significant zones, given the long time period covered, and considerable variation in pollen within each zone. This variation is heightened when comparing the diatom and sediment results. Sekhokong reflected low explanatory strength of pollen in explaining the diatom composition (*Section 6.2.2*), indicating the likelihood of a large region from which at least some of the pollen is derived. At a more local scale, however, Cyperaceae pollen tracks the percentage organic content of sediments closely. The ratio of Asteraceae: Poaceae pollen is particularly low throughout the profile, which by Norström et al.'s (2009) interpretation would indicate a summer rainfall regime throughout much of the past 13,200 cal. yr, appears not to reflect the higher resolution microclimatic pulses in the strength of the westerly belt that were identified for Sani Valley, potentially due to the differences in depositional environment.

SKP3: ~13,180-6,470 cal. yr BP

Zone SKP3 commences with a wet period, with the highest relative abundances of Cyperaceae pollen and the planktonic diatom species *Aulacoseira ambigua* for the profile. This period also comprises large proportions of the facultative planktonic *Fragilaria pinnata/ construens*, and Poaceae pollen (*Figures 6.2, 6.6*). This is indicative of a large wetland expanse, with at least ponds of shallow water, if standing water did not dominate the whole wetland. This wet period is followed immediately by a short-lived, but very dry, period from ~13,080-12,830 cal. yr BP, with a decrease in moisture represented by a drop in the relative abundance of planktonic diatoms, the proportion of Cyperaceae pollen, and the percentage organic content of sediments (*Figures 6.2, 6.6, 6.9*). Dry conditions are reflected by a peak in sand sized particles, in Poaceae pollen and in aerophilic diatoms (*Figures 6.2, 6.6, 6.9*). This suggests a rapid drying of the wetland, decreasing its spatial extent, replaced by the grassland conditions which dominate the broader landscape at present.

A return to wet conditions then occurs, and persists from ~12,660-10,850 cal. yr BP, with a marked dominance of Cyperaceae pollen, a peak in organic content, and a large proportion of planktonic diatoms relative to the remainder of the sequence (*Figures 6.2, 6.6, 6.9*). The

diatom record is dominated by epiphytic species during this period, indicating a large presence of macrophytes in the wetland (*Figure 6.6*). The percentage carbonate content is particularly low throughout the period, although the interpretation of this is unclear (*Figure 6.9*). Together, these proxies suggest a re-establishment of the size of the wetland to that of the beginning of the zone, but with shallow water restricted to small ponds, and the establishment of macrophytes, with herbs along the drier wetland edge. The zone commences with a peak in *Fragilaria* species (>40% of the pollen sum), tentatively indicating an abrupt period of cold conditions (*Figure 6.6*). This event coincides temporally with the Younger Dryas event (Abell & Plug, 2000). However, it seems not to have been a very cold event, as a broader range of diatom species remain present, and there is the continued presence of a range of plant pollen.

By ~10,550 cal. yr BP the relative abundance of Cyperaceae pollen had decreased to 15%, coinciding with a decrease in Asteraceae pollen and a peak in Poaceae pollen (*Figure 6.2*). This is simultaneous with a peak in aerophilic diatoms, and an abrupt rise in the percentage composition of sand-sized particles and an increase in the percentage composition of carbonates, but a decrease in the percentage composition of organic matter (*Figures 6.6, 6.9*). This indicates a sudden drying of the site, a disappearance of standing surface water and decreasing spatial extent of the wetland. The percentage organic composition of the sediments decreases more slowly, suggesting a rapid change from wetland to grassland species to maintain the organic input in the sediments (*Figure 6.9*). The low Asteraceae: Poaceae pollen ratio (*Figure 6.2*) could indicate warmer conditions associated with a further weakening in the westerlies, which would further increase the rate of peat production. Thereafter, a progressive increase in the relative abundance of Cyperaceae and Asteraceae pollen occurs, paired with a more pronounced decrease in Poaceae pollen which persists throughout the remainder of the profile (*Figure 6.2*). This is concurrent with a low relative abundance of planktonic diatoms, but large proportions of epiphytic species. This proxy evidence suggests that the region was slowly warming throughout this period, with surface conditions supporting macrophytes rather than deep standing water. The warmest period was likely at ~7,460 cal. yr BP, indicated by greatest pollen taxa diversity (*Figure 6.2*), which perhaps signals the middle, and warmest period, of the Holocene Altithermal (Neumann et al., 2014).

SKP2: ~6,420-1,200 cal. yr BP

Zone SKP2 is marked by variation in both precipitation and temperature. The onset of zone SKP2 is marked by an abrupt change in the pollen, diatom and sediment record (*Figures 6.2, 6.6, 6.9*). The gradual increase in Asteraceae and Cyperaceae pollen which comprised the terminal period of zone SKP3 is reversed by a sudden decrease, while Poaceae pollen rapidly increases (*Figure 6.2*). This is paired with the abrupt emergence of *Fragilaria famelica*, and of the group of aerophilic diatom species (*Figure 6.6*). The pollen and diatom composition would suggest a sudden extreme drying of the wetland, with establishment of grassland in its place, potentially during a period of comparatively colder temperatures than those immediately preceding it. This is followed by an increase in Cyperaceae pollen and decrease in Poaceae until ~5,450 cal. yr BP (*Figure 6.2*), indicating progressively wet conditions, at which point there is a peak in *Fragilaria* diatoms (*Figure 6.6*), indicating a second pulse of particularly cold conditions. A dry period follows, dominated by grassland conditions, which persists until ~3,700 cal. yr BP (*Figure 6.2*). The presence of consistent proportions of drought tolerant *Crassula*, Aizoaceae, Cheno-am, Apiaceae and *Anthospermum* pollen further indicates dry conditions, while the increase in species diversity suggests warmer temperatures (*Figure 6.2*).

The second half of the zone, from ~3,650-1,200 cal. yr BP, is marked by continuous fluctuations in the relative abundance of Poaceae, Cyperaceae and Asteraceae pollen, and in the ratios of planktonic, benthic and aerophilic diatoms (*Figures 6.2, 6.6*). Pronounced changes in the particle size distributions of sediments in each sample mark clearly defined sedimentary lenses (*Figure 6.9*), which were observed *in situ* during fieldwork (*Figure 3.13*). This period is characterised by the emergence and maintenance of *Fragilaria* species, indicating persistently cooler conditions throughout the zone (*Figure 6.6*). The pollen and sediment record, and changes in the ratios of aerophilic to planktonic diatom species (*Figures 6.2, 6.6, 6.9*), indicate rapid fluctuations in precipitation throughout the zone, which would have resulted in large variations in moisture availability, the amount of standing water in the wetland, and the size of the wetland. Wet phases, with greater wetland size and surface water depth, are indicated by peaks in benthic diatoms and Cyperaceae pollen

at ~3,430 cal. yr BP, ~3,350-3,270 cal. yr BP and ~3,106 cal. yr BP, and dry phases with smaller wetland extent and drier wetland surface indicated by increases in aerophilic diatoms, pollen from drought resistant plants and peaks in the percentage composition of gravel- and sand-sized sediment particles at ~3,400 cal. yr BP, ~2,785 cal. yr BP and ~1,550 cal. yr BP (*Figure 6.12*). A prolonged wet event is indicated from ~2,780-1,750 cal. yr BP, inferred from a peak in the benthic diatoms *Fragilaria famelica* and *Eunotia bilunaris*, and a high percentage composition of organic material in the sediment record (*Figures 6.6, 6.9*). This is followed by a very dry event, with a peak in aerophilic diatoms and highest relative abundance of Poaceae pollen in the sequence, which persists to the end of the zone (*Figures 6.2, 6.6*).

SKP1: ~1,150 cal. yr BP - Present

Zone SKP1 comprises only two samples, representing the period from ~1,150 cal. yr BP to present. The resolution of these samples prevents detailed climatic or environmental inferences for the individual samples. This zone is marked by an increase in the percentage organic composition of the sediment, an increase in the percentage of silt-sized particles, and an increase in the Asteraceae: Poaceae pollen ratio (*Figures 6.2, 6.9*), suggesting a shift to wetter, less seasonal and cooler conditions, with a strengthening of the westerly wind regime. The diatom record reflects a peak in *Fragilaria famelica* (*Figure 6.6*), the snow-tolerant diatom taxa, and of aerophilic species at the end of the sequence, indicating cold conditions. This may represent the same cold event detected in the Sani Valley sequence, coincident with the Little Ice Age (Tyson et al., 2000), but the date for this sample is inferred with a relatively high uncertainty (ca. last 100-200 years), and thus this cannot be confirmed. The termination of the zone is characterised by an increase in Asteraceae pollen, a decrease in Poaceae, and stable but low proportions of Cyperaceae (*Figure 6.2*). This is paired with a notably high relative abundance of *Crassula* pollen, and continued increases in *Crassula* and *Pentzia* pollen, which together with an increase in aerophilic diatoms would suggest a period of considerable drying to present conditions (*Figures 6.2, 6.6*). The abundance of *Crassula* pollen may also be indicative of human and animal disturbance of the wetland (Norström et al., 2009). The summary stratigraphic diagram indicating wet and dry, and warm and cold periods is presented in *Figure 6.12*.

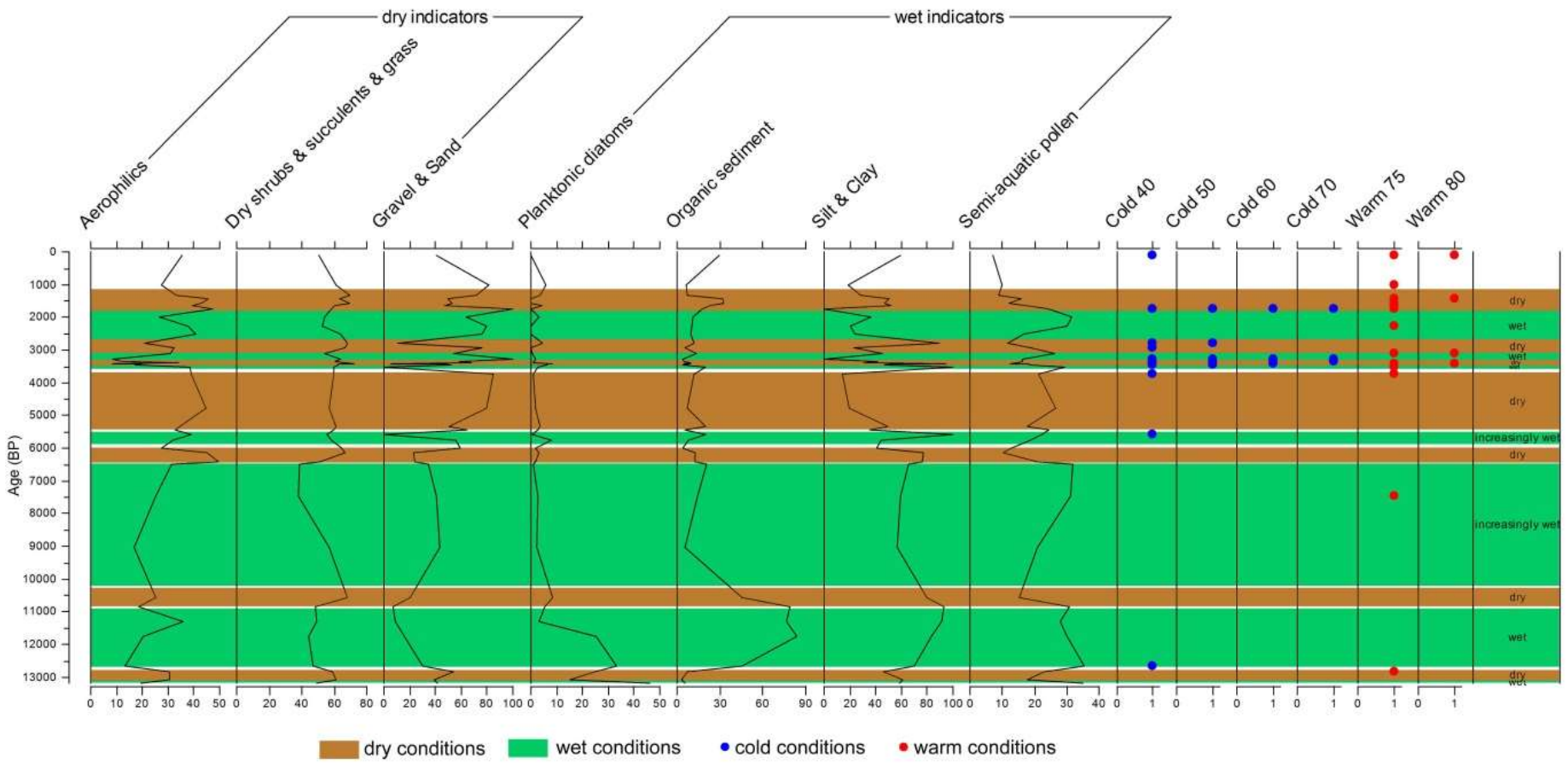


Figure 6.12: Summary diagram indicating the wet and dry, and cold and warm periods at Sekhokong from ~13,180 cal. yr - present, indicated by the pollen, diatom and sediment records. Cold 40, 50, 60, 70 refer to the index of percentage composition of Fragilaria diatom species; warm 75, 80 refer to the percentage species richness for pollen.

6.3.3 MAFADI WETLAND

The zones based on the CONISS analysis on the pollen results coincide with changes across all three of the proxies, indicating more clearly defined climate and environmental shifts at Mafadi Wetland than at the lower altitude sites. This suggests more clearly segregated environmental events than for the other two sites. The similarity in the timing of sudden shifts in each of the proxies may also be due to the high percentage of the diatom record explained by changes in the pollen PC1 curve for the site. All three proxies appear to reflect local conditions within the wetland. It is also notable that there is a significantly limited diversity of pollen and diatoms at Mafadi Wetland, compared to the lower altitude sites. This is likely due to the colder temperatures at this site, which few plants and diatoms can tolerate. At present, grasses and small shrubs cease mid-way up the slope between the wetland and Mafadi Summit (at ~3,380 m.asl), indicating that the site is located in close proximity to the terminal altitude for plant cover in eastern Lesotho (Grab, 1996a, 1999).

MP5: ~8,140-7,580 cal. yr BP

Zone MP5 is marked by a complete absence of pollen (*Figure 6.3*). The prolonged sterile pollen record suggests an absence of plants from this high altitude site. If this does reflect an absence of plants at Mafadi Wetland during this period, it would imply conditions either too dry or too cold to support plant life. Alternatively, an absence of pollen could indicate conditions which would compromise the preservation of pollen grains. For many other lower-altitude sites, the dissolution of pollen grains would be the common inference (cf. Gasse & Van Campo, 1998; Grab et al., 2005; Metwally et al., 2014). At Mafadi Wetland, the termination of vegetation cover occurs between the wetland and Mafadi Summit, thus already close to the terminal altitude for plant cover, indicating that an absence of plants in the region would not require a large change in the climate or environment (Grab, 1999). Furthermore, as the pollen likely reflects the plant communities within the immediate surrounds of the wetland, any changes in the altitudinal limits of plant growth would result in an absence of pollen in the profile. The diatom composition almost entirely comprises planktonic *Aulacoseira ambigua,* and facultative planktonic *Fragilaria pinnata/ construens* (*Figure 6.7*). The habitat of these species suggests the presence of shallow standing water (*Table 6.1*), which does not support an inference of conditions too dry to support plants.

Fragilaria pinnata/ construens are common in alpine lakes of east Africa, and survive under conditions of substantial ice cover and cold water temperatures (Schmidt et al., 2004; Ohlendorf et al., 2000; Wang et al., 2013). The diatom composition does not suggest pH conditions markedly different from the remainder of the core, and thus it is unlikely that the pollen was dissolved. It is thus inferred that this was a cold, but wet period, with temperatures too low to sustain plant life, resulting in a shift in plant communities down-slope. The percentage composition of carbonates and organic material in the sediments is low during this period (*Figure 6.10*), possibly a result of the lower temperatures decreasing productivity. The large percentage of silt-sized particles further confirms wetland presence in this zone (*Figure 6.10*). The very cold period at the beginning of this zone, marked by the highest percentage of *Fragilaria* diatom species in the sequence (*Figure 6.7*), is approximately coincident with the relatively short-lived '8.2 kyr' cold event (Mayewski et al., 2004; Alley & Ágústsdóttir, 2005; Chase et al., 2015b).

MP4: ~7,520-6,680 cal. yr BP

Pollen emerges at the commencement of this zone, with the pollen record dominated by Cyperaceae, suggesting at least localised wet patches (*Figure 6.3*). This is concurrent with a peak in Cheno-Am, Acanthaceae, *Crassula* and Aizoaceae, with the relatively high percentages of Poaceae and Asteraceae, suggesting warmer and drier conditions than in the preceding zone (*Figure 6.3*). This inference is supported by a decrease in the relative abundance of *Aulacoseira ambigua* and *Fragilaria pinnata/ construens* as the zone commences, replaced by an increase in aerophilic diatoms (*Eunotia praerupta, Pinnularia borealis* and *Pinnularia divergentissima, Figure 6.7*). The decrease in *Fragilaria* species further supports the pollen-based inference of warming during this period. This warming may reflect the Holocene Altithermal, but similar to the Sani Valley and Sekhokong record, this signal is weak as warming appears to have been insufficient to encourage a considerable up-slope shift in plant communities. The beginning of the zone is marked by an Asteraceae: Poaceae ratio of >0.5, suggesting weaker rainfall seasonality and a strengthening of the westerlies, but shifts to <0.5 for the remainder of the profile indicating the re-establishment of summer rainfall (*Figure 6.3*). This shift is concurrent with a sudden decrease in Cyperaceae and Asteraceae, a decrease in the percentage organic content of the

soil, and with an increase in the percentage of sand-sized sediment particles (*Figures 6.3, 6.10*). Paired with a second abrupt decrease in the proportion of planktonic and facultative planktonic diatoms, this is indicative of a dry period (*Figure 6.7*). The sustained population of planktonic *Aulacoseira ambigua* (*Figure 6.7*), however, suggests the continued presence of at least discrete ponds of surface water during this dry period.

MP3: ~6,610-5,700 cal. yr BP

Zone MP3 is marked by variations in the composition of pollen, diatoms and sediments throughout this time period (*Figures 6.3, 6.7, 6.10*). There is a larger proportion of epiphytic diatoms, which remains relatively constant throughout the zone (*Figure 6.7*), indicating more moist wetland conditions than in the previous zone, with a large macrophyte presence. The proportion of benthic and planktonic, relative to aerophilic, diatoms fluctuates throughout the zone (*Figure 6.7*), indicating distinct wet and dry pulses, resulting in changes from periods in which the wetland comprises shallow standing water (at least in ponds or flarks) to a drier wetland surface. The pollen record is characterised by fluctuations in Cyperaceae, Poaceae, Asteraceae, *Pentzia* and *Crassula* throughout, but with an overall increase in the relative abundance of Poaceae and decrease in the percentage of Asteraceae pollen (*Figure 6.3*). This indicates progressive drying, and the change in the Asteraceae: Poaceae ratio suggests an increase in precipitation seasonality. The period of slower accumulation commences at ~6,000 cal. yr BP and persists to the end of this zone, resulting in a lower temporal frequency of samples (as they were sampled at consistent depth). There is a peak in the percentage organic composition of sediments in the middle of this period, with the concurrent peak in Cyperaceae pollen indicating a discrete wet period, during an otherwise dry phase (*Figures 6.3, 6.10*). From a temperature perspective, there appears to have been a continuation of the warm conditions from the previous zone, further suggesting that this may represent the Holocene Altithermal. However, the inference of warmer conditions is made on the basis of a decrease in ice-tolerant diatom taxa and an increase in pollen species diversity, and consequently reflects a less cold event, rather than an objectively warm event.

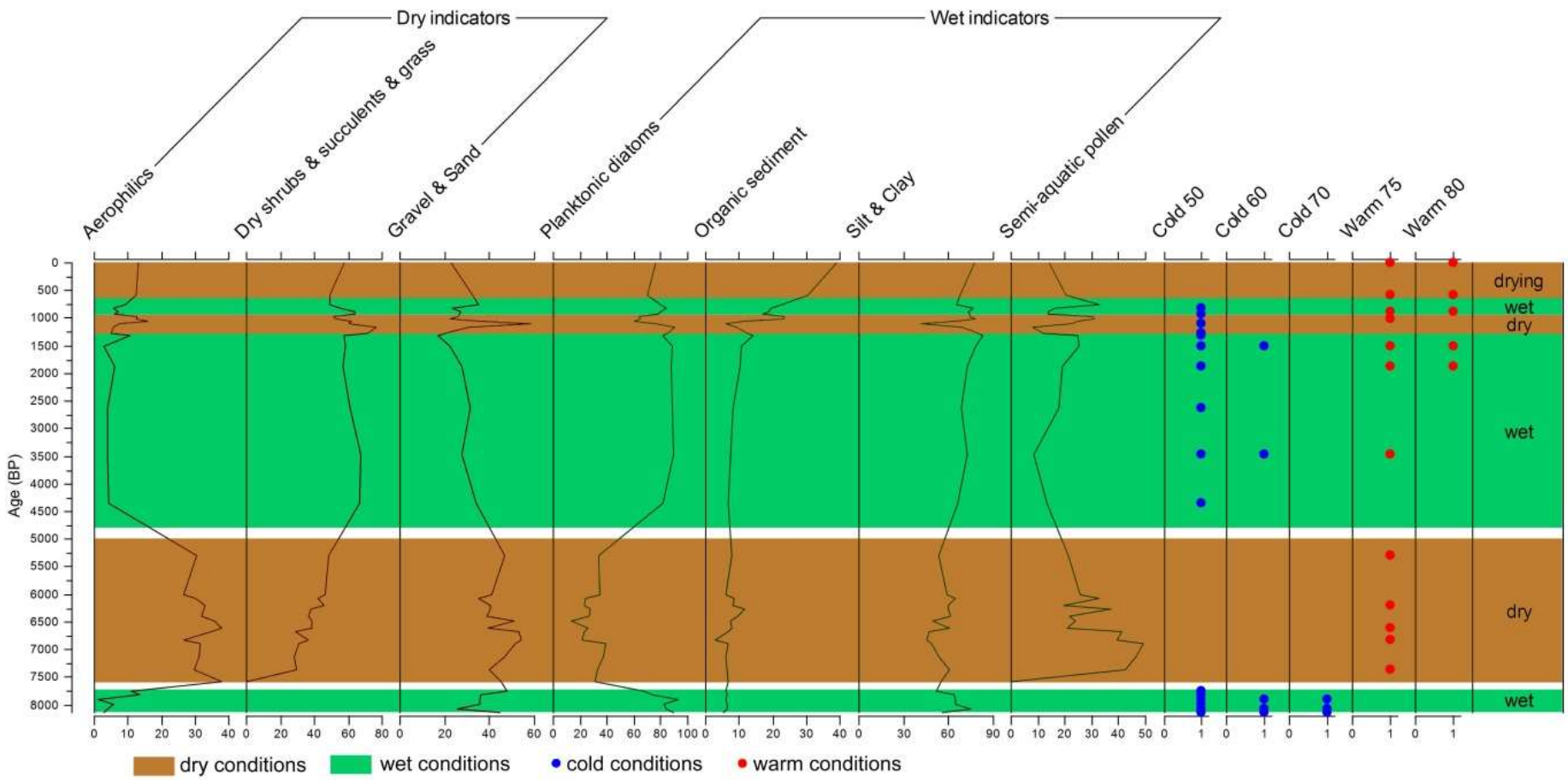


Figure 6.13: Summary diagram indicating the wet and dry, and cold and warm periods at Mafadi Wetland from ~8,140 cal. yr - present, indicated by the pollen, diatom and sediment records. Cold 40, 50, 60, 70 refer to the index of percentage composition of Fragilaria diatom species; warm 75, 80 refer to the percentage species richness for pollen.

MP2: ~5,600-1,100 cal. yr BP

The period of slow accumulation continues throughout much of this of this zone, but the sparse samples indicate a more consistent environment throughout this time period. This could be resulting from the lower temporal frequency of sampling, which does not facilitate the detection of more short-lived climate events, but the persistent relative abundance of both pollen and diatoms, and the slow, constant accumulation rate in this zone suggests that overall, the conditions were indeed relatively stable. The re-emergence of dominant *Aulacoseira ambigua* and *Fragilaria pinnata/ construens* indicates a wetland comprising shallow to deep surface water, while the sudden increase in *Fragilaria* species indicates a decrease in temperatures following the Holocene Altithermal (*Figure 6.7*). The relative abundance of benthic, epiphytic, epipelic, epilithic or aerophilic species all drop considerably to just above zero, indicating a decrease in diatom species diversity, suggesting a return to the conditions in zone MP5 with very cold temperatures and comparatively deep water (*Figure 6.7*). The relative abundance of Cyperaceae and Asteraceae is particularly low (*Figure 6.3*). The presence of large proportions of *Aulacoseira ambigua* prohibits an interpretation of dry conditions. The decrease in these pollen taxa therefore may be in response to the colder temperatures, which may have exceeded their cold tolerance. Alternately, the surface water extent of the wetland may have forced these plants to less suitable areas upslope. Notably, the highest relative abundance of Apiaceae in the profile is observed in this zone (*Figure 6.3*). This is most likely because this semi-aquatic species has a greater cold tolerance, as evidenced by its common presence at Marion Island (Nyakata & McGeogh, 2008). The dominant pollen group in this zone is Poaceae, which demonstrates little change in relative abundance throughout this period (*Figure 6.3*). There is also little change in the sedimentary properties in this zone (*Figure 6.10*). While the relative abundance of *Fragilaria pinnata/ construens* is as large as in zone MP5, the presence of pollen suggests that conditions were not as cold as during MP5 (*Figures 6.3, 6.7*). The difference in temperatures may only be seasonal: zone MP2 is characterised by an Asteraceae: Poaceae ratio of >0.5 (*Figure 6.3*) indicating summer rainfall and weakened westerlies, resulting in warmer summer conditions which may have resulted in seasonal growth of the plants producing pollen. The zone terminates with an increase in accumulation rate, and with a sudden peak in Poaceae pollen coupled with a decrease in the

relative abundance of Cyperaceae (*Figure 6.3*). This is concurrent with the highest relative abundance of *Aulacoseira ambigua* in the profile (*Figure 6.7*), indicating a sudden increase in moisture, with larger expanses of shallow to deep standing water. It is of interest to note that the adjacent diatomite bed discussed in *Section 5.4.6* temporally coincides roughly with this zone, which similarly suggests the existence of a very wet period, but with limited species diversity.

MP1: ~1,060 cal. yr BP - Present

Zone MP1 commences with fluctuations in Cyperaceae, Apiaceae, Asteraceae, Poaceae and *Crassula* pollen, paired with the re-emergence of both aerophilic and benthic diatom species (*Figures 6.3, 6.7*). This is indicative of warmer conditions than in the preceding zone, with a dry period responsible for a significant reduction in amount of surface water in the wetland. Notably, this period coincides with the Medieval Warm Period (Tyson et al., 2000). The pollen indicates finer-resolution moisture fluctuations, and fluctuations in the nature of the wetland, from one with shallow ponds to drier marshy conditions. This period is also characterised by a decrease in rainfall seasonality and an increase in the strength of the westerlies. At ~820 cal. yr BP there is a sudden peak in *Fragilaria* species (*Figure 6.7*) indicating an abrupt cold event, which is notably consistent with a cold event at Sani Valley, and contemporary with the beginning of the Little Ice Age. Notably this event is coupled with a brief peak in the Asteraceae: Poaceae ratio (*Figure 6.3*), suggesting a short-lived increase in the strength of the westerlies. From ~750 cal. yr BP the environmental proxies stabilise, with decrease in aerophilic diatoms, stable proportions of Asteraceae, and a slight change to Poaceae pollen from Cyperaceae, indicating an overall drying. This period witnesses a low relative abundance of *Fragilaria* species, which paired with an increase in the pollen taxa diversity through to a peak ~200 cal. yr BP may indicate a slight amelioration of temperatures following the onset of the Little Ice Age. The relative abundance of *Fragilaria* species demonstrates a slight increase at ~150 cal. yr BP (*Figure 6.7*) indicating a return to very cold temperatures, paired with another peak in the Asteraceae: Poaceae ratio (*Figure 6.3*) indicating a second short-lived increase in the strength of the westerlies, which coincides with the end of the Little Ice Age (Tyson et al., 2000). This coincides with the cold events at Sani Valley and Sekhokong and may provide a weak signal for a Little Ice Age event

(Tyson et al., 2000). It is notable that this event is reflected by a much weaker signal at Mafadi Wetland than at Sani Valley or Sekhokong, despite the colder temperatures at Mafadi Wetland. This may be because the cold threshold for plants and diatoms had already been exceeded prior to the ~150 cal. yr BP cold event, and thus further decreases in temperatures were not detected. It may also indicate a difference in lapse rates, with a weakening of the lapse rate under strengthened westerly conditions (Grab, 1997). The summary of these results is presented in *Figure 6.13.*

6.4 Lesotho Holocene Synthesis

This study comprises three geographically distinct study sites, which have slight variations in species composition and diversity for both pollen and diatoms, and differences in sedimentology. The profiles from the three sites span different time periods, and the proxies from these profiles are examined at varying temporal and sampling resolution. It is therefore valuable to explore the environmental and climatic shifts inferred from these proxies throughout the relative time periods shared by the three sites, and to determine the synchronicity of environmental and climate changes reconstructed for each of the sites. It is also of interest to compare the results from this study to the previously published environmental reconstructions for Lesotho, to determine the extent to which the changes observed in eastern Lesotho corroborate the earlier, lower-resolution analyses undertaken using pollen (Van Zinderen Bakker, 1955) and sedimentary characteristics (Marker, 1994, 1995, 1998), and to the work in central to western Lesotho which base environmental reconstructions on pollen (Grab et al., 2005), phytoliths (Grab et al., 2005; Parker et al., 2011), charcoal (Esterhuysen & Mitchell, 1996) and isotopes (Smith et al., 2002; Parker et al., 2011; Roberts et al., 2013). To facilitate the comparison of palaeoenvironmental changes reconstructed at a range of sites and using different proxies, the primary findings of published studies on dominant periods of warm or cold temperatures and/or dry or wet conditions (*Section 2.3.4, Figure 2.6*) are used. These published findings are compared to aridity and temperature indices developed for the three sites in this study (see *Section 6.3*). This aridity index involves the calculation of a ratio of the drought-resistant plant taxa, aerophilic diatoms and sand and gravel sediment size distribution to the semi-aquatic pollen, shallow to deep water diatoms, the organic content of the sediment and the

sediment distribution falling into the silt and clay classification. The intermediate cold index from the *Fragilaria* diatom species and species richness of 80% or higher is used to delineate periods of cold and warm temperatures at each of the sites respectively. To facilitate comparison between these sites, the periods of dry/wet and hot/cold conditions for each of the sites in this study, and each of the published studies for Lesotho, are presented visually (*Figure 6.14*).

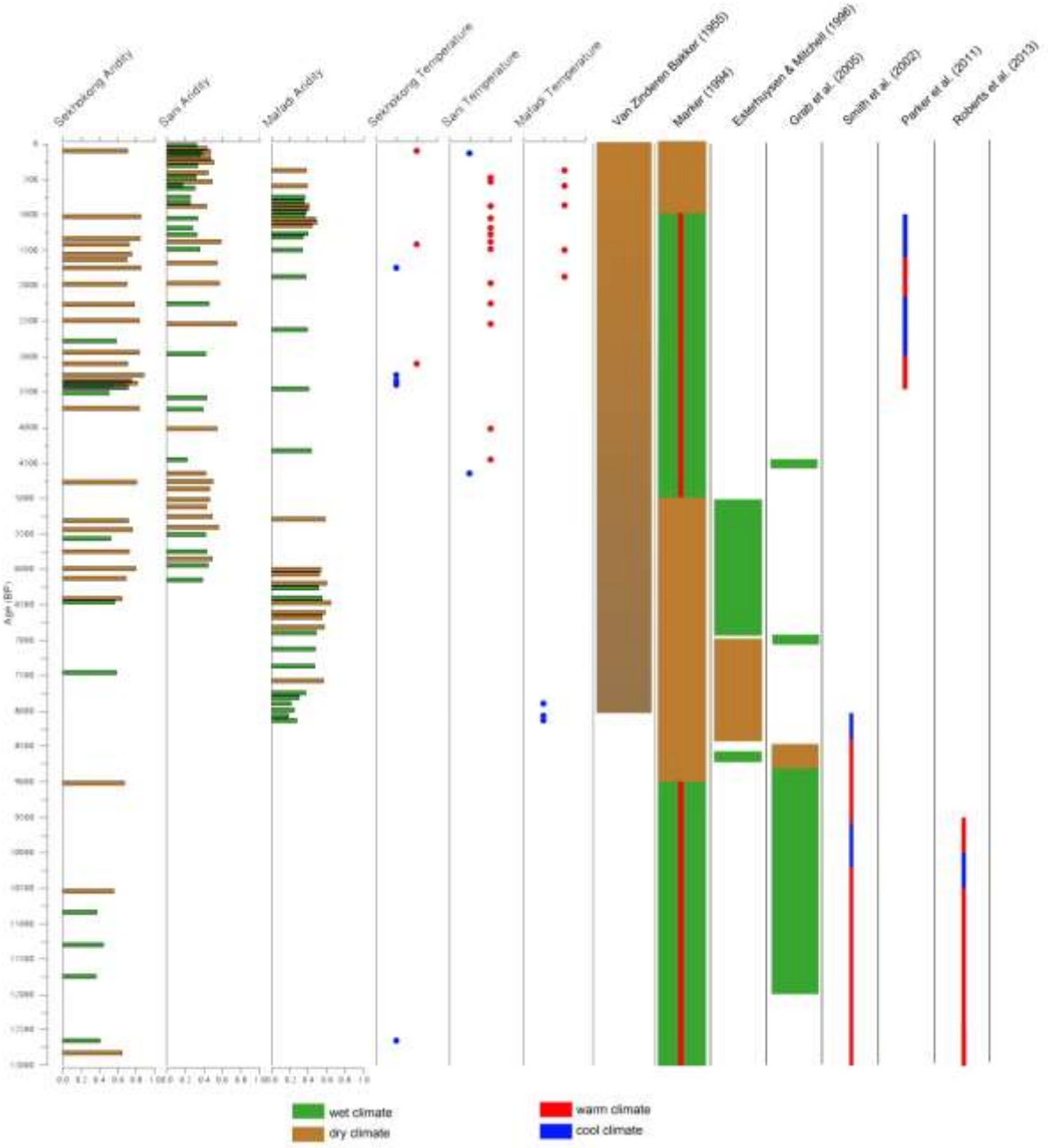


Figure 6.14: Reconstructed periods of dry and wet conditions, and warmer and extremely cold temperatures for Sani Valley, Sekhokong and Mafadi Wetland, and for the published proxy work for Lesotho.

6.4.1 Comparison Between Sites

Analysing only one site, or each of a number of sites entirely in isolation, can neglect landscape-scale climate and environmental variability, which are inherently captured by the pollen record. As the landscape variability is likely to have been as extensive in the past as at present, a radius of as much as 100km can be considered to have shared characteristics, thus providing motivation for the analysis of results between sites within this radius (Andrews & Bamford, 2008). For the eastern Lesotho sites in this study, there is considerable variance in the length of time periods spanned by the profiles, and the resultant temporal resolution afforded, for the different locations. Furthermore, the altitudinal difference between Mafadi Wetland and the lower altitude Sekhokong and Sani Valley sites (~400m) has the potential to provide preliminary information regarding tentative cold-temperature thresholds for vegetation in the eastern Lesotho highlands, and inferences relating to changes in lapse rates. The topographic differences between the three sites provide further variation in both the local environment, and the depositional characteristics of the environmental proxies. This section compares the proxy results and environmental reconstructions for Sani Valley, Sekhokong and Mafadi Wetland.

There are strong similarities in the pollen and diatom compositions for the three study sites, with few taxa particular to one site (*Tables 5.3, 5.7, 5.11; 5.4, 5.8, 5.12*). The relative abundance of the cold and ice tolerant *Fragilaria* species is notably higher at Mafadi Wetland than at the lower altitude, warmer Sani Valley and Sekhokong sites. Furthermore, the diversity in diatom species and pollen taxa is markedly lower at Mafadi Wetland than at Sani Valley and Sekhokong. Accumulation is also considerably slower at Mafadi Wetland than at the lower altitude sites, which due to the large organic content of the sediment at the three sites, can be attributed to slowly accumulating peat dominated sediment. The altitudinal difference between the sites therefore has a marked influence on the climate at the sites, which with a contemporary lapse rate in the eastern Lesotho highlands of 6.2°C/km (Grab, 1997), is to be expected. The associated change in species diversity, would suggest that this altitudinally driven temperature decrease between the sites exceeds a critical threshold for many plants, thus reducing the number of sufficiently cold-tolerant taxa which can inhabit Mafadi Wetland. From a geomorphological perspective, it is worth noting that Sekhokong, situated at the foot of a steep slope, is the only site at which gravel-

sized particles are measured (*Figure 6.9*). The site similarly has greater proportions of sand-sized particles throughout the profile (*Figure 6.9*), both of which result from a greater influence of colluvial sediment input (Marker, 1994). Thus, while a relative increase in sand- and gravel-sized particles compared to those of clay- and silt-size, should still be inferred as indicative of dry periods, the extremes in these comparisons are of geomorphological rather than climate derivation.

For all three sites, distinct periods of rapid and slow accumulation are apparent (*Figure 6.15*). Over the period ~4,750-1,250 cal. yr BP, all three sites experienced particularly slow rates of sediment accumulation (*Figure 6.15*). These similarities in the timing of the periods of slow accumulation at the three sites indicate a more regional climatic influence, rather than site-specific erosional influences. For Sekhokong, this was preceded by an earlier period of slow accumulation from ~12,500-6,750 cal. yr BP (*Figure 6.15*). The periods of slow accumulation could firstly be caused by a retardation of the accumulation of material. As the profiles from all three of the sites contain a large proportion of organic material, this would suggest either dry conditions, or conditions too warm for the partial decomposition of the organic matter into peat, but rather forming organic clay. Alternately, very cold conditions could reduce the vegetation density and the rate of decomposition, and similarly delay the accumulation of material (Baker et al., 2014). A contrasting interpretation is that these periods are indicative of heightened erosion, removing the surface sediment. It is notable that for palaeoenvironmental reconstructions based on sediment profiles in adjacent regions, Grab et al. (2005) and Norström et al. (2009) report age-depth records reflecting a coinciding period of slower accumulation. However, as the environmental significance of these periods cannot be deduced from the available evidence, no further inferences can be made at a local or regional scale (Norström et al., 2009).

Comparing the palaeoenvironmental reconstructions for the three sites, there is an overall agreement with regard to the timing of broadly defined wet and dry periods, while cold and warm events often are detected across more than one site (*Figure 6.14*). A higher cold temperature threshold was taken for Mafadi Wetland than for Sekhokong and Sani Valley, as the ~400m increase in altitude results in considerably colder temperatures at this site throughout the profile, and thus even during periods of warmer conditions, the climate

remained sufficiently cold to support large communities of *Fragilaria* species, in place of less cold-tolerant taxa.

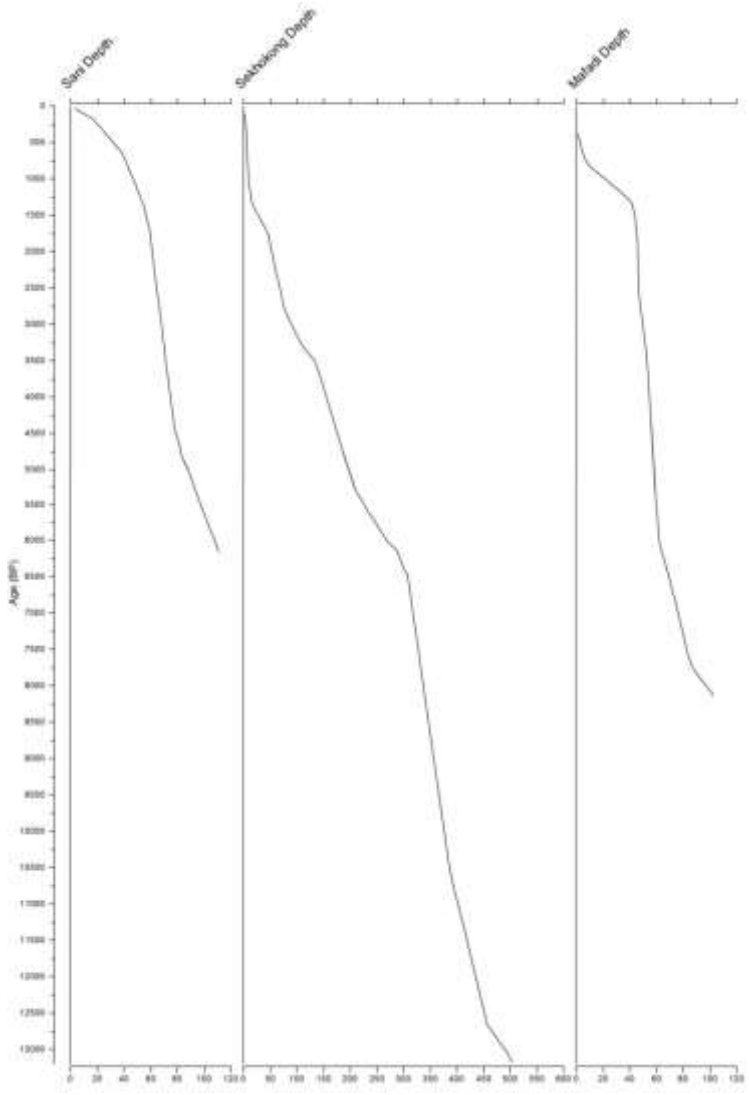


Figure 6.15: Age-depth relationship for the three study sites.

An exploration of the warm periods indicated by greater species diversity, and the timing of the cold events, indicates a warm late Holocene period across the three sites from 2,500-1,000 cal. yr BP (*Figure 6.14*), which would appear warmer than conditions at the time of the Holocene Altithermal (8,000-4,000 cal. yr BP: Chase & Meadows, 2007). Notably, all three sites provide evidence for very cold conditions at ~150 cal. yr BP (*Figure 6.14*), coincident with the end of the Little Ice Age (AD 1300-1800: Tyson et al., 2000). There is also evidence from both Sani Valley and Sekhokong of increased livestock presence in the region following this cold period, while there is no clear evidence from the less accessible and colder Mafadi Wetland, which must have been used for grazing only in recent decades.

At a finer scale, however, fluctuations in the climate reconstructions for each site are apparent, and variation in the timing of cohesive climatic events between sites is observed *(Figure 6.14)*. Climate events for the early Holocene can only be inferred from the Sekhokong record. These include a wet period from ~13,180-13,080 cal. yr BP, a dry period from ~13,080-12,830 cal. yr BP, concurrent with the Bølling-Allerød (Chase et al., 2015b), and a second wet event, commencing with a cold pulse, from ~12,660-10,850 cal. yr BP. From ~10,550-6,420 cal. yr BP, the Sekhokong record indicates dry conditions which are gradually becoming warmer and wetter. The temporal frequency of results is particularly low throughout this period. The record from Mafadi Wetland indicates cold, wet conditions from ~8,140-7,580 cal. yr BP, followed by warmer drier conditions from ~7,520-6,680 cal. yr BP.

Thereafter, differences are noted in the environmental reconstructions for the three sites (*Figure 6.14*). For Sekhokong, warmer, dry conditions are inferred for the period ~6,420-6,000 cal. yr BP, followed by cold and wet conditions from ~6,000-5,450 cal. yr BP. Warmer, dry conditions occur slightly later at Mafadi Wetland, extending from ~6,160-5,700 cal. yr BP, coinciding with the commencement of a longer wet period at Sani Valley, occurring from ~6,200-4,900 cal. yr BP. At Sekhokong, this is followed by a dry, warm period from ~5,450-3,700 cal. yr BP. At Sani Valley, a dry period is evident from ~4,770-4,470 cal. yr BP, but followed by a cold, wet period from ~4,460-2,260 cal. yr BP. At Mafadi Wetland, these cool, wet conditions cover a much longer period, from ~5,600-1,100 cal. yr BP. This prolonged period of cold and wet conditions possibly indicates snow accumulation at this high altitude bowl-shaped site. The more recent part of this period coincides with similarly cool, wet conditions at Sekhokong, from ~3,650-1,200 cal. yr BP. By contrast, dry conditions are evident at Sani Valley, from ~2,260-1,350 cal. yr BP. These variations in the timing of wet and dry periods for the three study sites may involve small-scale shifts in the extent of the westerly belt, or the influence of topographic boundaries to the transport of moisture derived either from the westerlies or from the Indian Ocean. Additionally, they may reflect the closer proximity of the spring-derived moisture at Sani Valley and Mafadi Wetland, providing continued moisture to the two sites during periods of regional drying. For all three sites, the period from ~1,000 cal. yr BP to present is characterised by progressive drying, with discrete wet events apparent in the higher resolution Sani Valley record. A pronounced

cold period is detected at all three sites at ca. 150 cal. yr BP, followed by progressive evidence of human disturbance from local (increase in livestock) to regional (deposition of pine pollen) scales.

Evidence for periods of potentially warmer temperatures (with greater pollen taxa diversity), and of extreme cold temperatures (with diatom communities dominated by *Fragilaria* species) were observed at each of the sites, although these were seldom supported by data from the other sites due to a lack of overlapping samples (*Figure 6.14*). At Sekhokong, pronounced cold events are detected at ~12,660 cal. yr BP and 5,450 cal. yr BP, with a third cold event occurring during the most recent 1,000 years, inferred to be between ~100-200 cal. yr BP (*Figure 6.14*). At Mafadi Wetland, cold conditions marked the beginning of the record, from ~8,140-7,580 cal. yr BP. A second period of particularly cold conditions is detected at ~150 cal. yr BP, coinciding with the cold period detected at Sekhokong and Sani Valley (*Figure 6.14*). An additional cold period is detected for Sani Valley at ~4,750 cal. yr BP (*Figure 6.14*). All three sites hold evidence for warm conditions from ~4,500 cal. yr BP to present (*Figure 6.14*); Sekhokong provides evidence for slight warming in the first half of the Holocene, with warmest conditions at ~7,460 cal. yr BP inferred from a peak in species diversity (*Figure 6.1*).

Similar variations in the timing of palaeoenvironmental events have been noted for studies undertaken in western Lesotho (*Figure 6.14*), and are attributed to the role of micro-climates in insulating and sheltering certain sites (Esterhuysen & Mitchell, 1996; Smith et al., 2002; Roberts et al., 2013). This, in particular, might explain the variations in the timing of climatic events, and at time periods of conflicting climates for the altitudinally comparable Sani Valley and Sekhokong. This may also explain some of the variations between the two lower altitude sites and Mafadi Wetland, with further variations possibly explained by the fluctuating lapse rates with altitude and throughout time, with the altitude of cloud belts influencing comparative temperatures between sites of varying altitude (Grab, 1997). The radius from which pollen is derived is also relevant, as with a broader region of transportation, the record will reflect predominantly regional conditions. The relationship between the diatom and pollen records (*Section 6.2.2.*) suggests that the Sekhokong pollen record may be indicative of more regional climatic and environmental changes than the

pollen record from Mafadi Wetland. Furthermore, with springs located in closer proximity to the Mafadi Wetland and Sani Valley sampling sites than at Sekhokong, these two sites may experience time lags for periods of drying as the sites continue to receive moisture from the springs. In many instances, an apparent disagreement between sites rather reflects a sampling gap for the one site, as is evident in *Figure 6.14*. For example, what would have been interpreted as a continuous dry period from ~500 cal. yr BP to present from the data from Sekhokong and Mafadi Wetland is found to be marked by distinct moist pulses from the samples covering a higher temporal resolution from Sani Valley. This further emphasises the importance of sampling at a high resolution in the core, to ensure high temporal resolution of samples throughout periods of slower accumulation.

6.4.2 Comparison with other studies in Lesotho

6.4.2.1 Eastern Lesotho Records

Comparing the results of this study with previously published palaeoenvironmental reconstructions undertaken in Lesotho, those from the eastern Lesotho highlands should reflect the greatest similarity due to their proximity, similar altitude, and the resultant climatic and vegetation parallels *(Figure 6.14)*. The closest comparison, based on study location and proxies, is the pollen analysis undertaken by Van Zinderen Bakker (1955), supplemented by the age-dates reported by Van Zinderen Bakker (1974) for what appears, by the description of the study location, to be the same wetland system. While the exact location of the coring site is not provided, it is described to be located on a tributary of the Malibamatso River in northeastern Lesotho (Van Zinderen Bakker, 1955; Schoeman, 1973; Van Zinderen Bakker & Werger, 1974). This pollen-based reconstruction suggests progressive regional aridification from 8,020 yr BP to present, and makes no comment on changes in temperature. These findings, while broad, are not consistent with the pollen, diatom or sediment results at Sani Valley, Sekhokong or Mafadi Wetland (*Figure 6.14*). At all three sites, the pollen record suggests substantial variability in moisture throughout the period 8,000 yr BP to present. Furthermore, at none of the sites is a progressive shift from Cyperaceae to Poaceae pollen detected. These discrepancies may be due to the low sampling frequency adopted in the Van Zinderen Bakker (1955) pollen record, at only at 10cm intervals throughout the 2m sediment profile. Furthermore, the study presents

changes in the relative abundance of only five pollen taxa, and bases the environmental reconstruction on relative shifts in Cyperaceae and Poaceae alone. Examining Van Zinderen Bakker's (1955) pollen diagram (*Figure 6.16*), much variation in the relative abundance of Cyperaceae pollen is apparent, which may correspond with wet periods in the records from Sani Valley, Sekhokong and Mafadi Wetland. Of further interest are the fluctuations in Apiaceae (Umbelliferae) pollen, which, similar to the results for Mafadi Wetland, does not always fluctuate in synchrony with the other semi-aquatic taxa, Cyperaceae (*Figure 6.16*).

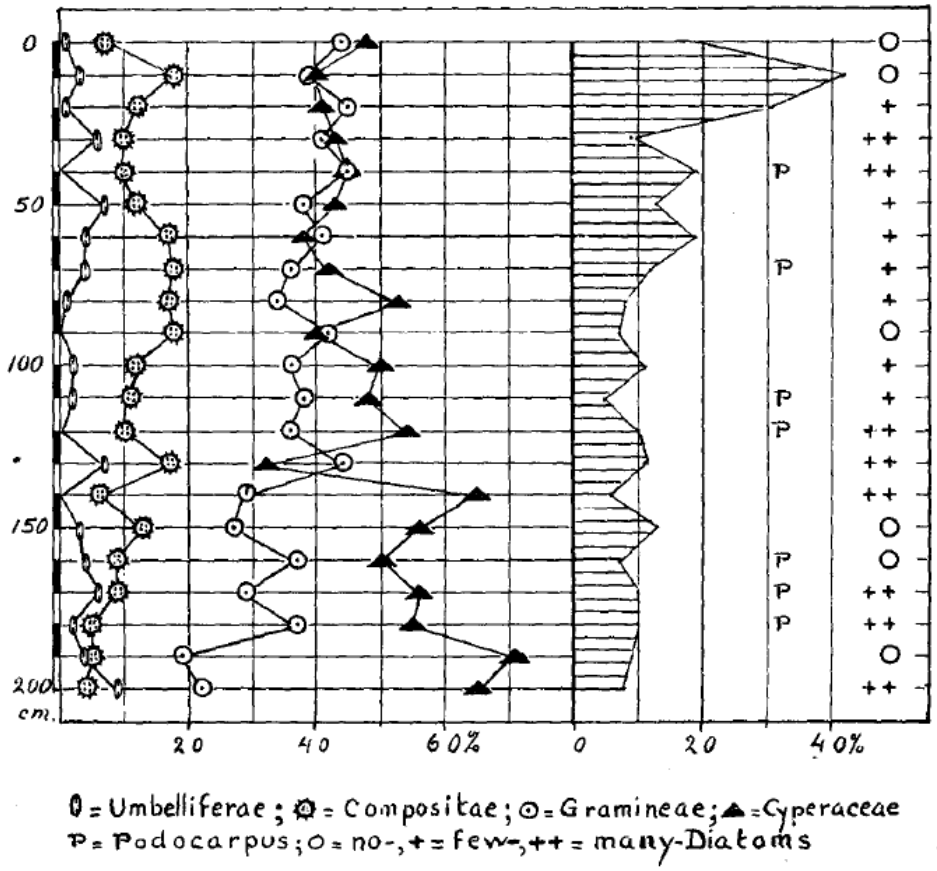


Figure 6.16: Van Zinderen Bakker's (1955) pollen diagram. The following changes in names of pollen taxa should be noted: Umbelliferae = Apiaceae, Compositae = Asteraceae, Gramineae = Poaceae.

Without confirmation that the basal date presented by Van Zinderen Bakker and Werger (1974) corresponds with the same profile, and without further dates to temporally constrain the timing of these fluctuations in Cyperaceae pollen, no further comparisons can be made. It should be noted that Van Zinderen Bakker (1955) did not frame the paper as a

palaeoenvironmental reconstruction for the region, or even a local site, but rather as a preliminary survey of the eastern Lesotho wetlands (Van Zinderen Bakker & Werger, 1974). It is only the lack of subsequent palaeoenvironmental work undertaken in the region which has placed perhaps undue significance on this pollen record.

The second palaeoenvironmental reconstruction for eastern Lesotho combined sedimentological results from Sekhokong (Sani Top) and Tlaeeng, a site located in northeastern Lesotho (*Figure 2.5*), to determine periods of environmental change for the broader highlands region (Marker, 1994, 1995, 1998). These findings are more consistent with this study (*Figure 6.14*). Agreement of results at Sekhokong is expected, as according to the maps, diagrams and descriptions presented by Marker (1994), her 'Sani Top' site was located in the same gulley system as the Sekhokong site. The agreement with the results from Sani Valley and Mafadi Wetland is of regional interest. Marker's (1994, 1998) sediment record and the inferred palaeoenvironmental history does, however, overlook many of the finer scale climatic and environmental pulses detected in this study for Sekhokong, as well as for Sani Valley and Mafadi Wetland *(Figure 6.14)*. With a lower sampling frequency than was used in this present study (Marker, 1994), and not exploring biological proxies which would have finer resolution thresholds than sediment properties, a broader-scale environmental reconstruction was inevitable (Grab et al., 2005). Marker's (1994) record begins with wet and warm conditions from 13,500-9,000 yr BP. The Sekhokong record reflects wet conditions for this period, although interrupted with marked dry periods towards the beginning (~13,080-12,830 cal. yr BP) and at the end (from ~10,550 cal. yr BP to the end of this period). The pollen and diatom records for Sekhokong do not suggest a particularly warm climate during this period, with the peak in *Fragilaria* species at ~12,660 cal. yr BP indicating a marked cold period. Notably though, the isotope records from western Lesotho demonstrate agreement with Marker (*Figure 6.14*), suggesting warm conditions from the onset of Marker's (1994) record until 10,500 cal. yr BP (Roberts et al., 2013) or 10,200 cal. yr BP (Smith et al., 2002). These isotope records may provide a more accurate record for warmer conditions, as given the very cold temperatures in the eastern Lesotho highlands above ~2,900m.asl, considerable warming would be required to exceed the minimum temperature thresholds of many less cold-tolerant plant and diatom taxa at or above such altitudes. Assuming greater accuracy from the isotope records, it is notable that

both isotope records agree on cold temperatures from 10,200-9,000 cal. yr BP, during which time Marker's (1994) record suggests continued warm conditions.

The onset of Marker's (1994) dry period at 9,000 yr BP is supported by a peak in the aridity at Sekhokong, with persistent dry conditions until ~6,420 cal. yr BP. The Mafadi Wetland record, by contrast, commences with very wet conditions indicated by the abundance of deep water *Aulacoseira ambigua*, with drier conditions commencing at Mafadi Wetland from ~7,520 cal. yr BP *(Figure 6.6)*. Results from western Lesotho, reconstructed from pollen and phytoliths, indicate a drying period from 8,600-8,450 cal. yr BP which supports the timing of this onset of aridity (Grab et al., 2005). Charcoal records from western Lesotho however indicate a wet period from 8,700-8,600 yr BP, in direct conflict with the records presented by Marker (1994), but indicate dry conditions from 8,500-7,000 yr BP (Esterhuysen & Mitchell, 1996) in agreement with Grab et al. (2005). The results from all three sites in this study support Marker's (1994) inference of dry conditions from at least 6,500-5,000 yr BP, although again this is in disagreement with the western Lesotho charcoal records which indicate wet conditions during this period (Esterhuysen & Mitchell, 1996; *Figure 6.14*). The pollen and phytolith record from western Lesotho (Grab et al., 2005) indicates a wet period at 7,000 cal. yr BP, and the charcoal records suggest wet conditions from 6,900 yr BP, both of which are in agreement with a wet pulse detected at Sani Valley, Sekhokong and Mafadi Wetland, but is temporally situated in the middle of Marker's (1994) dry period (*Figure 6.14*).

The dry period commencing at 5,000 yr BP reconstructed from sediments (Marker, 1994) corresponds with the results from Sani Valley, Sekhokong and Mafadi Wetland (*Figure 6.14*). However, significant wet periods occur during the period ~5,000-1,000 cal. yr BP at all three study sites, with more rapid fluctuations in the precipitation record towards the end of this period (*Figure 6.14*). For Sani Valley, a brief dry period between ~5,000-4,750 cal. yr BP is followed by wet conditions that persist for much of this period, interrupted only by a dry pulse from ~2,750-1,250 cal. yr BP. Broadly, the results from the three sites would suggest relatively warmer conditions during this period, although with marked cold pulses, supported by the phytolith and isotope data from Likoaeng (Parker et al., 2011). Notably, there is considerably more evidence from the pollen and diatom records for warmer

conditions during this period than Marker's (1994) earlier 'warm period'. The final zone in Marker's (1994) record extends from 1,000 yr BP to present, which is inferred to have been characterised by dry conditions. This is in agreement with the multi-proxy results from Sani Valley, Sekhokong and Mafadi Wetland, although marked wet pulses within this period are noted for Sani Valley (*Figure 6.14*). In contrast to the results of Marker (1994), data from all three sites suggest a continuation of the warmer temperatures during this period, although interrupted with a marked cold period leading up to ~150 cal. yr BP (*Figure 6.14*). The only other palaeoenvironmental and palaeoclimatic reconstructions spanning this period are the documentary-based reconstructions for Lesotho for last ca. 200 years (Grab & Nash, 2010; Nash & Grab, 2010), but these are at too high a temporal resolution to facilitate comparison with these coarser records.

6.4.2.2. Central and Western Lesotho Records

The precipitation reconstructions from western Lesotho cover shorter time periods than the records discussed for eastern Lesotho. The most comparable study, in terms of the proxies used, is the pollen and phytolith record for Tsoaing River Basin (Grab et al., 2005, *Figure 2.5*). However, as pollen could only be analysed for two samples in the profile (Grab et al., 2005), no direct comparison of the pollen records can be made. The wet period reconstructed for 12,000-8,600 cal. yr BP is in agreement with the Sekhokong record; although it does not provide evidence for the dry pulse at ~10,550 cal. yr BP recorded from the diatom, pollen and sediment records (*Figure 6.14*). The Tsoaing record reflects a dry pulse from 8,600-8,450 cal. yr BP. While this corresponds with a decrease in the percentage organic composition of sediments and a decrease in the relative abundance of planktonic diatoms at Sekhokong, it is not a marked wet period with reference to the rest of the multi-proxy record at Sekhokong (*Figure 6.14*). This may be due to the lower sampling frequency at Tsoaing (Grab et al., 2005), which may have resulted in sediments from wetter periods being sampled, or alternately could reflect the wetter conditions in eastern Lesotho resulting in less of a difference in precipitation at Sekhokong. The wet period reconstructed for Tsoiang at 7,000 cal. yr BP (Grab et al., 2005) corresponds with multi-proxy evidence for wet conditions at Sekhokong and Mafadi Wetland (*Figure 6.14*). Similarly, the wet conditions reconstructed at 4,500 cal. yr BP coincide with wet periods at Sani Valley,

Sekhokong and Mafadi Wetland, although the wet periods reconstructed in this study are longer-lived than that for Tsoaing, perhaps also reflecting the low sampling frequency at Tsoiang, as this wet event is represented by a single sample (*Figure 6.14*). The second precipitation record for western Lesotho derives from charcoal results from shelters at Tloutle, Ha Makotoko and Ntloana Tsoana (Esterhuysen & Mitchell, 1996; Esterhuysen et al., 1999; *Figure 2.5*). The onset of the wet period indicated by pollen and phytoliths at Tsoaing is consistent with the charcoal record, with a 100-year delay which could be attributed to the margin of uncertainty in the age-dates and comparison between calibrated and uncalibrated values. The first wet pulse in the charcoal record, centred at 8,700 yr BP is consistent with the multi-proxy data for Sekhokong, and could tentatively overlap with the wet period at the commencement of the Mafadi Wetland record, depending on the longevity of this period (*Figure 6.14*). The subsequent dry periods from the charcoal records do not align with any of the three sites (with the exception of short pulsed events), nor do they coincide with other studies from western Lesotho, with the exception of Marker's (1994) broad dry periods (*Figure 6.14*). It should be noted that proxy evidence from archaeological sites is limited in its accuracy as it represents the range of material brought into a shelter, rather than the full diversity of taxa in the local or regional environment at the time (Esterhuysen & Mitchell, 1996; Roberts et al., 2013). This may explain some of the inconsistencies with other palaeoenvironmental reconstructions in the region.

Isotope data from western Lesotho (Smith et al., 2002; Roberts et al., 2013), and for central Lesotho, paired with phytolith data at Likoaeng (Parker et al., 2012), provides evidence of fluctuations between periods of warmer and cooler temperatures in the late Quaternary. The isotope studies from western Lesotho indicate warm conditions from >13,500 cal. yr BP until some period between 10,500-10,200 cal. yr BP (Smith et al., 2002; Roberts et al., 2013). The disagreement between this warm period and the cool conditions inferred for Sekhokong is discussed in *Section 5.4.2.1.* This may suggest a strengthening of lapse rates during this period, which would result in a greater temperature variation in the highlands than the lowlands, or reflect micro-climates between the sites (Esterhuysen & Mitchell, 1996). The variation may also reflect anthropogenic bias in the material transported into the shelter, which may not include indicators of this cold period (Esterhuysen & Mitchell, 1996; Roberts et al., 2013). Both of the western Lesotho isotope records indicate cold periods of

ca. 500 years, but these do not coincide, extending from 10,200-9,600 cal. yr BP (Smith et al., 2002) and from 10,500-10,000 cal. yr BP (Roberts et al. 2013). This similarly may reflect differences in micro-climates between the sites, or possibly an improvement in age-dating methods between the time at which the two studies were undertaken (Esterhuysen & Mitchell, 1996; Smith et al., 2002). Irrespective of the reason, the discrepancy in timing is large relative to the duration of the event. Furthermore, during both of these periods, there is no evidence for a cold event in the Sekhokong record, which reflects a notably small relative abundance of *Fragilaria pinnata/ construens,* and an absence of *Fragilaria famelica,* with a greater dominance of less cold-tolerant taxa (*Figure 6.6*). For both isotope records, these cold events are bounded by warm periods, although again demonstrating little overlap, with warm conditions reported from 10,000-9,500 cal. yr BP (Roberts et al., 2013) and from 9,600-8,400 cal. yr BP (Smith et al., 2002). However, as the Roberts et al. (2013) isotope record terminates at 9,500 cal. yr BP, one cannot infer a cessation of warm conditions at this point. Warm conditions from the eastern Lesotho records in this study are inferred from an increase in the pollen species diversity, which does not occur during either of these periods. However, there is a markedly low relative abundance of *Fragilaria* species, indicating a greater proportion of diatoms with a lower snow or ice tolerance, from which slightly warmer conditions can be inferred (*Figure 6.6*). A cold period from 8,400-8,000 cal. yr BP represents the terminal period of the Smith et al. (2002) isotope record. This period corresponds with the commencement of the Mafadi Wetland record, which is marked by a particularly high relative abundance of the ice-tolerant *Fragilaria pinnata/ construens* species, indicating very cold temperatures in agreement with the isotope record (*Figure 6.7*). Due to a slower accumulation rate during this period, there are no data for Sekhokong at an equivalent date. The third isotope record is from central Lesotho at Likoaeng, which paired with phytolith analysis, spans a portion of the late Holocene, from 3,400-1,070 cal. yr BP (Parker et al, 2011; *Figure 2.5*). A cold pulse from 2,960-2,160 cal. yr BP (Parker et al., 2011), corresponds with the timing of a cold event at Sekhokong, and with a smaller proportional increase in *Fragilaria* species at Mafadi Wetland, but due to low diatom sampling frequency is not confirmed for Sani Valley (*Figure 6.14*). Thereafter, the isotope and phytolith record indicates increasingly warm conditions until 1,600 cal. yr BP, after which stable warm conditions persist to the end of the record. These warm conditions are in agreement with the increased pollen species diversity, and the relatively low abundance of

Fragilaria species at Sani Valley, Sekhokong and Mafadi Wetland during this period, but does not include the short-lived cold pulse detected for Sekhokong at ~1,750 cal. yr BP, nor the abrupt cold event at Mafadi Wetland at ~1,510 cal. yr BP (*Figure 6.14*). This may reflect a strengthening in lapse rates for this period, or alternatively a gap in sampling for Likoaeng for these two time slices. This period should therefore be interpreted as a warm period, interspersed by abrupt cold periods.

Much of the archaeological record for eastern Lesotho interprets pulses in occupation as periods of ameliorable climatic conditions conducive to settlement in the cold highland regions (cf. Carter, 1976; Plug, 1997; Mitchell et al., 1998; Plug & Mitchell, 2008; Stewart et al., 2012; Roberts et al., 2013). Tentative assumptions have been made that occupation would occur during warm periods, during which the highlands would provide greater security and a broader range of available food, or during dry periods in which eastern Lesotho provided one of the few reliable sources of water (Carter, 1976; Mitchell et al., 1998). No objective corroboration of these results, which does not rely on analysis of archaeological material, has been published. It is therefore of interest to analyse the climate reconstructions for Sani Valley, Sekhokong and Mafadi Wetland from this study for the time periods of occupation at various sites in Lesotho presented in the archaeological literature (*Table 6.2*). The majority of settlement periods correspond with either warm or wet climatic conditions reconstructed for the three sites in this study, supporting these hypotheses posed by the archaeologists. Settlement during periods with dry and cold conditions is only observed for Likoaeng, which is known to be a site favoured for its reliable fish supply (Plug et al., 2003; Parker et al., 2011), and is hypothesised to have been one of a group of sites used on a rotational seasonal basis (Mitchell et al., 2011) rather than occupied continuously throughout the year. The multi-proxy palaeoenvironmental reconstructions requested by Mitchell (1996) for Lesotho consequently serve to confirm the hypotheses regarding the climatic role in settlement patterns made by archaeologists, and provide greater support for their climatic inferences for periods prior to the Holocene.

Table 6.2: Climate reconstruction from Sani Valley, Sekhokong and Mafadi Wetland compared with the periods of human occupation at sites in Lesotho, as presented in the archaeological record.

Author	Year	Site	Occupation Periods	Climate (this study)
Mitchell et al.	1994	Hololo	AD 1660 (cal.) AD 1640 (cal.)	Dry, probably warm
Mitchell et al.	1994	Bohlahla	AD 1885-1914 (cal.) AD 1179 (cal.)	Wet, warm Average precipitation
Mitchell et al.	1994	Tloutle	AD 1272-1305 (cal.) AD 1446-1638 (cal.)	Wet, warm Warm, wet/dry
Esterhuysen & Mitchell	1996	Ha Makotoko	10,000-8,3700 yr BP	Wet, cold
Esterhuysen & Mitchell	1996	Ntloana Tsoana	12,100-8,780 yr BP	Wet, cold
Esterhuysen & Mitchell	1996	Tloutle	9,000-5,000 yr BP	Variable
Mitchell	1996a	Sehonghong	~6,000 yr BP ~7,000 yr BP ~10,000 yr BP ~11,000 yr BP ~12,000-12,500 yr BP ~20,000 yr BP ~25,000 yr BP	Dry Slightly wet Slightly dry Slightly wet Slightly wet, cold No data No data
Mitchell	1996b	Sehonghong	AD 850-1870 (cal.)	Fluctuating
Mitchell et al.	1998	Sehonghong	12,500-12,000 yr BP ~11,000 yr BP 9,800-9,300 yr BP	Slightly wet, cold Slightly wet No data
Mitchell et al.	2011	Likoaeng	1700-1000 BC (cal.) 1000-200 BC (cal.) AD 100 BC-250 (cal.) AD 800-899 (cal.)	Warm Warm, wet Warm, dry/wet Warm, wet
Parker	2011	Likoaeng	>3,380-2,860 cal. yr BP 2,860-2,440 cal. yr BP 2,510-2,150 cal. yr BP 2,070-1,600 cal. yr BP 1,260-1,070 cal. yr BP	Dry, cold → warm Dry, warm Dry, warm Dry, warm → cold Wet, warm
Stewart et al.	2012	Melikane	~80,000 cal. yr BP ~60,000 cal. yr BP ~50,000 cal. yr BP ~46,000-38,000 cal. yr BP ~24,000 cal. yr BP ~9,000 cal. yr BP ~3,000 cal. yr BP ~1,800 cal. yr BP	No data No data No data No data No data Dry Dry, warm Wet, warm
Roberts et al.	2013	Ntloana Tsoana	~61,000 cal. yr BP 57,000 cal. yr BP 14,200-9,600 cal. yr BP	No data No data Wet, cold pulse

6.4.2.3 Comparison with Studies at Sites Adjacent to Lesotho

The eastern Lesotho region is topographically and ecologically defined by the highlands, yet comparisons have been made with results from sites in western Lesotho which are at considerably lower altitude due to their geographic classification within the country of

Lesotho. It is of equivalent interest to compare the results from this study with those of adjacent lower altitude sites located within the South African region of the Drakensberg. This facilitates some consideration of the role of altitude and micro-climates in delineating climatic events. The two most relevant sites, based on the proxies used, their hydrology as wetlands, and their location within the humid eastern area of the SRZ, are the palaeoenvironmental reconstructions from Braamhoek Wetland in the Free State Drakensberg (Norström et al., 2009, 2014; Finné et al., 2010), and from Mahwaqa Mountain in the KwaZulu-Natal Drakensberg (Neumann et al., 2014).

The diatom composition for the profile at Braamhoek Wetland varies in a similar manner to the diatoms in the eastern Lesotho sites, indicating fluctuations in precipitation at the site, with wet conditions reflected by planktonic species, including *Aulacoseira ambigua,* and aerophilic species, including *Hantzschia amphioxys* (Finné et al., 2010). There is a greater relative abundance of planktonic species for the wet periods at Braamhoek, and these comprise a larger species diversity including a greater selection of *Aulacoseira*, as well as *Cyclotella* spp. and *Discotella* spp. (Finné et al., 2010). Conditions at Braamhoek appear considerably warmer throughout their profile than at Sani Valley, Sekhokong and Mafadi Wetland, as the ice and snow tolerant *Fragilaria pinnata/ construens* and *Fragilaria famelica* do not appear in the Braamhoek diatom record (Finné et al., 2010). Other diatoms found at both Braamhoek and the eastern Lesotho sites include *Eunotia praerupta* and *Gomphonema parvulum* (Finné et al., 2010). Many diatom taxa from Braamhoek are identified only to genus level, including diatoms from the genus *Stauroneis*, *Eunotia*, *Pinnularia* and *Gomphonema,* from which further overlaps may exist (Finné et al., 2010). There is considerable overlap in the pollen composition for Braamhoek and the eastern Lesotho sites, all of which are dominated by Cyperaceae, Poaceae and Asteraceae, with populations of *Crassula*, *Typha*, Aizoaceae, *Artemisia*, Cheno-Am, *Anthospermum*, *Erica*, *Passerina* and *Stoebe* (Norström et al., 2009). While this overlap in pollen composition can, in part, be explained by the wetland setting of the four sites (Norström et al., 2009), there is likely considerable species variation between the sites that cannot be detected due to the family level resolution of pollen analysis (Quick et al., 2011; Quick, 2013). Notably, because it is situated below the tree-line, the pollen record from Braamhoek includes a large relative abundance and greater species diversity of trees (Norström et al., 2009). These include

Podocarpus and *Olea* (Norström et al., 2009), which are detected intermittently in the records from the eastern Lesotho highlands, and may reflect one of the source regions of this pollen. It is interesting that, aside from the tree species, there does not appear to be particularly greater species diversity of pollen or diatoms from Braamhoek, but rather a noticeable shift to less cold-tolerant taxa.

The palaeoenvironmental reconstruction for Braamhoek Wetland is presented in a set of three papers: the first relies on pollen, charcoal and isotope results (Norström et al., 2009); the second is based on siliceous microfossils, presenting results from diatom and phytolith analysis (Finné et al., 2010); the third re-examines the pollen record, together with biomarkers and mineral magnetic properties (Norström et al., 2014). These three records provide slightly different environmental reconstructions, with variations in the dates for defined climatic periods (*Table 6.3*). Therefore, each of these records will be compared with the results from eastern Lesotho, and in particular, where possible the information from which these reconstructions were inferred will also be compared with similar raw data from Sani Valley, Sekhokong and Mafadi Wetland.

Table 6.3: Palaeoenvironmental reconstructions published for Braamhoek Wetland.

Study	Proxy	Dry	Wet
Norström et al. 2009	Pollen	16,000-13,700 cal. yr BP	13,700-12,800 cal. yr BP
	Charcoal	12,800-10,500 cal. yr BP	10,500-9,500 cal. yr BP
	Isotopes	9,500-8,200 cal. yr BP	
Finné et al. 2010	Diatoms	11,300-10,400 cal. yr BP	13,600 cal. yr BP
	Phytoliths	~<8,000-2,000 cal. yr BP	11,300 cal. yr BP
			10,400-10,000 cal. yr BP
			1,500 cal. yr BP-Present
Norström et al. 2014	Pollen	12,600-11,300 cal. yr BP	13,800-12,600 cal. yr BP
	Charcoal	7,000-2,000 cal. yr BP	10,200-8,500 cal. yr BP
	Biomarkers		2,000 cal. yr BP-Present
	Mineral magnetic properties		

From the Braamhoek Wetland diatom record, wet periods are inferred from peaks in the relative abundance of planktonic diatoms at 13,600 cal. yr BP, 11,300 cal. yr BP, and 10,400-10,000 cal. yr BP (Finné et al., 2010). Comparing these results with the diatom results from Sekhokong, only the event at ~13,600 cal. yr BP is tentatively detected. The Sekhokong record has a basal date of ~13,180 cal. yr BP, but commences with a high relative abundance of planktonic diatoms, which may have commenced ~420 years earlier. By contrast, both at ~11,300 cal. yr BP and between ~10,400-10,000 cal. yr BP, diatom records from Sekhokong

demonstrate cumulative relative abundance of planktonic and facultative planktonic species of less than 5%. The Braamhoek record reflects a rapid increase in *Gomphonema parvulum*, a pollution tolerant taxon, at the top of the core (most recent 500 years) which is interpreted as an increase in nutrients from livestock, and is consistent with the findings and interpretation of a shift to pollution and alkaline tolerant taxa at Sani Valley. The pollen record from Braamhoek has a marked increase in semi-aquatic taxa from 13,200 cal. yr BP, inferred to represent a wet event. This is timed more closely with the commencement of the Sekhokong record, and the wet conditions indicated by the sediments, pollen and diatoms (Norström et al., 2009; *Figure 6.12*). Notably, the 11,300 cal. yr BP wet event presented from the diatom results at Braamhoek (Finné et al., 2010) is not supported by the phytolith, pollen, charcoal or isotope results for the site (Norström et al., 2009). The wet period is, however, consistent with moist conditions at the time detected in pollen records from Wonderkrater (Scott et al., 2008), paired with cooler temperatures (Norström et al., 2009). The pollen, charcoal and isotope records suggest dry conditions after 11,300 cal. yr BP (Norström et al., 2009), which is consistent with the results from Sekhokong (*Figure 6.12*). The pollen and charcoal record from Braamhoek indicates a wet phase from 10,500-9,500 cal. yr BP (Norström et al., 2009), which is in agreement with the diatom records for the site (Finné et al., 2010). The siliceous microfossil record suggests dry conditions from the mid-Holocene (~8,000 cal. yr BP) to 1,500 cal. yr BP, followed by a return to wet conditions that persist until present conditions (Finné et al., 2010). This is in agreement with the pollen, biomarker and mineral magnetic properties for the site (Norström et al., 2014), but disagrees with Marker's (1994) palaeoenvironmental reconstruction for Sekhokong (Sani Top), which suggests dry conditions from 5,000-1,000 yr BP, and wet conditions thereafter, and occurs concurrent to a period of rapid moisture changes reconstructed for eastern Lesotho (*Figure 6.14*). The contradiction in the palaeoenvironmental reconstruction for this period is of interest, as the western Lesotho precipitation reconstructions do not extend earlier than 4,500 yr BP. The earlier section of this dry period at Braamhoek does, however, coincide with the charcoal (Esterhuysen & Mitchell, 1996), pollen and phytolith (Grab et al., 2005) records for western Lesotho, both indicative of marked wet periods. This may therefore imply some climatic boundary in the extent of the northward intrusion of the westerly belt, or an altitudinal obstruction to moist air from the Indian Ocean, to create a precipitation dipole between Braamhoek and Lesotho. The variations in the different

proxies results for Braamhoek, and the resultant inconsistencies in their palaeoenvironmental reconstructions, does, however, warrant concern.

The palaeoenvironmental reconstruction for Mahwaqa Mountain relies entirely on pollen results. Similar to the eastern Lesotho sites, Cyperaceae and Poaceae dominate the pollen sum, and relative changes in these two taxa are used to infer changes in moisture (Neumann et al., 2014). Notably, where Norström et al. (2009) infer higher proportions of Asteraceae pollen relative to Poaceae as indicative of decreased seasonality and the weakening of the westerlies, Neumann et al. (2014) infer this as representing considerable seasonal drying. The pollen sum for Mahwaqa Mountain comprises a large fynbos component, from which periods of cooler temperatures are inferred (Neumann et al., 2014). Similar to Braamhoek, the Mahwaqa Mountain site is situated below the tree-line and consequently the pollen sum comprises a significantly larger proportion of tree taxa than in the eastern Lesotho record (Neumann et al., 2014). Notably, increases in the relative abundance of *Podocarpus* pollen are inferred as indicative of wetter conditions (Neumann et al., 2014).

The Mahwaqa Mountain record begins with a cool period from 18,000-13,500 cal. yr BP, indicated by a dominance of *Erica* and Restionaceae pollen (Neumann et al., 2014). This period is not covered by the pollen record for the eastern Lesotho sites. It is followed by a period of progressive warming from 13,500 cal. yr BP, with the warmest conditions attained by 7,500 cal. yr BP, indicated by a decrease in the relative abundance of fynbos species (Neumann et al., 2014). The multi-proxy records for eastern Lesotho do not suggest particularly warm conditions in the early Holocene, with the Sekhokong record rather indicating a cold period at ~12,660 cal. yr BP, and the Mafadi Wetland record providing evidence for a cold period from ~8,140-7,580 cal. yr BP (*Figure 6.14*). While slightly warmer periods may not be detected in the proxy records of the high altitude sites, as temperatures remain below the threshold for less cold tolerant plants and diatoms, one would expect marked cold events to be detected at both the high and low altitude sites. The pollen and diatom records from Sekhokong and Mafadi Wetland both indicate warmer conditions after ~7,500 cal. yr BP, with a decrease in *Fragilaria* species and an increase in the diversity of pollen taxa (*Figures 6.2, 6.3, 6.6, 6.7*). It is notable that the progressive warming

commenced earlier at Sekhokong than at Mafadi Wetland, potentially indicating a delay in the Holocene Altithermal with altitude, which would imply a strengthening of lapse rates during this period (*Figure 6.14*). Compared to other palaeoenvironmental records for Lesotho, climate reconstructions from the sediment record for Sekhokong (Sani Top) suggest warm conditions until 9,000 BP (Marker, 1994), while isotope records from western Lesotho indicate warm conditions until 10,500/ 10,200 cal. yr BP, interrupted by a cool period, but re-established by 8,000 cal. yr BP (Smith et al., 2002; Roberts et al., 2013; *Figure 6.14*).

The Mahwaqa Mountain record thereafter suggests fluctuations in moisture, but warm conditions until 4,600 cal. yr BP (Neumann et al., 2014). This is in broad agreement with the results for eastern Lesotho, although fluctuations in both precipitation and temperatures are detected at all three sites (*Figure 6.14*). The driest period in the profile from Mahwaqa Mountain is inferred to occur from 4,600-3,500 cal. yr BP (Neumann et al., 2014). For Sani Valley, Sekhokong and Mafadi Wetland, the period of driest conditions occurs earlier, at ~5,500-4,000 cal. yr BP, with moist conditions established at all three sites by ~3,750 cal. yr BP (*Figure 6.14*). This may reflect the influence of the escarpment in blocking moisture, as the Mahwaqa Mountain site is situated at a lower altitude to the east of the Great Escarpment, and would thus receive moisture from the Indian Ocean, which cannot always reach the Lesotho highlands, particularly during periods of strengthened or more frequent coastal lows (Scott et al., 2012; Neumann et al., 2014). This dry period is followed by wet conditions at Mahwaqa Mountain from 3,500-800 cal. yr BP (Neumann et al., 2014), which is consistent with results from Mafadi Wetland and Sani Valley, although marked by pronounced dry pulses, but is not consistent with the multi-proxy record for Sekhokong which suggests dry conditions throughout this period (*Figure 6.14*). The Mahwaqa Mountain record concludes with the wettest conditions in the profile from 1,000 cal. yr BP to present (Neumann et al., 2014). This is consistent with the Braamhoek record (Norström et al., 2009, 2014, Finné et al., 2009) and for Sani Valley, but inconsistent with Sekhokong and Mafadi Wetland, both of which are consistent with Marker (1994), indicating dry conditions during this period (*Figure 6.14*). Evidence for pine exists in this final period (Neumann et al., 2014), consistent with the small percentage of pine detected in the pollen records from eastern Lesotho.

6.5 Regional to Global Comparisons

There is considerable regional variation in the palaeoenvironmental records for southern Africa, influenced by synoptic patterns, altitude, microclimates, and the contemporary environment of the site (Scott, 2002; Chase & Meadows, 2007; Burrough & Thomas, 2013), which has been highlighted by the differences between the environmental reconstructions for Sani Valley, Sekhokong and Mafadi Wetland. Climate models require high resolution, site specific data in order to facilitate greatest possible model certainty, and so the detection of regional variability in climate records is not only an accurate reflection of the contemporary conditions, but provides valuable information to ensure the development of models with large confidence margins (Jones et al., 2009). There are, however, large amplitude changes which have occurred during the Holocene, many of which have been prolifically reported for the Northern Hemisphere (Mayewski et al., 2004). It is of interest to determine whether these climate events are detected in the proxy records for the eastern Lesotho highlands, as the extent of teleconnections between the Northern and Southern Hemispheres is of further benefit to climate modellers, and to understanding the palaeoenvironmental history of southern Africa. This section first explores the global significance of the proxy records in this study. Thereafter, the large-amplitude global Holocene climate events are detailed, exploring their presence or absence in the eastern Lesotho record and in published palaeoenvironmental reconstructions from sites elsewhere in southern Africa.

6.5.1 Comparison of Proxy composition

Changes in the sedimentary record, while necessary to be interpreted in a wetland context, are not unique to a particular location, region or country. Regarding the diatom composition at Sani Valley, Sekhokong and Mafadi Wetland, there are three groups of species worth comment due to their presence in similar environments elsewhere in the world. The first are the *Fragilaria* species, which are interpreted as indicative of cold conditions when they dominate the diatom profiles in eastern Lesotho due to their ice- and snow-tolerance. These are cosmopolitan species, which appear in a range of high stress environments, but are dominant in high alpine wetlands and lakes in a range of locations, including Uganda (Panizzo et al., 2007; McGlynn et al., 2010), Switzerland (Lotter & Bigler, 2000; Ohlendorf et al., 2000), Canada (Karst-Riddoch et al., 2005), Finland (Shala et al., 2014) and Siberia

(Westover et al., 2006). The second are the pair of planktonic *Aulacoseira ambigua* and aerophilic *Hantzschia amphioxys,* which interchange throughout profiles to indicate periods of wet and dry conditions, at sites in South Africa (Finné et al., 2009), Mozambique (Sitoe et al., 2015), Australia (Gell & Little, 2007), and Canada (Hargan et al., 2015). The third is *Gomphonema parvulum*, which has a rapid increase in relative abundance at Sani Valley and Sekhokong in the most recent 200 years, and is interpreted to indicate an increase in livestock populations in the region. This species similarly appears predominantly in the top section of sediment profiles from South Africa (Finné et al., 2010), Tanzania (Barker et al., 2003), and Australia (Gell & Little, 2007). All of the diatom species identified at Sani Valley, Sekhokong and Mafadi Wetland have been previously recorded in Lesotho (Schoeman, 1973) and South Africa (Harding & Taylor, 2011). Such similarities within comparable environmental settings, environmental conditions, and environmental fluctuations elsewhere in the world demonstrate the value of this proxy for environmental reconstructions, and the global similarities in species. While the pollen record is specific to the vegetation of southern Africa, the dominant Poaceae, Cyperaceae and Asteraceae are common to wetland conditions globally, with shifts between Poaceae and Cyperaceae representing a cosmopolitan indicator of shifts between dry and wet conditions (Gasse & Van Campo, 1998).

6.5.2 Comparison the Synchronicity of Climatic Events

The palaeoenvironmental record for Sekhokong has a basal date of ~13,180 cal. yr BP, which marks the terminal phase of deglaciation following the LGM. Carbon isotope records from the Makapansgat speleothem, located in the SRZ of South Africa (*Figure 2.5*), indicate a shift towards wetter conditions during this phase, with the maximum precipitation attained by 13,000 cal. yr BP (Holmgren et al., 2003). This coincides with wet conditions at the start of the Sekhokong record. This is notable as the speleothem record suggests a progressive increase in moisture following the LGM (Holmgren et al., 2003), whereas evidence of glacial moraines in eastern Lesotho, and the snow accumulation requirements for these features, suggests a relatively wet LGM in the eastern Lesotho highlands (Mills et al., 2012). The variation between the wet LGM in Lesotho and dry conditions for the northern region of southern Africa is explained by a strengthening of the westerly belt (Finné et al., 2010; Mills

et al., 2012), but the convergence of wet conditions by 13,000 cal. yr BP may indicate a subsequent southerly shift of the ITCZ (Truc et al., 2013; Singarayer & Burrough, 2015).

The deglaciation period globally is interrupted by abrupt cold conditions from 13,000-11,500 cal. yr BP, driven by meltwater pulses in the Northern Atlantic, termed the Younger Dryas (Peteet, 1995; Mayewski et al., 1996; Abell & Plug, 2000). The marked cold period detected in the Sekhokong record by an increase in *Fragilaria* species and a decrease in pollen taxa diversity is dated to approximately ~12,660 cal. yr BP, which falls within this period. Evidence for this event is, however, scarce outside of the North Atlantic region, and often termed a Northern Hemisphere phenomenon (Abell & Plug, 2000). While isotope records from the archaeological sites in western Lesotho do not provide supporting evidence for this cold event with inferred warm conditions spanning this time period (Smith et al., 2002; Roberts et al., 2013), this may be a result of the cold dry conditions discouraging settlement during this period, and consequently not accumulating material in the excavated settlement. Evidence in support of a Younger Dryas event exists for other sites in southern Africa, including oxygen isotopes from mollusc shells at Elands Bay (Cohen et al., 1992), archaeological isotope evidence from Bushman's Rock Shelter in Limpopo Province, South Africa (Abell & Plug, 2000), a re-analysis of pollen data from Wonderkrater (Thackeray & Scott, 2006), and isotope records from hyrax middens in the Cederberg (Quick et al., 2011; Chase et al., 2015b). Thus, while the event was centred in the northern Atlantic, there is increasing evidence for a concurrent depression in temperatures in southern Africa, for which the Lesotho record provides new support.

A similar short-lived cold period driven by a large meltwater pulse in the northern Atlantic Ocean, often assumed to have influenced climates only in the Northern Hemisphere, is the '8.2 kyr' event (Mayewski et al., 2004; Alley & Ágústsdóttir, 2005). The very cold conditions which characterise the commencement of the Mafadi Wetland record from ~8,140-7,850 cal. yr BP, inferred from the dominance of ice-tolerant *Fragilaria pinnata/ construens*, coincides with this event. Although the Sekhokong record spans this period, there is a sampling gap from ~9,020-7,460 cal. yr BP, and hence cold conditions cannot be further corroborated for this period in eastern Lesotho. Isotope records from archaeological settlements in western Lesotho do, however, provide evidence for a cold event over the

same time period (Smith et al., 2002). Moreover, the phytolith records from Braamhoek indicate an increase in C_3 vegetation at 8,000 cal. yr BP (Finné et al., 2010). The Makapansgat speleothem record provides evidence for a cool event at 8,500 cal. yr BP (Holmgren et al., 2003), which may be synchronous with these events due to age uncertainties (Norström et al., 2009). Evidence for the '8.2kyr' event has most recently been reported for the southwestern Cape (Chase et al., 2015b). It would therefore appear that the cold events in the northern Atlantic due to meltwater pulses are detected in South Africa, providing valuable information regarding ocean heat transport during this deglaciation and early Holocene period.

The overall warming period associated with deglaciation continues until optimal conditions at the Holocene Altithermal (Wanner et al., 2015). The timing of this event is unclear, with discrepancies for much of southern Africa, but it appears broadly to span the period 7,500-6,500 cal. yr BP (Holmgren et al., 2003; Truc et al., 2013; Neumann et al., 2014; Wanner et al., 2015). There is no clear warm signal coinciding with this event for any of the eastern Lesotho sites, although a slight increase in plant and diatom species diversity, and decrease in *Fragilaria* species is noted for the three sites. This may be due to the cold temperatures at the sites, which would require substantial warming to exceed the thresholds of less cold-tolerant taxa and encourage range-shifts upslope. It is, however, notable that all three sites demonstrate a greater increase in pollen taxa diversity in the late Holocene than in the period coinciding with the Holocene Altithermal. This may indicate that lapse rates during this period were stronger than today, resulting in persistent cold conditions at high altitudes (Grab, 1997). It is notable, given this hypothesis, that there was no clear indication for Holocene Altithermal conditions at the lower-altitude Braamhoek Wetland (Norström et al., 2009, 2014; Finné et al., 2010), yet pollen records from the similarly low altitude Drakensberg site at Mahwaqa Mountain suggests a clearly defined Holocene Altithermal maximum at 6,500 cal. yr BP (Neumann et al., 2014). Unfortunately the isotope records from the archaeological shelter sites in western Lesotho do not span this period.

There has been recent discussion regarding the existence of the African Humid Period in southern Africa (Chase et al., 2009; Burrough & Thomas, 2013). This event spans the period 14,500-5,500 cal. yr BP, and has been detected in a range of records from western and

tropical Africa (Burrough & Thomas, 2013). Evidence from hyrax middens in Namibia for humid conditions during this period have raised hypotheses of such an event extending as far as 23°S (Chase et al., 2009), yet a review of palaeoclimatic records from southern Africa, with a particular focus on dryland conditions, is not in support of this view (Burrough & Thomas, 2013). The records from Sekhokong and Mafadi Wetland broadly suggest the presence of relatively wet conditions until ~6,500 cal. yr BP. This period is, however, marked by pronounced dry events. Precipitation reconstructions for other sites in eastern Lesotho similarly indicate marked dry periods throughout this time period. The prolonged wet periods in eastern Lesotho during this period would thus rather appear to be coincident with, rather than indicators of, an African Humid Period.

Climate and environmental change over the past 2,000 years is of interest at local through to global scales due to the more rapid climate fluctuations and the increase in the anthropogenic influence on the environment (Mayewski et al., 2004; Wanner et al., 2008, 2014). The climate event during this period which has attracted the greatest discussion in the southern African palaeoenvironmental context is the Little Ice Age, a short-lived cold event that occurred between AD 1300-1800 (Tyson et al., 2000; Wanner et al., 2008, 2015; Harrison et al., 2014). A peak in *Fragilaria* species and a decrease in pollen taxa diversity indicates an abrupt cold period at ~150 cal. yr BP for all thee eastern Lesotho sites, with a most prominent signal in the Sani Valley record. There is far more evidence for a Little Ice Age cold event in southern Africa (cf. Talma et al., 1974; Herbert, 1987; Talma & Vogel, 1992; Tyson & Lindesay, 1992; Brook et al., 1999; Holmgren et al., 2003; Sundqvist et al., 2013; Zinke et al., 2014), than there is for the Younger Dryas or '8.2kyr' event. Debate focuses more on precipitation during this period, with a current understanding that dry conditions occurred in the SRZ (Lee-Thorpe et al., 2001; Holmgren et al., 1999; Ekblom et al., 2008; Gillson & Ekblom, 2009; Neumann et al., 2010), but wet conditions in the WRZ (Stager et al., 2012; Weldeab et al., 2013). The multi-proxy results from Sani Valley would suggest that this event coincided with a period of wetter conditions, with a peak in Cyperaceae pollen. Results from Mafadi Wetland would support this inference, with the colder conditions contemporary with an increase in planktonic and facultative planktonic species, and an Asteraceae: Poaceae ratio indicative of a return to winter rainfall conditions. This would imply that the westerlies which dominate the WRZ were strengthened during this

period, yet not sufficiently to influence the interior plateau of South Africa, supporting Tyson and Lindesay's (1992) original hypothesis. Notably, for Sekhokong, this period is associated with proxy evidence for dry conditions. However, the sampling frequency was low during this period (1 sample per 500 years), and hence a rapid fluctuation in moisture would not have been detected. The second climate event during this period is the Medieval Warm Period, which precedes the Little Ice Age, occurring between AD 1000-1300 (Wanner et al., 2008). The only evidence in southern Africa for a Medieval Warm Period derives from high resolution speleothem isotope records (Tyson et al., 2000; Holmgren et al., 2003). It is therefore notable that warm conditions are inferred from a particularly low relative abundance of *Fragilaria* species and increase in pollen taxa diversity at both Sani Valley and Mafadi Wetland for this period. The Sekhokong record does not have samples with age-dates coinciding with this event. Regarding precipitation, a period of greater stability is noted for central southern Africa from ~2,000 cal. yr BP to present (Burrough & Thomas, 2013). The results from Sani Valley and Mafadi Wetland, for which a high temporal resolution of samples was achieved for this period, directly contradict these results, indicating rapid high amplitude fluctuations in precipitation throughout the period, supported at a global scale by Wanner et al. (2008). Evidence for increased anthropogenic influence on the local and regional environment, similar to that inferred from the pollen and diatom records at Sani Valley and Sekhokong, have been reported for a range of locations from AD ~1800 (cf. Baxter & Meadows, 1999; Neumann et al., 2008; Norström et al., 2009; Reinwarth et al., 2013; Neumann et al., 2011, 2014).

6.6 Future Research Trajectories

This research forms a pioneering study into the use of a multi-proxy approach to develop a continuous palaeoenvironmental reconstruction for the eastern Lesotho highlands region. The benefit of initiating such work in a region is that one is presented with a large choice in the selection of proxies and sites, factors that are more limited for regions in which palaeoenvironmental work has already been undertaken. There are, however, some methodological challenges in developing the optimal research approach for the study, particularly for a region where access to many of the sites is difficult. The viable coring depth, preservation of proxies, and the stratigraphic integrity of the sequences were

unknown before the field and laboratory work was undertaken. The presence of well-preserved fossil pollen and diatoms in the profiles from all three sites was unexpected, and greatly contributed to the richness of the results and subsequent palaeoenvironmental inferences. It has been hypothesised repeatedly over recent decades that the eastern Lesotho bogs are well suited to pollen and diatom preservation (Van Zinderen Bakker, 1955; Schoeman, 1973; Esterhuysen & Mitchell, 1996; Mitchell, 1996), which this study confirms for three discrete study sites, located in varied topographic settings at altitudes separated by 400m. Future pollen, diatom and sedimentary based palaeoenvironmental work consequently can, and should, be undertaken across a greater number of wetlands across eastern Lesotho, with less uncertainty regarding the presence and preservation of these proxies.

The eastern Lesotho highlands, referred to by Van Zinderen Bakker (1955) as the 'barren boggy wastes', is characterised by a large network of wetlands (Schwabe, 1995; Grundling et al., 2015). This provides potential for future work in the region. Analysis of more wetlands would be valuable in resolving the role of micro- and macro-topography, slope aspect, altitude and associated lapse rates, the potential role of fire, and the hydrological systems, in the spatial variation between palaeoenvironmental reconstructions in this study (Jones et al., 2009). A valuable approach to improve the understanding of regional variations in palaeoclimates is through conducting studies along transects spanning regions of known climate and environmental variability (Chase & Meadows, 2007). For the eastern Lesotho highlands, transects spanning large altitudinal ranges are of greatest value, particularly if they can be combined with previous studies from Mahwaqa Mountain (Neumann et al., 2014), Braamhoek Wetland (Norström et al, 2009, 2014; Finné et al., 2010), or with the palaeoenvironmental reconstructions for western Lesotho, particularly where such transects extend through the contemporary tree-line.

Accurate climate forecasting requires an understanding of regional microclimates (for which there still remains insufficient meteorological data) of the interaction between the climate and environment, and of long-term climate and environmental change (Jones et al., 2009). Such work would thus be of academic value, and would assist in the adaptation to climate change in this hydrologically important region. An increase in the number of study sites

investigated in eastern Lesotho should also include revisiting sites where archaeological and palaeogeomorphological work has been undertaken, to corroborate the evidence presented through these approaches, and to fill in the temporal gaps that arise from the pulsed nature of events.

A standalone pioneering study inevitably faces time and cost constraints, which limit the scope of a project. However, through the implementation of a pioneering study, a more informed approach can be made for future work, regarding site and proxy selection, and fieldwork methods, to make the most efficient use of time and money. In addition to increasing the number of wetland sites investigated in eastern Lesotho, increasing the number of proxies used in developing the palaeoenvironmental reconstructions would facilitate the corroboration of results, and the interpretation of a greater range of climate and environmental variables (Battarbee, 2000; Jones et al., 2009; Norström et al., 2014). The three proxies used in this study were selected on the basis of their confirmed presence in eastern Lesotho wetlands (Van Zinderen Bakker, 1955; Van Zinderen Bakker & Werger, 1974), continued calls for their analysis (Mitchell, 1996a), and the large range of palaeoenvironmental evidence available. Of value for comparison to the prolific archaeological work undertaken in Lesotho, would be the inclusion in continuous palaeoenvironmental reconstructions from sediment profiles of the proxies used in archaeological excavations in the region: isotopes, charcoal and phytoliths (Esterhuysen & Mitchell, 1996). Of these, isotopes offer the greatest value, as inferences on temperature changes in the highlands can most accurately be derived. It would be of particular interest to determine the oxygen isotopes from cleaned diatoms in the eastern Lesotho samples, from this and future studies, as it would afford a high resolution comparison of temperature and precipitation records for the site (Leng & Barker, 2006). Phytoliths arguably offer little additional value, as the eastern Lesotho highlands are dominated by C_3 vegetation, and the region is unlikely to have warmed sufficiently to promote considerable growth of C_4 plants from which temperature changes could be inferred (Finné et al., 2009; Parker et al., 2011). Predominant information would therefore concern the division between grasses and woody species, which can be obtained from the existing pollen records (Finné et al., 2009). The pollen slides prepared for this study have confirmed the presence of microcharcoal particles, which would be of value to investigate changes in fire regimes, and non-pollen

palynomorphs which could provide further information relating to the wetland conditions (Finch et al., 2009; Ekblom & Gillson, 2010; Van Geel et al., 2011). Proxies which may be present in the eastern Lesotho wetlands, and which would be of value to investigate, include geochemistry, biomarkers, ostracods, chironomids and cladocera. Recently, a project has been initiated in collaboration with researchers from the University of Stockholm, Sweden, to explore the geochemistry of sediment profiles from two wetlands in eastern Lesotho, in close proximity to the Sani Valley site, with a particular emphasis on detecting dust signals. Such international collaboration is essential in achieving these future research goals, particularly given the comparatively limited research capacity in southern Africa.

An increase in the number of wetland sites investigated, and in the number of proxies used, requires the support of high resolution age-dating, and the surveying of the contemporary flora of the local and regional environment. The marked changes in the accumulation rates for the sediment profiles obtained for Sani Valley, Sekhokong and Mafadi Wetland highlight the importance of high resolution dating. Diatomite beds (as described in *Section 5.4.6*), which may equally have developed through the slow, uniform accumulation of diatoms over thousands of years, or in one or many abrupt events spanning a few decades, further require a well constrained chronology to be of palaeoenvironmental value. Transfer functions are important to determining the environmental significance of fluctuations in the relative abundance of species, and relative changes between two groups. With disagreements in interpretation, such as the inference of Asteraceae pollen concerning seasonality (Norström et al., 2009; Neumann et al., 2014), the need for detailed evidence from the contemporary environment to inform these inferences becomes apparent.

For the broader southern African palaeoenvironmental community, this study further confirms the benefits of multi-proxy work, a methodological trajectory that is slowly growing, but which should be more actively pursued. Corroborating evidence across pollen, diatom and sediment records, and the improved resolution of environmental shifts which were detected, have contributed to the accuracy and confidence of inferences presented here. This study also demonstrates the value of diatoms as a proxy, and our unexpected discovery of diatoms in the profiles from Sani Valley and Sekhokong warrants greater

exploratory work to determine their abundance in sediment profiles from other southern African wetlands. With a considerable history of diatoms use in contemporary water quality assessments, and archives of diatom flora for much of southern Africa (Schoeman, 1973; Harding & Taylor, 2011), it is unfortunate that there has been such sparse use of this proxy in palaeoenvironmental studies (Partridge et al., 1993). Finally, through the value in corroborating climate and environmental inferences made from biological proxies, the often higher resolution fluctuations captured, and the information regarding the microtopographical setting which is provided, this study highlights the value of including sedimentary analyses in palaeoenvironmental reconstructions.

7. Conclusion

7.1 Introduction

The eastern Lesotho highlands are geographically distinct as the highest altitude region in southern Africa (Borg, 2012; Grundling et al., 2015). The climate of the highlands is of regional significance as they represent one of the few catchments where precipitation exceeds evaporation, and ensure the sustained supply of water to the South African interior via the Lesotho Highlands Water Scheme (Nüsser & Grab, 2002; Letšela, 2008; Grundling et al., 2015). The region hosts a population heavily dependent on subsistence agriculture, and are thus vulnerable to climate change and environmental threats (Ziervogel & Calder, 2003; Bisaro et al., 2010; Mpholo et al., 2012). An understanding of the nature and rate of climate change throughout the Holocene is thus of considerable value for the region. However, such research remains sparse, and the long-term climatic record for the region rests on inferences made from archaeological and palaeogeomorphological evidence, which for both disciplines stem from discrete and often extreme climatic events. To meet this knowledge gap of both academic and adaptation significance, the primary objective of this study was to develop a multi-proxy Holocene palaeoenvironmental and palaeoclimatic reconstruction for eastern Lesotho, using sediments. This was undertaken through the analysis of sediment properties, in conjunction with pollen and diatoms from sediment cores extracted from three sites in eastern Lesotho, the results and inferences of which are presented in this thesis. This chapter synthesises the work presented in the preceding chapters, first outlining the extent to which the study aims were achieved, then exploring the regional significance of the work, presenting an outline of the avenues for future work, and providing a final synopsis.

7.2 Achievement of Study Objectives

1) *To determine suitable sites, and extract sediment cores from peat bogs at three locations in eastern Lesotho constrained by altitude, latitude and depth of sediment.*

The three study sites selected for this study span a range of time periods, micro-topographies, and altitudes to facilitate both the comparison of results between sites, and

regional corroboration of the reconstructed palaeoenvironmental history. Sani Valley and Sekhokong are situated at comparable altitudes, and within a 10km radius, but span different time periods, from 13,180 cal. yr BP to present at Sekhokong, and from 6,200 cal. yr BP to present at Sani Valley. This ensures that the entire Holocene period is covered, with greater sampling frequency afforded for the late Holocene. Mafadi Wetland is altitudinally situated approximately 400m higher than Sani Valley and Sekhokong, and consequently provides a site from which altitudinal comparisons can be made. With a basal date of 8,140 cal. yr BP, Mafadi Wetland provides evidence for a large portion of the Holocene, yet at a higher resolution than the results for Sekhokong. While Sekhokong derives sediment from the adjacent mountain slopes, and receives pollen from a large geographic radius due to the large open valley geomorphology of the region surrounding the wetland, the Sani Valley and Mafadi Wetlands reflect more local conditions across all three proxies.

2) *To determine the species composition, richness and frequency from fossil pollen grains and diatoms isolated from high resolution sampling of discrete layers subsampled from the cores from each site;*
    a. *To determine changes in the frequency of each species throughout the depth of each core, and infer any dominant shifts in vegetation*
    b. *To determine differences in species composition and change between the study sites*

The results of the pollen analysis for Sani Valley, Sekhokong and Mafadi Wetland are presented in *Sections 5.2.3, 5.3.3* and *5.4.3* respectively. The results of the diatom analysis from these three sites are presented in *Sections 5.2.4, 5.3.4* and *5.4.4* respectively. The inference of the environmental and climatic significance of changes in the pollen and diatom communities, and discussions regarding the differences in species composition, richness and diversity between the three sites are discussed in *Section 6.3*. In summary, there are considerable similarities in the pollen and diatom composition for the three sites, and all three sites reflect pronounced shifts between dry and wet conditions with associated fluctuations in the wetland expanse. The pollen results do not reflect contemporary variations in plant species with altitude due to the family- to genera-specific resolution which pollen analysis affords. Pollen and diatom results indicate a decrease in species diversity between the lower altitude Sani Valley and Sekhokong sites, and the high altitude

Mafadi Wetland. This is inferred to be a consequence of lower temperatures at Mafadi Wetland given its higher altitude. The presence of *Chrysocoma* pollen throughout the Sani Valley profile is notable given the significance of the species *Chrysocoma ciliate* in invasives debates.

3) *To determine the sediment characteristics in each of the subsampled sediment layers, including the organic and carbonate composition and the particle size distribution of each sample*
    a. *To determine changes in the sediment properties throughout the core*
    b. *To determine changes in depositional environments throughout the core*

The results of sediment characteristics for Sani Valley, Sekhokong and Mafadi Wetland are presented in *Sections 5.2.2, 5.3.2* and *5.4.2* respectively. The inference of environmental and climatic conditions, and significance of changes in sedimentary characteristics of each profile, is discussed in *Section 6.3*. Fluctuations in the percentage of gravel- and sand-sized sediment particles relative to clay- and silt-sized particles, and changes in the percentage composition of organic material in the sediment record, corroborate the climate and environmental inferences made on the basis of pollen and diatom results for each of the three study sites.

4) *To temporally constrain the observed changes in sedimentology and proxy species composition through AMS dating of selected subsamples from cores from each of the study sites.*

A total of 21 radiocarbon AMS dates were obtained to temporally constrain the proxy results and palaeoenvironmental reconstructions for this study. These included five for Sani Valley (of which only four could be used), 11 for Sekhokong, and five for Mafadi Wetland. The calculation of accumulation rates, and the inference of dates for the samples at depths between these dates was undertaken using the BACON model. The acquisition of age-dates for samples across a range of depths in each of the profiles highlighted marked periods of slower accumulation, which were largely consistent for the three sites, and are likely to hold some climatic significance.

5) *To infer changes in past environments and climates from the shifts in species composition of fossil pollen and diatoms, and from the sedimentological changes through statistical analysis*
    a. *To determine the dominant environmental drivers responsible for the changes in proxies throughout the time period represented by the sediment cores*
    b. *To use the multiple proxies to corroborate results, and to provide information on a greater range of environmental variables.*

The statistical analysis of the results from the laboratory analysis for each of the environmental proxies is presented in *Chapter 5.* The palaeoenvironmental reconstruction for the three study sites, and the broader eastern Lesotho region, is presented in *Chapter 6,* following the theoretical and literary basis from which these inferences are made. A synthesis of this inferred palaeoenvironmental and palaeoclimatic reconstruction for the region is graphically presented in *Figure 6.14*. This commences with the late Pleistocene record for Sekhokong, which begins with a wet period from 13,180-13,080 cal. yr BP, followed by a dry period from 13,080-12,830 cal. yr BP, and a second wet event, commencing with a cold pulse, from 12,660-10,850 cal. yr BP. From 10,550-6,420 cal. yr BP, the Sekhokong record indicates dry conditions which slowly transition to a warmer and wetter climate. The record from Mafadi Wetland commences during this period, indicating cold, wet conditions from 8,140-7,580 cal. yr BP, followed by warmer dry conditions from 7,520-6,680 cal. yr BP. Thereafter, considerable differences are noted in the environmental reconstructions for the three sites. For Sekhokong, warm, dry conditions are inferred for the period 6,420-6,000 cal. yr BP, followed by cold and wet conditions from 6,000-5,450 cal. yr BP. Warm, dry conditions occur slightly earlier at Mafadi Wetland, extending from 6,160-5,700 cal. yr BP, coinciding with the commencement of a longer wet period at Sani Valley, occurring from 6,200-4,900 cal. yr BP. At Sekhokong, this is followed by a dry, warm period from 5,450-3,700 cal. yr BP. At Sani Valley, a dry period is evident from 4,770-4,470 cal. yr BP, but followed by a cold, wet period from 4,460-2,260 cal. yr BP. At Mafadi Wetland, these cool, wet conditions cover a considerably longer period, from 5,600-1,100 cal. yr BP. This more recent part of the period coincides with similarly cool, wet conditions at Sekhokong, from 3,650-1,200 cal. yr BP. By contrast, dry conditions are evident at Sani Valley, from 2,260-1,350 cal. yr BP. For all three sites, the period from 1,000 cal. yr BP to present is characterised by progressive drying, with discrete wet events apparent in the higher

resolution Sani Valley record. A pronounced cold event is detected at all three sites leading up to ca. 150 BP, followed by progressive evidence of human disturbance.

7.3 Regional Significance

The climate of the study sites is of regional significance due to the reliance of the South African interior on water from the Lesotho Highlands Water Scheme (Grundling, 2015). The region has acute climate sensitivity as a large proportion of the population is reliant on subsistence agriculture (Bisaro et al., 2010; Mpholo et al., 2012). Adaptation to climate change is thus of importance to ensure sustainable livelihoods of local populations and the economic viability of the country (Nüsser & Grab, 2002; Ziervogel & Calder, 2003). Timely and effective adaptation to climate change requires accurate climate forecasts ranging from seasonal to decadal scales, and the effective communication of these forecasts to the interested and affected parties (Ziervogel, 2004; Jones et al., 2009). However, such forecasts require high-resolution contemporary climate data, and the nature and rate of past climate change (Jones et al., 2009). As meteorological stations remain sparse for much of the eastern Lesotho highlands, and provide an inadequate historical record (Boelhouwers & Meiklejohn, 2002; Grab & Nash, 2010), an understanding of the nature of microclimates and altitudinal influence are necessary, for which the importance of proxy-based palaeoclimatic and palaeoenvironmental records is heightened.

The climate and environmental history of the individual study sites selected for this study is of further regional interest. The Sani Valley and Sekhokong sites are located within close proximity to the Sani Top border post and the Sani Top Lodge and Backpackers, and thus, relative to other parts of the eastern Lesotho highlands, the area receives a large number of tourists (Grab & Nüsser, 2001). To an extent, the continued success of this tourist destination is reliant on contemporary climate conditions, and the relatively pristine environment (Grab & Nüsser, 2001). Mafadi Wetland is of regional interest, as at 3,400m.asl, it is the highest altitude wetland in southern Africa. The environmental and climatic conditions at this wetland represent the most extreme high stress environment resulting from altitude, and presently represent the altitudinal threshold for the support of plant life.

The broad agreement in the palaeoenvironmental reconstructions for each of the three study sites, but the finer-scale fluctuations in climate which are detected for individual sites, highlights the extent to which palaeoenvironmental change is geographically heterogeneous, and the importance of micro-climates, the topographical setting of the site, and the role of altitude in exceeding the climatic thresholds of vegetation communities (*Figure 6.14*). Comparisons with previously published palaeoenvironmental reconstructions for the region further confirm these local variations in climate and environmental conditions, emphasising the need for continued palaeoenvironmental research in the region so as to better resolve these spatial and altitudinal variations in the detection of climate changes (*Figure 6.14*). To enhance understanding of vegetation thresholds associated with changes in the proxy record, contemporary climate and plant surveys for each of the study sites are essential. From a climate modelling perspective, these regional variations in the climate record are valuable for improving the resolution and accuracy of projections (Jones et al., 2009). An improved resolution of climate models is especially important in regions such as the eastern Lesotho highlands, characterised by considerable variations in topography, climate and ecology across short distances.

While considerable regional variation in climatic reconstructions is noted, both for the sites in this study and in comparison with previously published work, this study also provides evidence for globally synchronous climate events (*Figure 6.14*). Indicated predominantly by the relative abundance of *Fragilaria* diatom species, and in the diversity of pollen taxa, the eastern Lesotho palaeoenvironmental reconstruction presented in this study provides relatively strong evidence for the Younger Dryas, '8.2 kyr', and the Little Ice Age cold events. A weaker signal is detected for warm events, including tentative evidence for the Holocene Altithermal, with peak warming at 7,460 cal. yr BP, and for the Medieval Warm Period. While southern African analogues of many of these events have been confirmed from palaeoclimatic evidence elsewhere in southern Africa, with the exception of the '8.2 kyr' event detected in the western Lesotho isotope record (Smith et al., 2002), this represents the first confirmation of these events for Lesotho.

7.5 Application of Findings

The trajectories for future scientific work have been outlined in Section 6.6, based on the difficulties and successes of this project. In addition to continued palaeoenvironmental research in the region, it is important that results from this study be translated to accessible information for the population of Lesotho, and for the broader region of southern Africa. The agreement, on which the research permit for the work was granted, requires sharing the findings of this research with the Lesotho Government's Department of the Environment. The communication of these findings to the Lesotho Government, and the local population, is of importance in giving practical value to the otherwise solely academic pursuit which such a study entails. Findings from this study, together with existing work on contemporary climate and continued research into high resolution palaeoclimatic records for the region, are of potential value to climate modellers, in providing reconstructions of past climate cycles, and comparisons between sites with varying altitudes and micro-climates, which will assist with improving the resolution and accuracy of climate projections for the region. Reconstructions of the cycles between dry and wet periods throughout the Holocene for the three study sites improve the understanding of long term moisture fluctuations for the region, which may be of value in adaptation for sustainable maintenance of the Lesotho Highlands Water Scheme under continued climate change, with the hope of ensuring the continued economic sustainability of Lesotho. Thirdly, the environmental reconstructions for the three sites in this study provide valuable information on the climate and anthropogenic tolerances of vegetation communities in the region, which has the potential to improve the management of the eastern Lesotho wetlands. The preservation of these wetlands, in turn, is essential to any future palaeoenvironmental research in the region. Details regarding the dissemination of this knowledge have not yet been determined, but this is a priority once this study is complete.

7.6 Synthesis

This study analyses changes in the pollen, diatoms and the sedimentary properties, from subsampled sections of sediment profiles extracted from wetland sites at Sani Valley, Sekhokong and Mafadi Wetland in the eastern Lesotho highlands. These sediment profiles

are temporally constrained by a set of 21 radiocarbon AMS dates. Palaeoenvironmental reconstructions for each of these sites are made on the basis of inferences concerning the relative changes in these proxies. By adopting a multi-proxy approach, this study allows for the corroboration of the reconstructed climate and environmental histories for each of the sites, and facilitates the investigation into a wider range of environmental conditions. The study finds marked variability in precipitation and temperature in eastern Lesotho throughout the Holocene, and a notable influence of human disturbance in samples from the most recent 100 years. Many of the climate fluctuations are relatively unique to eastern Lesotho, and to the individual sites, yet temperature events of global significance are also detected, including the Younger Dryas, the '8.2kyr' event, the Holocene Altithermal, and the Little Ice Age. The success of this pioneering study in developing an environmental reconstruction for the eastern Lesotho highlands, strengthens the call for continued palaeoenvironmental research in the region.

REFERENCES

Aaby, B. (1976). Cyclic climatic variations in climate over the past 5 500 yr reflected in raised bogs. *Nature,* 263(5575): 281-284.

Abell, P.I. and Plug, I. (2000). The Pleistocene/ Holocene transition in South Africa: evidence for the Younger Dryas event. *Global Planetary Change,* 26: 173-179.

Alley, R.B., Mayewski, P.A., Sowers, T., Stuiver, M., Taylor, K.C. and Clark, P.U. (1997). Holocene climatic instability: A prominent, widespread event 8200 yr ago. *Geology,* 25(6): 483-486.

Alley, R.B. and Ágústsdóttir, A.M. (2005). The 8k event: Cause and consequences of a major Holocene abrupt climate change. *Quaternary Science Reviews,* 24: 1123-1149.

Ambrose, D.P. (1976). The Guide to Lesotho. *Winchester Press*: Johannesburg.

Anderson, N.J. (2000). Miniview: Diatoms, temperature and climate change. *European Journal of Phycology,* 35(4): 307-314.

Andren, E., Clarke, A., Telford, R., Weckstrom, K., Vilbaste, K., Aigars, J., Conley, D., Johnsen, T., Juggins, S. and Korhola, A. (2007). Defining reference conditions for coastal areas in the Baltic Sea. *Nordic Council of Ministries:* Copenhagen.

Andrews, P. and Bamford, M. (2008). Past and present vegetation ecology of Laetoli, Tanzania. *Journal of Human Evolution,* 54: 78-98.

Antoniades, D., Douglas, M.S.V. and Smol, J.P. (2005). Benthic diatom autecology and inference model development from the Canadian High Arctic Archipelago. *Journal of Phycology,* 41: 30-45.

Armstrong, H.A. and Brasier, M.D. (2005). Microfossils, second edition. *Blackwell Publishing*: Massachusetts.

Arthur, C., Mohapi, M. and Mitchell, P. (2011). Archaeology and dam projects in Lesotho. *Conservation and Management of Archaeological Sites,* 13(3): 231-252.

Avery, D.M. (1993). Last Interglacial and Holocene altithermal environments in South Africa and Namibia: micromammalian evidence. *Palaeogeography, Palaeoclimatology and Palaeoecology,* 101: 221-228.

Backéus, I. (1989). Flarks in the Maloti, Lesotho. *Geografiska Annaler, Series A, Physical Geography,* 71(1): 105-111.

Backwell, L.R., McCarthy, T.S., Wadley, L., Henderson, Z., Steininger, C.M., deKlerk, B., Barré, M., Lamothe, M., Chase, B.M., Woodborne, S., Susino, G.J., Bamford, M.K., Sievers, C.,

Brink, J.S., Rossouw, L., Pollarolo, L., Trower, G., Scott, L. and d'Errico, F. (2014). Multiproxy record of late Quaternary climate change and Middle Stone Age human occupation at Wonderkrater, South Africa. *Quaternary Science Reviews,* 99: 42-59.

Baker, A., Routh, J., Blaauw, M. and Roychoudhury, A.N. (2014). Geochemical records of palaeoenvironmental controls on peat forming processes in the Mfabeni 1land, Kwazulu Natal, South Africa since the Late Pleistocene. *Palaeogeography, Palaeoclimatology, Palaeoecology,* 395: 95-106.

Bangs, M., Battarbee, R.W., Flower, R.J., Jewson, D., Lees, J.A., Sturm, M., Vologina, E.G. and Mackay, A.W. (2000). Climate change in Lake Baikal: diatom evidence in an area of continuous sedimentation. *International Journal of Earth Science,* 89: 251-259.

Barber, H.G. and Haworth, E.Y. (1981). A guide to the morphology of the diatom frustule. Freshwater Biological Association Scientific Publication No. 44*, Freshwater Biological Association*: Cumbria, pp. 1-57.

Barker, P., Williamson, D., Gasse, F. and Gibert, E. (2003). Climatic and volcanic forcing revealed in a 50,000-year diatom record from Lake Massoko, Tanzania. *Quaternary Research,* 60: 368-376.

Barrable, A., Meadows, M.E. and Hewitson, B.C. (1998). Environmental reconstruction and climate modelling of the Late Quaternary in the winter rainfall region of the Western Cape, South Africa. *South African Journal of Science,* 98: 611-616.

Bateman, M.D., Holmes, P.J., Carr, A.S., Horton, B.P. and Jaiswal., M.K. (2004). Aeolianite and barrier dune construction spanning the last two glacial-interglacial cycles from the southern Cape coast, South Africa. *Quaternary Science Reviews,* 23: 1681-1698.

Battarbee, R.W. (2000). Palaeolimnological approaches to climate change, with special regard to the biological record. *Quaternary Science Reviews*, 19: 107–124.

Battarbee, R.W. and Kneen, M.J. (1982). The use of electronically counted microspheres in absolute diatom analysis. *Limnological Oceanography,* 27(1): 184-188.

Battarbee, R.W., Jones, V.J., Flower, R.J., Cameron, N.G., Bennion, H., Carvalho, L. and Juggins, S. (2001). Diatom analysis. In Smol, J.P., Birks, H.J.B. and Last, W.M. (eds.). Tracking environmental change using lake sediments, volume 3: Terrestrial, algal and siliceous indicators. *Kluver Academic Press*: Dordrecht.

Battarbee, R.W., Grytnes, J-A., Thompson, R., Appleby, P.G., Catalan, J., Korhola, A., Birks, H.J.B., Hoegaard, E. and Lami, A. (2002). Comparing palaeolimnological and instrumental evidence of climate change for remote mountain lakes over the last 200 years. *Journal of Palaeolimnology,* 28: 161-179.

Baxter, A.J. and Meadows, M.E. (1994). Palynological evidence for the impact of colonial settlement within lowland fynbos: A high resolution study from Verlorenvlei. southwestern Cape Province, South Africa. *Historical Biology*, 9: 61.

Baxter, A. and Meadows, M. (1999). Evidence for Holocene sea level changes at Verlorenvlei, Western Cape, South Africa. *Quaternary International* 56: 65-79.

Bell, J. (2011). 'The changing climate of livelihoods in Lesotho': The vulnerability of rural livelihoods in Phelantaba village, northern Lesotho, to climate variability and change. *Masters Dissertation submitted to the University of Johannesburg:* Johannesburg.

Bell, M. and Walker, M.J.C. (2013). Late Quaternary environmental Change: Physical and human perspectives. *Routledge:* Oxon, pp. 17-63

Bennett, K.D. and Willis, K.J. (2001). Pollen. In Smol, J.P., Birks, H.J.B. and Last, W.M. (eds.). Tracking environmental change using lake sediments, volume 3: Terrestrial Algal and siliceous indicators. *Kluwer Academic Publishers:* Dordrecht, pp. 5-32.

Bharwani, S., Shale, M., Tayor, A., Matin, N. and Downing, T. (2007). Integrating social vulnerability into water management in the Lesotho Highlands: The case of Ha Tsiu. *Proceedings of the International Conference on Adaptive and Integrated Water Management*: Basel.

Bird, J. (1965). Annals of Natal: 1495-1845. *Struik Publishers:* Cape Town, p. 24.

Birks, H.H. and Birks, H.J.B. (2014). Reconstructing Holocene climates from pollen and plant macrofossils. In Birks, J., Battarbee, R., Mackay, A. and Oldfield, F. (eds.). Global change in the Holocene. *Routledge:* London, pp. 342-357.

Birks, H.J.B., Lotter, A.F., Juggins, S. and Smol, J.P. (2012). Tracking environmental change using lake sediments, volume 5: Data handling and numerical techniques. *Springer:* Dordrecht.

Bisaro, A., Hinkel, J. and Kranz, N. (2010). Multilevel water, biodiversity and climate adaptation governance: evaluating adaptive management in Lesotho. *Environmental Science and Policy,* 13: 637-647.

Blaauw, M. (2010). Methods and code for 'classical' age-modelling of radiocarbon sequences. *Quaternary Geochronology,* 5: 512-518.

Blaauw, M. and Christen, J.A. (2011). Flexible paleoclimate age-depth models using an autoregressive gamma process. *Bayesian Analysis,* 6(3): 457-474.

Blaylock, R. (2004). Epidemiology of snakebite in Eshowe, KwaZulu-Natal, South Africa. *Toxicon,* 43(2): 159-166.

Boelhouwers, J.C. (1994). Periglacial landforms at Giant's Castle, Natal Drakensberg, South Africa. *Permafrost and Periglacial Processes,* 5: 129-136.

Boelhouwers, J. (2003). Quaternary slope development in the Lesotho highlands: review and alternative model. *South African Journal of Science,* 99: 44-46.

Boelhouwers, J.C. and Hall, K. (1990). Sani Pass. In Hanvey, P.M. (ed.). Field Guide to Geocryological Features in the Drakensberg. *Rhodes University:* Grahamstown.

Boelhouwers, J.C. and Meiklejohn, K.I. (2002). Quaternary periglacial and glacial geomorphology of Southern Africa: review and synthesis. *South African Journal of Science,* 98: 47-55.

Boelhouwers, J., Holness, S., Meiklejohn, I. and Sumner, P. (2002). Observations on a blockstream in the vicinity of Sani Pass, Lesotho Highlands, Southern Africa. *Permafrost and Periglacial Processes,* 13: 251-257.

Bolli, H., Saunders, J. and Perch-Nielsen, K. (1989). Plankton stratigraphy: Volume 2, radiolaria, diatoms, silicoflagellates, dinoflagellates and ichthyoliths. *Cambridge University Press:* Cambridge.

Booth, R. and Jackson, S. (2003). A high-resolution record of late-Holocene moisture variability from a Michigan raised bog, USA. *The Holocene,* 13(6): 863-876.

Borg, C. (2012). Mechanisms controlling valley asymmetry development at Abisko Northern Sweden and Sani Pass, Southern Africa. *Geotrycheriet Uppsala University*: Uppsala.

Borojevic, K. (2011). Interpreting, dating, and reevaluating the botanical assemblage from tell Kedesh: a case study of historical contamination. *Journal of Archaeological Science*, 38(4): 829-842.

Botha, G. and Porat, N. (2007). Soil chronosequence development in dunes on the southeast African coastal plain, Maputaland, South Africa. *Quaternary International,* 162-163: 111-132.

Bousman, B. and Scott, L. (1994). Climate or overgrazing: the palynological evidence for vegetation change in the eastern Karoo. *South African Journal of Science*, 90: 575-578

Brackley, I.J.A., Wallace, S., Galliers, R.M. and Lephoma, M. (1991). Geotechnical investigation for Katse Dam, Lesotho. In Blight, G.E., Fourie, A.B., Luker, I., Mouton, D.J. and Scheurenberg, R.J. (eds.). Proceedings of the conference on geotechnics in the African environment. *Balkema*: Rotterdam, pp. 351-358.

Bradley, R. (1999). Palaeoclimatology: Reconstructing climates of the Quaternary. *Academic Press Ltd.*: London.

Breman, E., Gillson, L. and Willis, K. (2011). How fire and climate shaped grass-dominated vegetation and forest mosaics in northern South Africa during past millennia. *The Holocene,* 22(12): 1427-1439.

Briggs, D. (1977). Sediments. *Butterworths:* London.

Bristow, D. (2010). Walking with demons: four weeks in the Drakensberg. In Ewart-Smith, C. (eds.). Twenty-one years of African travel writing. *Jacana Media:* Johannesburg, pp. 172-177.

Brook, G.A., Rafter, M.A., Railsback, L.B., Sheen, S.W. and Lundberg, J. (1999). A high-resolution proxy record of rainfall and ENSO since AD 1550 from layering in stalagmites from Anjohibe Cave, Madagascar. *The Holocene,* 9(6): 695-705.

Burrough, S.L., Breman, E. and Dodd, C. (2012). Can phytoliths provide and insight into past vegetation of the Middle Kalahari paleolakes during the late Quaternary? *Journal of Arid Environments,* 82: 113-116.

Burrough, S.L. and Thomas, D.S.G. (2013). Central southern Africa at the time of the African Humid Period: a new analysis of Holocene palaeoenvironmental and palaeoclimate data. *Quaternary Science Reviews,* 80: 29-46.

Butzer, K.A. (1973). Pleistocene 'periglacial' phenomena in southern Africa. *Boreas,* 2: 1-11.

Cain, C. (2009). Cultural heritage survey of Lesotho for the Maloti-Drakensberg Transfrontier Project, 2005-2006: Palaeontology, archaeology, history and heritage management. *The South African Archaeological Bulletin,* 64(189): 33-44.

Caljon, A.G. and Cocquyt, C.Z. (1992). Diatoms from surface sediments of the northern part of Lake Tanganyika. *Hydrobiologia,* 230: 135-156.

Camburn, K.E. and Charles, D.F. (2000). Diatoms of Low-Alkalinity Lakes in the Northeastern United States. *The Academy of the Natural Sciences of Philadelphia:* Philadelphia.

Carbutt, C. (2004). Vegetation survey for a wetland adjacent to Sani River. *Unpublished.*

Carbutt, C. (2012). The emerging invasive alien plants of the Drakensberg Alpine Centre, southern Africa. *Bothalia,* 42(2): 71-85.

Carbutt, C. and Edwards, T.J. (2004). The flora of the Drakensberg Alpine Centre. *Edinburgh Journal of Botany,* 60(3): 581-607.

Carbutt, C. and Edwards, T.J. (2006). The endemic and near-endemic angiosperms of the Drakensberg Alpine Centre. *South African Journal of Botany,* 72: 105-132.

Carmago, J.A. and Jiménez, A. (2007). Ecological responses of epilithic diatoms and aquatic macrophytes to fish farm pollution in a Spanish river. *Anales del Jardín Botánico de Madrid,* 64(2): 213-219.

Carr, A.S., Thomas, D.S.G., Bateman, M.D., Meadows, M.E. and Chase, B. (2006). Late Quaternary palaeoenvironments of the winter-rainfall zone of southern Africa: Palynological and sedimentological evidence from the Agulhas Plain. *Palaeogeography, Palaeoclimatology and Palaeoecology,* 239: 147-165.

Carr, A.S., Bateman, M.D., Roberts, D.L., Murray-Wallace, C.V., Jacobs, Z. and Holmes, P.J. (2010). The last interglacial sea-level high stand on the southern Cape coastline of South Africa. *Quaternary Research,* 73: 351-363.

Carr, A.S., Boom, A., Chase, B.M., Meadows, M.E. and Grimes, H.L. (2015). Holocene sea level and environmental change on the west coast of South Africa: evidence from plant biomarkers, stable isotopes and pollen. *Journal of Palaeolimnology,* 53: 415-432.

Carter, P.L. (1969). Moshebi's Shelter. *Lesotho,* 8: 13-23.

Carter, P.L. (1970). Late Stone Age exploitation patterns in southern Natal. *South African Archaeological Bulletin,* 25: 55-58.

Carter, P. (1976). The effects of climatic change on settlement in eastern Lesotho during the Middle and Later Stone Age. *World Archaeology,* 8: 197-206.

Carter, P.L., Mitchell, P.J. and Vinnicombe, P. (1988). Sehonghong: The Middle and Later Stone Age industrial sequence at a Lesotho rock-shelter. *British Archaeological Reports:* Oxford.

Chase, B.M. and Meadows, M.E. (2007). Late Quaternary dynamics of southern Africa's winter rainfall zone. *Earth Science Reviews,* 84: 103-138.

Chase, B.M., Meadows, M.E., Scott, L., Thomas, D.S.G., Marais, E., Sealy, J. and Reimer, P.J. (2009). A record of rapid Holocene climate change preserved in hyrax middens from southwestern Africa. *Geology*, 37: 703-706.

Chase, B.M., Quick, L.J., Meadows, M.E., Scott, L., Thomas, D.S.G. and Reimer, P.J. (2011). Late glacial interhemispheric climate dynamics revealed in South African hyrax middens. *Geology,* 39(1): 19-22.

Chase, B.M., Scott, L., Meadows, M.E., Gil-Romera, G., Boom, A., Carr, A.S., Reimer, P.J., Truc, L., Valsecchi, V. and Quick, L.J. (2012). Rock hyrax middens: A palaeoenvironmental archive for southern African drylands. *Quaternary Science Reviews,* 56: 107-125.

Chase, B.M., Boom, A., Carr, A.S., Meadows, M.E. and Reimer, P.J. (2013). Holocene climate change in southernmost South Africa: rock hyrax middens record shifts in southern westerlies. *Quaternary Science Reviews,* 82: 199-205.

Chase, B.M., Lim, S., Chevalier, M., Boom, A., Carr, A.S., Meadows, M.E. and Reimer, P.J. (2015a). Influence of tropical easterlies in southern Africa's winter rainfall zone during the Holocene. *Quaternary Science Reviews,* 107: 138-148.

Chase, B.M., Boom, A., Carr, A.S., Carré, M., Chevalier, M., Meadows, M.E., Pedro, J.B., Stager, J.C. and Reimer, P.J. (2015b). Evolving southwest African response to abrupt deglacial North Atlantic climate change events. *Quaternary Science Reviews,* 121: 132-136.

Cockroft, M.J., Wilkinson, M.J. and Tyson, P.D. (1987). The application of a present-day climatic mode to the Late Quaternary in southern Africa. *Climatic Change,* 10: 161-181.

Cocquyt, C. (2007). Diatom diversity in Hausburg Tarn, a glacial lake on Mount Kenya, east Africa. *Diatom Research,* 22(2): 255-285.

Coetzee, J.A. (1967). Pollen analytical studies in East and Southern Africa. *Palaeoecology of Africa,* 3: 1-146.

Coetzee, J.A. and Vogel, J.C. (1967). Evidence for the Paudorf Interstadial in Africa. *Palaeoecology of Africa*, 2: 100-101.

Cohen, A.L., Parkington, J.E., Brundrit, G.B. and Van Der Merwe, N.J. (1992). A Holocene marine climate record in mollusc shells from the southwest African coast. *Quaternary Research,* 38: 379-385.

Cohen, A.L. and Tyson, P.D. (1995). Sea-surface temperature fluctuations during the Holocene off the south coast of Africa: implications for terrestrial climate and rainfall. *The Holocene,* 5(3): 304-312

Cowling, R.M. and Hilton Taylor, C. (1994). Patterns of plant diversity and endemism in southern Africa: an overview. In Huntley, B.J. (ed) Botanical diversity in southern Africa. *National Botanical Institute:* Pretoria, pp. 31-52.

Craig, M.H., Kleinschmidt, I., Nawn, J.B, Le Sueur, D. ad Sharp, B.L. (2004). Exploring 30 years of malaria case data in KwaZulu-Natal, South Africa. Part 1. The impact of climatic factors. *Tropical Medicine & International Health,* 9(12): 1247-1257.

Craticula (n.d.). The European Diatom Database. Accessed on June 20, 2014 from http://craticula.ncl.ac.uk/Eddi/jsp/.

Daniau, A.L., Goñi, M.F.S., Martinez, P., Urrego, D.H., Bout-Roumazeilles, V., Desprat, S. and Marlon, J.R. (2012). Orbital-scale climate forcing of grassland burning in southern Africa. *PNAS,* 110(13): 5069-5073.

De Boer, E.J., Hooghiemstra, H., Florens, F.B.V., Baider, C., Engels, S., Dakos, V., Blaauw, M. and Bennett, K.D. (2013). Rapid succession of plant associations on the small ocean island of Mauritius at the onset of the Holocene. *Quaternary Science Reviews,* 68: 114-125.

Deacon, J. and Lancaster, I.N. (1988). Late Quaternary Palaeoenvironments of Southern Africa. *Clarendon Press:* Oxford.

Dean, W.E. (1999). The carbon cycle and biogeochemical dynamics in lake sediments. *Journal of Palaeolimnology,* 21(4): 375-393.

Deaton, B.C. (1987). Quantification of rock colour from Munsell Chips. *Journal of Sedimentary Petrology,* 57(4): 774-776.

Denys, L. (1994). Diatom assemblages along a former intertidal gradient: A palaeoecological study of a subboreal clay layer (western coastal plain, Belgium). *Netherlands Journal of Aquatic Ecology,* 28(1): 85-96.

Deschamps, C.L. (2006). A comparison of the biogeographical and geomorphological characteristics of gullied and non-gullied valley head mires in eastern Lesotho. *Master of Science Dissertation submitted to the University of the Witwatersrand:* Johannesburg.

Du Preez, P.J. and Brown, L.R. (2011). Impact of domestic animals on ecosystem integrity of Lesotho high altitude peatlands. In Grillo, O. and Venora, G. (eds.) Ecosystems biodiversity. *Intech*: Rijeka, pp. 249-270.

Duffin, K.I. (2008). The representation of rainfall and fire intensity in fossil pollen and charcoal records from a South African saVannah. *Review of Palaeobotany and Palynology,* 151: 59-71.

Duffin, K.I., Gillson, L. and Willis, K.J. (2008). Testing the sensitivity of charcoal as an indicator of fire events in saVanna environments: quantitative predictions of fire proximity, area and intensity. *Holocene*, 18: 279–291.

Dupont, L.M., Kim, J.H., Schneider, R.R. and Shi, N. (2004). Southwest African climate independent of Atlantic sea surface temperatures during the Younger Dryas. *Quaternary Research,* 61: 318-324

Dyer, T.G.J. and Marker, M.E. (1979). On some aspects of Lesotho hollows. *Geomorphology,* 23: 256-270.

Ekblom, A., Gillson, L., Risberg, J., Holmgren, K. and Chidoub, Z. (2008). Rainfall variability and vegetation dynamics of the lower Limpopo Valley, Southern Africa, 500 AD to present. *Palaeogeography, Palaeoclimatology, Palaeoecology,* 363-364: 68-78.

Ekblom, A. & Gillson, L. (2010). Fire history and fire ecology of Northern Kruger (KNP) and Limpopo National Park (PNL), southern Africa. *The Holocene,* 20(7): 1063-1077.

Ekblom, A., Risberg, J. and Holmgren, K. (2014a). Coastal forest and Miombo woodland history of the Vilankulo region, Mozambique. *The Holocene,* 18(8): 1247-1257.

Ekblom, A., Eichhorn, B., Sinclair, P., Badenhorst, S. and Berger, A. (2014b). Land use history and resource utilization from A.D. 400 to the present, at Chibuene, southern Mozambique. *Vegetation History and Archaeology,* 23(1): 15-32.

Erdtman, G. (1943). An Introduction to Pollen Analysis. *Waltham Mass:* New York.

Eriksson, P.G. (1981). A palaeoenvironmental analysis of the Clarens Formation in the Natal Drakensberg. *Transactions of the Geological Society of South Africa,* 84: 7-17.

Esterhuysen, A. and Mitchell, P. (1996). Palaeoenvironmental and archaeological implications of charcoal assemblages from Holocene sites in western Lesotho, Southern Africa. *Palaeoecology of Africa,* 24: 203-232.

Esterhuysen, A.B., Mitchell, P.J. and Thackeray, J.F. (1999). Climatic change across the Pleistocene/Holocene boundary in the Caledon River southern Africa: Results of a factor analysis of charcoal assemblages. *Southern African Field Archaeology,* 8: 28-34.

Faegri, K., Iversen, J. and Krzywinski, K. (1989). Textbook of Pollen Analysis. *The Blackburn Press:* New Jersey.

Fairbanks, R.G., Mortlock, R.A., Chiu, T.-C., Cao, L., Kaplan, A., Guilderson, T.P., Fairbanks, T.W., Bloom, A.L., Grootes, P.M. and Nadeau, M-J. (2005). Radiocarbon calibration curve spanning 0 to 50,000 years BP based on paired 230Th/234U/238U and 14C dates on pristine corals. *Quaternary Science Reviews,* 24: 1781-1796.

FAO 2003 Dejene, A., Midgley, S., Marake, M.V. and Ramasamy, S. (2011). Strengthening capacity for climate change adaptation in agriculture: experience and lessons from Lesotho. *Food and Agriculture Organization of the United Nations:* Rome.

Finch, A.A., Shaw, P.A., Weedon, G.P. and Holmgren, K. (2001).Trace element variation in speleothem aragonite: potential for palaeoenvironmental reconstruction. *Earth and Planetary Science Letters,* 186: 255-267.

Finch, J.M. and Hill, T.R. (2008). A late Quaternary pollen sequence from Mfabeni Peatland, South Africa: Reconstructing forest history in Maputaland. *Quaternary Research,* 70: 442-460.

Finkelstein, S.A., Peros, M.C. and Davis, A.M. (2005). Late Holocene palaeoenvironmental change in a Great Lakes coastal wetland: integrating pollen and diatom datasets. *Journal of Palaeolimnology,* 33: 1-12.

Finné, M., Norström, E., Risberg, J. and Scott, L. (2010). Siliceous microfossils as late-Quaternary paleo-environmental indicators at Braamhoek wetlands, South Africa. *The Holocene,* 20(5): 747-760.

Fletcher, M.S. and Moreno, P.I. (2012). Have the southern Westerlies changed in a zonally symmetric manner over the last 14,000 years? A hemisphere-wide take on a controversial problem. *Quaternary International,* 253: 32-46.

Foged, N. (1964). Freshwater diatoms from Spitsbergen. *Universitetsforlaget:* Oslo.

French, H.M. (1996). The periglacial environment, 2nd edition. *Longman:* London, p. 1-5.

Fritz, S.C., Juggins, S., Battarbee, R.W. and Engstrum, D.R. (1991). Reconstruction of past changes in salinity and climate using a diatom-based transfer function. *Nature,* 352: 706-708.

Gasse, F. (1986). East African diatoms: Taxonomy, ecological distribution. *Cramer:* Stuttgart.

Gasse, F. and Van Campo, E. (1998). A 40,000-yr Pollen and Diatom Record from Lake Tritrivakely, Madagascar, in the Southern Tropics. *Quaternary Research,* 49: 299-311.

Gasse, F. and Van Campo, E. (2001). Late Quaternary environmental changes from a pollen and diatom record in the southern tropics (Lake Tritrivakely, Madagascar). *Palaeogeography, Palaeoclimatology, Palaeoecology,* 167: 287-308.

Gell, P. and Little, F. (2007). Water quality history of Murrumbidgee River floodplain wetlands. *Land and Water Australia:* Canberra.

Giffen, M.H. (1966). Contributions to the diatom flora of South Africa II. Diatoms from the Hogsback region of the Amatola Mountains, Eastern Cape Province, South Africa. *Beifte zur Nova Hedwigia,* 21: 123-150.

Gillson, L. (2015a). Evidence of a tipping point in a southern African saVanna? *Ecological complexity,* 21: 78-86.

Gillson, L. (2015b). Biodiversity Conservation and Environmental Change. *Oxford University Press:* Oxford, pp. 54-114.

Gillson, L., Ekblom, A., Willis, K.J. and Froyd, C. (2008). Holocene palaeo-invasions: the link between pattern, process and scale in invasion ecology. *Landscape Ecology,* 23: 757-769.

Gillson, L. and Ekblom, A. (2009). Untangling anthropogenic and climatic influence on riverine forest in the Kruger National Park, South Africa. *Vegetation History Archaeobotany,* 18: 171-185.

Gil-Romera, G., Scott, L., Marais, E. and Brook, G.A. (2006). Middle- to late-Holocene moisture changes in the desert of northwest Namibia derived from fossil hyrax dung pollen. *The Holocene,* 16(8): 1073-1084.

Gil-Romera, G., Scott, L., Marais, E. and Brook, G.A. (2007). Late Holocene environmental change in the northwestern Namib Desert margin: New fossil pollen evidence from hyrax middens. *Palaeogeography, Palaeoclimatology, Palaeoecology,* 249: 1-17.

Gordon, N., García-Rodriguez, F. and Adams, J.B. (2012). Palaeolimnology of a coastal lake on the Southern Cape coast of South Africa: Sediment geochemistry and diatom distribution. *Journal of African Earth Sciences,* 75: 14-24.

Gorham, E. (1957). The development of peatlands. *Quarterly Review of Biology*, 32: 145-66.

Grab, S.W. (1996a). A note on the morphology of miniature sorted stripes at Mafadi Summit, High Drakensberg. *South African Geographical Journal,* 78(2): 59-63.

Grab, S. (1996b). Debris deposits in the high Drakensberg, South Africa: Possible indicators for plateau, niche and cirque glaciation. *Geomorphology,* 103: 389-403.

Grab, S.W. (1997). Analysis and characteristics of high altitude air temperature data from northern Lesotho: Implications for cryogeomorphic occurrences. *Geoöko Plus,* 4: 109-118.

Grab, S. (1999). Block and debris deposits in the High Drakensberg, Lesotho, southern Africa: Implications for high altitude slope processes. *Geografiska Annaler,* 81(1): 1-16.

Grab, S. (2000). Stone-banked lobes and environmental implications, High Drakensberg, Southern Africa. *Permafrost and Periglacial Processes,* 11: 177-187.

Grab, S. (2002a). Characteristics and palaeoenvironmental significance of relict sorted patterned ground, Drakensberg plateau, southern Africa. *Quaternary Science Reviews,* 21: 1729-1744.

Grab, S.W. (2002b). Turf exfoliation in the high Drakensberg, southern Africa. *Geografiska Annaler,* 84(1): 39-50.

Grab, S. (2002c). A note on needle-ice mound formation in the High Drakensberg, southern Africa. *Permafrost and Periglacial Processes,* 13: 315-318.

Grab, S. (2005). Aspects of the geomorphology, genesis and environmental significance of earth hummocks (thúfur, pounus): miniature cryogenic mounds. *Progress in Physical Geography,* 29(2): 139-155.

Grab, S.W. (2010). Alpine turf exfoliation pans in Lesotho, southern Africa: Climate-process-morphological linkages. *Geomorphology,* 114: 261-275.

Grab, S. (2012). On the burrowing impacts of ice rats Otomys sloggetti robertsi at a wetland fringe in the Afro-alpine zone, Lesotho. *South African Geographical Journal,* 94(1): 75-84.

Grab, S.W. (2013). Fine-scale variations of near-surface-temperature lapse rates in the High Drakensberg Escarpment, South Africa: Environmental Implications. *Arctic, Antarctic and Alpine Research,* 45(4): 500-514.

Grab, S. and Hall, K. (1996). North-facing hollows in the Lesotho/Drakensberg mountains: hypothetical palaeoenvironmental reconstructions? *South African Journal of Science,* 92: 183-184.

Grab, S. and Nüsser, M. (2001). Towards an integrated research approach for the Drakensberg and Lesotho mountain environments: A case study from the Sani Plateau region. *South African Geographical Journal,* 83: 64-68.

Grab, S.W. and Simpson, A.J. (2000). Climatic and environmental impacts of cold fronts over KwaZulu-Natal and the adjacent interior of southern Africa. *South African Journal of Science,* 96: 602-608.

Grab, S.W. and Deschamps, C.L. (2004). Geomorphological and Geoecological Controls and Processes Following Gully Development in Alpine Mires, Lesotho. *Artic, Antarctic and Alpine Research,* 36(1): 49-58.

Grab, S., Scott, L., Rossouw, L. and Meyer, S. (2005). Holocene palaeoenvironments inferred from a sedimentary sequence in the Tsoaing River Basin, western Lesotho. *CATENA,* 61: 49-62.

Grab, S.W., Mulder, N.A. and Mills, S.C. (2009). Spatial associations between longest-lasting winter snow cover and cold region landforms in the High Drakensberg, southern Africa. *Geografiska Annaler,* 91(2): 83-97.

Grab, S.W. and Nash, D.J. (2010). Documentary evidence of climate variability during cold seasons in Lesotho, southern Africa, 1833-1900. *Climate Dynamics,* 34: 473-499.

Grab, S.W. and Mills, S.C. (2011). Quaternary slope processes and morphologies in the upper Sehonghong Valley, eastern Lesotho. *Proceedings of the Geologists' Association,* 122: 179-186.

Grab, S.W., Mills, S.C. and Carr, S.J. (2012). Periglacial and glacial geomorphology. In Holmes, P. and Meadows, M. (eds.). Southern African geomorphology: Recent trends and new directions. *Sun Media*: Bloemfontein, pp. 231-266.

Grab, S.W. and Linde, J.H. (2014). Mapping exposure to snow in a developing African context: implications for human and livestock vulnerability in Lesotho. *Natural Hazards,* 71: 1537-1560.

Green, H., Pickering, R., Drysdale, R., Johnson, B.C., Hellstrom, J. and Wallace, M. (2015). Evidence for global teleconnections in a late Pleistocene speleothem record of water balance and vegetation change at Sudwala Cave, South Africa. *Quaternary Science Reviews,* 110: 114-130.

Grimm, E.C. (1987). CONISS: A FORTRAN 77 program for stratigraphically constrained cluster analysis by the method of incremental sum of squares. *Computers & Geosciences,* 13(1): 13-35.

Grundling, P.L., Linström, A., Fokkema, W. and Grootjans, A.P. (2015). Mires in the Maluti Mountains of Lesotho. *Mires and Peat*, 15(9): 1-11.

Gwimbi, P., Hachigonta, S., Sibanda, L.M. and Thomas, T.S. (2012). Southern African Agriculture and Climate Change: A comprehensive analysis – Lesotho. *International Food Policy Research Institute:* Washington.

Haas, L.J.M., Mazzei, L. and O'Leary, D.T. (2010). Lesotho Highlands Water Project, Communications Practices for Governance and Sustainability Improvement. World Bank Working Paper No. 200, *The World Bank*: Washington.

Haberyan, K. (1987). Fossil diatoms and the palaeolimnology of Lake Rukwa, Tanzania. *Freshwater Biology,* 17: 429-436.

Hall, K. (2010). The shape of glacial valleys and implications for southern African glaciation. *South African Geographical Journal,* 92: 35-44.

Hall, K. (2012). A reply to Dr Knight in regard to his comments relating to 'The shape of glacial valleys and implications for southern African glaciation' (Hall 2010). *South African Geographical Journal,* 94(1): 4-8.

Hancox, P.J. and Rubidge, B. (2001). Breakthroughs in the biodiversity, biogeography, biostratigraphy, and basin analysis of the Beaufort group. *Journal of African Earth Sciences,* 33(3): 563-577.

Hannah, L. (2010). Climate change biology. *Academic Press*: Burlington, pp. 22-30.

Hanvey, P.M. and Marker, M.E. (1992). Present-day periglacial microforms in the Lesotho Highlands: Implications for present and past climatic conditions. *Permafrost and Periglacial Processes,* 3: 353-361.

Hanvey, P.M. and Marker, M.E. (1994). Sedimentary sequences in the Tlaeeng Pass area, Lesotho. *South African Geographical Journal,* 76(2): 63-67.

Harding, W.R. and Taylor, J.C. (2011). The South African Diatom Index (SADI) – A preliminary index for indicating water quality in rivers and streams in southern Africa. Water Research Commission Report No. 1701/1/11. *WRC*: Pretoria.

Hargan, K.E., Rühland, K.M., Paterson, A.M., Finkelstein, S.A., Holmquist, J.R., MacDonald, G., Keller, W. and Smol, J.P. (2015). The influence of water-table depth and pH on the spatial distribution of diatom species in peatlands of the Boreal Shield and Hudson Plains, Canada. *Botany,* 93: 57-74.

Harper, G. (1969). Periglacial evidence in South Africa during the Pleistocene epoch. *Palaeoecology of Africa,* 4: 71-91.

Harrison, S., Rowan, A.V., Glasser, N.F., Knight, J., Plummer, M.A. and Mills, S.C. (2014). Little Ice Age glaciers in Britain: Glacier-climate modelling in the Cairngorm Mountains. *The Holocene,* 24(2): 135-140.

Hartnady, C.J.H. (1985). Uplift, faulting, seismicity, thermal spring and possible incipient volcanic activity in the Lesotho-Natal region, SE Africa: The Quathlamba Hotspot hypothesis. *Tectonics,* 4(4): 371-377.

Harwood, D.M. (2004). Diatomite. In Stoermer, E.F. and Smol, J.P. (eds.). The Diatoms: Applications for the Environmental and Earth Science. *Cambridge University Press*: Cambridge, pp. 436-443.

Heaton, T.H.E., Talma, A.S. and Vogel, J.C. (1986). Dissolved gas palaeotemperatures and 18O variations derived from groundwater near Uitenhage, South Africa. *Quaternary Research*, 25: 79-88.

Heine, K. (1987). Anthropogenic sedimentological changes during the Holocene in Southern Africa. *Striae,* 26: 41-50.

Heiri, O., Lotter, A.F. and Lemcke, G. (2001). Loss on ignition as a method for estimating organic and carbonate content in sediments: reproducibility and comparability of results. *Journal of Palaeolimnology,* 25: 101-110.

Hendey, Q.B. and Volman, T.P. (1986). Last Interglacial sea levels and coastal caves in the Cape Province, South Africa. *Quaternary International,* 25: 189-198.

Herbert, R.S. (1987). Late Holocene climatic change: the Little Ice Age and El Niño from planktonic foraminifera in sediments off Walvis Bay, South West Africa. Bulletin No. 18, Marine Geosciences Unit, Department of Geology, University of Cape Town. *UCT:* Cape Town.

Herzschuh, U. (2007). Reliability of pollen ratios for environmental reconstructions on the Tibetan Plateau. *Journal of Biogeography,* 34(7): 1265-1273.

Hicks, S. (2001). The use of annual arboreal pollen deposition values for delimiting tree-lines in the landscape and exploring models of pollen dispersal. *Review of Palaeobotany and Palynology,* 117: 1-29.

Higham, T. (1999). The 14C method. Retrieved on February 20, 2015 from http://www.c14dating.com/int.html

Hill, T.R. (1996). Statistical determination of sample size and contemporary pollen counts, Natal Drakensberg, South Africa. *Grana,* 35(2): 119-124.

Hinze, A., Pillay, N. and Grab, S. (2006). The burrow system of the African ice rat *Otomys sloggetti robertsi. Mammalian Biology – Zeitschrift für Saügetierkunde,* 71(6): 356-365.

Hogg, A.G., Hua, Q., Blackwell, P.G., Niu, M., Buck, C.E., Guilderson, T.P., Heaton, T.J., Palmer, J.G., Reimer, P.J., Reimer, R.W., Turney, C.S.M. and Zimmerman, S.R.H. (2013). SHCal13 Southern Hemisphere calibration, 0-50,000 years cal BP. *Radiocarbon*, 55(4): 1889-1903.

Holmes, P.J., Bateman, M.D., Carr, A.S. and Marker, M.E. (2007). The place of aeolian coversands in the geomorphic evolution of the southern Cape coast, South Africa. *South African Journal of Geology,* 110: 125-136.

Holmgren, K., Karlén, W. and Shaw, P.A. (1995). Paleoclimatic significance of the stable isotopic composition and petrology of a Late Pleistocene stalagmite from Botswana. *Quaternary Research,* 43: 320-328.

Holmgren, K., Karlén. W., Lauritzen, S.E., Lee-Thorp, J.A., Partridge, T.C., Piketh, S., Repinski, P., Stevenson, C., SVanered, O. and Tyson, P.D. (1999). A 3000-year high-resolution stalagmite-based record of palaeoclimate for northeastern South Africa. *The Holocene,* 9(3): 295-309.

Holmgren, K., Tyson, P.D., Moberg, A. and SVanered, O. (2001). A preliminary 3000-year regional temperature reconstruction for South Africa. *South African Journal of Science,* 97: 49-51.

Holmgren, K., Lee-Thorp, J.A., Cooper, G.R.J., Lundblad, K., Partridge, T.C., Scott, L., Sithaldeen, R., Talma, A.S. and Tyson, P.D. (2003). Persistent millennial-scale climatic

variability over the past 25,000 years in Southern Africa. *Quaternary Science Reviews,* 22: 2311-2326.

Holmgren, K., Risberg, J., Freudendahl, J., Achimo, M., Ekblom, A., Mugabe, J., Norström, E. and Sitoe, S. (2012). Water-level variations in Lake Nhauhache, Mozambique, during the last 2,300 years. *Journal of Palaeolimnology,* 48: 311-322.

Humphreys, A.J.B. (1987). Prehistoric seasonal mobility: what are we really achieving? *South African Archaeological Bulletin,* 42: 34-38.

Huntsman-Mapila, P., Ringrose, S., Mackay, A.W., Downey, W.S., Modisi, M., Coetzee, S.H., Tiercelin, J.J., Kampunzu, A.B. and Vanderpost, C. (2006). Use of the geochemical and biological sedimentary record in establishing palaeo-environments and climate change in the Lake Ngami basin, NW Botswana. *Quaternary International,* 148: 51-64.

Hutton, J. (1795). Theory of the Earth; with proofs and illustrations. *Creech*: Edinburgh.

Hydén, L. and Sekoli, T. (2001). Possibilities to forecast early summer rainfall in the Lesotho Lowlands from the El-Niño/ Southern Oscillation. *Water SA,* 26(1): 83-90.

Inouye, D. (2008). Effects of climate change on phenology, frost damage and floral abundance of montane wildflowers. *Ecology,* 89(2): 353-362.

IPCC (Intergovernmental Panel on Climate Change) (2013). Climate Change 2013: The Physical Science Basis. Chapter 12 - Long-term Climate Change: Projections, Commitments and Irreversibility. *Cambridge University Press*: New York. pp. 1029-1136.

Irving, S.J.E. and Meadows, M.E. (1997). Radiocarbon chronology and organic matter accumulation at Vankervelsvlei, Near Knysna, South Africa. *South African Geographical Journal,* 79(2): 101-105.

Jackson, S. (2012). Representation of flora and vegetation in Quaternary fossil assemblages: known and unknown knowns and unknowns. *Quaternary Science Reviews,* 49: 1-15.

Johansen, J.R. (2004). Diatoms of aerial habitats. In Stoermer, E.F. and Smol, J.P. (eds). The diatoms: Applications for the environmental and earth science. *Cambridge University Press*: Cambridge, pp. 264-273.

Johnson, B.J., Miller, G.H., Fogel, M.L. and Beaumont, P.B. (1997). The determination of the late Quaternary palaeoenvironments at Equus Cave, South Africa, using stable isotopes and amino acid racemization in ostrich eggshell. *Palaeogeography, Palaeoclimatology, Palaeoecology,* 136: 121-137.

Jones, P., Briffa, K., Osborn, T., Lough, J., Van Ommen, T., Vinther, B., Luterbacher, J., Wahl, E., Zwiers, F., Mann, M., Schmidt, G., Ammann, C., Buckley, B., Cobb, K., Esper, J., Goosse, H., Graham, N., Jansen, E., Kiefer, T., Kull, C., Küttel, M., Mosley-Thompson, E.,

Overpeck, J., Riedwyl, N., Schulz, M., Tudhope, A., Villalba, R., Wanner, H., Wolff, E. and Xoplaki, E. (2009). High-resolution palaeoclimatology of the last millennium: a review of current status and future prospects. *The Holocene,* 19(1): 3-49.

Juggins, S. (2007). C2, Software for ecological and palaeoecological data analysis and visualisation, User guide Version 1.5. Retrieved on 11 July 2014 from www.staff.ncl.ac.uk/stephen.juggins/software/code/C2.pdf

Juggins, S. (2013). Quantitative reconstructions in palaeolimnology: new paradigm or sick science? *Quaternary Science Reviews,* 64: 20-32.

Karst-Riddoch, T.L., Pisaric, M.F.J. and Smol, J.P. (2005). Diatom responses to 20th century climate-related environmental changes in high-elevation mountain lakes of the northern Canadian Cordillera. *Journal of Palaeolimnology,* 33: 265-282.

Kaufman, L. and Rousseeuw, P.J. (2009). Finding groups in data: An introduction to cluster analysis. *John Wiley & Sons:* New Jersey, pp. 87-98, 242-243.

Kent, M. and Coker, P. (1992). Vegetation description and analysis: A practical approach. *John Wiley & Sons*: Chichester. pp. 162-200.

Killick, D.J.B. (1963). An account of the plant ecology of the Cathedral Peak area of the Natal Drakensberg. *Memoirs of the Botanical Survey of South Africa:* Pretoria.

Killick, D.J.B. (1978). The Afroalpine region. In Werger, M.J.A. (ed.). Biogeography and ecology of southern Africa. *W. Junk*: The Hague, pp. 515–542.

Killick, D.J.B. (1990). A Field Guide: The Flora of the Natal Drakensberg. *Jonathan Ball and Ad. Donker Publishers*, Johannesburg.

Kirsten, K. (2008). Holocene environmental change at Groenvlei, Knysna, SouthAfrica: evidence from diatoms. *MSc Dissertation submitted to the University of Cape Town:* Cape Town.

Kirsten, K. (2014). Evidence of Holocene Environmental Change from Diatoms in Lake Sediments, Western Cape, South Africa. *PhD Thesis submitted to the University of Cape Town:* Cape Town.

Knight, J. (2012). The shape of glacial valleys: comment on Hall (2010). *South African Geographical Journal,* 94(1): 1-3.

Knight, J. and Harrison, S. (2014). Limitations of uniformitarianism in the Anthropocene. *Anthropocene,* 5: 71-75.

Kohfeld, K.E., Graham, R.M., de Boer, A.M., Sime, L.C., Wolff, E.W., Le Quéré, C. and Bopp, L. (2013). Southern Hemisphere westerly wind changes during the Last Glacial Maximum: paleo-data synthesis. *Quuaternary Science Reviews,* 68: 76-95.

Konert, M. and Vandenberghe, J.V. (1997). Comparison of laser grain size analysis with pipette and sieve analysis: a solution for the underestimation of the clay fraction. *Sedimentology,* 44: 523-535.

Körner, C. (2012). Treeline Climate. In Körner, C. (ed.). Alpine treelines: Functional ecology of the global high elevation tree limits. *Springer*: Basel, pp. 33-56.

Kramer, K. (2002). Diatoms of Europe (vol. 1-6). *A.R.G. Gantner Verlag K.G.*: Ruggel.

Krammer, K. and Lange-Bertalot, H. (1986). Süßwasserflora von Mitteleuropa (vol. 1-5). *VEB Gustav Fischer Verlag:* Jena.

Kristen, I., Fuhrmann, A., Thorpe, J., Röhl, U., Wilkes, H. and Oberhänsli, H. (2007). Hydrological changes in southern Africa over the last 200 Ka as recorded in lake sediments from the Tswaing impact crater. *South African Journal of Geology,* 110: 311-326.

Kudo, G. (1991). Effects of snow-free period on the phenology of alpine plants inhabiting snow patches. *Arctic and Alpine Research*, 23(4): 436-443.

Lamentowicz, M., Cedro, A., Galka, M., Goslar, T., Miotk-Szpiganowicz, G., Mitchell, E.A.D. and Pawlyta, J. (2005). Last millennium palaeoenvironmental changes from a Baltic bog (Poland) inferred from stable isotopes, pollen, plant macrofossils and testate amoebae. *Palaeogeography, Palaeoclimatology, Palaeoecology,* 265: 93-106.

Lancaster, N. (1982). Dunes on the Skeleton Coast, Namibia (South West Africa): Geomorphology and grain size relationships. *Earth Surface Processes and Landforms,* 7: 575-587.

Langdon, P., Barber, K. and Hughes, P. (2003). A 7500 year peat-based palaeoclimatic reconstruction and evidence for an 1100 year cyclicity in bog surface wetness from Temple Hill Moss, Pentland Hills, Southeast Scotland. *Quaternary Science Reviews,* 22(2): 259-274.

Lee, K. and Yoon, S-K. (2003). Ecological studies on Togyo Reservoir in Chulwon, Korea VI. The list of phytoplankton and periphyton. *Algae,* 18(4): 263-272.

Lee-Thorp, J.A., Holmgren, K., Lauritzen, S.E., Linge, H., Moberg, A., Partridge, T.C., Stevenson, C. and Tyson, P.D. (2001). Rapid climate shifts in the southern African interior throughout the mid to late Holocene. *Geophysical Research Letters,* 28(23): 4507-4510.

Legendre, P. and Birks, H.J.B. (2012a). Clustering and Partitioning. In Birks, H.J.B., Lotter, A.F., Juggins, S. and Smol, J.P. (eds.). Tracking environmental change using lake sediments, volume 5: Data handling and numerical techniques. *Springer:* Dordrecht, pp. 167-200.

Legendre, P. and Birks, H.J.B. (2012b). From Classical to Canonical Ordination. In Birks, H.J.B., Lotter, A.F., Juggins, S. and Smol, J.P. (eds.). Tracking environmental change using lake sediments, volume 5: Data handling and numerical techniques. *Springer:* Dordrecht, pp. 201-248.

Leng, M. J. and Barker, P. A. (2006). A review of the oxygen isotope composition of lacustrine diatom silica for palaeoclimate reconstruction. *Earth Science Reviews*, 75: 5-27.

Lepš, J. & Šmilauer, P. (2003). Multivariate analysis of ecological data using CANOCO. *Cambridge University Press:* Cambridge

Letšela, L.M.S. (2008). A participatory sustainability assessment framework for biodiversity conservation in rural areas. *PhD Thesis submitted to the University of the Free State:* Bloemfontein.

Lewis, C. (2005). Late Glacial and Holocene palaeoclimatology of the Drakensberg of the Eastern Cape, South Africa. *Quaternary International,* 129: 33-48.

Lewis, C.A. and Illinger, P.M. (2001). Late Quaternary glaciation in southern Africa: moraine ridges and glacial deposits at Mount Enterprise in the Drakensberg of the Eastern Cape Province, South Africa. *Journal of Quaternary Science,* 16(4): 365-374.

Linder, H.P. (1990). On the relationship between the vegetation and floras of the Afromontane and the Cape regions of Africa. *Mitteilungen aus dem Institut für Allgemeine Botanik Hamburg,* 23: 777-790.

Livingstone, D. (1975). Late Quaternary climatic change in Africa. *Annual Review of Ecology and Systematics,* 6: 249-280.

Lotter, A.F. and Bigler, C. (2000). Do diatoms in the Swiss Alps reflect the length of ice-cover. *Aquatic Sciences,* 62(2): 125-141.

Lotter, A.F. & Birks, H.J.B. (2003). The Holocene palaeolimnology of Sägistalsee and its environmental history – a synthesis. *Journal of Paleolimnology*, 30: 333–342.

Lyell, C. (1830). Principles of Geology. *John Murray*: London.

Mackay, A.W., Jones, V.J. and Battarbee, R.W. (2003). Approaches to Holocene climate reconstructions using diatoms. In Birks, J., Battarbee, R., Mackay, A. and Oldfield, F. (eds.). Global change in the Holocene. *Routledge:* London, pp. 294-309.

Mackay, A.W., Bezrukova, E.V., Leng, M.J., Meaney, M., Nunes, A., Piotrowska, N., Self, A., Shchetnikov, A., Shilland, E., Tarasov, P., Wang, L. and White, D. (2012). Aquatic ecosystem responses to Holocene climate change and biome development in boreal, central Asia. *Quaternary Science Reviews*, 41: 119-131.

Mackay, A.W., Bezrukova, E.V., Boyle, J.F., Holmes, J.A., Panizzo, V.N., Piotrowska, N., Shchetnikov, A., Shilland, E.M., Tarasov, P. and White, D. (2013). Multiproxy evidence for abrupt climate change impacts on terrestrial and freshwater ecosystems in the Ol'khon region of Lake Baikal, central Asia. *Quaternary International,* 290-291: 46-56.

Magill, R.E. (1987). Muci Austro-Africana III. Alpine mosses of Lesotho. *Journal of Bryology,* 14: 527-530.

Marake, M., Mokuku, C., Majoro, M. and Mokkitimi, N. (1998). Global change and subsistence rangelands in southern Africa: Resource availability, access and use in relation to rural livelihoods and welfare. *National University of Lesotho:* Maseru.

Marker, M.E. (1987). A note on marine benches of the southern Cape. *South African Journal of Geology,* 90: 120-124.

Marker, M.E. (1991). The evidence for cirque glaciation in Lesotho. *Permafrost and Periglacial Processes,* 2: 21-30.

Marker, M.E. (1994). Sedimentary sequences at Sani Top, Lesotho highlands, southern Africa. *The Holocene,* 4(4): 406-412.

Marker, M.E. (1995). Late Quaternary environmental implications from sedimentary sequences at two high altitude Lesotho sites. *South African Journal of Science,* 91: 294-298.

Marker, M.E. (1998). New radiocarbon dates from Lesotho. *South African Journal of Science,* 94: 239-240.

Marker, M.E and Whittington, G. (1971). Observations on some valley forms and deposits in the Sani Pass area, Lesotho. *South African Geographical Journal,* 53(1): 96-99.

Marker, M.E. and Miller, D.E. (1993). A mid-Holocene high stand of the sea at Knysna. *South African Journal of Science,* 89(2): 100-101.

Marsh, J.S. (1987). Basalt geochemistry and tectonic discrimination within continental flood basalt provinces. *Journal of Volcanology and Geothermal Research,* 32: 35-49.

Martin, A.R.H. (1959). The stratigraphy and history of Groenvlei, a South African coastal fen. *Australian Journal of Botany,* 7: 142-167.

Martin, A.R.H. (1962). Evidence relating to the Quaternary history of the Wilderness Lakes. *Transactions of the Geological Society of South Africa,* 64: 19-42.

Martin, A.R.H. (1968). Pollen analysis of Groenvlei lake sediments, Knysna (South Africa). *Review of Palaeobotany and Palynology,* 7: 107-144.

Masselink, G., Hughes, M. and Knight, J. (2014). Introduction to coastal processes and geomorphology, second edition. *Routledge*: Oxon.

Matlala, M.D., Taylor, J.C. and Harding W.R. (2011). Development of a diatom index for wetland health. Water Research Commission Report Number KV 270/11. *Water Research Commission*: Gezina.

Maud, R.R. (1968). Quaternary geomorphology and soil formation in coastal Natal. *Seitschrift fur Geomorphologie,* 7: 155-199.

Mayewski, P.A., Twickler, M.S., Whitlow, S.I., Meeker, L.D., Yang, Q., Thomas, J., Kreutz, K., Grootes, P.M., Morse, D.L., Steig, E.J., Waddington, E.D., Saltzman, E.S., Whung, P-Y. and Taylor, K.C. (1996). Climate change during the last deglaciation in Antarctica. *Science,* 272(2): 1636-1638.

Mayeweski, P.A., Rohling, E.E., Stager, J.C., Karlén, W., Maasch, K.A., Meeker, L.D., Meyerson, E.A., Gasse, F., Van Kreveld, S. Holmgren, K., Lee-Thorp, J., Rosqvist, G., Rack, F., Staubwasser, M., Schneider, R.R. and Steig, E.J. (2004). Holocene climate variability. *Quaternary Research,* 62(3): 243-255.

McCarthy, T. and Rubidge, B.S. (2005). The story of Earth and life: a southern African perspective on a 4.6-billion-year journey. *Struik:* Cape Town.

McCarthy, T.S., Ellery, W.N., Backwell, L., Marren, P., de Klerk, B., Tooth, S., Brandt, D. and Woodborne, S. (2010). The character, origin and palaeoenvironmental significance of the Wonderkrater spring mound, South Africa. *Journal of African Earth Sciences,* 58: 115-126.

McCormac, F.G., Hogg, A.G., Blackwell, P.G., Buck, C.E., Higham, T.F.G. and Reimer, P.J. (2004). SHCal04 Southern Hemisphere Calibration, 0-11.0 Cal Kyr BP. *Radiocarbon*, 4: 1087-1092.

McGlynn, G., Mackay, A.W., Rose, N.L., Taylor, R.G., Leng, M.J. and Engstrom, D.R. (2010). Palaeolimnological evidence of environmental change over the last 400 years in the Rwenzori Mountains of Uganda. *Hydrobiologia,* 648(1): 109-122.

Meadows, M.E. (1988). Late Quaternary Peat Accumulation in Southern Africa. *Catena,* 15: 459-472.

Meadows, M.E. (2007). Classics in physical geography revisited. Coetzee, J.A.1967: Pollen analytical studies in East and Southern Africa. *Palaeoecology of Africa* 3, 1-146. *Progress in Physical Geography,* 31(3): 313-317.

Meadows, M.E. (2012). Quaternary environments: Going forwards, looking backwards? *Progress in Physical Geography,* 35(4): 539-547.

Meadows, M.E. (2014). Recent methodological adVances in Quaternary palaeoecological proxies. *Progress in Physical Geography,* 38(6): 807-817.

Meadows, M.E. (2015). Seven decades of Quaternary palynological studies in southern Africa: a historical perspective. *Transactions of the Royal Society of South Africa,* 70(2): 103-108.

Meadows, M.E. and Linder, H.P. (1993). A palaeoecological perspective on the origin of Afromontane grasslands. *Journal of Biogeography,* 20(4): 345-355.

Meadows, M.E. and Sugden, J.M. (1993). The late Quaternary palaeoecology of a floristic kingdom: the southwestern Cape South Africa. *Palaeogeography, Palaeoclimatology, Palaeoecology,* 101: 271-281.

Meadows, M.E., Baxter, A.J. and Adams, T. (1994). The Late Holocene vegetation history of the lowland Fynbos, Verlorenvlei, southwestern Cape, South Africa. *Historical Biology,* 9:47–58.

Meadows, M.E., Baxter, A.J. and Parkington, J. (1996). Late Holocene environments at Verlorenvlei, Western Cape Province, South Africa. *Quaternary International,* 33: 81-95.

Meadows, M.E. and Baxter, A.J. (1999). Late Quaternary Palaeoenvironments of the southwestern Cape, South Africa: a regional synthesis. *Quaternary International,* 57/58: 193-206.

Meadows, M.E. and Baxter, A.J. (2001). Holocene vegetation history and palaeoenvironments at Klaarfontein Springs, Western Cape, South Africa. *The Holocene,* 11(6): 699-706.

Meadows, M.E., Chase, B.M. and Seliane, M. (2010). Holocene palaeoenvironments of the Cederberg and Swartruggens mountains, Western Cape, South Africa: Pollen and stable isotope evidence from hyrax dung middens. *Journal of Arid Environments,* 74: 786-793.

Metcalfe, S. (1993). Evolution of the Pretoria Saltpan – a diatom record spanning a full glacial-interglacial cycle. *Hydrobiologia,* 269: 159-166.

Metwally, A.A., Scott, L., Neumann, F.H., Bamford, M.K. and Oberhänsli, H. (2014). Holocene palynology and palaeoenvironments in the SaVanna Biome at Tswaing Crater, central South Africa. *Palaeogeography, Palaeoclimatology, Palaeoecology,* 402: 125-135.

Meyers, P.A. and Teranes, J.L. (2001). Sediment organic matter. In Last, W.M. and Smol, J.P. (eds.). Tracking environmental change using lake sediments, volume 2: Physical and Geochemical Methods. *Springer Science and Media:* Dordrecht, pp. 239-262

Milliman, J., Müller, G. and Förstner, F. (2012). Recent sedimentary carbonates: Part 1 marine carbonates. *Springer Verlag:* Berlin. pp. 3-15, 149-205.

Mills, S.C. (2006). The origin of slope deposits in the southern Drakensberg, eastern Lesotho. *PhD Thesis submitted to the University of the Witwatersrand:* Johannesburg.

Mills, S.C. and Grab, S.W. (2005). Debris ridges along the southern Drakensberg escarpment as evidence for Quaternary glaciation in southern Africa. *Quaternary International,* 129: 61-73.

Mills, S.C., Grab, S.W. and Carr, S.J. (2009a). Recognition and palaeoclimatic implications of late Quaternary niche glaciation in eastern Lesotho. *Journal of Quaternary Science,* 24(7): 647-663.

Mills, S.C., Grab, S.W. and Carr, S.J. (2009b). Late Quaternary moraines along the Sekhokong Range, eastern Lesotho: Contrasting the geomorphic history of north- and south-facing slopes. *Geografiska Annaler,* 91(2): 121-140.

Mills, S., Grab, S., Rea, B., Carr, S. and Farrow, A. (2012). Shifting westerlies and precipitation patterns during the Late Pleistocene in southern Africa determined using glacier reconstruction and mass balance modelling. *Quaternary Science Reviews,* 55: 145-159.

Mitchell, P.J. (1992). Archaeological research in Lesotho: A review of 120 years. *The African Archaeological Review,* 10: 3-34.

Mitchell, P.J. (1995). Revisiting the Robberg: New results and a revision of old ideas at Sehonghong Rock Shelter, Lesotho. *South African Archaeological Bulletin,* 50(161): 28-38.

Mitchell, P.J. (1996a). The late Quaternary of the Lesotho Highlands, southern Africa: Preliminary results and future potential of ongoing research at Sehonghong shelter. *Quaternary International,* 33: 35-43.

Mitchell, P.J. (1996b). The late Holocene assemblages with pottery. *South African Archaeological Bulletin,* 51(163): 17-25.

Mitchell, P.J., Parkington, J.E. and Yates, R. (1994). Recent Holocene archaeology in Western and Southern Lesotho. *South African Archaeological Bulletin,* 49(159): 33-52.

Mitchell, P., Parkington, J. and Wadley, L. (1998). A tale from three regions: The archaeology of the Pleistocene/Holocene transition in the Western Cape, the Caledon Valley and the Lesotho Highlands, Southern Africa. *Quaternary International,* 49/50: 105-115.

Mitchell, P., Plug, I., Bailey, G., Charles, R., Esterhuysen, A., Thorp, J., Parker, A. and Woodborne, S. (2011). Beyond the drip-line: a high-resolution open-air Holocene hunter-gatherer sequence from highland Lesotho. *Antiquity,* 85(330): 1225-1242

Mokotjomela, T., Schwaibold, U. and Pillay, N. (2009). Does the ice rat *Otomys sloggetti robertsi* contribute to habitat change in Lesotho? *Acta Oecologica,* 35: 437-443.

Moore, P. and Webb, J. (1978). An illustrated guide to pollen analysis. *Hodder and Stoughton:* London.

Mpholo, M., Mathaba, T. and Letuma, M. (2012). Wind profile assessment at Masitise and Sani in Lesotho for potential off-grid electricity generation. *Energy Conservation and Management,* 53: 118-127.

Mucina, L. and Rutherford, M.C. (2006). The vegetation of South Africa, Lesotho and Swaziland. *South African National Biodiversity Institute:* Cape Town.

Mulder, N. and Grab, S.W. (2009). Contemporary spatio-temporal patterns of snow cover over the Drakensberg. *South African Journal of Science,* 105: 228-233.

Nash, D.J., Meadows M.E., Gulliver, V.L. (2006). Holocene environmental change in the OkaVango Panhandle, northwest Botswana. *Quaternary Science Reviews,* 25(11-12): 1302-1322.

Nash, D.J. and Grab, S.W. (2010). 'A sky of brass and burning winds': documentary evidence of rainfall variability in the Kingdom of Lesotho, southern Africa, 1824-1900. *Climatic Change,* 101: 617-653.

Nel, W. and Sumner, P.D. (2005). First rainfall data from the KZN Drakensberg escarpment edge (2002 and 2003). *Water SA,* 31(3): 399-402.

Nel, W. and Sumner, P. (2008). Rainfall and temperature attributes on the Lesotho-Drakensberg escarpment edge, Southern Africa. *Geografiska Annaler,* 90(1): 97-108.

Neukom, R., Nash, D.J., Endfield, G.H., Grab, S.W., Grove, C.A., Kelso, C., Vogel, C.H. and Zinke, J. (2014). Multi-proxy summer and winter precipitation reconstruction for southern Africa over the last 200 years. *Climate Dynamics,* 42: 2713-2726.

Neumann, F.H., Stager, J.C., Scott, L., Venter, H.J.T and Weyhenmeyer, C. (2008). Holocene vegetation and climate records from Lake Sibaya, KwaZulu-Natal (South Africa). *Review of Palaebotany and Palynology,* 152: 113-128.

Neumann, F.H., Scott, L., Bousman, C.B. and Van As, L. (2010). A Holocene sequence of vegetation change at Lake Eteza, coastal KwaZulu-Natal, South Africa. *Review of Palaeobotany and Palynology,* 162: 39-53.

Neumann, F.H., Scott, L. and Bamford, M.K. (2011). Climate change and human disturbance of fynbos during the late Holocene at Princess Vlei, Western Cape, South Africa. *The Holocene,* 21(7): 1137-1149.

Neumann, F.H., Botha, G.A. and Scott, L. (2014). 18,000 years of grassland evolution in the summer rainfall region of South Africa: evidence from Mahwaqa Mountain, KwaZulu-Natal. *Vegetation History and Archaeobotany,* 23(6): 665-681.

Nixon, P.H. (1973). Lesotho Kimberlites. *Lesotho National Development Corporation:* Maseru.

Norström, E., Scott, L., Partridge, T., Risberg, J. and Holmgren, K. (2009). Reconstruction of environmental and climate changes at Braamhoek wetland, eastern escarpment South Africa, during the last 16 000 years with emphasis on the Pleistocene-Holocene transition. *Palaeogeography, Palaeoclimatology, Palaeoecology,* 271(3): 240-258.

Norström, E., Risberg, J., Gröndahl, H., Holmgren, K., Snowball, I., Mugabe, J.A. and Sitoe, S.R. (2012). Coastal paleo-environment and sea-level change at Macassa Bay, southern Mozambique, since c 6600 cal BP. *Quaternary International,* 260: 153-163.

Norström, E., Neumann, F.H., Scott, L., Smittenberg, R.H., Holmstrand, H., Lundqvist, S., Snowball, I., Sundqvist, H.S., Risberg, J. and Bamford, M. (2014). Late Quaternary vegetation dynamics and hydro-climate in the Drakensberg, South Africa. *Quaternary Science Reviews,* 105: 48-65.

Nüsser, M. and Grab, S. (2002). Land degradation and soil erosion in the eastern Highlands of Lesotho, Southern Africa. *Beiträge sur Physischen Geographie,* 133: 291-311.

Nyakatya, M.J. and McGeoch, M.A. (2008). Temperature variation across Marion Island associated with a keystone plant species (*Azorella selago* Hook. (Apiaceae)). *Polar Biology,* 31: 139-151.

Oberg, H., Norström, E., Malmström, M., Holmgren, K., Westerberg, L-O., Risberg, J., Eddudóttir, S.D., Andersen, T.J. and Mazuka, A. (2013). Environmental variability in northern Tanzania from AD 1000 to 1800, as inferred from diatoms and pollen in Lake Duluti. *Palaeogeography, Palaeoclimatology, Palaeoecology,* 374: 230-241.

Ohlendorf, C., Bigler, C., Goudsmit, G-H., Lemcke, G., Livingstone, D.M., Lotter, A.F., Müller, B. and Sturm, M. (2000). Causes and effects of long periods of ice cover on a remote high Alpine lake. *Journal of Limnology,* 59(1): 65-80.

Panizzo, V.N., Mackay, A.W., Ssemmanda, I., Taylor, R., Rose, N. and Leng, M.J. (2007). A 140-year record of recent changes in aquatic productivity in a remote, tropical alpine lake in the Rwenzori Mountain National Park, Uganda. *Journal of Palaeolimnology,* 40(1): 325-338.

Parker, A.G., Lee Thorp, J. and Mitchell, P.J. (2011). Late Holocene Neoglacial conditions from the Lesotho highlands, southern Africa: phytolith and stable carbon isotope evidence from the archaeological site of Likoaeng. *Proceedings of the Geologists' Association,* 122: 201-211.

Parmesan, C. and Yohe, G. (2003). A globally coherent fingerprint of climate change impacts across natural systems. *Nature,* 421: 37-42.

Parnell, A.C., Haslett, J., Allen, J.R.M., Buck, C.E. and Huntley, B. (2008). A flexible approach to assessing synchroneity of past events using Bayesian reconstructions of sedimentation history. *Quaternary Science Reviews,* 27: 1872-1885.

Parnell, A.C., Buck, C.E. and Doan, T.K. (2011). A review of statistical chronology models for high-resolution, proxy-based Holocene palaeoenvironmental reconstruction. *Quaternary Science Reviews,* 30: 2948-2960.

Partridge, T.C. (1999). Tswaing: Investigations into the origin, age and palaeoenvironments of the Pretoria Saltpan. *Council for Geosciences:* Pretoria.

Partridge, T.C. and Maude, R.R. (1987). Geomorphic evolution of southern Africa since the Mesozoic. *South African Journal of Geology,* 90(2): 179-208.

Partridge, T.C., Kerr, S.J., Metcalfe, S.E., Scott, L., Talma, A.S. and Vogel, J.C. (1993). The Pretoria Saltpan: a 200,000 year Southern African lacustrine sequence. . *Palaeogeography, Palaeoclimatology, Palaeoecology,* 101: 317-337.

Partridge, T.C., De Menocal, P.D., Lorentz, S.A., Paiker, M.J. and Vogel, J.C. (1997). Orbital forcing of climate over South Africa: A 200,000-year rainfall record from the Pretoria Saltpan. *Quaternary Science Reviews,* 16: 1125-1135.

Partridge, T.C., Scott, L. and Hamilton, J.E. (1999). Synthetic reconstructions of southern African environments during the Last Glacial Maximum (21-18 kyr) and the Holocene Altithermal (8-6 kyr). *Quaternary International,* 57/58: 207-214.

Patrick, R. & Reimer, C.W. (1975). The diatoms of the United States, exclusive of Alaska and Hawaii (vol. 1-2). Monographs of The Natural Academy of Natural Sciences of Philadelphia, Number 13, *Natural Academy of Natural Sciences*: Philadelphia.

Pepin, N. (2000). Twentieth century change in the climate record for the Front Range, Colorado, USA. *Arctic, Antarctic an Alpine Research,* 32(2): 135-146

Pepin, N. and Losleben, M. (2002). Climate change in the Colorado Rocky Mountains: free air versus surface temperature trends. *International Journal of Climatology,* 22(3): 311-329.

Peteet, D. (1995). Global Younger Dryas. *Quaternary International,* 28: 93-104.

Plug, I. (1993). The macrofaunal and molluscan remains from Tloutle, a Later Stone Age site in Lesotho, Southern Africa. *Field Archaeology,* 2: 44-48.

Plug, I. (1997). Late Pleistocene and Holocene Hunter-Gatherers in the Eastern Highlands of South Africa and Lesotho: A faunal interpretation. *Journal of Archaeological Science,* 24: 715-727.

Plug, I., Mitchell, P. and Bailey, G. (2003). Animal remains from Likoaeng, an open-air river site, and its place in the post-classic Wilton of Lesotho and eastern Free State, South Africa. *South African Journal of Science,* 99: 143-152.

Plug, I. and Mitchell, P.J. (2008). Fishing in the Lesotho highlands: 26,000 years of fish exploitation, with special reference to Sehonghong Shelter. *Journal of African Archaeology,* 6: 33-55.

Plug, I., Mitchell, P. and Bailey, G. (2010). Late Holocene fishing strategies in southern Africa as seen from Likoaeng, highland Lesotho. *Journal of Archaeological Science,* 27: 3111-3123.

Porat, N. and Botha, G. (2008). The luminescence chronology of dune development on the Maputaland coastal plain, southeast Africa. *Quaternary Science Reviews,* 27: 1024-1046.

Poulíčková, A., Špačková, J., Kelly, M.G., Duchoslav M. and Mann, D.G. (2008). Ecological variation within Sellaphora species complexes (Bacillariophyceae): specialists or generalists? *Hydrobiologia*, 614: 373-386

Prentice, I.C. (1985). Pollen representation, source area, and basin size: Toward a unified theory of pollen analysis. *Quaternary Research,* 23(1): 76-86.

Preston-Whyte, R.A. (1971). Diurnal wind variations over the Drakensberg escarpment at Sani Pass. *South African Geographical Journal,* 53(1): 89-92.

Quick, L.J. (2013). Late Quaternary palaeoenvironments of the southern Cape, South Africa: palynological evidence from three coastal wetlands. *PhD Thesis submitted to the University of Cape Town*: Cape Town.

Quick, L.J., Chase, B.M., Meadows, M.E., Scott, L. and Reimer, P.J. (2011). A 19.5 kyr vegetation history from the central Cederberg Mountains, South Africa: Palynological evidence from rock hyrax middens. *Palaeogeography, Palaeoclimatology, Palaeoecology,* 309: 253-270.

Quinlan, T. (1995). Grassland degradation and livestock rearing in Lesotho. *Journal of Southern African Studies,* 21(3): 491-507.

Ramsay, P.J. (1995). 9000 years of sea-level change along the southern African coastline. *Quaternary International,* 31: 71-75.

Ramsay, P.J. and Cooper, J.A.G. (2002). Late Quaternary Sea-Level Change in South Africa. *Quaternary Research,* 57: 82-90.

Reddering, J.S.V. (1988). Evidence for a middle Holocene transgression, Keurbooms estuary, South Africa. *Palaeoecology of Africa*, 19: 79-86.

Reinwarth, B., Franz, S., Baade, J., Haberzetti, T., Kasper, T., Daut, G., Helmschrot, J., Kirsten, K.L., Quick, L.J., Meadows, M.E. and Mäusbacher, R. (2012). A 700-year record on the effects of climate and human impact on the southern Cape coast inferred from lake sediments of Eilandvlai, Wilderness Embayment, South Africa. *Geografiska Annaler,* 95(4): 345-360.

Renaud, R. and Bamford, M.K. (2006). Results of a preliminary palynological analysis at Sibudu Cave. *Southern African Humanities,* 18(1): 235-240.

Renberg, I. (1990). A procedure for preparing large sets of diatom slides from sediment cores. *Journal of Palaeolimnology,* 4: 87-90.

Repinski, P., Holmgren, K., Lauritzen, S.E. and Lee-Thorp, J.A. (1999). A late Holocene climate record from a stalagmite, Cold Air Cave, Northern Province, South Africa. *Palaeogeography, Palaeoclimatology, Palaeoecology,* 150: 269-277.

Roberts, D.L., Bateman, M.D., Murray-Wallace, C.V., Carr, A.S. and Holmes, P.J. (2009). West Coast Dune Plumes: climate driven contrasts in dunefield morphogenesis along the western and southern South African Coasts. *Palaeogeography, Palaeoclimatology, Palaeoecology*, 271: 34-48.

Roberts, N. (2014). The Holocene, An Environmental History, 3rd ed. *Wiley Blackwell Publishing*: Oxford.

Roberts, P., Lee-Thorp, J.A., Mitchell, P.J. and Arthur, C. (2013). Stable carbon isotopic evidence for climate change across the late Pleistocene to early Holocene from Lesotho, southern Africa. *Journal of Quaternary Science,* 28(4): 360-369.

Rojas, M., Moreno, P.I., Kageyama, M., Crucifix, M., Hewitt, C., Abe-Ouchi, A., Ohgaito, R., Brady, E.C. and Hope, P. (2009). The Southern westerlies during the last glacial maximum in PMIP2 simulations. *Climate Dynamics*, 32: 525-548

Roqvist, G. (1990). Quaternary glaciations in Africa. *Quaternary Science Reviews,* 9: 281-297.

Rose, N.L. (2015). Spheroidal carbonaceous fly ash particles provide a globally synchronous stratigraphic marker for the Anthropocene. *Environmental Science and Technology,* 49(7): 4155-4162.

Rosen, D.Z., Lewis, C.A. and Illgner, P.M. (1999). Palaeoclimatic and archaeological implications of organic-rich sediments at Tiffendell Ski Resort, near Rhodes, Eastern Cape Province, South Africa. *Transactions of the Royal Society of South Africa,* 54(2): 311-321.

Rosseeuw, P.J. (1987). Silhouettes: A graphical aid to the interpretation and validation of cluster analysis. *Journal of Computational and Applied Mathematics,* 20: 53-65.

Rossel, R.A.V., Minasny, B., Roudier, P. and McBratney, A.B. (2006). Colour space models for soil science. *Geodema,* 133: 320-337.

Rouget, M., Richardson, D.M., Nel, J.L., Le Maitre, D.C., Egoh, B and Mgidi, T. (2004). Mapping the potential ranges of major plant invaders in South Africa, Lesotho and Swaziland using climatic suitability. *Diversity and Distributions,* 10: 475-484.

Round, F.E., Crawford, R.M. and Mann, D.G. (1990). The Diatoms: Biology and morphology of the genera. *Cambridge University Press:* Cambridge.

Rydgren, B. (1988). A geomorphological approach to soil erosion studies in Lesotho. *Geografiska Annaler,* 70(3): 255-262.

Ryżak, M. and Bieganowski, A. (2011). Methodological aspects of determining soil particle-size distribution using the laser diffraction method. *Journal of Plant Nutrition and Soil Science,* 174(4): 624-633.

Saarinen, T. and Petterson, G. (2006). Image analysis techniques. In Last, W.M. and Smol, J.P. (eds.). Tracking Environmental change using lake sediments: Volume 2: physical and geochemical methods. *Springer*: Dordrecht, pp. 23-82.

Schalke, H.J.W.G. (1973). The Upper Quaternary of the Cape Flats area (Cape Province, South Africa). *Scripta Geologica,* 15: 1-48.

Schmidt, F., Oberhänsli, H. and Wilkes, H. (2014). Biocoenosis response to hydrological variability in Southern Africa during the last 84 ka BP: A study of lipid biomarkers and compound-specific stable carbon and hydrogen isotopes from the hypersaline Lake Tswaing. *Global Planetary Change,* 112: 92-104.

Schmidt, R., Kamenik, C., Lange-Bertalot, H. and Klee, R. (2004). *Fragilaria* and *Staurosira* (Bacillariophyceae) from sediment surfaces of 40 lakes in the Austrian Alps in relation to environmental variables, and their potential for palaeoclimatology. *Journal of Limnology,* 63(2): 171-189.

Schmitz, G. and Rooyani, F. (1987). Lesotho geology, geomorphology, soils. *National University of Lesotho:* Maseru.

Schoeman, F.R. (1973). A systematical and ecological study of the diatom flora of Lesotho with special reference to the water quality. *V&R Printers:* Pretoria.

Schoeman, F.R. and Archibald, R.E.M. (1976). The diatom flora of southern Africa (no. 1-6). *Council of Scientific and Industrial Research:* Pretoria.

Schwabe, C. (1995). Alpine mires of the eastern highlands of Lesotho. In Cowan, G. (ed.). Wetlands in Southern Africa. *Department of Environmental Affairs and Tourism:* Pretoria.

Schwaibold, U. and Pillay, N. (2006). Behavioural strategies of the African ice rat *Otomys sloggetti robertsi* in the cold. *Physiology & Behaviour,* 88: 567-574.

Scott, L. (1976). Preliminary palynological results from the Alexandersfontein Basin near Kimberley. *Annuals of the South African Museum*, 71: 73-189.

Scott, L. (1982a). A Late Quaternary pollen record from the Transvaal Bushveld, South Africa. *Quaternary International,* 17: 339-370.

Scott, L. (1982b). Late Quaternary fossil pollen grains from the Transvaal, South Africa. *Review of Palaeobotany and Palynology,* 36: 241-278.

Scott, L. (1989). Climatic conditions in southern Africa since the Last Glacial Maximum, inferred from pollen analysis. *Palaeogeography, Palaeoclimatology, Palaeoecology,* 70: 345-353.

Scott, L. (1993). Palynological evidence for late Quaternary warming episodes in Southern Africa. *Palaeogeography, Palaeoclimatology, Palaeoecology,* 101: 229-235.

Scott, L. (1994). Palynology of late Pleistocene hyrax middens, south-western Cape Province, South Africa: a preliminary report. *Historical Biology*, 7: 71-81.

Scott, L. (1996). Palynology of hyrax middens: 2000 years of palaeo-environmental history in Namibia. *Quaternary International*, 33: 73-79.

Scott, L. (1999a). Vegetation history and climate in the SaVanna biome South Africa since 190,000 ka: a comparison of pollen data from the Tswaing Crater (the Pretoria Saltpan) and Wonderkrater. *Quaternary International,* 57/58: 215-223.

Scott, L. (1999b). Palynological analysis of the Pretoria Saltpan (Tswaing Crater) sediments and vegetation history in the bushveld saVannah biome, South Africa. In Partridge, T.C. (ed.). Tswaing – Investigations into the origin, age and palaeoenvironments of the Pretoria Saltpan. *Council for Geosciences:* Pretoria, pp. 143-166.

Scott, L. (2002). Grassland development under glacial and interglacial conditions in southern Africa: a review of pollen, phytolith and isotope evidence. *Palaeogeography, Palaeoclimatology, Palaeoecology,* 177: 47-57.

Scott, L. and Vogel, J.C. (1978). Pollen analysis of the thermal spring deposit at Wonderkrater (Transvaal, South Africa). *Palaeoecology of Africa*, 10: 155-162.

Scott, L. and Thackeray, J.F. (1987). Multivariate analysis of late Pleistocene and Holocene pollen spectra from Wonderkrater, Transvaal, South Africa. *South African Journal of Science,* 83: 93-98.

Scott, L. and Bousman, C.B. (1990). Palynological analysis of hyrax middens from southern Africa. *Palaeogeography, Palaeoclimatology, Palaeoecology*, 79: 367-379.

Scott, L. and Vogel, J.C. (1992). Short-term changes of climate and vegetation revealed by pollen analysis of hyrax dung in South Africa. *Review of Palaeobotany and Palynology*, 74: 283-291.

Scott, L., Steenkamp, M. and Beaumont, P.B. (1995). Palaeoenvironmental conditions in South Africa at the Pleistocene-Holocene transition. *Quaternary Science Reviews,* 14: 937-947.

Scott, L. and Vogel, J.C. (2000). Evidence for environmental conditions during the last 20 000 years in Southern Africa from ^{13}C in fossil hyrax dung. *Global and Planetary Change,* 26: 207-215.

Scott, L. and Nyakale, M. (2002). Pollen indications of Holocene palaeoenvironments at Florisbad spring in the central Free State, South Africa. *The Holocene,* 12(4): 497-503.

Scott, L., Holmgren, K., Talma, A.S., Woodborne, S. and Vogel, J.C. (2003). Age interpretation of the Wonderkrater spring sediments and vegetation change in the SaVanna Biome, Limpopo Province, South Africa. *South African Journal of Science,* 99: 484-488.

Scott, L., Marais, E. and Brook, G.A. (2004). Fossil hyrax dung and evidence of Late Pleistocene and Holocene vegetation types in the Namib Desert. *Journal of Quaternary Science,* 19(8): 829-832.

Scott, L., Bousman, C.B. and Nyakale, M. (2005). Holocene pollen from swamp, cave and hyrax dung deposits at Blydefontein (Kikvorsberge), Karoo, South Africa. *Quaternary International,* 129: 49-59.

Scott, L. and Rossouw, L. (2005). Reassessment of botanical evidence for palaeoenvironments at Florisbad, South Africa. *South African Archaeological Bulletin,* 60(182): 96-102.

Scott, L. and Woodborne, S. (2007). Pollen analysis and dating of Late Quaternary faecal deposits (hyraceum) in the Cederberg, Western Cape, South Africa. *Review of Palaeobotany and Palynology,* 144: 123-134.

Scott, L., Holmgren, K. and Partridge, T.C. (2008). Reconciliation of vegetation and climatic interpretations of pollen and other regional records from the last 60 thousand years in the SaVanna Biome of Southern Africa. *Palaeogeography, Palaeoclimatology, Palaeoecology,* 257: 198-206.

Scott, L., Neumann, F.H., Brook, G.A., Bousan, C.B., Norström, E. and Metwally, A.A. (2012). Terrestrial fossil-pollen evidence of climate change during the last 26 thousand years in Southern Africa. *Quaternary Science Reviews,* 32: 100-118.

Sene, K.J., Jones, D.A., Meigh, J.R. and Farquarson, F.A.K. (1998). Rainfall and flow variations in the Lesotho highlands. *International Journal of Climatology,* 18: 329-345.

Setty, M.G.A.P. (1966). Preparation and method of study of fossil diatoms. *Micropalaeontology,* 12(4): 511-514.

Shala, S., Helmens, K., Jansson, K., Kylander, M., Risberg, J. and Löwemark, L. (2014). Palaeoenvironmental record of glacial lake evolution during the Holocene at Sokli, NE Finland. *Boreas,* 43: 362-376.

Shi, N., Dupont, L.M., Beug, H.J. and Schneider, R. (1998). Vegetation and climate changes during the last 21 000 years in S.W. Africa based on a marine pollen record. *Vegetation History and Archaeobotany,* 7: 127-140.

Showers, K.B. (2005). Imperial gullies: Soil erosion and conservation in Lesotho. *Ohio University Press:* Athens, pp. 115-176.

Sime, L.C., Kohfeld, K.E., Le Quéré, C., Wolff, E.W., de Boer, A.M., Graham, R.M. and Bopp, L. (2013). Southern Hemisphere westerly wind changes during the Last Glacial Maximum: model-data comparison. *Quaternary Science Reviews,* 64: 104-120.

Simpson, G. and Birks, H.J.B. (2012). Statistical learning in palaeolimnology. In Birks, H.J.B., Lotter, A.F., Juggins, S. and Smol, J.P. (eds.). Tracking environmental change using lake sediments, volume 5: Data handling and numerical techniques. *Springer:* Dordrecht, pp. 249-330.

Singarayer, J.S. and Burrough, S.L. (2015). Interhemispheric dynamics of the African rainbelt during the late Quaternary. *Quaternary Science Reviews,* 124: 48-67.

Sitoe, S.R., Risberg, J., Norström, E., Snowball, I., Holmgren, K., Achimo, M. and Mugabe, J. (2015). Paleo-environment and flooding of the Limpopo River-plain, Mozambique, between c. AD 1200-2000. *CATENA,* 126: 105-116.

Smit, P. (1967). A geographical study. In Smit, P., Lestner, G.M.E., Van Wyk, A.J. and Van Der Merwe, E.J. (eds.). Lesotho. *The African Institute*: Pretoria.

Smith, J., Klein, R. and Huq, S. (2003). Climate change: Adaptive capacity and development. *Imperial College Press:* London.

Smith, J.M., Lee-Thorpe, J.A. and Sealy, J.C. (2002). Stable carbon and oxygen isotopic evidence for late Pleistocene to middle Holocene climatic fluctuations in the interior of southern Africa. *Journal of Quaternary Science,* 17(7): 683-695.

Smol, J.P., Birks, H.J.B., Lotter, A.F. and Juggins, S. (2012). The march towards the quantitative analysis of palaeolimnological data. In Birks, H.J.B., Lotter, A.F., Juggins, S.

and Smol, J.P. (eds.). Tracking environmental change using lake sediments, volume 5: Data handling and numerical techniques. *Springer:* Dordrecht, pp. 3-18.

Snoeijs, P. and Balashova, N. (eds.). (1998). Intercalibration and distribution of diatom species in the Baltic Sea (vol. 5). *Opulus Press Uppsala:* Uppsala.

Sonneman, J. A., Sincock, A., Fluin, J., Reid, M., Newall, P., Tibby, J. and Gell, P. (1999). An illustrated guide to common diatom species from temperate Australia – Identification guide 33. *CRC for Freshwater Ecology:* Albury.

Sparrow, G.W.A. (1967). Pleistocene periglacial topography in southern Africa. *Journal of Glaciology,* 6(46): 551-559.

Sperazza, M., Moore, J.N. and Hendrix, M.S. (2004). High-resolution particle size analysis of naturally occuring very fine-grained sediment through laser diffractometry: Research methods papers. *Journal of Sedimentary Research,* 74(5): 736-754.

Stager, J., Cumming, B. and Meeker, L. (2003). A 10 000-year high-resolution diatom record from Pilkington Bay, Lake Victoria, East Africa. *Quaternary Research,* 59: 172-181.

Stager, J.C., Mayewski, P.A., White, J., Chase, B.M., Neumann, F.H., Meadows, M.E., King, C.D. and Dixon, D.A. (2012). Precipitation variability in the winter rainfall zone of South Africa during the last 1400 yr linked to the austral westerlies. *Climate of the Past,* 8: 877-887.

Stager, J.C., Ryves, D.B., King, C., Madson, J., Hazzard, M., Neumann, F.H. and Maud, R. (2013). Late Holocene precipitation variability in the summer rainfall region of South Africa. *Quaternary Science Reviews,* 67: 105-120.

Steffen, W., Crutzen, P.J., McNeill, J.R. (2007). The Anthropocene: are humans now overwhelming the great forces of nature? *AMBIO*, 36: 614–621.

Stevenson, R.J. and Pan, Y. (2004). Assessing environmental conditions in rivers and streams with diatoms. In Stoermer, E.F. and Smol, J.P. (eds.). The Diatoms: Applications for the environmental and earth science. *Cambridge University Press*: Cambridge, pp. 11-40.

Stewart, B., Dewar, G., Morley, M., Inglis, R., Wheeler, M., Jacobs, Z. and Roberts, R. (2012). Afromontane foragers of the Late Pleistocene: Site formation, chronology and occupational pulsing at Melikane Rockshelter, Lesotho. *Quaternary International,* 270: 40-60.

Stoermer, E.F. and Smol, J.P. (2004). The Diatoms: Applications for the environmental and earth science. *Cambridge University Press*: Cambridge.

Strachan, K.L., Finch, J.M., Hill, T. and Barnett, R.L. (2014). A late Holocene sea-level curve for the east coast of South Africa. *South African Journal of Science,* 110 (1/2): 1-9

Strachan, K.L., Hill, T.R., Finch, J.M. and Barnett, R.L. (2015). Vertical zonation of foraminifera assemblages in Galpins Marsh, South Africa. *Journal of Foraminiferal Research,* 45(1): 29-41.

Stromquist, L., Lundén, B. and Chakela, Q. (1985). Sediment sources, sediment transfer in a small Lesotho catchment – a pilot study of the spatial distribution of erosion features and their variation with time and climate. *South African Geographical Journal,* 67(1): 3-13.

Stute, M. and Talma, A.S. (1997). Isotope techniques in the study of past and current environmental changes in the hydrosphere and the atmosphere. IAEA Vienna Symposium 1997, Isotopic techniques in the study of environmental change. *International Atomic Energy Agency:* Vienna, pp. 307-318.

Stuut, J.B., Prins, M.A., Schneider, R.R., Weltje, G.J., Jansen, F. and Postma, G. (2002). A 300-kyr record of aridity and wind strength in southwestern Africa: Inferences from grain-size distribution of sediments on Walvis Ridge, SE Atlantic. *Marine Geology,* 180: 221-233.

Sudan, P., Whitmore, G., Uken, R. and Woodborne, S. (2004). Quaternary evolution of the coastal dunes between Lake Hlabane and Cape St Lucia, KwaZulu-Natal. *South African Journal of Geology,* 107: 355-376.

Sumner, P. (2004a). Relict Sorted Patterned Ground in Lesotho. *Permafrost and Periglacial Processes,* 15: 89-93.

Sumner, P.D. (2004b). Geomorphic and climate implications of relict openwork block accumulations near Thabana-Ntlenyaya, Lesotho. *Geografiska Annaler,* 86(3): 289-302.

Sundqvist, H.S., Holmgren, K., Fohlmeister, J., Zhang, Q., Bar Matthews, M., Spötl, C. and Kömich, H. (2013). Evidence of a large cooling between 1690 and 1740 AD in southern Africa. *Scientific Reports,* 3: 1767.

Talma, A.S., Vogel, J.C. and Partridge, T.C. (1974). Isotopic contents of some Transvaal speleothems and their palaeoclimatic significance. *South African Journal of Science,* 70: 135-140.

Talma, A.S. and Vogel, J.C. (1992). Late Quaternary palaeotemperatures derived from a speleothem from Cango Caves, Cape Province, South Africa. *Quaternary Research,* 37: 203-213.

Ter Braak, C.J.F. (1987). Unimodal models to relate species to environment. *Groep Landbouwwiskunde:* Netherlands.

Thackeray, J.F. and Scott, L. (2006). The Younger Dryas in the Wonderkrater sequence, South Africa? *Annals of the Transvaal Museum,* 43: 111-112.

Traverse, A. (2007). Paleopalynology. *Springer:* Dordrecht.

Truc, L., Chevalier, M., Favier, C., Cheddadi, R., Meadows, M.E., Scott, L., Carr, A.S., Smith, G.F. and Chase, B.M. (2013). Quantification of climate change for the last 20,000 years from Wonderkrater, South Africa: Implications for the long-term dynamics of the Intertropical Convergence Zone. *Palaeogeography, Palaeoclimatology, Palaeoecology,* 386: 575-587.

Truter, A. (2014). Personal communication during laboratory training. September 2014.

Turner, S. and Plater, A. (2004). Palynological evidence for the origin and development of late Holocene wetland sediments: Mdlanzi Swamp, KwaZulu-Natal, South Africa. *South African Journal of Science,* 100: 220-229.

Tyson, P.D. (1986). Climatic change and variability in southern Africa. *Oxford University Press:* Cape Town

Tyson, P.D., Preston-Whyte, R.A. and Schulze, R.E. (1976). The climate of the Drakensberg. Natal Town and Regional Planning Reports 31. *The Natal Town and Regional Planning Commission:* Pietermaritzburg.

Tyson, P.D. and Lindesay, J.A. (1992). The climate of the last 2000 years in southern Africa. *The Holocene,* 2: 271-278.

Tyson, P.D., Karlén, W., Holmgren, K. and Heiss, G.A. (2000). The Little Ice Age and medieval warming in South Africa. *South African Journal of Science,* 96: 121-126.

Van Geel, B., Gelorini, V., Lyaruu, A., Aptroot, A., Rucina, S., Marchant, R., Sinninghe Damsté, J.S. and Verschuren, D. (2011). Diversity and ecology of tropical African fungal spores from a 25,000-year palaeoenvironmental record in southeastern Kenya. *Review of Palaeobotany and Palynology,* 164: 174-190.

Van Wilgen, B.W. and Richardson, D.M. (2012). Three centuries of managing introduced conifers in South Africa: Benefits, impacts, changing perceptions and conflict resolution. *Journal of Environmental Management,* 106: 56-68.

Van Zinderen Bakker, E.M. (1955). A Preliminary Survey of the Peat Bogs of the Alpine Belt of Northern Basotholand. *Acta Geographica,* 14: 413-422

Van Zinderen Bakker, E.M. (1957). A pollen analytical investigation of the Florisbad deposits (South Africa). In Clarke, J.D. (ed.). Proceedings of the Third-Pan-African Congress on Prehistory, Livingstone, 1955. *Chatto and Windus:* London, pp. 56-67.

Van Zinderen Bakker, E.M. (1969). The Pleistocene vegetation and climate of the basin. In Clark, J.D. (ed.). Kalambo Falls Prehistoric Site. *Cambridge University Press*: Cambridge, pp. 57-84.

Van Zinderen Bakker, E.M. (1972). Late Quaternary lacustrine phases in the southern Sahara and East Africa. *Palaeoecolology of Africa*, 6: 15-27.

Van Zinderen Bakker, E.M. (1976). The evolution of late Quaternary paleoclimates of Southern Africa. *Palaeoecology of Africa,* 9: 160-202.

Van Zinderen Bakker, E.M. (1981). The high mountains of Lesotho – a botanical paradise. *Veld and Flora*, 67: 106-108.

Van Zinderen Bakker, E.M. (1983). A late-glacial and post-glacial pollen record from the Namib Desert. *Palaeoecology of Africa,* 16: 421-428.

Van Zinderen Bakker, E.M. (1989). Middle Stone Age palaeoenviron-ments at Florisbad (South Africa). *Palaeoecology of Africa*, 20: 133-154.

Van Zinderen Bakker, E.M. (1995). Archaeology and palynology. *South African Archaeological Bulletin,* 50: 98-105.

Van Zinderen Bakker, E.M. and Butzer, K.W. (1973). Quaternary environmental changes in southern Africa. *Soil Science,* 116(3): 236-248.

Van Zinderen Bakker, E.M. and Werger, M.J.A. (1974). Environment, vegetation and phytogeography of the high-altitude bogs of Lesotho. *Vegetatio,* 29: 37-49.

Van Zinderen Bakker, E.M. and Coetzee, J.A. (1988). A review of late Quaternary pollen studies in east, central and southern Africa. *Review of Palaeobotany and Palynology,* 55: 155-174.

Venables, W.N. and Smith, D.M. (2015). An Introduction to R, Notes on R: A Programming Environment for Data Analysis and Graphics Version 3.1.3 (2015-03-09). Retrieved on 14 December 2014 from www.cran.r-project.org/manuals/r-release/R-intro.pdf

Walanus, A. and Nalepka, D. (2013). Information content of zero pollen counts in Holocene profiles. *The Holocene,* 23: 732-738.

Walker, M. (2005) Quaternary Dating Methods. *John Wiley and Sons Ltd.*: Chichester.

Walker, M., Ingersoll, R. and Webber, P. (1995). Effects of interannual climate variation on phenology and growth of two alpine forbs. *Ecology,* 76(4): 1067-1083.

Walsh, G. and Wepener, V. (2009). The influence of land use on water quality and diatom community structures in urban and agriculturally stressed rivers. *Water SA, 35(5): 579-594.*

Walther, S.C. and Neumann, F.H. (2011). Sedimentology, isotopes and palynology of late Holocene cores from Lake Sibaya and the Kosi Bay system (KwaZulu-Natal, South Africa). *South African Geographical Journal,* 93(2): 133-153.

Wang, L., Mackay, A.W., Leng, M.J., Rioual, P., Panizzo, V., Lu, H., Gu, Z., Chu, G., Han, J. and Kendrick, C. (2013). Influence of the ratio of planktonic to benthic diatoms on lacustrine organic matter $\delta^{13}C$ from Erlongwan maar lake, northeast China. *Organic Geochemistry,* 54: 62-68

Wanner, H., Beer, J., Bütikofer, J., Crowley, T., Cubasch, U., Flückiger, J., Goosse, H., Grosjean, M., Joos, F., Kalan, J.O., Küttel, M., Müller, S.A., Prentice, I.C., Solomina, O., Stocker, T.F., Tarasov, P., Wagner, M. and Stocker, T.F. (2008). Mid- to Late Holocene climatechange: an overview. *Quaternary Science Reviews,* 27: 1791-1828.

Wanner, H., Mercolli, L., Grosjean, M. and Ritz, S.P. (2015). Holocene climate variability and change: a data-based review. *Journal of the Geological Society,* 172(2): 254-263.

Weldeab, S., Stuut, J.B.W., Schneider, R.R. and Siebel, W. (2013). Holocene climate variability in the winter rainfall zone of South Africa. *Climate of the Past,* 9: 2347-2364.

West, R.G. (1968). Studying the past by pollen analysis. *Oxford University Press*: London.

Western diatoms (n.d.). Diatoms of the United States. Accessed on 20 June, 2014 from https://westerndiatoms.colorado.edu/

Westover, K.S., Fritz, S.C., Blyakharchuk, T.A. and Wright, H.E. (2006). Diatom palaeolimnological record of Holocene climatic and environmental change in the Altai Mountains, Siberia. *Journal of Palaeolimnology,* 35: 519-541.

Willis, K.J., Gillson, L., Bmcic, T.M. and Figueroa-Rangel, B.L. (2005). Providing baselines for biodiversity measurement. *Trends in Ecology and Evolution,* 20(3): 107-108.

Yang, J. (1990). Diatoms as indicators of lake trophic status. *MSc Dissertation submitted to Brock University:* Ontario.

Ziervogel, G. (2004). Targeting seasonal climate forecasts for integration into household level decisions: the case of smallholder farmers in Lesotho. *The Geographical Journal,* 170(1): 6-21.

Ziervogel, G. and Calder, R. (2003). Climate variability and rural livelihoods: assessing the impact of seasonal forecasts in Lesotho. *Area,* 35(4): 403-417.

Zinke, J., Loveday, B.R., Reason, C.J.C., Dullo, W.C. and Kroon, D. (2014). Madagascar corals track sea surface temperature variability in the Agulhas Current core region over the past 334 years. *Scientific Reports,* 4: 4393-4401.

Zunckel, K. (2003). Managing and conserving southern African grasslands with high endemism. *Mountain Research and Development,* 23(2): 113-118.

APPENDIX A: LABORATORY METHODS

A.1 POLLEN PREPARATION

1. Measure out 7g of each subsample into individual test tubes and label.

2. Add 45ml of 10% HCl to each of the samples and stir regularly in a beaker to dissolve carbonates.

3. Use a 500 micron sieve to remove roots and large organic particles. Add distilled water to the sieve to wash through small sized sediment and pollen. Sufficiently large spacing is required to prevent the removal of large pollen grains.

4. Sieved samples and distilled water stirred and placed in the centrifuge for 2 minutes at 3000rpm ("quick wash"). Decant. Add remaining solution to centrifuge tubes and centrifuge, decant. Repeat until all of the solution has been centrifuged.

5. Add 30ml 40% HF to re-combine centrifuged sample and leave overnight to remove silicates. Stir using stirring rod. Centrifuge for 5 minutes at 3000rpm. Decant. Add distilled water, centrifuge and decant. Repeat until the supernatant rinses clean.

6. Add 30ml 10% KOH to remove remaining organic material. Stir with stirring rod, decant into crucibles. Heat on hot plate for approx. 5 minutes until boiling. Return liquid to the washed centrifuge tubes. Centrifuge for 5 minutes at 3000rpm. Decant. Add distilled water, centrifuge and decant. Repeat until supernatant rinses clean.

7. Place sample in beakers, add 30ml super-saturated $ZnCl_2$ solution (155ml 10% HCl + 500g $ZnCl_2$ mix) for mineral separation. Pour into a tube bent in half, placed inside the centrifuge tubes. Centrifuge for 5 minutes. Bend the top of the tube, pour into a second clean centrifuge tube. Rise out the bent section using distilled water to include any pollen grains stuck to the side of the tube. Add distilled water to the second centrifuge tube to 45ml. Shake on shake machine. Centrifuge for 5 minutes at 3000r/min. Decant. Rinse with distilled water until all of the $ZnCl_2$ has been removed.

8. Perform acetolysis to remove cellulose: Add 15ml glacial acetic acid to sample. Shake on shake machine. Add glacial acetic acid to fill to 25ml. Centrifuge for 5 minutes at 3000rpm. Decant. Add a small amount of a 9:1 mixture of acetic anhydride and H_2SO_4. Place centrifuge tubes in a beaker of 80°C water for 3 minutes for acetolysis to occur. Transfer the centrifuge tubes into a beaker of cold water to stop acetolysis. Centrifuge for 5 minutes at 3000rpm and decant. Add 15ml glacial acetic acid to sample. Shake on shake machine. Centrifuge for 5 minutes at 3000rpm and decant. Add distilled water to 45ml, shake. Centrifuge for 5 minutes at 3000rpm and decant. Repeat 3 times

9. Preparing Slides: Heat glycerol jelly and slides. Number the slides according to the lab assigned sample numbers. Rinse sample (centrifuge) one last time, leaving behind some of the supernatant on decanting. Place 4 drops of glycerol jelly on a slide, followed by one drop of the corresponding sample mixture. Mix and spread using mixing rod. Remove any large particles which would obstruct the coverslip. Place back on the hot plate for a few minutes to allow the excess water to evaporate. Place coverslip on. Leave to cool. Wash the slide and permanently label.

A.2 Diatom Preparation

Due to the large number of samples, preparation was undertaken using a water bath, rather than a hot plate.

1. Weigh out 0.1g of wet sediment from each sample into separate centrifuge tubes. Record weights to four decimal points

2. Add 2ml 30% H_2O_2 to each sample. If no violent reaction occurs, add a further 3ml 30% H_2O_2. When any violent reactions have completed, place the test tube rack in the water bath, in the fume cupboard. Increase the water temperature to 70°C. Float hollow plastic spheres in the water bath to ensure that evaporation does not occur too rapidly.

3. Leave samples in the heated water bath, maintaining H_2O_2 levels, until all of the organic material has been removed. This may take a couple of hours to a few days.

4. Remove the test tubes from the water bath. Add 1-2 drops of 50% HCl to each tube to eliminate any remaining H_2O_2 and carbonates.

5. Top up test tubes with distilled water. Centrifuge at 1200rpm for 4 minutes. The supernatant liquid is decanted off and diatoms are re-suspended in more distilled water. Wash again a further four times.

6. In final wash, add a few drops of weak NH_3 solution to keep clays in suspension and prevent clumping of diatoms when slides are prepared.

7. In order to determine concentrations of diatoms, divinylbenzene microspheres are added in the final wash stage. A suspension of $5x10^5$ spheres is added to a few subsampled samples. Test slides are made to check the ratio of microspheres to diatoms. When the ratio has been corrected to 1:1, that concentration of microspheres can be added to each of the samples. For this study a concentration of $8.02x10^4$ microspheres was used with the original concentration of diatom solution for organic-rich samples, and a with a 100x dilution of the diatom solution for samples from diatomite-rich layers.

8. Using the 1ml pipette, place 0.5ml of well mixed diatom suspension on each cover slip. Cover the tray to keep off dust and leave to dry overnight. Once they have dried, heat the hotplate in the fume cupboard to 130°C.

9. Place 1 drop of Naphrax on a glass microscope slide. Invert the coverslip with the dried diatoms over the top. Heat the slide on the hotplate for 15 minutes to drive off the toluene in the Naphrax. Allow the slide to cool and check that the cover slip does not move.

A.3 Sediment Preparation

1. Compare each of the subsampled sediments to the Munsell Colour chart to determine the sediment colour. Record this.

2. Place sediment into small aluminium trays. Bake in the oven for 24 hours at 105°C to remove all water.

3. For each sample, weigh a crucible and record the weight. Fill the crucible with dry sediment and re-weigh, record the weight.

4. Place the crucible of dry sediment into the furnace and bake for 2 hours 45 minutes at 550°C to remove all organic matter. Once the furnace has cooled, remove the crucibles and re-weigh, record the weight. The proportion deficit in weight represents the percentage organic content of the sediment sample.

5. Place the crucible back into the furnace and bake for 4 hours 45 minutes at 950°C to remove carbonates. Once the furnace has cooled, remove the crucibles and re-weigh, record the weight. The proportion further deficit in weight represents the percentage carbonate content of the sediment sample.

6. Gently crush the sediment using a pestle and mortar to de-agglomerate any clumps of individual particles.

7. Using approximately one teaspoon of sediment reflecting a representative sample of the crushed sediment, make a slurry using water. Add a 1-3g representative sample of this slurry to the mastersizer beaker filled with water until the required obscuration range is attained. Run five particle size measurements per sample using the same standard operating procedure (SOP) for all samples, and capture the weighted average particle size distribution.

<u>Mastersizer Standard Operating Procedure</u>

- Particle type: non-spherical
- Material refractive index: 1.555 (clay)
- Material absorptive index: 0.1
- Dispersant: water (refractive index 1.33)
- Red light: 10 seconds background measurement
  10 seconds sample measurement
- Blue light: 10 seconds background measurement
  10 seconds sample measurement
- Number of measurements: 5
- Obscuration index: 5-15%
- Stirrer speed: 2560 RPM
- Ultrasound: 60 seconds before measurement at 30%
- No limits on result size range.

APPENDIX B: RAW PROXY DATA

B.1 SANI VALLEY MASTERSIZER PARTICLE SIZE RESULTS

Sample Number	Depth (cm)	-2	-1.5	-1	-0.5	0	0.5	1	1.5	2	2.5	3	3.5	4	4.5	5	5.5	6	6.5	7	7.5	8	8.5	9	9.5	10	10.5
S28	3-5	0.0	0.0	0.0	0.0	0.0	0.0	1.2	4.6	7.5	9.4	11.7	13.4	12.9	10.5	7.9	5.8	4.4	3.3	2.4	1.7	1.2	0.8	0.6	0.4	0.3	0.2
S1	6	0.0	0.0	0.0	0.0	0.0	0.8	4.2	9.1	12.9	14.0	12.2	9.5	8.0	7.1	5.8	4.3	3.2	2.4	1.9	1.4	1.0	0.8	0.6	0.4	0.3	0.1
S29	9-11	0.0	0.0	0.2	0.5	2.3	7.0	10.2	10.0	10.1	12.0	12.6	9.6	5.4	3.1	3.2	3.4	2.8	1.9	1.4	1.2	1.0	0.7	0.5	0.4	0.3	0.1
S9	12-14	0.0	0.0	0.0	0.0	0.0	0.8	4.2	7.9	8.6	8.0	8.4	9.5	9.9	9.0	7.5	6.1	4.9	3.9	3.1	2.4	1.8	1.3	1.0	0.7	0.6	0.4
J	15-17	0.0	0.0	0.0	0.0	0.0	0.2	2.1	5.9	8.4	9.5	10.4	11.0	10.5	9.1	7.5	6.0	4.8	4.3	2.5	2.3	1.7	1.3	1.0	0.7	0.5	0.4
S10	17-19	0.0	0.2	0.8	2.3	4.8	6.7	6.9	6.4	6.4	7.5	9.0	9.8	9.1	7.4	5.6	4.3	3.4	2.7	2.1	1.5	1.1	0.8	0.5	0.4	0.3	0.1
S2	19-22	0.0	0.0	0.0	0.1	0.8	2.4	4.6	7.8	12.6	14.9	12.2	7.9	6.2	6.3	5.9	4.7	3.5	2.8	2.2	1.7	1.2	0.8	0.6	0.4	0.3	0.1
S11	22-24	0.0	0.1	0.4	0.8	1.5	2.9	4.3	4.9	5.2	6.1	8.3	11.0	12.4	11.5	9.0	6.4	4.6	3.4	2.5	1.7	1.2	0.8	0.5	0.4	0.3	0.1
S12	27-29	0.0	0.2	1.0	2.0	3.4	4.5	4.9	4.5	4.3	5.3	7.5	10.0	11.3	10.7	8.7	6.4	4.7	3.5	2.5	1.7	1.1	0.7	0.5	0.3	0.3	0.1
I	30-32	0.0	0.0	0.0	0.0	0.0	0.1	0.9	1.9	2.5	3.4	6.0	9.9	13.4	14.7	13.3	10.3	7.4	5.5	4.0	2.7	1.6	1.0	0.7	0.5	0.4	0.2
S3	32-35	0.0	0.0	0.0	0.2	1.9	5.5	8.1	8.8	9.3	10.1	10.1	8.9	7.3	6.2	5.3	4.5	3.5	2.8	2.2	1.7	1.2	0.9	0.6	0.4	0.3	0.2
K	35-37	0.0	0.0	0.0	0.0	0.0	0.0	0.0	0.0	0.8	2.7	5.0	9.7	15.3	17.4	14.8	10.2	6.9	5.1	3.9	2.8	1.9	1.2	0.8	0.6	0.5	0.4
S13	37-39	0.0	0.0	0.0	0.0	0.2	1.0	2.1	2.7	2.9	3.6	6.1	10.2	13.5	13.9	11.6	8.5	6.3	5.0	4.0	2.9	2.0	1.3	0.9	0.6	0.5	0.3
H	40-42	0.0	0.0	0.0	0.0	0.1	0.7	1.8	2.7	3.1	4.1	6.8	10.4	12.9	13.1	11.5	9.0	6.8	5.3	4.1	2.9	1.8	1.1	0.8	0.5	0.4	0.2
S14	42-44	0.0	0.1	0.3	0.5	0.5	0.7	1.3	1.8	2.1	3.1	5.9	10.5	14.3	15.4	13.5	10.0	6.8	4.7	3.2	2.1	1.3	0.8	0.5	0.3	0.3	0.1
S4	43-45.5	0.0	0.4	1.5	2.4	2.5	2.2	2.1	2.8	4.3	6.6	9.2	10.5	10.1	9.6	9.3	8.2	6.3	4.4	2.9	1.9	1.2	0.7	0.5	0.3	0.2	0.0
S15	47-49	0.0	0.1	0.4	0.8	1.2	1.8	2.4	2.7	2.9	3.8	6.4	10.2	13.0	13.6	12.0	9.0	6.4	4.6	3.3	2.1	1.3	0.8	0.5	0.3	0.3	0.1
S30	49-52	0.0	0.0	0.2	0.3	0.4	0.7	1.1	1.5	2.6	5.1	8.7	12.0	13.4	13.3	12.0	9.3	6.5	4.5	3.0	2.0	1.2	0.8	0.5	0.3	0.2	0.1
S16	52-54	0.0	0.0	0.0	0.3	1.1	2.0	2.6	2.5	2.4	3.6	7.0	11.2	13.5	12.9	10.7	8.1	6.3	5.1	4.0	2.8	1.6	0.9	0.6	0.5	0.3	0.1
L	54-56	0.0	0.0	0.0	0.0	0.3	2.4	5.5	7.1	7.9	9.5	11.8	12.8	11.4	8.8	6.3	4.5	3.4	2.5	1.8	1.3	0.9	0.6	0.5	0.3	0.2	0.1
S5	56-58	0.0	0.4	1.4	1.8	1.3	1.0	2.7	5.5	6.1	4.0	2.0	2.4	4.3	7.5	11.9	11.6	8.4	6.1	5.3	4.5	3.5	2.7	2.1	1.6	1.3	0.8
G	58-60	0.0	0.0	0.0	0.1	0.9	3.1	6.0	8.3	9.8	10.7	10.9	9.9	8.1	6.4	5.2	4.3	3.6	3.0	2.5	2.0	1.6	1.3	1.0	0.7	0.5	0.4
S17	60-62	0.0	0.0	0.2	0.5	2.2	6.1	9.8	11.0	10.2	9.4	8.8	8.0	6.6	5.3	4.2	3.5	3.0	2.5	2.1	1.7	1.4	1.1	0.9	0.6	0.5	0.4

S18	62-64	0.0	0.0	0.0	0.1	0.9	2.9	6.0	9.2	11.3	11.7	11.0	9.5	7.7	6.1	4.9	3.9	3.2	2.6	2.2	1.8	1.5	1.2	0.9	0.7	0.6	0.4
F	64-66	0.0	0.1	0.4	1.5	4.1	7.6	10.2	11.2	11.1	10.5	9.3	7.7	6.2	5.0	3.9	3.0	2.2	1.6	1.3	1.0	0.7	0.5	0.4	0.3	0.2	0.0
S19	67-69	0.0	0.0	0.0	0.0	0.2	1.2	5.4	10.5	12.4	12.3	12.1	11.4	9.4	6.9	4.9	3.5	2.7	2.1	1.6	1.1	0.8	0.6	0.4	0.3	0.2	0.0
S6	71-73	0.0	0.2	0.8	2.0	4.3	6.6	7.3	6.9	6.7	7.6	8.7	8.9	7.8	6.4	5.3	4.6	4.0	3.3	2.6	1.9	1.4	1.0	0.7	0.5	0.4	0.2
S20	72-74	0.0	0.3	1.1	2.2	3.4	4.4	4.9	5.2	6.1	8.0	10.2	10.7	9.2	7.2	5.8	4.9	4.2	3.4	2.7	2.0	1.4	1.0	0.7	0.5	0.4	0.3
E	74-76	0.0	0.0	0.0	0.0	0.0	0.0	0.0	0.0	0.0	0.0	0.0	0.0	3.2	16.9	24.0	17.4	9.9	7.2	6.6	5.2	3.4	2.1	1.5	1.2	0.9	0.5
S21	77-79	0.0	0.2	0.9	2.3	4.6	7.0	8.4	9.1	9.9	10.6	10.0	8.0	6.1	4.8	4.0	3.2	2.5	2.1	1.7	1.4	1.1	0.8	0.6	0.4	0.3	0.3
D	80-82	0.0	0.0	0.2	0.8	2.4	5.2	7.4	8.3	9.0	9.7	9.9	9.1	7.9	6.5	5.3	4.2	3.4	2.7	2.1	1.7	1.3	1.0	0.7	0.5	0.4	0.3
S7	81.5-83.5	0.0	0.0	0.2	0.7	1.8	3.6	5.8	8.9	13.0	13.9	10.0	5.5	4.6	5.5	5.7	4.8	3.8	3.2	2.6	2.0	1.4	1.1	0.8	0.5	0.4	0.3
S22	83.5-85.5	0.0	0.1	0.5	1.5	3.1	4.8	6.2	8.6	11.8	12.8	10.9	8.3	6.7	5.7	4.7	3.5	2.6	2.1	1.8	1.4	1.1	0.8	0.5	0.4	0.3	0.2
S23	87-89	0.0	0.0	0.0	0.0	0.3	2.2	4.5	5.8	6.4	7.0	8.1	8.9	8.7	8.1	7.7	7.2	6.5	5.4	4.1	3.0	2.1	1.5	1.1	0.7	0.6	0.4
C	89-92	0.0	0.0	0.1	0.2	1.1	3.4	6.3	9.6	14.1	16.2	12.7	6.8	4.0	4.1	4.3	3.6	2.8	2.3	2.0	1.7	1.4	1.1	0.9	0.6	0.5	0.3
S24	92-94	0.0	0.0	0.0	0.5	3.4	8.2	11.3	11.2	9.7	9.0	8.6	7.5	5.9	4.7	4.0	3.4	2.8	2.3	1.9	1.5	1.2	1.0	0.7	0.5	0.4	0.2
B	95-97	0.0	0.0	0.0	0.0	0.4	2.4	5.2	7.2	8.3	9.4	10.3	9.9	8.4	7.1	6.1	5.2	4.3	3.6	3.0	2.5	1.9	1.5	1.2	0.8	0.7	0.4
S25	97-99	0.0	0.0	0.0	0.0	0.0	2.1	7.6	10.9	10.1	9.0	9.0	9.1	8.1	6.5	5.3	4.5	3.8	3.2	2.7	2.2	1.8	1.4	1.1	0.8	0.6	0.4
S26	102-104	0.0	0.0	0.0	0.2	1.9	6.1	9.7	10.5	9.4	8.6	8.4	7.9	6.7	5.4	4.6	4.0	3.4	3.0	2.5	2.1	1.7	1.3	1.0	0.7	0.6	0.4
A	104-106	0.0	0.0	0.0	0.0	0.5	3.1	7.3	10.0	10.5	10.0	9.6	8.8	7.5	6.1	5.0	4.2	3.6	3.1	2.6	2.2	1.8	1.4	1.1	0.7	0.6	0.4

B.2 SANI VALLEY POLLEN COUNTS

Sample Number	Midpoint Depth	Cyperaceae	Asteraceae total	Poaceae	*Crassula*	Acanthaceae	Aizoaceae	Apiaceae	Caryophylaceae	Cheno-Am	*Indigofera*	Gentianaceae	Geraniaceae	Liliaceae	Malvaceae	*Olea*	*Pinus*	*Podocarpus*	*Anthospermum*	*Passerina*	*Typha*	*Wydringtonia*	Total
S28	4	201	14	17	6		4	1	4	1	1			3									252
S1	6	176	23	45	7		2	1	1			1					1						257
S29	10	177	28	19	14	1	3	4	1								1	1		2			251
S9	13	159	24	53	4		3	1	1	2	1				1	2							251
S10	18	104	80	36	12			5	3	5	2			1						1	1		250
S2	20.5	101	73	54	8	1	1	1	3	6			1	2									251
S11	23	139	58	19	9		2	1	12	5			1	2	1					1	1		251
S12	28	83	107	43	7		1		2	4	1		1	1		1							251
S3	33.5	116	52	65	11		1	2	2	6				2									257
S13	38	112	70	49	6	1	1	1	1	4	1	1		1	2								250
S14	43	120	86	26	4		2	1	2	2		1		2	3						1		250
S4	44	82	103	60	1			1	1	2									1				251
S15	48	129	50	58	7	1	1		1				1					1			1		250
S30	50.5	172	30	44	4		1	0	2	1				1						1			256
S16	53	155	23	38	23			3	1	1	2			2		3							251
S5	57	108	57	56	8			5	4	6	1	2		1							2		250
S17	61	97	45	49	28	1	11	9	2	3	9	2				5					4		265
S18	63	139	43	34	6	1	10	2	2	1	5	3		1		1				1	2		251
S19	68	141	52	23	9	1	7	2	8			1		2		1		1		1	1		250
S6	72	141	46	43	4	1	6	3	1	3	2					1							251
S20	73	146	26	51	3	1	7	2	1	2	2	1		2	1	1			1	1	2		250
S21	78	167	25	33	8		3		5	2	3	1		2						1			250
S7	82.5	102	46	78	3		1	1	3	9		2		1							7		253

S22	84.5	111	55	53	4	2	5	2	4	2	1	3		2		2				1	3		250
S23	88	126	46	40	6		7	2	1	5	3	6		4		2					3		251
S24	93	138	28	45	7	2	5	4		3	10	4		1		1					2		250
S25	98	151	26	29	8	1	5	5	8	7	3	1				3			3				250
S26	103	144	35	28	10		6	12	3	1	1	1				6		2	1				250
S27	107	140	42	15	13	2	5	6	7	3	1	1		2		6			1	3	2	1	250
S8	111	113	43	66	6		2	6	1	4	3	1		1	1	1					2		250

B.3 Sani Valley Diatom Counts

Sample Number	Depth	*Aulacoseira ambigua*	*Fragilaria construens*	*Fragilaria pinnata*	*Fragilaria P/C girdle view*	*Cymbella laevis*	*Cymbella gracilis*	*Pinnularia viridis*	*Achnanthes minutissima*	*Gomphonema bohemicum*	*Gomphonema parvulum*	*Pinnularia borealis*	*Pinnularia divergentissima*	*Navicula trivialis*	*Navicula explanata*	*Gomphonema gracile*	*Diploneis ovalis*	*Eunotia praerupta*	*Fragilaria famelica*	*Stauroneis Phoenicenteron*	*Navicula laevissima*	*Navicula minima*	*Eunotia bilunaris*	*Diploneis parma*	*Sellaphora pupula*	*Denticula kuetzingii*	*Navicula pygmaea*	*Nitzschia palea*	*Hantzschia amphioxys*	*Stauroneis producta*
A	42-44	2				24					2	4	8	1	2	6	19	7	112	2		6	5	75	2			1	1	
B	33-35					33	12	12	4	4	6	5	7	1		6	14	5	103		1	4	5	46	1	1			6	
C	27-30					23	6	3				6	7			5	33	12	110	3			4	56	1	1			8	
D	18-20	1	1	4	4		3					1	5	1		1	24		198	1			4	35		1			2	
E	12-14		1	1		6					1	2	9			1	22	8	105	3	6	1	18	59	3				29	
F	2-4			3		4	6			2	6	33	16				14	2	31	3	1		7	97	7		1		47	
G	46-48		2			16	4				4	17	7	3		2	5	6	124	3	3	1		81		4			2	
H	28-30		1			63	6				6		3	1			1	13	144			4	15	11		4		1	10	
I	18-20	5	6	1	6	21	6		14	1	6	2	19	3		2	6	10	83		3	23	25	28	8	1		3	6	
J	3-5	4	13	10	49	8	9		21	3	3	3	6	10		1	10	2	39		13	6	10	18	14	19		4	4	2

Sample Number	Depth	*Cymbella selesiaca*	*Caloneis silicula*	*Pinnularia intermedia*	*Pinnularia gentilis*	Total	Microspheres	Weight of sample (g)	Dilution	Microsphere concentration	Diatom concentration
A	42-44				24	303	57	0.1002	10x	8.02 x 10^3	35567.0
B	33-35	4		6	14	300	65	0.1042	10x	8.02 x 10^3	28484.8
C	27-30			2	21	301	149	0.1032	10x	8.02 x 10^3	35736.2
D	18-20			2	16	304	261	0.1008	10x	8.02 x 10^3	17667.2
E	12-14			3	23	301	343	0.1014	10x	8.02 x 10^3	9605.0
F	2-4		2	1	20	303	253	0.1044	10x	8.02 x 10^3	7038.0
G	46-48				20	304	138	0.1026	10x	8.02 x 10^3	9341.3
H	28-30		7		13	303	68	0.1043	10x	8.02 x 10^3	16201.5
I	18-20	6	4		11	309	87	0.1025	10x	8.02 x 10^3	37015.4
J	3-5		13		12	306	69	0.1026	10x	8.02 x 10^3	42632.6

B.4 SEKHOKONG MASTERSIZER PARTICLE SIZE RESULTS

Sample number	Depth	-2	-1.5	-1	-0.5	0	0.5	1	1.5	2	2.5	3	3.5	4	4.5	5	5.5	6	6.5	7	7.5	8	8.5	9	9.5	10	10.5	11
SK1	0-5	0.0	0.0	0.0	0.0	0.0	0.2	0.8	2.1	4.4	7.4	11.0	15.0	17.2	15.5	10.6	5.7	3.1	2.2	1.7	1.2	0.7	0.5	0.4	0.3	0.2	0.0	0.0
SK2	7-12	0.0	0.5	2.1	3.6	4.5	4.0	2.4	2.9	10.3	16.7	14.4	8.6	6.8	7.1	6.3	3.9	2.1	1.2	1.0	0.7	0.4	0.3	0.2	0.1	0.0	0.0	0.0
SK3	14-19	0.0	0.0	0.0	0.0	0.0	0.0	0.4	2.6	6.1	9.2	12.0	15.3	17.0	14.7	9.5	4.8	2.6	1.9	1.4	0.9	0.5	0.4	0.3	0.2	0.2	0.0	0.0
SK4	20-25	0.0	0.0	0.1	0.3	1.0	1.7	2.3	2.9	4.8	8.4	12.7	15.4	14.7	11.3	7.4	4.6	3.3	2.7	2.1	1.5	1.0	0.7	0.5	0.4	0.3	0.1	0.0
SK5	29-34	0.0	0.1	0.5	1.2	2.2	3.0	3.4	3.9	5.9	9.1	11.7	12.2	10.8	8.6	6.4	4.8	3.9	3.3	2.7	2.1	1.5	1.0	0.7	0.5	0.4	0.2	0.0
SK6	35-40	0.0	0.2	0.6	1.0	1.2	2.0	3.7	5.9	7.7	8.1	8.2	9.1	10.1	9.7	7.9	5.9	4.7	3.9	3.2	2.3	1.6	1.1	0.8	0.6	0.5	0.3	0.0
SK7	42-7	0.0	0.1	0.5	0.9	1.9	2.9	3.1	10.3	30.6	34.5	14.2	0.9	0.0	0.0	0.0	0.0	0.0	0.0	0.0	0.0	0.0	0.0	0.0	0.0	0.0	0.0	0.0
SK8	50-55	0.0	0.0	0.0	0.0	0.9	3.1	4.6	4.5	4.6	6.2	9.0	12.2	13.5	11.8	8.5	5.7	4.1	3.1	2.4	1.7	1.2	0.9	0.7	0.5	0.5	0.3	0.0
SK9	58-62	0.0	0.3	1.6	3.1	4.5	4.9	5.0	6.5	9.5	11.7	11.5	9.7	8.1	6.6	5.0	3.4	2.3	1.8	1.4	1.0	0.7	0.5	0.4	0.3	-0.2	0.4	0.0
SK10	65-70	0.0	0.2	0.8	2.0	3.6	5.1	6.1	7.4	8.8	9.4	9.9	10.4	9.9	7.9	5.4	3.6	2.6	2.0	1.5	1.0	0.7	0.5	0.4	0.3	0.3	0.1	0.0
SK11	72-77	0.0	0.0	0.0	0.0	0.0	0.0	0.0	0.0	0.0	0.0	1.0	9.2	17.4	17.2	12.9	9.5	7.9	6.6	5.0	3.5	2.6	2.0	1.8	1.4	1.2	0.8	0.1
SK12	83-88	0.0	0.3	1.4	2.6	4.0	5.5	6.6	7.4	8.6	9.6	9.8	9.0	7.7	6.5	5.3	4.0	3.0	2.2	1.7	1.3	1.0	0.8	0.6	0.5	0.4	0.3	0.0
SK13	93-100	0.0	0.5	2.1	3.6	4.7	5.0	5.3	6.7	8.3	8.0	6.0	4.6	5.4	6.8	6.9	5.7	4.5	3.8	3.1	2.5	1.8	1.4	1.1	0.8	0.7	0.5	0.1
SK14	105-110	0.0	0.3	1.3	2.8	4.8	5.8	7.7	16.1	27.4	24.9	8.6	0.2	0.0	0.0	0.0	0.0	0.0	0.0	0.0	0.0	0.0	0.0	0.0	0.0	0.0	0.0	0.0
SK15	114-118	0.0	0.2	0.9	1.3	1.5	2.0	3.4	6.2	10.3	12.0	10.2	8.6	9.1	9.2	7.3	4.8	3.2	2.4	1.9	1.5	1.1	0.8	0.7	0.5	0.5	0.3	0.0
SK16	119-120	0.0	1.0	3.9	6.4	7.8	7.6	7.0	7.8	9.4	8.7	5.3	2.6	4.1	6.7	6.5	4.3	2.7	2.0	1.7	1.3	0.9	0.7	0.6	0.5	0.4	0.2	0.0
SK17	122-123	0.0	0.0	0.0	0.0	0.0	0.0	0.0	0.0	0.0	0.0	0.0	0.6	9.7	20.5	19.9	12.7	8.5	7.4	6.5	4.6	2.9	2.0	1.7	1.4	1.2	0.6	0.0
SK19	124-125	0.0	0.0	0.0	0.0	0.0	0.0	0.3	1.8	6.0	11.0	13.8	13.5	11.9	10.1	8.1	6.0	4.5	3.6	2.9	2.1	1.4	1.0	0.7	0.6	0.5	0.3	0.0
SK20	126-127	0.0	0.2	0.8	1.5	2.1	2.8	3.9	5.3	6.8	8.4	10.0	11.0	10.4	8.6	6.6	5.1	4.3	3.6	2.8	1.9	1.2	0.8	0.7	0.5	0.4	0.2	0.0
SK21	133-136	0.0	0.0	0.0	0.0	0.0	0.0	0.0	0.0	0.0	0.0	0.0	0.0	3.6	13.0	16.7	13.4	10.4	9.5	8.8	7.2	5.3	3.8	2.9	2.1	1.7	1.3	0.3
SK22	143-146	0.0	1.3	5.2	9.1	11.7	11.3	9.4	7.9	7.1	6.7	6.3	5.5	4.4	3.4	2.6	2.0	1.5	1.1	0.8	0.7	0.5	0.5	0.4	0.3	0.3	0.1	0.0
SK23	157-161	0.0	0.7	3.1	6.9	10.7	11.3	9.0	6.9	6.5	6.8	6.9	6.5	5.7	4.7	3.6	2.7	2.0	1.5	1.2	0.9	0.7	0.5	0.4	0.3	0.3	0.2	0.0
SK24	185-190	0.0	0.0	0.0	0.4	2.1	5.3	7.7	7.5	6.1	5.9	7.0	8.3	8.5	7.8	6.7	5.5	4.6	3.9	3.2	2.5	1.9	1.4	1.1	0.9	0.8	0.6	0.1
SK25	200-205	0.0	0.0	0.0	0.3	2.7	6.2	8.6	9.0	8.8	9.3	9.9	9.8	8.7	6.9	5.2	3.7	2.8	2.1	1.6	1.2	0.9	0.7	0.5	0.4	0.4	0.2	0.0
SK26	211-212	0.0	0.0	0.0	0.0	0.0	0.0	0.0	0.0	0.0	0.0	0.0	0.0	2.1	12.3	18.7	15.6	11.0	9.1	8.3	6.9	5.0	3.6	2.7	2.0	1.6	1.1	0.2
SK27	220-225	0.0	0.0	0.0	0.0	0.9	3.9	6.8	7.7	7.5	8.1	9.7	11.0	10.8	9.1	6.8	4.8	3.5	2.5	1.9	1.4	1.0	0.8	0.6	0.5	0.4	0.3	0.0

SK28	230-235	0.0	0.0	0.1	0.8	3.2	6.1	7.4	7.1	6.9	7.9	9.5	10.4	9.9	8.2	6.2	4.5	3.2	2.3	1.7	1.3	1.0	0.7	0.6	0.4	0.4	0.3	0.0
SK29	245-250	0.0	0.0	0.0	0.0	0.0	0.0	0.0	0.0	1.2	4.2	7.3	10.6	13.4	14.2	12.4	9.5	7.1	5.4	4.1	3.0	2.2	1.6	1.2	1.0	0.9	0.6	0.1
SK30	265-270	0.0	0.0	0.0	0.0	0.0	0.0	0.0	0.6	1.9	3.5	6.5	11.3	15.2	15.6	12.8	9.1	6.5	4.9	3.7	2.7	1.8	1.3	1.0	0.7	0.7	0.4	0.0
SK31	285-290	0.0	0.0	0.0	0.0	0.0	0.1	1.7	4.8	5.7	5.7	7.0	9.2	10.2	9.7	8.4	7.2	6.4	5.7	5.0	4.1	3.1	2.2	1.5	1.0	0.8	0.5	0.0
SK32	300-305	0.0	0.0	0.0	0.0	0.5	2.4	4.7	5.7	5.8	6.1	7.2	8.6	9.1	8.7	7.7	6.7	5.8	5.1	4.3	3.4	2.6	1.9	1.4	0.9	0.7	0.6	0.1
SK33	307-310	0.0	0.0	0.0	0.0	0.3	1.0	2.1	3.5	5.2	7.5	10.5	13.0	13.7	12.0	9.0	6.3	4.4	3.2	2.3	1.7	1.2	0.9	0.7	0.6	0.5	0.4	0.0
SK34	325-330	0.0	0.0	0.0	0.0	0.1	0.8	2.0	2.4	1.9	2.0	3.9	7.5	10.9	12.2	11.4	9.8	8.5	7.5	6.2	4.6	3.1	2.0	1.3	0.8	0.6	0.4	0.0
SK35	355-360	0.0	0.0	0.0	0.0	0.0	0.0	0.0	0.0	0.0	0.4	1.9	4.8	8.9	12.2	13.3	12.0	10.0	8.4	7.3	6.1	4.7	3.3	2.3	1.7	1.5	1.1	0.2
SK36	385-390	0.0	0.0	0.0	0.0	0.0	0.0	0.0	0.0	0.0	0.4	2.5	5.5	8.8	11.6	12.7	11.7	9.8	8.1	6.9	5.7	4.6	3.5	2.6	2.1	1.8	1.4	0.3
SK37	395-400	0.0	0.0	0.0	0.0	0.0	0.0	0.0	0.0	0.6	2.1	4.8	8.8	12.7	14.3	13.3	11.0	8.3	6.4	5.0	3.9	2.8	2.0	1.4	1.0	0.8	0.7	0.1
SK38	410-415	0.0	0.0	0.0	0.0	0.0	0.4	1.4	2.8	3.4	4.0	6.9	11.6	14.5	13.4	9.9	6.6	5.1	4.5	4.3	3.7	2.7	1.8	1.2	0.8	0.6	0.4	0.0
SK39	425-430	0.0	0.1	0.4	0.7	1.5	2.7	3.9	4.8	6.1	8.6	11.6	13.3	12.5	9.8	6.9	4.8	3.4	2.5	1.8	1.3	1.0	0.7	0.5	0.4	0.4	0.2	0.0
SK40	455-460	0.0	0.0	0.0	0.2	1.7	4.1	5.0	4.0	2.9	3.8	6.7	10.3	12.2	11.6	9.5	7.3	5.6	4.3	3.2	2.3	2.0	0.8	0.9	0.7	0.6	0.4	0.0
SK41	470-475	0.0	0.0	0.0	0.0	0.3	1.1	2.2	3.3	4.5	6.7	10.0	13.3	14.5	12.8	9.5	6.4	4.4	3.1	2.2	1.6	1.2	0.9	0.7	0.5	0.5	0.4	0.0
SK42	480-485	0.0	0.0	0.0	0.0	0.3	0.9	1.4	1.7	1.9	2.9	5.3	9.0	12.1	13.2	12.2	9.9	7.6	5.8	4.5	3.5	2.6	1.8	1.3	0.9	0.7	0.5	0.1
SK43	495-500	0.0	0.1	0.5	0.6	0.5	0.6	0.9	1.2	1.4	2.1	4.3	8.4	12.6	14.2	12.6	9.4	7.0	5.6	4.8	4.0	3.0	2.1	1.4	1.0	0.8	0.7	0.1
SK44	500-505	0.0	0.0	0.0	0.2	1.0	2.9	5.0	6.3	7.0	8.4	10.6	12.2	11.5	9.3	6.7	4.8	3.6	2.7	2.1	1.6	1.2	0.9	0.7	0.6	0.5	0.4	0.0

B.5 SEKHOKONG POLLEN COUNTS

Sample Number	Midpoint Depth	Cyperaceae	Poaceae	Asteraceae	*Crassula*	*Pentzia*	*Anthospermum*	*Passerina*	*Pinus*	*Podocarpus*	Apiaceae	Cheno-Am	*Indigofera*	Liliaceae	Ericaceae	Aizoaceae	*Vernonia*	*Olea*	Caryophylaceae	Geraniaceae	Malvaceae	Total
SK1	2.5	15	57	86	43	11	5	4	1		3	2	1	2		14		7				251
SK2	9.5	20	81	64	62	6	2	1	1		5					4	3	1	1			251
SK3	16.5	22	155	49	12	4						1		3		2	1	1				250
SK4	22.5	39	151	37	5	2		2			1		1	11		1			1			251
SK5	31.5	27	163	37	7	2					4	4		5			3		2			254
SK6	37.5	43	132	47	8	4	1					4		2		2			7			250
SK7	45.5	58	113	36	7	9	3				3	6		5		10						250
SK8	52.5	75	115	34	9						4	6				5			3			251
SK9	60	67	101	37	15			3			8	7		2		9	1					250
SK10	67.5	33	137	48	17						9	2		1		3						250
SK11	75.5	26	155	49	9	5					3			1		1			1			250
SK12	85.5	40	150	35	8						7	6				2			2			250
SK13	96.5	60	125	39	6	3		1			6	1		4		2	1		5			253
SK14	107.5	41	133	48	19	6								1		2						250
SK15	116	41	139	55	4	3		1				3				1			3			250
SK16	119.5	37	159	45	2			1				5	1	1								251
SK17	122.5	29	166	34	9	4		2			2	3		2		1			1			253
SK19	124.5	45	135	46	15	2						1	2	1		3						250
SK20	126.5	43	133	44	10	5	2	3			2	2		1		5					2	252
SK21	134.5	75	143	27	10	5					9	2	1	1		10					1	284
SK22	144.5	51	131	42	8	2		1			2	5		5		4						251
SK23	159																					0
SK24	187.5	67	133	40	6	4	2	2			1	1				1						257

SK25	202.5	43	131	50	9	4	1	3			1	5				3				250
SK26	211.5	61	133	36	6	2	1	2				8		1						250
SK27	222.5	56	123	53	7	2						3	1	2		3				250
SK28	232.5	45	132	55	4	2					2			2		7	1			250
SK29	247.5	31	144	57	12	1					1	3				1				250
SK30	267.5	26	167	58	5	2					1			2						261
SK31	287.5	56	131	73	5							1								266
SK32	302.5	80	81	73	12							1		1		3				251
SK33	308.5	81	82	72	7	1		1				8		5		1		1		259
SK34	327.5	54	133	57	14						2	5		1	1		1		1		269
SK35	357.5	37	150	41	17	3					1	2		1						252
Sk36	387.5	77	107	51	11	3						1				1				251
SK37	397.5	71	117	57	3	3						1			1					253
SK38	412.5	75	90	62	16	4						1		1			1			250
SK39	427.5	91	87	40	29						1	2	1		1	4		3		259
SK40	457.5	55	117	42	19	3					3	6	1			5	1			252
SK41	472.5	42	122	53	14	7					2	9				1				250
SK42	482.5	20	167	51	4	1					1	4		1					1	0
SK43	497.5	88	115	37	3	4		1		1		1						1		251
SK44	502.5	66	107	43	22	4					1	5			1	2		1		252

B.6 SEKHOKONG DIATOM COUNTS

Sample Number	Midpoint Depth	*Aulacoseira ambigua*	*Fragilaria construens*	*Fragilaria pinnata*	*Fragilaria girdle view*	*Cymbella laevis*	*Cymbella gracilis*	*Pinnularia viridis*	*Achnanthes minutissima*	*Gomphonema bohemicum*	*Gomphonema parvulum*	*Pinnularia borealis*	*Pinnularia divergentissima*	*Navicula trivialis*	*Navicula explanata*	*Gomphonema gracile*	*Diploneis ovalis*	*Eunotia praerupta*	*Fragilaria famelica*	*Stauroneis Phoenicenteron*	*Navicula laevissima*	*Navicula minima*	*Eunotia bilunaris*	*Eunotia exigua*	*Diploneis parma*	*Sellaphora pupula*	*Navicula insociabilis*	*Navicula salinarum*	*Denticula kuetzingii*	*Navicula pygmaea*	*Nitzschia palea*	*Hantzschia amphioxys*
SK1	2.5					4	4	7	10			29	13			12	17	22	120	1	2		3		4	7					3	24
SK2	9.5		18			1	5	1	38			23	14	1	20	14	5	9	93	1	1	2	13	2							4	33
SK3	16.5		8	1	2	4	6		19		2	30	17		12	3	6	14	61	1	7	27	23	3	7	3					8	27
SK4	22.5					7	7		9			26	56	1	6	9	4	6	64	2	17	10	9	3	28	1				1		18
SK5	31.5					3	7		5		8	21	38		10	6	3	8	52	7	9	22	12	8	28							32
SK6	37.5		2	3	8	8	11		4		6	20	29	1	4		10	5	30	4	8	18	30	14	26	11						28
SK7	45.5					2	3		4	6	2	16	20		1	2	2	7	116	8	3	12	30	6	29	9			1			2
SK8	52.5		4	2	3	4	15		13		22	18	21	1	3		9	9	44	8	14	17	39	11	9	3		1			3	15
SK9	60					1	19		8	3		20	16			3	4	25	94	7		7	16	4	27	1						21
SK10	67.5					2	24		2	2		18	17			2		8	104	2		7	13	4	35	6						45
SK11	75.5	6	1		7	3	4		3		6	25	3	1	5	2	3	8	164	2	12	5	8		3	3		3				22
SK12	85.5						17		7		4	21	25					11	149	3		9	10		21							23
SK13	96.5	1				3	32		5		3	14	12					7	107	3		11	16		14	8						47
SK14	107.5	2	3			1			1			9	4					2	263	2		1	1		4	1						7
SK15	116	1	3			2	7		7	1		6	9					8	219		3	6	8		5	3					2	9
SK16	119.5		1		2	2	8				16	20	16		5	2	3	14	116	1	3	4	16	1	5	12		2			2	45
SK17	122.5	1	24						17	2	7	4	8		1	5	1	2	168	2	2	3	28	2	1	4					4	9
SK19	124.5		19			6	3		23			9	24	1	12	4	5	3	131	3	3	2	21	4	18	3				1	1	2
SK20	126.5		19			3	4		15	1	2	4	35		10			2	142	11	2	6	20	3	4	1						7
SK21	134.5			2	6	15	26	7			4	24	17	2			2	16	72	2	2	6	14		11			2				47
SK22	144.5	2	1			1					1	12	8	2			2	5	133	3	3	1	15	2	44							46

SK23	199																																
SK24	187.5		6				25		6	3	2	31	31	3			6	3	62	6	2	4	10	2	25	3							40
SK25	202.5																																
SK26	211.5			7	4	8	7		1		5	13	11		3		14	2	79	3	18	7	21	2	24	8	2	3					41
SK27	222.5	3	6				3				9	36	3		6			12	138	3		9	9		9								45
SK28	232.5		2			7	6		16			42	12				6	6	105	5		5	11		10				2	1			45
SK29	247.5	4	21			2	3		15		3	15	16	3	7	1	7	13	79	5	1	14	14		12				4	3	9		35
SK30	267.5	1		2	3	2			7	3	18	16	14		2		14	1	61	4	15	30	28	9	10	12	1	6			6		33
SK31	287.5		9			7	9			2	2	22	38	2				23	53	6		7	25	4	38						2		16
SK32	302.5	1	4			5	8		5			17	48	1	5		3	12	46	6	5	18	12	4	16				1		2		54
SK33	308.5	1	2			2	2		13			7	20	2	5		1	7	103	3	1	16	29	1	20				1	1	4		41
SK34	327.5		2	1	5	28	11	2	11		17	5	17	2	1	5	6	21	40	6	4	6	47	10	19			2		1			8
SK35	357.5	3		3		21	2				25		18		4			8	1	8		4	110	30	6	8					1		19
Sk36	387.5	4	7	15		32	6		9		30	7	42		3	1	1	10		17	3	7	45	21	1	5							17
SK37	397.5	4		3	9	66	14	10	2		3	7	27	3			4	1	21	2	3	3	84	2	3	1				3			14
SK38	412.5			9		20	9				12	3	18				1	23	8	12		40	47	5	57	4							6
SK39	427.5	22	17	40		12	13		2		8	17	16		2			11	67	5	1	9	31	3	13	4					1		7
SK40	457.5		21	43	36	23	28	1	6		21	5	8	5	3	7		18	5	7		13	23	6	8								1
SK41	472.5	21	9	44		18	15		6		4	10	15			4	2	24	3	14	1	21	21	5	28					1	2		13
SK42	482.5																																
SK43	497.5	38		5	2	20	12	2		1	3	8	41	6	2		4	7	8	9		25	37	5	14	2				1			19
SK44	502.5	59		83		8	7				2	5	14	4		2		24	23	9	1	8	24	1	15	1			2				3

Sample Number	Midpoint Depth	*Stauroneis producta*	*Cymbella selesiaca*	*Caloneis silicula*	*Pinnularia intermedia*	*Gomphonema exigua*	*Cymbella cistula*	*Achnanthes coarctata*	*Diploneis didyma*	*Pinnularia gentilis*	Total	Microspheres	Weight of sample (g)	Dilution	Microsphere concentration	Diatom concentration
SK1	2.5			1						24	307	242	0.1020	10x	8.02 x 10^3	10174.1
SK2	9.5									7	305	280	0.1004	10x	8.02 x 10^3	8736.1
SK3	16.5			1	2					12	306	247	0.1031	0x	8.02 x 10^4	9935.7
SK4	22.5			7						12	303	80	0.1013	10x	8.02 x 10^3	30375.8
SK5	31.5			7						16	302	220	0.1046	10x	8.02 x 10^3	11009.3
SK6	37.5				1					20	301	90	0.1004	0x	8.02 x 10^4	26822.4
SK7	45.5		9	2						10	160	160	0.1014	10x	8.02 x 10^3	8020.0
SK8	52.5		7	1						10	306	162	0.1029	0x	8.02 x 10^4	15148.9
SK9	60			3						22	301	662	0.1003	10x	8.02 x 10^3	3646.6
SK10	67.5									11	302	306	0.1013	10x	8.02 x 10^3	7915.2
SK11	75.5		1		3					8	311	283	0.1043	0x	8.02 x 10^4	8813.5
SK12	85.5			4						7	311	182	0.1020	10x	8.02 x 10^3	13704.5
SK13	96.5			2						17	302	209	0.1011	10x	8.02 x 10^3	11588.7
SK14	107.5	1								1	303	284	0.1027	10x	8.02 x 10^3	8556.5
SK15	116									3	302	844	0.1023	10x	8.02 x 10^3	2869.7
SK16	119.5									8	304	205	0.1015	0x	8.02 x 10^4	11893.1
SK17	122.5	2					4			3	304	58	0.1005	10x	8.02 x 10^3	42035.9
SK19	124.5	1					5				304	127	0.1022	10x	8.02 x 10^3	19197.5
SK20	126.5		1	2			5			4	303	196	0.1007	10x	8.02 x 10^3	12398.3
SK21	134.5			5					1	22	305	533	0.1041	0x	8.02 x 10^4	4589.3
SK22	144.5	1		1						17	300	121	0.1032	10x	8.02 x 10^3	19884.3
SK23	199										0	300	0.1009	10x	8.02 x 10^3	6532.4
SK24	187.5	4		4			1			24	303	372	0.1021	10x	8.02 x 10^3	19323.8

SK25	202.5									0	411	0.1014	10x	8.02 x 10^3	5308.1
SK26	211.5		1	7		2		2	11	306	127	0.1021	0x	8.02 x 10^4	3676.8
SK27	222.5	9							21	321	485	0.1012	10x	8.02 x 10^3	28208.3
SK28	232.5	6	2	3				9	8	309	674	0.1008	10x	8.02 x 10^3	11701.9
SK29	247.5	2		4				7	7	306	87	0.1022	10x	8.02 x 10^3	11683.0
SK30	267.5	1		12		1			9	321	220	0.1038	0x	8.02 x 10^4	19222.5
SK31	287.5	7							31	303	208	0.1005	10x	8.02 x 10^3	11235.4
SK32	302.5	4		6					19	302	126	0.1023	10x	8.02 x 10^3	9067.4
SK33	308.5	3	2	1					16	304	217	0.1011	10x	8.02 x 10^3	6137.8
SK34	327.5	1					3		22	303	268	0.1025	0x	8.02 x 10^4	3147.5
SK35	357.5	1	2	2					24	300	392	0.1015	10x	8.02 x 10^3	6979.9
Sk36	387.5	3							26	312	795	0.1008	10x	8.02 x 10^3	4831.3
SK37	397.5			4			2		7	302	347	0.1023	0x	8.02 x 10^4	33790.9
SK38	412.5			3					23	300	498	0.1010	10x	8.02 x 10^3	21675.7
SK39	427.5		2			4			9	316	75	0.1005	10x	8.02 x 10^3	15574.3
SK40	457.5		7						5	300	111	0.1033	0x	8.02 x 10^4	6136.5
SK41	472.5		2			4			14	301	155	0.1004	10x	8.02 x 10^3	16912.9
SK42	482.5									0	410	0.1014	10x	8.02 x 10^3	20680.2
SK43	497.5		2	3					27	303	396	0.1001	0x	8.02 x 10^4	38750.0
SK44	502.5					5			10	310	147	0.1008	10x	8.02 x 10^3	10265.4

B.7 Mafadi Wetland Mastersizer Particle Size Results

Sample number	Depth	-2	-1.5	-1	-0.5	0	0.5	1	1.5	2	2.5	3	3.5	4	4.5	5	5.5	6	6.5	7	7.5	8	8.5	9	9.5	10	10.5	11
M1	0-2	0.0	0.0	0.0	0.0	0.0	0.0	0.1	0.5	1.4	2.8	6.0	11.8	17.1	18.0	14.3	9.1	5.7	4.1	3.1	2.2	1.4	0.8	0.5	0.4	0.3	0.2	0.0
M2	3-5	0.0	0.0	0.0	0.0	0.0	0.0	0.6	1.9	3.0	4.7	8.5	13.8	17.1	16.1	11.9	7.3	4.6	3.3	2.6	1.8	1.1	0.7	0.5	0.3	0.3	0.1	0.0
M3	6-8	0.0	0.0	0.0	0.0	0.0	0.9	2.8	4.0	4.0	4.6	7.2	11.3	14.3	14.0	10.9	7.4	5.2	4.1	3.3	2.4	1.5	0.9	0.6	0.4	0.3	0.1	0.0
M4	9-11	0.0	0.0	0.0	0.0	0.0	0.4	1.6	2.4	2.2	2.5	4.9	9.6	14.0	15.0	12.6	9.0	6.6	5.6	4.8	3.6	2.3	1.3	0.8	0.6	0.5	0.2	0.0
M5	12-14	0.0	0.0	0.0	0.1	0.5	1.2	1.7	1.6	1.5	2.9	6.3	11.1	14.5	14.4	11.6	8.3	6.3	5.3	4.4	3.3	2.1	1.2	0.7	0.5	0.4	0.2	0.0
M6	15-17	0.0	0.0	0.0	0.1	0.3	0.7	1.1	1.8	2.4	3.4	6.1	10.5	14.2	14.8	12.2	8.7	6.4	5.2	4.2	3.1	2.0	1.1	0.7	0.5	0.4	0.2	0.0
M7	18-20	0.0	0.0	0.0	0.0	0.4	1.2	1.8	1.9	2.1	3.1	5.7	9.8	13.5	14.3	12.2	9.1	6.8	5.5	4.4	3.2	2.0	1.2	0.8	0.4	0.5	0.2	0.0
M8	21-23	0.0	0.0	0.0	0.0	0.3	1.0	1.6	1.6	1.6	2.2	4.7	9.1	13.4	14.8	13.0	9.8	7.4	6.0	4.7	3.3	2.1	1.3	0.9	0.6	0.5	0.2	0.0
M9	24-26	0.0	0.0	0.0	0.0	0.0	0.0	0.0	0.4	4.3	8.6	10.8	12.1	12.9	12.1	9.8	7.2	5.5	4.4	3.5	2.6	1.9	1.3	1.0	0.7	0.6	0.4	0.0
M10	27-29	0.0	0.1	0.5	1.8	4.1	6.1	6.8	6.6	6.5	7.2	8.7	10.1	10.2	8.7	6.5	4.5	3.2	2.4	1.8	1.3	1.0	0.7	0.5	0.4	0.4	0.2	0.0
M11	30-32	0.0	0.0	0.0	0.0	0.0	0.0	0.2	1.6	4.1	5.9	8.0	10.9	12.9	12.4	10.0	7.5	6.0	5.5	4.9	3.8	2.5	1.4	0.9	0.7	0.5	0.3	0.0
M12	37-39	0.0	0.0	0.0	0.0	0.0	0.2	0.6	0.8	1.1	2.1	5.2	10.1	14.2	14.8	12.3	9.0	7.0	6.1	5.4	4.2	2.7	1.6	1.0	0.7	0.6	0.4	0.0
M13	40-42	0.0	0.0	0.0	0.0	0.2	0.3	0.8	1.1	0.9	1.3	3.8	8.7	13.0	13.9	11.8	9.1	7.8	7.4	6.8	5.3	3.3	1.8	1.1	0.8	0.6	0.4	0.0
M14	43-45	0.0	0.0	0.2	0.3	0.3	0.5	0.9	1.3	1.7	2.7	5.2	9.1	12.5	13.1	11.1	8.6	7.1	6.6	6.1	4.8	3.1	1.8	1.1	0.8	0.7	0.4	0.0
M15	46-48	0.0	0.0	0.0	0.0	0.2	1.2	2.4	3.1	3.2	3.7	5.5	8.5	11.0	11.4	9.9	8.0	6.9	6.5	6.1	4.8	3.1	1.8	1.1	0.8	0.6	0.4	0.0
M16	49-51	0.0	0.0	0.0	0.0	0.0	0.5	1.9	3.3	3.9	4.8	6.9	9.7	11.4	10.9	9.0	7.1	6.2	6.0	5.7	4.7	3.2	1.9	1.2	0.8	0.6	0.4	0.0
M17	52-54	0.0	0.0	0.0	0.0	0.0	0.3	1.7	3.1	3.4	4.0	6.1	9.2	11.2	10.9	9.0	7.2	6.5	6.6	6.5	5.4	3.6	2.0	1.2	0.9	0.7	0.4	0.0
M18	55-57	0.0	0.0	0.0	0.1	0.6	1.8	2.8	3.1	3.3	4.5	7.2	10.7	12.8	12.2	9.8	7.3	5.7	4.8	4.1	3.1	2.2	1.4	1.0	0.7	0.6	0.4	0.0
M19	58-60	0.0	0.0	0.1	0.2	0.5	1.8	3.6	4.6	5.3	7.1	10.3	13.3	13.7	11.5	8.3	5.6	3.9	2.9	2.2	1.6	1.1	0.8	0.6	0.5	0.4	0.2	0.0
M20	61-63	0.0	0.0	0.0	0.0	0.0	0.0	0.0	0.0	2.0	8.7	14.2	15.9	14.9	12.4	9.2	6.3	4.5	3.3	2.5	1.9	1.4	1.0	0.7	0.5	0.5	0.3	0.0
M21	64-66	0.0	0.1	0.3	0.5	1.1	2.4	3.5	3.6	3.8	5.3	8.3	11.8	13.2	11.9	9.1	6.4	4.9	3.9	3.0	2.2	1.6	1.1	0.8	0.6	0.5	0.3	0.0
M22	67-69	0.0	0.0	0.0	0.0	0.5	1.9	3.1	3.5	3.9	5.5	8.6	11.9	13.2	11.8	9.1	6.6	5.2	4.3	3.4	2.5	1.7	1.2	0.9	0.6	0.5	0.3	0.0
M23	70-72	0.0	0.0	0.0	0.2	0.9	2.3	3.4	3.6	3.8	5.1	8.2	11.9	13.5	12.1	9.1	6.5	4.9	3.9	3.0	2.3	1.6	1.2	0.9	0.6	0.5	0.4	0.0
M24	73-75	0.0	0.0	0.0	0.2	1.2	3.6	5.6	6.4	6.9	8.3	10.4	11.8	11.3	9.2	6.8	4.9	3.6	2.7	2.0	1.5	1.1	0.8	0.6	0.5	0.4	0.3	0.0
M25	62-64	0.0	0.0	0.0	0.0	0.0	0.3	1.3	2.6	3.7	5.5	9.0	12.7	14.2	12.8	9.9	7.2	5.5	4.3	3.3	2.4	1.8	1.2	0.9	0.7	0.6	0.4	0.0
M26	65-67	0.0	0.0	0.0	0.0	0.1	0.9	2.8	4.5	5.1	6.1	8.9	12.0	13.0	11.4	8.7	6.4	5.0	4.1	3.2	2.4	1.8	1.2	0.9	0.6	0.5	0.3	0.0

M27	68-70	0.0	0.0	0.0	0.0	0.0	1.0	3.9	6.5	7.8	8.9	10.7	12.1	11.5	9.4	7.2	5.3	4.0	3.1	2.3	1.8	1.3	1.0	0.8	0.6	0.5	0.3	0.0
M28	71-73	0.0	0.0	0.0	0.0	0.1	1.5	4.6	7.0	8.1	8.9	10.6	12.1	11.7	9.7	7.1	5.0	3.6	2.7	2.0	1.5	1.1	0.8	0.7	0.5	0.4	0.3	0.0
M29	74-76	0.0	0.0	0.0	0.1	0.5	2.0	4.3	6.2	7.3	8.6	10.5	11.9	11.6	9.8	7.5	5.4	4.0	2.9	2.1	1.5	1.1	0.8	0.7	0.5	0.5	0.3	0.0
M30	77-79	0.0	0.0	0.0	0.0	0.0	0.8	3.3	5.5	6.5	7.8	10.2	12.5	12.8	10.9	8.2	5.8	4.2	3.1	2.3	1.7	1.3	0.9	0.7	0.6	0.5	0.3	0.0
M31	80-82	0.0	0.0	0.0	0.0	0.1	0.9	2.6	3.9	4.9	6.5	9.1	11.7	12.8	11.8	9.4	6.9	5.0	3.8	2.8	2.1	1.6	1.2	0.9	0.8	0.7	0.5	0.0
M32	83-85	0.0	0.0	0.0	0.0	0.0	0.3	3.0	6.3	7.3	7.6	9.2	11.6	12.7	11.4	8.7	6.2	4.4	3.2	2.3	1.7	1.2	0.9	0.7	0.6	0.5	0.3	0.0
M33	86-88	0.0	0.0	0.2	0.6	1.9	4.2	5.8	5.8	5.5	6.1	8.0	10.1	11.0	10.2	8.2	6.1	4.4	3.2	2.4	1.7	1.3	1.0	0.8	0.6	0.6	0.4	0.0
M34	89-91	0.0	0.0	0.0	0.1	0.5	2.3	3.6	3.7	3.5	4.6	7.2	10.5	12.5	12.4	10.5	7.9	5.8	4.2	3.0	2.2	1.6	1.1	0.9	0.8	0.7	0.4	0.0
M35	92-94	0.0	0.0	0.1	0.3	0.8	1.5	2.7	3.5	4.1	-4.9	17.3	10.4	12.5	12.5	10.5	7.9	5.7	4.2	3.1	2.3	1.6	1.2	1.0	0.8	0.7	0.4	0.0
M36	96-98	0.0	0.0	0.0	0.0	0.0	0.7	1.9	3.7	4.8	5.7	7.8	10.8	12.6	12.2	10.1	7.6	5.7	4.2	3.2	2.4	1.8	1.3	1.1	0.9	0.8	0.5	0.0
M37	99-101	0.0	0.0	0.0	0.0	0.0	0.0	0.0	0.4	2.2	4.4	7.3	11.1	14.2	14.6	12.6	9.5	6.8	4.9	3.5	2.5	1.7	1.2	1.0	0.8	0.8	0.5	0.0
M38	102-104	0.0	0.0	0.0	0.5	2.0	4.8	6.5	5.9	4.6	4.8	6.6	8.9	10.5	10.4	9.1	7.1	5.3	3.8	2.7	1.9	1.3	1.0	0.8	0.6	0.6	0.4	0.0

B.8 MAFADI WETLAND POLLEN COUNTS

Sample Number	Depth	Cyperaceae	Poaceae	Asteraceae	*Crassula*	*Pentzia*	*Anthospermum*	*Passerina*	*Podocarpus*	Apiaceae	Acanthaceae	Cheno-Am	*Indigofera*	Liliaceae	Ericaceae	Aizoaceae	*Typha*	*Vernonia*	*Selago*	Amaryllidaceae	*Stoebe*	Caryophylaceae	Malvaceae	Total
M1	0-2	34	122	61	18	5	5	2	2	2	1	1	1											254
M2	3-5	48	107	65	7	7	3	2		3		1	5	2										250
M3	6-8	80	105	41	12	4	3	3		2		2												252
M4	9-11	37	129	69	10		3	1		5		5			1									260
M5	12-14	36	159	52	18		5	2		3	2	2	2			1								282
M6	15-17	37	151	54	15	2	4	2				3		1										269
M7	18-20	68	108	42	11		1	0		8		9		3										250
M8	21-23	74	120	39	8	1	2	0		5		2				3								254
M9	24-26	63	142	28	7	5	2	1						2		3								253
M10	27-29	58	147	37	6							1	2	1		1						3		256
M11	30-32	20	179	34	3	7						1	6			4								254
M12	37-39	30	167	31	6							7	7	1		1						2		252
M13	40-42	56	135	41	5	3				7		2	4											253
M14	43-45	56	133	34	7	3	2			8		6	3	1		1	2							256
M15	46-48	48	135	48	11	1	2	1		2		2	9	2	1									262
M16	49-51	41	145	47	7	2			1	4		3	5	2										257
M17	52-54	18	192	72	21	1	1			9		2	4					2						322
M18	55-57	24	144	45	18	3				9		1		5										249
M19	58-60	40	107	72	10	3				13		1		1		1		1				1	1	251
M20	61-63	60	99	63	11		1			4				2		5	1					4		250
M21	64-66	47	100	85	10	5	1			3		1				1	2					1		256
M22	67-69	51	77	104	12	1				4		2					2							253
M23	70-72	48	73	100	9	4	2			5		8				4								253

M24	73-75	94	72	52	12	1	2	1	4	3			1	4	2					2	250
M25	62-64	81	85	59	17	2			3			3	1	3	1					1	256
M26	65-67	111	83	69	25	5	1	1							3	1					299
M27	68-70	61	84	89	7	2				5							2	3			253
M28	71-73	102	59	75	7					2				4							249
M29	74-76	124	54	42	18	1					1	2		5	2			2	1		252
M30	77-79	117	45	62	18	1				1		1		5				2			252
M31	80-82	109	48	64	17				1	9		2		2	1	1	6				260
M32	83-85																				0
M33	86-88																				0
M34	89-91																				0
M35	92-94																				0
M36	96-98																				0
M37	99-101																				0
M38	102-104																				0

B.9 Mafadi Wetland Diatom Counts

Sample Number	Depth	*Aulacoseira ambigua*	*Fragilaria construens*	*Fragilaria pinnata*	*Fragilaria girdle view*	*Cymbella laevis*	*Cymbella gracilis*	*Pinnularia viridis*	*Achnanthes minutissima*	*Cyclotella meneghiana*	*Gomphonema bohemicum*	*Gomphonema parvulum*	*Pinnularia borealis*	*Pinnularia divergentissima*	*Navicula trivialis*	*Navicula explanata*	*Gomphonema gracile*	*Diploneis ovalis*	*Eunotia praerupta*	*Fragilaria famelica*	*Stauroneis Phoenicenteron*	*Navicula laevissima*	*Navicula minima*	*Eunotia bilunaris*	*Eunotia exigua*	*Diploneis parma*	*Sellaphora pupula*	*Navicula insociabilis*	*Navicula salinarum*	*Denticula kuetzingii*	*Navicula pygmaea*	*Nitzschia palea*
M1	0-2	97	8	77	52	9		2		2	1		18	6		1		1	13		2	1		2		1	2					
M2	3-5	95	19	92	16	5	7	9	2			4	9	9		1		4	12			4		2	4	4	3	1				
M3	6-8	99	15	85	47	9	2		1	1	1	1	5	13			3		4			1	1	5		2	2					
M4	9-11	97	13	87	60	5	3	2	1			9	4	11					2	1	4	2		4								
M5	12-14	135	11	54	44	9	3					7	3	16				3			4	1		8	1		2					
M6	15-17	82	14	80	62	13	3	2	1			7	2	11				2	3	1	1	3	2	6	5		2		1		2	
M7	18-20	63	13	94	24	11	1	8	3		1	5	4	26			1	3	5	1	2	6	1	10	8		1		3			
M8	21-23	69	7	73	48	9		3	9			8	4	24					7	2		4		17	10							
M9	24-26	82	13	63	26	6	2	6	1			13	6	18				1	23		6	9	1	11	6		1		1			
M10	27-29	71	36	102	21	4	2	8	4			7	3	7				2	10		6	8		2	2				1	1		
M11	30-32	157	18	91	5	2	1			4		4	2	6	1				9													
M12	37-39	83	38	104	29	4	5	1		4		3	1	12					2		1	4		2	3				1			
M13	40-42	71	24	136	21	2	4					2	7	16	2			2	6		2	4		1	1							
M14	43-45	87	22	137	29	7	1	2		2		3		6				1	2		1	3		3	1							
M15	46-48	94	23	128	22	2	1	6				1	4	11					3		1	1								2	1
M16	49-51	89	27	118	32	4	5	3					1	7				1	3	1	2	1			3				1			

M17	52-54	75	36	140	21	8	4					2	1	6					5													
M18	55-57	84	20	98	45	13	8			1		5	3	3					7		1	4		4								
M19	58-60	40	2	40	20	10	18	9	3			17	15	16				6	55	10	2	7	3	11	1				2		1	3
M20	61-63	32	4	49	23	17	10	13	2			22	23	14				7	39	7	2	9	1	23	4				3			3
M21	64-66	21	2	29	19	15	17	12	6			21	16	18	1		2	8	53	2	4	13	8	18	4							
M22	67-69	14	2	29	35	15	10	6	4			21	17	11		2	1	4	59	11	8	11		22	3						2	
M23	70-72	23	3	24	27	16	10	11	4			18	26	11	2	2	2	3	74	1	8	9		15	6							
M24	73-75	12	3	14	36	17	14	6	11			34	17	8	3	3	4	2	50	8	5	17	1	19								
M25	62-64	31	5	12	25	22	12	6	11			18	20	18	4	1	1	5	46	4	4	16	5	16	5							2
M26	65-67	25	7	30	21	11	6	5	5			15	21	19			2	7	48	13	8	15	2	16	4					4	2	
M27	68-70	13	4	12	11	16	10	5	4		3	21	20	24			7	6	56	12	7	9	7	27	3					1	1	3
M28	71-73	20	2	11	38	12	10	10	3		6	14	20	18			1	8	53	6	3	6	11	23	2				2			1
M29	74-76	29	5	34	50	11	8	7	2	3	4	7	19	9			1	8	55	9	5	3	3	14	3							
M30	77-79	32	3	33	45	11	9	5	5		3	5	12	10	3		4	3	69	8	9	2	5	12	1				1		1	1
M31	80-82	16	9	15	60	11	10	3	3			7	15	7	1		3	4	61	6	13	12	2	22			8					
M32	83-85	15	4	36	38	14	8		1			7	24	7			4	6	74	4	5	2		21	4					3	3	
M33	86-88	40	20	72	70	9	6		2			14	5	5					22	4	5	4	1	9	3							1
M34	89-91	61	13	100	47	5	3		2			8	7	12				4	17		2	2	1	4			1					
M35	92-94	44	13	90	134	3	2			1		1		3										5								
M36	96-98	80	4	41	124	3	3		12			2	5	3			2	3	5	4				3						1		
M37	99-101	41	11	71	129	6	4	1	2			4	3	3			1	1	4	2	2	1		5						1		
M38	102-104	22	8	92	147	5			8		1		1	6					2	1	2			1						1		

Sample Number	Depth	*Hantzschia amphioxys*	*Stauroneis producta*	*Cymbella selesiaca*	*Caloneis silicula*	*Amphora species girdle*	*Pinnularia intermedia*	*Pinnularia gentilis*	Total	Microspheres	Weight of sample (g)	Dilution	Microsphere concentration	Diatom concentration
M1	0-2	2			1			8	306	32	0.1023	10x	8.02 x 10^3	76691.3
M2	3-5	5						9	316	16	0.1057	10x	8.02 x 10^3	158395.0
M3	6-8	6						6	309	18	0.1024	10x	8.02 x 10^3	137676.7
M4	9-11							1	306	27	0.1037	100x	8.02 x 10^4	9089.3
M5	12-14							7	308	17	0.1002	10x	8.02 x 10^3	145303.5
M6	15-17	1						3	307	24	0.1025	100x	8.02 x 10^4	10258.9
M7	18-20	1	2					6	305	8	0.1024	10x	8.02 x 10^3	305762.5
M8	21-23	3						7	304	18	0.1017	10x	8.02 x 10^3	135448.9
M9	24-26	1					1	8	305	25	0.1013	10x	8.02 x 10^3	97844.0
M10	27-29							4	301	44	0.103	10x	8.02 x 10^3	54864.1
M11	30-32							1	301	4	0.1036	10x	8.02 x 10^3	603505.0
M12	37-39							3	300	20	0.1016	100x	8.02 x 10^4	12030.0
M13	40-42	2						6	309	12	0.1011	100x	8.02 x 10^4	20651.5
M14	43-45						1	4	312	18	0.1043	10x	8.02 x 10^3	139013.3
M15	46-48							5	305	15	0.1035	10x	8.02 x 10^3	163073.3
M16	49-51							3	301	18	0.1036	10x	8.02 x 10^3	134112.2
M17	52-54						1	5	304	32	0.1041	10x	8.02 x 10^3	76190.0
M18	55-57							6	302	21	0.1038	10x	8.02 x 10^3	115335.2
M19	58-60							11	302	124	0.1043	10x	8.02 x 10^3	19532.6
M20	61-63							6	313	34	0.104	10x	8.02 x 10^3	73831.2
M21	64-66	5			1		4	4	303	31	0.101	10x	8.02 x 10^3	78389.0
M22	67-69	5					2	7	301	41	0.1021	10x	8.02 x 10^3	58878.5
M23	70-72	2		1	2		1	4	305	23	0.1008	10x	8.02 x 10^3	106352.2
M24	73-75	3		4				9	300	55	0.1047	10x	8.02 x 10^3	43745.5

M25	62-64	2		3	2			6	302	27	0.1045	10x	8.02 x 10^3	89705.2
M26	65-67	3		1			1	11	302	53	0.1038	10x	8.02 x 10^3	45698.9
M27	68-70	3		3	1			15	304	56	0.1042	10x	8.02 x 10^3	43537.1
M28	71-73	7		4	2	1	1	11	306	65	0.1044	10x	8.02 x 10^3	37755.7
M29	74-76	4		1				8	302	91	0.1034	10x	8.02 x 10^3	26615.8
M30	77-79	1		3				10	306	81	0.1022	0x	8.02 x 10^4	302977.8
M31	80-82	3		3			2	8	304	94	0.1044	10x	8.02 x 10^3	25937.0
M32	83-85	4	2	3				14	303	287	0.104	0x	8.02 x 10^4	84671.1
M33	86-88	1						8	301	606	0.1013	0x	8.02 x 10^4	39835.3
M34	89-91	1			2			9	301	425	0.1005	0x	8.02 x 10^4	56800.5
M35	92-94				2			4	302	88	0.1003	0x	8.02 x 10^4	275231.8
M36	96-98	1		3				5	304	411	0.1036	0x	8.02 x 10^4	59320.7
M37	99-101	1						7	300	345	0.1016	0x	8.02 x 10^4	69739.1
M38	102-104							4	301	273	0.1044	0x	8.02 x 10^4	88425.6

B.10 Mafadi Diatomite Outcrop Mastersizer Particle Size Results

Sample number	Depth	-2	-1.5	-1	-0.5	0	0.5	1	1.5	2	2.5	3	3.5	4	4.5	5	5.5	6	6.5	7	7.5	8	8.5	9	9.5	10	10.5	11
M39	0-3	0.0	0.0	0.0	0.1	0.6	1.6	2.5	2.5	1.9	2.2	4.0	7.1	9.8	10.7	10.0	8.9	8.3	8.3	7.9	6.2	3.8	1.7	0.8	0.6	0.5	0.3	0.0
M40	3-6	0.0	0.0	0.0	0.0	0.0	0.0	0.0	0.0	0.4	1.9	4.4	8.0	11.4	12.7	11.7	9.9	8.9	8.5	7.9	6.3	3.9	1.8	0.9	0.6	0.5	0.3	0.0
M41	6-9	0.0	0.0	0.0	0.0	0.0	0.0	0.0	0.0	1.2	3.1	4.4	6.0	8.1	9.7	10.0	9.5	9.5	10.1	10.2	8.4	5.1	2.2	0.9	0.6	0.6	0.4	0.0
M42	9-12	0.0	0.0	0.0	0.0	0.0	0.0	0.3	0.8	0.9	1.0	2.2	4.9	8.3	10.6	11.1	10.6	10.2	10.5	10.3	8.3	5.0	2.2	1.0	0.7	0.6	0.4	0.0
M43	12-15	0.0	0.0	0.0	0.0	0.0	0.0	0.0	0.4	1.2	2.0	3.3	5.7	8.4	10.1	10.4	9.8	9.6	10.0	10.0	8.2	5.2	2.4	1.1	0.8	0.7	0.5	0.0
M44	15-18	0.0	0.0	0.0	0.0	0.0	0.4	1.5	2.0	1.7	1.9	3.2	5.6	8.0	9.5	9.8	9.2	9.1	9.7	9.9	8.2	5.2	2.4	1.1	0.7	0.7	0.4	0.0
M45	18-21	0.0	0.0	0.2	0.4	0.6	0.9	1.4	1.5	1.1	1.1	2.4	4.9	7.8	9.5	9.7	9.1	9.1	9.9	10.2	8.6	5.5	2.7	1.3	0.8	0.7	0.5	0.0
M46	21-24	0.0	0.0	0.0	0.0	0.0	0.7	2.8	4.0	3.4	2.8	3.7	5.8	8.0	9.0	8.8	8.1	8.1	8.7	8.8	7.4	4.7	2.3	1.1	0.7	0.6	0.4	0.0
M47	24-27	0.0	0.0	0.0	0.0	0.0	0.2	1.1	2.3	2.5	2.4	3.3	5.5	7.8	9.0	8.9	8.5	8.7	9.6	10.1	8.6	5.6	2.7	1.3	0.8	0.7	0.5	0.0
M48	27-30	0.0	0.0	0.0	0.0	0.0	0.2	0.9	1.8	1.9	1.6	2.3	4.5	7.2	9.0	9.3	8.8	9.0	10.1	10.9	9.5	6.2	3.0	1.4	0.9	0.8	0.6	0.0
M49	30-33	0.0	0.0	0.0	0.0	0.0	0.0	0.3	1.4	2.7	2.9	3.3	5.4	8.1	9.4	9.2	8.4	8.5	9.6	10.3	8.8	5.7	2.7	1.3	0.8	0.8	0.5	0.0
M50	33-36	0.0	0.0	0.0	0.0	0.3	1.7	3.1	3.1	2.2	2.2	3.5	6.0	8.4	9.4	9.0	8.1	7.9	8.6	9.0	7.5	4.8	2.3	1.1	0.7	0.7	0.5	0.0
M51	36-39	0.0	0.0	0.1	0.6	1.6	2.3	2.3	1.7	1.1	1.1	2.4	5.3	8.5	10.1	9.6	8.4	8.0	8.7	9.1	7.8	5.1	2.6	1.4	0.9	0.8	0.6	0.0
M52	39-42	0.0	0.0	0.0	0.3	1.1	2.0	2.0	1.3	0.7	1.0	2.3	4.5	6.9	8.7	9.8	10.3	10.7	11.0	10.3	7.9	4.7	2.1	1.0	0.7	0.6	0.3	0.0
M53	42-45	0.0	0.0	0.0	0.0	0.3	1.9	3.7	4.1	3.1	2.6	3.8	6.4	8.8	9.5	8.7	7.6	7.4	8.0	8.2	6.7	4.3	2.1	1.1	0.7	0.6	0.4	0.0
M54	45-48	0.0	0.0	0.0	0.6	2.1	3.4	3.4	2.5	1.8	2.1	3.9	6.9	9.2	9.5	8.5	7.5	7.5	7.8	7.6	6.1	4.0	2.3	1.3	0.8	0.6	0.5	0.0
M55	48-51	0.0	0.0	0.1	0.6	2.0	3.8	4.6	4.3	3.5	3.4	4.5	6.4	7.9	8.1	7.6	7.2	7.3	7.4	6.9	5.5	3.7	2.2	1.3	0.7	0.6	0.4	0.0
M56	51-54	0.0	0.0	0.0	0.4	1.7	3.3	3.9	3.2	2.3	2.6	4.6	7.5	9.3	9.1	8.1	7.4	7.3	7.4	6.9	5.5	3.8	2.3	1.4	0.8	0.7	0.5	0.0
M57	0-3	0.0	0.0	0.0	0.0	0.0	0.0	0.0	0.6	2.5	5.1	9.1	13.7	16.0	14.8	11.2	7.6	5.4	4.2	3.4	2.6	1.7	1.0	0.6	0.4	0.3	0.1	0.0
M58	3-6	0.0	0.0	0.0	0.0	0.0	0.0	0.2	0.7	1.3	2.9	7.0	12.9	16.6	15.9	12.1	8.1	5.8	4.7	3.9	2.9	2.0	1.3	0.8	0.5	0.4	0.2	0.0
M59	6-9	0.0	0.0	0.0	0.0	0.0	0.0	0.0	0.0	1.0	4.1	8.7	13.9	16.5	15.1	11.2	7.6	5.6	4.6	3.8	2.9	2.0	1.3	0.8	0.5	0.4	0.2	0.0
M60	9-12	0.0	0.0	0.0	0.0	0.0	0.0	0.0	0.0	0.0	0.0	0.0	0.1	6.5	18.6	21.0	14.1	8.8	7.5	7.3	5.9	4.0	2.5	1.6	1.0	0.8	0.5	0.0
M61	12-15	0.0	0.0	0.0	0.0	0.0	0.0	0.0	0.0	0.3	2.6	6.5	10.6	13.5	13.9	11.8	9.0	7.2	63.6	5.7	4.6	3.2	2.0	1.2	0.8	0.6	0.4	0.0
M62	15-18	0.0	0.0	0.0	0.0	0.0	0.0	0.0	0.0	0.0	1.2	4.5	8.9	12.5	13.7	12.3	9.9	8.2	7.3	6.6	5.3	3.8	2.4	1.5	0.9	0.7	0.4	0.0
M63	18-21	0.0	0.0	0.0	0.0	0.0	0.0	0.0	0.0	0.6	2.9	5.8	8.9	11.3	11.8	10.5	9.0	8.2	7.8	7.0	5.6	4.0	2.6	1.6	1.0	0.8	0.5	0.0
M64	21-24	0.0	0.0	0.0	0.0	0.0	0.0	0.0	0.0	0.2	1.5	3.5	6.1	8.9	10.8	11.3	10.7	10.2	10.1	9.5	7.6	4.7	2.3	1.1	0.7	0.6	0.4	0.0

M65	24-27	0.0	0.0	0.0	0.0	0.0	0.0	0.0	0.0	0.1	1.0	2.9	5.5	8.4	10.5	11.1	10.6	10.1	10.1	9.8	8.1	5.4	2.9	1.5	0.9	0.7	0.5	0.0
M66	27-30	0.0	0.1	0.3	0.5	0.5	1.3	2.9	3.5	2.6	2.0	2.8	5.0	7.4	8.8	9.0	8.7	8.8	9.2	9.1	7.5	4.8	2.4	1.1	0.7	0.6	0.4	0.0
M67	30-33	0.0	0.0	0.0	0.0	0.0	0.0	0.0	0.0	0.7	2.3	3.8	5.7	8.2	9.9	10.3	9.9	9.9	10.3	10.1	8.1	5.1	2.5	1.2	0.8	0.7	0.5	0.0
M68	33-36	0.0	0.0	0.0	0.0	0.0	0.0	0.1	1.3	3.5	4.0	4.1	5.7	8.2	9.7	9.6	8.9	8.9	9.3	9.1	7.4	4.8	2.4	1.2	0.8	0.6	0.5	0.0
M69	36-39	0.0	0.0	0.0	0.0	0.0	0.0	0.0	0.0	0.0	0.4	3.2	7.2	9.6	10.4	10.3	9.9	10.0	10.3	10.0	8.1	5.1	2.5	1.2	0.8	0.7	0.5	0.0
M70	39-42	0.0	0.0	0.0	0.0	0.0	0.0	0.0	0.3	0.5	0.7	1.9	4.8	8.2	10.4	10.7	10.0	9.9	10.6	10.7	9.0	5.8	2.9	1.4	0.9	0.8	0.6	0.0
M71	42-45	0.0	0.0	0.0	0.0	0.0	0.0	0.5	1.9	2.6	2.6	3.6	6.0	8.6	10.0	9.9	9.2	9.0	9.3	9.2	7.6	4.8	2.4	1.1	0.7	0.7	0.5	0.0
M72	45-48	0.0	0.0	0.0	0.0	0.0	0.2	1.2	2.1	2.0	2.0	3.1	5.4	7.9	9.4	9.5	8.9	8.9	9.5	9.8	8.3	5.5	2.8	1.4	0.9	0.8	0.5	0.0
M73	48-51	0.0	0.0	0.2	0.4	0.5	0.7	1.2	1.8	1.8	1.5	1.8	3.9	7.3	10.0	10.4	9.3	8.9	9.6	10.1	8.8	5.8	2.8	1.3	0.8	0.7	0.5	0.0
M74	51-54	0.0	0.0	0.0	0.1	0.3	0.7	1.0	1.7	2.4	2.9	3.9	6.2	8.7	9.8	9.3	8.3	8.1	8.8	9.2	7.8	5.1	2.5	1.2	0.8	0.7	0.4	0.0
M75	54-57	0.0	0.0	0.0	0.0	0.0	0.0	0.0	0.0	0.0	0.0	0.0	0.0	0.0	5.6	13.2	14.3	12.3	12.5	13.6	12.0	7.8	3.8	1.9	1.2	1.1	0.7	0.0
M76	57-60	0.0	0.0	0.2	0.9	2.5	3.9	4.5	4.1	3.2	2.4	3.0	5.5	8.1	8.9	8.1	7.3	7.3	7.6	7.4	6.0	3.9	2.2	1.2	0.8	0.6	0.4	0.0
M77	60-63	0.0	0.0	0.0	0.0	0.0	0.0	0.0	0.0	0.0	0.0	0.0	0.0	0.0	1.0	8.7	16.1	16.4	14.7	13.6	11.6	8.0	4.4	2.3	1.4	1.1	0.7	0.0

B.11 Mafadi Diatomite Outcrop Pollen Counts

Sample Number	Depth	Cyperaceae	Poaceae	Asteraceae	*Crassula*	*Pentzia*	*Anthospermum*	*Podocarpus*	Apiaceae	Acanthaceae	Cheno-Am	*Indigofera*	Liliaceae	Ericaceae	Aizoaceae	*Vernonia*	*Typha*	*Stoebe*	Caryophylaceae	Gentianaceae	Malvaceae	Amaryllidaceae	*Artemisia*	Geraniaceae	*Olea*	Malvaceae	*Passerina*	Total
M39	0-3	15	158	46	12	1			18										2								1	253
M40	3-6	25	162	43	4				10			1						1							1		3	250
M41	6-9	28	142	38	13	1		1	23	1					1				1			1			1		1	252
M42	9-12	25	142	35	11	1			26			1	2		3		2	1	1						2		1	253
M43	12-15	7	173	57	8				9	1	1				1		1		1									259
M44	15-18	8	153	67	12				5		1		1		1							1			2		1	252
M45	18-21	11	155	71	1				12				1									1						252
M46	21-24	10	160	55	6				10	1					3				2			2					1	250
M47	24-27	12	127	81	7	1			15	1	1	1		1	2		1					1					2	253
M48	27-30	18	107	96	7				29	3		1		1	1		2		1			3					1	270
M49	30-33	11	106	125					5						3		2											252
M50	33-36	11	111	66	12				37	2			1		3		4					3					3	253
M51	36-39	20	123	47	9				45	1	4		1	1			2		1									254
M52	39-42	20	132	53	6	2			19	2					2				1			2				1		240
M53	42-45	16	114	73	10				28	1	1		1		1		1		2			2						250
M54	45-48	31	136	49	13	1			27	1	1		1		1													261
M55	48-51	18	158	59	3				12		2		4		2				1			1						260
M56	51-54	39	107	63	9				27			1			1	2			4			2						255
M57	0-3	34	159	49	5	3			6	1	1	2	1		7				4				1					273
M58	3-6	37	139	49	8			3	12	1	1			1	2				7					1				261
M59	6-9	55	120	28	7	11		1	11	2	5	1		1		1	2		11		2			1				259
M60	9-12	29	142	47	10				8	1		3	2			2			6				1					251
M61	12-15	30	165	29	6	2			8		3								4			2		1				250

M62	15-18	49	121	30	8	8			12	1	2	3			1		1		5			3	7			251
M63	18-21	17	148	42	17	3			10		2	4	1			1			4			2	1			252
M64	21-24	23	108	62	25				19		3	1		2			3		1			5				252
M65	24-27	17	142	53	11		3		15	1	1			2	2							4	1			252
M66	27-30	39	127	52	9			1	12	3	2				2	1			1			3				252
M67	30-33	48	98	72	11	1	1		10	1			1	1	3							4				251
M68	33-36	50	94	57	16	1	1	1	16	6	1	1	3	1	2							2				252
M69	36-39	27	126	43	26	2	2		16	1	1			2	3	3			5			4				261
M70	39-42	56	90	60	17				13	3	1	2	2	1		1			1			3			1	251
M71	42-45	14	76	112	29				19	4		1	1	1	1				1	1		1				261
M72	45-48	34	81	85	24		4		15	2			2						1			5				253
M73	48-51	16	87	128	8	1	2		10	1		2							4			2				261
M74	51-54	28	102	97	8		4		7	2	1	1	2						2			3				257
M75	54-57	60	88	74	3	2			13	2		1		1				1	3			2				250
M76	57-60	43	94	70	5	1	2	1	19	8	2				1			1	1			2				250
M77	60-63	29	101	62	19	1	2		22	1	3	2			1				2			5				250

B.12 Mafadi Diatomite Outcrop Diatom Counts

Sample Number	*Aulacoseira ambigua*	*Fragilaria construens*	*Fragilaria pinnata*	*Fragilaria girdle view*	*Cymbella laevis*	*Cymbella gracilis*	*Pinnularia viridis*	*Achnanthes minutissima*	*Cyclotella meneghiana*	*Gomphonema bohemicum*	*Gomphonema parvulum*	*Pinnularia borealis*	*Pinnularia divergentissima*	*Navicula trivialis*	*Navicula explanata*	*Gomphonema gracile*	*Diploneis ovalis*	*Eunotia praerupta*	*Fragilaria famelica*	*Stauroneis Phoenicenteron*	*Navicula laevissima*	*Navicula minima*	*Eunotia bilunaris*	*Gomphonemopsis pseudexigua*	*Sellaphora pupula*	*Navicula salinarium*	*Caloneis Silicula*	*Nitzschia latens*	*Eunotia exigua*	*Diploneis parma*	*Sellaphora pupula*	*Navicula sp. Centre*	*Pinnularia gentilis*	Total
M39	22	40	115	116			1			5			1																				300
M39	46	53	73	102	3	3			2		5		2			1		1	1		1		4		1							3	301
M40	34	59	122	67	1		3	1	5	4		1	1	2	1			1	1					1									304
M41	40	46	111	87	1		1		4	3	1	1		11					1	2												1	310
M42	23	62	85	126	2			1	1																								300
M42	25	43	99	125	5		1		2	1	3								1														305
M43	33	61	121	79	3		1		4	1			1																				304
M44	59	74	90	56	3		1		8		4	3				1				2		1											302
M45	49	49	171	32	1		3							1																			306
M45	31	40	168	52	1				1				3					1	1	1		1	1										301
M46	32	54	114	75	4		3	1	9	2	1	6								2												1	304
M47	44	46	124	75	2				4			8														1							304
M48	47	55	105	86	3		2			2	1			1																			302
M48	51	30	114	108	3	2					3		1					1	1	2			2				1					1	320
M49	44	32	110	94	3	1	2	3	6		1	3				1			2														302
M50	55	47	98	88	1	3	4	1	6		3	1																					307
M51	90	40	82	65	4		6		15	1	1	1				1					1												307
M51	68	29	116	60	5	1	1				2							1	1	1			4									1	290
M52	84	28	90	83	2		4	3	4		1	3																				2	304
M53	60	36	101	80	1		4	2	11	3	1	1							1		1											1	303

M54	25	46	149	69	2		1	2	1		2		1	2			1													302
M55	38	67	122	49	3		5	3	7	1	2		4				0	3	1	1	1	1	1						1	310
M56	17	71	113	77	3	1	6		4			4	2	1				4			1	1								305
M57	45	49	78	99	7	2	2		10		1	3						2											2	300
M58	69	35	97	83	4				2		4		1						1	3	2									301
M59	30	32	121	98	2		1	1	7		1	3						1		1			3							301
M60	38	35	122	86	5		1		3	1		3						2	2										2	300
M61	33	32	120	89	8	3	3		2	1		3		2				1	2	4										303
M62	45	29	112	81	3		8		5	1		3	6					2		1	2							1	4	303
M63	36	31	89	111	11		4	1	3				2					4	2	2		1	5				1			303
M64	82	23	96	93	4	1	3		1		4		3	1				2		1										314
M65	56	41	114	54	6	1	5	2	2	1	1	6	6	2					1		1	2	2			1				304
M66	40	44	103	91	3				1		3	1	1			1		1		3	2		3		1				3	301
M67	39	26	63	167	1						2		3						1	1	1		1							305
M68	46	45	78	127	4		1						4	1					1	2	2		2						2	315
M69	29	39	84	135	1	1	2		5		2	1	2						2	1	3	1	2		1			1	1	313
M70	31	36	85	133		3	1		1		4	1				2		1	1	1	1	1	2						1	305
M71	31	28	109	121	4		2		2		3	1											1							302
M72	37	29	96	132	5					1	8		4							1		1	3						1	318
M73	57	20	125	86	6			1			4	1	2							2		2	2		1				2	311
M74	31	47	117	92	4		2	2			6	2	1					1			1	1	2							309
M75	41	26	97	130	4	2	1	1	1		2		2					1		1	1	1	1							312
M76	47	19	63	155	4						10	1						1	2	1			1						1	305
M77	46	28	121	83	5	1	2				1	1	4					1			2	1	4						2	302

APPENDIX C: ADDITIONAL DATA ANALYSIS

C.1 PRINCIPAL COMPONENTS ANALYSIS OUTPUT

C.1.1 SANI VALLEY POLLEN PCA

Importance of components:

	PC1	PC2	PC3	PC4	PC5	PC6	PC7	PC8	PC9	PC10
Eigenvalue	1.958	0.9732	0.6999	0.40418	0.37169	0.26704	0.18957	0.15548	0.14034	0.08187
Proportion	0.362	0.1799	0.1294	0.07472	0.06872	0.04937	0.03505	0.02874	0.02595	0.01514
Cumulative	0.362	0.5419	0.6713	0.74604	0.81476	0.86413	0.89917	0.92792	0.95386	0.969

Species scores

	PC1	PC2	PC3	PC4	PC5	PC6
Aizoaceae	-0.46129	0.450518	0.12551	-0.09731	0.44422	-0.21632
Apiaceae	-0.16441	0.559271	0.18319	0.20193	-0.23389	0.05186
Asteraceae general	1.46494	-0.11746	0.53672	-0.1419	0.05019	-0.23137
Chrysocoma	0.21467	0.222475	-0.01534	0.25696	0.28538	0.16331
Pentzchia	0.07681	0.092362	0.14447	0.24833	0.09354	0.05605
Vernonia	0.17836	-0.00688	0.00965	0.60203	0.33784	-0.01638
Caryophylaceae	-0.06155	-0.05758	0.42894	-0.10979	0.07274	0.41063
Cheno-Am	0.36735	0.303722	-0.03063	-0.24515	-0.2356	0.34357
Crassula	-0.25336	0.240064	0.31123	0.45733	-0.37618	0.08448
Cyperaceae	-1.11397	-0.44467	-0.08975	-0.09259	0.07347	0.02823
Indigofera	-0.23192	0.657791	-0.08118	-0.1114	-0.17305	-0.23119
Gentianaceae	-0.06383	0.505694	-0.07467	-0.18069	0.27519	0.03941
Olea	-0.2699	0.539241	0.18385	-0.03229	-0.14894	-0.22362
Poaceae	0.68975	0.195019	-0.96231	0.12052	-0.07269	0.02502
Typha	0.11812	0.545553	-0.01238	-0.15762	0.24682	0.29157

Site scores (weighted sums of species scores)

	PC1	PC2	PC3	PC4	PC5	PC6
S28	-1.23238	-0.82159	0.12534	-0.57843	0.02531	0.30996
S1	-0.63931	-0.75293	-0.73925	0.466973	0.39237	-0.15098
S29	-0.84388	-0.75098	0.50079	0.867432	-0.01173	-0.24593
S9	-0.45535	-0.30099	-0.9054	-0.48725	-0.42412	-0.49947
S10	0.74466	-0.02889	0.72339	-0.21846	-1.27263	0.20594
S2	0.82891	-0.32198	0.05208	0.678681	-0.06242	0.41225
S11	0.03106	-0.58182	1.27229	-0.6115	-0.02957	1.23559
S12	1.22067	-0.28196	0.67598	-0.68522	-0.58649	-1.20034
S3	0.46805	-0.30318	-0.5105	1.034851	-0.43212	0.49852
S13	0.65681	-0.23486	-0.08989	-0.13169	-0.18604	-0.54709
S14	0.61133	-0.39391	0.87259	-0.21628	0.91262	-0.18189
S4	1.47821	-0.59811	-0.11092	-0.05764	0.06599	-0.73251
S15	0.26436	-0.88567	-0.55436	0.520402	0.19243	-0.70058
S30	-0.37087	-1.06659	-0.62412	-0.31703	0.05782	0.18321
S16	-0.68138	-0.10008	-0.16566	0.930737	-1.74167	0.05707

S5	0.61054	0.35263	-0.30197	0.746819	0.01508	1.36038
S17	-0.05432	1.85358	0.25685	1.410627	-0.0611	-0.13353
S18	-0.27963	0.65189	0.08623	0.005577	1.22904	-0.523
S19	-0.28508	-0.17289	0.94832	0.850943	1.59512	0.21543
S6	-0.10814	0.0524	-0.23953	0.770972	0.5792	-0.62452
S20	-0.39873	0.31382	-0.79738	-0.68961	0.37956	-0.2301
S21	-0.67311	-0.4311	-0.20653	-0.44063	0.05875	0.34648
S7	0.71053	0.38855	-1.08586	-0.57249	0.45538	1.81568
S22	0.31958	0.54949	-0.091	-0.73622	0.47916	-0.09122
S23	-0.02258	0.82726	-0.0419	-0.9478	0.38999	-0.30443
S24	-0.44035	0.96061	-0.70458	-0.42394	-0.18065	-0.68961
S25	-0.63504	0.34234	0.33187	-0.77382	-0.65125	0.41548
S26	-0.59616	0.49092	0.64117	0.123268	-0.51397	-0.60895
S27	-0.51348	0.5235	1.40969	-0.36399	-0.26576	0.30234
S8	0.28508	0.72052	-0.72774	-0.15528	-0.40831	0.10584

C.1.2 SANI VALLEY DIATOM PCA

Importance of components:

	PC1	PC2	PC3	PC4	PC5	PC6	PC7	PC8	PC9
Eigenvalue	7.0084	4.0317	2.5839	1.29119	0.8679	0.47949	0.40841	0.23883	0.08764
Proportion	0.4123	0.2372	0.152	0.07596	0.05106	0.02821	0.02403	0.01405	0.00516
Cumulative	0.4123	0.6495	0.8015	0.87749	0.92855	0.95676	0.98079	0.99484	1

Species scores

	PC1	PC2	PC3	PC4	PC5	PC6
Achnanthes minutissima	-0.78972	0.02342	0.08652	0.120753	-0.17952	0.183889
Caloneis silicula	-0.55244	-0.01618	0.21665	-0.07358	0.223694	-0.07258
Cymbella laevis	0.0621	-0.61058	0.82771	0.270441	0.027339	0.06913
Cymbella gracilis	-0.22426	-0.01404	0.12533	0.176735	0.311737	0.285675
Diploneis ovalis	0.26203	0.23799	-0.3311	-0.1614	-0.2383	0.374659
Diploneis parma	0.68209	0.68386	-0.05569	0.298576	-0.22888	-0.11148
Eunotia bilunaris	-0.30458	-0.06527	0.29587	-0.49891	-0.17949	-0.01007
Eunotia praerupta	0.08331	-0.18385	0.4068	0.009958	-0.13225	-0.02939
Fragilaria pinnata/ construens	-1.51412	0.04442	-0.47984	0.044731	0.062121	-0.07095
Fragilaria famelica	0.59465	-0.94006	-0.49661	-0.11353	-0.02212	-0.08261
Hantzschia amphioxys	0.16192	0.5846	0.3741	-0.50451	0.232176	-0.06655
Navicula trivialis	-0.39544	-0.10075	-0.08801	0.217995	-0.00085	-0.08073
Navicula laevissima	-0.42441	0.23756	-0.01867	0.015904	-0.0703	-0.16929
Navicula minima	-0.42994	-0.2416	0.30587	0.091067	-0.37807	-0.09568
Pinnularia gentilis	0.21483	0.10496	-0.04209	0.001793	-0.06929	-0.04841
Pinnularia borealis	0.22737	0.65814	0.07252	0.345389	0.136663	-0.03813
Pinnularia divergentissima	-0.02788	0.2381	0.11777	-0.02272	-0.1689	-0.00866
Sellaphora pupula	-0.43678	0.37981	0.14082	-0.07531	-0.18528	0.072008

Site scores (weighted sums of species scores)

	PC1	PC2	PC3	PC4	PC5	PC6
J	-2.83398	0.55893	-0.63176	0.42123	0.45247	0.22572
I	-1.28429	-0.34262	0.91971	-0.2614	-1.56532	-0.10366
H	0.002511	-2.02562	1.48987	-0.79598	1.74007	-0.77689
G	0.640346	0.03309	-0.55218	2.238	0.52236	-1.77973
F	0.573466	2.60504	0.82564	-0.33367	1.19426	-0.07894
E	0.493527	0.57871	-0.10234	-2.06728	-1.01128	-1.13005
D	0.369506	-0.68974	-2.73078	-0.883	0.56998	0.32222
C	0.912384	-0.03652	0.07818	0.06245	0.06677	2.06751
B	0.337912	-0.38565	0.66469	0.81962	-0.06396	1.64867
A	0.78861	-0.29562	0.03899	0.80002	-1.90534	-0.39486

C.1.3 SEKHOKONG POLLEN PCA

Importance of components:

	PC1	PC2	PC3	PC4	PC5	PC6	PC7	PC8	PC9	PC10
Eigenvalue	1.252	1.0463	0.6296	0.4152	0.30949	0.26998	0.23586	0.15802	0.14069	0.12105
Proportion	0.2657	0.222	0.1336	0.08811	0.06568	0.05729	0.05005	0.03353	0.02986	0.02569
Cumulative	0.2657	0.4877	0.6213	0.70943	0.7751	0.8324	0.88245	0.91598	0.94584	0.97153

Species scores

	PC1	PC2	PC3	PC4	PC5	PC6
Cyperaceae	0.59146	1.35852	-0.15642	0.07931	-0.23839	-0.01333
Poaceae	0.80137	-0.94262	-0.17193	-0.15544	-0.12294	0.101216
Asteraceae	-0.41816	0.07884	0.69403	0.01469	0.2911	-0.23233
Crassula	-1.21637	0.1224	0.0388	-0.42286	-0.07618	0.143466
Pentzia	-0.37311	-0.24801	0.14382	0.52968	-0.41179	0.466176
Anthospermum	-0.3036	-0.02022	-0.14591	0.52611	0.26745	0.183757
Apiaceae	-0.36661	-0.21571	-0.80392	-0.26912	-0.05515	-0.1299
Cheno-Am	0.11532	0.23142	-0.44025	0.02259	0.66131	0.337967
Indigofera	-0.07956	0.02142	-0.03987	0.04543	-0.03933	-0.07305
Liliaceae	0.01988	-0.30343	-0.17523	0.53831	0.09511	-0.49513
Aizoaceae	-0.65666	0.16262	-0.57155	0.23564	-0.19092	-0.19314
Vernonia	-0.15952	-0.07525	-0.03887	-0.10355	0.01342	-0.11244
Olea	-0.39355	-0.07846	0.08821	0.10767	0.08228	0.005092
Caryophylaceae	0.06191	0.01489	-0.21607	-0.01561	0.06115	0.137709

Site scores (weighted sums of species scores)

	PC1	PC2	PC3	PC4	PC5	PC6
SK1	-2.41516	-0.17103	0.384731	1.110482	0.7853	-0.01506
SK2	-2.01514	-0.28271	0.405413	-0.74219	-0.2325	0.367357
SK3	-0.13797	-0.96808	0.491459	0.141511	-0.0589	-0.21698
SK4	0.35242	-0.68698	-0.18118	0.966156	-0.3984	-1.01603
SK5	0.332344	-0.99356	-0.37119	-0.25334	0.5084	-0.20313
SK6	0.160249	-0.16971	-0.00938	0.609562	0.3783	0.577017
SK7	-0.17895	0.16655	-0.95537	1.465215	-0.1923	0.167167
SK8	0.261185	0.71216	-0.99712	-0.67922	0.1533	0.053608
SK9	-0.35562	0.61981	-1.31017	-0.02224	0.622	-0.69899

SK10	-0.25788	-0.43359	-0.57566	-1.04111	0.2599	-0.80825
SK11	0.012874	-0.93645	0.163936	-0.197	-0.7336	-0.07298
SK12	0.314594	-0.30352	-0.93992	-1.05278	0.5091	0.191808
SK13	0.163671	0.01043	-0.7417	0.449278	-0.3233	-0.39795
SK14	-0.22385	-0.27871	0.632555	-0.00736	-1.0528	0.094402
SK15	0.364737	-0.21073	0.36672	0.247221	0.412	0.755785
SK16	0.823824	-0.47118	0.247554	0.015149	1.1133	-0.11593
SK17	0.178064	-0.87616	-0.43793	0.277057	0.1236	0.632179
SK19	-0.03622	-0.10605	0.284351	-0.09757	-0.4338	-0.17937
SK20	-0.04886	-0.25938	-0.13609	0.082908	-0.6991	-0.03385
SK21	0.028716	0.21462	-1.2617	0.101198	-1.2818	-0.06399
SK22	0.099584	-0.0646	-0.55165	0.600833	0.2945	-0.37501
SK24	0.331167	0.23168	-0.02694	0.375037	-0.4893	0.672298
SK25	-0.06446	-0.09821	-0.08288	0.303001	0.3747	0.841586
SK26	0.580921	0.18772	0.019686	0.51705	0.75	0.887402
SK27	0.214362	0.19998	0.246118	0.368038	0.028	-0.40688
SK28	0.06929	-0.24521	-0.00453	0.263076	-0.7442	-1.27053
SK29	0.007635	-0.45617	0.316737	-0.73151	0.3934	0.207406
SK30	0.374387	-1.00255	0.67178	-0.16963	-0.2053	-0.5824
SK31	0.502225	0.20115	0.977003	-0.56432	0.5184	-0.49151
SK32	-0.10288	1.11926	0.68218	-0.11114	0.2486	-1.23858
SK33	0.090721	1.02031	0.36495	0.883731	1.2245	-0.5601
SK34	0.166571	0.09022	0.151619	-0.85701	0.8449	-0.43713
SK35	0.098558	-0.50927	0.228838	-0.52354	-0.1396	0.451617
Sk36	0.146739	0.68395	0.717328	-0.109	-1.0495	0.005971
SK37	0.608269	0.47281	0.826573	0.080014	-0.261	0.216054
SK38	-0.09166	0.77278	0.959979	-0.00147	-0.2361	-0.0937
SK39	-0.33099	1.27314	-0.3397	-0.90866	-0.3224	-0.08966
SK40	-0.35134	0.28625	-0.44919	-0.53318	-0.2511	0.370257
SK41	-0.17781	-0.05184	0.037572	-0.26706	0.35	1.120496
SK43	0.74567	0.72246	0.321644	0.453751	-0.5622	0.829497
SK44	-0.24	0.59041	-0.12643	-0.44096	-0.2247	0.926096

C.1.4 SEKHOKONG DIATOM PCA

Importance of components:

	PC1	PC2	PC3	PC4	PC5	PC6	PC7	PC8	PC9	PC10
Eigenvalue	7.8719	2.9898	1.9175	1.622	1.29336	1.03186	0.82458	0.7629	0.60445	0.51898
Proportion	0.3498	0.1328	0.0852	0.07207	0.05747	0.04585	0.03664	0.0339	0.02686	0.02306
Cumulative	0.3498	0.4826	0.5678	0.63992	0.69739	0.74324	0.77988	0.8138	0.84064	0.8637

Species scores

	PC1	PC2	PC3	PC4	PC5	PC6
Aulacoseira ambigua	0.476536	-0.49047	0.51442	-0.02766	0.106575	-0.42816
Fragilaria pinnata/ construens	0.883098	-1.16892	0.059	0.19823	-0.30631	-0.23272
Cymbella laevis	0.899562	-0.01236	-0.01301	-0.07649	0.137155	0.47016
Cymbella gracilis	0.277936	0.246551	0.30007	0.15795	-0.34247	0.38639
Pinnularia viridis	0.09211	-0.00221	0.02351	0.12768	0.105593	0.33914
Achnanthes minutissima	-0.25745	-0.21194	-0.69952	0.2866	-0.37934	0.16536

Gomphonema bohemicum	-0.10744	0.103586	-0.03923	-0.26218	-0.13012	-0.03808
Gomphonema parvulum	0.637731	-0.01184	-0.23588	-0.20382	0.332563	-0.15704
Pinnularia borealis	-0.44293	0.332256	0.01565	0.36623	-0.2493	-0.08655
Pinnularia divergentissima	0.289119	0.450888	-0.22749	-0.05704	-0.31208	0.04951
Navicula explanata	0.00817	-0.11182	-0.57141	0.19436	-0.05828	-0.22656
Gomphonema gracilis	-0.03078	-0.15187	-0.27426	0.18162	-0.32579	0.21807
Diploneis ovalis	-0.03055	0.261132	-0.42308	0.25763	-0.02944	-0.05754
Eunotia praerupta	0.219061	0.048719	0.2867	0.09642	-0.32672	0.10179
Fragilaria famelica	-2.462	-0.34584	-0.0181	-0.50785	-0.02865	0.01593
Stauroneis phoenicenteron	0.367362	0.07792	0.01608	-0.17841	-0.18309	-0.1164
Navicula laevissima	-0.05152	0.136683	-0.52602	0.04147	-0.01231	-0.22793
Navicula minima	0.360056	0.300601	-0.07865	-0.10703	-0.31766	-0.4281
Eunotia bilunaris	0.853324	0.130107	-0.3265	-0.56899	0.267045	0.11546
Eunotia exigua	0.581233	0.217192	-0.3946	-0.29798	-0.0177	-0.0528
Diploneis parma	0.070905	0.656006	0.36525	-0.43574	-0.58414	-0.2169
Sellaphora pupula	-0.00338	0.125447	-0.25964	-0.3711	0.182494	-0.06971
Nitzschia palea	-0.0548	-0.11924	-0.25106	0.17793	0.016862	-0.18154
Hantzschia amphioxys	-0.34868	0.667545	0.13247	0.62711	0.399453	-0.25976
Stauroneis producta	-0.05371	0.036506	0.05999	0.09185	0.119684	-0.14152
Cymbella selesiaca	0.125954	-0.03519	-0.1129	-0.2523	-0.15404	-0.0475
Caloneis silicula	-0.01508	0.419535	-0.1089	0.02854	0.009558	-0.09636
Cymbella cistula	0.052534	-0.30943	0.01322	-0.0791	-0.14635	-0.09014
Diploneis didyma	-0.05437	0.017985	0.0155	0.14599	0.017561	-0.03537
Pinnularia gentilis	0.31248	0.559393	0.2193	0.05831	0.027977	-0.03398

Site scores (weighted sums of species scores)

	PC1	PC2	PC3	PC4	PC5	PC6
SK1	-0.91488	0.22097	-0.12226	1.157713	0.1886	1.65304
SK2	-0.52962	-0.96675	-1.39233	1.94468	-0.3031	0.70477
SK3	-0.03198	0.04758	-1.22161	1.016937	-0.5296	-0.56041
SK4	-0.25738	1.03236	-0.78676	0.446625	-1.1543	0.32361
SK5	0.01103	1.24298	-0.64758	0.401431	-0.6542	-0.57684
SK6	0.5838	0.73444	-0.66557	0.018695	-0.1639	-0.52848
SK7	-0.73863	0.96148	-0.9854	-3.0964	-1.6701	-0.15911
SK8	0.46498	0.24085	-1.36141	-0.19053	-0.108	-0.37779
SK9	-0.46609	0.88049	0.57675	-0.13383	-1.0246	0.8889
SK10	-0.60186	0.88481	0.94022	-0.2939	-0.3153	0.6954
SK11	-0.8319	-0.82439	-0.02154	0.180057	0.6717	-0.48928
SK12	-0.91674	0.438	0.76851	-0.21923	-0.3979	0.45865
SK13	-0.53247	0.68749	0.95097	-0.00924	0.5261	0.56329
SK14	-1.59991	-1.34806	0.88903	-0.84645	0.9107	0.26779
SK15	-1.25431	-0.92164	0.34753	-0.74604	0.2612	0.63623
SK16	-0.51952	0.11439	-0.15468	0.160198	1.1885	-0.15864
SK17	-0.72673	-1.71243	-0.98784	-0.71412	0.6489	-0.36001
SK19	-0.50404	-1.23819	-1.28228	-0.58292	-1.0674	0.57627
SK20	-0.44623	-1.03473	-0.86855	-0.85936	-0.3757	0.13619
SK21	-0.04943	0.55769	1.11911	0.960321	0.4738	1.07908
SK22	-0.76841	0.4689	1.03494	-0.47025	0.8748	-0.84593
SK24	-0.23219	0.89742	0.40669	0.632489	-0.5184	-0.30116
SK26	-0.12077	0.45884	-0.48274	0.050425	0.6371	-0.71105

SK27	-0.74451	-0.19364	1.18866	0.542573	0.9883	-1.22893
SK28	-0.69961	0.314	0.33046	1.099844	0.1001	0.41577
SK29	-0.19221	-0.45842	-0.23497	1.228051	-0.2889	-1.19033
SK30	0.05953	0.47135	-1.42963	-0.17034	1.0921	-1.9779
SK31	0.26296	0.61584	1.17226	-0.36719	-0.6583	0.16829
SK32	0.07786	0.94488	0.02176	1.142616	-0.3174	-0.82706
SK33	-0.43572	0.28815	-0.11843	0.042901	0.0928	-0.67217
SK34	0.72848	0.10398	-0.53709	-0.37335	-0.1103	1.54435
SK35	1.72674	0.48861	-0.49782	-1.24511	2.4403	0.25911
Sk36	1.82411	-0.00417	-0.83403	0.469777	0.9758	0.32742
SK37	1.0744	-0.12606	-0.19123	-0.20113	1.5587	2.25012
SK38	1.30901	0.87736	0.77271	-1.22628	-0.5765	-0.01268
SK39	0.5477	-1.40377	0.67321	-0.54324	-0.3389	-0.68841
SK40	1.57512	-1.61276	0.0299	0.387571	-1.2473	1.14263
SK41	1.48396	-0.70929	0.91272	0.669176	-1.4897	-0.68124
SK43	1.27038	0.47456	0.9232	-0.10864	0.3354	-0.61058
SK44	1.11505	-1.89312	1.76514	-0.15454	-0.6551	-1.13291

C.1.5 MAFADI WETLAND POLLEN PCA

Importance of components:

	PC1	PC2	PC3	PC4	PC5	PC6	PC7	PC8	PC9	PC10
Eigenvalue	1.3236	1.1943	0.6089	0.3477	0.25484	0.21641	0.16536	0.14425	0.12112	0.09003
Proportion	0.2912	0.2627	0.1339	0.0765	0.05606	0.04761	0.03638	0.03173	0.02664	0.01981
Cumulative	0.2912	0.5539	0.6878	0.7643	0.82041	0.86802	0.90439	0.93613	0.96277	0.98258

Species scores

	PC1	PC2	PC3	PC4	PC5	PC6
Cyperaceae	1.614914	-0.56548	0.05776	0.25872	0.082606	-0.20705
Poaceae	-1.64983	-0.31138	0.04475	0.05648	0.009625	0.070247
Asteraceae	0.49971	0.99656	-0.07109	-0.35862	-0.05314	-0.00869
Crassula	0.266297	0.15773	0.24402	0.16561	0.003604	0.379147
Pentzia	-0.14625	0.08915	0.4907	-0.19019	-0.28805	-0.40816
Anthospermum	-0.19605	0.11617	0.62787	0.21898	0.474298	-0.05151
Apiaceae	-0.29344	0.57521	-0.09998	0.73417	-0.30392	-0.20772
Cheno-Am	-0.08755	0.22275	-0.46474	0.16468	0.478538	-0.20404
Indigofera	-0.57635	-0.333	-0.21902	-0.17512	0.031493	-0.32148
Liliaceae	-0.00259	-0.22688	-0.11926	0.25757	-0.25584	0.209548
Aizoaceae	0.390609	-0.30048	-0.10356	-0.10366	-0.24603	0.023565
Acanthaceae	0.104696	0.08055	-0.09706	-0.0414	0.241061	0.105814

Site scores (weighted sums of species scores)

	PC1	PC2	PC3	PC4	PC5	PC6
M1	-0.4207	0.562784	1.195682	-0.2823	0.60218	0.16189
M2	-0.25085	0.254875	0.708184	-0.18373	-0.08793	-1.20646
M3	0.17135	-0.25605	1.165261	0.62973	0.77527	-0.61801
M4	-0.37216	0.792242	-0.12058	0.35895	0.89368	0.47187
M5	-0.60162	0.088159	0.253849	0.21141	1.04532	0.96108

M6	-0.50118	0.022751	0.830235	-0.35946	0.91197	1.00203
M7	0.03603	-0.00507	-0.7319	1.65243	0.55958	0.14471
M8	0.05337	-0.41861	0.207636	0.80792	0.09041	-0.3918
M9	-0.21155	-1.22194	1.168817	-0.13341	-0.33608	0.30528
M10	-0.31269	-1.05576	-0.6605	-0.42744	0.09247	0.55551
M11	-1.11663	-0.80699	-0.16188	-1.58129	-0.63441	-0.61767
M12	-0.90442	-0.94004	-1.33477	-0.59402	0.61857	0.31536
M13	-0.42196	-0.27446	-0.42275	0.34881	-0.37699	-1.37409
M14	-0.41008	-0.39914	-0.20191	1.02746	0.10258	-1.20454
M15	-0.49049	-0.34001	-0.02727	0.10592	0.37968	-0.35457
M16	-0.6194	-0.19567	-0.69322	0.09228	-0.39282	-0.50654
M17	-1.0126	0.769313	-0.15095	-0.08696	-0.21191	0.60303
M18	-0.73185	0.401387	-0.00469	0.80585	-1.26979	1.168
M19	-0.13925	0.909481	-0.25846	0.45316	-1.35262	-0.08416
M20	0.23982	0.033434	-0.02587	0.30997	-0.80308	1.01299
M21	0.06638	0.834728	0.445412	-0.5974	-0.46285	-0.30004
M22	0.3577	1.310552	-0.40644	-0.5384	-0.30736	0.06025
M23	0.35558	1.318116	-0.17759	-0.38259	0.06237	-0.89401
M24	0.71276	-0.08573	0.269457	0.70901	0.34341	-0.6035
M25	0.55478	-0.17211	0.188794	0.26758	-1.2853	0.5786
M26	0.76907	-0.14536	1.316644	-0.47125	0.14085	0.16638
M27	0.40151	0.648585	-0.53382	-1.26332	0.69914	-0.13354
M28	1.07465	-0.13803	-0.69533	-0.76971	0.24308	-0.06702
M29	1.17766	-1.12408	0.124908	-0.12629	-0.64143	0.19538
M30	1.34657	-0.4203	-0.08459	-0.35485	-0.29704	0.23731
M31	1.20018	0.052933	-1.18235	0.3719	0.89904	0.41629

C.1.6 MAFADI WETLAND DIATOM PCA

Importance of components:

	PC1	PC2	PC3	PC4	PC5	PC6	PC7	PC8	PC9	PC10
Eigenvalue	9.3921	1.17359	0.61541	0.41175	0.36121	0.28414	0.2328	0.21124	0.1792	0.15786
Proportion	0.6811	0.08511	0.04463	0.02986	0.02619	0.02061	0.01688	0.01532	0.013	0.01145
Cumulative	0.6811	0.76621	0.81084	0.8407	0.86689	0.8875	0.90438	0.9197	0.9327	0.94414

Species scores

	PC1	PC2	PC3	PC4	PC5	PC6
Achnanthes minutissima	0.47729	0.169208	0.270299	0.16898	-0.0048	0.328897
Aulacoseira ambigua	-1.45386	-0.9635	-0.26383	0.02893	-0.07822	0.051366
Cymbella laevis	0.5003	-0.02452	0.088632	0.048	-0.11992	-0.10357
Cymbella gracilis	0.60032	0.010674	-0.10132	-0.27908	-0.18771	0.028161
Diploneis ovalis	0.57091	-0.0872	-0.0405	0.06897	0.1416	0.03944
Eunotia praerupta	1.90247	0.141436	-0.48643	-0.15641	0.17551	-0.01989
Eunotia bilunaris	0.99121	0.037588	0.281548	0.22361	-0.17638	-0.20418
Eunotia exigua	0.31936	-0.27587	0.346105	0.03977	0.26073	-0.08007
Fragilaria pinnata/ construens	-1.85305	0.658295	0.17587	-0.09037	0.18373	-0.09728
Fragilaria famelica	0.7444	0.230946	0.066646	0.04007	-0.08762	0.248813
Gomphonema parvulum	0.84716	-0.20601	0.275951	-0.24502	-0.35284	-0.03636
Gomphonema gracilis	0.40906	0.134357	-0.08951	0.21091	-0.08306	0.04581

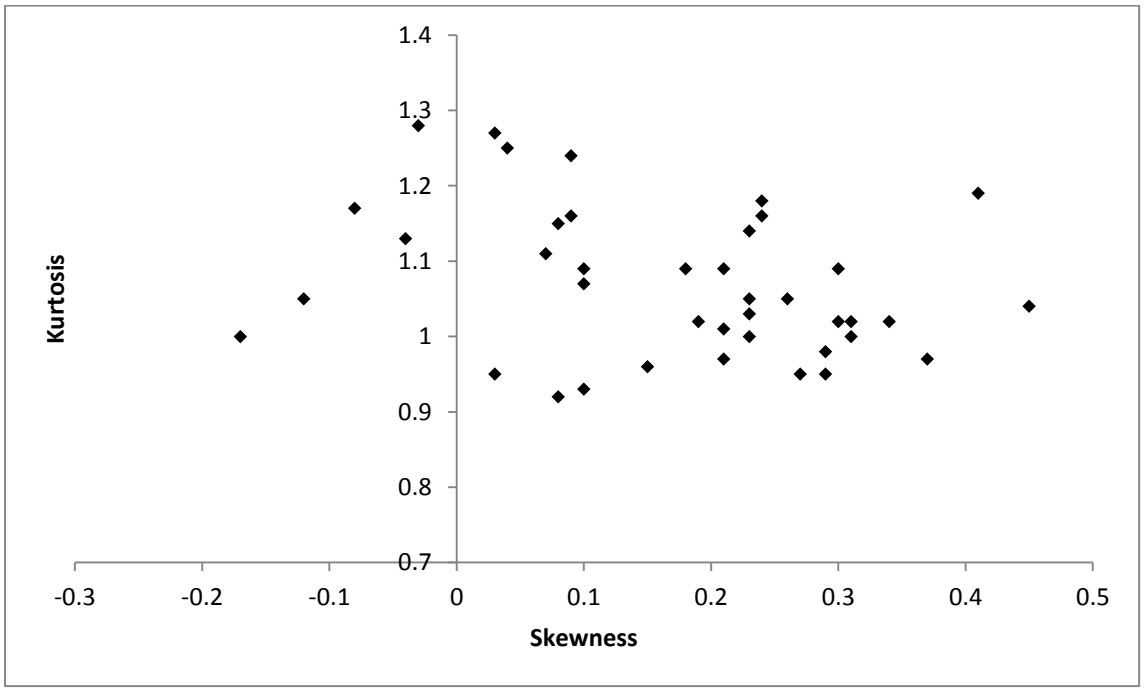
Hantzschia amphioxys	0.40107	0.009703	-0.04339	0.35185	0.09474	-0.06689
Navicula laevissima	0.67739	-0.20806	0.277987	-0.18638	0.03924	-0.19147
Navicula minima	0.49338	-0.07507	0.050528	0.11841	-0.03239	0.130444
Pinnularia viridis	0.57915	-0.30836	0.238509	-0.24294	0.40777	0.176474
Pinnularia borealis	0.95506	-0.08318	-0.26803	0.1053	0.12633	-0.02916
Pinnularia divergentissima	0.30357	-0.36769	0.267524	0.18639	0.08622	0.004185
Pinnularia gentilis	0.28626	0.071646	-0.06413	0.16407	0.015	-0.07859
Sellaphora pupula	-0.04068	-0.11779	-0.06556	0.20488	0.06293	-0.23361
Stauroneis phoenicenteron	0.49324	0.08472	-0.00315	-0.15325	0.08786	-0.2595

Site scores (weighted sums of species scores)

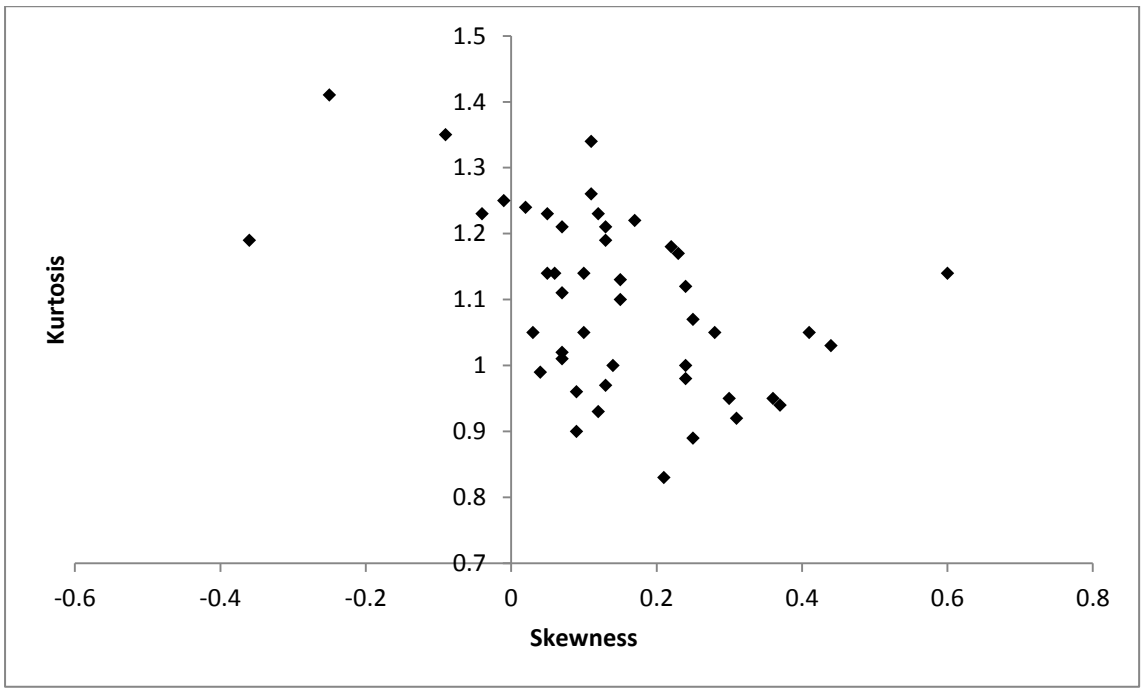
	PC1	PC2	PC3	PC4	PC5	PC6
M1	-0.49561	-0.43204	-1.65491	0.98558	1.306009	-0.74796
M2	-0.27634	-0.97503	-0.33056	0.29372	1.256388	0.28459
M3	-0.60841	-0.35448	-0.58196	2.00414	-0.69096	-0.15648
M4	-0.63795	-0.40428	0.373433	-0.75657	-0.85022	0.22922
M5	-0.66931	-1.54447	0.1321	0.77708	-1.58646	-1.12387
M6	-0.45791	-0.48947	0.955293	0.38164	-0.12567	-0.29523
M7	-0.16021	-0.637	1.595578	0.93352	0.99764	-0.12359
M8	-0.19786	-0.53127	1.808552	1.53118	0.211385	0.47324
M9	0.05442	-1.16663	0.422439	-0.22465	0.56088	-1.18616
M10	-0.37865	-0.19628	0.644291	-1.33111	1.081185	0.03423
M11	-0.85858	-1.30689	-1.79098	-0.38076	-1.05249	1.18349
M12	-0.75442	-0.30273	0.539648	-0.75641	-0.03168	-0.46575
M13	-0.59853	0.08443	-0.2922	0.05755	0.557607	-0.80497
M14	-0.82467	-0.07822	0.53802	-0.61943	0.025693	-0.40445
M15	-0.85047	-0.33298	-0.43184	-0.69011	0.974523	0.63088
M16	-0.83304	-0.10692	-0.24761	-0.79812	1.145884	0.57619
M17	-0.90135	0.50732	-0.71692	-0.55038	-0.4737	0.33491
M18	-0.59246	0.06402	-0.50599	-0.92108	-1.33652	-0.95404
M19	0.78836	-0.44279	-0.41373	-1.14213	-0.28598	1.22154
M20	0.76371	-0.36112	0.60632	-0.93505	0.000373	0.18412
M21	1.08497	-0.41049	0.485339	-0.28891	0.095085	0.42025
M22	1.0366	0.50174	0.276545	-0.44874	-0.09469	-0.50509
M23	1.02514	-0.19847	-0.39563	-0.93192	0.745391	-0.55813
M24	1.12415	0.51264	0.4151	-0.63245	-1.53555	0.35789
M25	1.02123	-0.68177	0.481239	0.05125	-0.40584	0.56623
M26	0.97288	-0.10578	0.27505	0.30086	0.241149	0.13985
M27	1.35623	-0.15544	0.205939	0.91867	-0.88139	0.30192
M28	1.05434	-0.13739	-0.00815	0.71146	0.235054	0.5841
M29	0.70846	0.37207	-0.6143	0.15102	0.958713	0.42253
M30	0.72189	0.5019	-1.03111	0.0487	0.43865	0.83547
M31	0.84777	0.88677	-0.68111	0.25521	0.175619	-1.60504
M32	0.85768	1.03112	-1.3406	0.79597	0.036906	-1.24719
M33	-0.03949	0.90317	0.365212	-0.57219	-0.78685	-0.79212
M34	-0.28679	0.27373	-0.48691	0.30944	-0.17371	-0.56546
M35	-1.05821	1.4208	0.669889	-0.03941	-0.64676	-0.27876
M36	-0.58123	0.62409	-0.45131	1.10169	-0.6785	2.22255
M37	-0.52898	1.3769	0.401881	-0.07997	-0.17147	0.0741
M38	-0.82736	2.29125	0.783943	0.49072	0.764316	0.73702

C.2 Skewness: Kurtosis Plots

C.2.1 Sani Valley



C.2.2 Sekhokong



C.2.3 MAFADI WETLAND

